Université de Montréal

Identification of Transcriptional Regulators Functions in the Human Fungal Pathogen *Candida albicans* using Functional Genomics

Par
Aline Khayat

Institut de Recherche en Immunologie et Cancer
Programme de Biologie Moléculaire
Faculté de Médecine

Thèse présentée à la Faculté de Médecine
en vue de l'obtention du grade de *Philosophiæ Doctor* (PhD)
en Biologie Moléculaire
option Biologie des Systèmes

Janvier, 2017

Résumé

Candida albicans, une levure pathogène de l'humain, cause des infections envahissantes chez les individus immunodéprimés. *C. albicans* peut changer sa morphologie entre les formes levures et filamenteuses, un déterminant de virulence considérable qui est influencé par plusieurs facteurs environnementaux comme le pH, le sérum, les nutriments, et le farnesol, une molécule de la détection du quorum. Le génome de *C. albicans* a été séquencé et à date, plusieurs gènes codant des régulateurs de transcription (RT) restent incaracterisés. Basé sur des criblages à grande-échelle, il a été possible d'attribuer des phénotypes à certains des RT incaractérisés, cependant, leurs cibles traduisant ces phénotypes restent inconnues. Le but de cette thèse était d'étudier les fonctions biologiques de RT sélectionnés et d'établir des réseaux transcriptionnels chez *C. albicans*. J'ai utilisé des approches génétiques et génomiques afin d'identifier et de caractériser le regulon de ces RT, ce qui a permis de déterminer leur fonctions biologiques. Notre groupe avait identifié Fcr1p, un RT dont la délétion augmente la filamentation et la tolérance à plusieurs antifongiques. Cependant, le mécanisme sous-jacent reste inconnu. Dans le Chapitre 2, j'ai identifié le régulon d'Fcr1p et j'ai trouvé qu'il régule ses cibles de façon complexe étant en même temps un activateur et un répresseur d'expression de gènes. J'ai démontré que Fcr1p agit comme répresseur direct des gènes de l'assimilation et du métabolisme de l'azote. L'expression de plusieurs de ces cibles était dépendante d'Fcr1p en conditions d'épuisement d'azote. J'ai montrés que Fcr1p agit aussi comme répresseur indirect de gènes hyphe-spécifiques ainsi qu'un activateur indirect de transport et de métabolisme du carbone et de gènes levure-spécifiques. De plus, la suréxpression d'Fcr1p abolit la filamentation sur le milieu Spider, confirmant que c'est un répresseur de filamentation. Dans le Chapitre 3, j'ai décris un crible génétique basé sur un principe de co-culture pour identifier des mutants de RT défectueux en production de farnesol. Conséquemment, les RT Ada2p, Cas5p, Fgr15p, Cas1p, et Rlm1p,

impliqués dans le maintien de la paroi cellulaire, ont été identifiés. La quantification du farnesol intracellulaire de ces mutants a confirmé que le défaut observé peut être attribué à un défaut de la biosynthèse de farnesol plutôt qu'à un défaut de sécrétion de celui-ci. Pour comprendre le mécanisme responsable de ce défaut, nous avons commencé par caractériser le régulon de Cas5p par des analyses de profilages d'expression et de localisation. J'ai montré que Cas5p se lie à des gènes impliqués dans le catabolisme des hydrocarbures et la production d'énergie. Cas5p induit aussi des gènes impliqués dans le catabolisme des hydrocarbures et des lipides et réprime des gènes impliqués dans le métabolisme primaire, montrant que Cas5p régule plusieurs voies métaboliques, notamment celle du carbone. En plus des fonctions d'Ada2p et Rlm1p dans la liaison et/ou la régulation de gènes du catabolisme des hydrocarbures, nos résultats appuient avec la proposition que le farnesol constitue une traduction du métabolisme du carbone cellulaire. Dans l'ensemble, ces résultats ont aidé à élucider le rôle d'Fcr1p ainsi que 5 autres RT dans la régulation de voies métaboliques fondamentales influençant le dimorphisme, un attribut crucial de la virulence chez *C. albicans.*

Mots-Clés: *Candida albicans*, azote, carbone, métabolisme, assimilation, farnesol, détection du quorum, filamentation, régulation transcriptionnelle, génomique fonctionnelle.

Abstract

Candida albicans, an important human fungal pathogen, causes life-threatening invasive infections in immuno-compromised individuals. It switches between yeast and filamentous forms. This dimorphism is a considerable virulence attribute and one that is influenced by many environmental factors, such as pH, serum, nutrients and farnesol, a quorum sensing molecule. The genome of *C. albicans* has been sequenced and to date, many of the genes encoding transcriptional regulators (TRs) remain uncharacterized. Based on large-scale screens, it was possible to assign phenotypes to some of the uncharacterized TRs, however the targets of these TRs that mediate these phenotypes remain to be identified. The aim of this thesis work was to understand the normal biological function of selected TRs and construct transcriptional networks in *C. albicans.* I used genetic and genomic approaches to identify and characterize the regulon of these TRs, which helped to define their biological functions. Our group has previously identified Fcr1p, a zinc cluster TR whose deletion increases cell tolerance to multiple drugs and enhances filamentation. However, the mechanism by which it mediates these phenotypes is still unknown. In Chapter 2, I identified the regulon of Fcr1p and found that it regulates its targets in a complex manner since it can act both as an activator and as a repressor of gene expression. I have shown that Fcr1p acts as a direct negative regulator of genes involved in nitrogen source assimilation and metabolism. The Fcr1p-dependent expression of a number of its targets also occurs under nitrogen starvation conditions. Results also showed that Fcr1p is an indirect negative regulator of hyphal-specific genes, and an indirect positive regulator of carbon source transport and metabolism, as well as yeast-specific genes. Furthermore, Fcr1p overexpression abrogates filamentation on Spider medium confirming that it is a negative regulator of filamentation. In Chapter 3, I describe a genetic screen based on a co-culture assay with *A. nidulans* to identify TR mutants defective in farnesol production. Our results

identified Ada2p, Cas5p, Fgr15p, Cas1p, and Rlm1p, five TRs involved in cell wall integrity. Intracellular farnesol quantification in these mutants confirmed that the observed defect in farnesol production could be attributed to impairment in farnesol biosynthesis rather than export of this molecule. To get an insight into the molecular mechanism responsible for this defect, we started by identifying the regulon of Cas5p using expression and location profiling. Results showed that Cas5p binds genes involved in carbohydrate catabolism and energy production. Cas5p also upregulates genes involved in carbohydrate and lipid catabolism and downregulates genes involved in primary metabolism, indicating that Cas5p is involved in the regulation of many pathways, with a clear involvement in carbon metabolism. Coupled to the known function of Ada2p and Rlm1p in binding and/or regulating genes involved in carbohydrate catabolism, our results support the proposition that farnesol is a metabolic read-out of the cell carbon metabolic activity. Taken together, these results helped elucidate the role of Fcr1p as well as five other TRs in the regulation of central metabolic pathways that influence morphological switching, a crucial attribute of *C.albicans* virulence.

Keywords: *Candida albicans*, nitrogen, carbon, metabolism, assimilation, farnesol, quorum sensing, filamentation, transcriptional regulation, functional genomics.

Table of contents

List of Tables

Chapter 2

Chapter 3

List of Figures

Chapter 1

Chapter 2

Chapter 3

Chapter 4

List of Abbreviations

5-FC: 5-Fluorocytosine

5-FOA: 5-fluor-orotic acid

ABC: ATP-binding cassette

ALS: Agglutinin-Like Sequence

AmB : Amphotericin B

APC: Antigen presenting cell

Cas9: CRISPR-associated 9

CDR1: Candida drug resistance 1

CFEM: Common in several fungal extracellular membranes

CGD: Candida genome database

ChIP-chip: Chromatin immunoprecipitation on chip

ChIP-seq: Chromatin immunoprecipitation- sequencing

CRISPR: Clustered regularly interspaced short palindromic repeats

CRP: Cyclic AMP receptor protein

CWI: Cell wall integrity

dsDNA: double strand DNA

ESCRT: endosomal-sorting complex required for trafficking

FCZ: Fluconazole

FOH: Farnesol

FPP: Farnesyl pyrophosphate

FRT: Flip recombinase target sequences

FXR: Farnesol X receptor

GFP: Green fluorescent protein

GOF: Gain of Function

GST: Glutathione S-transferase

gRNA: Guide RNA

GTP: Guanosine triphosphate

HA: Hemagglutinin

HDACi: Histone deacetylase inhibitors

H&E: Hematoxylin & eosin

HOG: High osmolarity glycerol

HS1: Hot spot 1

HSL: homoserine lactone

ICL: isocitrate lyase

Kb: Kilobase

KDa: Kilodalton

LFAB: Lipid Formulations of Amphotericin B

MIC: Minimum inhibitory concentration

MAPK: mitogen-activated protein kinase

MCC: Membrane Compartment of Can1

MDR1: Multidrug resistance 1

MFS: Major facilitator superfamily

MRR1: Multidrug resistance regulator 1

MTL: Mating type locus

MW: Molecular weight

NCR: Nitrogen Catabolite Repression

NTE: N-terminal extension

ORF: open reading frame

PAS: Periodic acid-Schiff

PAMP: pathogen-associated molecular patterns

PKA: protein kinase A

PKC: protein kinase C

PLB: Phospholipases

PPase: Phosphatase

PRR: pattern recognition receptors

P-S6: Phosphorylated Subunit 6

PTM: post-translational modification

QS: quorum sensing

QSM: Quorum sensing molecules

RNA-seq: RNA-sequencing

RNS: Reactive nitrogen species

ROS: Reactive oxygen species

SAP: Secreted aspartyl protease

SEM: Scanning electron microscopy

SOD: Superoxide dismutase

SRE: Sterol responsive element

SREBP: Sterol regulatory element-binding proteins

TAC1: Transcriptional activator of *CDR* genes 1

TAP: tandem affinity purification

TCA: Tricarboxylic acid

TF: Transcription factor

Th1/Th17: T helper 1/T helper 17

TNFα: Tumor necrosis factor α

TOR: Target of Rapamycin

TR: Transcriptional regulator

tracrRNA: Trans-activating CRISPR RNA

TSA: Trichostatin A

TSC: Two-component-system

TSS: transcription start site

uORF: upstream open reading frame

UTR: untranslated region

YFP: Yellow fluorescent protein

To my parents,

and to my brothers,

who are the most precious gift in the world.

Acknowledgements

First of all, I would like to thank my supervisor Dr. Martine Raymond for hosting me in her research unit during my PhD studies, where I received a scientific training of the highest quality. During the course of my studies, she taught me valuable skills such as critical thinking, attention to detail, distanciation, patience and perseverance. I also thank her for giving me the opportunity to present my work at different occasions, especially at the 12th ASM Conference on Candida and Candidiasis, where I got the chance to meet renowned scientists in the field. In addition to her academic support, she was also supportive in times of crisis.

Thanks also go to past and present members of the Raymond lab, more particularly Sandra Weber, who was more like an older sister than a lab manager. I thank her for her assistance and for caring about me at the personal level too. I am grateful for having the team of Dr. Alain Verreault as my lab neighbors, for their friendliness, and their enjoyable spirit. I also owe many thanks to Rahul Ghugari and Sarah Tsao for their support during the difficult times and for being such good listeners.

I would like to express my gratitude to the Faculty of Medicine Molecular biology program at Université de Montréal for granting me many scholarships. I am also grateful for the Candida Genome Database for providing a precious resource without which most of my studies, analyses, and experiments wouldn't have been possible. I also extend my thanks to all IRIC staff, facilities and platforms, particularly Christian Charbonneau for his assistance and advice in microscopy and Illustrator, and Suzanne Renaud from administration for her assistance, her professionalism and most importantly for her extreme politeness and smiling face all year round. I would also like to thank Dr. Brian Wilhelm, Dr. Luis Rockeach, Dr. Joachim Morschhäuser, and Dr. Jean-Claude Labbé for accepting to review and evaluate my thesis.

Last but not least, I am blessed with a supportive and understanding family and relatives who continue to prove that I am not alone in this world despite the distances that separate us. I also thank Joe for his support and patience during the last phase of my PhD and especially during the writing period. I am also glad and lucky to have true and caring friends scattered all over the planet who were there for me through the ups and downs and who are too numerous to list here.

Chapter 1

1. Chapter 1: Introduction

C. albicans belongs to the Fungi Kingdom, the Ascomycota phylum, the Saccharomycotina subphylum, the *Candidaceae* family, the genus *Candida,* and the species *albicans*. The Ascomycota phylum is the largest of the Fungi phyla and is characterized by a specific structure called “ascus” that covers the spores during meiosis. *C. albicans* is closely related to the “baker’s yeast” *Saccharomyces cerevisiae* which also belongs to the Saccharomycotina subphylum. As opposed to *S. cerevisiae*, *C. albicans* is diploid, presents a number of karyotypic variations, and has no meiotic division (Scannell *et al.*, 2007).

Generally, *Candida* species are harmless commensals of skin and genitourinary tracts of healthy individuals. On occasions when host immunity is impaired, these fungi can progress and cause a variety of infections. *Candida albicans* is the most commonly isolated *Candida* species in nosocomial candidiasis, however, other *Candida* species such as *Candida glabrata*, *Candida tropicalis*, *Candida parapsilosis* and *Candida dubliniensis*, are becoming more and more prevalent. *Candida albicans* is one of the *Candida spp*. that are dimorphic and can transition between the yeast and the filamentous morphologies. It can cause superficial as well as systemic infections due to a remarkable battery of virulence attributes (McManus & Coleman, 2014). Currently a few antifungals exist for the treatment of *Candida albicans* infections, however their effectiveness has been compromised by the frequent emergence of resistance. Genetic manipulations to study this organism have been difficult due to its genetic composition (see section 1.6.1), however, the sequencing of its genome has facilitated these tasks and allowed large-scale genomic studies. Since then, efforts have been directed towards the

characterization of genes of unknown functions but also to the reconstruction of transcriptional networks to better understand the mechanisms underlying *C. albicans* patho-biology.

1.1. *Candida albicans* Morphology

1.1.1. Macroscopic morphology

Candida albicans yeast colonies are whitish and smooth in appearance. Under certain circumstances, colonies with rough surface are seen which usually contain a mix of yeast and hyphal forms (see section 1.3.1), reflecting some type of morphological diversity (Homann *et al.*, 2009). A particular type of colonies is also seen when culturing the mating-competent cell type known as opaque. As opposed to the normal yeast (white) colonies, opaque colonies are large and greyish in color but for better visualization Phloxin B stain is sometimes used (Figure 1.1) (Slutsky *et al.*, 1987)(see section 1.3.2).

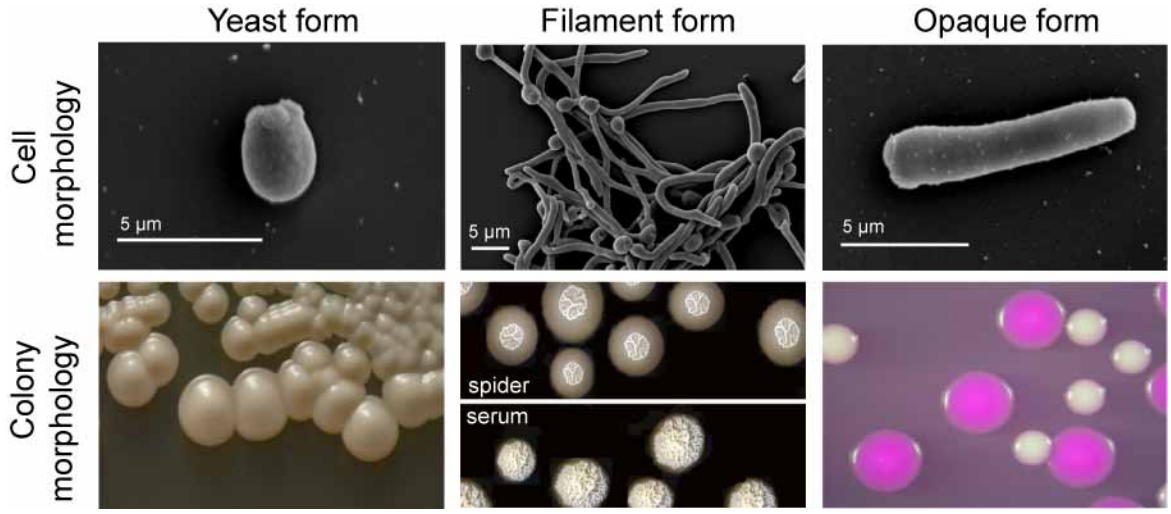

Figure 1.1. *Candida albicans* morphology.

The upper panel depicts the main *Candida albicans* cellular morphologies under scanning electron microscopy (SEM). The lower panel shows the typical colony morphologies

corresponding to each type of cells. White yeast cells have an ovoid shape and form whitish creamy colonies on sabouraud agar (selective medium). Hyphal cells display filamentous extensions and appear as an intertwined network. When grown on filament inducing culture media, they form colonies with rough surface (such as on media containing serum). They also invade the underlying agar, which appears as a crown-like halo surrounding the center of the colony (such as on spider medium). Opaque cells are typically elongated and form greyish colonies that can be stained in pink when grown on medium containing Phloxin B. Adapted from (Al-Akeel R, 2013; Elson *et al.*, 2009; Morschhauser, 2010; Si *et al.*, 2013).

1.1.2. Microscopic morphology

Candida albicans cells are polymorphic cells that can exist in different morphological forms: yeast, hyphae, pseudohyphae, chlamydospores and opaque (Si *et al.*, 2013). Yeast cells possess the typical round to ovoid shape of budding yeast, while hyphae are narrow elongated cells with parallel cell walls with no constrictions (Figure 1.1). Pseudohyphae, on the other hand, are elongated in shape, however wider than hyphal elongations, presenting constrictions, branches, and multiple nuclei (P. Sudbery *et al.*, 2004). Pseudohyphal growth results from cell division without detachment of daughter cells (Chaffin *et al.*, 1998). Chlamydospores are spore-like rounded cells that have a thick wall and a high content of carbohydrates and lipids. This cell type develops when cells encounter harsh environmental conditions such as extreme temperatures, nutrient starvation or hypoxia (Whiteway & Bachewich, 2007). Opaque cells, which are the mating-competent form of *Candida albicans*, are typically elongated cells. Even though they have the same amount of DNA as yeast (white) cells, they are significantly larger, heavier and less prone to form filaments (Figure 1.1) (Slutsky *et al.*, 1987). Just as white cells, opaque cells proliferate by budding (Morschhauser, 2010).

Like other eukaryotic cells, *Candida albicans* cells have different cellular compartments each with a specific role that is vital to the cell biology. For example, the

cell surface is also of particular importance. It is not only responsible for vital functions for fungal survival such as adhesion and invasion but also contains important components of host immune recognition (see sections 1.3.4 and 1.3.6). Due to its key importance, *Candida albicans* cell surface has been the target of many antifungals (see section 1.4). The fungal cell wall, an important constituent of the cell surface compartement, has been the focus of many studies. It has been long thought that the role of the cell wall was only confined to conferring structural and protective properties. However, recent advances in the field have shown that the cell wall fulfils a wide range of functions that demonstrate its highly dynamic and plastic structure making it essential for a number of physiological processes (see section 1.3.12). Electron microscopic visualization of the fungal cell wall reveals a layering aspect. More specifically, the cell wall is mainly composed of two layers. The external layer, which is rich in N- and O-linked glycoproteins, and the internal layer, which contains more of the β-1,3 and β-1,6-glucan, as well as chitin (Figure 1.2) (Chaffin *et al.*, 1998; Netea *et al.*, 2015). Carbohydrates, β-1,3 and β-1,6-glucan, chitin and mannans, constitute roughly 80% of wall mass, while proteins and lipids constitute a minority of the total cell wall components (Chaffin *et al.*, 1998). The cell wall also contains a certain amount of proteins destined for excretion. These are transiently located within the cell wall for this purpose (Chaffin *et al.*, 1998). Cell wall composition with regards to structure and distribution of the various components is rearranged upon morphological switching. This rearrangement exposes new fungal epitopes, which accounts for the immunogenicity of the hyphal forms (Shibata *et al.*, 2007).

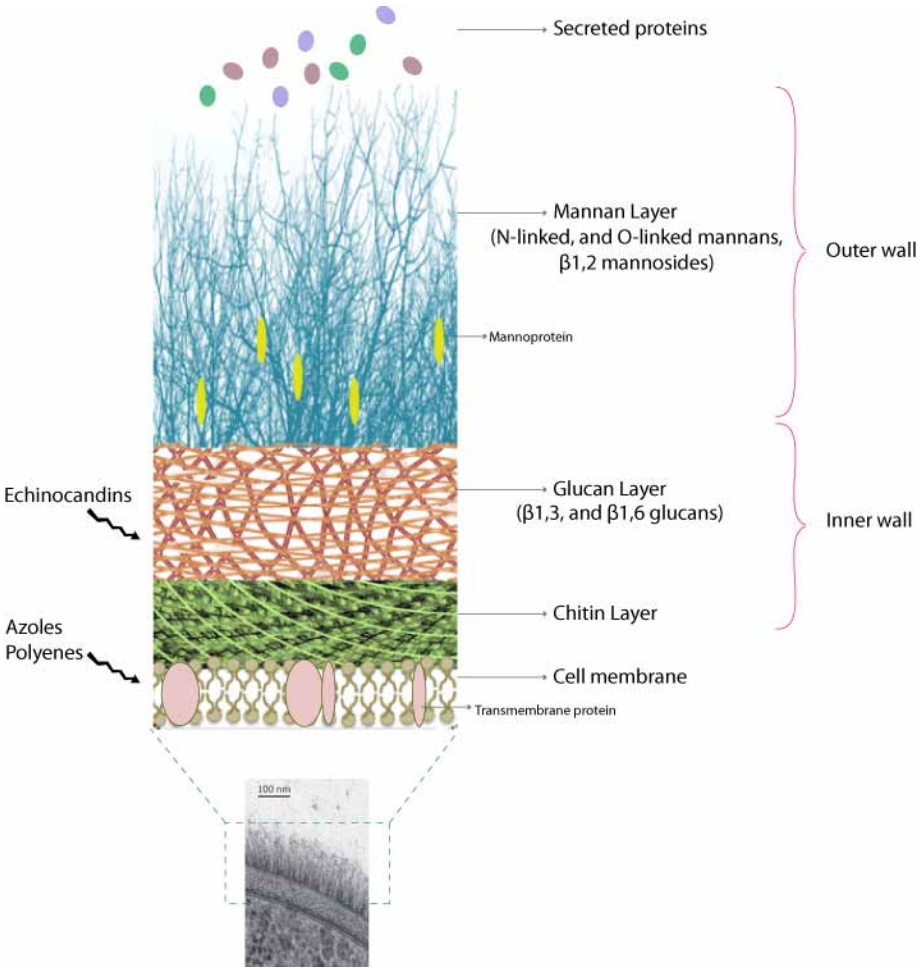

Figure 1.2. *Candida albicans* cell surface composition.

Illustrated here are the main components of *Candida albicans* cell surface: the outer cell wall, containing mannans and mannosylated proteins, the inner cell wall (the skeletal component) containing β-glucans and chitin, and the cell membrane, containing the phospholipid bilayer and transmembrane proteins. The bottom of the figure shows a microscopic view of the general cell surface structure. Adapted and modified from (Gow *et al.*, 2011; Grubb *et al.*, 2008; Perez-Garcia LA, 2012).

1.2. Infections and Host Immunity

1.2.1. Epidemiology

Under normal conditions, *Candida albicans* exists as part of the normal commensal flora of humans. Commensal colonization with *Candida albicans* is estimated to be as high as 30-55% in immuno-competent adults (Millsop & Fazel, 2016). However, upon weakening of the host immunological status or breach of protective barriers, *Candida* cells gain a proliferative advantage and an access to non-commensal sites, thereby causing disease. Bloodstream infections of *Candida* species are between the fourth and seventh leading cause of hospital-acquired blood infections (Antinori *et al.*, 2016; Lionakis, 2014) and *Candida albicans* continues to be the most commonly isolated species (50-90%) in diagnosed candidiasis (Martins *et al.*, 2014; Pfaller & Diekema, 2007). In addition, mortality rates associated with blood stream infections range from 30 to 70% and the clinical management of these infections in the US costs around 1 billion dollars per year (Mathe & Van Dijck, 2013). Therefore, *C. albicans* infections constitute a burden on hospital medicine.

The increasing incidence of *Candida* infections is owed in part to the rise in invasive medical interventions such as catheters, tubing, bone marrow and organ transplantation as well as aggressive chemotherapy. This has given *C. albicans* easier access to non-commensal sites, thereby increasing the risk of hospital acquired infections (Eggimann *et al.*, 2015). On the other hand, the selective pressure incurred by the use of large-spectrum antibiotics, also offered a proliferative advantage for *C. albicans* cells at commensal sites (Eggimann *et al.*, 2003).

A DNA-fingerprinting analysis has shown that *Candida albicans* strains harvested from hospital-acquired infection sites could have two possible origins; either from patient's

commensal sites or through cross-contamination from health care workers (Marco *et al.*, 1999). In an attempt to limit the transition from colonization to invasiveness, the medical community has been gradually implementing standard guidelines for proper and adequate prescription of prophylactic antifungal treatments based on objective parameters such as colonization index, *Candida* score, high-risk medical interventions, as well as potential patient-related predisposing factors (Eggimann & Pittet, 2014; Eggimann *et al.*, 2015).

1.2.2. Types of infections

Candida albicans is responsible for a wide range of clinical conditions ranging from superficial mucosal infections to disseminated systemic infections. The most common mucocutaneous infections associated with *Candida albicans* are oral thrush (also known as oropharyngial candidiasis) and vulvo vaginal, and esophageal candidiasis (J. Kim & Sudbery, 2011). Superficial mucosal infections cause irritations, burning, and whitish or red (erythematous) depositions at the affected site (Fidel, 2002; Millsop & Fazel, 2016). These infections can occur in single or recurrent episodes in healthy individuals following hormonal, corticosteroid or antibiotic therapy (Fidel, 2002). Invasive candidiasis includes blood infections, known as candidemia, and organ infections, known as deep-seated candidiasis (Antinori *et al.*, 2016). Depending on the location of the infection, corresponding specific symptoms can be manifested such as symptoms associated with liver damage, kidney failure, respiratory dysfunction as well as abdominal infections (Antinori *et al.*, 2016). These infections occur when yeast cells access the bloodstream causing candidemia and organ infections such as endocarditis, meningitis and peritonitis (Martins *et al.*, 2014). This type of infections is most commonly associated with high mortality rates.

Biofilm-associated infections are a particular type of infections that arise from colonization of biomaterial surfaces and medical devices. Yeast cells within this particular

microenvironment are extremely notorious as they are intrinsically resistant to antifungals and immune recognition. In addition, biofilms constitute an important site of dissemination giving access to internal visceral organs and causing various types of invasive candidiasis. Clinical management of biofilm-borne infections represents a significant and costly challenge in the clinical setting (Nobile & Johnson, 2015). Biofilm structure and regulation are discussed in more details in a later section (see section 1.3.5).

1.2.3. Host immunity and defense mechanisms

Commensal *Candida albicans* cells are mostly in the yeast phase and elicit the adaptive immunity that tolerates their presence (Cassone, 2013). However, the switch to the hyphal form induces the expression of fungal antigens such as Hyr1p and Hwp1p that are recognized by the host immune system as foreign antigens and therefore elicit an immune reaction to eradicate the fungal cells (Cassone, 2013; Y. Wang *et al.*, 2015). In general, host immunity against fungal cells is achieved by a combination of specific (adaptive) and non-specific (innate) responses.

The innate immune response constitutes the first line of defense against pathogenic invaders and consists of physical and chemical barriers. For instance, the skin constitutes a protective barrier against microorganisms whereas cilia of the respiratory tract ensure their effective elimination (Levitz, 1992). Other examples include epithelial cells that produce β–defensins with fungistatic activity (Fidel, 2002; Netea *et al.*, 2015), macrophages and endothelial cells that ensure phagocytosis of microbial cells, and while blood polymorphonuclears that secrete chemokines and chemoattractants and recruit other immune cells to the site of infection (Fidel, 2002; Jimenez-Lopez & Lorenz, 2013). Resident antagonistic microbial flora also controls pathogens by secreting apoptotic chemicals that inhibit proliferation of competing microorganisms (Levitz, 1992). Among the described innate immunity mechanisms is iron sequestration, whereby the host keeps

iron reserves protein-bound to prevent their utilization by foreign organisms (D. A. Davis, 2009) (Almeida *et al.*, 2009). Finally, new evidence has shown that the host body temperature itself also contributes to protection against certain fungal pathogens that grow typically at lower temperatures (Bieganska, 2014).

The adaptive immunity can be divided into cell-mediated and humoral immunity (Figure 1.3). Cell mediated immunity to *Candida* has been shown to rely mainly on the presence of specific CD4+ and CD8+ cells (Ashman *et al.*, 2004; Fidel, 2002). In addition, a Th0/Th1 response manifested by the production of IL-2, interferon-γ, TNF-α amongst others, is also generally considered as protective against *Candida* invasion (Fidel, 2002). In contrast, the humoral anti-*Candida* response characterized by the production of IgA, IgG and IgM, is generally considered insufficient on its own and rather requires complementary immune mechanisms to efficiently clear an infection (Fidel, 2002). The adaptive immunity also participates in the recognition and control of *Candida* commensal forms. Immunological testing of asymptomatic healthy carriers revealed the presence of immune effectors such as responsive T-cells as well as specific blood, skin and mucosal anti-*Candida* antibodies (Fidel, 2002). More thorough reviews on host immunity and defense mechanisms against *Candida albicans* cells are detailed elsewhere (Ashman *et al.*, 2004; Romani, 2000).

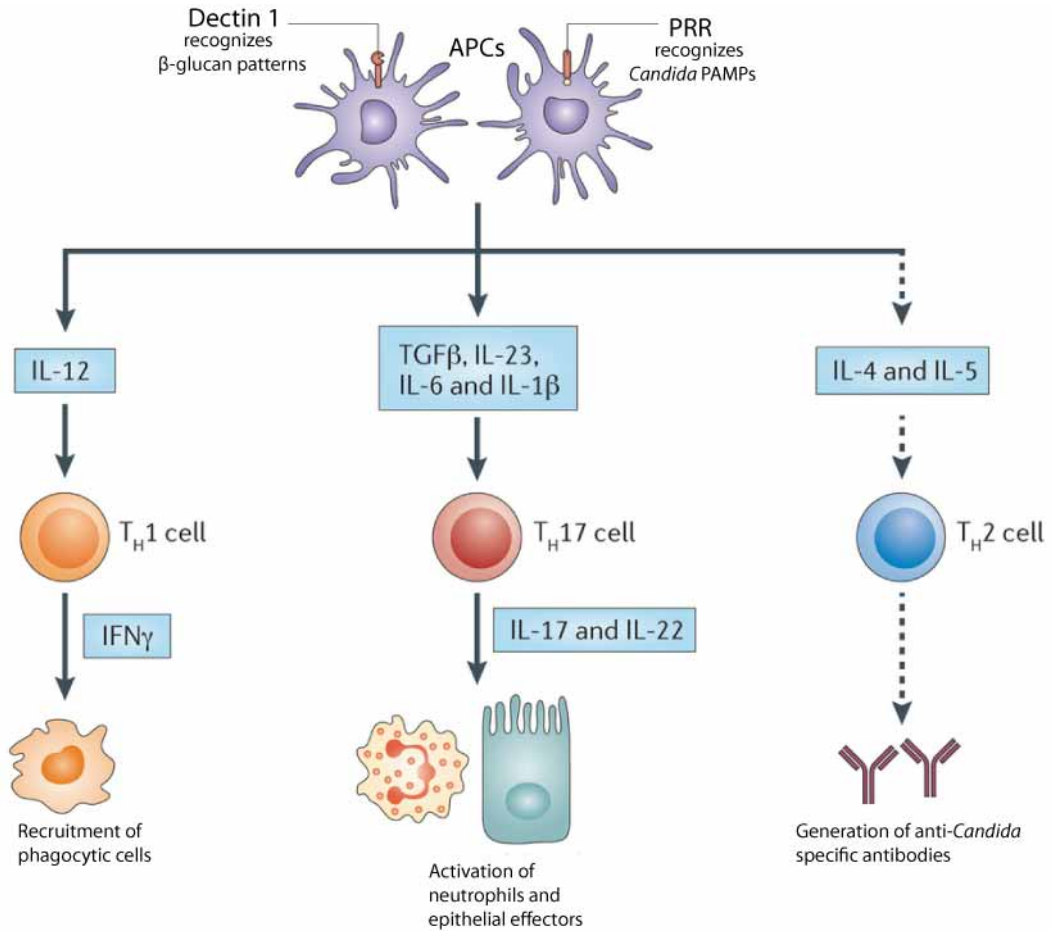

Figure 1.3. Main anti-*Candida albicans* immunity mechanisms.

After detection of *Candida albicans* cells by host recognition mechanisms, a wide range of responses is generated, however for simplicity reasons only three types of responses are illustrated in this figure. Among the most important recognition receptors are Dectin 1, which recognizes β–glucan patterns and PRR, which recognizes *Candida* PAMPs, both of which located on antigen-presenting cells (APC). The Th1 response is induced by the production of IL-12, which activates Th1 cells, the production of IFNγ, and initiation of phagocytosis. The Th17 response is triggered by TGFβ and the interleukins-6, -23, and 1β followed by production of pro-inflammatory cytokines interleukins-17 and -22 and the activation of the neutrophil and epithelial effectors. The Th2 response, which has a minor importance in *Candida albicans* immunity, starts with the production of the interleukins-4 and -5 and ultimately results in the production of antibodies(Cassone, 2013).

1.3. Pathogenic determinants and virulence

Candida albicans virulence potential relies on key pathogenic determinants that allow survival in harsh host niches and successful maintenance of infection. The most important virulence traits are discussed in this section.

1.3.1. Filamentation

One of the most important and most studied virulence attributes of *Candida albicans* is its ability to transition between yeast and hyphal forms, both of which are important for the many aspects of establishing an infection. For example, hyphal extensions are essential for disruption and penetration of epithelial cells and for escaping from macrophages whereas yeast cells allow dissemination through the blood stream to access the various host organs (Saville *et al.*, 2003). It has been long thought that filaments are tightly coupled to virulence. However, recent studies have shown that cells locked in either morphology are less or non virulent. These findings indicate that it is the ability of cells to undergo the switch between the two morphologies that confers adaptability to changes in environmental conditions. Therefore, the morphological switch itself confers virulence rather than either one of the morphological states alone (Braun *et al.*, 2001). In addition, filamentation and timely initiation of yeast or hyphal programs is also central to biofilm formation and dynamics.

1.3.1.1. Environmental cues

Phenotypic switching is triggered by a battery of various environmental and host stimuli (Figure 1.4). For example, conditions that allow the maintenance of the yeast form include an acidic medium or high cell density. On the other hand, filamentous growth is promoted by a neutral to alkaline medium or by low cell density (D. A. Davis, 2009; Mayer *et al.*, 2013). Morphologic transition in response to cell density is regulated by a process

called quorum sensing (see section 1.3.9). Besides pH and cell density, other factors promote the yeast-hyphal switch including serum, hypoxia, semi-solid matrix environment, elevated temperature, increased CO_2 pressure, nitrogen and carbon starvation (Figure 1.4). All of these environmental cues are relevant to *in vivo* conditions. For example, serum is an essential constituent of the blood, the typical temperature inside the human host is 37ºC, and the CO_2 level in internal organs is higher than the atmospheric one (P. E. Sudbery, 2011; P. Sudbery *et al.*, 2004). It is also well recognized that filamentation inside macrophages is triggered by important cues such as hypoxia, high CO_2 level, and alkaline pH (Miramon *et al.*, 2013). Furthermore, it has been proposed that alcalinization of the *C. albicans* surrounding medium in addition to the presence of ROS, both signal cells to filament within phagocytes (Jimenez-Lopez & Lorenz, 2013).

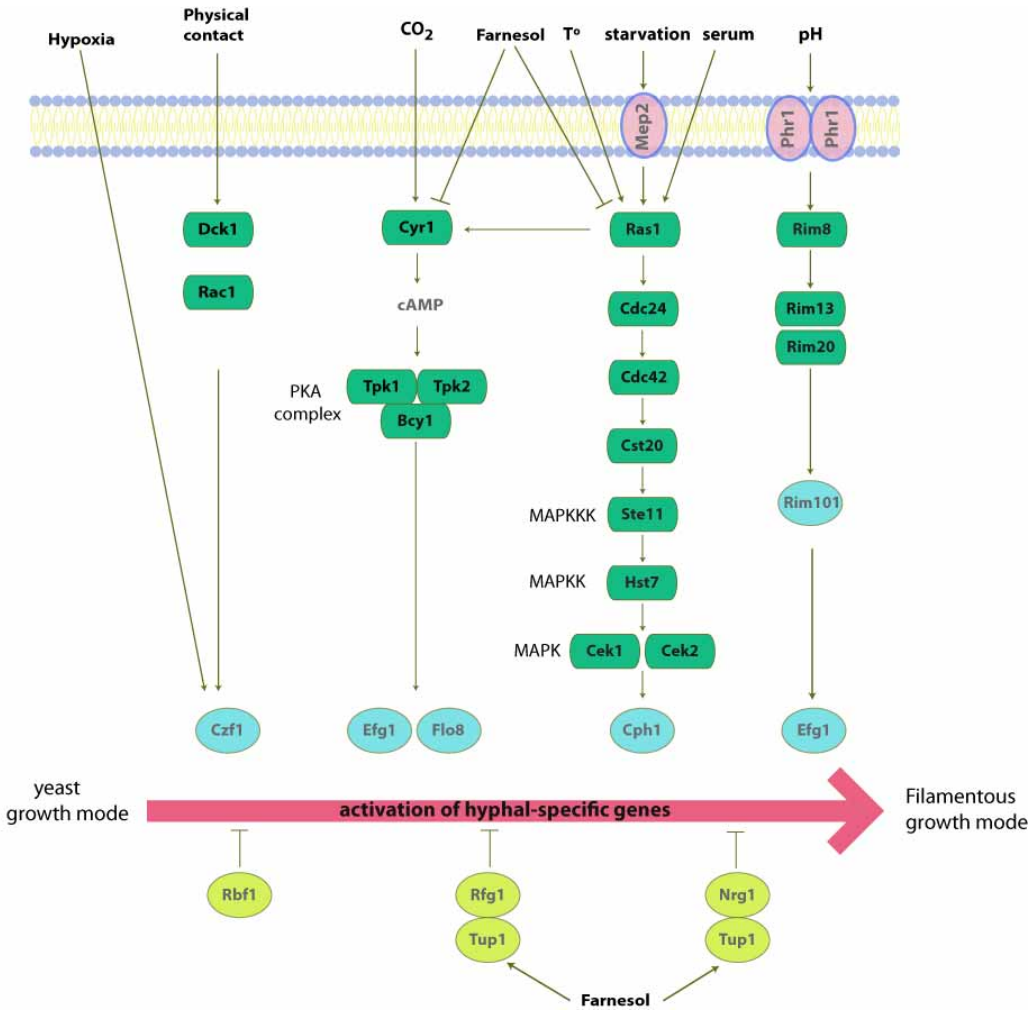

Figure 1.4. Simplified signal transduction pathways regulating filamentous growth. Inducing environmental stimuli (such as temperature, serum or pH) target different signal transduction pathways (such as cAMP or MAP kinase pathways), which in turn activate transcription factors (such as Efg1p, Cph1p, or Flo8p) involved in filamentation. The cascade ultimately leads to the expression of hyphal-specific genes (such as *HWP1*, *ECE1*, or *ALS3*). On the other hand, inhibiting environmental stimuli (such as farnesol) activate repressor transcription factors (such as Tup1p or Nrg1p) that prevent the expression of hyphal-specific genes. PKA, protein kinase A; MAPK: mitogen-activated protein kinase. Adapted and modified from (Huang, 2012; P. E. Sudbery, 2011).

1.3.1.2. Signal transduction pathways

Following detection of an environmental stimulus by external sensors, an interconnected web of signal transduction pathways is activated leading to activation of

transcription factors that regulate the expression of hyphae- and hyphae-associated genes (Figure 1.4). Signaling pathways involved in yeast-hyphal switch include MAP kinase and cAMP/PKA pathways (Dhillon *et al.*, 2003), RIM101 pathway (D. A. Davis, 2009), Protein kinase c (PKC) pathway (Kumamoto, 2005), Tor signaling pathway (Bastidas *et al.*, 2009), high-osmolarity glycerol (HOG) pathway (Roman *et al.*, 2005), as well as other pathways.

1.3.1.3. Transcriptional regulation

Transcription factors (TF) that promote filamentation include Czf1p, Cph1p, Cph2p, Efg1p, Rim101p, Tec1p, and Flo8p. On the other hand, TFs that block the filamentous program include Nrg1, Tup1, Rfg1, Rbf1, and Efg1p (Dhillon *et al.*, 2003; Huang, 2012; P. E. Sudbery, 2011). In some instances the regulation of filamentation is complex and context-dependent such as in the case of the transcription factor Efg1p that promotes filamentation in aerobic conditions and represses it under anaerobic conditions (Giusani *et al.*, 2002; Setiadi *et al.*, 2006). Under other circumstances, TF expression level dictates the phenotypic outcome as is the case with *UME6*. High expression levels correlate with hyphal formation whereas low levels correlate with a yeast morphology (Carlisle *et al.*, 2009). Condition-specific transcription factors also control filamentation. For example, under embedded conditions, the transcription factor Czf1p is responsible for the morphogenetic switch inducing contact-mediated filamentation (D. H. Brown, Jr. *et al.*, 1999). This is achieved by relieving the repressive pressure of Efg1 on the filamentous process (Giusani *et al.*, 2002). Finally, hypoxia-induced filamentation is under the positive regulation of Upc2p and the negative regulation of Bcr1p (Synnott *et al.*, 2010).

1.3.1.4. Gene expression

A major transcriptional reprogramming of the cell induces hyphal growth. Many studies have shown that a large number of genes are differentially regulated upon hyphal switch under various conditions (Grumaz *et al.*, 2013; Nantel *et al.*, 2002). Expression of some of those genes is specifically associated with the particular inducing stimulus, while others are common to all stimuli. In particular, 8 genes (*ALS3, ECE1, HGT2, HWP1, IHD1, RBT1, DCK1* and orf19.2457) were recently found to be differentially regulated in response to a number of filament-inducing stimuli, defining a core set of genes that are specific to the hyphal program (Martin *et al.*, 2013). Interestingly, filamentation is not only characterized by expression the hyphal program genes but also independent genes encoding proteins related to virulence such as adhesins (Als3p and Hwp1p) and proteases of the Sap family (Sap4p and Sap5p) (see sections 1.3.4 and 1.3.6) (Kumamoto & Vinces, 2005; Mayer *et al.*, 2013).

1.3.2. White-opaque switching

Candida albicans undergoes another type of phenotypic switching called the white-opaque switch that is controlled by the mating type locus (MTL). The MTL locus in *Candida albicans* is usually heterozygous having two different alleles *MTLa* and *MTLα* located on chromosome 5. Their products form the a1-α2 complex, which represses the TF Wor1p, the master transcriptional regulator of white-opaque switching (Miller & Johnson, 2002). For the white-opaque switch to occur, homozygozity at the MTL locus has first to be achieved to yield cells that are purely *MTLa* or *MTLα (Lockhart et al., 2002)*. It was shown that loss of one copy of chromosome 5 followed by duplication of the remaining copy is the most common mechanism of acquiring homozygosity at the MTL locus, producing cells that are either *MTLa/a* or *MTLα/α* (W. Wu *et al.*, 2005). The absence of the a1-α2 repressor in MTL homozygous strains results in derepression of

Wor1p, which drives the switch to the opaque phase. Mating occurs between a cells and α cells, resulting in tetraploids that produce the a1-α2 repressor and switch back to the white phase. The resulting tetraploids revert to the diploid state by a process known as concerted chromosome loss (Morschhauser, 2010). Positive transcriptional regulators of the white-to-opaque switch include Czf1p, Wor2p, and the recently characterized Wor4p, while negative regulation is achieved by Efg1p (Morschhauser, 2010) (Lan *et al.*, 2002; Lohse & Johnson, 2016). Many genes exhibit differential expression proper to each cell type and therefore confer phenotypic as well as metabolic attributes that explain their differential adaptability with respect to the different host niches (Lan *et al.*, 2002; Morschhauser, 2010). Many of the genes differentially expressed play a role in adhesion, virulence, cellular membrane composition, as well as stress response genes (Lan *et al.*, 2002). Among the genes that are expressed in a phase-specific manner, *SAP1* and *OP4* are preferentially expressed in the opaque phase, while *WH11* and *RME1* are considered white-specific transcripts (C. A. Kvaal *et al.*, 1997; C. Kvaal *et al.*, 1999; Strauss *et al.*, 2001; Tsong *et al.*, 2003).

The white-opaque transition is a prerequisite for mating but is also considered as a virulence attribute (Ramirez-Zavala *et al.*, 2008). White-opaque switching is reversible and occurs at low frequency to allow mating and therefore generate diversity (Lockhart *et al.*, 2002; Ramirez-Zavala *et al.*, 2008). The switching rate in natural strains occurs at relatively low frequency, however the WO-1 strain has a switching rate as high as 10^{-2} (Slutsky *et al.*, 1987). In addition to stochastic spontaneous switching, environmental cues have also been shown to enhance the frequency of the switch, such as the anaerobic conditions encountered in the intestines but also the elevated concentration of CO_2 within tissues (Huang *et al.*, 2009; Ramirez-Zavala *et al.*, 2008). Exposure to high temperatures also results in an increase in the opaque-to-white transition, indicating that the white

phase may be better adapted to the physiological temperature (37º) of internal organs (Slutsky *et al.*, 1987). It is thought that transitioning between cell types allows better adaptation to different niches but is also useful for effective immune evasion (Strauss *et al.*, 2001). In this regard, opaque cells are better at avoiding recognition by leukocytes due to their inability to produce a specific chemoattractant (Geiger *et al.*, 2004). Furthermore, it was shown that in a systemic mouse model, cells in the white state were more virulent than opaque cells(C. A. Kvaal *et al.*, 1997; C. Kvaal *et al.*, 1999). However, opaque cells had more adhesive and tissue invasion properties and therefore were more virulent in skin infection models(C. A. Kvaal *et al.*, 1997; C. Kvaal *et al.*, 1999). Opaque cells also induce white cells to form biofilms and hence contribute to pathogenesis via colonization of medical devices (Daniels *et al.*, 2006).

1.3.3. Metabolic adaptation

Energy-efficient assimilation of nutrients and metabolic adaptability are key for successful colonization as well as infection by pathogenic fungi. *Candida albicans* is a metabolically flexible pathogen capable of adapting its metabolism to the available nutrients within the resident niche. Nutritional adaptability therefore allows persistence and is often correlated with enhanced pathogenic potential (Ene *et al.*, 2012; Lorenz & Fink, 2001).

In the presence of preferred sources of nutrients, control mechanisms known as carbon and nitrogen catabolite repression are active. In these conditions, cells preferentially assimilate and metabolize those rich nutrients as sources of energy and use them as building blocks for proteins, lipids, nucleic acids, and carbon-rich molecules, amongst others (Fleck *et al.*, 2011; Flores *et al.*, 2000). In the absence of preferred sources, a shift in the transcriptional program allows activation of alternative metabolic pathways to extract the so-called “non-preferred” nutrient sources. A recycling system is also activated

to breakdown non-vital intracellular molecules and use them as building blocks essential for running vital functions (Miramon *et al.*, 2013).

An example of nutrient supply fluctuations is illustrated by the intracellular phagocytic environment that is glucose-deficient as compared to the blood, liver and brain environments which are glucose-rich (Fleck *et al.*, 2011; Lorenz *et al.*, 2004). As the intraphagocytic environment mimics nutritional starvation, *C. albicans* switches to the use of lipids and amino acids as precursor molecules (Brock, 2009; Mayer *et al.*, 2013). Gluconeogenic molecules that can be used as energy sources include citrate, pyruvate, acetate, glycerol, ethanol, and lactate (Brock, 2009; Ene *et al.*, 2012). Expression of aspartic proteinases encoded by the *SAP* gene family exposes additional nutrient sources, notably proteins, resulting from host tissue damage (Fleck *et al.*, 2011; Naglik *et al.*, 2003). In addition, genes encoding proteins relevant to nitrogen transport, such as Can1p, Gap1p, and Mep1p, are also upregulated to acquire the exposed extracellular nitrogen sources (Brock, 2009; Lorenz *et al.*, 2004; Miramon *et al.*, 2013). Furthermore, vital trace elements (such as iron and copper) that are essential for optimal fungal enzymatic activity are most of the times hidden away (bound to host proteins) from microorganisms (D. A. Davis, 2009). Fungal metabolic flexibility, manifested by the expression of a wide array of permeases, transporters and extracellular hydrolytic enzymes allows access to these hidden resources (A. J. Brown *et al.*, 2007; Nailis *et al.*, 2010).

1.3.4. Adhesion

The *Candida albicans* genome harbors a gene family known as the Agglutinin-Like Sequence (*ALS*) family, which encodes a number of cell-surface adhesins. These glycoproteins participate in cell adhesion and attachment to inert surfaces as well as live tissues (Hoyer & Cota, 2016). This gene family presents a lot of allelic variations within the same strain, each of which with a unique function. This allelic variation contributes to

diversity and therefore adaptability to the encountered colonization surface (Hoyer *et al.*, 2008). The deletion of one *ALS* gene results in a compensatory mechanism to restore adhesive properties (X. Zhao *et al.*, 2005). Expression of some *ALS* genes occurs downstream of transcription factors involved in filamentous growth. For example, the *ALS1* and *ALS3* genes are regulated by the morphological regulator Efg1p (Braun & Johnson, 2000), while *ALS3* is activated by Tec1p (promoting filamentation) and repressed by Nrg1p and Tup1p (inhibition of filamentation) (Argimon *et al.*, 2007). In addition to the *ALS* gene family, the products of other genes also have adherence properties, some of which are secretory proteins, while others are surface-bound proteins. Examples of these genes include *PGA10*, *HWP2*, and *PBR1*, *SAP1*, *HYR3*, and *HWP1* (Finkel *et al.*, 2012; Staab & Sundstrom, 1998). Transcriptional regulation of adherence is also achieved by a number of other transcription factors such as Bcr1p, Ace2p, Zap1p, Cas5p, Zcf28p and the chromatin modulator Snf5p (Finkel *et al.*, 2012).

Candida albicans is recognized as a highly adhesive yeast, which accounts for much of its virulence. Strains in which adhesion genes have been deleted are less virulent and more rapidly cleared by the host immune system in comparison with wild type strains (X. Zhao *et al.*, 2004; X. Zhao *et al.*, 2005). Also, a number of adhesins have been associated with epithelial invasion and destruction (Phan *et al.*, 2007; X. Zhao *et al.*, 2004). As adherence is crucial for biofilms, Als proteins are also implicated in the establishment of these particular *C. albicans* microenvironments (see section 1.3.5). Also, given their vital importance to *Candida albicans* biology, some Als proteins have also been investigated as potential targets in the generation of vaccines (see section 1.4.6). Therefore, it seems that the existence of a gene family that specifically mediates adhesion implies the importance of such trait for *Candida albicans* pathology.

1.3.5. Biofilms

Candida albicans biofilms are organized communities of cells in different morphological stages that form on inert material such as medical devices. Within the biofilm, yeast, hyphae as well as pseudohyphal cells can be found intertwined in a carbohydrate-rich extracellular matrix (Figure 1.5). Initiation of the biofilm starts with the attachment stage where yeast cells adhere to the inert surface. Then hyphal forms start to appear with gradual deposition of the matrix material such as mannose and glucose. The final step, referred to as the maturation stage is characterized by an increase in the extracellular matrix volume and dissemination of yeast cells out of the biofilm to establish a new biofilm elsewhere or a bloodstream candidemia (Figure 1.5) (Chandra *et al.*, 2001; Ramage *et al.*, 2009). Important molecules such as farnesol and pheromones are secreted within biofilms. Farnesol, a quorum-sensing molecule orchestrates the interchange between yeast and hyphal morphologies that are essential for the establishment of a healthy biofilm structure (see section 1.3.9) (Deveau & Hogan, 2011). On the other hand, pheromones are also important for biofilm biology. It was shown that in a given cell population, a minority of cells exist in the opaque phase and signal white cells through pheromones to form biofilms, which in turn provide a suitable environment for switching and mating (Daniels *et al.*, 2006). Genes with differential expression in biofilm structures include ergosterol biosynthesis genes such as *ERG25* and *ERG9*, and β–glucan biosynthetic genes such as *SKN1* and *KRE,* as well as adhesion genes such as *ALS* genes (Hoyer *et al.*, 2008; Mathe & Van Dijck, 2013). It has also been shown that the transcriptional response induced in biofilms is largely similar to the response to hypoxic conditions, indicating that hypoxic adaptation is also essential for maintenance of biofilms (Sellam, Al-Niemi*, et al.*, 2009).

Clinically, it has been shown that more than 80% of reported cases of microbial infections can be associated with biofilm structures and that the probability of developing a biofilm-associated infection is approximately 30% (Mathe & Van Dijck, 2013; Nobile & Johnson, 2015). Biofilms are regarded as a serious clinical burden due to their recalcitrance and difficulty to eradicate. They also display intrinsic resistance to many antifungals (Nobile & Johnson, 2015). Biofilm-associated drug resistance could be due to a number of factors, including the protective effect of the thick extracellular matrix combined with differential genes expression such as genes involved in quorum sensing and drug efflux pumps (Chandra *et al.*, 2001; Jabra-Rizk *et al.*, 2004). The condensed extracellular matrix also allows persistence by protecting resident biofilm cells from the host immune system (Mathe & Van Dijck, 2013).

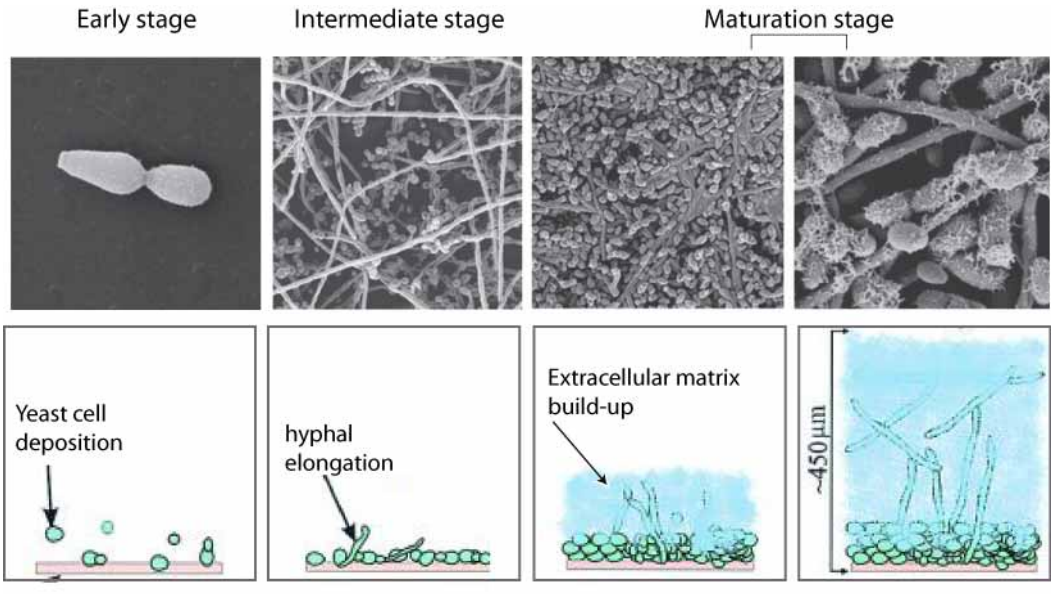

Figure 1.5. Developmental stages of biofilm formation.
The upper panel presents the different developmental stages of a typical biofilm on polymerized plastic surface as seen by scanning electron microscopy (SEM). The lower panel shows a schematic illustrating those same stages. The establishment or early phase starts by deposition of yeast cells onto the inert surface. Some cells start to

elongate as contact sensing is activated. During the intermediate stage, a web of filamentous cells will begin to form. The maturation stage is typically characterized by the buildup of the dense extracellular matrix followed by detachment of yeast cells to colonize other sites. Adapted and modified from (Chandra *et al.*, 2001; Ramage *et al.*, 2009).

1.3.6. Tissue Invasion

Host tissue invasion is an important virulence trait that allows the fungal pathogen to access non-commensal sites and progression of infection. Tissue invasion is mediated by distinctive mechanisms such as induced endocytosis and active penetration of hyphal extensions, which results in an apparent tissue infiltration (Figure 1.6) (Grubb *et al.*, 2008). These mechanisms rely on the coordinate expression of cell-surface proteins and extracellular enzymes. For example, the expression of the *C. albicans* invasins Als3p and Ssa1p induce endocytosis of fungal cells into epithelial and endothelial cells by binding to host cadherins (Cassone & Cauda, 2012; Phan *et al.*, 2007; Sun *et al.*, 2010; W. Yang *et al.*, 2014). Moreover, tissue invasion not only allows access to non-commensal sites but also allows the acquisition of nutrients from host tissues by execreting proteolytic enzymes and hydrolases such lipases, proteases, and hydrolases (Hube *et al.*, 2000; Leidich *et al.*, 1998; Niewerth & Korting, 2001; Stehr *et al.*, 2004). Interestingly the *C. albicans* genome has a repertoire of gene families for those enzymes, the secreted aspartyl proteases (Sap) family constituted of 10 SAP genes (*SAP1-10*), the phospholipases (*PLB*) gene family (*PLB1-5*), and the lipases (*LIP1-10*), underscoring the importance of these enzymes in the disease process. In addition to degrading E-cadherin (human transmembrane proteins), aspartic proteases actively participate in immune evasion by hydrolyzing and neutralizing host antibodies and proteins of the complement cascade (see section 1.3.7) (Cassone, 2013; Cassone & Cauda, 2012; Gropp *et al.*, 2009)

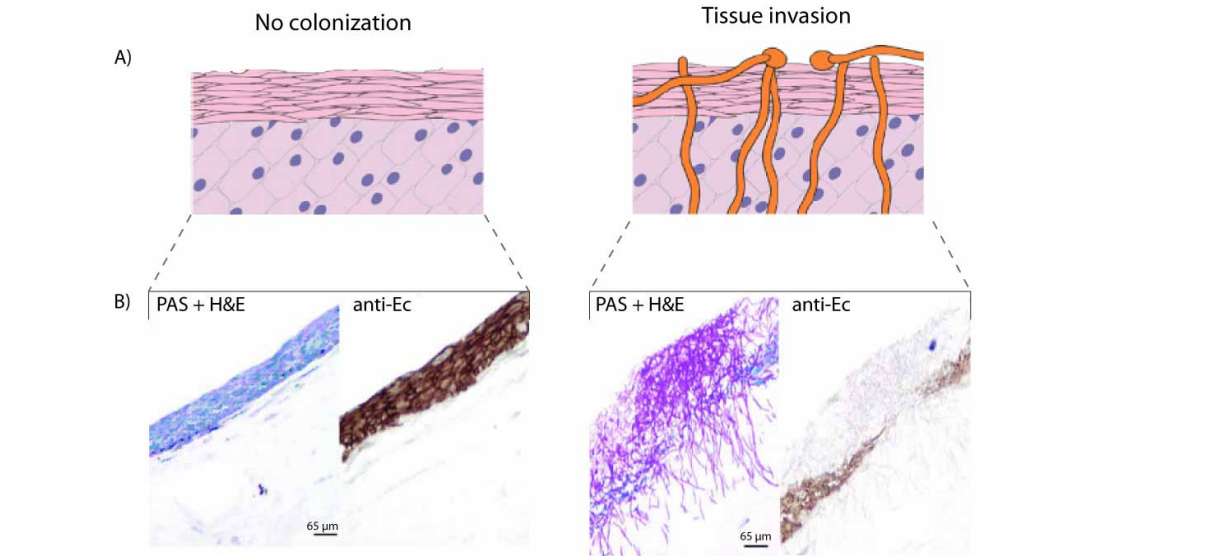

Figure 1.6. Tissue invasion by *Candida albicans*.

Tissue invasion of oral epithelilum by *Candida albicans* cells. **(A)** schematic illustration of a normal germ free oral mucosal epithelium (left) and *Candida*-invaded oral mucosal epithelium (right). **(B)** immunohistochemistry sections of a normal (left) and *Candida*-invaded (right) oral mucosa. Sections were stained either with periodic acid-Schiff (PAS, which stains polysaccharides in pink) and hematoxylin-eosin (H&E, which stains nuclei in blue) or anti-E-cadherin antibodies (anti-Ec). The tissue sections invaded by *Candida albicans* show evidence of infiltration by the yeast hyphal extensions accompanied by tissue destruction evidenced by the loss of E-cadherin (brown color). Adapted and modified from (Villar *et al.*, 2007; D. Wilson *et al.*, 2009).

1.3.7. Quorum Sensing

Quorum sensing (QS) is a form of microbial communication that uses signaling molecules to transmit cell density information to surrounding cells. This mechanism allows the concerted expression of genes that confer virulence and survival attributes. The signaling molecules or quorum sensing molecules (QSMs) are produced and sensed by the same type of cells, hence the name auto-inducers. At low cell density, each cell produces QSMs; as the cells divide and cell density increases, the amount of QSMs in the

surrounding builds up until a trigger threshold is exceeded. QSMs are sensed by the cell population, which then translate, and process the message into a transcriptional response (Figure 1.7) (Hogan, 2006).

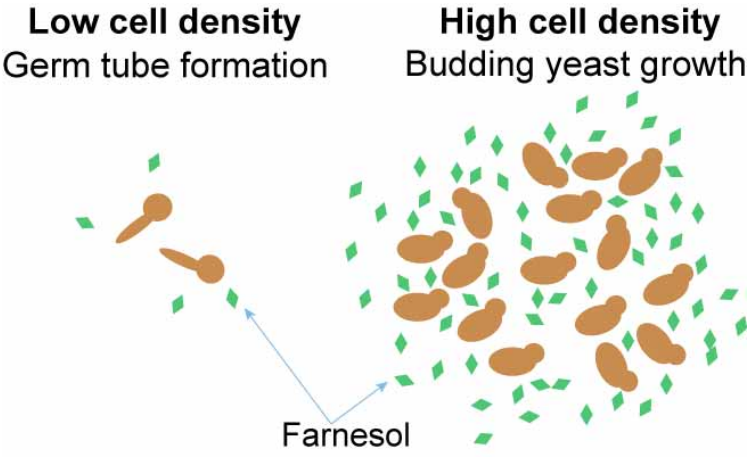

Figure 1.7. The principle of *C. albicans* farnesol-mediated quorum sensing. Simplified illustration representing the main principle underlying farnesol-mediated quorum sensing in *C. albicans*. At low cell density (<10^6 cells/ml), *C. albicans* cells produce the quorum sensing molecule farnesol in proportional amounts to the total number of viable cells. Under such conditions, cells tend to form germ tubes. Whereas at high cell density (≥10^6 cells/ml), farnesol accumulates beyond a certain threshold, which blocks this morphological switch, resulting in a majority of budding yeast population. Figure (not to scale) drawn based on (Hornby *et al.*, 2001).

The first reported eukaryotic QSM was farnesol, a sesqueterpene alcohol and an extremely interesting molecule with multiple functions in eukaryotic cells. Farnesol is by far the most studied quorum-sensing molecule (Hornby *et al.*, 2001). This molecule is produced by an alternative branching from the ergosterol biosynthesis pathway involving the Dpp2p and Dpp3p enzymes (Navarathna, Hornby*, et al.*, 2007; Nickerson *et al.*, 2006). Since ergosterol and farnesol have a common biosynthetic pathway upstream of farnesyl pyrophosphate (FPP) (Hornby *et al.*, 2003; Hornby & Nickerson, 2004), treatment with

sterol biosynthesis blockers such as azoles leads to the accumulation of farnesol (Figure 1.8)(Hornby & Nickerson, 2004). Farnesol inhibits filamentous growth at a cell density beyond 10^6 cells/ml (Figure 1.7) (Wongsuk *et al.*, 2016). It is believed that farnesol achieves repression of hypha-specific genes through inhibition of the MAP kinase and the cAMP signaling pathways (Figure 1.4) (Hall *et al.*, 2011; Sato *et al.*, 2004).

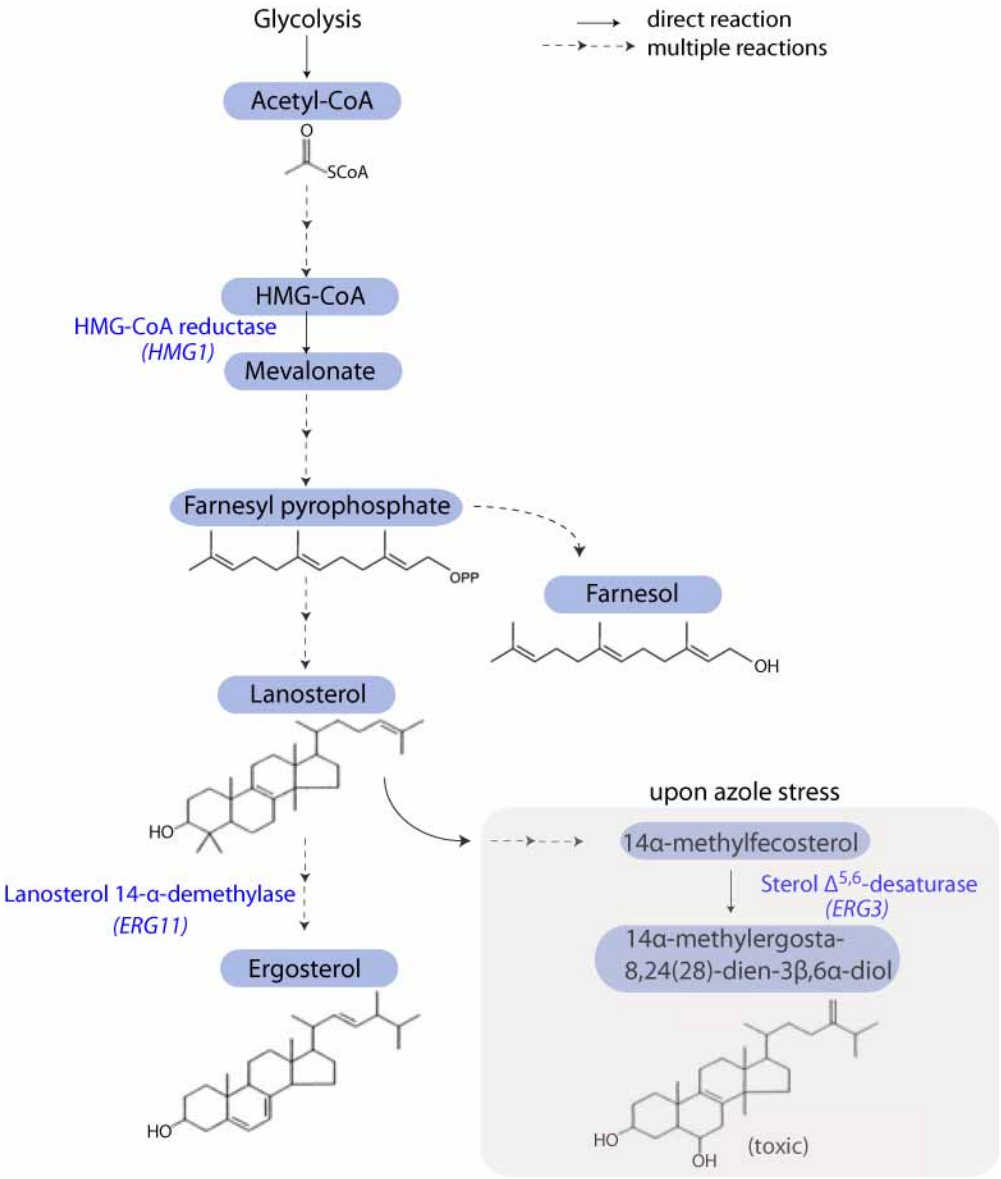

Figure 1.8. The ergosterol biosynthesis pathway.

Simplified overview of the main steps of the ergosterol biosynthetic pathway with branches illustrating the reactions that occur upon azole treatment and in the alternative pathway of farnesol biosynthesis. Briefly, acetyl-CoA molecules feed from glycolysis into the pathway of ergosterol biosynthesis. After several enzymatic reactions the end product of the pathway is ergosterol the main sterol of fungal membranes. Upon treatment with azoles, an alternative branch of the pathway (at the level of lanosterol) gives rise to the toxic sterol analogue 14α-methylergosta-8,24(28)-dien-3β, 6α-diol catalyzed by the Erg3p enzyme. Another alternative branch of the pathway (at the level of farnesyl pyrophosphate, FPP) also gives rise to the quorum sensing molecule farnesol. Straight arrows illustrate single-reaction steps. Dotted arrows illustrate multiple reaction steps. In blue are selected main enzymes of the pathway with the corresponding gene encoding them in parenthesis. Pathway reconstructed based on (Martel *et al.*, 2010; Nickerson *et al.*, 2006).

Given the effect of farnesol on the morphological switch in *Candida albicans* and since biofilms are highly dependent on the capacity of cells to transition between the two morphologies, farnesol is also believed to play a role in the dynamics of biofilm formation (Deveau & Hogan, 2011). Different studies have shown that farnesol plays a dual role with respect to biofilms. For instance, exposure to farnesol in early stages of biofilm formation, especially before adherence and germination, inhibits the development of a structurally mature biofilm (Ramage *et al.*, 2002). However, at the later stages such as the maturation step, farnesol is produced within the biofilm community to allow the control of the population size and to promote dispersal of yeast cells for colonization of new sites (Nickerson *et al.*, 2006; Wongsuk *et al.*, 2016). QS is believed to contribute to the pathogenicity of *Candida albicans* as farnesol has been shown to play a role in immune evasion by modulating the host responses to *Candida albicans*. It was shown to negatively affect the viability of macrophages and to induce the production of toxic intracellular reactive oxygen species (ROS) within macrophages (Abe S, 2009).

Interestingly, farnesol confers anti-ROS protective properties to *Candida albicans* cells (Westwater *et al.*, 2005). Moreover, it was shown that farnesol posseses immunomodulatory properties. Farnesol was able to prevent the production of important host cytokines notably interleukin-12 and interferon-gamma in a murine intravenous infection model (Navarathna, Nickerson*, et al.*, 2007). In several microorganisms, induction of apoptosis in response to *Candida albicans* farnesol allows *Candida* cells to eliminate microbial competition within host niches (Albuquerque & Casadevall, 2012). More specifically, Semighini *et al* have shown that farnesol produced by *Candida albicans* cells induces apoptosis in *Aspergillus nidulans* (Semighini *et al.*, 2006). Finally, high doses of farnesol are deleterious to *Candida albicans* cells and act synergistically with antifungals. Farnesol was shown to interfere with ABC-transporters mediated efflux and reduced the minimum inhibitory concentration of amphotericin B, fluconazole, and caspofungin (Sharma, 2011). Therefore, this molecule is being currently investigated in combination therapies (Cordeiro *et al.*, 2013; Jabra-Rizk *et al.*, 2006)

Other QSM molecules have also been identified in *Candida albicans* such as isoamyl alcohol, and 1-dodecanol for example which inhibit the yeast-hyphal switch, while tyrosol that is produced in the lag growth phase promotes the switch in the opposite direction (Martins M, 2007; (H. Chen *et al.*, 2004). Quorum sensing molecules produced by other organsims also affect *Candida albicans* cell behavior. Among the exogenous the QSMs influencing *Candida albicans* morphology, 3-oxo-C12-homoserine lactone (HSL) that is produced by the bacterium *Pseudomonas aeruginosa* triggers inhibition of *Candida albicans* filamentation (Hall *et al.*, 2011)

1.3.8. Cell wall maintenance and cell wall integrity pathway

The fungal cell wall is of great importance with regards to the fungal lifestyle within the human host. It not only confers rigidity and a permeability barrier but also mediates

important interactions with the surrounding environment. It is subjected to many environmental stresses such as oxidative stress, temperature challenges, pH fluctuations, nutritional deficiencies, host immune effectors, and antifungal agents (Dichtl *et al.*, 2016). In addition, the cell wall contributes to cell adherence and modulates the host immunity (Chaffin *et al.*, 1998). It follows that this fungal structure has attracted particular scientific interest as a potential antifungal target. Interestingly, it has been shown that the cell wall undergoes constant remodeling in response to environmental conditions, which allows it to adapt and survive in different host niches. Therefore the composition of the cell wall at any given point is the balance between biosynthesis and restructuring processes (Dichtl *et al.*, 2016). This balance is regulated by the cell wall integrity pathway (CWI), which detects environmental changes and dictates the suitable adaptation output (Dichtl *et al.*, 2016).

The cell wall integrity and maintenance pathway is composed of cell-surface sensors such as Dfi1p, Rhb1p, Rho1p, and Msb2p, which activate downstream signaling cascades such as Cek1p and Mkc1p MAPK pathways as well as Hog1p, calcineurin and protein kinase pathways (Dichtl *et al.*, 2016; Ernst & Pla, 2011). In addition to the PKC-MAPK kinases, other kinases have also been shown to be involved in cell wall integrity and damage response. A recent screen has shown that a large number of kinases actually participate in this adaptive response. These kinases include CbK1p, Vps34p, Tpk1p and Gin4p (Blankenship *et al.*, 2010).

Transcriptional regulators of the cell wall integrity and damage responses involve the transcription factors Rlm1p, Cas5p, Sko1p and Efg1p (Bruno *et al.*, 2006; Delgado-Silva *et al.*, 2014; Ernst & Pla, 2011). A recent study revealed a novel negative transcriptional regulator of cell wall integrity by demonstrating that deletion of *CZF1* resulted in enhanced tolerance to cell wall perturbing agents, most probably due to the observed upregulation

of genes involved β-glucan biosynthesis (Dhamgaye *et al.*, 2012). Downstream effector genes involved in cell wall maintenance include *CHS1, CHS2, CHS3* (encoding chitin synthases) and *PMT1*, *PMT2*, *PMT3* (encoding mannosyl-transfereases) (Ernst & Pla, 2011).

Interestingly, many genes involved in cell wall biogenesis are also important players of the filamentation program. For example, the transcriptional regulator Czf1p regulates filamentation under embedded conditions but also plays a role in cell wall maintenance (D. H. Brown, Jr. *et al.*, 1999; Dhamgaye *et al.*, 2012), while Efg1p regulates the hyphal switch as well as cell wall dynamics (Bockmuhl & Ernst, 2001; Sohn *et al.*, 2003). This is consistent with the fact that for the cell to undergo a morphological switch, its outer cell wall has also to be remodeled accordingly.

1.3.9. Other Pathogenic Determinants

1.3.9.1. Immune evasion

As seen in section 1.2.3, *Candida albicans* is confronted by the host immune system that tries to eradicate the fungal offender and terminate the infection process. However, *Candida albicans* uses a number of escape mechanisms in order to avoid immune surveillance and escape host immune defense mechanisms. For instance, *Candida* surface antigens have the remarkable ability to bind and neutralize an important component of the innate immunity known as the complement system (Jimenez-Lopez & Lorenz, 2013; Luo *et al.*, 2011). It has also been reported that some cell wall components such as glycolipids may act as apoptotic agents against macrophages (Miramon *et al.*, 2013). Furthermore, fungal epitopes recognized by the host such as β-glucans, mannans and chitin are usually linked to proteins localized at the cell surface. However, some of these antigens are hidden away from immune recognition as a mechanism of immune

evasion (Jimenez-Lopez & Lorenz, 2013; Wheeler & Fink, 2006). Several reports have shown that any imbalance in the distribution and composition of cell surface components exposes immunogenic antigens. In addition, one of the most studied immune evasion mechanisms is escape of phagocytosis by hyphal induction. Following phagocytosis by macrophages, yeast cells switch to hyphal morphology and pierce the macrophage membrane. This phenomenon usually inflicts considerable damage to the engulfing phagocytes (Ghosh *et al.*, 2009; Lorenz *et al.*, 2004). Interestingly, Bain *et al* have elegantly provided the first evidence that fungal phagocyte escape can occur by mere exocytosis without damage to host macrophages (Bain *et al.*, 2012). For better appreciation of this phenomenon, readers are invited to consult the live imaging of this video article (Bain *et al.*, 2012).

1.3.9.2. Adaptation to Hypoxia

Oxygen levels differ according to the host niche encountered. For instance, superficial sites such as the skin are typically oxygen-rich whereas deep tissues such as visceral organs or even the lungs are considered oxygen-poor sites (Butler, 2013; Ernst & Tielker, 2009). Therefore, oxygen sensing and adaptation to hypoxic environments is crucial for *Candida albicans* virulence in terms of survival in deep tissues but also in biofilm microenvironments.

It is known that *Candida albicans* cells exposed to low levels of oxygen switch to the hyphal growth mode. In addition to upregulation of hyphae-specific genes, other hallmarks of the adaptation to hypoxic conditions include upregulation of genes involved in glycolysis and fermentation as well as downregulation of respiratory genes (Setiadi *et al.*, 2006).

1.3.9.3. Oxidative and nitrosative stress adaptation

During the initial stages of *C. albicans* infection, yeast cells are confronted with the innate immune system, most notably the macrophages. Engulfment by macrophages forces *C. albicans* to resist the harsh environment generated by the intracellular production of reactive oxygen species (ROS) and reactive nitrogen species (RNS), which possess fungicidal and fungistatic properties, respectively, and promote *Candida albicans* killing (A. J. Brown *et al.*, 2014; Jimenez-Lopez & Lorenz, 2013). ROS are further metabolized into toxic molecules such as hydrogen peroxide, hydroxyl radicals and hypochlorous acid, whereas RNS are metabolized into nitrates. ROS also react with RNS to further amplify the toxic insult (Duhring *et al.*, 2015). To counteract these effects, *C. albicans* activates a specific response to detoxify oxidative molecules and ensure its survival. The hallmark of this response is the upregulation of genes encoding detoxifying and neutralizing enzymes such as glutathione transferase, thioredoxin reductase, glutathione reductase(Wang *et al.*, 2006), glutathione peroxidase, extracellular as well as cell surface-bound superoxide dismutases (SODs) (Frohner *et al.*, 2009), and catalases(Duhring *et al.*, 2015), but also genes involved in DNA repair (Lorenz *et al.*, 2004). Thus it appears that this fungal pathogen has evolved this mechanism of defense against oxidative stress in response to the exposure to a typical situation that is often encountered within the host.

1.3.9.4. pH stress resistance

Depending on the occupied niche within the host, *Candida albicans* is challenged with a wide range of pH to which it has to adapt to ensure survival. For example, blood pH is usually considered slightly alkaline (around 7.4) whereas vaginal pH is more acidic (around 4). In addition to site-specific pH differences, changes can also vary in one specific niche according to circumstances such as the oral cavity before and after sugar fermentation by resident bacteria or the vagina outside and during menstruation (D. A.

Davis, 2009). pH is important for optimal physiological functioning of fungal enzymes but also for ion-gradient import through the plasma membrane (D. A. Davis, 2009). Therefore, pH adaptation mechanisms are essential for fungal adaptation and survival. In *C. albicans,* environmental pH is sensed via the Rim101p signal transduction pathway and the preferential expression of the β-galactosidase, Phr1p in neutral-alkaline environment, and Phr2p in acidic environment (D. Davis, 2003; Muhlschlegel & Fonzi, 1997).

1.4. Antifungals used for systemic therapy

A small range of antifungals have been developed so far in order to control fungal infections, more specifically *Candida albicans* infections. The fact these are eukaryotic cells has made it more difficult to develop an antifungal that is devoid of toxic effects in humans. So far, the most commonly used antifungals for the treatment of *Candida* systemic infections include polyenes, 5-fluorocytosine, azoles and echinocandins. All of these compounds have their advantages as well as their limitations. In addition, some of them may become inefficient in the light of the emergence of drug resistance (see section 1.5). Therefore there is a pressing need for the development of new antifungals.

1.4.1. Polyenes

Polyenes are macrolides derived from the bacterial species *Streptomyces.* Polyenes interact with ergosterol, the main sterol of fungal membranes, which interferes with the membrane permeability leading to eventual cell death. Of the main polyenes used in antifungal therapies, nystatin is produced by the bacterium *Streptomyces noursei* and was one of the commonly used topical antifungals in the past (Moudgal & Sobel, 2010). However, for the treatment of systemic infections, another polyene known as Amphotericin B (AmB) is usually administered intravenously (Moudgal & Sobel, 2010). One of the down sides of AmB is that it is associated with high tissue toxicity, notably in

the kidneys. To decrease toxicity effects, lipid formulations of AmB (LFABs) have been developped such as liposomal amphotericin B, amphotericin B colloidal dispersion and amphotericin B lipid complex. These formulations offer the advantage of reduced nephrotoxicity while keeping the efficacy of AmB (Bellmann, 2007).

1.4.2. 5-Fluorocytosine

The antimetabolite 5-fluorocytosine (5-FC) has antifungal activity against various *Candida* species and other fungi (Pfaller *et al.*, 2002; Vermes *et al.*, 2000). It is metabolized to 5-fluorouracil and therefore interferes with RNA and DNA synthesis. Due to high frequency of resistance, 5-FC has been more popular in combination therapies with AmB. There have also been concerns about toxicity associated with a 5-FC based treatment(Moudgal & Sobel, 2010).

1.4.3. Azoles

Azole amtimycotic agents target the cytochrome P450, lanosterol 14-α-demethylase (or Erg11p, encoded by the *ERG11* gene), which catalyzes the conversion of lanosterol to ergosterol (Figure 1.8). Binding and inhibition of P450 enzymatic activity leads to decreased ergosterol content in the plasma membrane and accumulation of toxic metabolites. The resulting alterations in membrane permeability, osmotic deregulation and oxidative stress cause a growth arrest, hence the fungistatic effect of azole antifungals (Akins, 2005; Kelly *et al.*, 1995).

Azole drugs can be mainly subdivided into two main groups, the imidazoles and the triazoles, containing two and three nitrogens in their azole ring, respectively(Odds *et al.*, 2003). Imidazole drugs include ketoconazole, miconazole, and clotrimazole. Imidazoles were among the first azoles used clinically. Their efficacy was restricted for the treatment

of superficial candidiasis. In this class of azoles, only ketoconazole is still used in clinic (Moudgal & Sobel, 2010).

Following imidazoles, triazoles were designed with an improved binding affinity to Erg11p. Triazole antifungals include fluconazole and itraconazole (1st generation), and voriconazole and posaconazole (2nd generation) (Moudgal & Sobel, 2010; Odds *et al.*, 2003). Fluconazole has been extensively used in the clinic and many studies have demonstrated its effectiveness in invasive candidiasis (Winston *et al.*, 2000) (Anaissie *et al.*, 1996). In addition, according to the "clinical practice guideline for the management of candidiasis", fluconazole is still recommended as one of the first line antifungals (Pappas *et al.*, 2016). Second generation triazoles have broader spectrum of activity against a number of fungal agents and better specificity and have been approved for clinical use (Sable *et al.*, 2008).

Due to their good bioavailability, toxicity profile, and spectrum of action, azoles have been widely used not only for the treatment of superficial and systemic candidiasis but also as prophylaxis regimens for the prevention of fungal infections in high-risk subjects(Spampinato & Leonardi, 2013). However, potential drug interactions are to be considered for azole treatments especially in immunocompromised patients (Bellmann, 2007). Most importantly, azole drugs have been associated with frequent emergence of drug resistance, which is of clinical concern (see section 1.5.1)

1.4.4. Echinocandins

Echinocandins are semi-synthetic lipopeptides that block β-(1,3)-D-glucan synthase thereby compromising the biosynthesis of β-(1,3)-D-glucan, one of the major cell wall components(Denning, 2003). This in turn leads to an imbalance in cell wall composition, which interferes with osmotic homeostasis leading to cell death. Hence echinocandins

are fungicidal against *Candida* species and represent a good alternative for treatment of azole-resistant strains (S. C. Chen *et al.*, 2011) .

Echinocandins are considered relatively costly(S. C. Chen *et al.*, 2011). They are usually administered intravenously and interactions with other drugs are generally not a concern (Bellmann, 2007). Echinocandins have been shown to have synergistic and additive effects if combined with an azole or a polyene drug (S. C. Chen *et al.*, 2011). The pharmacokinetic and pharmacodynamics properties of echinocandins have been extensively reviewed elsewhere (S. C. Chen *et al.*, 2011). The first FDA approved echinocandin for clinical use was caspofungin (Barchiesi *et al.*, 1999). It results in more side effects than the other echinocandins currently used (Eschenauer *et al.*, 2007). Advantages of caspofungin include “post-antifungal effect”, which is the sustained effect of the antifungal after it has been withdrawn or after short exposure, and a proven effectiveness against *Candida* biofilms (Manavathu *et al.*, 2004; Moudgal & Sobel, 2010). The second approved echinocandin antifungal was micafungin which proved its effectiveness in several clinical trials of esophageal candidiasis (Pettengell *et al.*, 2004) with superior antifungal activity as compared to caspofungin (Cappelletty & Eiselstein-McKitrick, 2007; Pfaller & Diekema, 2010). Unlike other echinocandins, micafungin has been approved for use as a prophylactic agent (Hiramatsu *et al.*, 2008). Anidulafungin was approved after micafungin and has good activity against *Candida* species (Moudgal & Sobel, 2010). It is unique in that it is metabolized via the biliary tract rather than the liver (Eschenauer *et al.*, 2007). A new improved echinocandin, CD101, is currently being investigated as an alternative to the treatment of emerging echinocandin-resistant strains. So far, it has been shown to be effective *in vitro* against *Candida* and *Aspergillus* species (Y. Zhao *et al.*, 2016). Echinocandins are currently recommended as initial therapy in the treatment of invasive candidiasis (Pappas *et al.*, 2016).

1.4.5. New compounds under investigation

In the last few years, interest and investigation of new molecules has increased due to the high incidence of drug resistance even towards new classes of antifungals notably echinocandins. Among the new compounds currently under investigation in vitro are : mohangamide A and mohangamide B that specifically inhibit the glycoxylate pathway enzyme, isocitrate lyase (ICL), and compromise gluconeogenesis and hence virulence. ICL is not found in mammalian cells, which makes those two compounds good drug targets for *C. albicans* (X. Li *et al.*, 2015). The compounds 4- and 5-substituted 1,2,3-triazoles modulate the two-component-system (TSC) portion of the high osmolarity glycerol 1 (Hog1p) mitogen-activated protein kinase (MAPK) signaling pathway (Diner, 2011). Their effect is deleterious to fungal cells but not to mammalian cells since TSC is not conserved in the latter ones. Structural differences between human and fungal lipases have also been exploited to test the efficacy of quinine and ebelactone B as potential inhibitors of *C. albicans* growth (X. Li *et al.*, 2015). Shikonin was also shown to interfere with reactive oxygen species equilibrium in *C. albicans* (Miao *et al.*, 2012). Finally, modulation of histone H3 lysine 56 acetylation was also suggested as an antifungal strategy (Wurtele *et al.*, 2010). Thus, it appears that as many potential molecules are being identified, there is hope in the development of new antifungals, however scant funding of those studies may impede the rapid development and implementation of such treatments.

1.4.6. Vaccines:

Due to the limited options offered by treatment regimens and the increased incidence of drug resistance, part of the *Candida albicans* community has turned to put more effort into prevention of candidiasis. Even though the development of vaccines targeted against *Candida albicans* infections proved to be tedious and complicated, this field recently

witnessed great advancements with the design of immunogenic and protective formulations. Most of the vaccines under investigation combine *Candida albicans* specific antigens with an adjuvant to maximize the immune response.

The protein vaccines that have passed Phase I clinical trials consisted of the surface adhesin Als3 and the secreted aspartyl protease Sap2. Both were able to induce protective humoral and cellular immunity such as IgA antibodies, cytokines as well as T helper 1 and T helper 17 (Th1/Th17) responses (X. J. Wang *et al.*, 2015). Other fungal antigens currently under investigation as potential protein vaccines include the stress-induced chaperone Hsp90 and the cell wall GPI-anchored protein Hyr1 (X. J. Wang *et al.*, 2015). The drawback of such vaccines is that they are targeted against a single fungal antigen, which may still result in immune evasion by a surrogate *Candida albicans* pathogenicity mechanism (Cassone, 2013).

Live attenuated vaccines have also been investigated as potential vaccines such as a *tet-NRG1 Candida albicans* strain that elicited a relatively good immunological response in animal models(Saville *et al.*, 2009). However, this type of vaccines contains a wide range of antigens that have not yet been fully identified and tested individually and therefore are less likely to be approved for use in humans in the near future (X. J. Wang *et al.*, 2015).

It is now widely accepted that a good *Candida albicans* vaccine should follow a number of considerations: 1) it should be able to elicit an immune response that does not completely eliminate the commensal form of the fungus but rather keeps it from switching to the filamentous invasive forms; 2) the fungal antigens to be targeted should therefore be hyphal-specific and induce specific antibody-mediated immunity; 3) the response induced by the administration of the vaccine should generate memory cells that will be activated upon future fungal invasion; 4) the immunity generated should be a combination of cellular and humoral responses to offer the maximum protection possible; and 5) a

multivalent vaccine, combining multiple tested and approved fungal immunogens would be more likely to produce a broad-spectrum protection against *Candida albicans* infections (Cassone, 2013; X. J. Wang *et al.*, 2015). It can therefore be concluded that efforts towards generating a good anti-*Candida albicans* vaccine must be multiplied in order to accelerate this particular field of research.

1.5. Mechanisms of Antifungal Resistance

1.5.1. Azole resistance

The ease of use and accessibility of azole drugs have encouraged their use in prophylactic regimens among high-risk patients such as patients with HIV infection to prevent oropharyngeal / esophageal candidiasis, or organ transplant patients to prevent invasive candidiasis or abdominal surgery patients to prevent cadidemia. Nevertheless, the fungistatic nature of azole drugs and their prolonged overuse in the clinical setting has created a selective pressure on *Candida albicans* strains and resulted in the emergence of acquired azole resistance. A number of azole resistance mechanisms have been identified which can exist individually or in combination in clinical isolates. Molecular mechanisms mediating azole antifungal resistance can be grouped under four main categories: 1) decreased intracellular drug accumulation, 2) altered target protein structure, 3) increased target protein concentration, and 4) reduced drug toxicity.

1.5.1.1. Decreased intracellular drug accumulation

One of the most important resistance mechanisms and one that has deserved much investigation is the active drug efflux outside the cell via the up-regulation of drug efflux pumps. The increased export of the drug greatly reduces its effect and promotes cell survival. Drug efflux pumps belong to two main families, the ATP-binding cassette (ABC) transporters, such as Cdr1p and Cdr2p, and the major facilitator superfamily (MFS), such

as Mdr1p (Tsao *et al.*, 2009; Wirsching *et al.*, 2000) (Hiller *et al.*, 2006). ABC transporters typically use ATP hydrolysis for mediating the energy-dependent transport of the drug (Cannon *et al.*, 2009; Goncalves *et al.*, 2016; Smriti *et al.*, 2002).

On the other hand, MFS transporters use the proton gradient across the cell membrane for active drug export (Pao *et al.*, 1998; Wirsching *et al.*, 2000) (Cannon *et al.*, 2009). In contrast to Cdr1p and Cdr2p, which have been implicated in the transport of multiple azole compounds, Mdr1p transport is more specific to fluconazole (Goncalves *et al.*, 2016).

The transcriptional regulation of the *CDR1*/ *CDR2* and *MDR1* genes is under the control of zinc cluster transcription factors, Tac1p and Mrr1p, respectively. GOF mutations in Tac1p have been linked to up-regulation of *CDR1* and *CDR2* in a number of clinical azole-resistant isolates. Similarly, GOF mutations in Mrr1p result in the overexpression of *MDR1* and therefore contribute to azole resistance (Coste *et al.*, 2004; Dunkel, Blass*, et al.*, 2008; Morschhauser *et al.*, 2007; Znaidi *et al.*, 2007).

It has been long thought that the TF Mrr2p mediates solely yeast cell adherence (Finkel *et al.*, 2012). However, recent insights have shown that this TF is also involved in fluconazole resistance via the control of *CDR1* expression (Schillig & Morschhauser, 2013; X. J. Wang *et al.*, 2015).

1.5.1.2. Altered target protein structure

Alteration of the target enzyme is also a frequent mechanism of azole resistance in *C. albicans*. Changes in the active site of the Erg11 protein result from point mutations in the *ERG11* gene. Such conformational changes decrease the binding affinity of the drug thereby compromising its effectiveness (Akins, 2005; Lamb *et al.*, 2000; White, 1997). Many Amino acid substitutions in Erg11p have been described in azole-resistant clinical isolates, however, they do not all contribute equally to the resistance profile (Flowers *et al.*,

2012; Morio *et al.*, 2010). Interestingly, the majority of the mutations described for Erg11p in the context of resistance were located in 3 specific regions, the N-terminal segment and the heme binding sites, which are essential for enzymatic function (Marichal *et al.*, 1999; Noel, 2012).

1.5.1.3. Increased target protein cellular concentration

A frequent mechanism that has been associated with azole resistance is the upregulation of the *ERG11* gene encoding a lanosterol demethylase, which is the target of azoles (White & Silver, 2005). The increase in target molecules overcomes the effect of the drug and results in the drug tolerance reported in many clinical strains (Akins, 2005; Perea *et al.*, 2001).

Transcriptional regulation of *ERG11* is mediated by the zinc cluster transcription factor Upc2p. In fact, this TF also positively regulates ergosterol biosynthesis genes via its binding to sterol responsive elements (SRE) located in the promoter of several *ERG* genes, including *ERG11* (MacPherson *et al.*, 2005; Silver *et al.*, 2004). Gain of function (GOF) mutations in Upc2p lead to a hyperactive variant of the TF and result in overexpression of *ERG11* (Dunkel, Liu*, et al.*, 2008; Flowers *et al.*, 2012; Hoot *et al.*, 2011).

1.5.1.4. Reduced drug-induced toxicity

Emergence of loss-of-function mutations in the *ERG3* gene encoding an ergosterol desaturase in the ergosterol biosynthesis pathway has been linked to clinical azole resistance. In addition, *Candida albicans* strains carrying different Erg3p loss-of-function mutations were also resistant to various azole compounds in vitro. The mechanism behind the resistant phenotype is that a defective Erg3p enzyme is no longer capable of catalyzing the reaction that produces the toxic ergosterol analogue that results from an

azole exposure (Figure 1.8). Therefore, loss-of-function mutations in this ergosterol desaturase prevent the formation of toxic derivatives (Kelly *et al.*, 1997; Martel *et al.*, 2010).

1.5.1.5. Aneuploidies

Genome plasticity and aneuploidies have also been associated with azole resistance. For instance, chromosome 5 harbors a number of important genes such as *TAC1* encoding a transcriptional regulator controlling drug efflux pumps, *ERG11* encoding an important enzyme in the ergosterol biosynthetic pathway and an important target for azole drugs, and *MTL* that is essential for mating. Formation of an isochromosome 5 allows adaptability to environmental stresses and the acquisition of drug resistance. One arm of chromosome 5 is lost and the remaining one is duplicated resulting in the isochromosome (Selmecki *et al.*, 2006; Selmecki *et al.*, 2008).Gene duplication also contributes to azole resistance either due to chromosome duplication or due to isochromosome formation. Both genomic alterations have been often reported for *C. albicans* strains owing to its highly plastic genome and contributing to the amplification of drug resistance (Morschhauser, 2016).

1.5.2. Echinocandin resistance

Even though resistance to echinocandin antifungals is much less frequent than azole resistance, an increasing number of cases have been reported in the last few years, especially for *Candida* species (Goncalves *et al.*, 2016; Pfaller *et al.*, 2013; Spampinato & Leonardi, 2013). Echinocandin antifungal resistance is mostly attributed to point mutations in the genes *FKS1* and *FKS2* encoding subunits of the β-(1,3)-glucan synthase enzyme (Ben-Ami *et al.*, 2011; Desnos-Ollivier *et al.*, 2008; Odds *et al.*, 2003). More specifically, most of the mutations that are reported to be associated with echinocandin resistance are

concentrated in two conserved regions in the *FKS1* gene, called the “hot spots” HS1 and HS2 (Ben-Ami *et al.*, 2011; Lackner *et al.*, 2014). These mutations bring about conformational changes compromising the enzyme binding affinity to echinocandins and therefore limits their antifungal potential (Perlin, 2015).

It has been noted that mutations in Fks1p enzyme have been correlated with increased chitin content and reduced fitness in fly and mouse infection models. In these same strains, echinocandin resistance correlated with compromised growth and hyphal formation (Ben-Ami *et al.*, 2011). Another study has also shown that an increase in chitin content in *C. albicans* cells, secondary or not to Fks1p mutations, also leads to echinocandin resistance and treatment failure in a murine model (Lee *et al.*, 2012).

Most recently, evidence has shown that an increase of cell wall chitin content in response to echinocandin treatment might be a contributor to the observed echinocandin resistance, and that this phenomenon was partly mediated by the activation of the MAPKKK signaling pathway (Dichtl *et al.*, 2016). Therefore, increased chitin content is now recognized as an additional resistance mechanism to the echinocandin class of antifungals.

1.6. The *Candida albicans* genome and genetic approaches

The *C. albicans* genome is relatively difficult to manipulate genetically due to the fact that its genome is diploid with the absence of a complete sexual cycle, the use of a noncanonical CUG codon, as well as the absence of centromeric plasmids (De Backer *et al.*, 2000). Very few genetic tools were available and research progress in this field was very slow until the sequencing of the genome. The sequence of the *Candida albicans* genome using the reference strain SC5314 was published in 2004 by Jones *et al* which revealed new insights about the genome structure and composition (Jones *et al.*, 2004). The sequencing and the annotation of the genome also allowed the development of functional genomic tools adapted for this organism (see section 1.6.3). In addition, the availability of an official database

specifically for *Candida albicans* and related species, Candida Genome Database (CGD), provided excellent tools complementary to any study in this organism. CGD combines genome sequences, experimental information, analysis tools as well as related literature that is freely accessible online (Skrzypek *et al.*, 2016). An array of studies using these techniques then allowed rapid advancements in the knowledge of *Candida albicans* pathogenicity, drug resistance mechanisms as well as other important biological processes.

1.6.1. Genome Composition and Characteristics

The *Candida albicans* genome is diploid (about 16 MB) consisting of approximately 6000 genes distributed on eight chromosomes, chromosomes 1 to 7 and chromosome R (Braun *et al.*, 2005; Butler *et al.*, 2009). *Candida albicans* belongs to the CUG clade having a genetic code that uses the CUG codon that codes for a serine in place of a leucine (Butler *et al.*, 2009; Santos & Tuite, 1995). After the sequencing of the genome, a lot of polymorphisms between gene alleles were found. It also revealed that the *Candida albicans* genome encodes a number of gene families that are involved in important cellular processes such as adhesins (ALS family), extracellular proteases (SAP family), superoxide dismutase (SOD family) and oligopeptide transporters (OPT family), amongst others (Jones *et al.*, 2004). One of the striking characteristics of the *Candida albicans* genome is that it is highly plastic; chromosomal abnormalities as well as aneuploidies are often found in a number of strains (De Backer *et al.*, 2000; Magee *et al.*, 1992) . Such genomic plasticity allows *Candida albicans* to generate diversity and acquire further adaptability to specific environments or stresses. Other diversity mechanisms include chromosomal rearrangements, translocations, and chromosome truncations (Selmecki *et al.*, 2010). Genome plasticity has also been correlated with the loss of heterozygosity and formation of an isochromosome 5 as explained in section 1.5.1.5 (Selmecki *et al.*, 2006; Selmecki *et al.*, 2008)

1.6.2. Genetic manipulations

1.6.2.1. URA blaster strategy

This strategy uses the *URA3* marker (encoding the orotidine-5'-phosphate decarboxylase enzyme), that can be looped out by culturing on 5-fluor-orotic acid (5-FOA) which allows the recycling of the marker for use in a subsequent cycle to delete the second allele of the gene of interest. The strain typically used for this genetic manipulation is CAI-4, which has a deleted *URA3* gene (De Backer *et al.*, 2000; Fonzi & Irwin, 1993). This strategy presents some limitations especially as to virulence studies because of reports demonstrating that *URA3* gene expression levels differ according to its genomic location, which can mask the effect of the gene under study (Staab & Sundstrom, 2003) . The URA blaster technique has been used in the process of generation of the BWP17 parental strain (R. B. Wilson *et al.*, 1999).

1.6.2.2. SAT1 flipper strategy

This gene deletion strategy has gained popularity due to the use of a dominant selectable marker without the use of auxotrophies. *SAT1* encodes a nourseothricin resistance gene that has been adapted for use in *Candida albicans*. This has proven particularly useful when generating strains to be used in transcriptomics and gene expression profiling. The method uses the Flip recombinase system (Figure 1.9) (Reuss *et al.*, 2004; Sasse & Morschhauser, 2012).

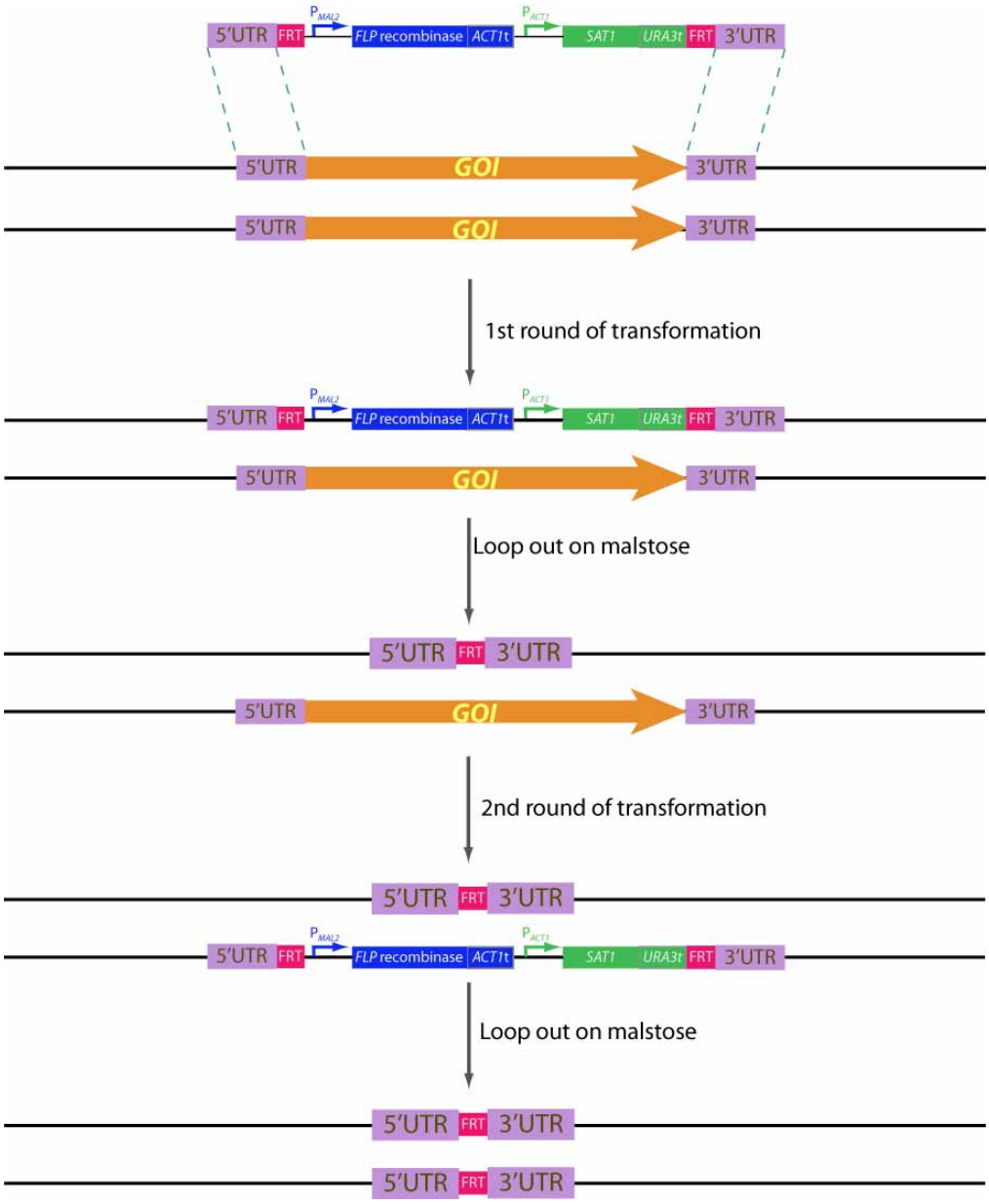

Figure 1.9. *SAT1* flipper strategy.

This strategy relies on the use of a selectable dominant marker with no involvement of auxotrophies. The cassette contains the *SAT1* marker and the flip recombinase gene under the control of the *MAL2* promoter. The whole cassette is flanked by FRT sequences that enable excision of the cassette and homologous sequences to the upstream and downstream regions of the target gene. The first round of transformation integrates the cassette at the first allele. The cassette is then excised in the presence of maltose due to the recombination of the FRT sequences. The marker is then recycled and used in

another round of transformation and selection on maltose to generate the deletion at the second allele. One FRT sequence remains at each allele. GOI: gene of interest, UTR: untranslated region, P: promoter, FLP: flip recombinase, FRT: flip recombinase target sequences, t: terminator. Figure (not to scale) drawn based on (Reuss *et al.*, 2004; Samaranayake & Hanes, 2011).

1.6.2.3. Epitope-tagging

A particular protein can be fused either with an epitope to allow easy immunological detection and purification or with a fluorescent protein to allow microscopic visualization and localization within the cellular compartments. The most used tagging epitopes include hemagglutinin (HA), which was used in chapters 2 and 3, c-myc (MYC), and tandem affinity purification (TAP). Fluorescent-protein tags include but not limited to green fluorescent protein (GFP), red fluorescent protein (RFP), and yellow fluorescent protein (YFP). These strategies either use the *URA3* marker or the *SAT1* marker in the same way as for gene deletion (Figure 1.10) (Lavoie *et al.*, 2008).

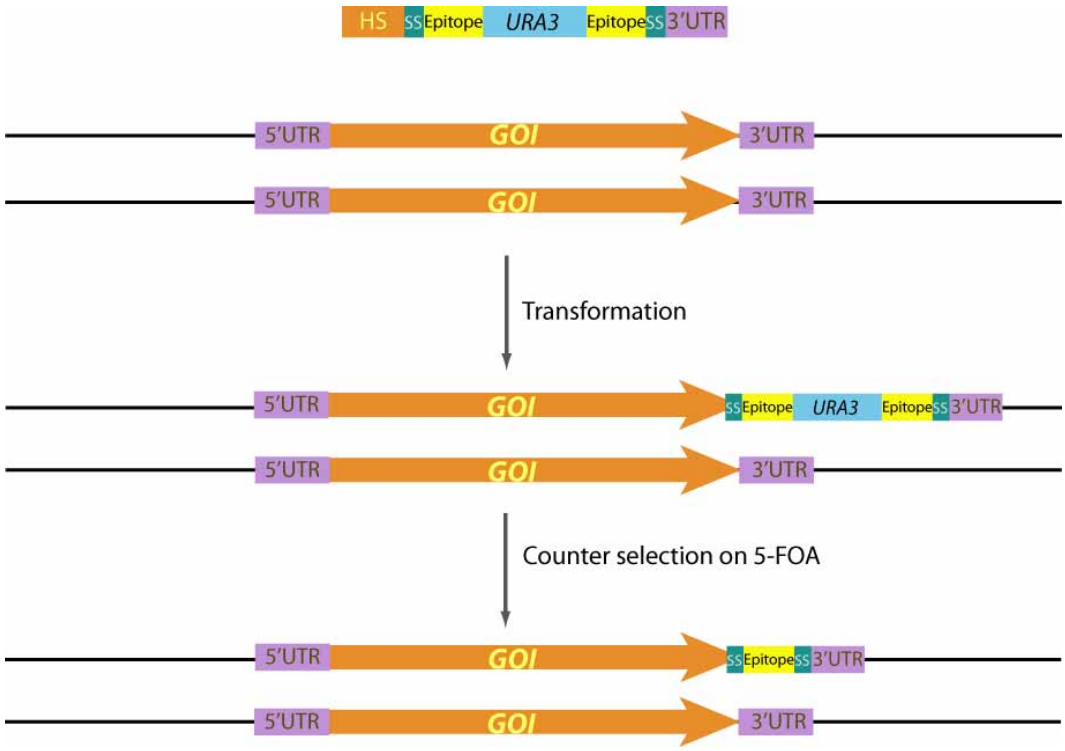

Figure 1.10. Epitope tagging strategy.

Schematic example of the cassette and strategy for epitope tagging at the C-terminus of a target gene. The cassette contains the *URA3* marker flanked by sequences coding for the epitope then by sequences specific to the origin vector, then by sequences homologous the target gene terminal sequences and sequences from the target gene 3'UTR. After transformation, the cassette is integrated at one allele. Selection on 5-FOA allows the loop out of the *URA3* marker. GOI: gene of interest, UTR: untranslated region, SS: specific sequence. Figure (not to scale) drawn based on (Liu *et al.*, 2007).

1.6.2.4. Genome Editing

As discussed above, *Candida albicans* genome is very complex and the existence of aneuploid strains is not uncommon. In addition, genetic manipulations in this organism present many challenges to scientists that require lengthy manipulations.

In the past few years, an interest in clustered regularly interspaced short palindromic repeats (CRISPR) has emerged in the scientific literature describing an RNA-based

bacterial adaptive immune system that can be engineered and adapted to different model systems, including human cells, to edit genes (Pennisi, 2013). Briefly, the technology known as genome editing or gene surgery is based on the expression of a fused guide RNA (gDNA) and a trans-activating CRISPR RNA (tracrRNA) that is complementary to a target DNA sequence. This complex recruits an endonuclease known as (CRISPR-associated 9) Cas9 that cleaves the DNA sequence at the recognition site triggering error-prone cellular repair mechanisms. Following the repair a mutation will have been introduced resulting in gene disruption (Figure 1.11). Different adaptations of the system can be used not only to disrupt genes but also to perform gene replacement, and modulate gene expression (Pennisi, 2013). Recently, the CRISPR-Cas9 genome editing technology has been adapted to *Candida albicans* will allow rapid modifications of the genome and accelerate gene function discoveries (Min *et al.*, 2016; Vyas *et al.*, 2015).

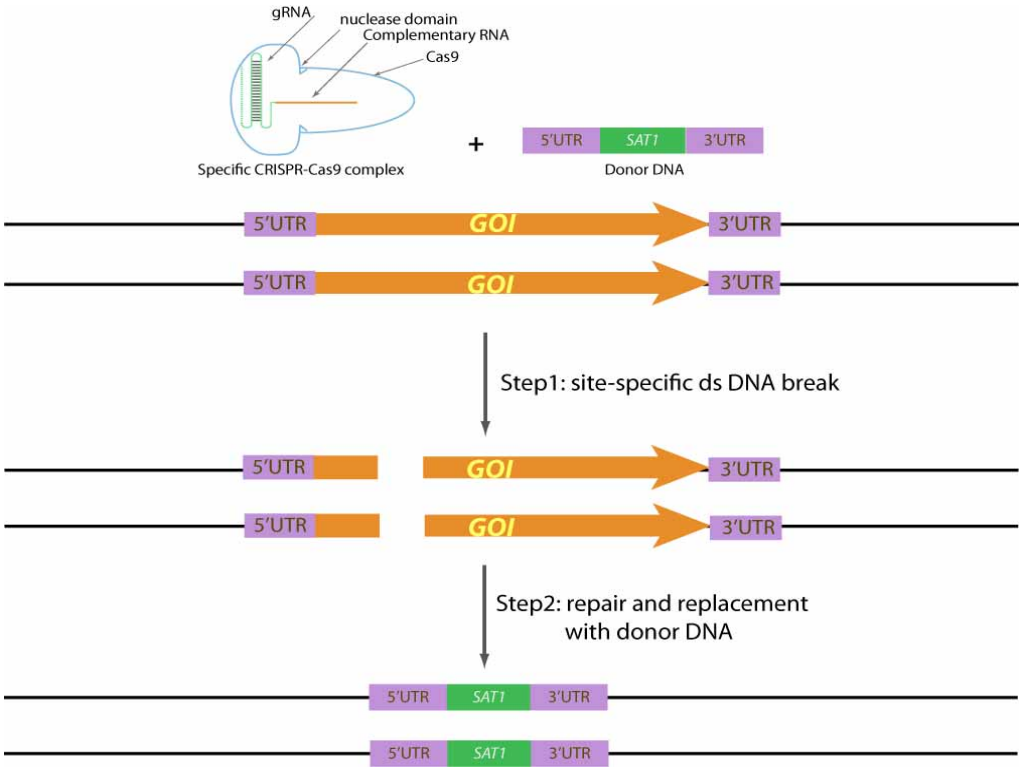

Figure 1.11. CRISPR-Cas9 technology.

The CRISPR-Cas9 complex is designed to contain a guide RNA (gRNA) with a complementary RNA that recognizes the desired target sequence. Upon recognition and binding, the target sequence is cleaved at the nuclease sites of the Cas9 protein. The resulting dsDNA break is replaced by the donor DNA that is flanked by upstream and downstream sequences of the target sequence. Figure (not to scale) drawn based on (Min *et al.*, 2016; Pennisi, 2013).

1.6.3. Functional Genomics

The sequencing and the annotation of the *Candida albicans* genome as well as the availability of priceless resources and tools provided by CGD allowed a surge of large-scale genomic studies that identified gene functions and reconstructed transcriptional networks regulating major *Candida albicans* biological processes. This has made it possible to design, develop and implement functional genomics tools to study genetic interactions. Gene knockout libraries and transposon mutant libraries are now available for researchers to conduct large-scale functional screens to identify gene-phenotype relationships. Notably, the GRACE^{TM} collection that relies on a combination of gene replacement and conditional expression allowed the study of essential genes (Roemer *et al.*, 2003). Furthermore, large-scale studies have harnessed these tools and resources with the sequencing technology to provide a better resolution of genome-wide changes and responses to different stimuli (Dhamgaye *et al.*, 2012; Lohse & Johnson, 2016). For example, the integration of location and expression profiles allowed the conceptualization of transcriptional networks (Figure 1.12). The binding sites of a TF are identified and the responding genes as well as the nature of the interaction (positive or negative regulation) are established.

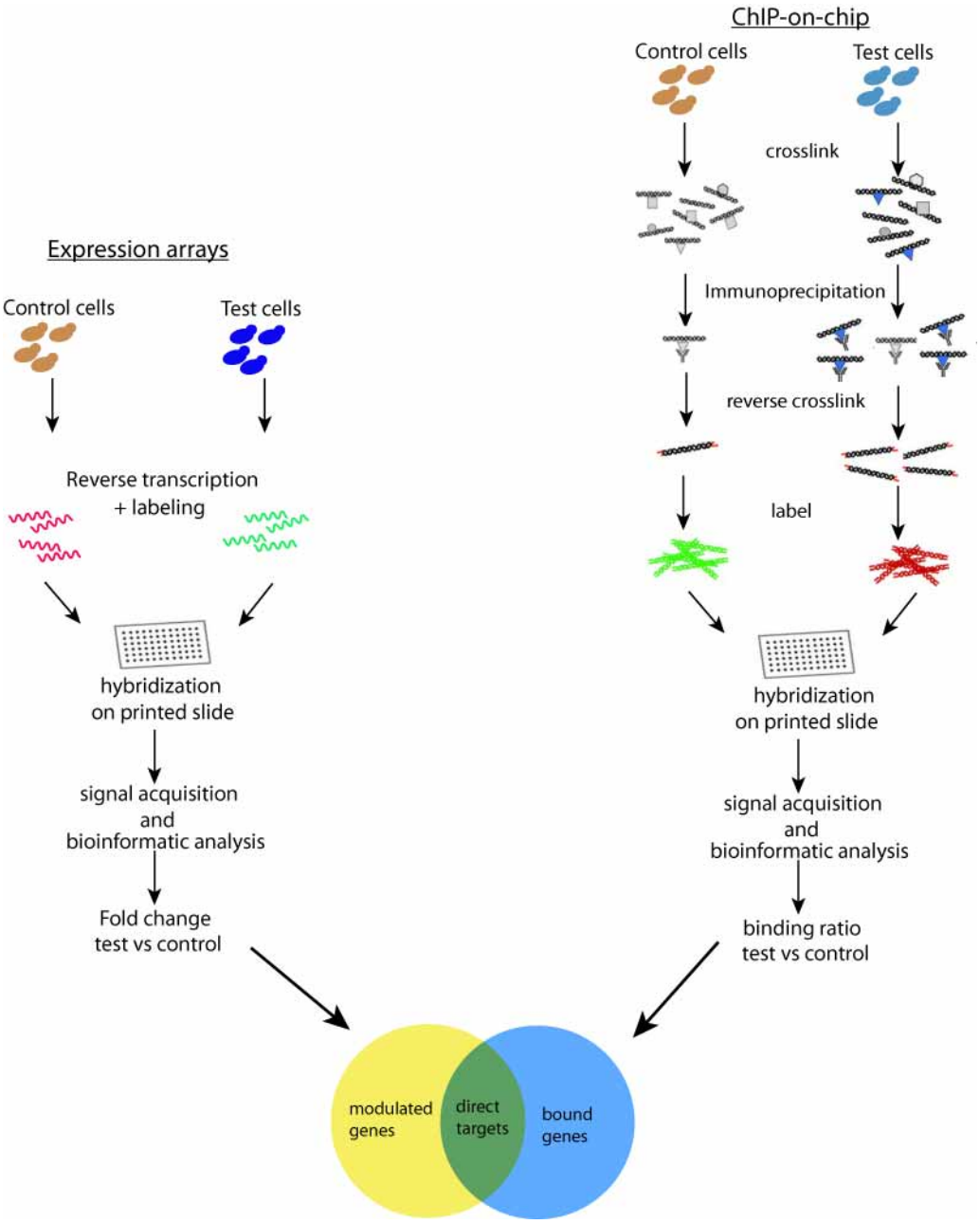

Figure 1.12. Overview of expression and location profiling workflow.

Brief overview of the main steps of RNA profiling on arrays and ChIP-on-chip assays. For expression arrays, RNA extracted from control and test cells is reverse transcribed. Differential florescent labeling is applied followed by hybridization on printed array. The signal intensities are then compared and analyzed with bioinformatic tools. A fold change (ratio) is then generated comparing gene expression in the test cells to that of control cells. For ChIp-on-chip, DNA and proteins from test and control cells are cross-linked then

immunoprecipitated. A reverse crosslink step dissociates proteins from the DNA. This latter is then labeled with fluorescent dyes before hybridization on arrays. The signal intensities are then compared, analyzed and mapped to a genome browser using bioinformatic tools. A binding ratio is then generated comparing the protein enrichments (across the genome, for tiling arrays and at promoter regions, for promoter arrays) in the test cells to that of control cells. The combination of binding targets and modulated genes lists allows the identification of direct targets and the elucidation of regulons and transcriptional networks. Figure adapted and modified based on (Wyrick & Young, 2002).

These approaches have been used in a number of studies to reconstruct transcriptional networks underlying important processes such as the response to hypoxia, the regulation of carbohydrate metabolism, biofilm formation, and hyphal switch (Askew *et al.*, 2009; Fox *et al.*, 2015; Grumaz *et al.*, 2013; Sellam *et al.*, 2014). Of the many insights that could be gained from these genome-wide approaches was the discovery of new previously unannotated transcribed regions and detecting changes in lengths of untranslated regions (UTRs) (Bruno *et al.*, 2010)as well as the identification of novel transcripts that may reveal novel ORFs or regulatory RNAs (Dhamgaye *et al.*, 2012; Sellam *et al.*, 2010). Genome wide analyses have also shown that genes of the *Candida albicans* genome have relatively short UTRs (50-80 nucleotides) and that genes with long 5'UTRs have been found in genes coding for transcriptional regulators of the hyphal morphological switch (Sellam *et al.*, 2010). The have also revealed alternative transcription start sites for genes encoding transcriptional regulators such as Efg1p and Tac1p (Dhamgaye *et al.*, 2012; Lachke *et al.*, 2003).

1.7. Rationale and Objectives

The *Candida albicans* genome contains a large number of genes coding for transcriptional regulators (TR); however, the biological function of many of them is still unknown. Given that transcriptional regulation is at the basis of many molecular mechanisms underlying and mediating important biological processes in *C. albicans*, it is predicted that

many of the TR with unknown function may as well play essential roles in *Candida albicans* patho-biology.

The first objective of this work was to elucidate the transcriptional network under the control of Fcr1p, a TR that is involved in negative regulation of drug resistance and in filamentous growth. The identification of this TR regulon would help to understand the mechanism by which it mediates its associated phenotypes. It would also help to predict and test whether this TR has other potential biological function(s) (Chapter 2). The second objective was to identify the transcriptional network that controls the production of the quorum-sensing molecule, farnesol. The use of a phenotypic screen of a transposon mutant library of transcriptional regulators would allow the identification of candidate TRs involved in the production of this molecule. This would also give an indication as to the biological pathways that may be implicated in this process (Chapter 3).

To achieve these goals, approaches that coupled genetic and functional genomic tools (ChIP-chip and expression profiling on microarrays) were used in combination with a genetic screen. These approaches allowed the unraveling of transcriptional regulator biological functions as well as the elucidation of new transcriptional networks. These findings will add to the construction of the complex hub of general transcriptional networks governing important biological processes in the opportunistic yeast *Candida albicans*.

Chapter 2

2. Chapter 2: Genome-wide Location and Expression Analyses of the *Candida albicans* Fcr1p Transcription Factor Regulon

This chapter is presented as a manuscript in preparation for PLOS One

Aline Khayat (AK), Osman Zin Al-Abdin (OZAA), Martine Raymond (MR)

Author Contributions

Osman Zin-al-Abdin	Tagged Fcr1p and performed the ChIP-chip assay
Aline Khayat	Analyzed the ChIP-chip & GO term results and generated figure 2.1 Performed experiments, analyzed results and generated figures 2.2, 2.3, and 2.4. Wrote the abstract, introduction, results, discussion, conclusion, and part of the methods section
Martine Raymond	Conceived and supervised the project; corrected the different versions of the manuscript

Genome-wide Location and Expression Analyses of the *Candida albicans* Fcr1p Transcription Factor Regulon

Short Title: Regulon of the *Candida albicans* transcription factor Fcr1p

Aline Khayat[1], Osman Zin Al-Abdin[1,#a], Martine Raymond[1,2*]

[1]Institute for Research in Immunology and Cancer, Université de Montréal, Montreal, Quebec, Canada

[2]Department of Biochemistry and Molecular Medicine, Université de Montréal, Montreal, Quebec, Canada

[#a] Current Address: King Saud University, Princess Al-Johara Al-Ibrahim Center for Cancer Research, Prostate Cancer Research Chair, College of Medicine, Prostate Cancer Research Chair, Riyadh, Saudi Arabia.

Author Contribution:

Conceived and designed the experiments: AK, OZAA, MR. Performed the experiments: AK, OZAA. Analyzed the data: AK, MR. Generated the figures: AK. Wrote the paper: AK, MR

* Corresponding author

E-mail: martine.raymond@umontreal.ca

2.1. Abstract

C. albicans, an opportunistic commensal of the human microbial flora, is among the leading causes of death in the immunocompromised population. One of its main virulence factors is attributed to its morphological transition between yeast and hyphal forms. The *C. albicans* genome comprises many transcription factors, important proteins that regulate vital cellular processes. However, the function of many of TFs is still unknown. In this study, we used combined genetic and genomic approaches to investigate the biological functions of Fcr1p, a TF belonging to the fungal-specific family of zinc cluster regulators. ChIP-chip analyses showed that Fcr1p binds predominantly to genes involved in nitrogen source uptake, metabolism and utilization. Fcr1p was found to bind within the open reading frame (ORF) of its targets, possibly through an association with the transcriptional or chromatin remodeling machinery. Expression profiling assays using an *fcr1*ΔΔ deletion mutant as well as an *FCR1* overexpressing strain revealed that Fcr1p can function both as an activator and a repressor of gene expression. Mining of the bound and modulated genes identified 17 direct target genes, 10 of which were downregulated and involved in nitrogenous compounds transport (*DUR3*, *MEP1*, *CAN2*, *NUP*, *OPT1*, *OPT9*, *FCY2*, *FCY24*), utilization (*DUR1,2*) and regulation (*GAT1*). These results indicate that Fcr1p functions as a repressor of nitrogen assimilation. Our results also showed that Fcr1p is an activator of yeast-specific genes (*YWP1, RME1*) and a repressor of hyphae-specific genes (*HWP1, ECE1*). Consistent with this, *FCR1* overexpression was shown to abrogate hyphae formation on solid spider medium, demonstrating that Fcr1p is a repressor of filamentation. Finally, many TF-encoding genes were found to be regulated by Fcr1p (*GAT1*, *STP1 (orf19.5917), RME1*, *WOR1*, *TYE7*, *ECE1*, others), suggesting that Fcr1p regulates many of its targets indirectly.

2.2. Introduction

C. albicans is an important opportunistic human fungal pathogen. It is part of the normal microbial flora and exists as a commensal at several host sites such as the skin, the mucosal surfaces of the oral cavity and the gastrointestinal and genitourinary tracts. However, *C. albicans* is capable of causing severe mucosal or invasive infections when the host conditions become permissive to fungal proliferation (Spampinato & Leonardi, 2013). These infections occur particularly in severely immunocompromised patients, for example AIDS patients or patients undergoing immunosuppressive drug treatment following organ transplantations or having chemotherapy for cancer treatment. Depending on the host immunological status, the antifungal treatment adopted, and the fungal cell susceptibility, these infections can range anywhere between benign to lethal (Eggimann & Pittet, 2014; J. Kim & Sudbery, 2011).

C. albicans is a polymorphic organism which undergoes a reversible transition between different morphological forms including yeast, hyphae, and pseudohyphae (J. Kim & Sudbery, 2011). This ability to change from yeast to filamentous forms is a major virulence determinant of this organism, allowing cells to grow within different host niches (Cooney & Klein, 2008). For instance, the yeast form is necessary to produce dissemination within the blood stream, while hyphal projections allow the penetration of intraepithelial junctions and the evasion of phagocytes (Berman & Sudbery, 2002; Zhu & Filler, 2010). Furthermore, *C. albicans* can grow as biofilms on inert surfaces such as clinical implanted devices. Biofilm cells are characterized by a timely coordination between the hyphal and yeast forms in addition to displaying multi-drug resistance. Hence this phenotypic transition has been extensively studied in *C. albicans* and other medically important fungi (Han *et al.*, 2011; J. Kim & Sudbery, 2011; Mayer *et al.*, 2013; Whiteway & Bachewich, 2007). The filamentous program has been shown to be induced by many different environmental stimuli such as high

temperature, serum, contact with solid matrix, oxygen and nutrient limitation, and pH stress. Each of these environmental cues triggers a different signalling cascade that ultimately converge into a core set of effector genes, leading to the formation of hyphae or pseudohyphae. Transcription factors (TFs) such as Cph1p, Efg1p, Tec1p and Czf1p activate hyphae-specifc genes whereas TFs such as Nrg1p and Rfg1p repress those genes (Han *et al.*, 2011; P. E. Sudbery, 2011). *C. albicans* is also capable of another type of phenotypic transition known as the white-opaque switching controlled by TFs such as Wor1p and Wor2p, with opaque cells being the mating-competent form (Morschhauser, 2010; Whiteway & Bachewich, 2007). In addition to phenotypic transitions, metabolic adaptation is also an important virulence determinant of *C. albicans*, which allows it to adapt and extract the available nutrients in each particular niche. This metabolic flexibility is manifested by the expression of a wide array of permeases, transporters and extracellular hydrolytic enzymes (A. J. Brown *et al.*, 2007)(Nallis , 2010) .

C. albicans infections are often treated with azole drugs, such as fluconazole, that target the biosynthesis of ergosterol, the major sterol of fungal membranes, or with echinocandins such as caspofungin, which interfere with the biosynthesis of the fungal cell wall (Moudgal & Sobel, 2010). However, the management of *C. albicans* infections is challenging, partly due to the emergence of drug-resistant strains frequently encountered while using azoles. Azole resistance is caused by the upregulation of drug efflux pumps of the ABC transporter family such as Cdr1p and Cdr2p, the major facilitator transporter Mdr1p, or the ergosterol biosynthetic enzyme, Erg11p (Morschhauser, 2016; Morschhauser *et al.*, 2007; Tsao *et al.*, 2009). The constitutive upregulation of these genes is mediated by the acquisition of gain-of-function mutations in TFs of the zinc cluster family: Tac1p, Mrr1p, and Upc2p, respectively (Coste *et al.*, 2004; Dunkel, Liu*, et al.*, 2008; Morschhauser *et al.*, 2007). In addition, it has been recently shown that *CDR1* is under the control of Mrr2p and that

mutations in the latter induces overexpression of *CDR1* (Schillig & Morschhauser, 2013; X. J. Wang *et al.*, 2015). Mutations in the *ERG11* gene have also been shown to contribute to azole resistance (Flowers *et al.*, 2012). On the other hand, echinocandins resistance is correlated with mutations in the *FKS1* gene, encoding a glucan synthase, which is the target of echinocandins (Balashov *et al.*, 2006).

C. albicans is a diploid organism whose genome (28.6 Mb) has been sequenced and annotated (Inglis *et al.*, 2012). It contains 6198 genes, a large fraction of these (72%) are still uncharacterized. A major task for the *Candida* community is now to assign functions to these genes, with the goals of gaining a better understanding of the biology of this medically important fungus and identifying fungal-specific proteins representing potential antifungal drug targets. For example, zinc cluster transcription factors possess a conserved fungal-specific DNA binding motif (MacPherson *et al.*, 2006). They are involved in the regulation of a spectrum of important cellular processes including carbon source utilization (Gal4p, Rgt1p, Suc1p), filamentation (Czf1p, Ume6p, Ahr1p) and drug resistance (Tac1p, Mrr1p, Mrr2p, Upc2p) (Finkel *et al.*, 2012; Han *et al.*, 2011; MacPherson *et al.*, 2006; Mayer *et al.*, 2013; Morschhauser, 2011). The *C. albicans* genome comprises 82 zinc cluster TFs (Schillig & Morschhauser, 2013), many of unknown function.

We previously identified the *FCR1* (*Fluconazole Resistance 1*) gene by functional complementation of an azole hypersensitive *Saccharomyces cerevisiae* strain with a *C. albicans* multi-copy genomic DNA library (Talibi & Raymond, 1999). *FCR1* was found to code for a zinc cluster TF whose deletion in *C. albicans* increased cell resistance to multiple drugs and whose overexpression enhanced susceptibility to these drug, demonstrating that Fcr1p functions as a negative regulator of drug resistance in *C. albicans* (Talibi & Raymond, 1999). This function was possibly through derepression of the *CDR1* transporter gene (Shen *et al.*, 2007). Genome-wide expression studies have shown that *FCR1* is upregulated in biofilm cells

as compared to planktonic cells (Nett *et al.*, 2009) and downregulated in biofilms upon treament with farnesol, a quorum sensing molecule (Cao *et al.*, 2005). Finally, it was found in a genetic screen using a transposon mutant library that an *fcr1* mutant displays enhanced filamentation (Uhl *et al.*, 2003). In this study, we have combined genetic and genomics approaches to investigate Fcr1p biological functions.

2.3. Materials and Methods

2.3.1. *C. albicans* strains

C. albicans strains used in this study are listed in Table II.1. Cells were routinely grown in YPD (1% yeast extract, 2% peptone, 2% dextrose) or YPD 2% agar plates at 30ºC and subsequently diluted for each specific assay (see assay specifications below). For nitrogen starvation conditions, cells were grown in yeast nitrogen base medium (YNB) without amino acids and ammonium sulfate. Cells were harvested as indicated.

Table II. 1. Strains used in this study.

Strain name	Parent	Relevant genotype or feature	Reference
SC5314		*FCR1*/*FCR1*	(Gillum *et al.*, 1984)
KO	SC5314	*fcr1*Δ::FRT/*fcr1*Δ::FRT	This study
CAI4		*FCR1*/*FCR1*; *ura3Δ::imm434/ura3Δ::imm434*	(Fonzi & Irwin, 1993)
Fcr1p-HA_3	CAI4	*FCR1/FCR1-HA*$_3$	This study
KO_c	CAI4	*fcr1*Δ::*hisG*/*fcr1*Δ::*hisG*	(Talibi & Raymond, 1999)
EV[a]	KO_c	*fcr1*Δ::*hisG*/*fcr1*Δ::*hisG* [YPB-ADH]	(Talibi & Raymond, 1999)
OE[b]	KO_c	*fcr1*Δ::*hisG*/*fcr1*Δ::*hisG* [YPB-ADH/*FCR1*]	(Talibi & Raymond, 1999)

[a] Empty vector

[b] Overexpression.

2.3.2. Chromatin immunoprecipitation and data analysis

Three independent cultures (50 mL each) of strains CAI4 (untagged) and Fcr1p-HA_3 (tagged) were grown in YPD medium at 30ºC to an OD_{600} of 1.0-1.2. The subsequent steps of DNA crosslinking, DNA shearing, ChIP, and DNA labeling with Cy dyes were conducted as described previously (Znaidi *et al.*, 2009). Labeled DNA from the tagged strain (Fcr1p-HA_3, Cy5-labeled) and the corresponding untagged control strain (CAI4, Cy3-labeled) were mixed and hybridized to *C. albicans* whole-genome tiled-oligonucleotide DNA microarray based on assembly 19 (*n* = 3) (Srikantha *et al.*, 2006). Hybridization was performed as recommended by the manufacturer (NimbleGen® systems, Inc). Scanning of the slides was performed using a GenePix 4000B scanner (Molecular Devices). Scanned images were pre-processed using the NimbleScan™ software (version 2.4, NimbleGen® systems, Inc). General Feature Format (GFF) reports were created for the Cy5 (tagged strain) and Cy3 (untagged control strain) intensity signals from each independent replicate, then imported into the TileScope software (http://tilescope.gersteinlab.org:8080/mosaic/pipeline.html) and quantile normalization was applied to the data (Zhang *et al.*, 2007). The parameters used were as follows: window size of 400 bp, MaxGap of 60 bp and MinRun of 120 bp. The replicate data were combined and peak-finding (i.e. Fcr1p binding sites) was performed using the following criteria: pseudo-median signal threshold of ≥ 1.5-fold and p-value cut-off of ≤ 0.01. Signal intensities were mapped to an in-house *C. albicans* genome browser. Gene Ontology (GO) term analysis was performed by uploading gene lists into the GO Term finder tool available at the Candida Genome Database website (http://www.candidagenome.org/).

2.3.3. Quantitative PCR validation of the ChIP-Chip data

An aliquot of the precipitated ChIP DNA from CAI4 and Fcr1p-HA_3 (n=3) was set aside for q-PCR analysis to confirm Fcr1p binding. ChIP DNA was quantified by PicoGreen DNA kit (Invitrogen) according to the manufacturer's instructions. The *SPS4* gene was used as an

endogenous control since no Fcr1p enrichment was detected at this locus. Relative quantification (enrichment) was calculated based on the detected C_t (threshold cycle) of each sample using the formula $RQ = 2^{-\Delta\Delta Ct}$, where $\Delta C_t = C_{t\ target\ gene} - C_{t\ SPS4}$, and $\Delta\Delta C_t = \Delta C_{t\ tagged\ strain} - \Delta C_{t\ untagged\ strain}$. For this assay, specific primers for *FGR23*, intergenic region upstream of *ORF19.1611* and two independent regions (α and β) within the *MEP1* ORF were used (Supplementary Table II.1).

2.3.4. Transcriptional profiling assays and data analysis

Three independent cultures (50 mL each) of strains SC5314, KO,EV, and OE were grown in YPD medium to an OD_{600} of 1.0, at which point they were harvested and snap-freezed in liquid nitrogen. The OE strain took more time (≈ 30 minutes) to reach the same OD as the other strains and consequently was harvested at a later time. Total RNA was extracted using the hot phenol method as previously described (Schmitt *et al.*, 1990). RNA samples were further purified using Qiagen RNeasy kit columns as per manufacturer's instructions. RNA was then quantified using a NanoDrop Spectrophotometer ND-1000 (NanoDrop Technologies, Inc.) and its integrity was assessed using a 2100 Bioanalyzer (Agilent Technologies). Cy3-labeled CTP cRNA was produced with 50 ng of total RNA using the Low Input Quick Amp Labeling Kit, according to manufacturer's instructions (Agilent Technologies, Inc). The labeled cRNA (1.65 µg) were fragmented and hybridized to *C. albicans* assembly 21-based Agilent custom-made DNA microarray 4 x 44K (Synnott *et al.*, 2010). The arrays were incubated in an Agilent hybridization oven at 65ºC for 17 hours at 10 rpm. They were washed and scanned with an Agilent DNA Microarray Scanner C. All these steps were done according to Agilent One-Color Microarray-Based Gene Expression Analysis protocol (Agilent Technologies, Inc). The expression profiling assays were performed at the McGill University and Genome Quebec Innovation Center (Montreal, Canada). Output from the Agilent Feature Extraction software were read into R, preprocessed and tested for differential expression

using functions from the Bioconductor R (Gentleman, 2005) and Limma (Smyth, 2005). Specifically, the *normexp* method with an offset value of 16 was used for global background adjustment, followed by quantile normalization and a $\log_2$ transformation. Within-array duplicate spots were summarized by averaging, using the function *avereps*. The annotation for probes was retrieved from the chromosomal feature file for *C. albicans* (C_albicans_SC5314) available at *candidagenome.org*. Benjamini-Hochberg false discovery rate was below 0.1 (10%). Gene Ontology (GO) term analysis was performed as described above for the ChIP-chip data.

2.3.5. Northern blotting

The SC5314 and KO strains were grown in YPD medium to an OD_{600} of 1.0 or 18.0. For nitrogen starvation, strains were grown in YNB to a final OD_{600} of 1.0. Subsequently, 50 ODs of cells were collected and RNA was prepared using a hot phenol method as previously described (Schmitt *et al.*, 1990). RNA (18 µg) was loaded on gel (1% agarose, 7.5% formaldehyde) for electrophoresis. The gel was subsequently washed with distilled water. Gel Images were acquired using Syngene bioimaging system (Synoptics Group, Cambridge UK). RNA was then transferred to a nylon membrane (Hybond-N; Amersham Pharamacia Biotech). RNA was hybridized with α ^{32}P-radiolabeled DNA probes as described previously (MacPherson *et al.*, 2005)(Supplementary Table II.1). All probes used consisted of a PCR-amplified DNA fragment derived from the open reading frame of the gene as indicated in the Supplementary Table II.1. Membranes were exposed to an imaging plate (Molecular Dynamics) and the corresponding signals detected by a PhosphorImager (Fuji LAS-5000).

2.3.6. Filamentation assay

Overnight cultures were washed and diluted in PBS to an OD_{600} of 0.1. Subsequently, 15 µL of cells were streaked on spider plates (1% nutrient broth, 1% mannitol, 0.2% potassium phosphate, 1.36% agar, pH 7.2). Plates were incubated at 37ºC for 7 days. Colonies were visualized with a Leica stereomicroscope and photographed using a Canon camera with 8x magnification.

2.4. Results and Discussion

2.4.1. Genome-wide location profiling of Fcr1p

2.4.1.1. Fcr1p binds within the coding region of its target genes

To understand the biological functions of Fcr1p, we first sought to identify its bound targets by performing a ChIP-chip experiment. To this end, the protein was tagged with a triple hemagglutinin epitope at its C-terminus (Supplementary Figure 2.1). For the ChIp-chip assay, the tagged Fcr1p-HA_3 strain and untagged CAI4 control cells were grown under standard growth conditions in rich medium at 30ºC, and harvested in log phase at an optical density OD_{600} of 1.0. The DNA was crosslinked, immunoprecipitated, purified, labeled and hybridized to *C. albicans* whole-genome NimbleGen™ tiling arrays (Srikantha *et al.*, 2006). Mapping of the signal intensities to an in-house genome browser revealed a particular binding profile whereby Fcr1p was bound to its targets within their entire coding region, as exemplified by the tilemaps at the *GDH3, RHR2, DUR1,2, CAN2,* and *MEP1* loci (Figure 2.1A). ChIP-PCR was used to further test Fcr1p enrichment at the *MEP1* locus. *FGR23* and the intergenic region between *orf19.1610* and *orf19.1611* in the same contig as *MEP1* were also tested as negative controls as they displayed below threshold signal intensities. Results

showed that Fcr1p binding within the *MEP1* gene was enriched by about 0.4 fold (Log2 folds) in the tagged strain as compared to the untagged strain, while the *FGR23* gene the *orf19.1610*-*orf19.1611* intergenic region were enriched by 0.14 and 0.08 folds (Log2 folds), respectively (Figure 2.1B). This is consistent with the ChIP-chip results in which Fcr1p binding was enriched by 2.5 fold at the *MEP1* locus but not significantly enriched at the two other tested loci (Supplementary Table II.2-A). Taken together, these results showed that Fcr1p binds to the entire coding region of its target genes, unlike the vast majority of TFs which bind to discrete sequences in the promoter region. To generate such a profile, it is likely that Fcr1p binds DNA indirectly, maybe through an association with proteins of the transcriptional or chromatin remodeling machinery. For example, it is possible that Fcr1p interacts and travels with RNA polymerase II across the transcribed region of its targets, in a manner similar to that of the transcription elongation factor pTEFb (Zhou *et al.*, 2012) or yeast-expressed p53 (S. Kim *et al.*, 2011). Interestingly, the *S. cerevisiae* Sum1p TF has been shown to be co-enriched with the histone deacetylases Hst1p and Sir2p at the ORFs of many highly expressed RNA polymerase II-transcribed genes functioning in processes such as fermentation, glycolysis, and translation (M. Li *et al.*, 2013). Although the mechanism of Sum1p binding to the ORFs was not characterized, it was proposed that this complex be associated with a “poised state” of the TF to allow rapid transcriptional repression of metabolic genes during diauxic shift (M. Li *et al.*, 2013). Based on these observations, we propose that the molecular mechanisms underlying Fcr1p binding to the coding region of its targets are intimately linked to its function, which deserves future investigation.

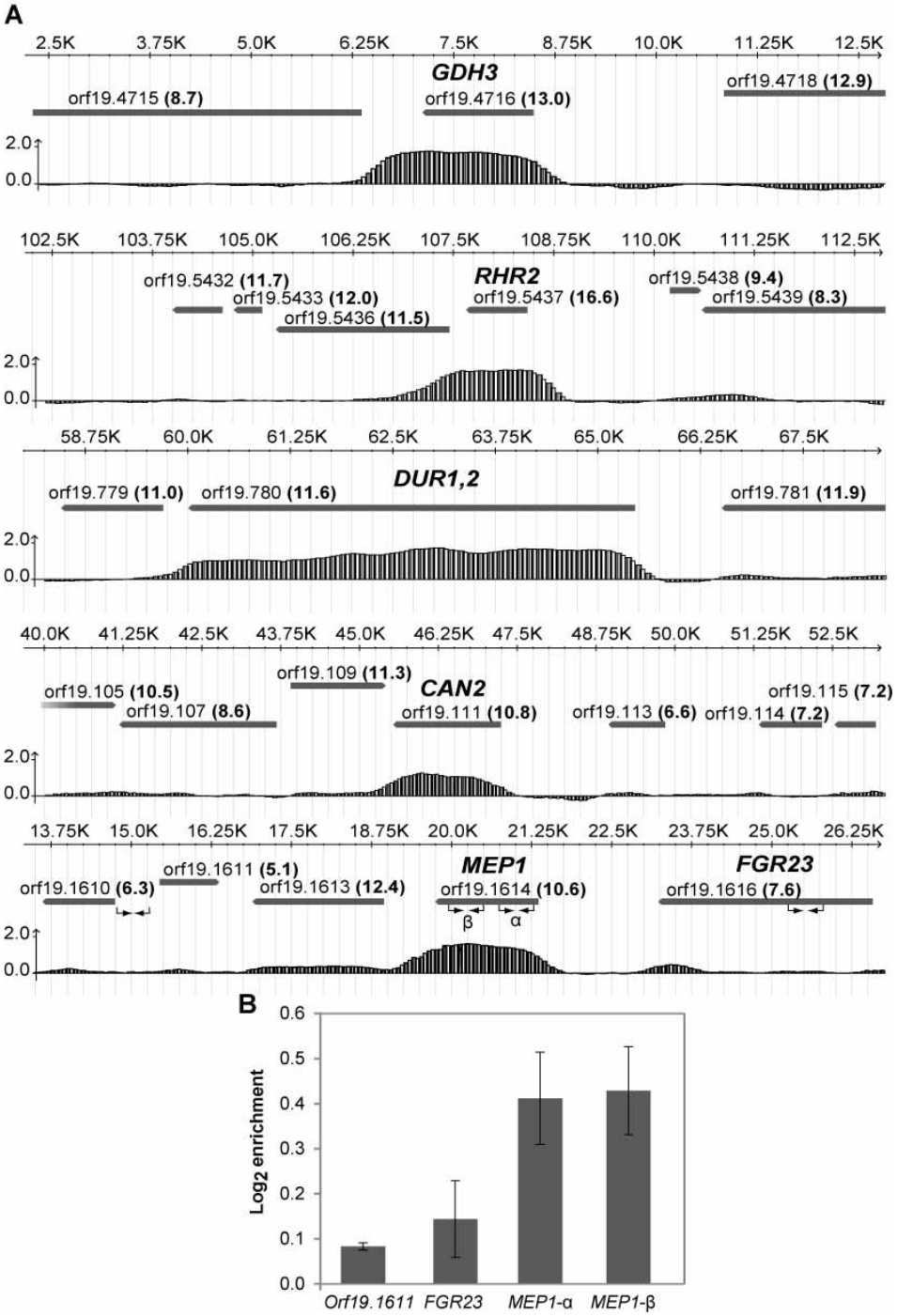

Figure 2.1. Fcr1p binds within the coding region of its target genes.

(A) Fcr1p location profile at selected target genes. The tilemaps in the genome browser views shows the signal intensity for each of the oligonucleotide probes spanning the Watson and Crick strands on the tiling array. The orientation of each ORF is depicted by the arrowed gray

rectangle. The *x*-axis represents the genomic positions in the contigs and the *y*-axis represents log_2-transformed signal intensities (n=3) illustrating Fcr1p enrichment at selected target genes: *GDH3, RHR2, DUR1,2, CAN2,* and *MEP1.* Small arrows in the lowermost panel (*MEP1*) indicate the position of primer pairs used for qPCR validation. α and β represent two independent primer sets within the *MEP1* ORF. Numbers in parenthesis correspond to the average raw expression levels of the genes obtained in the expression profiling experiment. The average represents the calculated mean of the values of two probes from each of the triplicate slides for the indicated gene in SC5314. **(B)** qPCR validation of Fcr1p enrichment at the *MEP1* locus. ChIP DNA from CAI4 and CAI4/Fcr1p-HA_3 (n=3) was analyzed by q-PCR with two primer pairs (α and β, illustrated in panel A) within the *MEP1* gene as well as primer pairs for the gene *FGR23* and *orf19.1610-orf19.1611* intergenic region. Error bars represent the standard deviation for Fcr1p enrichment at each locus.

2.4.1.2. Fcr1p binds to genes involved in nitrogen sources uptake, metabolism and regulation

The ChIP-chip experiment identified binding of Fcr1p to 144 genes, with an enrichment ratio ≥ 1.5 fold and a *p*-value ≤ 0.01 (Supplementary Table II.2-A). GO term analysis by biological process, considering a significance cut-off at a *p*-value ≤ 0.05, yielded 16 functional categories (Supplementary Table II.2-B), the most significant ones including "Nitrogen compound transport" (21 genes), "Amino acid transmembrane transport" (10 genes), "Nitrogen utilization" (6 genes), "Alpha-amino acid catabolic process" (7 genes), and "Glutamate metabolism" (5 genes), suggesting a role for Fcr1p in nitrogen assimilation and metabolism (Figure 2.2). Interestingly, many genes encoding (or predicted to encode) transporters of different nitrogen sources were enriched for Fcr1p binding, including basic amino acids (*CAN1, CAN2, CAN3*), general amino acids (*GAP2, GAP5, GAP6*), oligopeptides (*OPT1, OPT4, OPT9*, *IFC3*, *PTR22*, *orf19.2292*), asparagine/glutamine (*GNP1*, *orf19.7566*), methionine (*MUP1*), urea (*DUR3*), ammonium (*MEP1*), dicarboxylic amino acid (*DIP5*), and polyamine (*TPO3*) (Supplementary Table II.2-A). These results suggest that Fcr1p regulates

nitrogen source uptake by *C. albicans* cells. In addition, Fcr1p was bound to a number of genes coding for nitrogen metabolic enzymes such as glutamate synthases (*GLT1, GLN1*), glutamate dehydrogenase (*GDH3*), 1-pyrroline-5-carboxylate dehydrogenase, for glutamate biosynthesis (*PUT2*), proline oxidase (*PUT1*), and urea amydolyase (*DUR1,2*) (Supplementary Table II.2-A). Two genes coding for transcription factors controlling nitrogen utilization (*GAT1*, *STP1(orf19.5917*) were also bound by Fcr1p. Finally, "*de novo* IMP biosynthesis" (5 genes) and "nucleoside monophosphate biosynthetic process" (7 genes) were highly enriched among the GO terms. Fcr1p was bound to the *ADE1, ADE4, ADE5,7, ADE6, ADE13*, *RNR21*, *RNR22* and *ADK1* genes involved in *de novo* purine biosynthesis, to the *URA1* gene involved in *de novo* pyrimidine biosynthesis and to the *FCY2* and *FCY24* genes encoding putative purine-cytosine permeases. This suggests that Fcr1p also regulates nucleotide *de novo* biosynthesis and salvage pathways and thus the flow of nitrogen into molecules with nitrogen-containing precursors (Ljungdahl & Daignan-Fornier, 2012). Taken together, our ChIP-chip data strongly suggest that Fcr1p is involved in regulating nitrogen uptake, metabolism and utilization in *C. albicans*.

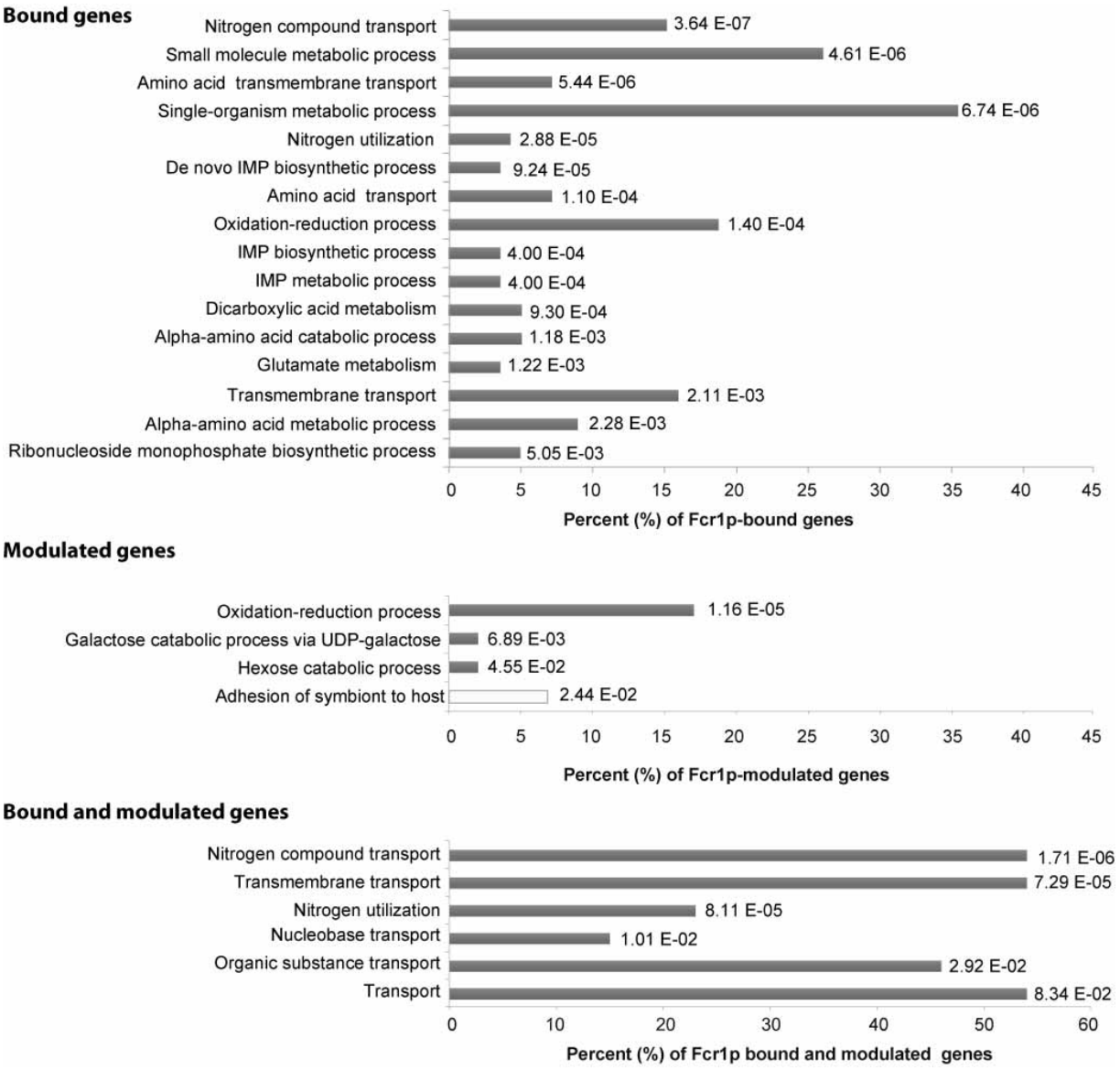

Figure 2.2. Gene Ontology (GO) enrichment analysis for Fcr1p bound genes

A) Process GO terms for genes bound by Fcr1p. **B)** Process GO terms for genes modulated by FCR1 overexpression. Grey bars represent upregulated terms, white bar represents downregulated terms **C)** Process GO terms for genes bound and modulated Fcr1p. The *x*-axis represents the percentage of genes assigned to a specific term. Corresponding adjusted *p*-values are indicated next to each bar. GO terms by function and component can be found in Supplementary Tables II.2-B and II.3-D.

2.4.1.3. Fcr1p binds to genes encoding membrane-associated proteins

Interestingly, GO term analysis by cellular component revealed enrichment of target genes coding for proteins located at the plasma membrane (24 genes; *p*-value = 0.0027) (Supplementary Table II.2-B). In addition to genes coding for nitrogen compound transporters, Fcr1p was also bound to genes encoding transporters of other molecules such as glycerophosphocholine (*GIT3*), manganese (*CCC1*), copper (*CRP1*), and antibiotic (*QDR1*), as well as a predicted transporter of unknown function (*orf19.4550*). This suggests a broader role for Fcr1p in controlling the uptake of various compounds at the level of the plasma membrane. In line with this, a GO term analysis by molecular function revealed that "Transmembrane transport activity" (26 genes) was highly enriched among Fcr1p bound genes (Supplementary Table II.2-B). Taken together, these results indicate a potential role for Fcr1p as a regulator of the assimilation of many compounds in general and more specifically nitrogenous compounds at the level of the plasma membrane, possibly contributing to general cellular homeostasis or adaptative responses to particular stimuli.

2.4.2. Genome-wide expression profiling of Fcr1p

2.4.2.1. Fcr1p functions as an activator and a repressor of gene expression

We next used genome-wide expression profiling as a complementary approach to characterize the Fcr1p regulon. For this, a *fcr1*ΔΔ mutant (KO) was constructed in strain SC5314 (wt) using the dominant selectable marker *SAT1* (Reuss *et al.*, 2004) (see supporting information and Supplementary Figure 2 for details on the strain construction). Three independent cultures of the SC5314 wild type and mutant *fcr1*ΔΔ strains were grown in YPD medium and harvested in log phase at an OD_{600} of 1.0, the growth condition also used for the

ChIP-chip experiment. Total RNA was extracted, converted to cDNA and hybridized to *C. albicans* DNA microarray (Synnott *et al.*, 2010). In order to rule out the possibility of random or non-specific binding of Fcr1p to transcribed regions in general, we have examined the raw expression data of the transcripts in wild-type strain SC5314. This analysis showed that genes that were not bound by Fcr1p were nevertheless expressed under the growth conditions used for the location and expression experiments, demonstrating that binding of Fcr1p is specific for its target genes and is independent of their transcriptional status (Figure 2.1). Comparative data analysis revealed that only a few genes were significantly modulated in the mutant relative to the wild type strain (2 downregulated and 7 upregulated genes; ≥ 2.0 fold; p-value ≤ 0.01) (Supplementary Table II.3-A). Interestingly, four of the upregulated genes are involved in biological adhesion and biofilm formation (*PBR1*, *ECE1*, *HWP1*, *ALS3*), suggesting that Fcr1p may repress these processes.

The very small number of genes identified by this approach suggested that Fcr1p function may be masked by redundancy with other TFs and/or that Fcr1p has low activity under the standard growth conditions used for the experiment in the absence of knowledge of the Fcr1p activating stimuli. A similar situation has been encountered in several studies using gene deletion and inactivation approaches to decipher TF function (Banerjee *et al.*, 2008; Homann *et al.*, 2009; MacPherson *et al.*, 2005; Noble *et al.*, 2010; Vandeputte *et al.*, 2011). We therefore turned to a TF overexpression approach that has proven to be a useful alternative method to discover new TF functions (Chua *et al.*, 2006; Sopko *et al.*, 2006). Overexpression appears to mimic transcription factor physiological activation and has been shown to increase both the sensitivity and relevance of the results (Chua *et al.*, 2006; Sopko *et al.*, 2006). In some other cases, dubious binding can also occur due to overexpression resulting in false positive results. It has also been reported that genes with inherently low occupancy are also likely to display a false negative profile in overexpression approaches

(Tang *et al.*, 2006; Znaidi *et al.*, 2009). We thus compared the expression profile of a CAI4 strain in which the *FCR1* gene was deleted (contains the empty YPB-ADH vector as a control; designated EV) to that of the same strain containing the YPB-ADH-FCR1 expression vector that expresses *FCR1* at high levels from the strong *ADH1* promoter (designated OE) (Talibi & Raymond, 1999). Comparing the expression profile of these two strains revealed that 175 genes were upregulated and 73 genes were downregulated in the OE strain relative to the control strain (≥ 2 fold; p-value ≤ 0.01) (Supplementary Table II.3-B), demonstrating that Fcr1p can function both as an activator and a repressor. GO term analysis of the upregulated genes yielded biological processes pertaining to galactose catabolism (*GAL1*, *GAL7*, *GAL10*) while analysis of the downregulated genes yielded biological processes relating to cell adhesion (*WOR1*, *HYR1*, *URA3*, *ALS1*, *ALS2*) and substrate-specific transmembrane transporter activity (*DUR3*, *GIT1*, *MEP1*, *FCY2*, *CNH1*, *CAN2*, *HGT12*, *NUP*, *OPT1*, *FCY24*). Genes involved in galactose catabolism and cell adhesion were not bound by Fcr1p, suggesting that they are indirect targets of Fcr1p, while many of the genes with transmembrane transporter activity were bound by Fcr1p, and thus likely to be direct targets (see below).

2.4.2.2. Fcr1p regulates genes involved in different biological processes

Further analysis of the Fcr1p direct and indirect targets identified a number of potential functions for Fcr1p, including nitrogen homeostasis, yeast-hyphae transition, and stress adaptation.

2.4.2.2.1. Nitrogen metabolism

Mining of the genes bound and modulated by Fcr1p yielded a list of 17 direct target genes (Table II.2 and Supplementary Table II.4-A), with 7 downregulated genes involved in

nitrogen transport (*DUR3*, *MEP1*, *FCY2*, *CAN2*, *NUP*, *OPT1*, *FCY24*). These results indicate that Fcr1p negatively regulates nitrogen source uptake.

Table II.2. Genes bound and modulated by Fcr1p

Gene name	Binding[a]	Expression[b]	Description
Upregulated			
HSP21	1.8	5.0	Small heat shock protein
orf19.510	1.5	2.6	Protein of unknown function
ADH5	1.7	2.1	Putative alcohol dehydrogenase
orf19.7296	1.8	2.0	Putative cation conductance protein
Downregulated			
orf19.1691	1.6	-2.0	Plasma-membrane-localized protein
orf19.4287	1.6	-2.1	Putative oxidoreductase
UBA4	1.6	-2.1	Putative ubiquitin activating protein
GAT1	1.6	-2.2	GATA-type TF; regulator of nitrogen utilization
MEP1	2.5	-2.2	Ammonium permease
FCY2	1.6	-2.3	Purine-cytosine permease of pyrimidine salvage
DUR3	1.7	-2.5	Spermidine transporter
FCY24	1.6	-2.6	Putative nucleoside transporter
OPT9	2.4	-2.6	Probable pseudogene; similar to *OPT1*
DUR1,2	2.6	-2.7	Urea amidolyase; hydrolyzes urea to CO2
OPT1	2.5	-2.9	Oligopeptide transporter
CAN2	2.0	-3.0	Basic amino acid permease
NUP	1.9	-5.1	Nucleoside permease

[a] Linear binding ratio (from S2 Table)

[b] Expression ratio (from S3 Table)

Interestingly, the GATA transcription factor gene *GAT1* (and its effector gene *MEP1*), which was shown to be partly involved in nitrogen catabolite repression, was also among the downregulated targets of Fcr1p (Limjindaporn *et al.*, 2003). In addition, *GAT1* was also shown to be involved in the regulation of pathogenicity genes such as the *SAP* genes and therefore *gat1* mutants displayed attenuated virulence in mouse animal models (Limjindaporn *et al.*, 2003). This places Fcr1p upstream of an important nitrogen and virulence regulator and

implicates that Fcr1p may participate in the repression of nitrogen-dependent genes in the presence of preferable nitrogen sources. Fcr1p also negatively regulates genes needed for coping with nitrogen starvation conditions such as *DUR1,2* and *OPT1*, encoding an oligopeptide transporter, further confirming its role in the energy-efficient use of available nitrogen sources (Ramachandra *et al.*, 2014). Furthermore, 8 of the 17 Fcr1p direct targets (*orf19.510, ADH5, orf19.7296, MEP1, DUR3, OPT9, DUR1,2,* and *OPT1*) were also modulated in the same direction in a nitrogen starvation growth medium (Ramachandra *et al.*, 2014).

In *Saccharomyces cerevisiae*, nutrient sensing is mediated by components of the TOR pathway, whereby they dictate the phosphorylation state of nitrogen-responsive TFs and therefore determine their intracellular location and transcriptional activity. In this sense TOR pathway links NCR to the overall transcriptional and translational activity of nutrient-deprived cells (Rodkaer & Faergeman, 2014). In the same manner, it's plausible that Fcr1p may lie downstream of the TOR signalling pathway and controls nitrogen-responsive genes.

To test for the role of *FCR1* in nitrogen homeostasis predicted by our genomic results, the *fcr1*ΔΔ mutant, *FCR1* overexpressing and control strains were cultured in liquid medium containing different sources of nitrogen and their growth was monitored by Growth Curve Analysis (GCA). The *fcr1*ΔΔ mutant and *FCR1* overexpressing strain did not show any noticeable change at the level of different growth parameters (final OD, doubling time, lag time; data not shown). This is however not so surprising because of the redundancy that exists in the control of nitrogen acquisition in yeast (Coffman *et al.*, 1996; Coffman *et al.*, 1997; Magasanik & Kaiser, 2002). It has been shown that, when one regulator of this pathway is disturbed, many feedback loops take over to compensate, making the

transcriptional readout of target genes the only good indicator of TF deregulation (Ljungdahl & Daignan-Fornier, 2012; Magasanik & Kaiser, 2002; Ramachandra *et al.*, 2014).

To investigate whether Fcr1p regulates its targets in response to nitrogen deprivation, cells were grown either in YPD or YNB only (nitrogen starvation). For YPD, the SC5341 and *fcr1*ΔΔ strains were grown in YPD medium and harvested at log phase (OD_{600}= 1.2; conditions mimicking profiling conditions) and stationary phase (OD_{600}= 18; conditions mimicking nutritional deprivation). For the nitrogen starvation, cells were grown to log phase (OD_{600}= 1.0). Northern blotting with an *FCR1* probe showed that *FCR1* has the same level of expression at both low and high cell densities. On the other hand, the *FCR1* band displayed a shorter message in the medium lacking nitrogen as compared to rich medium, indicating the existence of a different transcriptional start site or termination site under those conditions. A slight increase in *FCR1* expression in starvation can be noted, however, this has not been quantified by qRT-PCR (Figure 2.3-A). Examination of Fcr1p target genes revealed that *OPT1*, encoding an oligopeptide transporter, displayed a double band possibly due to the presence of antisense regulation for this gene. In addition, *OPT1* is not highly modulated in YPD, however, it is highly derepressed in nitrogen starvation (YNB) in the absence of Fcr1p. Furthermore, *HSP30*, encoding a putative heat shock protein and one of the most highly modulated genes in the *FCR1* overexpression strain, is upregulated at high cell density and more so under starvation and this upregulation is totally dependent on Fcr1p. Taken together these data indicate that Fcr1p responds to nitrogen sources and that it regulates its target genes in nitrogen deprivation conditions.

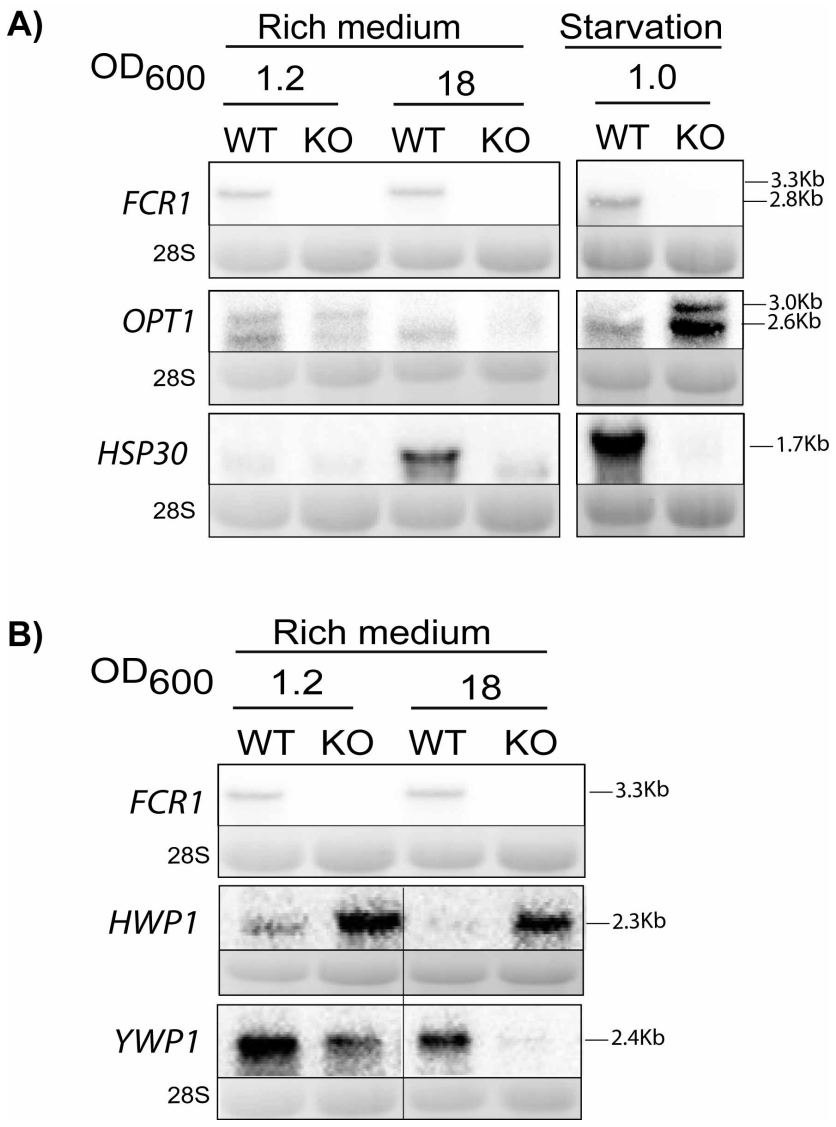

Figure 2. 3. Northern blot analysis of selected Fcr1p targets

The indicated strains were grown either in YPD (and harvested at log phase (OD = 1.2) or at high cell density (OD = 18), and in YNB without ammonium sulfate and without amino acids (and harvested at log phase (OD = 1.0). RNA was extracted and subjected to Northern hybridization with **A)** the *FCR1*, *OPT1*, and *HSP30* probes, and **B)** the *FCR1*, *HWP1*, and *YWP1* probes. All probes used consisted of a DNA fragment derived from the open reading frame of the corresponding gene as indicated in Supplementary Table II.1. 28S RNA is shown below as control. Samples were migrated on the same gel.

2.4.2.2.2. Yeast-hyphae transition

Interestingly, genes involved in the hyphal program were downregulated upon *FCR1* overexpression (*ALS1*, *ALS2*, *FGR17*), suggesting that Fcr1p negatively regulates the hyphal growth mode. We have looked at a recent study that analyzed the transcriptomic changes incurred by the hyphal switch, and we have found that 9 of the hyphal specific genes (*PGA23, PGA10, PGA45, SOD5, EBP1, HYR1, orf19.2452, orf19.6200, orf19.2059*) and 6 of the yeast specific genes (*MNN22, SOU1, RME1, WH11, orf19.5572, orf19.670.2*) detected in this study were downregulated and upregulated, respectively by *FCR1* overexpression (Grumaz *et al.*, 2013). These observations further reinforce the Fcr1p positive role in the yeast growth mode. We thus examined the *FCR1*-regulated expression of yeast- and hyphae-specific genes, using Northern blot analysis (Figure 2.3-B). The SC5341 and *fcr1*ΔΔ strains were grown in YPD medium and harvested at log phase (OD_{600}= 1.2) and at stationary phase (OD_{600}= 18). Results showed that the yeast-specific gene *YWP1* is less expressed in the *fcr1*ΔΔ mutant as compared to the wild type control at both low and high cell density whereas the hyphae-specific gene (*HWP1*) was derepressed in the *fcr1*ΔΔ mutant under the same conditions (Figure 2.3-B). We also examined the expression of the *RME1* gene encoding a TF of the zinc finger family that was recently shown to be expressed as a yeast-specific gene (Grumaz *et al.*, 2013). Taken together, these results suggest that Fcr1p plays a positive role regulating yeast-specific genes and a negative role in regulating hypae-specific genes.

To test this hypothesis at the phenotypic level, a filamentation assay was performed on solid spider medium. Unlike previously reported (Uhl *et al.*, 2003), we did not observe a clear hyperfilamentous phenotype in the *fcr1*ΔΔ mutant (Figure 2.4, top panel). However, we found that *FCR1* overexpression completely abrogated filamentation as compared to the control strain (Figure 2.4, bottom panel). This situation is similar to the filamentous regulator Rfg1p for which a phenotype is detectable upon *RFG1* overexpression but not deletion (Cleary *et al.*,

2010). Repression of filamentation upon *FCR1* overexpression was not observed in liquid spider medium (data not shown), suggesting that Fcr1p may inhibit filamentation through the contact-mediated filamentation pathway. These results suggest that Fcr1p is a positive regulator of yeast-associated genes and a negative regulator of filamentation on semi-solid matrix, the mechanism of which remains to be elucidated.

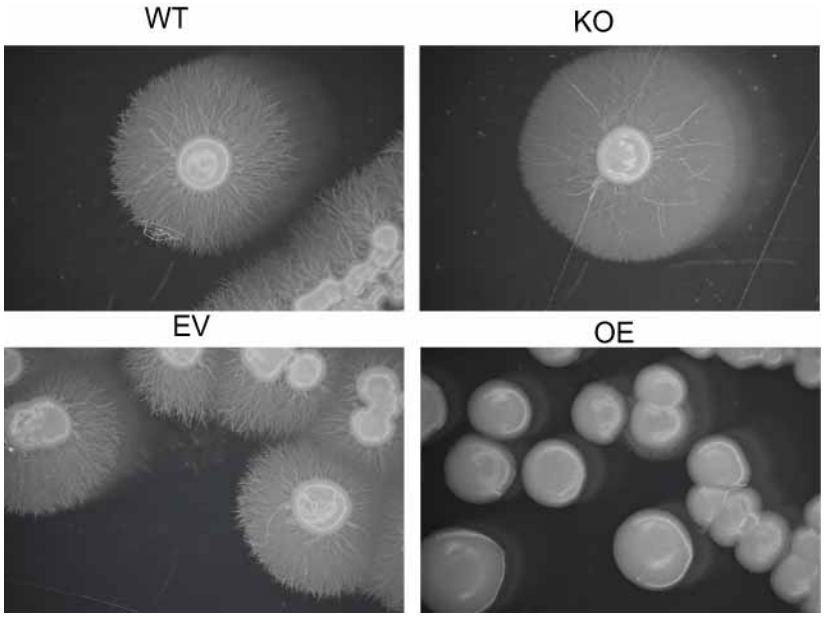

Figure 2.4. Fcr1p overexpression represses filamentation

Growth on Spider solid media. Strains SC5314 (WT), KO, EV and OE were plated on spider plates at 37°C for 7 days and pictures taken with Leica stereomicroscope at 8x magnification.

2.4.2.2.3. Stationary phase and stress response genes

FCR1 overexpression also resulted in the modulation of a number of genes involved in stress response such as *SOD4*, encoding a superoxide dismutase, *HSP30* and *HSP31*, encoding putative heat shock proteins, and also *STP4, HSP21*, *HGT10* and *ORF19.7085,* that are known to be induced during core stress response and in stationary phase cultures (Frohner *et al.*, 2009; Horak, 2013; Mayer *et al.*, 2012). Interestingly, *HSP30* was the most

strongly upregulated gene in the *FCR1* overexpression strain, yet its expression was not changed in the *fcr1*ΔΔ mutant and it was not bound by Fcr1p. Northern blotting with an *HSP30* probe confirmed that *HSP30* is strongly upregulated by overexpressing *FCR1* (Data not shown). It also revealed that *HSP30* is strongly induced at high cell density and that this induction requires *FCR1* (Figure 2.3). Northern blot results also show that *HSP30* is induced under nitrogen starvation condition and that this induction is Fcr1p-depenedent (Figure 2.3). These results show that *HSP30* is indirectly regulated by Fcr1p under normal biological conditions and under stress conditions, demonstrating the usefulness of our overexpression strategy in discovering Fcr1p targets. They also showed that Fcr1p is functional at high cell density and in nitrogen limiting conditions. Taken together, these results suggest that Fcr1p may participate in the cellular response to stress

2.4.2.2.4. Transcriptional regulators

Only a minority of the modulated genes were bound by Fcr1p, suggesting that a majority of the modulated genes are indirect targets of Fcr1p, at least under the experimental conditions used (Supplementary Table II.4-A). Therefore, Fcr1p might be mediating its action through intermediate TFs. Interestingly; our ChIP-chip experiment identified two TFs encoding genes bound by Fcr1p: *STP1 (orf19.5917)* regulating *SAP2*, a secreted aspartyl proteinase, and *GAT1* regulating nitrogen utilization confirming a potential role for Fcr1p in the regulation of nitrogen assimilation. Expression profiling also revealed modulation of a number of transcriptional regulators such as *RME1*, encoding a yeast-specific zinc finger protein (Figure 2.3), and *EFH1*, encoding a regulator of filamentous growth, confirming an Fcr1p role in the regulation of the hyphal switch.

Rme1p is a zinc finger protein that blocks meiosis and promotes sporulation in *S.cerevisiae*. In *C. albicans*, Rme1p, is expressed in white cells, however, its exact function is still not well characterized. A recent study demonstrated that in the dairy yeast, *Kluveromyces lactis*,

Rme1p participates in the rewiring of the ancient mating circuit, where it serves as an intermediate to integrate starvation signals into the circuit. In *K. lactis* sporulation and meiosis genes are under the repressive control of Rme1p (Booth *et al.*, 2010).

Fcr1p was also found to regulate *RGT1*, encoding a regulator of glucose transporters but also the genes encoding the glycolysis regulators *GAL4* and *TYE7,* indicating that Fcr1p is also involved in the assimilation and metabolism of carbon, which is also required in the nutrient-poor stationary phase. Collectively, these data further confirm our hypothesis about Fcr1p involvement in nitrogen assimilation, yeast-associated genes and stationary phase.

2.5. Conclusion

In conclusion, metabolic processes lie at the center of cell survival and therefore it is only logical that the regulation of the corresponding metabolic genes has to be redundant in order to avoid potential major imbalances. In this study, we have found that Fcr1p is involved in the regulation of metabolic and morphological processes that are important for survival and adaptation such as the metabolism and utilization of nitrogen and the yeast-hyphae morphological switch. This explains the lack of a specific phenotype upon deregulation of Fcr1p. Furthermore, we have shown that Fcr1p is an atypical zinc cluster transcription factor that binds within open reading frames. Even though this study has elucidated a number of potential Fcr1p roles in *Candida albicans* cells, the fact that a large number of the Fcr1p bound genes (35%) and modulated genes (11%) are yet uncharacterized ORFs, leaves the space to imply that the full spectrum of Fcr1p function still remains to be identified.

2.6. Acknowledgments

We would like to thank Dr. Mike Snyder, Stanford University, for the design of the *C. albicans* tiling arrays and Dr. Geraldine Butler, University College Dublin, for the design of the *C. albicans* expression array. We are grateful to the Candida Genome Database for providing

a very useful analysis platform through their website. We also wish to acknowledge the McGill University and Génome Québec Innovation Center for the RNA profiling experiment. We also thank Sandra Weber for her valuable advice. This work was supported by Grant MOP 42384 to MR from the Canadian Institute of Health Research. The Institute for Research in Immunology and Cancer is supported by the Canada Foundation for Innovation and the Fonds de la Recherche en Santé du Québec.

2.7. Supporting Information

Construction of an Fcr1p-HA_3 tagged strain for ChIP-chip analysis:

An *FCR1*-tagging cassette was amplified from plasmid pCaMPY-3×HA (Liu *et al.*, 2007) using primers MR1825 and MR1826 (Supplementary Table II.1). These primers contain homologous sequences to the *FCR1* C-terminus as well as specific sequences within the pCaMPY-3×HA vector as described previously (Liu *et al.*, 2007). The resulting fragment (1,921 bp), containing 134 bp of sequences homologous to the terminal sequences of the *FCR1* ORF (except for the stop codon), the *C. albicans URA3* marker flanked by direct repeats of the 3×HA epitope-encoding sequences and 134 bp of sequences homologous to the 3' untranslated region of the *FCR1* gene, was used to transform strain CAI4 (Supplementary Figure 2.1). Transformations were conducted using a modified standard lithium acetate procedure as described previously (MacPherson *et al.*, 2005). The transformed cells were plated on SD-ura plates and incubated for 3 days at 30°C to select for integrants of the tagging cassette. Counter-selection of the *URA3* gene in these clones was carried out on plates containing 5-FOA as described previously (Boeke *et al.*, 1984) (Supplementary Figure 2.1). Looping out of the *URA3* gene was performed to minimize potential transcriptional interference by the 3'UTR-integrated marker and ensure normal

expression of the tagged gene. The colonies were then analysed by western blotting as described below.

The resulting strain CAI4/Fcr1p-HA_3 was analyzed by Western blotting to confirm proper epitope tagging (Supplementary Figure 2.1). A total of 20 OD of cells was harvested and frozen at -80ºC. Pellets were thawed on ice and resuspended in 100 µl of extraction buffer (TE buffer supplemented with 5 µg/ml of each pepstatin, aprotinin, and leupeptin and 1 mM phenylmethylsulfonyl). Acid-washed glass beads (75 µl) were added and cell lysis was carried out at 4ºC by vortexing at maximum speed for 4 min followed by centrifugation at 3000 rpm. Proteins were quantified by Bradford Protein assay (Bio-Rad laboratories). Proteins (15 µg) were loaded on SDS- 8% Polyacrylamide gel. Protein transfer was carried out on a nitrocellulose membrane using a Trans Blot SD Semi-Dry transfer apparatus (Bio-Rad). The membrane was then stained with Ponceau S staining solution (0.1% Ponceau S; 5% acetic acid) and scanned as a loading and transfer control. Immunoblotting was performed using mouse anti-HA monoclonal antibody (Santa Cruz Biotechnology) at a 1:1000 dilution. HA-tagged Fcr1p proteins were subsequently detected using Western Lightning® Plus-ECL (PerkinElmer, Inc, USA).

A chemiluminescent signal was detected in the CAI4/Fcr1p-HA_3 lane (tagged strain) but not in the CAI4 lane (untagged control) around 75 kDa, corresponding roughly to the predicted molecular weight (67 kDa) of the tagged protein (Supplementary Figure 2.1), which confirmed the successful tagging of Fcr1p. We also observe a slower migrating band of smeary appearance and of lesser intensity, which suggests that the Fcr1p protein is subject to post-translational modification, possibly phosphorylation.

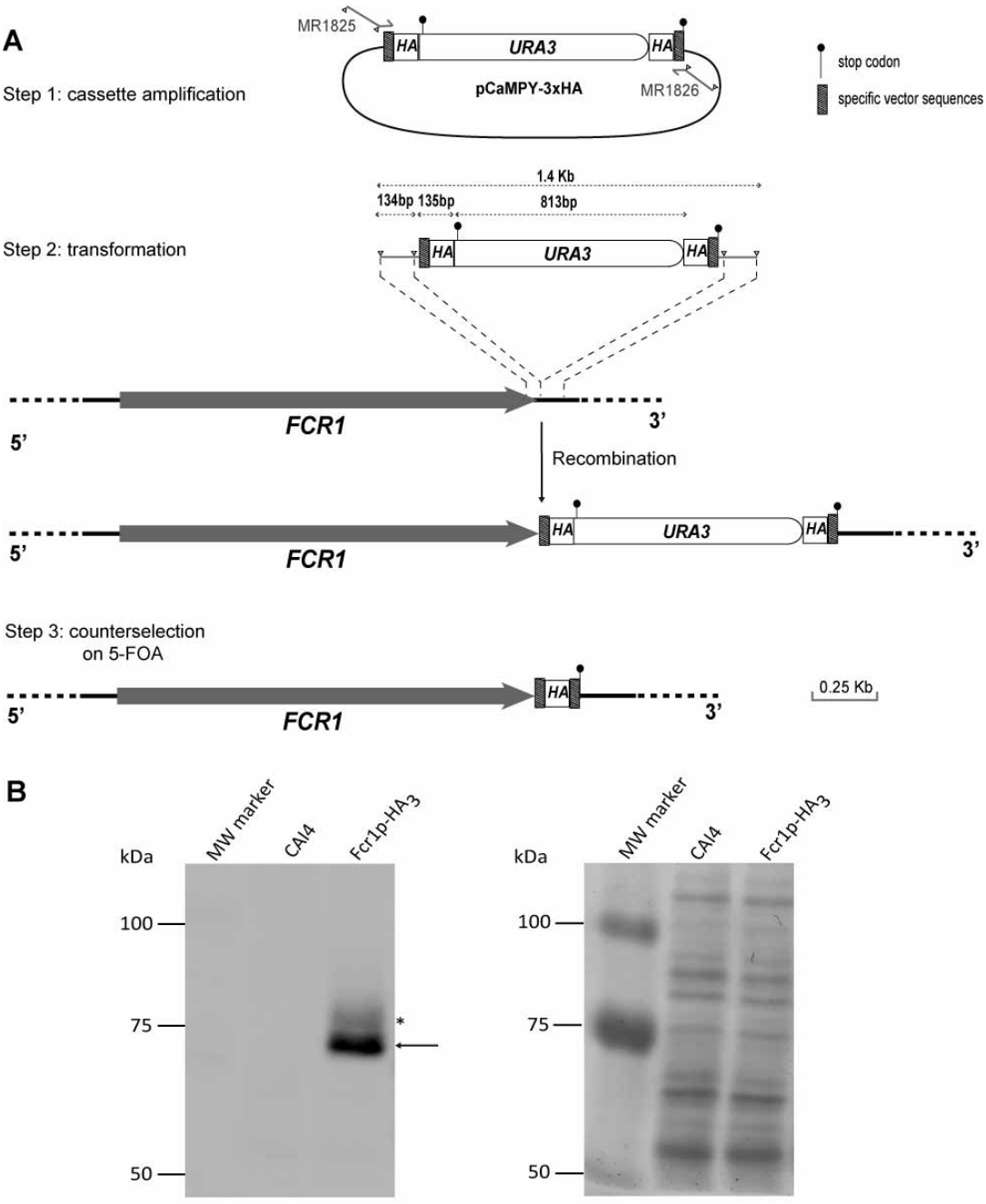

Supplementary Figure 2.1. Epitope-tagging of Fcr1p.

(A) Schematic representation of the *FCR1* epitope tagging strategy. The top panel illustrates the amplification of the 3xHA tagging cassette from plasmid pCaMPY-3xHA (step 1). The middle panel illustrates the PCR amplified tagging cassette and the configuration of the *FCR1* locus after transformation and homologous recombination (step 2). The bottom panel illustrates the final configuration of the *FCR1* locus after excision of the *URA3* gene (step 3).

The stop codon is represented by the black circle. Sequences homologous to the *FCR1* sequences are delimited by small triangles. Hatched boxes represent sequences specific to the pCaMPY-3xHA vector that contain the annealing sequences for the tagging primers. Dashed lines represent integration of the tagging cassette at the target locus. **(B)** Protein extracts from strains CAI4 and CAI4/Fcr1p-HA_3 were analyzed by Western blotting (left panel) using an anti-HA monoclonal antibody. The molecular weight markers are indicated on the left. The Fcr1p-HA_3 protein is indicated by the arrow. A more slowly migrating form of the protein is shown by the star. PonceauS staining is shown (right panel) as a protein loading and transfer control.

Construction and characterization of *fcr1*Δ/Δ homozygous mutants in SC5314

We constructed an *fcr1*Δ/Δ mutant in the SC5314 background using a PCR-based method and the dominant selectable marker *SAT1,* to avoid potential effects of auxotrophic markers on the gene expression profiles. A first round of PCR was used to amplify the *SAT1-FLP* cassette from plasmid pSFS2A (Reuss *et al.*, 2004), using primers MR2652 and MR2653 (Supplementary Figure 2.1 A, Supplementary Table II.1). This generated a DNA fragment containing the entire *SAT1-FLP* cassette flanked by 60 bp of the upstream and downstream regions of the *FCR1* gene. A second round of PCR was used to extend the previous fragment using primers MR2654 and MR2655 (Supplementary Table II.1), thereby generating the *FCR1-SAT1-FLP* cassette containing the entire *SAT1-FLP* cassette flanked by 120 bp of the upstream and downstream regions of the *FCR1* gene. The resulting cassette containing the dominant selectable nourseothricin resistance marker *SAT1* and the *FLP* recombinase gene, flanked by the FRT recombination target sequences (Supplementary Figure 2.2), was used to transform *C. albicans* strain SC5314 by electroporation as described previously (De Backer *et al.*, 1999). The correct nourseothricin-resistant (Nou^R) integrants were selected on YPD agar plates supplemented with 200 µg/ml of nourseothricin (Werner

BioAgents, Jena, Germany). Clones with the correct genotype, as determined by PCR analysis, were sub-cultured in YPM (1% yeast extract, 2% peptone and 2% maltose) to induce expression of the *FLP* recombinase gene and excise the cassette from the first deleted allele. A second round of transformation, excision and selection was performed to delete the second *FCR1* allele using the same *FCR1-SAT1-FLP* cassette used for the first allele. PCR verification was done at each step of the process (Supplementary Figure 2.2.B and 2.2.C). Genomic DNA (100 ng), prepared as described previously (Rose, 1990), was used in each PCR amplification reaction. The resulting PCR products were run on 1% agarose gel, scanned and images were acquired using Syngene bioimaging system (Synoptics Group, Cambridge UK) (Supplementary Figure 2.2.C). A combination of three sets of primers was used to confirm the correct genotype. PCR analysis using primers MR1851 and MR1888 (Supplementary Table II.1), which flank the entire *FCR1* locus (Supplementary Figure 2.2.B), yielded a band of 2.6 kb for the wild-type allele, 5.3 kb for the allele with the *SAT1-FLP* cassette integration, and 1.2 kb for the allele where only the FRT sequence remains replacing the *FCR1* target allele after excision of the *SAT1-FLP* cassette (Supplementary Figure 2.2.C). PCR analysis using primers MR1851 and MR2005 (Supplementary Figure 2.2.B) yielded a band of 1.7 kb resulting from the amplification of the 5' junction of the *SAT1-FLP* cassette upstream of the *FCR1* locus, confirming integration of the cassette at the *FCR1* locus (Supplementary Figure 2.2.C). The PCR product resulting from the amplification of the 3' junction of the *SAT1-FLP* cassette downstream of the *FCR1* locus using primers MR1888 and MR2004 (Supplementary Figure 2.2.B) was a band of 472 bp, confirming *SAT1-FLP* cassette excision from the *FCR1* locus (Supplementary Figure 2.2.C). Two independent *fcr1*Δ/Δ mutants were generated, however, for simplicity purposes, only one mutant is presented in the study (referred to as KO).

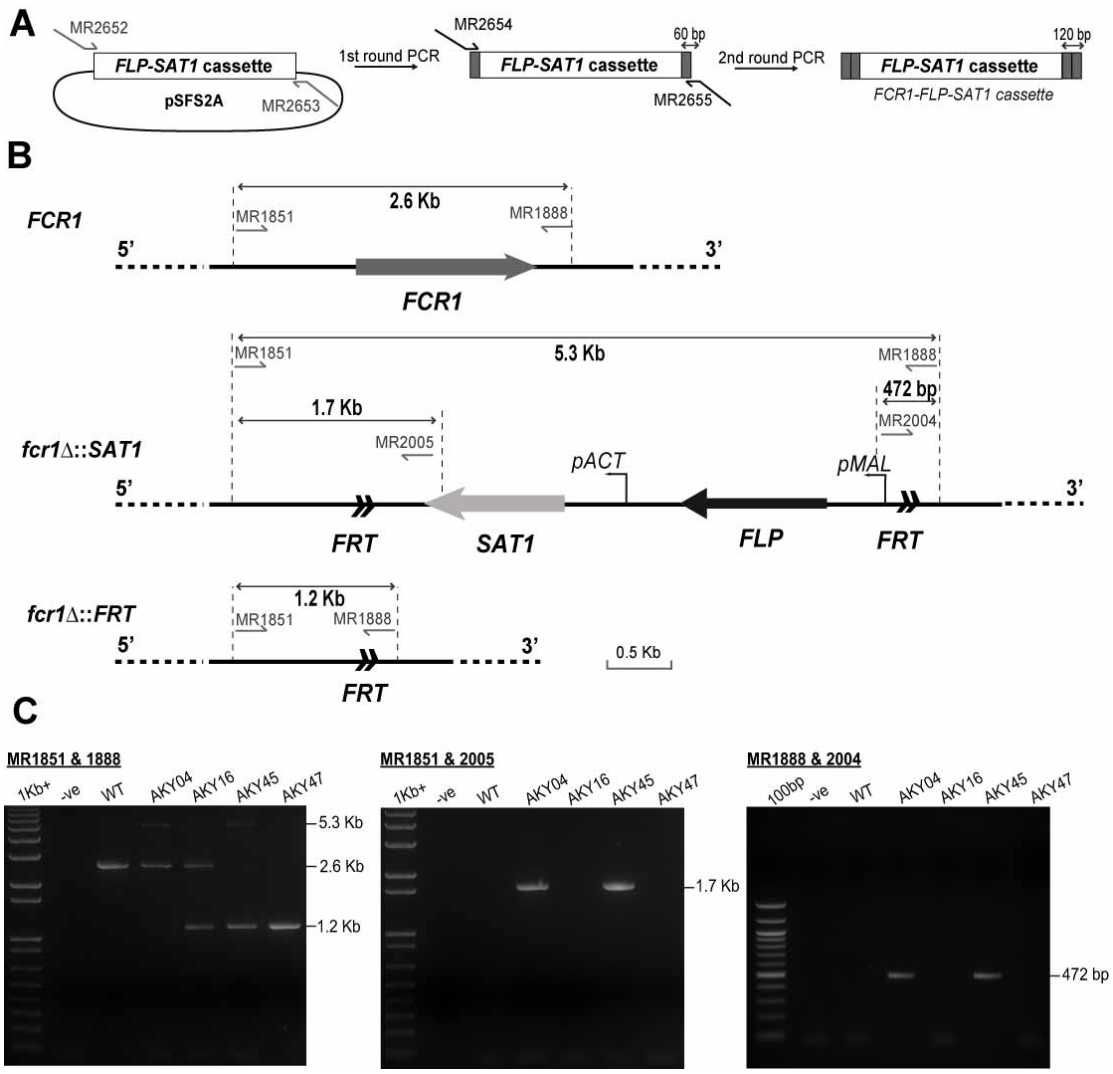

Supplementary Figure 2. 2 Construction of an fcr1ΔΔ mutant in SC5314.

(A) Schematic representation of the **s**equential PCR amplification of the *FCR1-SAT1-FLP* cassette from pSFS2A. Arrows represent primers used in the 1st round (in grey) and 2nd round (in black) of PCR. The resulting *FCR1-SAT1-FLP* deletion cassette is shown in the right panel where the *SAT1-FLP* cassette is flanked by 120 bp of *FCR1* sequences. **(B)** Schematic representation of the *FCR1* locus. The top panel represents the wild type *FCR1* allele; the middle panel represents the *FCR1* allele replaced by integration of the *SAT1* cassette(Reuss *et al.*, 2004). The *SAT1* cassette components are from left to right: *FRT*, FLP recombination target sequence; *SAT1*, nourseothricin resistance marker; *ACT1t*, *ACT1* transcriptional terminator sequence; *FLP*, FLP-recombinase gene; *pMAL*, maltose promoter sequence; *FRT*, FLP recombination target sequences. The bottom panel represents the knocked-out allele replaced by the *FRT* sequence AFTER loop-out of the *SAT1* cassette. The corresponding

genotype at the *FCR1* locus is indicated on the left of each panel. Only one allele is represented. A second round of transformation allowed the deletion of the second allele using the same strategy. **(C)** Agarose gel analysis of the PCR products. For simplicity, a representative of clone for each step is shown on the gels. PCR products from SC5314 (WT), AKY04 (*SAT1* integration at the first allele), AKY16 (*SAT1* excision from the first allele), AKY45 (*SAT1* integration at the second allele), and AKY47 (*SAT1* excision from the second allele) are shown. The left panel shows PCR products resulting from the amplification of the *FCR1* locus using primer pairs MR1851 and MR1888 (Supplementary Table II.1) which flank the *FCR1* locus. The middle panel shows PCR products resulting from the amplification of the 5' junction of the *SAT1-FLP* cassette upstream of the *FCR1* locus using primers MR1851 and MR2005 (Supplementary Table II.1). The right panel shows PCR products resulting from the amplification of the 3' junction of the *SAT1-FLP* cassette downstream of the *FCR1* locus using primers MR1888 & MR2004 (Supplementary Table II.1). The size of the DNA fragments is indicated on the right of each gel

References

Boeke, J. D., F. LaCroute, and G. R. Fink. "A Positive Selection for Mutants Lacking Orotidine-5'-Phosphate Decarboxylase Activity in Yeast: 5-Fluoro-Orotic Acid Resistance." *Mol Gen Genet* 197, no. 2 (1984): 345-6.

De Backer, M. D., D. Maes, S. Vandoninck, M. Logghe, R. Contreras, and W. H. Luyten. "Transformation of Candida Albicans by Electroporation." *Yeast* 15, no. 15 (1999): 1609-18.

Liu, T. T., S. Znaidi, K. S. Barker, L. Xu, R. Homayouni, S. Saidane, J. Morschhauser, A. Nantel, M. Raymond, and P. D. Rogers. "Genome-Wide Expression and Location Analyses of the Candida Albicans Tac1p Regulon." *Eukaryot Cell* 6, no. 11 (2007): 2122-38.

MacPherson, S., B. Akache, S. Weber, X. De Deken, M. Raymond, and B. Turcotte. "Candida Albicans Zinc Cluster Protein Upc2p Confers Resistance to Antifungal Drugs and Is an Activator of Ergosterol Biosynthetic Genes." *Antimicrob Agents Chemother* 49, no. 5 (2005): 1745-52.

Reuss, O., A. Vik, R. Kolter, and J. Morschhauser. "The Sat1 Flipper, an Optimized Tool for Gene Disruption in Candida Albicans." *Gene* 341 (2004): 119-27.

Rose, M. D., F. Winston, and P. Hieter. . *Methods in Yeast Genetics: A Laboratory Course Manual.* Cold Spring Harbor, NY: Cold Spring Harbor Laboratory Press, 1990.

Schneider, B. L., W. Seufert, B. Steiner, Q. H. Yang, and A. B. Futcher. "Use of Polymerase Chain Reaction Epitope Tagging for Protein Tagging in Saccharomyces Cerevisiae." *Yeast* 11, no. 13 (1995): 1265-74.

Chapter 3

3. Chapter 3: A Genetic Screen in *Candida albicans* Identifies Transcriptional Regulators of Farnesol-Dependent Quorum Sensing

This chapter is presented as a manuscript in preparation for PLOS Pathogens

Aline Khayat[1] (AK), Weiwei Liu[1] (WL), Martine Raymond (MR)

[1]Equal contribution

Author Contributions

Weiwei Liu	Wrote part of the results and methods sections Performed the screen and generated figure 3.1 Performed the FOH quantification, and analyzed the results Performed the FCZ- treatment and analyzed the results Performed the microscopy and R2A assay and generated figures 3.4 & 3.5 Performed the Western and generated figure 3.6 Tagged Cas5p & performed ChIp-chip assay, and analyzed the results
Aline Khayat	Wrote the abstract, introduction, discussion & conclusion, and part of the results and methods sections Re-wrote the results section previously written by Weiwei Analyzed the ChIP-chip & GO term results and generated figure 3.7 Analyzed the results of FOH quantification and generated figure 3.2 Analyzed the results of FCZ treatment and generated figure 3.3 Designed and supervised a trainee for the generation of the mutant Prepared RNA for profiling and performed Northern validations and troubleshooting for expression assays Analyzed the expression data, GO terms and generated figure 3.8
Martine Raymond	Conceived and supervised the project; corrected the different versions of the manuscript

A Genetic Screen in *Candida albicans* Identifies Transcriptional Regulators of Farnesol-Dependent Quorum Sensing

Short Title: *C.albicans* Transcription factors regulating farnesol production

Khayat Aline[1&], Weiwei Liu[1&], Martine Raymond[1,2*]

[1]Institute for Research in Immunology and Cancer, Université de Montréal, Montreal, Quebec, Canada H3T 1J4, [2] Département de Biochimie et médecine moléculaire, Université de Montréal, Montreal, Quebec, Canada H3C 3J7
In preparation for PLoS Pathogens

Author Contribution:

Conceived and designed the experiments: WL, AK, MR. Performed the experiments: WL, AK. Analyzed the data: WL, AK, MR. Generated the figures: WL, AK. Wrote the paper: AK, WL, MR.

[&] Equal contribution
* Corresponding author
E-mail: **martine.raymond@umontreal.ca**

3.1. Abstract

Morphogenic switch in *Candida albicans* is closely linked to its pathogenic potential. Farnesol, a quorum sensing molecule, is a negative regulator of the yeast-to-hyphae switch. Some aspects of farnesol sensing have been documented, however, the transcriptional regulators (TRs) of farnesol production are not well characterized. To address this issue, we established a genetic screen based on a co-culture assay with *Aspergillus nidulans* to identify *C. albicans* TR mutants defective in farnesol production. Such mutants allow the growth of *A. nidulans* due to low or no farnesol production. We identified Ada2p, Cas5p, Fgr15p, Cas1p, and Rlm1p, five TRs involved in cell wall integrity as candidate genes in this screen. Extracellular farnesol quantification in these TR mutants confirmed that the observed defect can be attributed to an impairment in farnesol production. Intracellular farnesol levels diminished proportionally to extracellular levels, consistent with a defect in farnesol biosynthesis. To get an insight into the molecular mechanism underlying the farnesol defect in the *cas5*ΔΔ mutant, we used genomic approaches combining location and expression profiling to identify the Cas5p regulon. Our results showed that Cas5p binds genes involved in carbohydrate catabolism (*GAL1, ADH2, PDC11*) and energy production (*GMP1, AOX1, PGK1*). Cas5p also upregulates genes involved in carbohydrate catabolism (*GAL1*, *GAL7*, and *ADH2)* as well as genes involved in lipid catabolism (*LIP1, PXP2, PEX5*). It also dowregulates genes involved in ribosome biogenesis (*RPS21, SSF1, HAS1*) and primary metabolism (*PMM1, ERG2, RHR2*). These results indicate that Cas5p is involved in the regulation of many pathways, with a clear involvement in carbon metabolism. Coupled to the known function of Ada2p and Rlm1p in binding and/or regulating genes involved in carbohydrate catabolism, our results support the proposition that farnesol is a metabolic read-out of the cell carbon metabolic activity.

3.2. Introduction

Candida albicans, a dimorphic and opportunistic yeast, is one of the leading causes of invasive candidiasis (Arendrup, 2010; Sanguinetti *et al.*, 2015). Most of its virulence potential is attributed to its ability to switch its morphology between yeast and hyphal forms. It disseminates in the blood stream via the yeast form and/or inflicts localized organ infection by tissue barrier penetration via the hyphal form (Mayer *et al.*, 2013).

This morphological switch is also very important for biofilm formation on medical devices. Biofilms are regarded as a serious clinical problem since they are particularly notorious, having increased resistance to a wide range of antifungal agents and making the eradication of the infection a challenging task (Ramage *et al.*, 2009). The formation of solid biofilms requires a timely activation of the yeast and filamentous programs with the progressive deposition of carbohydrate-rich extracellular matrix (Chandra *et al.*, 2001)

The yeast-to-hyphae transition is a reversible switch that is activated by a number of environmental cues such as temperature, solid matrix, serum and nutritional starvation, which trigger signal transduction pathways that activate the transcriptional regulators (TRs) Cph1p, Tec1p, and Efg1p, and ultimately, upregulating the expression of hyphae-specific genes. On the other hand, transcriptional repression of hyphae-specific genes is mediated by the transcriptional repressors Nrg1p, and Rfg1p and the co-repressor Tup1p (P. E. Sudbery, 2011). In addition, the quorum sensing molecule farnesol prevents filamentous growth by activating the TFs Nrg1p, Rfg1p, and Rbf1p (Enjalbert & Whiteway, 2005; Hogan *et al.*, 2004).

Quorum sensing (QS), a cell density-dependent intercellular communication process, is mediated by quorum sensing molecules (QSM), which are produced and sensed by the same type of cells. When QSMs exceed a threshold, they trigger a signal transduction pathway leading to the concerted expression of QS-dependent genes that are important for survival (Han *et al.*, 2011). Farnesol, a sesquiterpene alcohol, was the first QS molecule to be

identified in *C. albicans* (Hornby *et al.*, 2001). Farnesol is produced in an alternative pathway branching from the sterol biosynthesis pathway by two consecutive dephosphorylation reactions mediated by the enzymes Dpp2p and Dpp3p (Navarathna, Hornby*, et al.*, 2007; Nickerson *et al.*, 2006). Since farnesol and ergosterol share the same biosynthetic pathway upstream of farnesyl pyrophosphate (FPP), molecules like azoles or zaragozic acid, that block ergosterol biosynthesis beyond the FPP branching point, cause an increased accumulation of farnesol (Hornby *et al.*, 2003; Hornby & Nickerson, 2004). FPP is also an important branching point for the metabolism of other lipids such as geranylgeraniol, geranylgeranyl diphosphate, and dolichol diphosphate (Nickerson *et al.*, 2006). In line with its inhibitory effect on filamentous growth, farnesol is important in controlling the dynamics of biofilm maturation as it promotes the yeast form, thereby allowing cells to disseminate from the biofilm to seed other potential locations and start new biofilms (Nickerson *et al.*, 2006). Farnesol is also important for survival of *C. albicans* cells in a polymicrobial niche where production of this molecule allows the elimination of competing mircroorganisms. It also confers antioxidant protection properties shielding cells from oxidative damage (Albuquerque & Casadevall, 2012; Westwater *et al.*, 2005) .

C. albicans morphogenesis is influenced by environmental factors that are translated by signal transduction pathways and transcription factors. Farnesol influences many of these pathways at different levels. It has been shown that Hog1p, which is involved in osmotic stress response, is activated in the presence of farnesol (Smith *et al.*, 2004), while farnesol was unable to block filamentous growth in a *chk1* mutant (Kruppa *et al.*, 2004). In addition, farnesol inhibits filamentation by inhibiting the cAMP and Cek1p MAP kinase pathways (Davis-Hanna *et al.*, 2008; Roman *et al.*, 2009). Furthermore, farnesol promotes expression of the transcriptional repressor Tup1p at the RNA and protein levels (Kebaara *et al.*, 2008) and has a positive role in cell wall integrity via activation of Mkc1p (Roman *et al.*, 2009).

Recently, six mutants unresponsive to farnesol were identified, including the TF mutants *czf1*ΔΔ, *rlm1*ΔΔ, *stp2*ΔΔ and *yap3*ΔΔ, however only the mechanism underlying the defect in the *czf1*ΔΔ mutant was investigated (Langford *et al.*, 2013). Finally, the zinc homeostasis regulator Zap1p has been identified as a positive regulator of farnesol production in biofilms (Ganguly *et al.*, 2011).

Even though research interest in fungal quorum sensing has risen over the past few years, many aspects of the molecular mechanisms of farnesol-dependent QS in *C. albicans* are still poorly characterized, such as the regulation of biosynthesis, the transport system, the sensing network and the receptors involved, as well as farnesol binding proteins and their subcellular localization. In addition, the regulation of the production, export and detection of farnesol is still unknown. The aim of this study was to identify transcriptional regulators involved in the production of farnesol. Since farnesol-mediated quorum sensing, filamentation, and virulence are closely linked, elucidation of the mechanisms regulating farnesol-dependent QS would allow understanding its role in important biological processes relevant to the pathobiology of *C. albicans.*

3.3. Results

3.3.1. Screen for *C. albicans* genes regulating farnesol production

To identify *C. albicans* transcriptional regulators involved in the production of farnesol, a screen was conducted based on the published finding that farnesol produced by *C. albicans* cells induces apoptosis in the filamentous fungus *Aspergillus nidulans* and therefore hinders its growth (Semighini *et al.*, 2006). For that, a collection of 142 *C. albicans* TR mutants, generated by random transposon insertion, was screened by a co-culture assay with *A. nidulans* (Supplementary table III.1). Our results showed that 22 TR transposon mutants

failed to inhibit *A. nidulans* growth over a period of 72 hours, ranging from weak to no inhibition, suggesting a defective farnesol production in those mutants (Table III.1). Interestingly, 6 of those TR-encoding genes, *CAS1, CAS4, CAS5, FGR15, ADA2*, and *RLM1*, had previously been identified in a screen for hypersusceptibility to caspofungin due to cell wall defects (Bruno *et al.*, 2006), suggesting a possible link between cell wall integrity and farnesol production. We therefore selected these genes for further investigation.

Table III. 1. Genes identified in the phenotypic screen*

Hyphal growth	*CPH1* (orf19.4433) *CPH2* (orf19.1187) *TEC1* (orf19.5908) *ACE2* (orf19.6124)
Biofilm formation	*BCR1* (orf19.723)
Caspofungin susceptibility	*CAS1* (orf19.1135) *CAS4* (orf19.1694) *CAS5* (orf19.4670) *FGR15* (orf19.2054) *ADA2* (orf19.2331) *RLM1* (orf19.4662)
SPS-sensing pathway	*STP2* (orf19.4961) *STP3* (orf19.5917)
Utilization of carbon sources	*MIG1* (orf19.4318)
Uncharacterized genes	*SFP1* (orf19.5953) *MDM34* (orf19.1826) *ZCF14* (orf19.2647) *ZCF18* (orf19.3405) *ZCF23* (orf19.4450) *ZCF39* (orf19.7583) orf19.6781 orf19.6850

*Farnesol has not been quantified in these mutants

To ascertain the role of these TRs in farnesol production, we performed the co-culture assay with deletion mutants (*ada2*ΔΔ*, cas5*ΔΔ*, cas1*ΔΔ*, fgr15*ΔΔ, and *rlm1*ΔΔ) and revertants (*ADA2*-Rev, *CAS5*-Rev, *CAS1*-Rev, *FGR15*-Rev and *RLM1*-Rev) of these TRs in the BWP17 background (Table III.2), except for the mutant of the *CAS4* gene, which appears to be an essential gene (Bruno *et al.*, 2006).

Table III. 2. *C. albicans* strains used in this study.

Strain Name	Strain ID	Genotype	Parent	Reference
BWP17	BWP17	*ura3Δ::λimm434/ura3Δ:: λimm434 arg4::hisG/arg4::hisG his1::hisG/his1::hisG*	RM1000	(R. B. Wilson *et al.*, 1999)
	CJN523	*ura3Δ::λimm434/ura3Δ::λimm434 arg4::hisG/arg4::hisG his1::hisG/his1::hisG cas1::Tn7-UAU1/cas1::Tn7-URA3*	BWP17	(Nobile & Mitchell, 2005)
	CJN958	*ura3Δ::λimm434/ura3Δ::λimm434 arg4::hisG/arg4::hisG his1::hisG/his1::hisG cas4::Tn7-UAU1/cas4::Tn7-URA3*	BWP17	(Nobile & Mitchell, 2005)
	CJN432	*ura3Δ::λimm434/ura3Δ::λimm434 arg4::hisG/arg4::hisG his1::hisG/his1::hisG cas5::Tn7-UAU1/cas5::Tn7-URA3*	BWP17	(Nobile & Mitchell, 2005)
	CJN831	*ura3Δ::λimm434/ura3Δ::λimm434 arg4::hisG/arg4::hisG his1::hisG/his1::hisG fgr15::Tn7-UAU1/fgr15::Tn7-URA3*	BWP17	(Nobile & Mitchell, 2005)
	CJN863	*ura3Δ::λimm434/ura3Δ::λimm434 arg4::hisG/arg4::hisG his1::hisG/his1::hisG ada2::Tn7-UAU1/ada2::Tn7-URA3*	BWP17	(Nobile & Mitchell, 2005)
	BRY429	*ura3Δ::λimm434/ura3Δ::λimm434 arg4::hisG/arg4::hisG his1::hisG/his1::hisG rlm1::Tn7-UAU1/rlm1::Tn7-URA3*	BWP17	Unpublished
cas1ΔΔ	VIC1039	*cas1Δ::ARG4/cas1Δ::URA3 his1::hisG/his1::hisG*	BWP17	(Bruno *et al.*, 2006)
fgr15ΔΔ	VIC1045	*fgr15Δ::ARG4/fgr15Δ::URA3 his1::hisG/his1::hisG*	BWP17	(Bruno *et al.*, 2006)
ada2ΔΔ	VIC1057	*ada2Δ::ARG4/ada2Δ::URA3 his1::hisG/his1::hisG*	BWP17	(Bruno *et al.*, 2006)
cas5ΔΔ	VIC1075	*cas5Δ::ARG4/cas5Δ::URA3 his1::hisG/his1::hisG*	BWP17	(Bruno *et al.*, 2006)
rlm1ΔΔ	VIC1090	*rlm1Δ::ARG4/rlm1Δ::URA3 his1::hisG/his1::hisG*	BWP17	(Bruno *et al.*, 2006)
CAS1-Rev	VIC1039-REV4	*cas1Δ::ARG4/cas1Δ::URA3 pCAS1::HIS1::his1::hisG/his1::hisG*	VIC1039	This study
FGR15-Rev	VIC1045-REV1	*fgr15Δ::ARG4/fgr15Δ::URA3 pFGR15::HIS1::his1::hisG/his1::hisG*	VIC1045	This study
ADA2-Rev	VIC1197	*ada2Δ::ARG4/ada2Δ::URA3 pADA2::HIS1::his1::hisG/his1::hisG*	VIC1057	(Bruno *et al.*, 2006)
CAS5-Rev	VIC1190	*cas5Δ::ARG4/cas5Δ::URA3 pCAS5::HIS1::his1::hisG/his1::hisG*	VIC1075	(Bruno *et al.*, 2006)
RLM1-Rev	VIC1209	*rlm1Δ::ARG4/rlm1Δ::URA3 pRLM1::HIS1::his1::hisG/his1::hisG*	VIC1090	(Bruno *et al.*, 2006)
Cas5p-HA_3	CU6-2	*CAS5/CAS5-HA_3*	BWP17	This study
SC5314	SC5314	Wild type		(Gillum *et al.*, 1984)
cas5ΔΔ$_S$		*cas5Δ*::FRT/*cas5Δ*::FRT	SC5314	This study

As expected, the wild type BWP17 strain compromised the growth of *A. nidulans* (Figure 3.1A). The *ada2*ΔΔ mutant completely failed to inhibit *A. nidulans* growth as evidenced by the overlaying *A. nidulans* colonies, whereas co-culture with the remaining mutants revealed different levels of *A. nidulans* growth impairment, ranging from weak to strong impairment (Figure 3.1B). These results confirmed the data obtained with the transposon mutants. On the other hand, the co-culture assay performed with the revertant strains showed reduced *A. nidulans* growth as compared to the mutant strains, confirming that the observed phenotype can be attributed to the deletion of the corresponding gene (Figure 3.1C). Taken together, these results suggested that Ada2p, Cas5p, Fgr15p, Cas1p, and Rlm1p may regulate farnesol production.

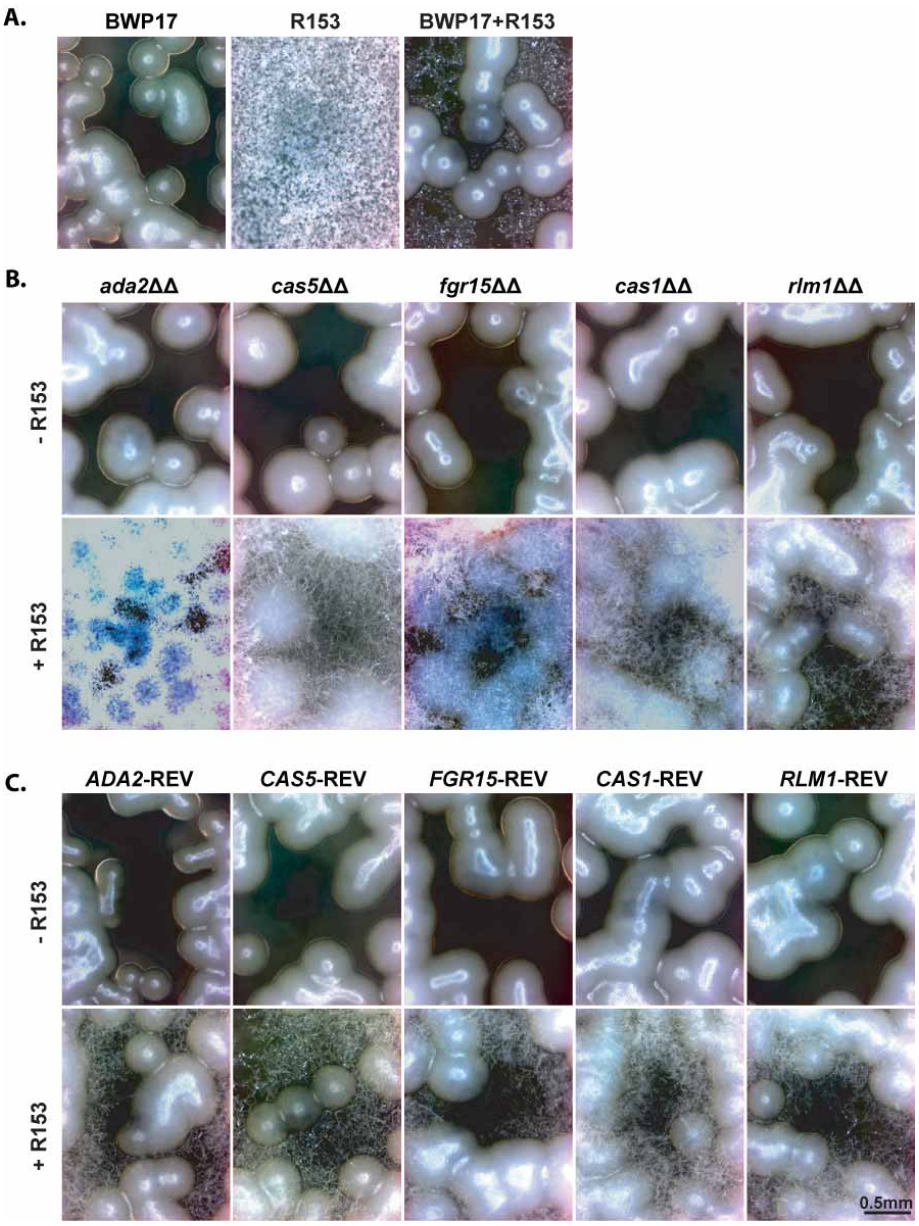

Figure 3.1. Macroscopic morphology of the *C. albicans* farnesol regulators mutants co-cultured with *A. nidulans*.

Colony morphologies of *C. albicans* and *A. nidulans* co-culture assays after 24 hrs of incubation on YPD plates at 30°C. **(A)** From left to right, colony morphology for *C. albicans* wild type strain BWP17, the *A. nidulans* R153 strain, and BWP17 co-cultured with R153. **(B)** *C. albicans* strains *ada2*ΔΔ, *cas5*ΔΔ, *fgr15*ΔΔ, *cas1*ΔΔ, and *rlm1*ΔΔ each co-cultured with or without the *A. nidulans* R153 strain, as indicated. **(C)** *C. albicans* strains *ADA2*-REV, *CAS5*-

REV*, FGR15*-REV*, CAS1*-REV*,* and *RLM1*-REV were each co-cultured with or without the *A. nidulans* R153 strain, as indicated.

3.3.2. The identified regulators are involved in farnesol biosynthesis

To determine whether the inability of these mutants to cause wild type levels of *A. nidulans* growth inhibition was really due to a defect in farnesol production, we quantified extracellular farnesol in the 5 TR mutants as well as their revertants by HPLC. The total amount of the extracted farnesol was normalized to the dry cell weight of the originating culture. The results showed that, under these conditions, BWP17 produced 0.06 mg of farnesol per g of dry cell weight, slightly less than farnesol amounts detected in some other wild type strains (Hornby & Nickerson, 2004), possibly owing to strain and growth conditions differences. In contrast, farnesol was undetectable in the *ada2*ΔΔ mutant, indicating that farnesol production in this mutant is strongly impaired. In addition, farnesol was reduced by 12-, 22-, 36-, and 52-folds in the *cas5*ΔΔ*, fgr15*ΔΔ, *cas1*ΔΔ*,* and *rlm1*ΔΔ mutants, respectively, as compared to the wild type control strain BWP17 (Figure 3.2A). On the other hand, a clear increase in farnesol production was observed in the revertant strains compared to the mutants (Figure 3.2A). These results correlate with the increased *A. nidulans* growth observed in the co-culture assay and demonstrate a reduction of extracellular farnesol levels produced by those 5 TR mutants.

To differentiate whether the reduction in extracellular farnesol was due to a defect in farnesol export or biosynthesis, intracellular farnesol was quantified from the same strains. Our results showed that intracellular levels of farnesol in the mutants were reduced almost to the same extent as observed for the extracellular farnesol, with *ada2*ΔΔ showing the most drastic impairment (undetectable farnesol level) (Figure 3.2B). Similarly, farnesol levels increased in the revertant strains. These data indicate that the reduced extracellular farnesol in those mutants can be attributed to a defect in the biosynthesis of farnesol rather than its export.

Collectively, these results indicate that the TRs Ada2p, Cas5p, Fgr15p, Cas1p, and Rlm1p regulate farnesol biosynthesis.

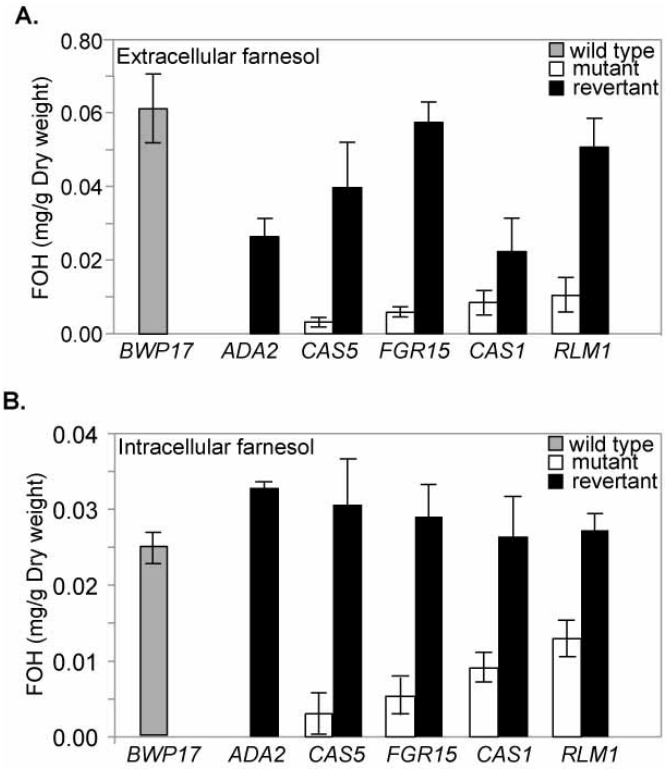

Figure 3.2 Quantification of extracellular and intracellular farnesol

Strains BWP17, *ada2*ΔΔ, *cas5*ΔΔ*, fgr15*ΔΔ*, cas1*ΔΔ*,* and *rlm1*ΔΔ as well as the revertant strains *ADA2*-REV, *CAS5*-REV*, FGR15*-REV*, CAS1*-REV*,* and *RLM1*-REV were grown to saturation for the extraction and quantification of **(A)** extracellular (n=4 for the wt and the mutant strains; n=3 for the revertant strains) as well as **(B)** intracellular farnesol production (n=3). Farnesol (in mg) was normalized to the dry cell weight (in g) of the originating culture (see materials and methods). Error bars represent standard deviation.

3.3.3. Investigation of fluconazole-induced extracellular farnesol production

To test whether fluconazole-induced farnesol production is affected in these TR mutants, BWP17, as well as the 5 TRs and their corresponding revertants, were grown for 24

hrs in YPD in the presence or absence of 1 µg/ml of fluconazole. Quantification of extracellular farnesol showed an 8-fold increase in farnesol levels in BWP17 when fluconazole was present in the medium. Whereas fluconazole was unable to induce the production of farnesol in the *ada2*ΔΔ mutant. On the other hand, fluconazole induced farnesol production by 33, 20, 4, and 2 folds in the *cas5*ΔΔ, *cas1*ΔΔ, *fgr15*ΔΔ, and *rlm1*ΔΔ mutants, respectively, when compared to the untreated controls (Figure 3.3). These data showed that some of the mutants are able to respond to fluconazole treatment better than others, suggesting that they may regulate farnesol production via different molecular mechanisms.

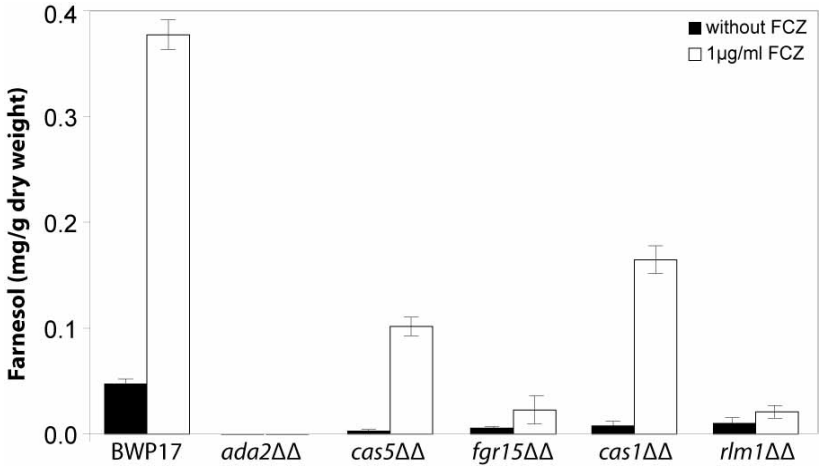

Figure 3.3. Quantification of farnesol production in response to fluconazole treatment. Extracellular farnesol was quantified from strains BWP17, *ada2*ΔΔ, *cas5*ΔΔ, *fgr15*ΔΔ, *cas1*ΔΔ, and *rlm1*ΔΔ grown to saturation in the presence or absence of 1 µg/ml fluconazole (FCZ). Farnesol (in mg) was normalized to the dry cell weight (in g) of the originating culture (see materials and methods). Error bars represent standard deviation (n=3).

3.3.4. Investigation of exogenous farnesol sensing

Since the 5 mutants were impaired in farnesol production and farnesol is necessary to block the yeast-to-filament transition, it was of interest to investigate the constitutive

filamentation status of these mutants. For that, the mutants as well as their respective revertants were grown in YPD to saturation for microscopic examination. Unlike the wild type strain BWP17, which grew as yeast cells, the *cas5*ΔΔ and *fgr15*ΔΔ mutants grew as a mix of hyphae and yeast cells, suggesting that the levels of extracellular farnesol produced by these mutants are not sufficient to completely inhibit filamentous growth (Figure 3.4). This observation is in line with the results of published large-scale screens showing that *cas5*ΔΔ and *fgr15*ΔΔ (Filamentous Growth Regulator 15) mutants display enhanced filamentation (Homann *et al.*, 2009; Uhl *et al.*, 2003). Conversely, the *cas1*ΔΔ and *rlm1*ΔΔ mutants grew as yeast cells, possibly because the levels of extracellular farnesol produced by these cells are high enough to inhibit filamentation. Interestingly, the *ada2*ΔΔ mutant, that does not produce farnesol, grew also as yeast cells, compatible with its reported afilamentous phenotype in Spider medium (Pukkila-Worley *et al.*, 2009). We observed that the *ada2*ΔΔ cells formed large aggregates, seemingly due to a defect in cell septation (Figure 3.4). All the revertant strains grew exclusively as yeast, like the wild type control. Therefore, it seems that the residual farnesol produced by some of these mutants can still achieve repression of the filamentation in rich medium at high cell density.

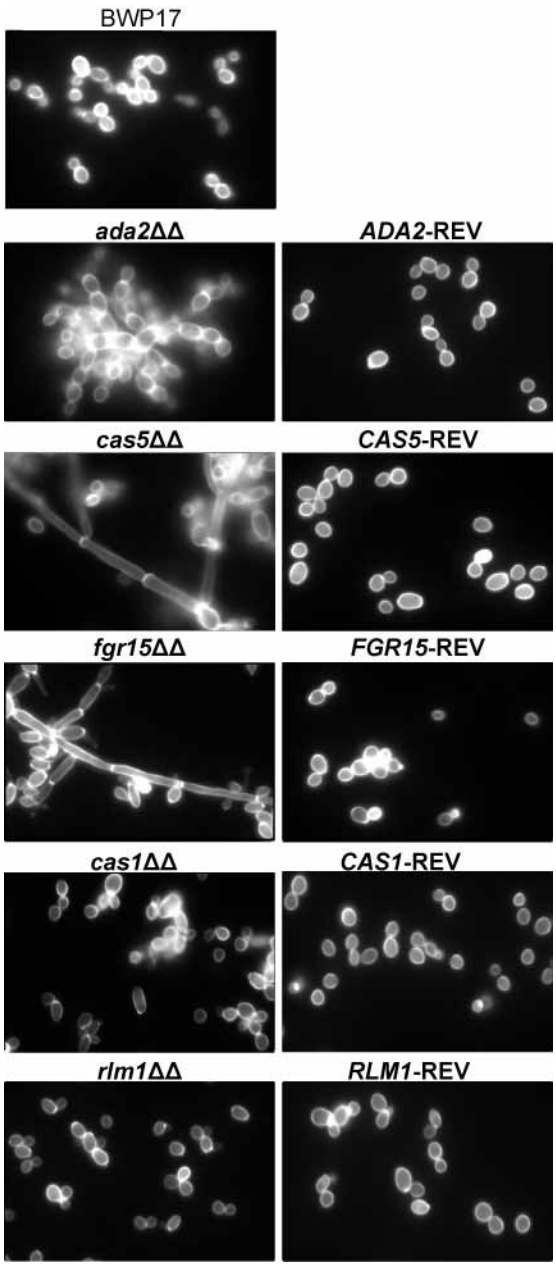

Figure 3.4. Microscopic characterization of the farnesol regulators mutants
Strains BWP17, *ada2ΔΔ*, *cas5ΔΔ, fgr15ΔΔ, cas1ΔΔ,* and *rlm1ΔΔ* were grown to saturation in YPD and stained with calcofluor white for microscopic visualization.

To determine whether farnesol production is linked to farnesol sensing, the mutants as well as their respective revertants were grown overnight in the filament-inducing medium R2A (Ross J, 2010), in the absence or presence of a high concentration of exogenous farnesol. All

strains grew exclusively as hyphae in the R2A medium, indicating that the 5 regulators are not required for filamentation under this condition (Figure 3.5). On the other hand, filamentation was abrogated by farnesol in the wild type strain and in the *ada2*ΔΔ, *cas5*ΔΔ, and *cas1*ΔΔ mutants, indicating that these strains are still able to respond to farnesol. The *fgr15*ΔΔ mutant grew exclusively as hyphae. As mentioned earlier, the *fgr15*ΔΔ mutant is already constitutively filamentous which may explain its unresponsiveness to farnesol, having already passed the commitment step beyond which farnesol is no longer effective (Nickerson *et al.*, 2006). The *rlm1*ΔΔ grew as a mix of hyphae, pseudohyphae and yeast cells, indicating that this mutant has a decreased ability to respond to exogenous farnesol, consistent with previously reported observations (Langford *et al.*, 2013). These data indicate that Rlm1p may regulate farnesol sensing under certain conditions.

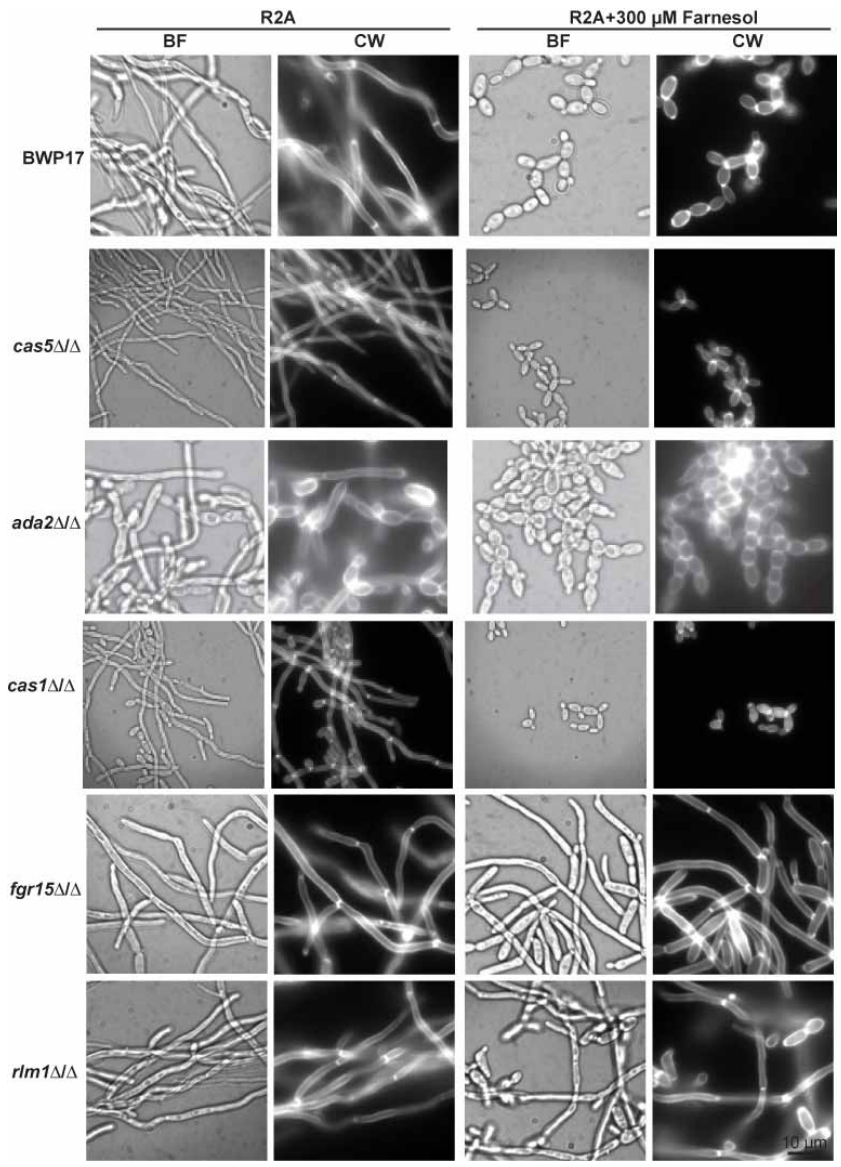

Figure 3.5. Analysis of cellular morphology in response to exogenous farnesol.
Strains BWP17, *ada2*ΔΔ, *cas5*ΔΔ, *fgr15*ΔΔ, *cas1*ΔΔ, and *rlm1*ΔΔ were grown to saturation in R2A medium (to induce filamentation) in the presence or absence of 300 µM of farnesol. Shown are microscopic morphologies of calcofluor white-stained cells in bright field (BF) and under fluorescent excitation (CW).

3.3.5. Identification of the Cas5p regulon

Cas5p was chosen for further investigation because *cas5*ΔΔ was one of the most affected mutants and also because of its role in important biological processes such as virulence as well as echinocadin and azole resistance (Bruno *et al.*, 2006; Chamilos *et al.*, 2009; Pukkila-Worley *et al.*, 2009; Vasicek *et al.*, 2014). To understand how Cas5p may regulate farnesol biosynthesis, we sought to identify its regulon, using a ChIP-chip assay to identify all the Cas5p-bound genes. For this, a tagged Cas5p-HA_3 strain was constructed and analyzed by Western blotting by growing the cells in YPD at 30°C at a starting OD of 0.1 and harvesting them at different time points (Figure 3.6). This experiment showed that the Cas5p-HA_3 protein is most abundant at low cell density and decreases with time.

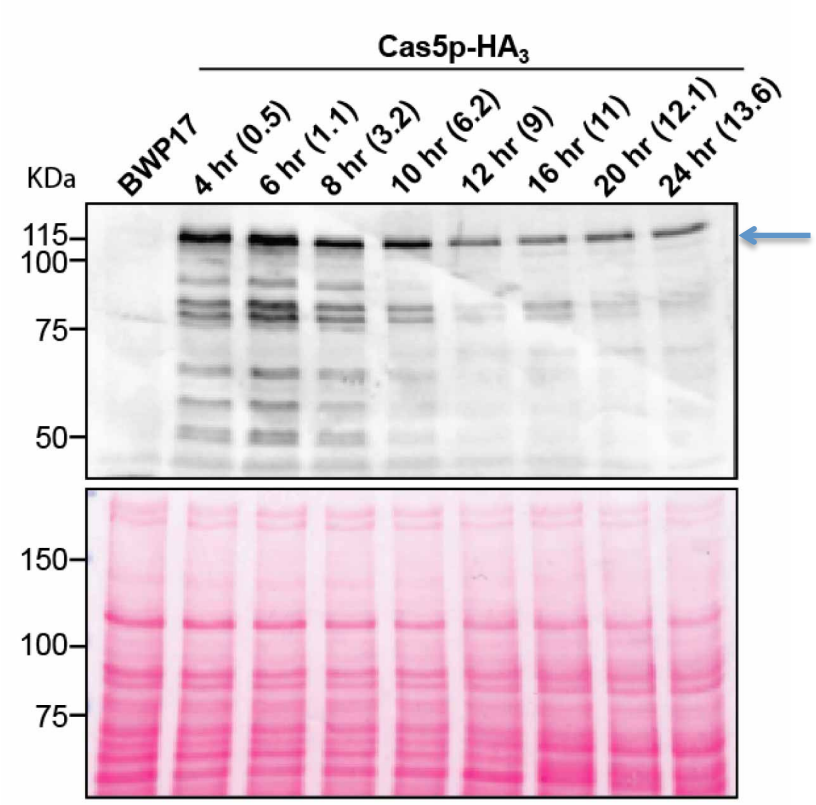

Figure 3.6. Western blot analysis of Cas5p-HA_3 at different cell densities.
Protein extracts from strains BWP17 and Cas5p-HA_3 harvested at the indicated time points after dilution (corresponding OD_{600} are indicated between parenthesis) were analyzed by

Western blotting using an anti-HA monoclonal antibody. The position of the molecular weight markers is indicated on the left. The Cas5p-HA_3 protein is indicated by the arrow. Additional Cas5p-specific faster migrating bands are also detected in the lanes corresponding to the tagged protein but not in the untagged control (BWP17), probably due to protein degradation (Figure 3.6). Ponceau S staining is shown (bottom panel) as a protein loading and transfer control.

For the ChIp-Chip assay, the tagged Cas5p-HA_3 strain and untagged BWP17 control cells were grown in rich medium at 30ºC, and harvested at early log phase (optical density OD_{600} of 0.7. DNA was crosslinked, immunoprecipitated, labeled and hybridized to *C. albicans* whole-genome NimbleGen™ tiling arrays (Srikantha *et al.*, 2006). Mapping of the signal intensities to an in-house genome browser revealed that, unlike typical transcription factors, Cas5p binds to the majority of its targets within their coding region, suggesting an association with the chromatin or transcriptional machinery rather than direct DNA binding at these loci (Figure 3.7A). The ChIP-Chip results identified binding of Cas5p to 233 genes, with an enrichment ratio ≥ 1.5 fold and a *p*-value ≤ 0.01 (Supplementary table III.3-A). GO term analysis by biological process and a significance cut-off at a *p*-value ≤ 0.01, identified 82 functional categories (Supplementary table III.3-B), the most significant ones including “pyruvate metabolism” (16 genes; *p*-value = 1.25E-14), “carbohydrate catabolism” (21 genes; *p*-value = 3.58E-14), “coenzyme metabolism” (20 genes; *p*-value = 1.27E-10), and “pyridine-containing compound metabolism” (19 genes; p-value = 3.36E-10). Interestingly, among the GO terms retrieved were also the categories pertaining to the “generation of precursor metabolites and energy” (23 genes; *p*-value = 1.48E-07), “cofactor metabolism” (23 genes; *p*-value = 2.98E-06), “response to oxidative stress” (31 genes; *p*-value = 8.08E-06), “monosaccharide transport” (9 genes; *p*-value = 6.60E-04), and “NADH metabolism” (5 genes; *p*-value = 5.12E-03) (Fig 7B). Cas5-p was also bound to genes encoding glucose transporters including many members of the *HGT* family such as *HGT1, HGT2, HGT6,* but also genes encoding kinases involved in glucose transport such as *SHA3* and *HXK2.* Furthermore, genes coding for transcription factors involved in the regulation of glycolysis were also enriched for Cas5p binding such as *TYE7*, *GAL4*, and *MIG1*, suggesting a role for Cas5p in

carbon assimilation and metabolism. In addition, Cas5-p was also enriched at genes involved in the generation of precursor molecules pertaining to many different pathways such as *NDE1* (putative NADH-dehydrogenase), *ENO1* (enolase), *TDH3* (NAD-linked glyceraldehyde-3-phosphate dehydrogenase), *ACH1* (acetyl-coA hydrolase), *OLE1* (stearoyl-CoA desaturase), and *FDH3* (formaldehyde dehydrogenase). Collectively, these data indicate that Cas5p is involved in the regulation of energy generation, more particularly in carbon acquisition and metabolism.

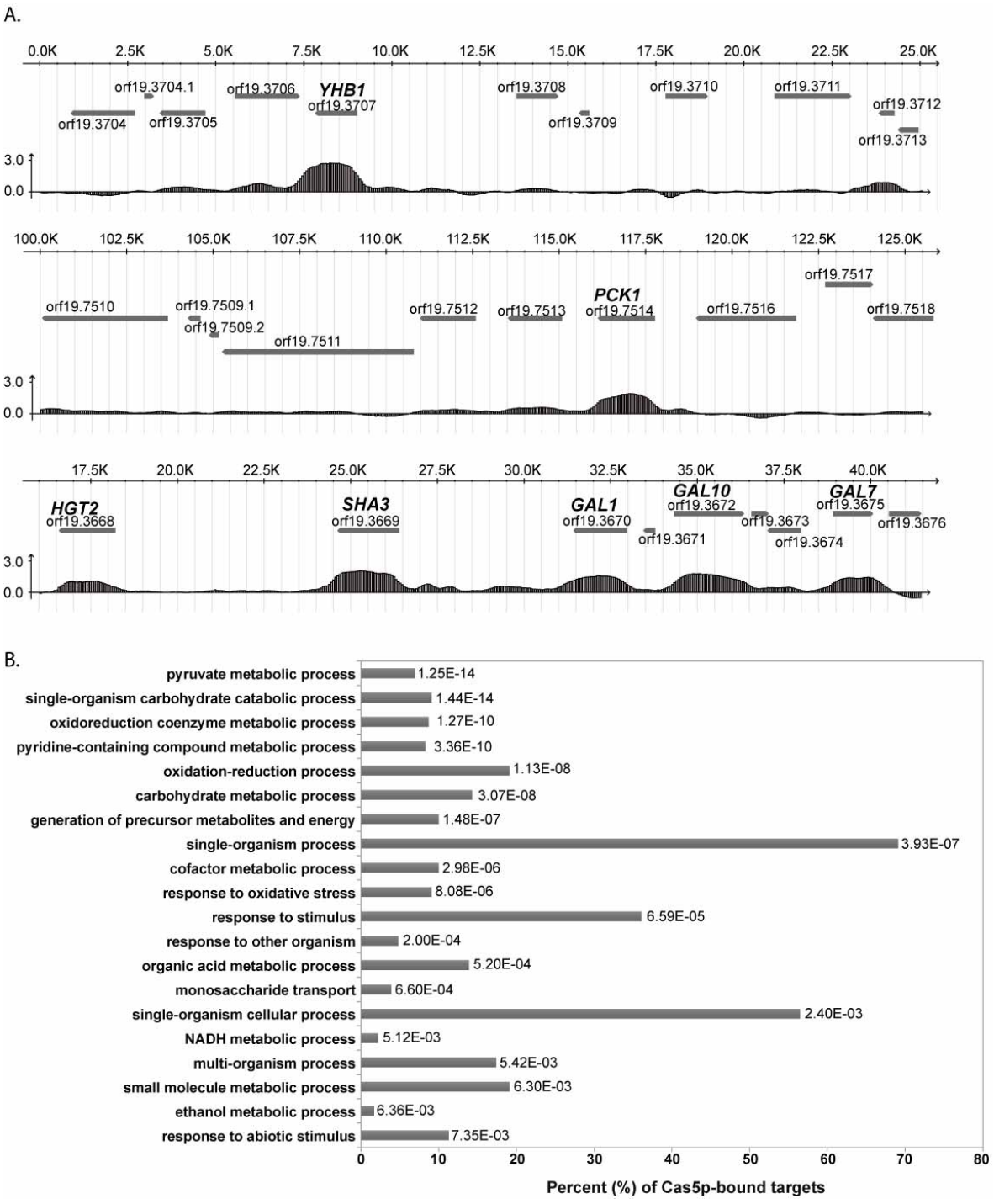

Figure 3.7. Cas5p location profile and Gene Ontology (GO) enrichment analysis for Cas5p bound genes.

(A) Cas5p location profile at selected target genes. Mapping of the ChIP-Chip hits to a *Candia albicans* assembly 19-based in-house genome browser. The x-axis represents the corresponding genomic positions, and the y-axis represents $\log_2$-transformed signal

intensities (n=3) illustrating Cas5p enrichment at the target genes *YHB1* and *PCK1,* as well as target genes within the *GAL* locus, namely, *HGT2*, *SHA3*, *GAL1, GAL10* and *GAL7.* Tiles represent the $\log_2$ pseudo-median signal intensities collected from each of the probes spanning the Watson and Crick strands on the tiling array. Arrows represent ORF orientation on the corresponding strand. **(B)** Top 20 GO terms for targets bound by Cas5p based on REVIGO mother term sorting (Supek *et al.*, 2011). The x-axis represents the percent of Cas5p target genes assigned to a specific term. Corresponding adjusted p-values are indicated next to each bar.

To determine the role of Cas5p in regulating gene expression, a *CAS5* deletion mutant (*cas5*$\Delta\Delta_S$) devoid of auxotrophies was generated from the SC5314 wild-type strain using the dominant selectable marker *SAT1* (Reuss *et al.*, 2004) and used for genome-wide expression profiling analysis. Briefly, strains SC5314 and *cas5*$\Delta\Delta_S$ were grown in YPD medium and harvested at low cell density (OD_{600} of 0.7) and high cell density (OD_{600} of 13-14), two conditions used for the ChIP-chip and farnesol quantification assays, respectively. Total RNA was extracted, converted to cDNA and hybridized to custom *C. albicans* GE Microarray (Synnott *et al.*, 2010). We found that, at low cell density, very few genes were modulated (19 upregulated and 8 downregulated genes; ≥ 1.5 fold; p-value ≤ 0.01; Supplementary table III.4-A) to which no significant GO term enrichment could be associated but which included genes encoding GPI-linked proteins (*PGA31*, *RBR1*, *PGA26*, *PGA6*) and adhesin (*ALS3*). At high cell density, 840 genes were modulated (579 upregulated and 261 downregulated genes; ≥ 1.5 fold; p-value ≤ 0.01; Supplementary table III.4-B), suggesting that Cas5p may be more active at regulating gene expression at high cell density (directly or indirectly). GO term analysis revealed downregulation in the mutant of many metabolic processes such as lipid modification (13 genes; *p*-value = 8.80E-8), lipid catabolism (15 genes; *p*-value = 1.07E-7), peroxisome organization (12 genes; *p*-value = 1.50E-4), arginine metabolism (6 genes; *p*-value = 1.83E-3), carbohydrate transport (9 genes; *p*-value = 6.67E-3), and monosaccharide

catabolism (6 genes; *p*-value = 8.97E-3) (Figure 3.8 and Supplementary table III.4-C). On the other hand, there was an upregulation of ribosome biogenesis (154 genes; *p*-value = 3.21E-84), organic cyclic compound metabolism (239 genes; *p*-value = 1.82E-28), nitrogen compound metabolism (256 genes; *p*-value = 1.02E-27), primary metabolism (368 genes; *p*-value = 6.69E-26), and DNA strand elongation involved in DNA replication (13 genes; *p*-value = 2.70E-4) (Figure 3.8 and Supplementary table III.4-C). Visual inspection of the list of modulated genes revealed downregulation of genes encoding proteins involved in glucose transport (*HGT2*, *HGT10*, *HGT13*, *HGT17*, *HGT19*, *HXT5*) and galactose metabolism (*GAL1, GAL10, GAL7*) as well as the *STD1* gene encoding a putative transcription factor involved in the control of glucose-regulated gene expression (Sexton *et al.*, 2007). Collectively, these data show that Cas5p is involved in the regulation of many cellular pathways, with a clear positive involvement in energy metabolism, more specifically in lipid and carbon metabolism and acquisition, which could explain the farnesol biosynthesis defect of the *cas5*ΔΔ mutant (see Discussion).

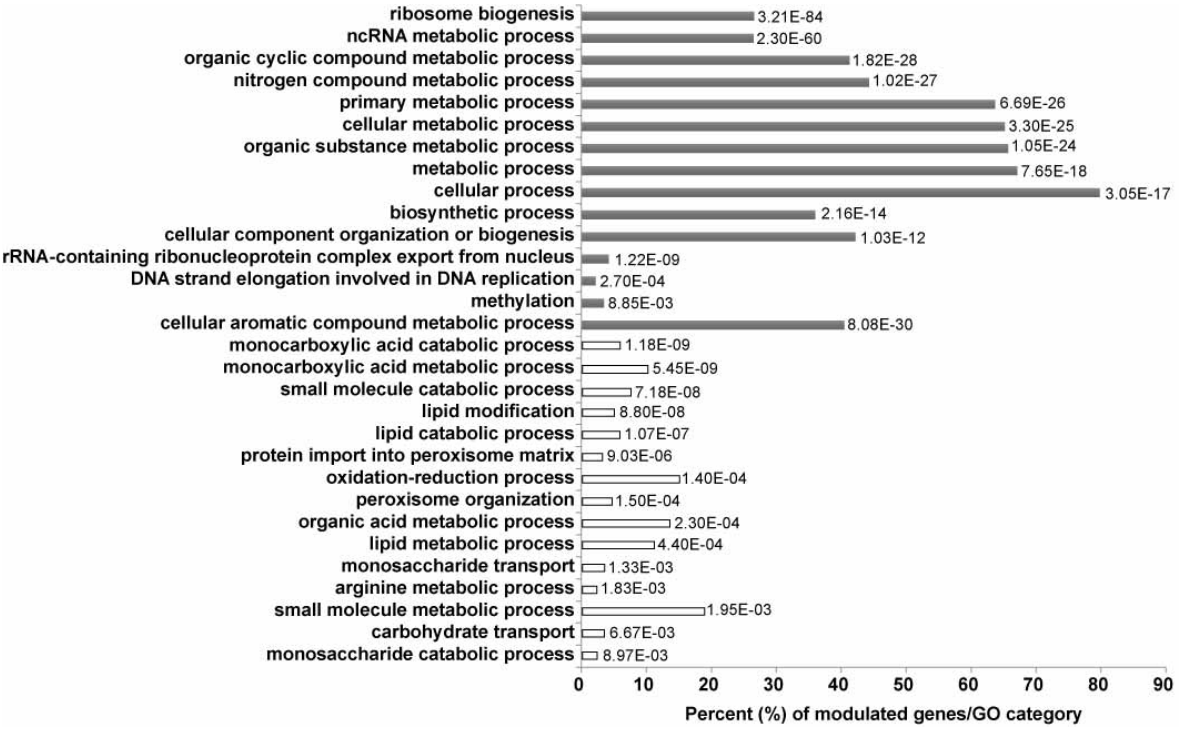

Figure 3.8. Gene Ontology (GO) enrichment analysis for Cas5p modulated genes
Process GO term analysis illustrating the top 20 overrepresented GO categories for the Cas5p modulated genes based on REVIGO mother term sorting (Supek F, 2011). The x-axis represents the percent of Cas5p target genes assigned to a specific term. Grey bars represent upregulated terms, white bar represents downregulated terms. Corresponding adjusted p-values are indicated next to each bar.

3.4. Discussion

3.4.1. Identification of a genetic screen as readout of farnesol production

In this study, we have established and validated a genetic screen to identify transcriptional regulators involved in farnesol production, based on the finding that farnesol produced by *C. albicans* induces apoptosis in *A. nidulans* (Semighini *et al.*, 2006). This allowed the identification of 5 transcriptional regulators, Ada2p, Cas5p, Fgr15p, Cas1p, Rlm1p that are involved in the biosynthesis of farnesol (Figure 3.1). Extracellular and

intracellular farnesol quantification by HPLC confirmed the decreased levels of farnesol in those mutants (Figure 3.2). Therefore, this screen can serve as a useful tool to identify mutants that are defective in farnesol production. Furthermore, such a screen can be adapted and automated to screen additional libraries of mutants to identify potential transporters, kinases, or even enzymes and chromatin modulators involved in farnesol production. This will help uncovering new mechanisms relevant to the physiology and regulation of farnesol production.

3.4.2. Regulators of farnesol production may operate via different mechanisms

Based on the results of the phenotypic assays, some of these TRs can be clustered together. For example, the mutants *ada2*ΔΔ and *cas5*ΔΔ can be clustered together because they display the most defects with regards to the levels of farnesol they produce as shown by co-culture and HPLC assays. Also, these mutants show the strongest susceptibility to caspofungin (25 ng/ml) and a drastic gene expression defect with regards to regulation of the core caspofungin responsive genes (Bruno *et al.*, 2006). In addition, they also respond to exogenous farnesol by inhibiting filamentous growth. Similarly, the mutants *fgr15*ΔΔ and *rlm1*ΔΔ can be clustered together because they display the least defects with regards to levels of farnesol and they are both the least responsive to the addition of exogenous farnesol. These mutants also showed slight sensitivity to caspofungin (25 ng/ml) (Bruno *et al.*, 2006). On the other hand, the *cas1*ΔΔ mutant appears to have an intermediate phenotype between the two clusters of regulators. The *cas1*ΔΔ mutant is among the least impaired in farnesol levels and the least sensitivity to caspofungin (Bruno *et al.*, 2006), but retains responsiveness to exogenous farnesol treatment. Finally, it seems that farnesol biosynthesis is a multifactorial process. It is plausible that these regulators mediate farnesol production via distinct mechanisms. Given that the production of farnesol from the ergosterol pathway is under the

action of the enzymes Dpp2p and Dpp3p (Navarathna, Hornby*, et al.*, 2007; Nickerson *et al.*, 2006), we have checked our profiling data for modulation of *DPP2* and *DPP3* expression levels. We have found that none of those two genes was modulated under these conditions. This observation implies that a defect (if any) of farnesol biosynthesis potentially caused by these enzymes would be at a translational or post-translational modification level. Therefore, an examination of Dpp2p and Dpp3p enzymatic activity would give us an insight into the functionality of these enzymes in the farnesol defective mutants. Enzymatic activity can be tested by using protein extracts from the farnesol deficient mutants and purification of the enzymes Dpp2p and Dpp3p. The purified enzymes can then be used in enzymatic assays in presence of the labeled substrate farnesyl pyrophosphate. The products of the reactions can then be analyzed by thin-layer chromatography as previously described (W. I. Wu *et al.*, 1996).

3.4.3. Identification of Cas5p biological functions

To gain insight into the mechanism of farnesol biosynthesis, one TR was chosen for detailed inspection. The mutant *ada2*ΔΔ had the most drastic effect with regards to farnesol production, but since Ada2p is a chromatin regulator, its deregulation is expected to affect many pathways. The next most affected mutant was *cas5*ΔΔ*,* hence hinting to an important role for Cas5p in the farnesol biosynthesis pathway. A genomic approach to determine the bound and modulated targets of Cas5p was used to identify the targets that mediate the farnesol biosynthesis defect of the *cas5*ΔΔ mutant. We have found that Cas5p binds to genes involved in carbohydrate metabolism, mainly glycolytic genes. We have also shown that Cas5p upregulates genes involved in fatty acid oxidation and carbohydrate catabolism, reflecting a role in energy production. Consistent with its reported role in cell wall stress response, deletion of *CAS5* resulted in an upregulation of PGA family genes (*PGA10, PGA13, PGA30, PGA45*), as well as cell wall biogenesis genes (*CHS2, CHS3, PMI1,* and *PMM1)* (Bruno *et al.*, 2006). On the other hand, Cas5p binds and downregulates genes involved in cell

adhesion such as *TEC1, ALS1, DEF1,* which is reflective of a change in cell wall properties. Furthermore, the absence of a functional Cas5p caused the upregulation of the genes *SOD3, SOD5* and *RHR2*, possibly due to an adaptive response to osmotic stress following the cell wall defect. Interestingly, there was an upregulation of many genes associated with ribosome biogenesis (*RPS21, SSF1, HAS1*) in the *cas5*ΔΔ mutant reflecting an uncontrolled energy expenditure on a process that is ought to be downregulated at high cell density (Warner JR, 1999). Accordingly, it seems that Cas5p is involved in the regulation of many pathways with a clear involvement in carbon metabolism, which could explain the farnesol deficient phenotype.

3.4.4. Farnesol biosynthesis is linked to carbon metabolism

The genomic analysis of the Cas5p regulon in combination with the genomic data available in the literature about Ada2p (location profile) and Rlm1p (expression profile) helped to further reveal a strong connection among 3 of the identified farnesol regulators. A large number of Cas5p targets involved in carbon metabolism and glycolysis were also bound by Ada2p (Sellam, Askew*, et al.*, 2009). It has also been shown that a large number of caspofungin-responsive genes that are dependent on Cas5p, were also dependent on Ada2p implying that the co-recruitment of the 2 TRs may be needed for the activation of common target genes (Bruno *et al.*, 2006). This comes in support for the fact that *ada2*ΔΔ*,* and *cas5*ΔΔ had almost the same phenotype in our assays. Furthermore, *GAL4,* encoding the regulator of glycolytic genes was bound by Cas5p and Ada2p and regulated by Rlm1p (Delgado-Silva *et al.*, 2014), indicating that these TFs have a tight control over the glycolytic pathway. Similarly to what was reported for *RLM1* deletion, *CAS5* deletion caused an upregulation of genes involved in the use of alternative carbon sources (*GCV2, RMS1*), indicating that alternative sources, rather than glucose, are used as the main carbon source in those mutants. In addition, the *GAL* genes *GAL1, GAL10, GAL7* were bound by Cas5p and modulated by both Cas5p (at high cell density) and Rlm1p (Delgado-Silva *et al.*, 2014). Furthermore, we have found that Cas5p also downregulates the gene *IDI1*, whose ortholog(s) play a role in the biosynthesis of farnesyl diphosphate, a precursor of

sesquiterpenes. Interestingly, it also happens that Rlm1p downregulates *IDI1* (Delgado-Silva *et al.*, 2014), which is inline with their role in farnesol biosynthesis. Therefore, it seems that the TRs that regulate farnesol biosynthesis also regulate carbon metabolism. Interestingly, it appears that Cas5p also regulates genes involved in lipid metabolism, glucose uptake, energy source and acetyl-CoA. Therefore, since those TFs regulate both farnesol production and central carbon metabolism, and since farnesol is a carbon-rich molecule, then farnesol may be regarded as a metabolic product serving as a signalling molecule, which carries a metabolic message relayed to surrounding cells through quorum sensing. Therefore, farnesol-mediated quorum sensing may be the readout of the cellular glycolytic activity reflecting energy levels and its production.

3.5. Conclusion

In conclusion, the literature has provided evidence for a link between cell wall biogenesis and carbohydrate metabolism. Here we suggest the possibility of a link between those two processes with farnesol biosynthesis, whereby the flow of carbon within *C.albicans* metabolic system is translated into farnesol production. Farnesol is in turn sensed by the neighbouring biomass as an indicator of carbon abundance in the surrounding medium. Further studies in this area should shed more light on the exact mechanism whereby cells achieve the co-regulation of these complex processes.

3.6. Materials And Methods

3.6.1. *C. albicans* strains and culture conditions

All strains used in this study are listed in Table III.2 and Supplementary table III.1. Strains were routinely grown at 30°C in YPD medium containing 1% yeast extract (EMD Biosciences, Darmstadt, Germany), 2% Bacto peptone (BD Biosciences, Sparks, MD), and 2% glucose (Sigma, St. Louis, MO). For solid medium, 2% agar (Difco, BD) was added. Complementation

of strains *cas1*ΔΔ and *fgr15*ΔΔ was mainly carried out as described in Bruno et al. (Bruno *et al.*, 2006).

3.6.2. *C. albicans* transformation

C. albicans transformations were performed by electroporation (Reubb O, 2004) using the GenePulserII system (Bio-Rad) and 0.2 cm gap cuvettes (electric pulse of 1.8 kV, 25 µF and 200 Ω). Transformed *C. albicans* cells were washed once with 800 µl of 1 M sorbitol, resuspended in 200 µl of the selective synthetic medium lacking histidine (0.67% nitrogen base, 2% glucose, and 0.2% amino acid mix without histidine), and then plated on the same synthetic solid medium for histidine prototrophy selection. The Ura+ transformants were grown in synthetic complete (SC) medium lacking uracil (SC-ura) (Sherman F, 1991), or in SC medium lacking uracil and containing 0.1% 5-fluoro-orotic acid (Toronto Research Chemicals Inc., North York, ON, Canada) and 0.005% uridine (Sigma, St. Louis, MO) (Boeke *et al.*, 1984).

3.6.3. Co-culture assay and microscopic analysis

A spore suspension (25 µl) from the *A. nidulans* R153 strain at a concentration of $8x10^5$ was mixed with 25 µl of *C. albicans* cells at an OD_{600} of 0.1, then plated on 55mm- YPD plates and incubated at 30°C for 24 h. An equivalent concentration of *C. albicans* cells was mixed with 25 µl of sterile water and plated similarly as a negative control. Microscopic examination was done using a LEICA MZ FLIII fluorescence stereomicroscope equipped with a dark field and 100x magnification. Pictures were acquired with a Canon Micropublisher camera. Assays were repeated independently for 2-4 times.

3.6.4. Extraction of extracellular and intracellular farnesol

Extracellular and intracellular farnesol were extracted as previously described in Hornby et al, and Navarathna et al, respectively (Hornby *et al.*, 2001; Navarathna *et al.*, 2005) with minor

modifications as described below. *C. albicans* strains were inoculated in 200 ml of liquid YPD medium at an OD_{600} of 0.01, and then incubated at 30°C for 24 h (250 rpm). Cells from 100 ml of culture were harvested at 4°C by centrifugation at 3500 rpm for 10 min to determine the dry weight, which will be used to normalize the farnesol concentration. The remaining 100-ml culture was centrifuged similarly to separate the cells and the supernatant, which will then be used to measure the intracellular and extracellular farnesol, respectively. To measure intracellular farnesol, cells were washed with 50 ml of sterile water and resuspended in 5 of ml sterile water. Cell suspensions were frozen in liquid nitrogen and disrupted with a Freezer Mill (SPEX CetriPrep, Metuchen, NJ) as previously described (Tsao *et al.*, 2009). Cell breakage was greater than 96% as determined by CFU (colony forming unit) on YPD plate. The supernatant containing the intracellular farnesol was separated from cell debris at 4°C by centrifugation at 4500 rpm for 5 min. Intracellular farnesol was subsequently extracted by adding 5 ml of ethyl acetate and vortexing for 5 min. The organic supernatant was collected at 4°C by centrifugation at 5000 rpm for 30 min then evaporated at 35°C. The resulting residues were suspended in 200 µl of 4:1 methanol-H_2O mixture and filtered (0.45 µm- pore-size nylon membrane filter) for analysis by HPLC and/or GC/MS. Results represent the average of three independent experiments. To measure extracellular farnesol, supernatant from the 100 ml-culture was filtered (0.45 µm-pore-size sterile syringe filter) and farnesol was extracted by vigorous shaking with 25 ml of ethyl acetate. The sample was then dehydrated by anhydrous sodium sulfate and evaporated at 35°C. The resulting residues were suspended in 200 µl of 4:1 methanol-H_2O mixture and filtered (0.45 µm- pore-size nylon membrane filter) for analysis by HPLC and/or GC/MS. Results represent the average of four independent experiments except for the revertant strains where results represent the average of three independent experiments. The concentration of farnesol is expressed as mg of

farnesol normalized to the dry cell weight of the originating culture, hence the unit “mg/g dry weight”.

3.6.5. HPLC and GC/MS

High-performance liquid chromatography (HPLC) analysis employed a Waters (Milford, Mass.) pump model 510 and a Waters Tunnable Absorbance Detector model 486. Data were analyzed using ChemStation for LC systems vB.04.01 SP1 software (Agilent Technologies). A 1.8 µm ZORBAX SB-C18 column (4.6x20 mm) was used. Standard concentrations ranged from 0.05 mg/ml to 1 mg/ml farnesol. Gas chromatography-mass spectrometry (GC/MS) was occasionally used to confirm farnesol detection. Data were analyzed using the same software mentioned above.

3.6.6. Fluconazole treatment

Cells were diluted to a final OD_{600} of 0.01 in 100 ml of YPD medium in the presence or absence of 1µg/ml of fluconazole (Sigma). Cells were harvested after incubation at 30ºC for 24hrs. Extraction of extracellular farnesol was carried out as described above.

3.6.7. Filamentation assays and microscopic analysis

To induce hyphal growth, strains were grown in R2A medium which was prepared according to Reasoner and Geldreich (Reasoner DJ, 2009) by mixing 0.05% yeast extract, 0.05% Bacto proteose peptone (BD Biosciences, Sparks, MD), 0.05% casamino acids (Difco, Sparks, MD), 0.05% glucose, 0.05% soluble starch, 0.03% K_2HPO_4 (Fisher Scientific, Fair Lawn, NJ), 0.005% $MgSO_4 \cdot 7H_2O$ (Fisher Scientific, Fair Lawn, NJ), and 0.03% sodium pyruvate (Life Technologies, Grand Island, NY). *C. albicans* cells were diluted to a final OD_{600} of 10^{-4} in R2A medium in the presence or absence of 300 µM exogenous farnesol (Sigma), and incubated at 37°C overnight. Cells were subsequently stained with calcofluor white (Fluorescent Brightener 28, Sigma) at a final concentration of 1 µg/ml for microscopic

examination using a Zeiss Axio-Imager Z1 microscope equipped with a DAPI filter and 630x magnification. Images were acquired with the Axiocam

3.6.8. Construction of an Cas5p-HA3 tagged strain

An *CAS5*-tagging cassette was amplified from plasmid pCaMPY-3×HA (Liu *et al.*, 2007) using primers MR2549 and MR2550 (Supplementary table III.2). These primers contain homologous sequences to the *CAS5* C-terminus as well as specific sequences within pCaMPY-3×HA vector as described previously (Schneider BL, 1995). The resulting fragment (1,893 bp), containing 120 bp of sequences homologous to the terminal sequences of the *CAS5* ORF (except for the stop codon), the *C. albicans URA3* marker flanked by direct repeats of the 3×HA epitope-encoding sequences and 120 bp of sequences homologous to the 3' untranslated region of the *CAS5* gene, was used to transform strain BWP17. Transformations were conducted using a modified standard lithium acetate procedure as described previously (MacPherson *et al.*, 2005). The transformed cells were plated on SD-ura plates and incubated for 3 days at 30°C to select for integrants of the tagging cassette. Counterselection of the *URA3* gene in these clones was carried out on plates containing 5-FOA as descibed previously (Boeke *et al.*, 1984). Loop-out of the *URA3* marker, allows the chromosomal expression at a normal level without interference with the transcription of the 3'UTR. DNA sequencing was performed to confirm the in-frame integration of the tagging cassette and to ensure the absence of unintended mutations.

3.6.9. Protein extraction and Western blot analysis

Total protein extracts of *C. albicans* cells were prepared as follows. Overnight cultures were diluted into fresh YPD medium to an OD_{600} of 0.1 and incubated at 30°C. Cells (20 OD) were harvested at the indicated times. Cell pellets were resuspended in 150 µl of extraction buffer (10 mM Tris-HCl pH7.5; 400 mM NaCl; 10% glycerol; 1 mM sodium orthovanadate; 50 mM

sodium fluoride; 50 mM sodium β-glycerophosphate; 10 mM β-mercaptoethanol; 1 μM MG132 and protease inibitors; 1 mM phenylmethylsulfonyl fluoride; leupeptin, pepstatin, and aprotinin at 5 μg/ml each), then frozen in liquid nitrogen and stored at -80°C. For protein extraction, 100 μl of ice-cold glass beads were and cells were broken by vortexing five successive cycles of 1 min each, separate by 1-min breaks. Total proteins were recovered by centrifugation at 5000 rpm for 30 sec at 4°C. Protein concentrations were determined with the micro-BCA protein assay kit (Pierce, Rockford, IL). Total protein extracts (50 μg) were separated by low-bis SDS-PAGE (8% acrylamide, 150:1 acrylamide/bisacrylamide ratio); which was either stained with Coomassie or transferred to a nitrocellulose membrane with a Trans Blot SD semi-dry transfer apparatus (Bio-Rad). The membrane was stained with Ponceau reagent (0.1% Ponceau S in 5% acetic acid) prior to immunodetection. A mouse anti-HA monoclonal antibody (1:1000 dilution; Santa Cruz Biotech) was used for the immunodetection of Cas5p-HA_3. The protein was subsequently detected using the ECL chemiluminescence kit (SuperSignal chemiluminescennt substrate, Pierce, Rockford, IL). The experiment was repeated five times.

3.6.10. ChIP-on-chip and data analysis

Three independent cultures (50 mL each) of strains BWP17 (untagged) and Cas5p-HA_3 (tagged) were grown in YPD medium at 30ºC to an OD_{600} of 0.7. The subsequent steps of DNA crosslinking, DNA shearing, ChIP, and DNA labeling with Cy dyes were conducted as described previously(Znaidi *et al.*, 2009). Labeled DNA from the tagged strain (Cas5p-HA_3, Cy5-labeled) and the corresponding untagged control strain (BWP17, Cy3-labeled) were mixed and hybridized to *C. albicans* whole-genome tiled-oligonucleotide DNA microarray based on assembly 19 (n = 3) (Srikantha *et al.*, 2006). Hybridization, General Feature Format (GFF) reports acquisition and TileScope analysis were done as previously described (Khayat A, unpublished). Peak-finding (i.e. Cas5p binding sites) was performed using the following

criteria: pseudo-median signal threshold of ≥ 1.5-fold and p-value cut-off of ≤ 0.01. Signal intensities were mapped to an in-house *C. albicans* genome browser. Gene Ontology (GO) term analysis were performed by uploading gene lists into the GO Term Finder tool available at the Candida Genome Database website (http://www.candidagenome.org/). Significance cut-off was set at a *p*-value ≤ 0.01.

3.6.11. Transcriptional profiling assays and data analysis

Three independent cultures (50 mL each) of strains SC5314, cas5ΔΔ$_s$ were grown in YPD medium and harvested at low cell density (OD_{600} of 0.7) or at high cell density (OD_{600} of 13-14). The cas5 mutant strain took more time (around 3 hrs and 12 hrs more for the low and high cell density conditions, respectively) to reach the same OD as the wild type and consequently was harvested at a later time. Total RNA was extracted using the hot phenol method as previously described (Schmitt *et al.*, 1990). RNA samples were further purified using Qiagen RNeasy kit columns as per manufacturer's instructions. RNA was then quantified using a NanoDrop Spectrophotometer ND-1000 (NanoDrop Technologies, Inc.) and its integrity was assessed using a 2100 Bioanalyzer (Agilent Technologies). Cy3-labeled CTP cRNA was produced with 50 ng of total RNA using the Low Input Quick Amp Labeling Kit, according to manufacturer's instructions (Agilent Technologies, Inc). The labeled cRNA was then normalized at 1.65 µg, fragmented and hybridized to *C. albicans* assembly 19-based custom-made GE Microarray 4 x 44K (Synnott *et al.*, 2010). The arrays were incubated in an Agilent hybridization oven at 65ºC for 17 hours at 10 rpm. They were washed and scanned with an Agilent DNA Microarray Scanner C. All these steps were done according to Agilent One-Color Microarray-Based Gene Expression Analysis protocol (Agilent Technologies, Inc). Bioanalyzer and expression profiling assays were performed at the McGill University and Genome Quebec Innovation Center (Montreal, Canada). Output from the Agilent Feature Extraction software were read into R, preprocessed and tested for differential

expression using functions from the Bioconductor R (Gentleman, 2005)and Limma Package (Smyth, 2005). Specifically, the *normexp* method with an offset value of 16 was used for global background adjustment, followed by quantile normalization and a $\log_2$ transformation. Within-array duplicate spots were summarized by averaging using the function *avereps*. The annotation for probes was retrieved from the chromosomal feature file for *C. albicans* (C_albicans_SC5314) available at *candidagenome.org*. Benjamini-Hochberg false discovery rate was below 0.1 (10%). Gene Ontology (GO) term analysis and GO Slim analyses were performed as described above for ChIP-chip.

3.7. Acknowledgments

We would like to thank Dr. Aron Mitchell, Columbia University, for providing the mutant strains, Dr. Mike Snyder, Stanford University, for the design of the *C. albicans* tiling arrays and Dr. Geraldine Butler, University College Dublin, for the design of the *C. albicans* expression array. We are grateful to the Candida Genome Database for providing a unique and essential platform through their website. We also wish to acknowledge the McGill University and Génome Québec Innovation Center for the RNA profiling experiment. We thank Dr. Mauricio Corredor for initiating the screen, François Bourdeau for generating the *cas5* mutants, and Sandra Weber for technical advice on the ChIP-Chip assay. This work was supported by a grant (203691) from the *Natural Sciences and Engineering Research Council* of Canada to MR. The Institute for Research in Immunology and Cancer is supported by the Canada Foundation for Innovation and the Fonds de la Recherche en Santé du Québec.

Chapter 4

4. Chapter 4: Discussion and Future Perspectives

With the sequencing and annotation of the *C.albicans* genome, *Candida* research has entered the post-genomics era. Systems biology approaches are being harnessed by fungal researchers all over the world in an attempt to reconstruct the cellular and metabolic landscape of *C. albicans* both under the commensal as well as the pathogenic state. In contrast to studying individual genes or molecules, complex biological questions can now be answered at the global level, by designing and interpreting large-scale assays. The purpose of this work was to combine genetics and functional genomics to elucidate transcriptional regulator functions and construct transcriptional networks in *Candida albicans*.

4.1. Fcr1p is involved in nutrient assimilation and metabolism

4.1.1. Nitrogen Assimilation and Metabolism

As seen in Chapter 2, I have shown that Fcr1p is involved in the regulation of genes coding for nitrogen metabolic enzymes and nitrogen compound transporters. However, in rich medium, there was no observable phenotype as growth of the *fcr1*ΔΔ mutant in rich medium was not affected when compared to the growth of the corresponding wild type strain (data not shown). In addition, very few genes were differentially expressed in the *fcr1*ΔΔ mutant under those conditions. This may be because Fcr1p may not be active in rich medium. On the other hand, the role of Fcr1p in the regulation of its target genes was more evident when cells were grown under nitrogen starvation conditions. Fcr1p targets were differentially expressed when Fcr1p was abscent and in nitrogen depelete conditions. As seen in Chapter 2, *FCR1* expression was slightly induced in a nitrogen starvation medium and the expression of the Fcr1p-targets, *YWP1* and *RME1,* was responsive to the lack of nitrogen and this response was dependent on the presence of Fcr1p (Figure 4.1A). These findings are consistent with

the previously reported results for transcriptional networks governing the response to nitrogen deprivation in *Candida albicans*, where *FCR1* and *RME1* were upregulated, whereas *YWP1* was downregulated in response to nitrogen starvation (Ramachandra *et al.*, 2014). Although these three genes are yeast-specific and were regulated similarly in serum-induced filamentation (Grumaz *et al.*, 2013), it appears that they respond differently when in nitrogen depletion conditions.

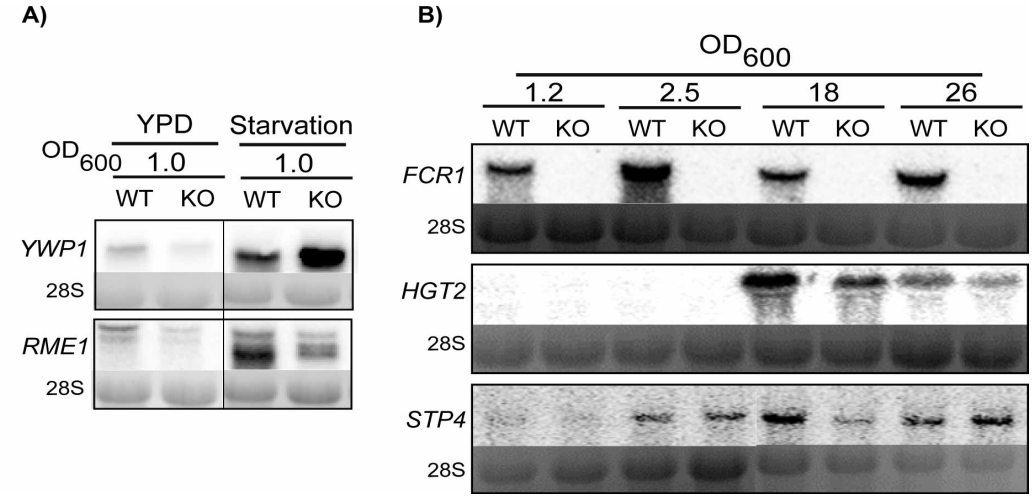

Figure 4.1. Northern blots for Fcr1p targets.
A) The *fcr1ΔΔ* knockout strain and the wild type SC5314 were grown to an OD of 1 in YPD or Yeast Nitrogen Base without amino acids and without ammonium sulfate (nitrogen starvation). RNA was extracted and subjected to Northern hybridization with the *YWP1* and *RME1* specific probes. Samples were migrated on the same gel. **B)** In a preliminary experiment, the same strains were grown in YPD and harvested at different cell densities as indicated. RNA was extracted and subjected to Northern hybridization with the *FCR1*, *HGT2*, and *STP4* specific probes. 28S RNA is shown below as control.

4.1.2. Sugar Assimilation and Metabolism

Interestingly, close inspection of the genes modulated in the *FCR1* overexpressing strain revealed upregulation of many genes encoding sugar transporters such as *HGT1*, *HGT2*, and *HGT10* as well as genes encoding enzymes of carbon metabolism such as

GAL10, *GAL102*, and *HSX11*. In addition, *RGT1*, encoding a transcriptional repressor of fermentable sugar transporters as well as glycolysis enzymes and functioning downstream of the Hgt4p sugar sensor, was also upregulated (see section 4.5.2), consistent with a role of Fcr1p in the import and metabolism of sugars (Sexton *et al.*, 2007). It has also been shown that *FCR1* is derepressed in a *mig1*ΔΔ mutant, indicating that Fcr1p is under the control of the carbon catabolite repressor Mig1p, further reinforcing a role for Fcr1p in carbon metabolism (Murad *et al.*, 2001). These observations imply that Fcr1p may also be involved in the response to sugar availability and acquisition. As the different transporters regulated by Fcr1p have different glucose specificities and sensitivities (V. Brown *et al.*, 2006), It would be interesting to investigate the expression of *FCR1* in response to glucose deprivation and in different concentrations of glucose, both at the RNA and protein levels.

Collectively these results imply that Fcr1p responds to nutritional cues and that it regulates genes involved in nutrient acquisition and metabolism, specifically nitrogen and sugars.

4.2. The expression of *FCR1* and its targets are subject to cell density effects

My expression profiling experiments revealed a significantly larger number of modulated genes in the *FCR1* overexpressing strain as compared to the *fcr1*ΔΔ mutant strain. Therefore, I speculated that the standard conditions under which I grew my cells for the profiling experiments (rich medium, early log) may not be the conditions under which Fcr1p is the most active. I also hypothesized that among the genes specifically modulated by the overexpression of *FCR1*, I might find additional Fcr1p targets. To test this, I have looked for

genes that were modulated in the *FCR1* overexpression strain but were not modulated in the fcr1 mutant strain *fcr1*ΔΔ. These genes might be examples of potential Fcr1p target genes that I could not detect using expression profiling only in the *fcr1*ΔΔ mutant strain. The gene *HSP30* was chosen as a candidate gene for such an analysis. Northern blotting with an *HSP30* probe (that was modulated only upon *FCR1* overexpression) revealed that this gene is in fact under the control of Fcr1p, however, only in the instance of high cell density, condition at which the expression of *HSP30* is strongly induced in an *FCR1*-dependant manner (Figure 2.3A). Similarly, the expression of the genes *HGT2*, encoding a glucose transporter, and *STP4* (preliminary data), encoding a transcription factor, was not detected at low cell density, however, they were both upregulated at high cell density and this upregulation required a functional Fcr1p protein at OD 18 (Figure 4.1B). I also noted that *FCR1* expression pattern fluctuates across the different cell densities, indicating that Fcr1p and its targets are subject to cell density effects. Further preliminary inspection of Fcr1p target gene expression with respect to varied range of cell densities (OD 1.2, 2.5, 5, 14, 15, 18, and 26) revealed even more complex regulation. For example, *RME1* was downregulated in the *fcr1*ΔΔ mutant at an OD of 1.2 corresponding to the expression profiling conditions. However a more pronounced effect of Fcr1p on the expression of this gene could be seen at ODs 2.5, 5, 14, and 15 but not at higher cell densities (data not shown). On the other hand, Fcr1p-dependent regulation of other targets could only be seen at a single time point such as in the case of *CAN2* and *HAP43* which were regulated by Fcr1p only at OD 26, but also in the case of *STP4*, *GDH2*, and *PLB1*, which were regulated in an Fcr1p-dependent manner only at OD 18, 14, and 5, respectively (data not shown). Using the same line of thought, I have extended my Northern blot analysis to Fcr1p targets that were only detected in the ChIP-chip assay. Similarly, *FCR1*-dependent expression of *GDH3* and *GLN1* could only be seen at an OD of 5 and 26, respectively. Taken together, these results lead me to the conclusion that

Fcr1p activity is dependent on cell density and that Fcr1p also regulates genes whose expression responds to cell density. Furthermore, as demonstrated by others (Chua *et al.*, 2006; Schillig & Morschhauser, 2013), gene overexpression has allowed me to identify Fcr1p targets that could not be detected simply by examining the expression profile of the *fcr1*ΔΔ mutant under standard conditions. Location profiling has also identified Fcr1p targets whose expression could only be detected when examining cell density variations. Therefore, by adopting a combination of different genomic approaches, it was possible to identify more Fcr1p targets than it would have been possible using a single approach.

4.3. Harnessing of the phenotypic screen

In Chapter 3, we have established and validated a phenotypic screen for the identification of transcriptional regulators involved in farnesol production. We have used a co-culture assay that proved to be successful as a readout for mutants that are defective in farnesol production based on their inability to inhibit the growth of *Aspergilus nidulans*. It would be interesting to extend this screen to study other libraries of mutants such as kinase and transporter mutants, or eventually to complete mutant collections (Blankenship *et al.*, 2010; Homann *et al.*, 2009; Vandeputte *et al.*, 2011). Such large-scale investigations would however require automation of the screen. This can be achieved using a similar co-culture assay using an *A. nidulans* strain expressing GFP-α-tubulin. Inhibition of *A. nidulans* growth can therefore be monitored using a fluorescence reader (Szewczyk & Oakley, 2011). Potential candidates (or hits) can then be selected for further characterization and functional assays to determine their role in farnesol production. Therefore, this screen is a very useful tool that can be used to shed light on important regulators and effectors that are involved in the metabolism and control of farnesol production.

4.4. Farnesol regulators link energy metabolism to quorum sensing

In this thesis work I present the first evidence of a link between metabolism, energy production and farnesol biosynthesis as well as the identification of important regulators of farnesol production by the means of a systematic screen in *Candida albicans*. Interestingly, the 5 TRs, Ada2p, Cas5p, Cas1p, Fgr15p and Rlm1p, share the regulation of many important cellular processes, most notably metabolism of energy, more particularly carbon metabolism (Bruno *et al.*, 2006; Delgado-Silva *et al.*, 2014; Vasicek *et al.*, 2014) (Figure 4.2).

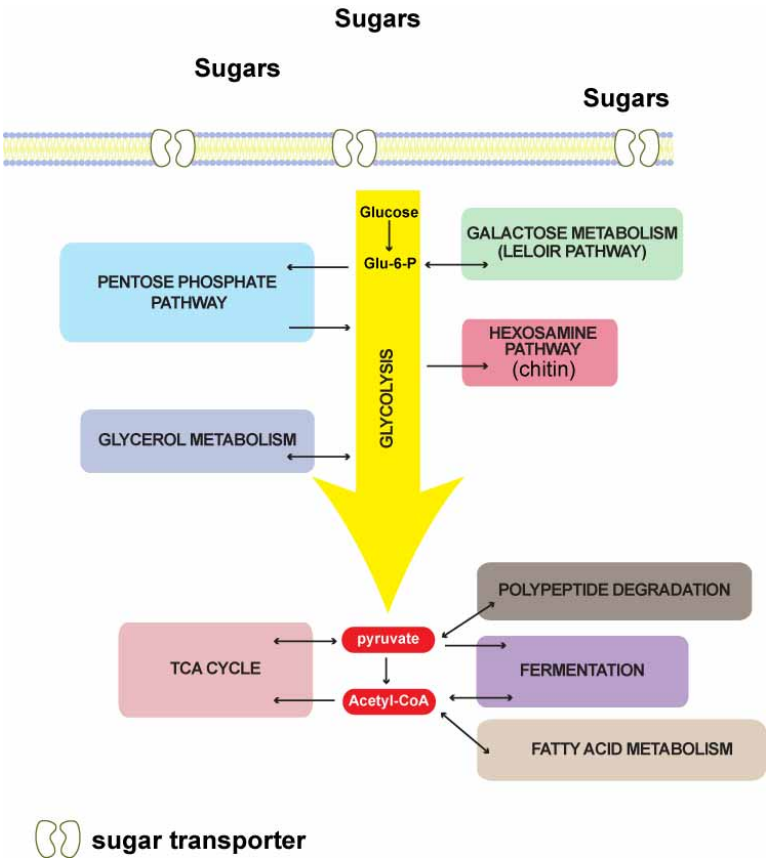

Figure 4.2. Schematic representation of the central carbon metabolism in *C. albicans*. Central carbon metabolism scheme in *C. albicans*. Various metabolites feed into and out of the glycolysis pathway linking important metabolic pathways such as the Leloir pathway, the

TCA cycle, the fatty acid metabolic pathway, the hexosamine pathway, the polypeptide degradation pathway, the fermentation pathway, the glycerol metabolism pathway and the pentose phosphate pathway, all of which converging on the common molecules pyruvate and acetyl-CoA.

In addition to farnesol biosynthesis, Ada2p, Cas5p, Cas1p, Fgr15p and Rlm1p are involved in cell wall integrity, control of glycolysis, stress response and lipid metabolism. However, the exact molecular mechanism by which they mediate the control of these processes is still not clear. Currently, I have available the location profile of Ada2p (Sellam, Askew*, et al.*, 2009), the expression profile of an *rlm1*ΔΔ mutant (Delgado-Silva *et al.*, 2014), as well as the regulon of Cas5p which indicate that these regulators share the biological process of carbon metabolism. Establishment of the complete regulons of those 5 TRs would give me a better idea about the molecular mechanisms by which they mediate these important processes (Figure 4.3).

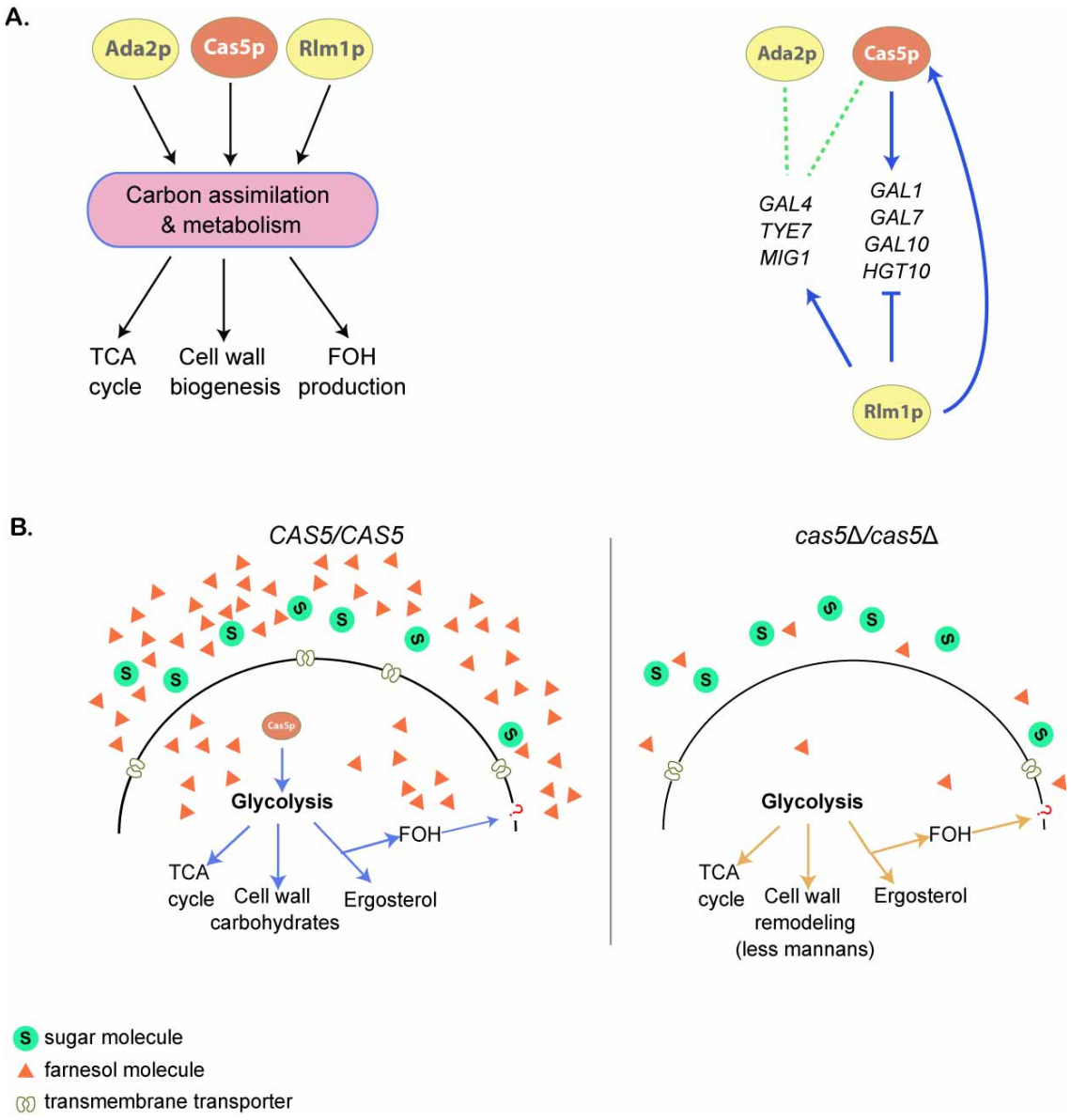

Figure 4.3. Schematic model for farnesol biosynthesis regulation.

A) Left panel: Commonly regulated pathways by the three farnesol biosynthesis regulators, Ada2p, Cas5p, and Rlm1p, as shown by integration of genomics data available for those regulators. **Right panel:** minimal transcriptional network inferred from genomics data showing the relationship among the three farnesol regulators. Genes represented here were selected among a list of genes that are targets of at least two of the three regulators and that function in the acquisition and metabolism of carbon sources. Continuous blue lines indicate regulation at the RNA level and dotted green lines represent DNA binding. **B)** Proposed model for the metabolic deregulation that occurs in the absence of the TR Cas5p and which

results in a decrease in normal farnesol levels. Model in a wild type cell (left panel), model in a *cas5*ΔΔ mutant strain (right panel), blue arrows represent normal flow of metabolites, orange arrows represent deregulated flow of metabolites, question mark represents unknown export mechanism. TCA: Tricarboxylic acid; FOH: Farnesol

4.5. Unresolved Questions

My PhD studies have led to many new and interesting findings but have also left me with many unresolved questions and many hypotheses that would be interesting to address.

4.5.1. In-ORF binding

In this work I have shown results of location profiling for two transcriptional regulators, Fcr1p and Cas5p. In both cases, an atypical enrichment profile was detected within the entire open reading frame of their target genes. This type of binding has been reported only scarcely in the literature due to the fact that intergenic arrays were more frequently used than tiling arrays to study TF binding sites (Caselle *et al.*, 2002; van Helden *et al.*, 1998). In addition, ChIP-seq technology that allows detection of in-ORF binding is not widely accessible and requires a lot of computational expertise. In general, even though some instances of intragenic binding were reported in a few studies, a link with transcriptional control could not be established with certainty (Ishihama *et al.*, 2016; Minch *et al.*, 2015; Shimada *et al.*, 2008). Usually elongation factors typically assume in-orf genomic locations such as in the case of the p-TEFb elongation factor. p-TEFb was suggested to maintain the transcribed region in a nucleosome-free state (Zhou *et al.*, 2012). Furthermore, the tumor suppressor p53 was shown to physically interact with the large subunit of the RNA polymerase II in a manner that is dependent on the core DNA binding domain of p53 (Balakrishnan & Gross, 2008; S. Kim *et al.*, 2011). Furthermore, it was recently reported in *E. coli* that CRP (Cyclic AMP receptor protein) binds intragenic regions. Detailed investigation of this profile demonstrated the presence of a small gene embedded in the coding region of a

larger gene, making it look like the CRP regulator is bound inside the ORF of the larger gene (Haycocks & Grainger, 2016). Even fewer studies about gene-specific TF intragenic binding in yeast were reported. For example, our group has reported this type of atypical binding for the TF Cap1p in *C. albicans*. Binding of Cap1p was most probably related to its functionality as hyperactivating the TF resulted in an enhancement of in-orf binding (Znaidi *et al.*, 2009). In *S. cerevisiae*, intragenic binding has been associated with the regulation of metabolism. The transcriptional repressor Sum1 was shown to rapidly induce repression of genes involved in glycolysis upon entry into the diauxic shift (M. Li *et al.*, 2013). Even though, typical histone modification mechanisms were ruled out, the exact mechanism of the repression could not be ascertained (M. Li *et al.*, 2013). In this thesis work, tiling arrays were used, which allowed the detection of such atypical binding for Fcr1p and Cas5p. Strikingly, both TRs are involved in the control of metabolic pathways as was shown for Sum1 in *S. cerevisiae* (M. Li *et al.*, 2013). So I asked whether this type of atypical binding could be correlated with the functionality of the TRs. In the case of Fcr1p and with respect to nitrogen-dependent targets, we were able to correlate intragenic binding with gene repression. In the case of Cas5p, the TR was bound to carbon catabolism genes at low cell density; however these genes were not modulated by Cas5p under these conditions. On the other hand, carbon catabolic genes were repressed in a Cas5p-dependent manner at high cell density. Therefore, it would be interesting to know whether Cas5p still binds within the ORFs of these genes at high cell density. To ascertain this functionality, it would be interesting to perform a ChIP-chip assay at high cell density in order to investigate whether Cas5p shifts or leaves its genomic location under such conditions. On the other hand, another interesting possibility is to test for the possible involvement of histone modifications. For that, enrichment for histone acetylation marks using ChIP at Fcr1p or Cas5p targets in the corresponding TR mutants versus wild type would be used (M. Li *et al.*, 2013). Finally, as genome-wide approaches are being adopted, scientists

are becoming more flexible with long-standing paradigms about typical TF binding, DNA recognition and transcriptional control and have just started to accept the exceptions (Carroll *et al.*, 2006; Haycocks & Grainger, 2016). The scientific field has started to address these as significant events that deserve attention and further investigation.

4.5.2. Mechanism of inhibition of filamentation

I have shown in Chapter 2 that Fcr1p overexpression represses filamentation. Examining my expression profiling data did not allow me to detect differential expression of any of the master regulators of filamentous growth in *Candida albicans* such as Flo8p, Efg1p, Cph1p, Rfg1p, Nrg1p or Tup1p. This could be due to the fact that the expression profiling experiment was not done under filament-inducing conditions. Inspection of their respective proteins would probably be more informative as to their involvement in Fcr1p-dependent repression of the hyphal switch. However, I have found that *RFX2* was upregulated in the *FCR1*-overexpressing cells. *RFX2* encodes a transcriptional repressor whose deletion results in upregulation of hyphal-specific genes and a hyperfilamentous phenotype (Hao *et al.*, 2009). I have also found that *RGT1* is upregulated in the *FCR1* overexpressing strain. Interestingly, deletion of *RGT1* has been shown to result in a hyperfilamentous phenotype due to uncontrolled expression of sugar transporters (see section 4.1.2) (Sexton *et al.*, 2007). In addition, I have also detected upregulation of *RME1* encoding a zinc finger protein that is a yeast-specifc gene, however, the physiologic function of *RME1* in *C. albicans* has not yet been determined. These data hint to the fact that upregulation of yeast-specific genes as well as the genes coding for the transcriptional regulators *RFX2, RGT1* and *RME1* may possibly underlie the abrogation of filamentation in the *FCR1* overexpressing strain. To test this hypothesis, it would be interesting to delete them in the *FCR1* overexpressing strain, using the CRISPR technology (section 1.6.2.4), to determine their effect on *FCR1*-repressed

filamentation. Preliminary results indicate that overexpression of *RME1* in a wild-type strain does not repress filamentation.

4.5.3. Mechanism operating upstream of Fcr1p

As seen in section 4.1, my results strongly suggest that Fcr1p is implicated in the regulation of nutrient acquisition and metabolism, more specifically nitrogen and sugar sources. The next question that emerges is about the identity of the mechanism operating upstream of Fcr1p. **i)** In preliminary experiments, I have shown that in cells grown in standard conditions (rich medium, early log), the Fcr1p protein displayed a downshift following phosphatase treatment indicating that Fcr1p is subject to post-translational phosphorylation (Figure 4.4A), **ii)** as seen in Chapter 2, the *FCR1* transcript size differed between nitrogen replete and nitrogen deplete conditions. Furthermore, the transcripts of the Fcr1p targets *OPT1*, *HSP30*, and *RME1* also displayed different transcript sizes, the biological significance of which is still unclear (Figure 2.3A and Figure 4.1). Multiple RNA isoforms have been described for Nitrogen Catabolite Repression (NCR)-responsive regulators such as Gat1p in *Saccharomyces cerevisiae*. Due to differential transcriptional initiation sites but also due to premature termination, different isoforms of *GAT1* are generated in response to nitrogen source (Georis *et al.*, 2015). *GAT1* and NCR are regulated by the TOR pathway (Georis *et al.*, 2015). Given my demonstrated role of Fcr1p in the regulation of nitrogen-dependent genes and glucose-dependent genes, both of which are typically responsive to nutritional signals and TOR-dependent regulation (Chowdhury & Kohler, 2015), I speculate that Fcr1p and some of the Fcr1p targets may be subject to a similar regulatory mechanism (Figure 4.4B). In order to investigate the signaling relationship between Fcr1p and TOR, it would be interesting to study the phosphorylation status of Fcr1p in response to treatment with rapamycin in rich medium. Pharmacological inhibition of TOR pathway by the TOR inhibitor rapamycin results in a decrease in the phosphorylated form of S6 (P-S6), inhibition of cellular growth and

induction of nitrogen responsive genes (Chowdhury & Kohler, 2015; Liao *et al.*, 2008). Therefore, if Fcr1p phosphorylation is TOR-dependent then dephosphorylation of Fcr1p would be expected when wild type cells are treated with rapamycin in rich medium. It would also be interesting to test whether Fcr1p is dephosphorylated in wild type cells exposed to nitrogen depletion conditions. This would help determine whether the Fcr1p-dependent regulation of nitrogen genes under nitrogen starvation is dependent on the phosphorylation status of this TF. Furthermore, it has been shown that PKA signaling promotes P-S6 levels in response to glucose availability while P-S6 levels where reduced upon treatment with the cAMP inhibitor, farnesol (Chowdhury & Kohler, 2015). Since carbon metabolic genes were also under the control of Fcr1p, it would be interesting to test whether the phosphorylation state of Fcr1p is regulated by the availability of glucose and whether Fcr1p functions downstream of PKA. For that a phosphatase treatment of protein extracts from wild type cells grown in the absence or presence of glucose and farnesol can be tested.

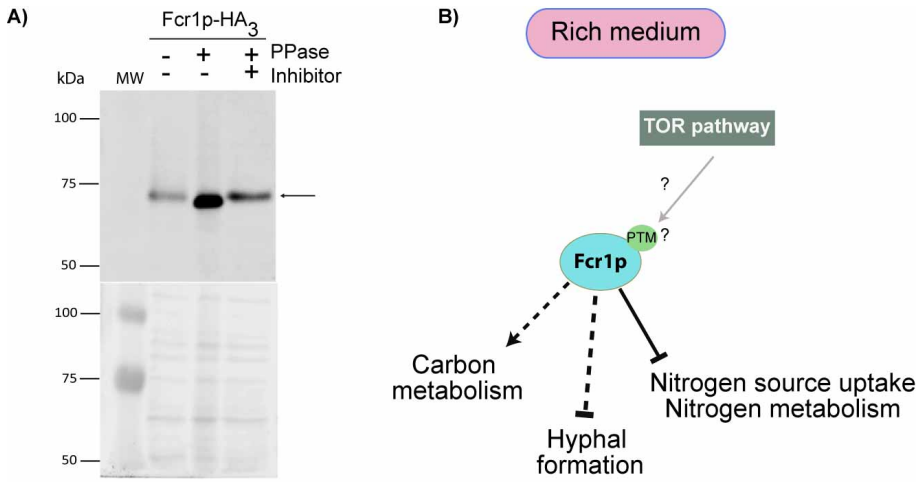

Figure 4.4. Proposed model for Fcr1p mode of action.

Phosphatase Assay. Protein extracts from strain CAI4/Fcr1p-HA_3 treated with phosphatase (PPase) in the presence or absence of phosphatase inhibitor were analyzed by Western blotting (upper panel) using an anti-HA monoclonal antibody. The molecular weight markers (MW) are indicated on the left. The Fcr1p-HA_3 protein is indicated by the arrow. PonceauS

staining is shown (lower panel) as a protein loading and transfer control. KDa: Kilodalton. **B)** Schematic Illustration depicting a proposed model for Fcr1p mode of action as suggested by our current findings. Continuous lines represent direct regulation, dotted lines represent indirect regulation, question mark and grey arrow represent possible pathway under investigation. PTM: post-translational modification

4.5.4. Azole resistance

FCR1 was first discovered by functional complementation of the fluconazole hypersensitivity of a *pdr1 pdr3 Saccharomyces cerevisiae* strain where its expression caused an upregulation of the *PDR5* gene encoding an ABC multidrug transporter homologous to Cdr1p and Cdr2p (Talibi & Raymond, 1999). However in *C. albicans,* deletion of *FCR1* in the CAI4 background was found to cause mild azole resistance (Talibi & Raymond, 1999). I have evaluated our *fcr1*ΔΔ mutant constructed in the SC5314 background for azole resistance, using a fluconazole MIC assay (Figure 4.5). Unlike what I observed in the CAI4 background (Talibi & Raymond, 1999), I found no difference in fluconazole susceptibility in the constructed mutants as compared to the wild type control, SC5314. This could be due to inherent differences in strain backgrounds such as karyotype abnormalities (Selmecki *et al.*, 2010). As previously reported, the *FCR1* overexpressing strain displayed in my hands an enhanced susceptibility to fluconazole (Figure 4.5). Shen et al. had obtained our *FCR1* overexpressing strain and looked at the molecular mechanism behind this azole hypersusceptibility (Shen *et al.*, 2007). Their results showed that *FCR1* overexpression resulted in azole hypersusceptibility due to *CDR1* repression (Shen *et al.*, 2007). Conversely, my data did not show binding of Fcr1p to *CDR1* and my overexpression profiling data did not reveal any modulation at the level of known players of azole resistance such as *CDR1, ERG11,* and *UPC2* (Supplementary Table II.3-B). Furthermore, confirmation Northern blots did not show any modulation of these genes (data not shown). These discrepencies could be due to the fact that my results could not be directly compared to the Shen et al. study

because my profiling assay was not done in the presence of azoles while their experiments were done in the presence of 20 µg/ml of fluconazole. In addition, my experiments used standard protocols where cells were analyzed at log phase (for the genomics assay) and after 48 h (for the MIC assay), while Shen *et al* have grown their cells for 25 days! (Shen *et al.*, 2007). The fact that my results show enhanced susceptibility to fluconazole without any modulation of known players of azole resistance can be explained by the previously stated assumption that TF deletion may not reveal tremendous phenotypic changes that are otherwise obvious by overexpressing the TF. This can also be partly explained by the fact that the growth medium in our profiling experiments did not contain azoles or because one (or more) of the modulated genes plays a yet unknown role in azole susceptibility. On the other hand, our group had previously shown that Fcr1p is a negative regulator of resistance to different drugs such as brefedin A, and ketoconazole (Talibi & Raymond, 1999) and my profiling results show a notable deregulation of many transporters. Therefore, it is possible that this multiple drug resistance is secondary to a deregulation in transporters at the level of the cell membrane. To address this, genes coding for candidate transporters could be overexpressed in the *fcr1* mutant or deleted in the *FCR1* overexpression strain and tested for drug susceptibility.

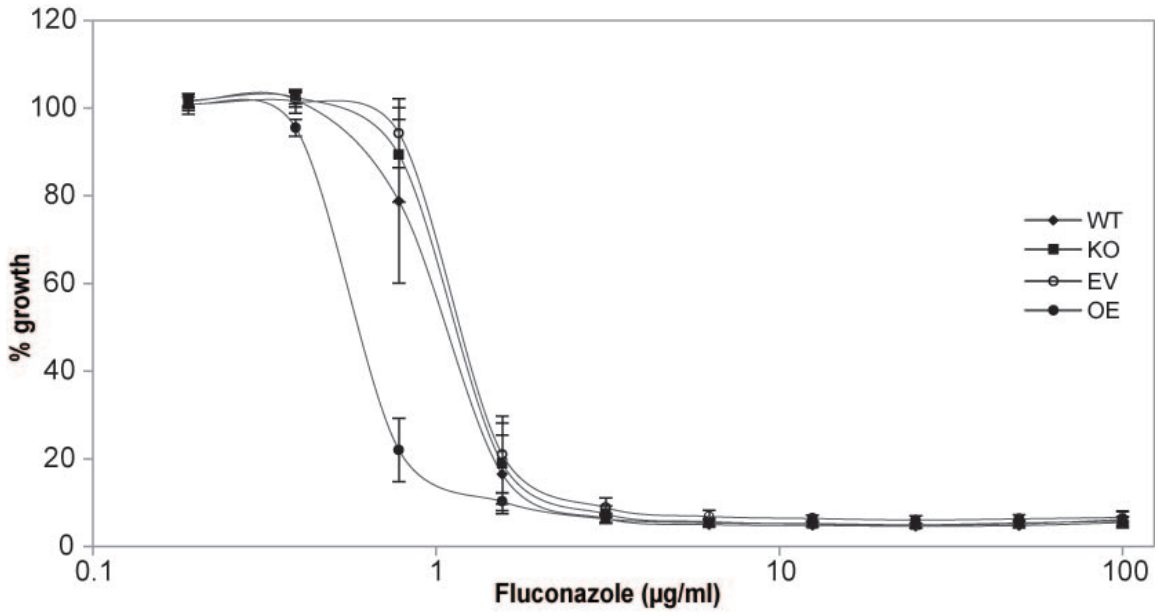

Figure 4.5. Fluconazole MIC assay

Fluconazole (FCZ) susceptibility testing by microtiter plate assay comparing, the strains SC5314 (WT), the *fcr1*ΔΔ mutant in the SC5314 background, *fcr1*ΔΔ mutant in the CAI4 background containing the empty vector strain (EV) and the *FCR1* overexpressing strain (OE).

4.5.5. The farnesol receptor

Many aspects of the molecular mechanisms of farnesol-dependent quorum sensing in *Candida albicans* are poorly characterized. One of the very intriguing questions is about the identification of a farnesol receptor in *Candida albicans*. Therefore, it would be interesting to identify and test potential receptors for this molecule. In mammalians, the nuclear receptor farnesol X receptor (FXR) which is a transcription factor, was identified by a screen of potential farnesol ligands. It forms a heterodimer with the retinoid X receptor to achieve, along with ligand binding, transcriptional control of target genes. It was found that farnesol as well as farnesol metabolites bind and activate FXR in the liver and the intestines, to regulate bile acid homeostasis (Fayard *et al.*, 2001; Forman *et al.*, 1995). Farnesol, via activation of FXR, also activates the degradation of HMG-CoA reductase, a key enzyme in the biosynthesis of cholesterol (Niesor *et al.*, 2001). More recently, an odorant binding protein was identified in

Chilo suppressalis, an insect that attacks rice crops. CsupOBP8 acts as a chemoreceptor, which binds and transports farnesol amongst other plant volatiles (K. Yang *et al.*, 2016). Therefore, since these proteins have known affinity to farnesol, the *Candida albicans* genome can be searched for putative proteins having structural features (such as α-helices enclosing a hydrophobic pocket) that are similar to the ligand-binding domain of the FXR or the CsupOBP8, which can then be tested for binding affinity to farnesol using the competitive fluorescence-binding assay described in Yang et al (Pelosi *et al.*, 2014; K. Yang *et al.*, 2016). Alternatively, a genetic screen can also be carried out by growing mutant libraries at 30ºC and 37ºC in the presence or absence of farnesol. *C. albicans* grows as filaments at 37ºC and addition of farnesol prevents this transition (see sections 1.3.1.1 and 1.3.9). Therefore, mutant colonies growing in filamentous forms at 37ºC on a medium containing farnesol can be considered as farnesol-resistant. Among the identified mutants, potential farnesol receptor mutants may be detected, which can then be selected for secondary screens and further investigation (Langford *et al.*, 2013).

4.5.6. The galactose transporter

It has been shown that galactose metabolism has been transcriptionally rewired in *C. albicans* and that its regulation differs in many aspects from its regulation in baker's yeast (Rokas & Hittinger, 2007). In *S. cerevisiae*, Gal2 has been identified as the galactose permease whereas a galactose transporter has not yet been identified in *C. albicans*. I have seen in Chapter 3 that Cas5p binds and regulates multiple genes that are clustered in the same locus such as *GAL1*, *GAL7*, *GAL10*, that are involved in galactose metabolism but also the genes *HGT2* (encoding a putative glucose transporter) and *SHA3* (encoding a S/T kinase) that are involved in sugar transport (Figure 3.7A). Their presence in the same locus, bound and regulated by the same factor, may imply coordinated gene expression or regulation for those genes. Therefore it is possible that the Hgt2p transporter may also be

able to transport galactose. Eukaryotic genes are not randomly clustered; especially yeast genes (98%) are clustered in the same regulatory regions. For example, the *GAL1*, *GAL7*, *GAL10* genes are also clustered in *S. cerevisiae* as well (Slot & Rokas, 2010). There is also evidence to suggest that adjacently clustered genes often pertain to the same or related functional category and are often co-expressed, a phenomenon known as "multi-gene regulation" (Hurst *et al.*, 2004; Kruglyak & Tang, 2000). In addition, some sugar transporters in *S. cerevisiae such as HXT9, HXT11, and HXT17* also have some affinity for galactose. Taken together these data suggest that Hgt2p may also have some affinity to galactose, which warrants a future investigation.

4.6. A common transcriptional network for Fcr1p and Cas5p

As mentioned in Chapter 1, the aim of this thesis work was to construct transcriptional networks. In line with this, I have found that Fcr1p and Cas5p share a lot of similarities indicating that both regulators share potentially common regulatory pathways. Therefore I have put together data to generate a representative minimal transcriptional network that encompasses both TRs. First both regulators share an atypical binding profile within open reading frames of their targets and that may be related to their function in metabolic pathways and regulation of metabolic genes (see section 4.5.1) (Figure 4.6). As seen in Chapters 2 and 3, both regulators are potentially more active at high cell density, which also coincides with nutritional depletion of the growth medium.

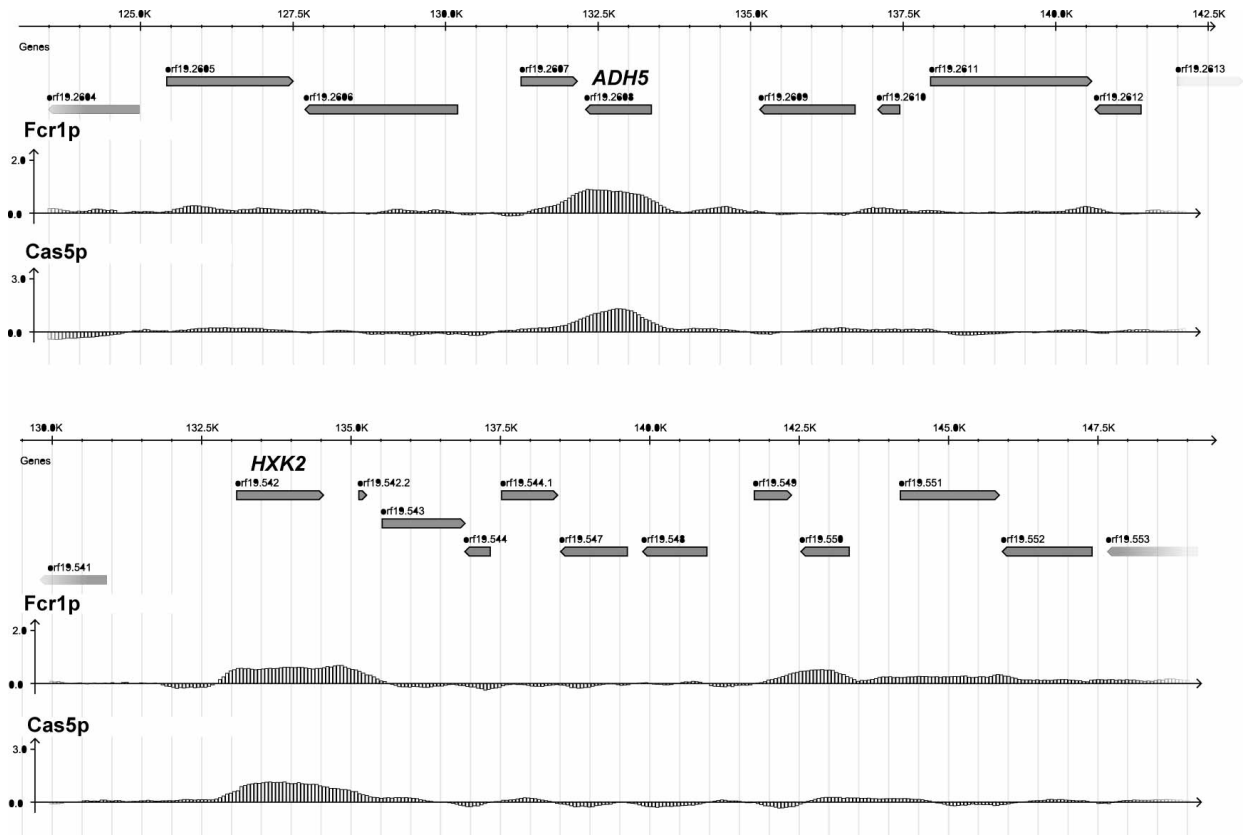

Figure 4.6. Location profile for Common Fcr1p and Cas5p targets.
Tilemaps for selected Fcr1p and Cas5p common targets. The genome browser views shows the signal intensity for each of the oligonucleotide probes spanning the Watson and Crick strands on the tiling arrays. The *x*-axis represents the genomic positions in the contigs and the *y*-axis represents $\log_2$-transformed signal intensities (n=3) illustrating Fcr1p and Cas5p enrichment at selected target genes: *ADH5,* and *HXK2.*

Second, I have found that Cas5p is bound to *FCR1* and that it positively regulates *FCR1* expression at low (below cutoff) and high cell density (data not shown). Furthermore, Fcr1p and Cas5p were bound to 28 common genes and regulated 62 other common genes at high cell density, implying a potential functional and/or physical interaction between the two regulators. Those common genes mainly function in cellular processes such as transport, carbon and nitrogen metabolism, indicating that Fc1p and Cas5p may participate in the same regulatory pathways (Figure 4.7). However, it was not possible to find any gene that is bound

and regulated by both factors, probably owing to that fact that the location profiling assays were done at low cell density (standard laboratory conditions). Collectively, these data indicate that Cas5p lies upstream of Fcr1p and that both regulators collaborate in the regulation of genes associated with nutrient acquisition and metabolism under the studied conditions. In order to achieve a better resolution of the transcriptional network encompassing Cas5p and Fcr1p, a ChIP-Chip or ChIP-Seq assay would be interesting to do at high cell density to ascertain the relationship between those two regulators. It would then be possible to differentiate whether Cas5p mediates the regulation of common genes via positive regulation of *FCR1* or that Cas5p and Fcr1p regulate the same set of genes, however, through distinct intermediates. As shown in Figure 4.7B, Fcr1p and Cas5p control other transcriptional regulators such as *STP4*, *RME1* and *ZCF15* (shown in red). Determining the regulons of those regulators would add to this model and help reconstruct an even more complex transcriptional network. Finally, Cas5p and Fcr1p also play a role in the regulation of hyphal switch through distinct mechanisms. Fcr1p is a negative regulator of filamentation and yeast-specific genes and Cas5p control this morphological switch via regulation of quorum sensing. Therefore, it appears that both TRs share the control of key *C. albicans* virulence traits, hyphal switch and metabolic adaptation.

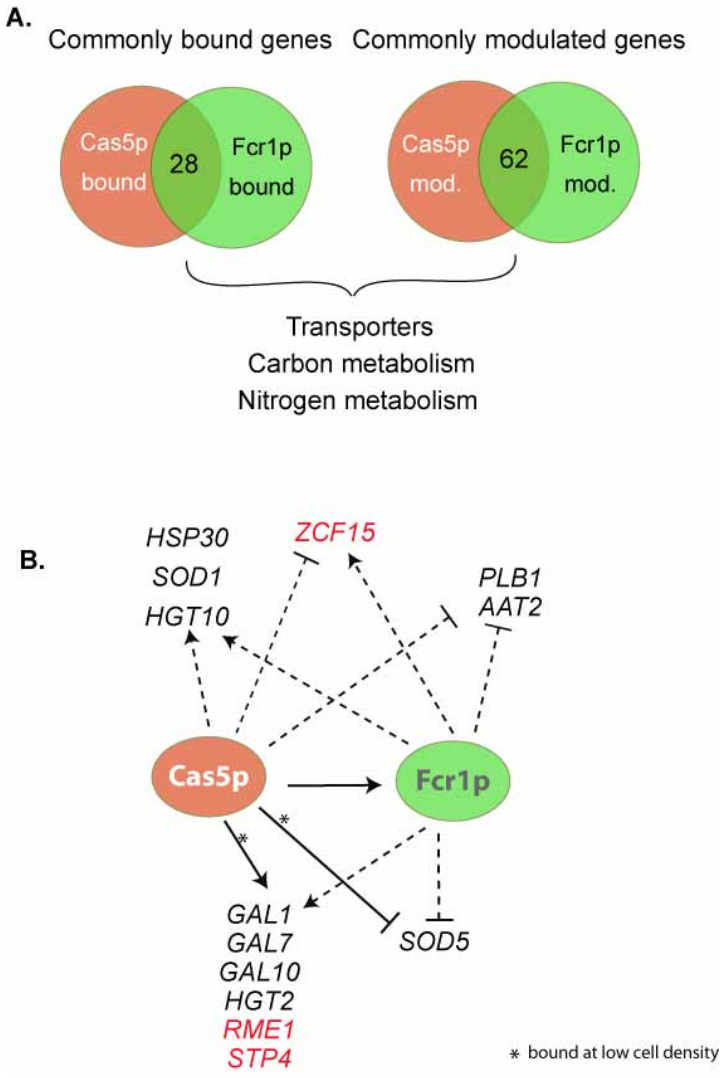

Figure 4.7. Example of constructed Fcr1p and Cas5p transcriptional network. Venn diagrams showing the overlap of genes bound and genes regulated by Fcr1p and Cas5p. The lists of commonly bound genes (28 genes) and commonly regulated genes (62 genes) do not overlap, however, the cellular processes represented by these gene lists indicate that both TRs are involved in the control of transporters as well as carbon and nitrogen metabolism. **B)** Schematic construction of a minimal transcriptional network based on our functional genomics data obtained for the transcriptional regulators Fcr1p and Cas5p. Continuous lines represent direct regulation, dotted lines represent indirect regulation, and genes in red represent genes that encode transcriptional regulators.

4.7. Conclusion

In conclusion, in this thesis work I have uncovered new players in metabolism and assimilation of nutrient sources. I have provided insight into the regulation of farnesol biosynthesis by showing the first example of transcriptional regulators involved in this process. I have also provided the first evidence of a link between metabolism and quorum sensing. Finally, the use of genetics and functional genomics allowed me to meet my objective of identifying transcription factor functions and to contribute to construction of transcriptional networks governing important cellular processes relevant to *Candida albicans* patho-biology.

5. References

Akins, R. A. "An Update on Antifungal Targets and Mechanisms of Resistance in Candida Albicans." *Med Mycol* 43, no. 4 (2005): 285-318.

Al-Akeel R, El-Kersh T, Al-Sheikh Y, Al-Ahmadey Z. "Prevalence and Comparison for Detection Methods of Candida Species in Vaginal Specimens from Pregnant and Non Pregnant Saudi Women." *African journal of microbiology research* 7, no. 7 (2013): 56-65.

Albuquerque, P., and A. Casadevall. "Quorum Sensing in Fungi--a Review." *Med Mycol* 50, no. 4 (2012): 337-45.

Almeida, R. S., D. Wilson, and B. Hube. "Candida Albicans Iron Acquisition within the Host." *FEMS Yeast Res* 9, no. 7 (2009): 1000-12.

Anaissie, E. J., S. E. Vartivarian, D. Abi-Said, O. Uzun, H. Pinczowski, D. P. Kontoyiannis, P. Khoury, K. Papadakis, A. Gardner, Raad, II, J. Gilbreath, and G. P. Bodey. "Fluconazole Versus Amphotericin B in the Treatment of Hematogenous Candidiasis: A Matched Cohort Study." *Am J Med* 101, no. 2 (1996): 170-6.

Antinori, S., L. Milazzo, S. Sollima, M. Galli, and M. Corbellino. "Candidemia and Invasive Candidiasis in Adults: A Narrative Review." *Eur J Intern Med* (2016).

Arendrup, M. C. "Epidemiology of Invasive Candidiasis." *Curr Opin Crit Care* 16, no. 5 (2010): 445-52.

Argimon, S., J. A. Wishart, R. Leng, S. Macaskill, A. Mavor, T. Alexandris, S. Nicholls, A. W. Knight, B. Enjalbert, R. Walmsley, F. C. Odds, N. A. Gow, and A. J. Brown. "Developmental Regulation of an Adhesin Gene During Cellular Morphogenesis in the Fungal Pathogen Candida Albicans." *Eukaryot Cell* 6, no. 4 (2007): 682-92.

Ashman, R. B., C. S. Farah, S. Wanasaengsakul, Y. Hu, G. Pang, and R. L. Clancy. "Innate Versus Adaptive Immunity in Candida Albicans Infection." *Immunol Cell Biol* 82, no. 2 (2004): 196-204.

Askew, C., A. Sellam, E. Epp, H. Hogues, A. Mullick, A. Nantel, and M. Whiteway. "Transcriptional Regulation of Carbohydrate Metabolism in the Human Pathogen Candida Albicans." *PLoS Pathog* 5, no. 10 (2009): e1000612.

Baek, Y. U., S. J. Martin, and D. A. Davis. "Evidence for Novel Ph-Dependent Regulation of

Candida Albicans Rim101, a Direct Transcriptional Repressor of the Cell Wall Beta-Glycosidase Phr2." *Eukaryot Cell* 5, no. 9 (2006): 1550-9.

Bain, J. M., L. E. Lewis, B. Okai, J. Quinn, N. A. Gow, and L. P. Erwig. "Non-Lytic Expulsion/Exocytosis of Candida Albicans from Macrophages." *Fungal Genet Biol* 49, no. 9 (2012): 677-8.

Baker, A., I. A. Graham, M. Holdsworth, S. M. Smith, and F. L. Theodoulou. "Chewing the Fat: Beta-Oxidation in Signalling and Development." *Trends Plant Sci* 11, no. 3 (2006): 124-32.

Balakrishnan, S. K., and D. S. Gross. "The Tumor Suppressor P53 Associates with Gene Coding Regions and Co-Traverses with Elongating Rna Polymerase Ii in an in Vivo Model." *Oncogene* 27, no. 19 (2008): 2661-72.

Balashov, S. V., S. Park, and D. S. Perlin. "Assessing Resistance to the Echinocandin Antifungal Drug Caspofungin in Candida Albicans by Profiling Mutations in Fks1." *Antimicrob Agents Chemother* 50, no. 6 (2006): 2058-63.

Banerjee, M., D. S. Thompson, A. Lazzell, P. L. Carlisle, C. Pierce, C. Monteagudo, J. L. Lopez-Ribot, and D. Kadosh. "Ume6, a Novel Filament-Specific Regulator of Candida Albicans Hyphal Extension and Virulence." *Mol Biol Cell* 19, no. 4 (2008): 1354-65.

Barchiesi, F., A. M. Schimizzi, A. W. Fothergill, G. Scalise, and M. G. Rinaldi. "In Vitro Activity of the New Echinocandin Antifungal, Mk-0991, against Common and Uncommon Clinical Isolates of Candida Species." *Eur J Clin Microbiol Infect Dis* 18, no. 4 (1999): 302-4.

Barker, K. S., and P. D. Rogers. "Recent Insights into the Mechanisms of Antifungal Resistance." *Curr Infect Dis Rep* 8, no. 6 (2006): 449-56.

Bastidas, R. J., J. Heitman, and M. E. Cardenas. "The Protein Kinase Tor1 Regulates Adhesin Gene Expression in Candida Albicans." *PLoS Pathog* 5, no. 2 (2009): e1000294.

Bellmann, R. "Clinical Pharmacokinetics of Systemically Administered Antimycotics." *Curr Clin Pharmacol* 2, no. 1 (2007): 37-58.

Ben-Ami, R., G. Garcia-Effron, R. E. Lewis, S. Gamarra, K. Leventakos, D. S. Perlin, and D. P. Kontoyiannis. "Fitness and Virulence Costs of Candida Albicans Fks1 Hot Spot Mutations Associated with Echinocandin Resistance." *J Infect Dis* 204, no. 4 (2011): 626-35.

Berman, J., and P. E. Sudbery. "Candida Albicans: A Molecular Revolution Built on Lessons

from Budding Yeast." *Nat Rev Genet* 3, no. 12 (2002): 918-30.

Bieganska, M. J. "Two Fundamentals of Mammalian Defense in Fungal Infections: Endothermy and Innate Antifungal Immunity." *Pol J Vet Sci* 17, no. 3 (2014): 555-67.

Blankenship, J. R., S. Fanning, J. J. Hamaker, and A. P. Mitchell. "An Extensive Circuitry for Cell Wall Regulation in Candida Albicans." *PLoS Pathog* 6, no. 2 (2010): e1000752.

Bockmuhl, D. P., and J. F. Ernst. "A Potential Phosphorylation Site for an a-Type Kinase in the Efg1 Regulator Protein Contributes to Hyphal Morphogenesis of Candida Albicans." *Genetics* 157, no. 4 (2001): 1523-30.

Boeke, J. D., F. LaCroute, and G. R. Fink. "A Positive Selection for Mutants Lacking Orotidine-5'-Phosphate Decarboxylase Activity in Yeast: 5-Fluoro-Orotic Acid Resistance." *Mol Gen Genet* 197, no. 2 (1984): 345-6.

Bonhomme, J., M. Chauvel, S. Goyard, P. Roux, T. Rossignol, and C. d'Enfert. "Contribution of the Glycolytic Flux and Hypoxia Adaptation to Efficient Biofilm Formation by Candida Albicans." *Mol Microbiol* 80, no. 4 (2011): 995-1013.

Booth, L. N., B. B. Tuch, and A. D. Johnson. "Intercalation of a New Tier of Transcription Regulation into an Ancient Circuit." *Nature* 468, no. 7326 (2010): 959-63.

Braun, B. R., and A. D. Johnson. "Tup1, Cph1 and Efg1 Make Independent Contributions to Filamentation in Candida Albicans." *Genetics* 155, no. 1 (2000): 57-67.

Braun, B. R., D. Kadosh, and A. D. Johnson. "Nrg1, a Repressor of Filamentous Growth in C.Albicans, Is Down-Regulated During Filament Induction." *EMBO J* 20, no. 17 (2001): 4753-61.

Braun, B. R., M. van Het Hoog, C. d'Enfert, M. Martchenko, J. Dungan, A. Kuo, D. O. Inglis, M. A. Uhl, H. Hogues, M. Berriman, M. Lorenz, A. Levitin, U. Oberholzer, C. Bachewich, D. Harcus, A. Marcil, D. Dignard, T. Iouk, R. Zito, L. Frangeul, F. Tekaia, K. Rutherford, E. Wang, C. A. Munro, S. Bates, N. A. Gow, L. L. Hoyer, G. Kohler, J. Morschhauser, G. Newport, S. Znaidi, M. Raymond, B. Turcotte, G. Sherlock, M. Costanzo, J. Ihmels, J. Berman, D. Sanglard, N. Agabian, A. P. Mitchell, A. D. Johnson, M. Whiteway, and A. Nantel. "A Human-Curated Annotation of the Candida Albicans Genome." *PLoS Genet* 1, no. 1 (2005): 36-57.

Brock, M. "Fungal Metabolism in Host Niches." *Curr Opin Microbiol* 12, no. 4 (2009): 371-6.

Brown, A. J., G. D. Brown, M. G. Netea, and N. A. Gow. "Metabolism Impacts Upon Candida Immunogenicity and Pathogenicity at Multiple Levels." *Trends Microbiol* 22, no. 11 (2014): 614-22.

Brown, A. J., S. Budge, D. Kaloriti, A. Tillmann, M. D. Jacobsen, Z. Yin, I. V. Ene, I. Bohovych, D. Sandai, S. Kastora, J. Potrykus, E. R. Ballou, D. S. Childers, S. Shahana, and M. D. Leach. "Stress Adaptation in a Pathogenic Fungus." *J Exp Biol* 217, no. Pt 1 (2014): 144-55.

Brown, A. J., F. C. Odds, and N. A. Gow. "Infection-Related Gene Expression in Candida Albicans." *Curr Opin Microbiol* 10, no. 4 (2007): 307-13.

Brown, D. H., Jr., A. D. Giusani, X. Chen, and C. A. Kumamoto. "Filamentous Growth of Candida Albicans in Response to Physical Environmental Cues and Its Regulation by the Unique Czf1 Gene." *Mol Microbiol* 34, no. 4 (1999): 651-62.

Brown, V., J. A. Sexton, and M. Johnston. "A Glucose Sensor in Candida Albicans." *Eukaryot Cell* 5, no. 10 (2006): 1726-37.

Bruno, V. M., S. Kalachikov, R. Subaran, C. J. Nobile, C. Kyratsous, and A. P. Mitchell. "Control of the C. Albicans Cell Wall Damage Response by Transcriptional Regulator Cas5." *PLoS Pathog* 2, no. 3 (2006): e21.

Bruno, V. M., Z. Wang, S. L. Marjani, G. M. Euskirchen, J. Martin, G. Sherlock, and M. Snyder. "Comprehensive Annotation of the Transcriptome of the Human Fungal Pathogen Candida Albicans Using Rna-Seq." *Genome Res* 20, no. 10 (2010): 1451-8.

Butler, G. "Hypoxia and Gene Expression in Eukaryotic Microbes." *Annu Rev Microbiol* 67 (2013): 291-312.

Butler, G., M. D. Rasmussen, M. F. Lin, M. A. Santos, S. Sakthikumar, C. A. Munro, E. Rheinbay, M. Grabherr, A. Forche, J. L. Reedy, I. Agrafioti, M. B. Arnaud, S. Bates, A. J. Brown, S. Brunke, M. C. Costanzo, D. A. Fitzpatrick, P. W. de Groot, D. Harris, L. L. Hoyer, B. Hube, F. M. Klis, C. Kodira, N. Lennard, M. E. Logue, R. Martin, A. M. Neiman, E. Nikolaou, M. A. Quail, J. Quinn, M. C. Santos, F. F. Schmitzberger, G. Sherlock, P. Shah, K. A. Silverstein, M. S. Skrzypek, D. Soll, R. Staggs, I. Stansfield, M. P. Stumpf, P. E. Sudbery, T. Srikantha, Q. Zeng, J. Berman, M. Berriman, J. Heitman, N. A. Gow, M. C. Lorenz, B. W. Birren, M. Kellis, and C. A. Cuomo. "Evolution of Pathogenicity and Sexual Reproduction in Eight Candida Genomes." *Nature* 459, no. 7247 (2009): 657-62.

Buu, L. M., and Y. C. Chen. "Impact of Glucose Levels on Expression of Hypha-Associated Secreted Aspartyl Proteinases in Candida Albicans." *J Biomed Sci* 21 (2014): 22.

Cannon, R. D., E. Lamping, A. R. Holmes, K. Niimi, P. V. Baret, M. V. Keniya, K. Tanabe, M. Niimi, A. Goffeau, and B. C. Monk. "Efflux-Mediated Antifungal Drug Resistance." *Clin Microbiol Rev* 22, no. 2 (2009): 291-321, Table of Contents.

Cao, Y. Y., Y. B. Cao, Z. Xu, K. Ying, Y. Li, Y. Xie, Z. Y. Zhu, W. S. Chen, and Y. Y. Jiang. "Cdna Microarray Analysis of Differential Gene Expression in Candida Albicans Biofilm Exposed to Farnesol." *Antimicrob Agents Chemother* 49, no. 2 (2005): 584-9.

Cappelletty, D., and K. Eiselstein-McKitrick. "The Echinocandins." *Pharmacotherapy* 27, no. 3 (2007): 369-88.

Carlisle, P. L., M. Banerjee, A. Lazzell, C. Monteagudo, J. L. Lopez-Ribot, and D. Kadosh. "Expression Levels of a Filament-Specific Transcriptional Regulator Are Sufficient to Determine Candida Albicans Morphology and Virulence." *Proc Natl Acad Sci U S A* 106, no. 2 (2009): 599-604.

Carroll, J. S., C. A. Meyer, J. Song, W. Li, T. R. Geistlinger, J. Eeckhoute, A. S. Brodsky, E. K. Keeton, K. C. Fertuck, G. F. Hall, Q. Wang, S. Bekiranov, V. Sementchenko, E. A. Fox, P. A. Silver, T. R. Gingeras, X. S. Liu, and M. Brown. "Genome-Wide Analysis of Estrogen Receptor Binding Sites." *Nat Genet* 38, no. 11 (2006): 1289-97.

Caselle, M., F. Di Cunto, and P. Provero. "Correlating Overrepresented Upstream Motifs to Gene Expression: A Computational Approach to Regulatory Element Discovery in Eukaryotes." *BMC Bioinformatics* 3 (2002): 7.

Cassone, A. "Development of Vaccines for Candida Albicans: Fighting a Skilled Transformer." *Nat Rev Microbiol* 11, no. 12 (2013): 884-91.

Cassone, A., and R. Cauda. "Candida and Candidiasis in Hiv-Infected Patients: Where Commensalism, Opportunistic Behavior and Frank Pathogenicity Lose Their Borders." *AIDS* 26, no. 12 (2012): 1457-72.

Caudron, F., and Y. Barral. "Septins and the Lateral Compartmentalization of Eukaryotic Membranes." *Dev Cell* 16, no. 4 (2009): 493-506.

Chaffin, W. L., J. L. Lopez-Ribot, M. Casanova, D. Gozalbo, and J. P. Martinez. "Cell Wall and Secreted Proteins of Candida Albicans: Identification, Function, and Expression." *Microbiol Mol Biol Rev* 62, no. 1 (1998): 130-80.

Chamilos, G., C. J. Nobile, V. M. Bruno, R. E. Lewis, A. P. Mitchell, and D. P. Kontoyiannis. "Candida Albicans Cas5, a Regulator of Cell Wall Integrity, Is Required for Virulence in Murine and Toll Mutant Fly Models." *J Infect Dis* 200, no. 1 (2009): 152-7.

Chandra, J., D. M. Kuhn, P. K. Mukherjee, L. L. Hoyer, T. McCormick, and M. A. Ghannoum. "Biofilm Formation by the Fungal Pathogen Candida Albicans: Development, Architecture, and Drug Resistance." *J Bacteriol* 183, no. 18 (2001): 5385-94.

Chen, H., M. Fujita, Q. Feng, J. Clardy, and G. R. Fink. "Tyrosol Is a Quorum-Sensing Molecule in Candida Albicans." *Proc Natl Acad Sci U S A* 101, no. 14 (2004): 5048-52.

Chen, S. C., M. A. Slavin, and T. C. Sorrell. "Echinocandin Antifungal Drugs in Fungal Infections: A Comparison." *Drugs* 71, no. 1 (2011): 11-41.

Chen, Y., Q. Yu, H. Wang, Y. Dong, C. Jia, B. Zhang, C. Xiao, L. Xing, and M. Li. "The Malfunction of Peroxisome Has an Impact on the Oxidative Stress Sensitivity in Candida Albicans." *Fungal Genet Biol* 95 (2016): 1-12.

Chiranand, W., I. McLeod, H. Zhou, J. J. Lynn, L. A. Vega, H. Myers, J. R. Yates, 3rd, M. C. Lorenz, and M. C. Gustin. "Cta4 Transcription Factor Mediates Induction of Nitrosative Stress Response in Candida Albicans." *Eukaryot Cell* 7, no. 2 (2008): 268-78.

Chowdhury, T., and J. R. Kohler. "Ribosomal Protein S6 Phosphorylation Is Controlled by Tor and Modulated by Pka in Candida Albicans." *Mol Microbiol* 98, no. 2 (2015): 384-402.

Chua, G., Q. D. Morris, R. Sopko, M. D. Robinson, O. Ryan, E. T. Chan, B. J. Frey, B. J. Andrews, C. Boone, and T. R. Hughes. "Identifying Transcription Factor Functions and Targets by Phenotypic Activation." *Proc Natl Acad Sci U S A* 103, no. 32 (2006): 12045-50.

Cleary, I. A., P. Mulabagal, S. M. Reinhard, N. P. Yadev, C. Murdoch, M. H. Thornhill, A. L. Lazzell, C. Monteagudo, D. P. Thomas, and S. P. Saville. "Pseudohyphal Regulation by the Transcription Factor Rfg1p in Candida Albicans." *Eukaryot Cell* 9, no. 9 (2010): 1363-73.

Coffman, J. A., R. Rai, T. Cunningham, V. Svetlov, and T. G. Cooper. "Gat1p, a Gata Family Protein Whose Production Is Sensitive to Nitrogen Catabolite Repression, Participates in Transcriptional Activation of Nitrogen-Catabolic Genes in Saccharomyces Cerevisiae." *Mol Cell Biol* 16, no. 3 (1996): 847-58.

Coffman, J. A., R. Rai, D. M. Loprete, T. Cunningham, V. Svetlov, and T. G. Cooper. "Cross Regulation of Four Gata Factors That Control Nitrogen Catabolic Gene Expression in Saccharomyces Cerevisiae." *J Bacteriol* 179, no. 11 (1997): 3416-29.

Cooney, N. M., and B. S. Klein. "Fungal Adaptation to the Mammalian Host: It Is a New World, after All." *Curr Opin Microbiol* 11, no. 6 (2008): 511-6.

Cordeiro, R. A., C. E. Teixeira, R. S. Brilhante, D. S. Castelo-Branco, M. A. Paiva, J. J. Giffoni Leite, D. T. Lima, A. J. Monteiro, J. J. Sidrim, and M. F. Rocha. "Minimum Inhibitory Concentrations of Amphotericin B, Azoles and Caspofungin against

Candida Species Are Reduced by Farnesol." *Med Mycol* 51, no. 1 (2013): 53-9.

Coste, A. T., M. Karababa, F. Ischer, J. Bille, and D. Sanglard. "Tac1, Transcriptional Activator of Cdr Genes, Is a New Transcription Factor Involved in the Regulation of Candida Albicans Abc Transporters Cdr1 and Cdr2." *Eukaryot Cell* 3, no. 6 (2004): 1639-52.

Daniels, K. J., T. Srikantha, S. R. Lockhart, C. Pujol, and D. R. Soll. "Opaque Cells Signal White Cells to Form Biofilms in Candida Albicans." *EMBO J* 25, no. 10 (2006): 2240-52.

Davis, D. "Adaptation to Environmental Ph in Candida Albicans and Its Relation to Pathogenesis." *Curr Genet* 44, no. 1 (2003): 1-7.

Davis, D., J. E. Edwards, Jr., A. P. Mitchell, and A. S. Ibrahim. "Candida Albicans Rim101 Ph Response Pathway Is Required for Host-Pathogen Interactions." *Infect Immun* 68, no. 10 (2000): 5953-9.

Davis, D. A. "How Human Pathogenic Fungi Sense and Adapt to Ph: The Link to Virulence." *Curr Opin Microbiol* 12, no. 4 (2009): 365-70.

Davis, D. A., V. M. Bruno, L. Loza, S. G. Filler, and A. P. Mitchell. "Candida Albicans Mds3p, a Conserved Regulator of Ph Responses and Virulence Identified through Insertional Mutagenesis." *Genetics* 162, no. 4 (2002): 1573-81.

Davis-Hanna, A., A. E. Piispanen, L. I. Stateva, and D. A. Hogan. "Farnesol and Dodecanol Effects on the Candida Albicans Ras1-Camp Signalling Pathway and the Regulation of Morphogenesis." *Mol Microbiol* 67, no. 1 (2008): 47-62.

De Backer, M. D., D. Maes, S. Vandoninck, M. Logghe, R. Contreras, and W. H. Luyten. "Transformation of Candida Albicans by Electroporation." *Yeast* 15, no. 15 (1999): 1609-18.

De Backer, M. D., P. T. Magee, and J. Pla. "Recent Developments in Molecular Genetics of Candida Albicans." *Annu Rev Microbiol* 54 (2000): 463-98.

Delgado-Silva, Y., C. Vaz, J. Carvalho-Pereira, C. Carneiro, E. Nogueira, A. Correia, L. Carreto, S. Silva, A. Faustino, C. Pais, R. Oliveira, and P. Sampaio. "Participation of Candida Albicans Transcription Factor Rlm1 in Cell Wall Biogenesis and Virulence." *PLoS One* 9, no. 1 (2014): e86270.

Denning, D. W. "Echinocandin Antifungal Drugs." *Lancet* 362, no. 9390 (2003): 1142-51.

Desnos-Ollivier, M., S. Bretagne, D. Raoux, D. Hoinard, F. Dromer, and E. Dannaoui.

"Mutations in the Fks1 Gene in Candida Albicans, C. Tropicalis, and C. Krusei Correlate with Elevated Caspofungin Mics Uncovered in Am3 Medium Using the Method of the European Committee on Antibiotic Susceptibility Testing." *Antimicrob Agents Chemother* 52, no. 9 (2008): 3092-8.

Deveau, A., and D. A. Hogan. "Linking Quorum Sensing Regulation and Biofilm Formation by Candida Albicans." *Methods Mol Biol* 692 (2011): 219-33.

Dhamgaye, S., M. Bernard, G. Lelandais, O. Sismeiro, S. Lemoine, J. Y. Coppee, S. Le Crom, R. Prasad, and F. Devaux. "Rna Sequencing Revealed Novel Actors of the Acquisition of Drug Resistance in Candida Albicans." *BMC Genomics* 13 (2012): 396.

Dhillon, N. K., S. Sharma, and G. K. Khuller. "Signaling through Protein Kinases and Transcriptional Regulators in Candida Albicans." *Crit Rev Microbiol* 29, no. 3 (2003): 259-75.

Dichtl, K., S. Samantaray, and J. Wagener. "Cell Wall Integrity Signalling in Human Pathogenic Fungi." *Cell Microbiol* (2016).

Doedt, T., S. Krishnamurthy, D. P. Bockmuhl, B. Tebarth, C. Stempel, C. L. Russell, A. J. Brown, and J. F. Ernst. "Apses Proteins Regulate Morphogenesis and Metabolism in Candida Albicans." *Mol Biol Cell* 15, no. 7 (2004): 3167-80.

Douglas, L. M., and J. B. Konopka. "Fungal Membrane Organization: The Eisosome Concept." *Annu Rev Microbiol* 68 (2014): 377-93.

Douglas, L. M., H. X. Wang, and J. B. Konopka. "The Marvel Domain Protein Nce102 Regulates Actin Organization and Invasive Growth of Candida Albicans." *MBio* 4, no. 6 (2013): e00723-13.

Duhring, S., S. Germerodt, C. Skerka, P. F. Zipfel, T. Dandekar, and S. Schuster. "Host-Pathogen Interactions between the Human Innate Immune System and Candida Albicans-Understanding and Modeling Defense and Evasion Strategies." *Front Microbiol* 6 (2015): 625.

Dunkel, N., J. Blass, P. D. Rogers, and J. Morschhauser. "Mutations in the Multi-Drug Resistance Regulator Mrr1, Followed by Loss of Heterozygosity, Are the Main Cause of Mdr1 Overexpression in Fluconazole-Resistant Candida Albicans Strains." *Mol Microbiol* 69, no. 4 (2008): 827-40.

Dunkel, N., T. T. Liu, K. S. Barker, R. Homayouni, J. Morschhauser, and P. D. Rogers. "A Gain-of-Function Mutation in the Transcription Factor Upc2p Causes Upregulation of Ergosterol Biosynthesis Genes and Increased Fluconazole Resistance in a Clinical Candida Albicans Isolate." *Eukaryot Cell* 7, no. 7 (2008): 1180-90.

Eggimann, P., J. Garbino, and D. Pittet. "Management of Candida Species Infections in Critically Ill Patients." *Lancet Infect Dis* 3, no. 12 (2003): 772-85.

Eggimann, P., and D. Pittet. "Candida Colonization Index and Subsequent Infection in Critically Ill Surgical Patients: 20 Years Later." *Intensive Care Med* 40, no. 10 (2014): 1429-48.

Eggimann, P., Y. A. Que, J. P. Revelly, and J. L. Pagani. "Preventing Invasive Candida Infections. Where Could We Do Better?" *J Hosp Infect* 89, no. 4 (2015): 302-8.

Elson, S. L., S. M. Noble, N. V. Solis, S. G. Filler, and A. D. Johnson. "An Rna Transport System in Candida Albicans Regulates Hyphal Morphology and Invasive Growth." *PLoS Genet* 5, no. 9 (2009): e1000664.

Ene, I. V., A. K. Adya, S. Wehmeier, A. C. Brand, D. M. MacCallum, N. A. Gow, and A. J. Brown. "Host Carbon Sources Modulate Cell Wall Architecture, Drug Resistance and Virulence in a Fungal Pathogen." *Cell Microbiol* 14, no. 9 (2012): 1319-35.

Enjalbert, B., and M. Whiteway. "Release from Quorum-Sensing Molecules Triggers Hyphal Formation During Candida Albicans Resumption of Growth." *Eukaryot Cell* 4, no. 7 (2005): 1203-10.

Ernst, J. F., and J. Pla. "Signaling the Glycoshield: Maintenance of the Candida Albicans Cell Wall." *Int J Med Microbiol* 301, no. 5 (2011): 378-83.

Ernst, J. F., and D. Tielker. "Responses to Hypoxia in Fungal Pathogens." *Cell Microbiol* 11, no. 2 (2009): 183-90.

Eschenauer, G., D. D. Depestel, and P. L. Carver. "Comparison of Echinocandin Antifungals." *Ther Clin Risk Manag* 3, no. 1 (2007): 71-97.

Fayard, E., K. Schoonjans, and J. Auwerx. "Xol Inxs: Role of the Liver X and the Farnesol X Receptors." *Curr Opin Lipidol* 12, no. 2 (2001): 113-20.

Fidel, P. L., Jr. "Immunity to Candida." *Oral Dis* 8 Suppl 2 (2002): 69-75.

Finkel, J. S., W. Xu, D. Huang, E. M. Hill, J. V. Desai, C. A. Woolford, J. E. Nett, H. Taff, C. T. Norice, D. R. Andes, F. Lanni, and A. P. Mitchell. "Portrait of Candida Albicans Adherence Regulators." *PLoS Pathog* 8, no. 2 (2012): e1002525.

Fleck, C. B., F. Schobel, and M. Brock. "Nutrient Acquisition by Pathogenic Fungi: Nutrient Availability, Pathway Regulation, and Differences in Substrate Utilization." *Int J Med Microbiol* 301, no. 5 (2011): 400-7.

Flores, C. L., C. Rodriguez, T. Petit, and C. Gancedo. "Carbohydrate and Energy-Yielding Metabolism in Non-Conventional Yeasts." *FEMS Microbiol Rev* 24, no. 4 (2000): 507-29.

Flowers, S. A., K. S. Barker, E. L. Berkow, G. Toner, S. G. Chadwick, S. E. Gygax, J. Morschhauser, and P. D. Rogers. "Gain-of-Function Mutations in Upc2 Are a Frequent Cause of Erg11 Upregulation in Azole-Resistant Clinical Isolates of Candida Albicans." *Eukaryot Cell* 11, no. 10 (2012): 1289-99.

Flowers, S. A., B. Colon, S. G. Whaley, M. A. Schuler, and P. D. Rogers. "Contribution of Clinically Derived Mutations in Erg11 to Azole Resistance in Candida Albicans." *Antimicrob Agents Chemother* 59, no. 1 (2015): 450-60.

Fonzi, W. A., and M. Y. Irwin. "Isogenic Strain Construction and Gene Mapping in Candida Albicans." *Genetics* 134, no. 3 (1993): 717-28.

Forman, B. M., E. Goode, J. Chen, A. E. Oro, D. J. Bradley, T. Perlmann, D. J. Noonan, L. T. Burka, T. McMorris, W. W. Lamph, R. M. Evans, and C. Weinberger. "Identification of a Nuclear Receptor That Is Activated by Farnesol Metabolites." *Cell* 81, no. 5 (1995): 687-93.

Fox, E. P., C. K. Bui, J. E. Nett, N. Hartooni, M. C. Mui, D. R. Andes, C. J. Nobile, and A. D. Johnson. "An Expanded Regulatory Network Temporally Controls Candida Albicans Biofilm Formation." *Mol Microbiol* 96, no. 6 (2015): 1226-39.

Fradin, C., M. Kretschmar, T. Nichterlein, C. Gaillardin, C. d'Enfert, and B. Hube. "Stage-Specific Gene Expression of Candida Albicans in Human Blood." *Mol Microbiol* 47, no. 6 (2003): 1523-43.

Frohner, I. E., C. Bourgeois, K. Yatsyk, O. Majer, and K. Kuchler. "Candida Albicans Cell Surface Superoxide Dismutases Degrade Host-Derived Reactive Oxygen Species to Escape Innate Immune Surveillance." *Mol Microbiol* 71, no. 1 (2009): 240-52.

Galan-Diez, M., D. M. Arana, D. Serrano-Gomez, L. Kremer, J. M. Casasnovas, M. Ortega, A. Cuesta-Dominguez, A. L. Corbi, J. Pla, and E. Fernandez-Ruiz. "Candida Albicans Beta-Glucan Exposure Is Controlled by the Fungal Cek1-Mediated Mitogen-Activated Protein Kinase Pathway That Modulates Immune Responses Triggered through Dectin-1." *Infect Immun* 78, no. 4 (2010): 1426-36.

Ganguly, S., A. C. Bishop, W. Xu, S. Ghosh, K. W. Nickerson, F. Lanni, J. Patton-Vogt, and A. P. Mitchell. "Zap1 Control of Cell-Cell Signaling in Candida Albicans Biofilms." *Eukaryot Cell* 10, no. 11 (2011): 1448-54.

Geiger, J., D. Wessels, S. R. Lockhart, and D. R. Soll. "Release of a Potent Polymorphonuclear Leukocyte Chemoattractant Is Regulated by White-Opaque Switching in Candida Albicans." *Infect Immun* 72, no. 2 (2004): 667-77.

Gentleman, V. Carey, S. Dudoit, R. Irizarry, W. Huber "Bioconductor R." *Bioinformatics and Computational Biology Solutions using R* (2005).

Georis, I., A. Feller, J. J. Tate, T. G. Cooper, and E. Dubois. "Nitrogen Catabolite Repression-Sensitive Transcription as a Readout of Tor Pathway Regulation: The Genetic Background, Reporter Gene and Gata Factor Assayed Determine the Outcomes." *Genetics* 181, no. 3 (2009): 861-74.

Georis, I., J. J. Tate, F. Vierendeels, T. G. Cooper, and E. Dubois. "Premature Termination of Gat1 Transcription Explains Paradoxical Negative Correlation between Nitrogen-Responsive Mrna, but Constitutive Low-Level Protein Production." *RNA Biol* 12, no. 8 (2015): 824-37.

Ghosh, S., D. H. Navarathna, D. D. Roberts, J. T. Cooper, A. L. Atkin, T. M. Petro, and K. W. Nickerson. "Arginine-Induced Germ Tube Formation in Candida Albicans Is Essential for Escape from Murine Macrophage Line Raw 264.7." *Infect Immun* 77, no. 4 (2009): 1596-605.

Gillum, A. M., E. Y. Tsay, and D. R. Kirsch. "Isolation of the Candida Albicans Gene for Orotidine-5'-Phosphate Decarboxylase by Complementation of S. Cerevisiae Ura3 and E. Coli Pyrf Mutations." *Mol Gen Genet* 198, no. 2 (1984): 179-82.

Giusani, A. D., M. Vinces, and C. A. Kumamoto. "Invasive Filamentous Growth of Candida Albicans Is Promoted by Czf1p-Dependent Relief of Efg1p-Mediated Repression." *Genetics* 160, no. 4 (2002): 1749-53.

Goncalves, S. S., A. C. Souza, A. Chowdhary, J. F. Meis, and A. L. Colombo. "Epidemiology and Molecular Mechanisms of Antifungal Resistance in Candida and Aspergillus." *Mycoses* (2016).

Gow, N. A., F. L. van de Veerdonk, A. J. Brown, and M. G. Netea. "Candida Albicans Morphogenesis and Host Defence: Discriminating Invasion from Colonization." *Nat Rev Microbiol* 10, no. 2 (2011): 112-22.

Gropp, K., L. Schild, S. Schindler, B. Hube, P. F. Zipfel, and C. Skerka. "The Yeast Candida Albicans Evades Human Complement Attack by Secretion of Aspartic Proteases." *Mol Immunol* 47, no. 2-3 (2009): 465-75.

Grubb, S. E., C. Murdoch, P. E. Sudbery, S. P. Saville, J. L. Lopez-Ribot, and M. H. Thornhill. "Candida Albicans-Endothelial Cell Interactions: A Key Step in the Pathogenesis of

Systemic Candidiasis." *Infect Immun* 76, no. 10 (2008): 4370-7.

Grumaz, C., S. Lorenz, P. Stevens, E. Lindemann, U. Schock, J. Retey, S. Rupp, and K. Sohn. "Species and Condition Specific Adaptation of the Transcriptional Landscapes in Candida Albicans and Candida Dubliniensis." *BMC Genomics* 14 (2013): 212.

Hall, R. A., K. J. Turner, J. Chaloupka, F. Cottier, L. De Sordi, D. Sanglard, L. R. Levin, J. Buck, and F. A. Muhlschlegel. "The Quorum-Sensing Molecules Farnesol/Homoserine Lactone and Dodecanol Operate Via Distinct Modes of Action in Candida Albicans." *Eukaryot Cell* 10, no. 8 (2011): 1034-42.

Han, T. L., R. D. Cannon, and S. G. Villas-Boas. "The Metabolic Basis of Candida Albicans Morphogenesis and Quorum Sensing." *Fungal Genet Biol* 48, no. 8 (2011): 747-63.

Hao, B., C. J. Clancy, S. Cheng, S. B. Raman, K. A. Iczkowski, and M. H. Nguyen. "Candida Albicans Rfx2 Encodes a DNA Binding Protein Involved in DNA Damage Responses, Morphogenesis, and Virulence." *Eukaryot Cell* 8, no. 4 (2009): 627-39.

Haycocks, J. R., and D. C. Grainger. "Unusually Situated Binding Sites for Bacterial Transcription Factors Can Have Hidden Functionality." *PLoS One* 11, no. 6 (2016): e0157016.

Herrero, E., J. Ros, G. Belli, and E. Cabiscol. "Redox Control and Oxidative Stress in Yeast Cells." *Biochim Biophys Acta* 1780, no. 11 (2008): 1217-35.

Hiller, D., S. Stahl, and J. Morschhauser. "Multiple Cis-Acting Sequences Mediate Upregulation of the Mdr1 Efflux Pump in a Fluconazole-Resistant Clinical Candida Albicans Isolate." *Antimicrob Agents Chemother* 50, no. 7 (2006): 2300-8.

Hiramatsu, Y., Y. Maeda, N. Fujii, T. Saito, Y. Nawa, M. Hara, T. Yano, S. Asakura, K. Sunami, T. Tabayashi, A. Miyata, K. Matsuoka, K. Shinagawa, K. Ikeda, K. Matsuo, and M. Tanimoto. "Use of Micafungin Versus Fluconazole for Antifungal Prophylaxis in Neutropenic Patients Receiving Hematopoietic Stem Cell Transplantation." *Int J Hematol* 88, no. 5 (2008): 588-95.

Hogan, D. A. "Talking to Themselves: Autoregulation and Quorum Sensing in Fungi." *Eukaryot Cell* 5, no. 4 (2006): 613-9.

Hogan, D. A., A. Vik, and R. Kolter. "A Pseudomonas Aeruginosa Quorum-Sensing Molecule Influences Candida Albicans Morphology." *Mol Microbiol* 54, no. 5 (2004): 1212-23.

Homann, O. R., J. Dea, S. M. Noble, and A. D. Johnson. "A Phenotypic Profile of the Candida Albicans Regulatory Network." *PLoS Genet* 5, no. 12 (2009): e1000783.

Hoot, S. J., A. R. Smith, R. P. Brown, and T. C. White. "An A643v Amino Acid Substitution in Upc2p Contributes to Azole Resistance in Well-Characterized Clinical Isolates of Candida Albicans." *Antimicrob Agents Chemother* 55, no. 2 (2011): 940-2.

Horak, J. "Regulations of Sugar Transporters: Insights from Yeast." *Curr Genet* 59, no. 1-2 (2013): 1-31.

Hornby, J. M., E. C. Jensen, A. D. Lisec, J. J. Tasto, B. Jahnke, R. Shoemaker, P. Dussault, and K. W. Nickerson. "Quorum Sensing in the Dimorphic Fungus Candida Albicans Is Mediated by Farnesol." *Appl Environ Microbiol* 67, no. 7 (2001): 2982-92.

Hornby, J. M., B. W. Kebaara, and K. W. Nickerson. "Farnesol Biosynthesis in Candida Albicans: Cellular Response to Sterol Inhibition by Zaragozic Acid B." *Antimicrob Agents Chemother* 47, no. 7 (2003): 2366-9.

Hornby, J. M., and K. W. Nickerson. "Enhanced Production of Farnesol by Candida Albicans Treated with Four Azoles." *Antimicrob Agents Chemother* 48, no. 6 (2004): 2305-7.

Hoyer, L. L., and E. Cota. "Candida Albicans Agglutinin-Like Sequence (Als) Family Vignettes: A Review of Als Protein Structure and Function." *Front Microbiol* 7 (2016): 280.

Hoyer, L. L., C. B. Green, S. H. Oh, and X. Zhao. "Discovering the Secrets of the Candida Albicans Agglutinin-Like Sequence (Als) Gene Family--a Sticky Pursuit." *Med Mycol* 46, no. 1 (2008): 1-15.

Huang, G. "Regulation of Phenotypic Transitions in the Fungal Pathogen Candida Albicans." *Virulence* 3, no. 3 (2012): 251-61.

Huang, G., T. Srikantha, N. Sahni, S. Yi, and D. R. Soll. "Co(2) Regulates White-to-Opaque Switching in Candida Albicans." *Curr Biol* 19, no. 4 (2009): 330-4.

Hube, B., F. Stehr, M. Bossenz, A. Mazur, M. Kretschmar, and W. Schafer. "Secreted Lipases of Candida Albicans: Cloning, Characterisation and Expression Analysis of a New Gene Family with at Least Ten Members." *Arch Microbiol* 174, no. 5 (2000): 362-74.

Hurst, L. D., C. Pal, and M. J. Lercher. "The Evolutionary Dynamics of Eukaryotic Gene Order." *Nat Rev Genet* 5, no. 4 (2004): 299-310.

Inglis, D. O., M. B. Arnaud, J. Binkley, P. Shah, M. S. Skrzypek, F. Wymore, G. Binkley, S. R. Miyasato, M. Simison, and G. Sherlock. "The Candida Genome Database Incorporates Multiple Candida Species: Multispecies Search and Analysis Tools with Curated Gene and Protein Information for Candida Albicans and Candida Glabrata."

Nucleic Acids Res 40, no. Database issue (2012): D667-74.

Ishihama, A., T. Shimada, and Y. Yamazaki. "Transcription Profile of Escherichia Coli: Genomic Selex Search for Regulatory Targets of Transcription Factors." *Nucleic Acids Res* 44, no. 5 (2016): 2058-74.

Jabra-Rizk, M. A., W. A. Falkler, and T. F. Meiller. "Fungal Biofilms and Drug Resistance." *Emerg Infect Dis* 10, no. 1 (2004): 14-9.

Jabra-Rizk, M. A., M. Shirtliff, C. James, and T. Meiller. "Effect of Farnesol on Candida Dubliniensis Biofilm Formation and Fluconazole Resistance." *FEMS Yeast Res* 6, no. 7 (2006): 1063-73.

Jacobsen, I. D., D. Wilson, B. Wachtler, S. Brunke, J. R. Naglik, and B. Hube. "Candida Albicans Dimorphism as a Therapeutic Target." *Expert Rev Anti Infect Ther* 10, no. 1 (2012): 85-93.

Jimenez-Lopez, C., and M. C. Lorenz. "Fungal Immune Evasion in a Model Host-Pathogen Interaction: Candida Albicans Versus Macrophages." *PLoS Pathog* 9, no. 11 (2013): e1003741.

Jin, Y., L. P. Samaranayake, Y. Samaranayake, and H. K. Yip. "Biofilm Formation of Candida Albicans Is Variably Affected by Saliva and Dietary Sugars." *Arch Oral Biol* 49, no. 10 (2004): 789-98.

Jones, T., N. A. Federspiel, H. Chibana, J. Dungan, S. Kalman, B. B. Magee, G. Newport, Y. R. Thorstenson, N. Agabian, P. T. Magee, R. W. Davis, and S. Scherer. "The Diploid Genome Sequence of Candida Albicans." *Proc Natl Acad Sci U S A* 101, no. 19 (2004): 7329-34.

Karababa, M., E. Valentino, G. Pardini, A. T. Coste, J. Bille, and D. Sanglard. "Crz1, a Target of the Calcineurin Pathway in Candida Albicans." *Mol Microbiol* 59, no. 5 (2006): 1429-51.

Kebaara, B. W., M. L. Langford, D. H. Navarathna, R. Dumitru, K. W. Nickerson, and A. L. Atkin. "Candida Albicans Tup1 Is Involved in Farnesol-Mediated Inhibition of Filamentous-Growth Induction." *Eukaryot Cell* 7, no. 6 (2008): 980-7.

Kelly, S. L., D. C. Lamb, A. J. Corran, B. C. Baldwin, and D. E. Kelly. "Mode of Action and Resistance to Azole Antifungals Associated with the Formation of 14 Alpha-Methylergosta-8,24(28)-Dien-3 Beta,6 Alpha-Diol." *Biochem Biophys Res Commun* 207, no. 3 (1995): 910-5.

Kelly, S. L., D. C. Lamb, D. E. Kelly, N. J. Manning, J. Loeffler, H. Hebart, U. Schumacher,

and H. Einsele. "Resistance to Fluconazole and Cross-Resistance to Amphotericin B in Candida Albicans from Aids Patients Caused by Defective Sterol Delta5,6-Desaturation." *FEBS Lett* 400, no. 1 (1997): 80-2.

Kennedy, M. J., A. L. Rogers, L. R. Hanselmen, D. R. Soll, and R. J. Yancey, Jr. "Variation in Adhesion and Cell Surface Hydrophobicity in Candida Albicans White and Opaque Phenotypes." *Mycopathologia* 102, no. 3 (1988): 149-56.

Kim, J., and P. Sudbery. "Candida Albicans, a Major Human Fungal Pathogen." *J Microbiol* 49, no. 2 (2011): 171-7.

Kim, S., S. K. Balakrishnan, and D. S. Gross. "P53 Interacts with Rna Polymerase Ii through Its Core Domain and Impairs Pol Ii Processivity in Vivo." *PLoS One* 6, no. 8 (2011): e22183.

Kirchhoff, L. V., S. Hieny, G. M. Shiver, D. Snary, and A. Sher. "Cryptic Epitope Explains the Failure of a Monoclonal Antibody to Bind to Certain Isolates of Trypanosoma Cruzi." *J Immunol* 133, no. 5 (1984): 2731-5.

Kruglyak, S., and H. Tang. "Regulation of Adjacent Yeast Genes." *Trends Genet* 16, no. 3 (2000): 109-11.

Kruppa, M., B. P. Krom, N. Chauhan, A. V. Bambach, R. L. Cihlar, and R. A. Calderone. "The Two-Component Signal Transduction Protein Chk1p Regulates Quorum Sensing in Candida Albicans." *Eukaryot Cell* 3, no. 4 (2004): 1062-5.

Kumamoto, C. A. "A Contact-Activated Kinase Signals Candida Albicans Invasive Growth and Biofilm Development." *Proc Natl Acad Sci U S A* 102, no. 15 (2005): 5576-81.

Kumamoto, C. A., and M. D. Vinces. "Contributions of Hyphae and Hypha-Co-Regulated Genes to Candida Albicans Virulence." *Cell Microbiol* 7, no. 11 (2005): 1546-54.

Kvaal, C., S. A. Lachke, T. Srikantha, K. Daniels, J. McCoy, and D. R. Soll. "Misexpression of the Opaque-Phase-Specific Gene Pep1 (Sap1) in the White Phase of Candida Albicans Confers Increased Virulence in a Mouse Model of Cutaneous Infection." *Infect Immun* 67, no. 12 (1999): 6652-62.

Kvaal, C. A., T. Srikantha, and D. R. Soll. "Misexpression of the White-Phase-Specific Gene Wh11 in the Opaque Phase of Candida Albicans Affects Switching and Virulence." *Infect Immun* 65, no. 11 (1997): 4468-75.

Lachke, S. A., T. Srikantha, and D. R. Soll. "The Regulation of Efg1 in White-Opaque Switching in Candida Albicans Involves Overlapping Promoters." *Mol Microbiol* 48, no. 2 (2003): 523-36.

Lackner, M., M. Tscherner, M. Schaller, K. Kuchler, C. Mair, B. Sartori, F. Istel, M. C. Arendrup, and C. Lass-Florl. "Positions and Numbers of Fks Mutations in Candida Albicans Selectively Influence in Vitro and in Vivo Susceptibilities to Echinocandin Treatment." *Antimicrob Agents Chemother* 58, no. 7 (2014): 3626-35.

Lamb, D. C., D. E. Kelly, T. C. White, and S. L. Kelly. "The R467k Amino Acid Substitution in Candida Albicans Sterol 14alpha-Demethylase Causes Drug Resistance through Reduced Affinity." *Antimicrob Agents Chemother* 44, no. 1 (2000): 63-7.

Lan, C. Y., G. Newport, L. A. Murillo, T. Jones, S. Scherer, R. W. Davis, and N. Agabian. "Metabolic Specialization Associated with Phenotypic Switching in Candidaalbicans." *Proc Natl Acad Sci U S A* 99, no. 23 (2002): 14907-12.

Langford, M. L., J. C. Hargarten, K. D. Patefield, E. Marta, J. R. Blankenship, S. Fanning, K. W. Nickerson, and A. L. Atkin. "Candida Albicans Czf1 and Efg1 Coordinate the Response to Farnesol During Quorum Sensing, White-Opaque Thermal Dimorphism, and Cell Death." *Eukaryot Cell* 12, no. 9 (2013): 1281-92.

Lavoie, H., A. Sellam, C. Askew, A. Nantel, and M. Whiteway. "A Toolbox for Epitope-Tagging and Genome-Wide Location Analysis in Candida Albicans." *BMC Genomics* 9 (2008): 578.

Lee, K. K., D. M. Maccallum, M. D. Jacobsen, L. A. Walker, F. C. Odds, N. A. Gow, and C. A. Munro. "Elevated Cell Wall Chitin in Candida Albicans Confers Echinocandin Resistance in Vivo." *Antimicrob Agents Chemother* 56, no. 1 (2012): 208-17.

Leidich, S. D., A. S. Ibrahim, Y. Fu, A. Koul, C. Jessup, J. Vitullo, W. Fonzi, F. Mirbod, S. Nakashima, Y. Nozawa, and M. A. Ghannoum. "Cloning and Disruption of Caplb1, a Phospholipase B Gene Involved in the Pathogenicity of Candida Albicans." *J Biol Chem* 273, no. 40 (1998): 26078-86.

Levitz, S. M. "Overview of Host Defenses in Fungal Infections." *Clin Infect Dis* 14 Suppl 1 (1992): S37-42.

Li, M., V. Valsakumar, K. Poorey, S. Bekiranov, and J. S. Smith. "Genome-Wide Analysis of Functional Sirtuin Chromatin Targets in Yeast." *Genome Biol* 14, no. 5 (2013): R48.

Li, X., Y. Hou, L. Yue, S. Liu, J. Du, and S. Sun. "Potential Targets for Antifungal Drug Discovery Based on Growth and Virulence in Candida Albicans." *Antimicrob Agents Chemother* 59, no. 10 (2015): 5885-91.

Liao, W. L., A. M. Ramon, and W. A. Fonzi. "Gln3 Encodes a Global Regulator of Nitrogen Metabolism and Virulence of C. Albicans." *Fungal Genet Biol* 45, no. 4 (2008): 514-26.

Limjindaporn, T., R. A. Khalaf, and W. A. Fonzi. "Nitrogen Metabolism and Virulence of Candida Albicans Require the Gata-Type Transcriptional Activator Encoded by Gat1." *Mol Microbiol* 50, no. 3 (2003): 993-1004.

Lionakis, M. S. "New Insights into Innate Immune Control of Systemic Candidiasis." *Med Mycol* 52, no. 6 (2014): 555-64.

Liu, T. T., S. Znaidi, K. S. Barker, L. Xu, R. Homayouni, S. Saidane, J. Morschhauser, A. Nantel, M. Raymond, and P. D. Rogers. "Genome-Wide Expression and Location Analyses of the Candida Albicans Tac1p Regulon." *Eukaryot Cell* 6, no. 11 (2007): 2122-38.

Ljungdahl, P. O., and B. Daignan-Fornier. "Regulation of Amino Acid, Nucleotide, and Phosphate Metabolism in Saccharomyces Cerevisiae." *Genetics* 190, no. 3 (2012): 885-929.

Lockhart, S. R., C. Pujol, K. J. Daniels, M. G. Miller, A. D. Johnson, M. A. Pfaller, and D. R. Soll. "In Candida Albicans, White-Opaque Switchers Are Homozygous for Mating Type." *Genetics* 162, no. 2 (2002): 737-45.

Lohse, M. B., and A. D. Johnson. "Identification and Characterization of Wor4, a New Transcriptional Regulator of White-Opaque Switching." *G3 (Bethesda)* 6, no. 3 (2016): 721-9.

Lopez-Ribot, J. L., R. K. McAtee, L. N. Lee, W. R. Kirkpatrick, T. C. White, D. Sanglard, and T. F. Patterson. "Distinct Patterns of Gene Expression Associated with Development of Fluconazole Resistance in Serial Candida Albicans Isolates from Human Immunodeficiency Virus-Infected Patients with Oropharyngeal Candidiasis." *Antimicrob Agents Chemother* 42, no. 11 (1998): 2932-7.

Lorenz, M. C., J. A. Bender, and G. R. Fink. "Transcriptional Response of Candida Albicans Upon Internalization by Macrophages." *Eukaryot Cell* 3, no. 5 (2004): 1076-87.

Lorenz, M. C., and G. R. Fink. "The Glyoxylate Cycle Is Required for Fungal Virulence." *Nature* 412, no. 6842 (2001): 83-6.

Luo, S., A. M. Blom, S. Rupp, U. C. Hipler, B. Hube, C. Skerka, and P. F. Zipfel. "The Ph-Regulated Antigen 1 of Candida Albicans Binds the Human Complement Inhibitor C4b-Binding Protein and Mediates Fungal Complement Evasion." *J Biol Chem* 286, no. 10 (2011): 8021-9.

MacPherson, S., B. Akache, S. Weber, X. De Deken, M. Raymond, and B. Turcotte. "Candida Albicans Zinc Cluster Protein Upc2p Confers Resistance to Antifungal

Drugs and Is an Activator of Ergosterol Biosynthetic Genes." *Antimicrob Agents Chemother* 49, no. 5 (2005): 1745-52.

MacPherson, S., M. Larochelle, and B. Turcotte. "A Fungal Family of Transcriptional Regulators: The Zinc Cluster Proteins." *Microbiol Mol Biol Rev* 70, no. 3 (2006): 583-604.

Magasanik, B., and C. A. Kaiser. "Nitrogen Regulation in Saccharomyces Cerevisiae." *Gene* 290, no. 1-2 (2002): 1-18.

Magee, P. T. "Fungal Pathogenicity and Morphological Switches." *Nat Genet* 42, no. 7 (2010): 560-1.

Magee, P. T., L. Bowdin, and J. Staudinger. "Comparison of Molecular Typing Methods for Candida Albicans." *J Clin Microbiol* 30, no. 10 (1992): 2674-9.

Manavathu, E. K., M. S. Ramesh, I. Baskaran, L. T. Ganesan, and P. H. Chandrasekar. "A Comparative Study of the Post-Antifungal Effect (Pafe) of Amphotericin B, Triazoles and Echinocandins on Aspergillus Fumigatus and Candida Albicans." *J Antimicrob Chemother* 53, no. 2 (2004): 386-9.

Marco, F., S. R. Lockhart, M. A. Pfaller, C. Pujol, M. S. Rangel-Frausto, T. Wiblin, H. M. Blumberg, J. E. Edwards, W. Jarvis, L. Saiman, J. E. Patterson, M. G. Rinaldi, R. P. Wenzel, and D. R. Soll. "Elucidating the Origins of Nosocomial Infections with Candida Albicans by DNA Fingerprinting with the Complex Probe Ca3." *J Clin Microbiol* 37, no. 9 (1999): 2817-28.

Marichal, P., L. Koymans, S. Willemsens, D. Bellens, P. Verhasselt, W. Luyten, M. Borgers, F. C. Ramaekers, F. C. Odds, and H. V. Bossche. "Contribution of Mutations in the Cytochrome P450 14alpha-Demethylase (Erg11p, Cyp51p) to Azole Resistance in Candida Albicans." *Microbiology* 145 (Pt 10) (1999): 2701-13.

Martchenko, M., A. Levitin, H. Hogues, A. Nantel, and M. Whiteway. "Transcriptional Rewiring of Fungal Galactose-Metabolism Circuitry." *Curr Biol* 17, no. 12 (2007): 1007-13.

Martel, C. M., J. E. Parker, O. Bader, M. Weig, U. Gross, A. G. Warrilow, N. Rolley, D. E. Kelly, and S. L. Kelly. "Identification and Characterization of Four Azole-Resistant Erg3 Mutants of Candida Albicans." *Antimicrob Agents Chemother* 54, no. 11 (2010): 4527-33.

Martin, R., D. Albrecht-Eckardt, S. Brunke, B. Hube, K. Hunniger, and O. Kurzai. "A Core Filamentation Response Network in Candida Albicans Is Restricted to Eight Genes." *PLoS One* 8, no. 3 (2013): e58613.

Martins, M., M. Henriques, J. Azeredo, S. M. Rocha, M. A. Coimbra, and R. Oliveira. "Morphogenesis Control in Candida Albicans and Candida Dubliniensis through Signaling Molecules Produced by Planktonic and Biofilm Cells." *Eukaryot Cell* 6, no. 12 (2007): 2429-36.

Martins, N., I. C. Ferreira, L. Barros, S. Silva, and M. Henriques. "Candidiasis: Predisposing Factors, Prevention, Diagnosis and Alternative Treatment." *Mycopathologia* 177, no. 5-6 (2014): 223-40.

Mathe, L., and P. Van Dijck. "Recent Insights into Candida Albicans Biofilm Resistance Mechanisms." *Curr Genet* 59, no. 4 (2013): 251-64.

Mayer, F. L., D. Wilson, and B. Hube. "Candida Albicans Pathogenicity Mechanisms." *Virulence* 4, no. 2 (2013): 119-28.

Mayer, F. L., D. Wilson, I. D. Jacobsen, P. Miramon, S. Slesiona, I. M. Bohovych, A. J. Brown, and B. Hube. "Small but Crucial: The Novel Small Heat Shock Protein Hsp21 Mediates Stress Adaptation and Virulence in Candida Albicans." *PLoS One* 7, no. 6 (2012): e38584.

McManus, B. A., and D. C. Coleman. "Molecular Epidemiology, Phylogeny and Evolution of Candida Albicans." *Infect Genet Evol* 21 (2014): 166-78.

Miao, H., L. Zhao, C. Li, Q. Shang, H. Lu, Z. Fu, L. Wang, Y. Jiang, and Y. Cao. "Inhibitory Effect of Shikonin on Candida Albicans Growth." *Biol Pharm Bull* 35, no. 11 (2012): 1956-63.

Miller, M. G., and A. D. Johnson. "White-Opaque Switching in Candida Albicans Is Controlled by Mating-Type Locus Homeodomain Proteins and Allows Efficient Mating." *Cell* 110, no. 3 (2002): 293-302.

Millsop, J. W., and N. Fazel. "Oral Candidiasis." *Clin Dermatol* 34, no. 4 (2016): 487-94.

Min, K., Y. Ichikawa, C. A. Woolford, and A. P. Mitchell. "Candida Albicans Gene Deletion with a Transient Crispr-Cas9 System." *mSphere* 1, no. 3 (2016).

Minch, K. J., T. R. Rustad, E. J. Peterson, J. Winkler, D. J. Reiss, S. Ma, M. Hickey, W. Brabant, B. Morrison, S. Turkarslan, C. Mawhinney, J. E. Galagan, N. D. Price, N. S. Baliga, and D. R. Sherman. "The DNA-Binding Network of Mycobacterium Tuberculosis." *Nat Commun* 6 (2015): 5829.

Miramon, P., L. Kasper, and B. Hube. "Thriving within the Host: Candida Spp. Interactions with Phagocytic Cells." *Med Microbiol Immunol* 202, no. 3 (2013): 183-95.

Mitchell, B. M., T. G. Wu, B. E. Jackson, and K. R. Wilhelmus. "Candida Albicans Strain-Dependent Virulence and Rim13p-Mediated Filamentation in Experimental Keratomycosis." *Invest Ophthalmol Vis Sci* 48, no. 2 (2007): 774-80.

Morio, F., C. Loge, B. Besse, C. Hennequin, and P. Le Pape. "Screening for Amino Acid Substitutions in the Candida Albicans Erg11 Protein of Azole-Susceptible and Azole-Resistant Clinical Isolates: New Substitutions and a Review of the Literature." *Diagn Microbiol Infect Dis* 66, no. 4 (2010): 373-84.

Morschhauser, J. "Regulation of White-Opaque Switching in Candida Albicans." *Med Microbiol Immunol* 199, no. 3 (2010): 165-72.

Morschhauser, J. "Nitrogen Regulation of Morphogenesis and Protease Secretion in Candida Albicans." *Int J Med Microbiol* 301, no. 5 (2011): 390-4.

Morschhauser, J. "The Development of Fluconazole Resistance in Candida Albicans - an Example of Microevolution of a Fungal Pathogen." *J Microbiol* 54, no. 3 (2016): 192-201.

Morschhauser, J., K. S. Barker, T. T. Liu, B. Warmuth J. Bla, R. Homayouni, and P. D. Rogers. "The Transcription Factor Mrr1p Controls Expression of the Mdr1 Efflux Pump and Mediates Multidrug Resistance in Candida Albicans." *PLoS Pathog* 3, no. 11 (2007): e164.

Moudgal, V., and J. Sobel. "Antifungals to Treat Candida Albicans." *Expert Opin Pharmacother* 11, no. 12 (2010): 2037-48.

Muhlschlegel, F. A., and W. A. Fonzi. "Phr2 of Candida Albicans Encodes a Functional Homolog of the Ph-Regulated Gene Phr1 with an Inverted Pattern of Ph-Dependent Expression." *Mol Cell Biol* 17, no. 10 (1997): 5960-7.

Mulhern, S. M., M. E. Logue, and G. Butler. "Candida Albicans Transcription Factor Ace2 Regulates Metabolism and Is Required for Filamentation in Hypoxic Conditions." *Eukaryot Cell* 5, no. 12 (2006): 2001-13.

Murad, A. M., C. d'Enfert, C. Gaillardin, H. Tournu, F. Tekaia, D. Talibi, D. Marechal, V. Marchais, J. Cottin, and A. J. Brown. "Transcript Profiling in Candida Albicans Reveals New Cellular Functions for the Transcriptional Repressors Catup1, Camig1 and Canrg1." *Mol Microbiol* 42, no. 4 (2001): 981-93.

Naglik, J. R., S. J. Challacombe, and B. Hube. "Candida Albicans Secreted Aspartyl Proteinases in Virulence and Pathogenesis." *Microbiol Mol Biol Rev* 67, no. 3 (2003): 400-28, table of contents.

Nailis, H., S. Kucharikova, M. Ricicova, P. Van Dijck, D. Deforce, H. Nelis, and T. Coenye. "Real-Time Pcr Expression Profiling of Genes Encoding Potential Virulence Factors in Candida Albicans Biofilms: Identification of Model-Dependent and -Independent Gene Expression." *BMC Microbiol* 10 (2010): 114.

Nantel, A., D. Dignard, C. Bachewich, D. Harcus, A. Marcil, A. P. Bouin, C. W. Sensen, H. Hogues, M. van het Hoog, P. Gordon, T. Rigby, F. Benoit, D. C. Tessier, D. Y. Thomas, and M. Whiteway. "Transcription Profiling of Candida Albicans Cells Undergoing the Yeast-to-Hyphal Transition." *Mol Biol Cell* 13, no. 10 (2002): 3452-65.

Navarathna, D. H., J. M. Hornby, N. Hoerrmann, A. M. Parkhurst, G. E. Duhamel, and K. W. Nickerson. "Enhanced Pathogenicity of Candida Albicans Pre-Treated with Subinhibitory Concentrations of Fluconazole in a Mouse Model of Disseminated Candidiasis." *J Antimicrob Chemother* 56, no. 6 (2005): 1156-9.

Navarathna, D. H., J. M. Hornby, N. Krishnan, A. Parkhurst, G. E. Duhamel, and K. W. Nickerson. "Effect of Farnesol on a Mouse Model of Systemic Candidiasis, Determined by Use of a Dpp3 Knockout Mutant of Candida Albicans." *Infect Immun* 75, no. 4 (2007): 1609-18.

Navarathna, D. H., K. W. Nickerson, G. E. Duhamel, T. R. Jerrels, and T. M. Petro. "Exogenous Farnesol Interferes with the Normal Progression of Cytokine Expression During Candidiasis in a Mouse Model." *Infect Immun* 75, no. 8 (2007): 4006-11.

Netea, M. G., L. A. Joosten, J. W. van der Meer, B. J. Kullberg, and F. L. van de Veerdonk. "Immune Defence against Candida Fungal Infections." *Nat Rev Immunol* 15, no. 10 (2015): 630-42.

Nett, J. E., A. J. Lepak, K. Marchillo, and D. R. Andes. "Time Course Global Gene Expression Analysis of an in Vivo Candida Biofilm." *J Infect Dis* 200, no. 2 (2009): 307-13.

Nickerson, K. W., A. L. Atkin, and J. M. Hornby. "Quorum Sensing in Dimorphic Fungi: Farnesol and Beyond." *Appl Environ Microbiol* 72, no. 6 (2006): 3805-13.

Niesor, E. J., J. Flach, I. Lopes-Antoni, A. Perez, and C. L. Bentzen. "The Nuclear Receptors Fxr and Lxralpha: Potential Targets for the Development of Drugs Affecting Lipid Metabolism and Neoplastic Diseases." *Curr Pharm Des* 7, no. 4 (2001): 231-59.

Niewerth, M., and H. C. Korting. "Phospholipases of Candida Albicans." *Mycoses* 44, no. 9-10 (2001): 361-7.

Nobile, C. J., and A. D. Johnson. "Candida Albicans Biofilms and Human Disease." *Annu*

Rev Microbiol 69 (2015): 71-92.

Nobile, C. J., and A. P. Mitchell. "Regulation of Cell-Surface Genes and Biofilm Formation by the C. Albicans Transcription Factor Bcr1p." *Curr Biol* 15, no. 12 (2005): 1150-5.

Nobile, C. J., N. Solis, C. L. Myers, A. J. Fay, J. S. Deneault, A. Nantel, A. P. Mitchell, and S. G. Filler. "Candida Albicans Transcription Factor Rim101 Mediates Pathogenic Interactions through Cell Wall Functions." *Cell Microbiol* 10, no. 11 (2008): 2180-96.

Noble, S. M., S. French, L. A. Kohn, V. Chen, and A. D. Johnson. "Systematic Screens of a Candida Albicans Homozygous Deletion Library Decouple Morphogenetic Switching and Pathogenicity." *Nat Genet* 42, no. 7 (2010): 590-8.

Noel, T. "The Cellular and Molecular Defense Mechanisms of the Candida Yeasts against Azole Antifungal Drugs." *J Mycol Med* 22, no. 2 (2012): 173-8.

Odds, F. C., A. J. Brown, and N. A. Gow. "Antifungal Agents: Mechanisms of Action." *Trends Microbiol* 11, no. 6 (2003): 272-9.

Pao, S. S., I. T. Paulsen, and M. H. Saier, Jr. "Major Facilitator Superfamily." *Microbiol Mol Biol Rev* 62, no. 1 (1998): 1-34.

Pappas, P. G., C. A. Kauffman, D. R. Andes, C. J. Clancy, K. A. Marr, L. Ostrosky-Zeichner, A. C. Reboli, M. G. Schuster, J. A. Vazquez, T. J. Walsh, T. E. Zaoutis, and J. D. Sobel. "Executive Summary: Clinical Practice Guideline for the Management of Candidiasis: 2016 Update by the Infectious Diseases Society of America." *Clin Infect Dis* 62, no. 4 (2016): 409-17.

Pelosi, P., R. Mastrogiacomo, I. Iovinella, E. Tuccori, and K. C. Persaud. "Structure and Biotechnological Applications of Odorant-Binding Proteins." *Appl Microbiol Biotechnol* 98, no. 1 (2014): 61-70.

Pennisi, E. "The Crispr Craze." *Science* 341, no. 6148 (2013): 833-6.

Perea, S., J. L. Lopez-Ribot, W. R. Kirkpatrick, R. K. McAtee, R. A. Santillan, M. Martinez, D. Calabrese, D. Sanglard, and T. F. Patterson. "Prevalence of Molecular Mechanisms of Resistance to Azole Antifungal Agents in Candida Albicans Strains Displaying High-Level Fluconazole Resistance Isolated from Human Immunodeficiency Virus-Infected Patients." *Antimicrob Agents Chemother* 45, no. 10 (2001): 2676-84.

Perez-Garcia LA, Diaz-Jimenez DF, Lopez-Esparza A, Mora-Montes HM. "Role of Cell Wall Polysaccharides During Recognition of Candida Albicans by the Innate Immune System." *Journal of Glycobiology* 1, no. 102 (2012).

Perlin, D. S. "Mechanisms of Echinocandin Antifungal Drug Resistance." *Ann N Y Acad Sci* 1354 (2015): 1-11.

Pettengell, K., J. Mynhardt, T. Kluyts, W. Lau, D. Facklam, D. Buell, and F. K. South African Study Group. "Successful Treatment of Oesophageal Candidiasis by Micafungin: A Novel Systemic Antifungal Agent." *Aliment Pharmacol Ther* 20, no. 4 (2004): 475-81.

Pfaller, M. A., and D. J. Diekema. "Epidemiology of Invasive Candidiasis: A Persistent Public Health Problem." *Clin Microbiol Rev* 20, no. 1 (2007): 133-63.

Pfaller, M. A., and D. J. Diekema. "Epidemiology of Invasive Mycoses in North America." *Crit Rev Microbiol* 36, no. 1 (2010): 1-53.

Pfaller, M. A., S. A. Messer, L. Boyken, H. Huynh, R. J. Hollis, and D. J. Diekema. "In Vitro Activities of 5-Fluorocytosine against 8,803 Clinical Isolates of Candida Spp.: Global Assessment of Primary Resistance Using National Committee for Clinical Laboratory Standards Susceptibility Testing Methods." *Antimicrob Agents Chemother* 46, no. 11 (2002): 3518-21.

Pfaller, M. A., S. A. Messer, L. N. Woosley, R. N. Jones, and M. Castanheira. "Echinocandin and Triazole Antifungal Susceptibility Profiles for Clinical Opportunistic Yeast and Mold Isolates Collected from 2010 to 2011: Application of New Clsi Clinical Breakpoints and Epidemiological Cutoff Values for Characterization of Geographic and Temporal Trends of Antifungal Resistance." *J Clin Microbiol* 51, no. 8 (2013): 2571-81.

Phan, Q. T., C. L. Myers, Y. Fu, D. C. Sheppard, M. R. Yeaman, W. H. Welch, A. S. Ibrahim, J. E. Edwards, Jr., and S. G. Filler. "Als3 Is a Candida Albicans Invasin That Binds to Cadherins and Induces Endocytosis by Host Cells." *PLoS Biol* 5, no. 3 (2007): e64.

Pukkila-Worley, R., A. Y. Peleg, E. Tampakakis, and E. Mylonakis. "Candida Albicans Hyphal Formation and Virulence Assessed Using a Caenorhabditis Elegans Infection Model." *Eukaryot Cell* 8, no. 11 (2009): 1750-8.

Qin, J., M. J. Li, P. Wang, M. Q. Zhang, and J. Wang. "Chip-Array: Combinatory Analysis of Chip-Seq/Chip and Microarray Gene Expression Data to Discover Direct/Indirect Targets of a Transcription Factor." *Nucleic Acids Res* 39, no. Web Server issue (2011): W430-6.

Ramachandra, S., J. Linde, M. Brock, R. Guthke, B. Hube, and S. Brunke. "Regulatory Networks Controlling Nitrogen Sensing and Uptake in Candida Albicans." *PLoS One* 9, no. 3 (2014): e92734.

Ramage, G., E. Mowat, B. Jones, C. Williams, and J. Lopez-Ribot. "Our Current

Understanding of Fungal Biofilms." *Crit Rev Microbiol* 35, no. 4 (2009): 340-55.

Ramage, G., S. P. Saville, B. L. Wickes, and J. L. Lopez-Ribot. "Inhibition of Candida Albicans Biofilm Formation by Farnesol, a Quorum-Sensing Molecule." *Appl Environ Microbiol* 68, no. 11 (2002): 5459-63.

Ramirez-Zavala, B., O. Reuss, Y. N. Park, K. Ohlsen, and J. Morschhauser. "Environmental Induction of White-Opaque Switching in Candida Albicans." *PLoS Pathog* 4, no. 6 (2008): e1000089.

Reales-Calderon, J. A., N. Aguilera-Montilla, A. L. Corbi, G. Molero, and C. Gil. "Proteomic Characterization of Human Proinflammatory M1 and Anti-Inflammatory M2 Macrophages and Their Response to Candida Albicans." *Proteomics* 14, no. 12 (2014): 1503-18.

Reasoner, D. J., and E. E. Geldreich. "A New Medium for the Enumeration and Subculture of Bacteria from Potable Water." *Appl Environ Microbiol* 49, no. 1 (1985): 1-7.

Reuss, O., A. Vik, R. Kolter, and J. Morschhauser. "The Sat1 Flipper, an Optimized Tool for Gene Disruption in Candida Albicans." *Gene* 341 (2004): 119-27.

Rodkaer, S. V., and N. J. Faergeman. "Glucose- and Nitrogen Sensing and Regulatory Mechanisms in Saccharomyces Cerevisiae." *FEMS Yeast Res* 14, no. 5 (2014): 683-96.

Roemer, T., B. Jiang, J. Davison, T. Ketela, K. Veillette, A. Breton, F. Tandia, A. Linteau, S. Sillaots, C. Marta, N. Martel, S. Veronneau, S. Lemieux, S. Kauffman, J. Becker, R. Storms, C. Boone, and H. Bussey. "Large-Scale Essential Gene Identification in Candida Albicans and Applications to Antifungal Drug Discovery." *Mol Microbiol* 50, no. 1 (2003): 167-81.

Rokas, A., and C. T. Hittinger. "Transcriptional Rewiring: The Proof Is in the Eating." *Curr Biol* 17, no. 16 (2007): R626-8.

Roman, E., R. Alonso-Monge, Q. Gong, D. Li, R. Calderone, and J. Pla. "The Cek1 Mapk Is a Short-Lived Protein Regulated by Quorum Sensing in the Fungal Pathogen Candida Albicans." *FEMS Yeast Res* 9, no. 6 (2009): 942-55.

Roman, E., C. Nombela, and J. Pla. "The Sho1 Adaptor Protein Links Oxidative Stress to Morphogenesis and Cell Wall Biosynthesis in the Fungal Pathogen Candida Albicans." *Mol Cell Biol* 25, no. 23 (2005): 10611-27.

Romani, L. "Innate and Adaptive Immunity in Candida Albicans Infections and Saprophytism." *J Leukoc Biol* 68, no. 2 (2000): 175-9.

Ross J, Barbeau J, Emami E. "Influence of Farnesol on Candida Albicans Biofilms from Oral and Vaginal Strains." 96-97: American Society of Microbiology, 2010.

Sable, C. A., K. M. Strohmaier, and J. A. Chodakewitz. "Advances in Antifungal Therapy." *Annu Rev Med* 59 (2008): 361-79.

Samaranayake, D. P., and S. D. Hanes. "Milestones in Candida Albicans Gene Manipulation." *Fungal Genet Biol* 48, no. 9 (2011): 858-65.

Sanguinetti, M., B. Posteraro, and C. Lass-Florl. "Antifungal Drug Resistance among Candida Species: Mechanisms and Clinical Impact." *Mycoses* 58 Suppl 2 (2015): 2-13.

Santos, M. A., and M. F. Tuite. "The Cug Codon Is Decoded in Vivo as Serine and Not Leucine in Candida Albicans." *Nucleic Acids Res* 23, no. 9 (1995): 1481-6.

Sasse, C., N. Dunkel, T. Schafer, S. Schneider, F. Dierolf, K. Ohlsen, and J. Morschhauser. "The Stepwise Acquisition of Fluconazole Resistance Mutations Causes a Gradual Loss of Fitness in Candida Albicans." *Mol Microbiol* 86, no. 3 (2012): 539-56.

Sasse, C., and J. Morschhauser. "Gene Deletion in Candida Albicans Wild-Type Strains Using the Sat1-Flipping Strategy." *Methods Mol Biol* 845 (2012): 3-17.

Sato, T., T. Watanabe, T. Mikami, and T. Matsumoto. "Farnesol, a Morphogenetic Autoregulatory Substance in the Dimorphic Fungus Candida Albicans, Inhibits Hyphae Growth through Suppression of a Mitogen-Activated Protein Kinase Cascade." *Biol Pharm Bull* 27, no. 5 (2004): 751-2.

Saville, S. P., A. L. Lazzell, A. K. Chaturvedi, C. Monteagudo, and J. L. Lopez-Ribot. "Efficacy of a Genetically Engineered Candida Albicans Tet-Nrg1 Strain as an Experimental Live Attenuated Vaccine against Hematogenously Disseminated Candidiasis." *Clin Vaccine Immunol* 16, no. 3 (2009): 430-2.

Saville, S. P., A. L. Lazzell, C. Monteagudo, and J. L. Lopez-Ribot. "Engineered Control of Cell Morphology in Vivo Reveals Distinct Roles for Yeast and Filamentous Forms of Candida Albicans During Infection." *Eukaryot Cell* 2, no. 5 (2003): 1053-60.

Scannell, D. R., G. Butler, and K. H. Wolfe. "Yeast Genome Evolution--the Origin of the Species." *Yeast* 24, no. 11 (2007): 929-42.

Schillig, R., and J. Morschhauser. "Analysis of a Fungus-Specific Transcription Factor Family, the Candida Albicans Zinc Cluster Proteins, by Artificial Activation." *Mol Microbiol* 89, no. 5 (2013): 1003-17.

Schmitt, M. E., T. A. Brown, and B. L. Trumpower. "A Rapid and Simple Method for Preparation of Rna from Saccharomyces Cerevisiae." *Nucleic Acids Res* 18, no. 10 (1990): 3091-2.

Schneider, B. L., W. Seufert, B. Steiner, Q. H. Yang, and A. B. Futcher. "Use of Polymerase Chain Reaction Epitope Tagging for Protein Tagging in Saccharomyces Cerevisiae." *Yeast* 11, no. 13 (1995): 1265-74.

Sellam, A., T. Al-Niemi, K. McInnerney, S. Brumfield, A. Nantel, and P. A. Suci. "A Candida Albicans Early Stage Biofilm Detachment Event in Rich Medium." *BMC Microbiol* 9 (2009): 25.

Sellam, A., C. Askew, E. Epp, H. Lavoie, M. Whiteway, and A. Nantel. "Genome-Wide Mapping of the Coactivator Ada2p Yields Insight into the Functional Roles of Saga/Ada Complex in Candida Albicans." *Mol Biol Cell* 20, no. 9 (2009): 2389-400.

Sellam, A., H. Hogues, C. Askew, F. Tebbji, M. van Het Hoog, H. Lavoie, C. A. Kumamoto, M. Whiteway, and A. Nantel. "Experimental Annotation of the Human Pathogen Candida Albicans Coding and Noncoding Transcribed Regions Using High-Resolution Tiling Arrays." *Genome Biol* 11, no. 7 (2010): R71.

Sellam, A., F. Tebbji, M. Whiteway, and A. Nantel. "A Novel Role for the Transcription Factor Cwt1p as a Negative Regulator of Nitrosative Stress in Candida Albicans." *PLoS One* 7, no. 8 (2012): e43956.

Sellam, A., M. van het Hoog, F. Tebbji, C. Beaurepaire, M. Whiteway, and A. Nantel. "Modeling the Transcriptional Regulatory Network That Controls the Early Hypoxic Response in Candida Albicans." *Eukaryot Cell* 13, no. 5 (2014): 675-90.

Selmecki, A., A. Forche, and J. Berman. "Aneuploidy and Isochromosome Formation in Drug-Resistant Candida Albicans." *Science* 313, no. 5785 (2006): 367-70.

Selmecki, A., A. Forche, and J. Berman. "Genomic Plasticity of the Human Fungal Pathogen Candida Albicans." *Eukaryot Cell* 9, no. 7 (2010): 991-1008.

Selmecki, A., M. Gerami-Nejad, C. Paulson, A. Forche, and J. Berman. "An Isochromosome Confers Drug Resistance in Vivo by Amplification of Two Genes, Erg11 and Tac1." *Mol Microbiol* 68, no. 3 (2008): 624-41.

Semighini, C. P., J. M. Hornby, R. Dumitru, K. W. Nickerson, and S. D. Harris. "Farnesol-Induced Apoptosis in Aspergillus Nidulans Reveals a Possible Mechanism for Antagonistic Interactions between Fungi." *Mol Microbiol* 59, no. 3 (2006): 753-64.

Setiadi, E. R., T. Doedt, F. Cottier, C. Noffz, and J. F. Ernst. "Transcriptional Response of Candida Albicans to Hypoxia: Linkage of Oxygen Sensing and Efg1p-Regulatory Networks." *J Mol Biol* 361, no. 3 (2006): 399-411.

Sexton, J. A., V. Brown, and M. Johnston. "Regulation of Sugar Transport and Metabolism by the Candida Albicans Rgt1 Transcriptional Repressor." *Yeast* 24, no. 10 (2007): 847-60.

Shen, H., M. M. An, J. Wang de, Z. Xu, J. D. Zhang, P. H. Gao, Y. Y. Cao, Y. B. Cao, and Y. Y. Jiang. "Fcr1p Inhibits Development of Fluconazole Resistance in Candida Albicans by Abolishing Cdr1 Induction." *Biol Pharm Bull* 30, no. 1 (2007): 68-73.

Sherman, F. "Getting Started with Yeast." *Methods Enzymol* 194 (1991): 3-21.

Shibata, N., A. Suzuki, H. Kobayashi, and Y. Okawa. "Chemical Structure of the Cell-Wall Mannan of Candida Albicans Serotype a and Its Difference in Yeast and Hyphal Forms." *Biochem J* 404, no. 3 (2007): 365-72.

Shimada, T., A. Ishihama, S. J. Busby, and D. C. Grainger. "The Escherichia Coli Rutr Transcription Factor Binds at Targets within Genes as Well as Intergenic Regions." *Nucleic Acids Res* 36, no. 12 (2008): 3950-5.

Shingu-Vazquez, M., and A. Traven. "Mitochondria and Fungal Pathogenesis: Drug Tolerance, Virulence, and Potential for Antifungal Therapy." *Eukaryot Cell* 10, no. 11 (2011): 1376-83.

Si, H., A. D. Hernday, M. P. Hirakawa, A. D. Johnson, and R. J. Bennett. "Candida Albicans White and Opaque Cells Undergo Distinct Programs of Filamentous Growth." *PLoS Pathog* 9, no. 3 (2013): e1003210.

Silver, P. M., B. G. Oliver, and T. C. White. "Role of Candida Albicans Transcription Factor Upc2p in Drug Resistance and Sterol Metabolism." *Eukaryot Cell* 3, no. 6 (2004): 1391-7.

Skrzypek, M. S., J. Binkley, and G. Sherlock. "How to Use the Candida Genome Database." *Methods Mol Biol* 1356 (2016): 3-15.

Slot, J. C., and A. Rokas. "Multiple Gal Pathway Gene Clusters Evolved Independently and by Different Mechanisms in Fungi." *Proc Natl Acad Sci U S A* 107, no. 22 (2010): 10136-41.

Slutsky, B., M. Staebell, J. Anderson, L. Risen, M. Pfaller, and D. R. Soll. ""White-Opaque Transition": A Second High-Frequency Switching System in Candida Albicans." *J Bacteriol* 169, no. 1 (1987): 189-97.

Smith, D. A., S. Nicholls, B. A. Morgan, A. J. Brown, and J. Quinn. "A Conserved Stress-Activated Protein Kinase Regulates a Core Stress Response in the Human Pathogen Candida Albicans." *Mol Biol Cell* 15, no. 9 (2004): 4179-90.

Smriti, S. Krishnamurthy, B. L. Dixit, C. M. Gupta, S. Milewski, and R. Prasad. "Abc Transporters Cdr1p, Cdr2p and Cdr3p of a Human Pathogen Candida Albicans Are General Phospholipid Translocators." *Yeast* 19, no. 4 (2002): 303-18.

Smyth, G. K. . "Limma: Linear Models for Microarray Data." *Bioinformatics and Computational Biology Solutions Using R and Bioconductor* (2005).

Sobel, J. D. "Vulvovaginal Candidosis." *Lancet* 369, no. 9577 (2007): 1961-71.

Sohn, K., C. Urban, H. Brunner, and S. Rupp. "Efg1 Is a Major Regulator of Cell Wall Dynamics in Candida Albicans as Revealed by DNA Microarrays." *Mol Microbiol* 47, no. 1 (2003): 89-102.

Sopko, R., D. Huang, N. Preston, G. Chua, B. Papp, K. Kafadar, M. Snyder, S. G. Oliver, M. Cyert, T. R. Hughes, C. Boone, and B. Andrews. "Mapping Pathways and Phenotypes by Systematic Gene Overexpression." *Mol Cell* 21, no. 3 (2006): 319-30.

Sosinska, G. J., P. W. de Groot, M. J. Teixeira de Mattos, H. L. Dekker, C. G. de Koster, K. J. Hellingwerf, and F. M. Klis. "Hypoxic Conditions and Iron Restriction Affect the Cell-Wall Proteome of Candida Albicans Grown under Vagina-Simulative Conditions." *Microbiology* 154, no. Pt 2 (2008): 510-20.

Spampinato, C., and D. Leonardi. "Candida Infections, Causes, Targets, and Resistance Mechanisms: Traditional and Alternative Antifungal Agents." *Biomed Res Int* 2013 (2013): 204237.

Srikantha, T., A. R. Borneman, K. J. Daniels, C. Pujol, W. Wu, M. R. Seringhaus, M. Gerstein, S. Yi, M. Snyder, and D. R. Soll. "Tos9 Regulates White-Opaque Switching in Candida Albicans." *Eukaryot Cell* 5, no. 10 (2006): 1674-87.

Staab, J. F., and P. Sundstrom. "Genetic Organization and Sequence Analysis of the Hypha-Specific Cell Wall Protein Gene Hwp1 of Candida Albicans." *Yeast* 14, no. 7 (1998): 681-6.

Staab, J. F., and P. Sundstrom. "Ura3 as a Selectable Marker for Disruption and Virulence Assessment of Candida Albicans Genes." *Trends Microbiol* 11, no. 2 (2003): 69-73.

Stehr, F., A. Felk, A. Gacser, M. Kretschmar, B. Mahnss, K. Neuber, B. Hube, and W. Schafer. "Expression Analysis of the Candida Albicans Lipase Gene Family During

Experimental Infections and in Patient Samples." *FEMS Yeast Res* 4, no. 4-5 (2004): 401-8.

Strauss, A., S. Michel, and J. Morschhauser. "Analysis of Phase-Specific Gene Expression at the Single-Cell Level in the White-Opaque Switching System of Candida Albicans." *J Bacteriol* 183, no. 12 (2001): 3761-9.

Strijbis, K., J. van den Burg, W. F. Visser, M. van den Berg, and B. Distel. "Alternative Splicing Directs Dual Localization of Candida Albicans 6-Phosphogluconate Dehydrogenase to Cytosol and Peroxisomes." *FEMS Yeast Res* 12, no. 1 (2012): 61-8.

Sudbery, P., N. Gow, and J. Berman. "The Distinct Morphogenic States of Candida Albicans." *Trends Microbiol* 12, no. 7 (2004): 317-24.

Sudbery, P. E. "Growth of Candida Albicans Hyphae." *Nat Rev Microbiol* 9, no. 10 (2011): 737-48.

Sun, J. N., N. V. Solis, Q. T. Phan, J. S. Bajwa, H. Kashleva, A. Thompson, Y. Liu, A. Dongari-Bagtzoglou, M. Edgerton, and S. G. Filler. "Host Cell Invasion and Virulence Mediated by Candida Albicans Ssa1." *PLoS Pathog* 6, no. 11 (2010): e1001181.

Supek, F., M. Bosnjak, N. Skunca, and T. Smuc. "Revigo Summarizes and Visualizes Long Lists of Gene Ontology Terms." *PLoS One* 6, no. 7 (2011): e21800.

Synnott, J. M., A. Guida, S. Mulhern-Haughey, D. G. Higgins, and G. Butler. "Regulation of the Hypoxic Response in Candida Albicans." *Eukaryot Cell* 9, no. 11 (2010): 1734-46.

Szewczyk, E., and B. R. Oakley. "Microtubule Dynamics in Mitosis in Aspergillus Nidulans." *Fungal Genet Biol* 48, no. 10 (2011): 998-9.

Talibi, D., and M. Raymond. "Isolation of a Putative Candida Albicans Transcriptional Regulator Involved in Pleiotropic Drug Resistance by Functional Complementation of a Pdr1 Pdr3 Mutation in Saccharomyces Cerevisiae." *J Bacteriol* 181, no. 1 (1999): 231-40.

Tang, L., X. Liu, and N. D. Clarke. "Inferring Direct Regulatory Targets from Expression and Genome Location Analyses: A Comparison of Transcription Factor Deletion and Overexpression." *BMC Genomics* 7 (2006): 215.

Thewes, S., M. Kretschmar, H. Park, M. Schaller, S. G. Filler, and B. Hube. "In Vivo and Ex Vivo Comparative Transcriptional Profiling of Invasive and Non-Invasive Candida Albicans Isolates Identifies Genes Associated with Tissue Invasion." *Mol Microbiol* 63, no. 6 (2007): 1606-28.

Tsao, S., F. Rahkhoodaee, and M. Raymond. "Relative Contributions of the Candida Albicans Abc Transporters Cdr1p and Cdr2p to Clinical Azole Resistance." *Antimicrob Agents Chemother* 53, no. 4 (2009): 1344-52.

Tsong, A. E., M. G. Miller, R. M. Raisner, and A. D. Johnson. "Evolution of a Combinatorial Transcriptional Circuit: A Case Study in Yeasts." *Cell* 115, no. 4 (2003): 389-99.

Uhl, M. A., M. Biery, N. Craig, and A. D. Johnson. "Haploinsufficiency-Based Large-Scale Forward Genetic Analysis of Filamentous Growth in the Diploid Human Fungal Pathogen C.Albicans." *EMBO J* 22, no. 11 (2003): 2668-78.

van Helden, J., B. Andre, and J. Collado-Vides. "Extracting Regulatory Sites from the Upstream Region of Yeast Genes by Computational Analysis of Oligonucleotide Frequencies." *J Mol Biol* 281, no. 5 (1998): 827-42.

Vandeputte, P., F. Ischer, D. Sanglard, and A. T. Coste. "In Vivo Systematic Analysis of Candida Albicans Zn2-Cys6 Transcription Factors Mutants for Mice Organ Colonization." *PLoS One* 6, no. 10 (2011): e26962.

Vasicek, E. M., E. L. Berkow, V. M. Bruno, A. P. Mitchell, N. P. Wiederhold, K. S. Barker, and P. D. Rogers. "Disruption of the Transcriptional Regulator Cas5 Results in Enhanced Killing of Candida Albicans by Fluconazole." *Antimicrob Agents Chemother* 58, no. 11 (2014): 6807-18.

Vermes, A., H. J. Guchelaar, and J. Dankert. "Flucytosine: A Review of Its Pharmacology, Clinical Indications, Pharmacokinetics, Toxicity and Drug Interactions." *J Antimicrob Chemother* 46, no. 2 (2000): 171-9.

Villar, C. C., H. Kashleva, C. J. Nobile, A. P. Mitchell, and A. Dongari-Bagtzoglou. "Mucosal Tissue Invasion by Candida Albicans Is Associated with E-Cadherin Degradation, Mediated by Transcription Factor Rim101p and Protease Sap5p." *Infect Immun* 75, no. 5 (2007): 2126-35.

Vyas, V. K., M. I. Barrasa, and G. R. Fink. "A Candida Albicans Crispr System Permits Genetic Engineering of Essential Genes and Gene Families." *Sci Adv* 1, no. 3 (2015): e1500248.

Walton, P. A. "Import of Stably-Folded Proteins into Peroxisomes." *Ann N Y Acad Sci* 804 (1996): 76-85.

Wang, H. X., L. M. Douglas, V. Aimanianda, J. P. Latge, and J. B. Konopka. "The Candida Albicans Sur7 Protein Is Needed for Proper Synthesis of the Fibrillar Component of the Cell Wall That Confers Strength." *Eukaryot Cell* 10, no. 1 (2011): 72-80.

Wang, X. J., X. Sui, L. Yan, Y. Wang, Y. B. Cao, and Y. Y. Jiang. "Vaccines in the Treatment of Invasive Candidiasis." *Virulence* 6, no. 4 (2015): 309-15.

Wang, Y., Y. Y. Cao, X. M. Jia, Y. B. Cao, P. H. Gao, X. P. Fu, K. Ying, W. S. Chen, and Y. Y. Jiang. "Cap1p Is Involved in Multiple Pathways of Oxidative Stress Response in Candida Albicans." *Free Radic Biol Med* 40, no. 7 (2006): 1201-9.

Wang, Y., J. Y. Liu, C. Shi, W. J. Li, Y. Zhao, L. Yan, and M. J. Xiang. "Mutations in Transcription Factor Mrr2p Contribute to Fluconazole Resistance in Clinical Isolates of Candida Albicans." *Int J Antimicrob Agents* 46, no. 5 (2015): 552-9.

Warner, J. R. "The Economics of Ribosome Biosynthesis in Yeast." *Trends Biochem Sci* 24, no. 11 (1999): 437-40.

Westwater, C., E. Balish, and D. A. Schofield. "Candida Albicans-Conditioned Medium Protects Yeast Cells from Oxidative Stress: A Possible Link between Quorum Sensing and Oxidative Stress Resistance." *Eukaryot Cell* 4, no. 10 (2005): 1654-61.

Wheeler, R. T., and G. R. Fink. "A Drug-Sensitive Genetic Network Masks Fungi from the Immune System." *PLoS Pathog* 2, no. 4 (2006): e35.

White, T. C. "The Presence of an R467k Amino Acid Substitution and Loss of Allelic Variation Correlate with an Azole-Resistant Lanosterol 14alpha Demethylase in Candida Albicans." *Antimicrob Agents Chemother* 41, no. 7 (1997): 1488-94.

White, T. C., and P. M. Silver. "Regulation of Sterol Metabolism in Candida Albicans by the Upc2 Gene." *Biochem Soc Trans* 33, no. Pt 5 (2005): 1215-8.

Whiteway, M., and C. Bachewich. "Morphogenesis in Candida Albicans." *Annu Rev Microbiol* 61 (2007): 529-53.

Wilson, D., S. Thewes, K. Zakikhany, C. Fradin, A. Albrecht, R. Almeida, S. Brunke, K. Grosse, R. Martin, F. Mayer, I. Leonhardt, L. Schild, K. Seider, M. Skibbe, S. Slesiona, B. Waechtler, I. Jacobsen, and B. Hube. "Identifying Infection-Associated Genes of Candida Albicans in the Postgenomic Era." *FEMS Yeast Res* 9, no. 5 (2009): 688-700.

Wilson, R. B., D. Davis, and A. P. Mitchell. "Rapid Hypothesis Testing with Candida Albicans through Gene Disruption with Short Homology Regions." *J Bacteriol* 181, no. 6 (1999): 1868-74.

Winston, D. J., J. W. Hathorn, M. G. Schuster, G. J. Schiller, and M. C. Territo. "A Multicenter, Randomized Trial of Fluconazole Versus Amphotericin B for Empiric Antifungal Therapy of Febrile Neutropenic Patients with Cancer." *Am J Med* 108, no.

4 (2000): 282-9.

Wirsching, S., S. Michel, and J. Morschhauser. "Targeted Gene Disruption in Candida Albicans Wild-Type Strains: The Role of the Mdr1 Gene in Fluconazole Resistance of Clinical Candida Albicans Isolates." *Mol Microbiol* 36, no. 4 (2000): 856-65.

Wongsuk, T., P. Pumeesat, and N. Luplertlop. "Fungal Quorum Sensing Molecules: Role in Fungal Morphogenesis and Pathogenicity." *J Basic Microbiol* 56, no. 5 (2016): 440-7.

Wu, W., C. Pujol, S. R. Lockhart, and D. R. Soll. "Chromosome Loss Followed by Duplication Is the Major Mechanism of Spontaneous Mating-Type Locus Homozygosis in Candida Albicans." *Genetics* 169, no. 3 (2005): 1311-27.

Wu, W. I., Y. Liu, B. Riedel, J. B. Wissing, A. S. Fischl, and G. M. Carman. "Purification and Characterization of Diacylglycerol Pyrophosphate Phosphatase from Saccharomyces Cerevisiae." *J Biol Chem* 271, no. 4 (1996): 1868-76.

Wurtele, H., S. Tsao, G. Lepine, A. Mullick, J. Tremblay, P. Drogaris, E. H. Lee, P. Thibault, A. Verreault, and M. Raymond. "Modulation of Histone H3 Lysine 56 Acetylation as an Antifungal Therapeutic Strategy." *Nat Med* 16, no. 7 (2010): 774-80.

Wyrick, J. J., and R. A. Young. "Deciphering Gene Expression Regulatory Networks." *Curr Opin Genet Dev* 12, no. 2 (2002): 130-6.

Yang, K., Y. Liu, D. J. Niu, D. Wei, F. Li, G. R. Wang, and S. L. Dong. "Identification of Novel Odorant Binding Protein Genes and Functional Characterization of Obp8 in Chilo Suppressalis (Walker)." *Gene* 591, no. 2 (2016): 425-32.

Yang, W., L. Yan, C. Wu, X. Zhao, and J. Tang. "Fungal Invasion of Epithelial Cells." *Microbiol Res* 169, no. 11 (2014): 803-10.

Zhang, Z. D., J. Rozowsky, H. Y. Lam, J. Du, M. Snyder, and M. Gerstein. "Tilescope: Online Analysis Pipeline for High-Density Tiling Microarray Data." *Genome Biol* 8, no. 5 (2007): R81.

Zhao, X., S. H. Oh, G. Cheng, C. B. Green, J. A. Nuessen, K. Yeater, R. P. Leng, A. J. Brown, and L. L. Hoyer. "Als3 and Als8 Represent a Single Locus That Encodes a Candida Albicans Adhesin; Functional Comparisons between Als3p and Als1p." *Microbiology* 150, no. Pt 7 (2004): 2415-28.

Zhao, X., S. H. Oh, K. M. Yeater, and L. L. Hoyer. "Analysis of the Candida Albicans Als2p and Als4p Adhesins Suggests the Potential for Compensatory Function within the Als Family." *Microbiology* 151, no. Pt 5 (2005): 1619-30.

Zhao, Y., W. B. Perez, C. Jimenez-Ortigosa, G. Hough, J. B. Locke, V. Ong, K. Bartizal, and D. S. Perlin. "Cd101: A Novel Long-Acting Echinocandin." *Cell Microbiol* (2016).

Zhou, Q., T. Li, and D. H. Price. "Rna Polymerase Ii Elongation Control." *Annu Rev Biochem* 81 (2012): 119-43.

Zhu, W., and S. G. Filler. "Interactions of Candida Albicans with Epithelial Cells." *Cell Microbiol* 12, no. 3 (2010): 273-82.

Znaidi, S., K. S. Barker, S. Weber, A. M. Alarco, T. T. Liu, G. Boucher, P. D. Rogers, and M. Raymond. "Identification of the Candida Albicans Cap1p Regulon." *Eukaryot Cell* 8, no. 6 (2009): 806-20.

Znaidi, S., X. De Deken, S. Weber, T. Rigby, A. Nantel, and M. Raymond. "The Zinc Cluster Transcription Factor Tac1p Regulates Pdr16 Expression in Candida Albicans." *Mol Microbiol* 66, no. 2 (2007): 440-52.

SUPPLEMENTARY DOCUMENTS

SUPPLEMENTARY TABLE II.1_PRIMERS USED IN THIS STUDY

Gene	Primer ID	Position (bp relative to ATG)	Primer Sequence (5'-3')	Amplicon Size (bp)
FCR1 HA-tagging[a]	MR1825	1418	AACCATTAAGTCCATCTGATGATGCTATTGTTTATCCTACAAATCAATTT ACTAATAGACCAGCTACGGTGTCCACTTTTGGTGGTGGGTTAGATGTG TTGGTGGATAATTCATTGGATCCTTTCTTCAATATTagggaacaaaagctgg	1921
	MR1826	1688	ATAATTGAAACAAAACCGTATTAGAATAACATAAAAAAGAAAATCATC ACATAGCTTCAATGTAACCAGACAAATAAAAAACCTTAAATAGAAAGG GGGAACAGAAAACCCTCCCATTCACTTAGGATTACTATctatagggcgaatt gg	
MEP1-α ChIP-PCR	MR2363	481	TGTCCCGTGGTTTATTGGAT	74
	MR2364	555	ACCAGCATAATCTAAAGCACCTG	
MEP1-β ChIP-PCR	MR2365	875	TGGCTGCTACTCCTTCTTCAG	75
	MR2366	950	CAAACTATCCCAGCAGTAATACCTAA	
FGR23 ChIP-PCR	MR2367	1822	CTGGAACTATCAGTGTCGTCTACTTT	65
	MR2368	1887	TCCCAGACATTTACCACTAGCA	
Orf19.1611 ChIP-PCR[b]	MR2369	-664	AGTCAAGTTATTGTTTCCCCTGA	89
	MR2370	-575	AGCAATTGGTAGCATCATCTTTT	
SPS4 ChIP-PCR	MR1137	-635	TACAGTTGCCCCAGTCAACA	43
	MR1138	-593	TGTCTTGGAACGGAAACTCA	
FCR1 deletion; first round[c]	MR2652	-60	TTTGCTTGATTTCTTTTTCCTTGCTTCAAATTTTCAAATTTCCTTTCCTTTT TACCAAATGAGCTCCACCGCGGTGGCGGCCGCT	4337
	MR2653	1614	TAAAAAACCTTAAATAGAAAGGGGGAACAGAAAACCCTCCCATTCACT TAGGATTACTATGGTACCGGGCCCCCCCTCGAGGAA	
FCR1 deletion; second round	MR2654	-120	ATAACTCCTCCAAATAATATTTTCTTTTTTGCTTCCCTTATTTTATTTTTTA TTTACATATTTGCTTGATTTCTTTTTCC	4457
	MR2655	1674	ACCGTATTAGAATAACATAAAAAAGAAAATCATCACATAGCTTCAATG TAACCAGACAAATAAAAAACCTTAAATAGAAA	
Verification of *FCR1* deletion	MR1851	-992	CCAACTCTTCATTTTGAGCTCTCT	1153[d]
	MR1888	1640	ACATAGCTTCAATGTAACCAGACA	
Verification of *SAT1* integration	MR2004	356	TAAATTTGTGTTGTTCGGTGACTCCATCAC	472[e]

	MR2005	3473	TCTCATATGAAAATTTCGGTGATCCCTGAG	1736[e]
FCR1 probe	MR1684	409	ACTGGTGTGGTTGCTCCTATAA	973
	MR1685	1381	CAACACTGCCAGCACCAATAT	
HSP30 probe	MR2673	279	GGGCTATACTTGGATTTTGACAG	632
	MR2674	910	CTTCAGTAGCAGTTGGAGCATGT TC	
HWP1 probe	MR2681	246	GCCATGTGACTATCCACAACAGCC	643
	MR2682	888	GGCTTCAGTAGTAGTGGTTGGAAC	
YWP1 probe	MR2713	480	TTACGTTCCAGGTTCAAGTT	531
	MR2714	1010	TCATCACAAGCAACAACAGT	
OPT1 probe	MR2210	331	TTGTTCAGTTTCCATAGTCCCTCA	947
	MR2211	1278	CATGGAAGCAAATGGTGTGTGTT	

[a] bases in lower case represent sequences homologous to sequences from plasmid pCaMPY-3xHA

[b] probe located in the intergenic region upstream of orf19.1611

[c] underlined bases represent annealing sequences within plasmid pSFS2A

[d] product size in the final knockout (after loop out of the SAT1 cassette)

[e] product size for SAT1 integration at the target allele (combination PCR; see supplementary Figure 2.2)

SUPPLEMENTARY TABLE II.2A_Fcr1p BINDING HITS

Systematic Name	Standard Name*	Linear Binding Ratio	Description
*Genes with an asterix appear twice (2 hits within the same gene)			
orf19.4716	GDH3	3.0	Uncharacterized ORF||Protein described as similar to NADP-glutamate dehydrogenase; hyphal downregulated expression; transcription is regulated by Nrg1p, Plc1p; downregulated by Efg1p; upregulated by Rim101p at pH 8; ciclopirox olamine induced
orf19.5437	RHR2	2.7	Verified ORF||Putative glycerol 3-phosphatase; roles in osmotic tolerance, glycerol accumulation in response to salt; regulated by macrophage, stress response, yeast-hyphal switch, pheromone, GCN4, HOG1, NRG1, TUP1; antigenic in murine systemic infection
orf19.780	DUR1,2	2.6	Verified ORF||Urea amidolyase, contains urea carboxylase and allophanate hydrolase activities needed to hydrolyze urea to CO2; required for utilization of urea as nitrogen source and for hyphal switch in macrophages; transcription is regulated by Nrg1p
orf19.6993	GAP2	2.5	Uncharacterized ORF||Protein similar to amino acid permeases; ketoconazole, flucytosine repressed; induced by histidine, and induction requires Ssy1p; regulated by Nrg1p, Tup1p; shows colony morphology-related gene regulation by Ssn6p
orf19.2602	OPT1	2.5	Verified ORF||Oligopeptide transporter; transports 3-to-5-residue peptides; alleles are distinct, one has intron; not ABC or PTR type transporter; suppresses S. cerevisiae ptr2-2 mutant defects; induced by BSA or peptides; Stp3p, Hog1p regulated
orf19.6224	orf19.6224	2.5	Uncharacterized ORF||Predicted ORF in Assemblies 19, 20 and 21
orf19.6257	GLT1	2.5	Uncharacterized ORF||Putative glutamate synthase; alkaline downregulated; transcription is downregulated in both intermediate and mature biofilms
orf19.1614	MEP1	2.5	Verified ORF||Ammonium permease; Mep1p is a more efficient ammonium permease than Mep2p, whereas Mep2p has additional regulatory role; not essential for viability; 11 predicted transmembrane regions; low mRNA abundance; hyphal downregulated
orf19.2584	OPT9	2.4	Probable pseudogene similar to fragments of OPT1 oligopeptide transporter gene; decreased expression in hyphae compared to yeast-form cells; transcriptionally induced upon phagocytosis by macrophage
orf19.1868	RNR22	2.4	Uncharacterized ORF||Protein described as ribonucleoside diphosphate reductase; shows colony morphology-related gene regulation by Ssn6p; RNA abundance regulated by tyrosol and cell density
orf19.691	GPD2	2.3	Uncharacterized ORF||Similar to glycerol 3-P dehydrogenases; regulated by Ssn6p, Nrg1p, Efg1p; induced upon osmotic and oxidative stress (via Hog1p), cell wall regeneration, macrophage/pseudohyphal growth, core stress response; possibly essential (UAU1 method)
orf19.1817	orf19.1817	2.3	Predicted ORF from Assembly 19; removed from Assembly 20
orf19.2942	DIP5	2.2	Verified ORF||Putative permease for dicarboxylic amino acids; mutation confers hypersensitivity to toxic ergosterol analog; transcriptionally induced upon phagocytosis by macrophage; Gcn4p-regulated; upregulated by Rim101p at pH 8

orf19.2989	GOR1	2.1	Ortholog(s) have glyoxylate reductase activity, role in glyoxylate catabolic process and cytosol, mitochondrion, nucleus localization
orf19.646	GLN1	2.1	Uncharacterized ORF||Protein described as similar to glutamate synthase; regulated by Tsa1p, Tsa1Bp under H2O2 stress conditions
orf19.1847	ARO10	2.0	Uncharacterized ORF||Aromatic decarboxylase of the Ehrlich fusel oil pathway of aromatic alcohol biosynthesis; pH-regulated (alkaline downregulated); protein abundance is affected by URA3 expression in the CAI-4 strain background
orf19.111	CAN2	2.0	Uncharacterized ORF||Putative amino acid permease; transcription is regulated by Nrg1p and Tup1p; caspofungin induced; flucytosine induced; shows colony morphology-related gene regulation by Ssn6p; ; fungal-specific (no human or murine homolog)
orf19.406	ERG1	2.0	Verified ORF||Squalene epoxidase, catalyzes epoxidation of squalene to 2,3(S)-oxidosqualene in the ergosterol biosynthetic pathway; essential; target of allylamine antifungal drugs; uses NADH as a reducing cofactor, while S. cerevisiae Erg1p uses NADPH
orf19.1311	SPO75	2.0	Uncharacterized ORF||Similar to S. cerevisiae sporulation protein; fungal-specific (no human or murine homolog)
orf19.4784	CRP1	2.0	Verified ORF||Copper transporter of the plasma membrane; P1-type ATPase (CPx type); mediates Cu resistance; similar to proteins of Menkes and Wilson disease; copper-induced; Tbf1p-activated; suppresses Cu sensitivity of S. cerevisiae cup1 null mutant
orf19.238	CCP1	2.0	Uncharacterized ORF||Similar to cytochrome-c peroxidase N terminus; transcription is negatively regulated by Rim101p or alkaline pH; transcription induced by interaction with macrophage or low iron; oxygen-induced activity
orf19.97	CAN1	2.0	Verified ORF||Amino acid permease, transports basic amino acids; complements lysine transport mutation; contains 10 predicted transmembrane regions and 3 predicted N-glycosylation sites; transcriptionally induced upon phagocytosis by macrophage
orf19.1207	orf19.1207	2.0	Dubious ORF||Predicted ORF in Assemblies 19, 20 and 21
orf19.633	orf19.633	1.9	Uncharacterized ORF||Protein described as a putative methyltransferase; decreased expression in hyphae compared to yeast-form cells; expression regulated during planktonic growth
orf19.2803	HEM13	1.9	Verified ORF||Coproporphyrinogen III oxidase; antigenic in human/mouse; localizes to yeast-form cell surface, not hyphae; soluble in hyphae; iron-regulated expression; macrophage-downregulated; not Rfg1p regulated, farnesol-induced; possibly essential
orf19.5000	CYB2	1.9	Uncharacterized ORF||Protein described as precursor protein of cytochrome b2; transcriptionally regulated by iron; expression greater in high iron; alkaline downregulated; shows colony morphology-related gene regulation by Ssn6p
orf19.6570	NUP	1.9	Verified ORF||Nucleoside permease; adenosine and guanosine are substrates, whereas cytidine, adenine, guanine, uridine, uracil are not; similar to a nucleoside permease of S. pombe; possibly processed by Kex2p
orf19.7196	orf19.7196	1.9	Uncharacterized ORF||Protein described as a vacuolar protease; upregulated in the presence of human neutrophils
orf19.6659	GAP6	1.9	Uncharacterized ORF||Putative general amino acid permease; Plc1p-regulated; Gcn4p-regulated; fungal-specific (no human or murine homolog)

orf19.7676	XYL2	1.9	Verified ORF||Protein described as similar to D-xylulose reductase; immunogenic in mouse; soluble protein in hyphae; Hog1p-induced; induced during cell wall regeneration; caspofungin or fluconazole-induced; Mnl1p-induced in weak acid stress
orf19.1756	GPD1	1.9	Uncharacterized ORF||Protein similar to S. cerevisiae glycerol-3-phosphate dehydrogenase (enzyme of glycerol biosynthesis); biofilm-induced expression; regulated by Efg1p; regulated by Tsa1p, Tsa1Bp under H2O2 stress conditions
orf19.4777	DAK2	1.8	Uncharacterized ORF||Protein described as similar to dihydroxyacetone kinase; transcription is decreased upon yeast-hyphal switch; fluconazole-induced; caspofungin repressed; protein detected by mass spec in stationary phase cultures
orf19.5750	SHM2	1.8	Verified ORF||Cytoplasmic serine hydroxymethyltransferase; complements the glycine auxotrophy of an S. cerevisiae shm1 null shm2 null gly1-1 triple mutant; antigenic in human; soluble protein in hyphae; farnesol-upregulated in biofilm
orf19.2841	PGM2	1.8	Uncharacterized ORF||Protein not essential for viability; similar to S. cerevisiae Pgm2p, which is phosphoglucomutase
orf19.6559	orf19.6559	1.8	Uncharacterized ORF||Predicted ORF in Assemblies 19, 20 and 21; protein level decreased in stationary phase cultures
orf19.4737	TPO3	1.8	Verified ORF||Possible role in polyamine transport; MFS-MDR family; transcription induced by Sfu1p, regulated upon white-opaque switching; decreased expression in hyphae compared to yeast-form cells; regulated by Nrg1p; fungal-specific
orf19.3940.1	CUP1	1.8	Verified ORF||Metallothionein, involved in copper resistance; transcription is induced by copper
orf19.4836	URA1	1.8	Verified ORF||Dihydroorotate dehydrogenase (DHODH); enzyme of de novo pyrimidine biosynthesis; putative bipartite mitochondrial targeting motif, membrane spanning region; transcription is regulated upon yeast-hyphal switch, or by Nrg1p, Mig1p, Tup1p
orf19.1034	orf19.1034	1.8	Uncharacterized ORF||Predicted ORF in Assemblies 19, 20 and 21; caspofungin repressed
orf19.789	PYC2	1.8	Uncharacterized ORF||Putative pyruvate carboxylase, binds to biotin cofactor; up-regulated in mutant lacking the Ssk1p response regulator protein, upon benomyl treatment, or in an azole-resistant strain overexpressing MDR1
orf19.3521	ARH2	1.8	Uncharacterized ORF||Predicted ORF in Assemblies 19, 20 and 21
orf19.5305	RHD3	1.8	Verified ORF||GPI-anchored cell wall protein; transcription decreased upon yeast-hyphal switch; transcriptionally regulated by iron; expression greater in high iron; clade-associated gene expression; possibly an essential gene (by UAU1 method)
orf19.3264	CCE1	1.8	Uncharacterized ORF||Putative Holliday junction resolving enzyme; similar to S. cerevisiae Cce1p
orf19.5917	STP3	1.8	Verified ORF||Transcription factor; regulates SAP2, OPT1 expression and thereby protein catabolism for nitrogen source; activated via amino-acid-induced proteolytic processing; macrophage/pseudohyphal-repressed
orf19.951	orf19.951	1.8	Uncharacterized ORF||Predicted ORF in Assemblies 19, 20 and 21; transcription downregulated upon yeast-hyphal switch; fluconazole-induced; possibly spurious ORF (Annotation Working Group prediction)
orf19.6937	PTR22	1.8	Oligopeptide transporter involved in uptake of di-/tripeptides; regulated by Stp2 and Stp3; transcript induced upon phagocytosis by macrophage; repressed by Rim101 at pH 8; flow model biofilm induced
orf19.822	HSP21	1.8	Small heat shock protein; role in stress response and virulence; fluconazole-downregulated; induced in cyr1 or ras1 mutant; stationary phase enriched protein; detected in some, not all, biofilm extracts; Spider biofilm induced
orf19.7296	orf19.7296	1.8	Verified ORF||Predicted ORF in Assemblies 19, 20 and 21; similar to stomatin mechanoreception protein; induced by Rgt1p

orf19.5784	AMO1	1.7	Putative peroxisomal copper amine oxidase
orf19.4674.1	CRD2	1.7	Verified ORF||Metallothionein; role in adaptation to growth with high concentration of copper ions; basal transcription is cadmium-repressed; regulated by Ssn6p; complements copper sensitivity of an S. cerevisiae cup1 null mutant
orf19.915	orf19.915	1.7	Uncharacterized ORF||Predicted ORF in Assemblies 19, 20 and 21
orf19.1843	ALG6	1.7	Uncharacterized ORF||Putative glucosyltransferase involved in cell wall mannan biosynthesis; transcription is elevated in chk1, nik1, and sln1 homozygous null mutants; repressed by nitric oxide; possibly essential gene, disruptants not obtained by UAU1 method
orf19.2608	ADH5	1.7	Verified ORF||Putative alcohol dehydrogenase; soluble protein in hyphae; expression is regulated upon white-opaque switching; fluconazole-induced; antigenic during murine systemic infection; regulated by Nrg1p, Tup1p; macrophage-downregulated protein
orf19.5079	CDR4	1.7	Verified ORF||Putative transporter of ATP-binding cassette (ABC) superfamily; fluconazole, Sfu1p, Hog1p, core stress response induced; caspofungin repressed; fluconazole resistance is not affected by mutation or correlated with expression
orf19.3870	ADE13	1.7	Verified ORF||Enzyme of adenine biosynthesis; soluble protein in hyphae; not induced during GCN response, in contrast to the S. cerevisiae ortholog; repressed by nitric oxide
orf19.385	GCV2	1.7	Uncharacterized ORF||Putative protein of glycine catabolism; downregulated by Efg1p; Hog1p-induced; upregulated by Rim101p at acid pH; transcription is activated in the presence of elevated CO2; protein detected by mass spec in stationary phase cultures
orf19.3966	CRH12	1.7	Verified ORF||Putative cell wall protein, member of the CRH family; transcription is regulated by Nrg1p and Tup1p; alkaline upregulated by Rim101p; repressed during cell wall regeneration
orf19.6317	ADE6*	1.7	Uncharacterized ORF||Enzyme of adenine biosynthesis; not induced during GCN response, in contrast to the S. cerevisiae ortholog; protein detected by mass spec in stationary phase cultures
orf19.6317	ADE6*	1.7	Uncharacterized ORF||Enzyme of adenine biosynthesis; not induced during GCN response, in contrast to the S. cerevisiae ortholog; protein detected by mass spec in stationary phase cultures
orf19.3442	orf19.3442	1.7	Uncharacterized ORF||Predicted ORF in Assemblies 19, 20 and 21
orf19.5282	orf19.5282	1.7	Uncharacterized ORF||Putative protein of unknown function; mRNA binds to She3p; decreased expression in hyphae compared to yeast-form cells; regulated by Efg1p and Efh1p; intron in 5'-UTR; transcriptionally activated by Mnl1p under weak acid stress
orf19.2825	DRE2	1.7	Putative cytosolic Fe-S protein assembly protein; a-specific transcript; regulated by Sef1, Sfu1, and Hap43; rat catheter and Spider biofilm induced
orf19.5288	IFE2	1.7	Uncharacterized ORF||Protein described as an alcohol dehydrogenase; decreased expression in hyphae compared to yeast-form cells; Efg1p-regulated; fluconazole-induced; Hog1p-induced; increased expression in response to prostaglandins
orf19.3967	PFK1	1.7	Verified ORF||Alpha subunit of phosphofructokinase (PFK), which is Pfk1p, Pfk2p heteromultimer; PFK is activated by fructose 2,6-bisphosphate or AMP, inhibited by ATP; activity reduced on hyphal induction; phagocytosis-downregulated; fluconazole-induced

orf19.164	orf19.164	1.7	Uncharacterized ORF||Predicted ORF in Assemblies 19, 20 and 21
orf19.489	DAP1	1.7	Uncharacterized ORF||Protein similar to S. cerevisiae Dap1p, which is a protein related to mammalian membrane-associated progesterone receptors involved in response to DNA damage; induced in core stress response; Hog1p regulated; clade-associated expression
orf19.6656	DUR3	1.7	Uncharacterized ORF||Putative protein of unknown function, transcription is upregulated in clinical isolates from HIV+ patients with oral candidiasis; alkaline downregulated; amphotericin B induced; shows colony morphology-related gene regulation by Ssn6p
orf19.1067	GPM2	1.7	Verified ORF||Protein described as phosphoglycerate mutase; decreased expression in hyphae compared to yeast-form cells; macrophage/pseudohyphal-repressed; induced by high levels of peroxide stress, farnesol-induced
orf19.7459	orf19.7459	1.7	Uncharacterized ORF||Predicted ORF in Assemblies 19, 20 and 21; fluconazole-induced; ketoconazole-repressed
orf19.5280	MUP1	1.7	Uncharacterized ORF||Alkaline upregulated by Rim101p
orf19.2839	CIRT4B	1.7	Uncharacterized ORF||Decreased transcription is observed in an azole-resistant strain that overexpresses CDR1 and CDR2
orf19.2669	orf19.2669	1.7	Uncharacterized ORF||Predicted ORF in retrotransposon Tca4 with similarity to the Pol region of retrotransposons encoding reverse transcriptase, protease and integrase; downstream from RHD2 with similarity to the Gag region encoding nucleocapsid-like protein
orf19.4274	PUT1	1.7	Uncharacterized ORF||Alkaline upregulated by Rim101p
orf19.508	QDR1	1.6	Uncharacterized ORF||Putative transporter of antibiotic resistance; transcription is regulated by Nrg1p and Tup1p; caspofungin repressed; expression is regulated upon white-opaque switching
orf19.4550	orf19.4550	1.6	Uncharacterized ORF||Predicted membrane transporter, member of the drug:proton antiporter (12 spanner) (DHA1) family, major facilitator superfamily (MFS)
orf19.4617	orf19.4617	1.6	Uncharacterized ORF||Predicted ORF in Assemblies 19, 20 and 21
orf19.3303	orf19.3303	1.6	Uncharacterized ORF||Predicted ORF in Assemblies 19, 20 and 21
orf19.7611	TRX1	1.6	Uncharacterized ORF||Similar to thioredoxin; biofilm, benomyl, flucytosine, peroxide induced; amphotericin B, caspofungin repressed; upregulated in the presence of human neutrophils; macrophage-downregulated gene
orf19.5061	ADE5,7	1.6	Verified ORF||Enzyme of adenine biosynthesis; interacts with Vps34p; required for hyphal growth and virulence; flucytosine induced; not induced during GCN response, in contrast to the S. cerevisiae ortholog
orf19.6948	CCC1	1.6	Verified ORF||Putative manganese transporter, required for normal filamentous growth; mRNA binds to She3p and is localized to hyphal tips; repressed by nitric oxide and alkaline pH; shows colony morphology-related regulation by Ssn6p
orf19.333	FCY2	1.6	Verified ORF||Putative purine-cytosine permease of pyrimidine salvage; similar to S. cerevisiae Fcy2p; mutation associated with resistance to flucytosine in clinical isolates; transposon mutation affects filamentation; farnesol-upregulated in biofilm
orf19.3820	orf19.3820*	1.6	Uncharacterized ORF||Predicted ORF in Assemblies 19, 20 and 21; clade-associated gene expression
orf19.3820	orf19.3820*	1.6	Uncharacterized ORF||Predicted ORF in Assemblies 19, 20 and 21; clade-associated gene expression

orf19.1275	GAT1*	1.6	Verified ORF||Zinc finger transcriptional regulator of nitrogen utilization; required for nitrogen catabolite repression and utilization of isoleucine, tyrosine and tryptophan N sources; required for virulence in a mouse systemic infection model
orf19.1275	GAT1*	1.6	Verified ORF||Zinc finger transcriptional regulator of nitrogen utilization; required for nitrogen catabolite repression and utilization of isoleucine, tyrosine and tryptophan N sources; required for virulence in a mouse systemic infection model
orf19.411	orf19.411	1.6	Uncharacterized ORF||Protein described as similar to GTPase regulators; possibly spurious ORF (Annotation Working Group prediction); transcriptionally regulated by iron; expression greater in low iron; transcriptionally activated by Mnl1p under weak acid stress
orf19.787	orf19.787	1.6	Uncharacterized ORF||Predicted ORF in Assemblies 19, 20 and 21
orf19.3974	PUT2	1.6	Uncharacterized ORF||Alkaline upregulated; protein detected by mass spec in exponential and stationary phase cultures
orf19.2308	orf19.2308	1.6	Uncharacterized ORF||Predicted ORF in Assemblies 19, 20 and 21
orf19.6983	orf19.6983	1.6	Uncharacterized ORF||Predicted ORF in Assemblies 19, 20 and 21; repressed by nitric oxide
orf19.5519	GCV1	1.6	Uncharacterized ORF||Protein described as T subunit of glycine decarboxylase; transcription is negatively regulated by Sfu1p
orf19.5229	orf19.5229	1.6	Uncharacterized ORF||Predicted ORF in Assemblies 19, 20 and 21
orf19.2762	AHP1	1.6	Verified ORF||Putative alkyl hydroperoxide reductase; immunogenic in mouse; biofilm-induced; fluconazole-induced; amphotericin B, caspofungin, alkaline downregulated; induced in core stress response; regulated by Ssk1p, Nrg1p, Tup1p, Ssn6p, Hog1p
orf19.5514	orf19.5514	1.6	Uncharacterized ORF||Predicted ORF in Assemblies 19, 20 and 21
orf19.7566	orf19.7566	1.6	Uncharacterized ORF||Putative protein of unknown function, transcription is upregulated in clinical isolates from HIV+ patients with oral candidiasis; alkaline upregulated by Rim101p; fungal-specific (no human or murine homolog)
orf19.2292	orf19.2292	1.6	Oligopeptide transporter; transcriptionally induced upon phagocytosis by macrophage; fungal-specific (no human or murine homolog); merged with orf19.176 in Assembly 20
orf19.1235	HOM3	1.6	Uncharacterized ORF||Putative L-aspartate 4-P-transferase; fungal-specific (no human or murine homolog); regulated by Gcn2p and Gcn4p
orf19.2371	orf19.2371	1.6	Uncharacterized ORF||Putative Gag protein of retrotransposon Tca2; separated by a stop codon from Pol protein orf19.2372; both likely translated as single polyprotein that includes nucleocapsid-like protein (Gag), reverse transcriptase, protease, and integrase
orf19.84	CAN3	1.6	Uncharacterized ORF||Predicted ORF in Assemblies 19, 20 and 21; expression is regulated upon white-opaque switching
orf19.1407	orf19.1407	1.6	Predicted ORF from Assembly 19; merged with orf19.6117 in Assembly 20
orf19.539	LAP3	1.6	Uncharacterized ORF||Protein described as an aminopeptidase; transcription is positively regulated by Sfu1p; transcription is repressed in response to alpha pheromone in SpiderM medium; clade-associated gene expression; virulence-group-correlated expression

orf19.1107	orf19.1107	1.6	Uncharacterized ORF||Predicted ORF in Assemblies 19, 20 and 21
orf19.176	OPT4	1.6	Verified ORF||Oligopeptide transporter; detected at germ tube plasma membrane by mass spectrometry; transcriptionally induced upon phagocytosis by macrophage; fungal-specific (no human or murine homolog); merged with orf19.2292 in Assembly 20
orf19.5058	SMI1	1.6	Uncharacterized ORF||Decreased mRNA abundance observed in cyr1 homozygous null mutant hyphal cells; caspofungin repressed; possibly an essential gene, disruptants not obtained by UAU1 method
orf19.7331	FCY24	1.6	Uncharacterized ORF||Putative transporter; more similar to S. cerevisiae Tpn1p, which is a vitamin B6 transporter, than to purine-cytosine permeases; transcription is regulated by Nrg1p
orf19.2132	orf19.2132	1.6	Uncharacterized ORF||Predicted ORF in Assemblies 19, 20 and 21; possibly spurious ORF (Annotation Working Group prediction)
orf19.4287	orf19.4287	1.6	Uncharacterized ORF||Predicted ORF in Assemblies 19, 20 and 21; clade-associated gene expression
orf19.391	UPC2*	1.6	Verified ORF||Transcriptional regulator of ergosterol biosynthetic genes and sterol uptake; binds ERG2 promoter; has Zn(2)-Cys(6) binuclear cluster; induced upon ergosterol depletion, by azoles, anaerobicity; macrophage/pseudohyphal-repressed
orf19.391	UPC2*	1.6	Verified ORF||Transcriptional regulator of ergosterol biosynthetic genes and sterol uptake; binds ERG2 promoter; has Zn(2)-Cys(6) binuclear cluster; induced upon ergosterol depletion, by azoles, anaerobicity; macrophage/pseudohyphal-repressed
orf19.3641	orf19.3641	1.6	Expression is regulated upon white-opaque switching; merged with orf19.84 in Assembly 20
orf19.1233	ADE4*	1.6	Uncharacterized ORF||Predicted ORF in Assemblies 19, 20 and 21; flucytosine induced
orf19.1233	ADE4*	1.6	Uncharacterized ORF||Predicted ORF in Assemblies 19, 20 and 21; flucytosine induced
orf19.1799	GAP5*	1.6	Putative general amino acid permease; fungal-specific (no human or murine homolog)
orf19.1799	GAP5*	1.6	Putative general amino acid permease; fungal-specific (no human or murine homolog)
orf19.1193	GNP1	1.6	Uncharacterized ORF||Protein described as similar to asparagine and glutamine permease; fluconazole or caspofungin induced; transcription is regulated by Nrg1p, Mig1p, Tup1p, Gcn2p, Gcn4p, and alkaline regulated by Rim101p; fungal-specific
orf19.5612	BMT4	1.6	Verified ORF||Putative beta-mannosyltransferase, required for elongation of beta-mannose chains on the acid-labile fraction of cell wall phosphopeptidomannan; member of a 9-gene family; regulated by Tsa1p, Tsa1Bp
orf19.3353	orf19.3353	1.6	Uncharacterized ORF||Protein described as similar to a mitochondrial complex I intermediate-associated protein; fluconazole-downregulated
orf19.3175	orf19.3175	1.6	Uncharacterized ORF||Predicted ORF in Assemblies 19, 20 and 21; alkaline downregulated; repressed by nitric oxide; virulence-group-correlated expression
orf19.6959	HOM32	1.6	Putative L-aspartate 4-P-transferase; fungal-specific (no human or murine homolog); removed from Assembly 20
orf19.1862	orf19.1862	1.6	Uncharacterized ORF||Possible stress protein; increased transcription is associated with CDR1 and CDR2 overexpression or fluphenazine treatment; transcription regulated by Sfu1p, Nrg1p, Tup1p
orf19.5641	CAR2	1.6	Verified ORF||Alkaline upregulated; mutation confers hypersensitivity to toxic ergosterol analog, and to amphotericin B

orf19.5911	CMK1	1.6	Uncharacterized ORF||Expression is regulated upon white-opaque switching; biochemically purified Ca2+/CaM-dependent kinase is soluble, cytosolic, monomeric, and serine-autophosphorylated
orf19.1691	orf19.1691	1.6	Verified ORF||Predicted ORF in Assemblies 19, 20 and 21; fluconazole-induced; filament induced; Hog1p-induced; regulated by Nrg1p, Tup1p; increased expression in response to prostaglandins
orf19.6117	orf19.6117	1.6	Uncharacterized ORF||Predicted ORF in Assemblies 19, 20 and 21
orf19.3810	orf19.3810	1.6	Uncharacterized ORF||Predicted ORF in Assemblies 19, 20 and 21
orf19.7612	CTM1	1.6	Uncharacterized ORF||Predicted ORF in Assemblies 19, 20 and 21; regulated by Gcn2p and Gcn4p; transcriptionally activated by Mnl1p under weak acid stress
orf19.118	FAD2	1.6	Verified ORF||Delta-12 fatty acid desaturase, involved in production of linoleic acid, which is a major component of membranes
orf19.5801	RNR21*	1.6	Uncharacterized ORF||Protein described as similar to ribonucleoside-diphosphate reductase; regulated by tyrosol and cell density; transcription is upregulated in response to treatment with ciclopirox olamine; fluconazole or flucytosine induced
orf19.5801	RNR21*	1.6	Uncharacterized ORF||Protein described as similar to ribonucleoside-diphosphate reductase; regulated by tyrosol and cell density; transcription is upregulated in response to treatment with ciclopirox olamine; fluconazole or flucytosine induced
orf19.2324	UBA4	1.6	Uncharacterized ORF||Predicted ORF in Assemblies 19, 20 and 21; increased expression in response to prostaglandins; clade-associated gene expression
orf19.6660	orf19.6660	1.6	Uncharacterized ORF||Putative protein of unknown function; mRNA binds to She3p; predicted ORF in Assemblies 19, 20 and 21
orf19.1979	GIT3	1.6	Glycerophosphocholine permease; white cell specific transcript; fungal-specific; alkaline repressed; caspofungin, macrophage/pseudohyphal-repressed; flow model biofilm induced; Spider biofilm induced
orf19.6973	orf19.6973	1.6	Uncharacterized ORF||Predicted ORF in Assemblies 19, 20 and 21; regulated by Gcn2p and Gcn4p
orf19.768	SYG1	1.6	Uncharacterized ORF||Protein not essential for viability; similar to S. cerevisiae Syg1p, which is a plasma membrane protein that may be involved in signal transduction
orf19.2655	BUB3	1.6	Uncharacterized ORF||Protein similar to S. cerevisiae Bub3p, which is a kinetochore checkpoint component; induced under hydroxyurea treatment
orf19.683	orf19.683	1.6	Predicted ORF from Assemblies 19 and 20; identical to orf19.3391; merged with orf19.3391 in Assembly 20 (see Locus History)
orf19.6640	TPS1	1.6	Verified ORF||Trehalose-6-phosphate synthase; role in hyphal growth and virulence in mouse systemic infection; upregulated in presence of human neutrophils; macrophage/pseudohyphal-repressed after 16h; detected by mass spec in stationary phase cultures
orf19.2375	orf19.2375	1.6	Predicted ORF from Assembly 19; orf19.2371, orf19.2372, and orf19.2375 are similar to the Tca2 (pCal) retrotransposon, which is present in strain hOG1042 as 50 to 100 copies of a linear dsDNA; removed from Assembly 20

orf19.3718	orf19.3718	1.6	Gene fragment (probable assembly 19 error); 5' end of OPT4-2 allele (oligopeptide transporter); fungal-specific (no human or murine homolog); transcriptionally induced upon phagocytosis by macrophage; merged with orf19.176 in Assembly 20
orf19.2866	orf19.2866	1.6	Uncharacterized ORF||Predicted ORF in Assemblies 19, 20 and 21
orf19.7445	orf19.7445	1.5	Uncharacterized ORF||Predicted ORF in Assemblies 19, 20 and 21
orf19.3749	IFC3	1.5	Verified ORF||Oligopeptide transporter; transcriptionally induced upon phagocytosis by macrophage; induced by BSA or peptides; fluconazole-induced; upregulated by Rim101p at pH 8; virulence-group-correlated expression; no human or murine homolog
orf19.3391	ADK1	1.5	Uncharacterized ORF||Putative adenylate kinase; decreased expression in hyphae compared to yeast-form; macrophage-induced protein; adenylate kinase release used as a marker for cell lysis; possibly an essential gene, disruptants not obtained by UAU1 method
orf19.2768	AMS1	1.5	Uncharacterized ORF||Putative alpha-mannosidase; transcription is regulated by Nrg1p; induced during cell wall regeneration
orf19.6637	orf19.6637	1.5	Uncharacterized ORF||Predicted ORF in Assemblies 19, 20 and 21
orf19.1205	orf19.1205	1.5	Predicted ORF from Assembly 19; transcription is negatively regulated by Sfu1p; removed from Assembly 20
orf19.7484	ADE1	1.5	Verified ORF||Phosphoribosylaminoimadazole succinocarboxamide synthetase, enzyme of adenine biosynthesis; not induced during GCN response, in contrast to the S. cerevisiae ortholog; fungal-specific (no human or murine homolog)
orf19.922	ERG11	1.5	Verified ORF||Lanosterol 14-alpha-demethylase, member of cytochrome P450 family that functions in ergosterol biosynthesis; target of azole antifungals; may contribute to drug resistance; azole- or biofilm-induced; subject to hypoxic regulation
orf19.510	orf19.510	1.5	Uncharacterized ORF||Predicted ORF in Assemblies 19, 20 and 21; possibly spurious ORF (Annotation Working Group prediction)
orf19.542	HXK2	1.5	Uncharacterized ORF||Protein described as hexokinase II; antigenic in human; downregulated in the presence of human neutrophils; regulated by Efg1p; fluconazole-induced; shows colony morphology-related gene regulation by Ssn6p
orf19.5961	orf19.5961	1.5	Uncharacterized ORF||Predicted ORF in Assemblies 19, 20 and 21; described as similar to S. cerevisiae Nas6p proteasome component; induced upon adherence to polystyrene; regulated by Gcn2p and Gcn4p

SUPPLEMENTARY TABLE II.2B_GO TERM ANALYSIS OF BOUND GENES

GO term	Cluster frequency	Background frequency	adj. p-value	Gene(s) annotated to the term
nitrogen compound transport	21 out of 138 genes, 15.2%	203 out of 6525 background genes, 3.1%	3.64E-07	CAN2:GNP1:MEP1:OPT4:GAP5:OPT1:DIP5:FCY2:IFC3:TPO3:CDR4:MUP1:NUP:DUR3:GAP6:PTR22:GAP2:FCY24:orf19.7566:CAN3:CAN1
small molecule metabolic process	36 out of 138 genes, 26.1%	633 out of 6525 background genes, 9.7%	4.61E-06	FAD2:ADE4:HOM3:GPD1:ARO10:RNR22:PGM2:GOR1:ARH2:orf19.3810:GCV2:ADE13:UPC2:PUT2:ERG1:PUT1:GDH3:DAK2:URA1:DAP1:CYB2:ADE5,7:LAP3:RHR2:GCV1:CAR2:SHM2:RNR21:GLT1:ADE6:GLN1:orf19.683:ADE1:TRX1:DUR1,2:ERG11
amino acid transmembrane transport	10 out of 138 genes, 7.2%	43 out of 6525 background genes, 0.7%	5.44E-06	CAN2:GNP1:GAP5:DIP5:MUP1:GAP6:GAP2:orf19.7566:CAN3:CAN1
single-organism metabolic process	49 out of 138 genes, 35.5%	1073 out of 6525 background genes, 16.4%	6.74E-06	FAD2:ADE4:HOM3:GPD1:ALG6:ARO10:RNR22:CCP1:ADH5:HEM13:PGM2:GOR1:orf19.3175:orf19.3303:orf19.3442:ARH2:orf19.3810:GCV2:ADE13:UPC2:PUT2:ERG1:PUT1:orf19.4287:GDH3:DAK2:URA1:DAP1:CYB2:ADE5,7:IFE2:LAP3:RHR2:GCV1:CAR2:SHM2:AMO1:RNR21:GLT1:ADE6:GLN1:orf19.683:GPD2:orf19.7459:ADE1:TRX1:XYL2:DUR1,2:ERG11
nitrogen utilization	6 out of 138 genes, 4.3%	12 out of 6525 background genes, 0.2%	2.88E-05	MEP1:OPT4:OPT1:IFC3:GLN1:DUR1,2
'de novo' IMP biosynthetic process	5 out of 138 genes, 3.6%	8 out of 6525 background genes, 0.1%	9.24E-05	ADE4:ADE13:ADE5,7:ADE6:ADE1
amino acid transport	10 out of 138 genes, 7.2%	58 out of 6525 background genes, 0.9%	1.10E-04	CAN2:GNP1:GAP5:DIP5:MUP1:GAP6:GAP2:orf19.7566:CAN3:CAN1
oxidation-reduction process	26 out of 138 genes, 18.8%	418 out of 6525 background genes, 6.4%	1.40E-04	GPD1:ALG6:RNR22:CCP1:ADH5:HEM13:PGM2:GOR1:orf19.3175:orf19.3442:orf19.3810:GCV2:PUT2:ERG1:PUT1:orf19.4287:GDH3:URA1:IFE2:AMO1:RNR21:GLT1:GPD2:orf19.7459:XYL2:ERG11

IMP metabolic process	5 out of 138 genes, 3.6%	10 out of 6525 background genes, 0.2%	4.00E-04	ADE4:ADE13:ADE5,7:ADE6:ADE1
IMP biosynthetic process	5 out of 138 genes, 3.6%	10 out of 6525 background genes, 0.2%	4.00E-04	ADE4:ADE13:ADE5,7:ADE6:ADE1
dicarboxylic acid metabolic process	7 out of 138 genes, 5.1%	30 out of 6525 background genes, 0.5%	9.30E-04	ADE13:PUT2:PUT1:GDH3:GLT1:GLN1:ADE1
alpha-amino acid catabolic process	7 out of 138 genes, 5.1%	31 out of 6525 background genes, 0.5%	1.18E-03	ARO10:GCV2:PUT2:PUT1:LAP3:GCV1:CAR2
glutamate metabolic process	5 out of 138 genes, 3.6%	12 out of 6525 background genes, 0.2%	1.22E-03	PUT2:PUT1:GDH3:GLT1:GLN1
transmembrane transport	22 out of 138 genes, 15.9%	363 out of 6525 background genes, 5.6%	2.11E-03	CAN2:GNP1:MEP1:OPT4:GAP5:GIT3:OPT1:DIP5:IFC3:orf19.4550:TPO3:QDR1:MUP1:orf19.6117:NUP:DUR3:GAP6:PTR2:GAP2:orf19.7566:CAN3:CAN1
alpha-amino acid metabolic process	13 out of 138 genes, 9.4%	138 out of 6525 background genes, 2.1%	2.28E-03	HOM3:ARO10:orf19.3810:GCV2:PUT2:PUT1:GDH3:LAP3:GCV1:CAR2:SHM2:GLT1:GLN1
ribonucleoside monophosphate biosynthetic process	7 out of 138 genes, 5.1%	38 out of 6525 background genes, 0.6%	5.05E-03	ADE4:ADE13:URA1:ADE5,7:ADE6:orf19.683:ADE1
glutamate biosynthetic process	4 out of 138 genes, 2.9%	8 out of 6525 background genes, 0.1%	5.67E-03	PUT2:PUT1:GDH3:GLT1
carboxylic acid transport	10 out of 138 genes, 7.2%	89 out of 6525 background genes, 1.4%	6.42E-03	CAN2:GNP1:GAP5:DIP5:MUP1:GAP6:GAP2:orf19.7566:CAN3:CAN1
organic acid transport	10 out of 138 genes, 7.2%	90 out of 6525 background genes, 1.4%	7.10E-03	CAN2:GNP1:GAP5:DIP5:MUP1:GAP6:GAP2:orf19.7566:CAN3:CAN1
nucleoside monophosphate biosynthetic process	7 out of 138 genes, 5.1%	40 out of 6525 background genes, 0.6%	7.22E-03	ADE4:ADE13:URA1:ADE5,7:ADE6:orf19.683:ADE1

organonitrogen compound metabolic process	26 out of 138 genes, 18.8%	515 out of 6525 background genes, 7.9%	7.33E-03	ADE4:HOM3:GPD1:ARO10:UBA4:HEM13:orf19.3303:orf19.3810:GCV2:ADE13:PUT2:PUT1:GDH3:URA1:ADE5,7:LAP3:GCV1:CAR2:SHM2:AMO1:GLT1:ADE6:GLN1:orf19.683:ADE1:DUR1,2
oligopeptide transmembrane transport	4 out of 138 genes, 2.9%	9 out of 6525 background genes, 0.1%	1.00E-02	OPT4:OPT1:IFC3:PTR22
cellular amino acid catabolic process	7 out of 138 genes, 5.1%	43 out of 6525 background genes, 0.7%	1.19E-02	ARO10:GCV2:PUT2:PUT1:LAP3:GCV1:CAR2
ribonucleoside monophosphate metabolic process	7 out of 138 genes, 5.1%	43 out of 6525 background genes, 0.7%	1.19E-02	ADE4:ADE13:URA1:ADE5,7:ADE6:orf19.683:ADE1
ion transmembrane transport	11 out of 138 genes, 8.0%	116 out of 6525 background genes, 1.8%	1.20E-02	CAN2:GNP1:MEP1:GAP5:DIP5:MUP1:GAP6:GAP2:orf19.7566:CAN3:CAN1
carbohydrate metabolic process	17 out of 138 genes, 12.3%	266 out of 6525 background genes, 4.1%	1.48E-02	GPM2:GPD1:ALG6:orf19.2308:AMS1:PGM2:CRH12:PFK1:DAK2:SMI1:HXK2:RHR2:BMT4:TPS1:GPD2:PYC2:HSP21
oxidoreductase activity	30 out of 138 genes, 21.7%	422 out of 6525 background genes, 6.5%	2.01E-07	FAD2:GPD1:RNR22:UBA4:CCP1:ADH5:AHP1:HEM13:GOR1:orf19.3175:orf19.3442:ARH2:orf19.3810:GCV2:PUT2:ERG1:PUT1:orf19.4287:GDH3:URA1:CYB2:IFE2:GCV1:AMO1:RNR21:GLT1:GPD2:TRX1:XYL2:ERG11
transmembrane transporter activity	26 out of 138 genes, 18.8%	356 out of 6525 background genes, 5.5%	1.78E-06	CAN2:GNP1:MEP1:OPT4:GAP5:GIT3:OPT1:DIP5:FCY2:IFC3:orf19.4550:TPO3:CRP1:CDR4:QDR1:MUP1:NUP:DUR3:GAP6:PTR22:CCC1:GAP2:FCY24:orf19.7566:CAN3:CAN1
amino acid transmembrane transporter activity	10 out of 138 genes, 7.2%	46 out of 6525 background genes, 0.7%	3.49E-06	CAN2:GNP1:GAP5:DIP5:MUP1:GAP6:GAP2:orf19.7566:CAN3:CAN1
substrate-specific transmembrane transporter activity	23 out of 138 genes, 16.7%	311 out of 6525 background genes, 4.8%	1.13E-05	CAN2:GNP1:MEP1:OPT4:GAP5:GIT3:OPT1:DIP5:FCY2:IFC3:TPO3:CRP1:MUP1:NUP:DUR3:GAP6:PTR22:CCC1:GAP2:FCY24:orf19.7566:CAN3:CAN1

transporter activity	26 out of 138 genes, 18.8%	430 out of 6525 background genes, 6.6%	8.11E-05	CAN2:GNP1:MEP1:OPT4:GAP5:GIT3:OPT1:DIP5:FCY2:IFC3:orf19.4550:TPO3:CRP1:CDR4:QDR1:MUP1:NUP:DUR3:GAP6:PTR22:CCC1:GAP2:FCY24:orf19.7566:CAN3:CAN1
substrate-specific transporter activity	23 out of 138 genes, 16.7%	367 out of 6525 background genes, 5.6%	2.20E-04	CAN2:GNP1:MEP1:OPT4:GAP5:GIT3:OPT1:DIP5:FCY2:IFC3:TPO3:CRP1:MUP1:NUP:DUR3:GAP6:PTR22:CCC1:GAP2:FCY24:orf19.7566:CAN3:CAN1
carboxylic acid transmembrane transporter activity	10 out of 138 genes, 7.2%	71 out of 6525 background genes, 1.1%	2.50E-04	CAN2:GNP1:GAP5:DIP5:MUP1:GAP6:GAP2:orf19.7566:CAN3:CAN1
organic anion transmembrane transporter activity	11 out of 138 genes, 8.0%	91 out of 6525 background genes, 1.4%	3.50E-04	CAN2:GNP1:GAP5:GIT3:DIP5:MUP1:GAP6:GAP2:orf19.7566:CAN3:CAN1
organic acid transmembrane transporter activity	10 out of 138 genes, 7.2%	74 out of 6525 background genes, 1.1%	3.70E-04	CAN2:GNP1:GAP5:DIP5:MUP1:GAP6:GAP2:orf19.7566:CAN3:CAN1
oxidoreductase activity, acting on the CH-NH2 group of donors	5 out of 138 genes, 3.6%	14 out of 6525 background genes, 0.2%	9.50E-04	GCV2:GDH3:GCV1:AMO1:GLT1
anion transmembrane transporter activity	12 out of 138 genes, 8.7%	122 out of 6525 background genes, 1.9%	1.10E-03	CAN2:GNP1:MEP1:GAP5:GIT3:DIP5:MUP1:GAP6:GAP2:orf19.7566:CAN3:CAN1
oligopeptide transmembrane transporter activity	4 out of 138 genes, 2.9%	8 out of 6525 background genes, 0.1%	1.80E-03	OPT4:OPT1:IFC3:PTR22
ion transmembrane transporter activity	17 out of 138 genes, 12.3%	248 out of 6525 background genes, 3.8%	1.89E-03	CAN2:GNP1:MEP1:GAP5:GIT3:DIP5:TPO3:CRP1:MUP1:NUP:DUR3:GAP6:CCC1:GAP2:orf19.7566:CAN3:CAN1
L-amino acid transmembrane transporter activity	5 out of 138 genes, 3.6%	17 out of 6525 background genes, 0.3%	2.80E-03	GNP1:DIP5:MUP1:GAP2:CAN1
plasma membrane	24 out of 140 genes, 17.1%	476 out of 6525 background genes, 7.3%	2.70E-03	CAN2:MEP1:orf19.1691:OPT1:AHP1:DIP5:orf19.3718:IFC3:ERG1:orf19.4550:TPO3:CRP1:CDR4:QDR1:RHD3:SHM2:DUR3:PTR22:CCC1:GAP2:orf19.7296:SYG1:ERG11:CAN1

membrane	48 out of 140 genes, 34.3%	1406 out of 6525 background genes, 21.5%	8.93E-03	CAN2:GNP1:SPO75:MEP1:orf19.1691:GAP5:ALG6:GIT3:CCP1:OPT1:AHP1:AMS1:DIP5:CCE1:FCY2:ARH2:orf19.3718:IFC3:UPC2:ERG1:orf19.4550:TPO3:CRP1:URA1:CDR4:QDR1:MUP1:RHD3:orf19.5514:SHM2:orf19.6117:orf19.6224:NUP:DUR3:GAP6:orf19.683:PTR22:CCC1:GAP2:orf19.7296:FCY24:orf19.7445:orf19.7459:orf19.7566:SYG1:CAN3:ERG11:CAN1

SUPPLEMENTARY TABLE II.3A_MODULATED GENES IN THE *fcr1* MUTANT

Standard Name	Systematic Name	FC (fcr1ΔΔ /wt)	adj.P.Val	Description
HNM3	orf19.2587	2.6	8.62E-02	Putative transporter; Hap43, flucytosine repressed; possibly essential, disruptants not obtained by UAU1 method; Spider biofilm induced
ECE1	orf19.3374	2.4	6.52E-02	Hypha-specific protein; regulated by Rfg1, Nrg1, Tup1, Cph1, Efg1, Hog1, farnesol, phagocytosis; fluconazole-induced; rat catheter and Spider biofilm induced; flow model biofilm repressed; Bcr1-repressed in RPMI a/a biofilms
CHA1	orf19.1996	2.2	1.91E-03	Similar to catabolic ser/thr dehydratases; repressed by Rim101; induced in low iron; regulated on white-opaque switch; filament induced; Tn mutation affects filamentation; flow model biofilm induced; Spider biofilm repressed
ALS3	orf19.1816	2.2	2.56E-02	Cell wall adhesin; epithelial adhesion, endothelial invasion; alleles vary in adhesiveness; immunoprotective in mice; binds SspB adhesin of S. gordonii in mixed biofilm; induced in/required for Spider biofilm; flow model biofilm repressed
orf19.4273	orf19.4273	2.0	6.51E-02	Putative mitochondrial membrane protein; ortholog of S. cerevisiae Sls1; coordinates expression of mitochondrially-encoded genes; Hap43-induced
HWP1	orf19.1321	2.0	5.96E-02	Hyphal cell wall protein; host transglutaminase substrate; opaque-, a-specific, alpha-factor induced; at MTLa side of conjugation tube; virulence complicated by URA3 effects; Bcr1-repressed in RPMI a/a biofilms; Spider biofilm induced
PBR1	orf19.6274	2.0	3.25E-02	Protein of unknown function; required for cohesion, adhesion, and RPMI biofilm formation; induced by alpha pheromone in white cells; fluconazole-induced; Spider biofilm induced
orf19.4706	orf19.4706	-2.0	1.85E-02	Protein of unknown function; induced in cyr1 or ras1 mutant; induced by fluconazole, by alpha pheromone in SpiderM medium and during oralpharyngeal candidasis; Spider biofilm induced
RME1	orf19.4438	-2.7	1.80E-03	Zinc finger protein; controls meiosis in S. cerevisae; white-specific transcript; upregulation correlates with clinical development of fluconazole resistance; Upc2-regulated in hypoxia; flow model biofilm induced; Spider biofilm repressed

SUPPLEMENTARY TABLE II.3B_MODULATED GENES IN THE *FCR1* OE STRAIN

Standard Name	Systematic Name	FC (OE/fcr1 ΔΔ)	adj.P.Val	Description
HSP30	orf19.4526	26.1	2.72E-06	Putative heat shock protein; fluconazole repressed; amphotericin B induced; Spider biofilm induced; rat catheter biofilm induced
HSP31	orf19.3664	24.8	4.91E-07	Putative 30 kda heat shock protein; repressed during the mating process; rat catheter biofilm induced
orf19.5785	orf19.5785	23.4	7.79E-08	Protein of unknown function; upregulated in a cyr1 or ras1 null mutant; induced by nitric oxide
orf19.3988	orf19.3988	16.2	1.63E-06	Putative adhesin-like protein; induced by Mnl1 under weak acid stress; rat catheter and Spider biofilm induced
orf19.1774	orf19.1774	14.6	8.84E-04	Predicted dehydrogenase; transcript upregulated in an RHE model of oral candidiasis; virulence-group-correlated expression; Spider biofilm repressed
orf19.6688	orf19.6688	8.5	1.63E-06	Protein of unknown function; expression decreases by benomyl treatment or in an azole-resistant strain overexpressing MDR1; Spider biofilm induced
RME1	orf19.4438	8.0	4.89E-06	Zinc finger protein; controls meiosis in S. cerevisae; white-specific transcript; upregulation correlates with clinical development of fluconazole resistance; Upc2-regulated in hypoxia; flow model biofilm induced; Spider biofilm repressed
orf19.4907	orf19.4907	7.5	1.43E-05	Putative protein of unknown function; Hap43p-repressed gene; increased transcription is observed upon fluphenazine treatment; possibly transcriptionally regulated by Tac1p; induced by nitric oxide; fungal-specific (no human/murine homolog
HGT1	orf19.4527	7.4	1.85E-05	High-affinity MFS glucose transporter; induced by progesterone, chloramphenicol, benomyl; likely essential for growth; protein newly produced during adaptation to the serum; rat catheter and Spider biofilm induced
HAP41	orf19.740	7.0	6.42E-05	Putative Hap4-like transcription factor; Hap43-repressed; not required for response to low iron; induced by Mnl1 under weak acid stress; Spider biofilm induced
orf19.4911	orf19.4911	6.6	2.66E-06	BED zinc finger protein; predicted DNA binding protein; Spider biofilm repressed
MET3	orf19.5025	6.4	3.63E-06	ATP sulfurlyase; sulfate assimilation; repressed by Met, Cys, Sfu1, or in fluconazole-resistant isolate; Hog1, caspofungin, white phase-induced; induced on biofilm formation, even in presence of Met and Cys; Spider, F-12/CO2 biofilm induced
CFL2	orf19.1264	6.2	1.85E-05	Oxidoreductase; iron utilization; Sfu1/Sef1/Hap43/Nrg1/Tup1/Rim101 regulated; alkaline/low iron/fluphenazine/ciclopirox olamine, flucytosine, fluconazole, Spider/flow model/rat catheter biofilm induced; caspofungin/amphotericin B repressed
STP4	orf19.909	5.9	7.28E-05	C2H2 transcription factor; induced in core caspofungin response; colony morphology-related gene regulation by Ssn6; induced by 17-beta-estradiol, ethynyl estradiol; rat catheter and Spider biofilm induced
RBT5	orf19.5636	5.8	2.69E-05	GPI-linked cell wall protein; hemoglobin utilization; Rfg1, Rim101, Tbf1, Fe regulated; Sfu1, Hog1, Tup1, serum, alkaline pH, antifungal drugs, geldamycin repressed; Hap43 induced; required for RPMI biofilms; Spider biofilm induced

YDC1	orf19.3104	5.6	4.92E-06	Alkaline dihydroceramidase; involved in sphingolipid metabolism; Mob2-dependent hyphal regulation; transcript is regulated by Nrg1 and Mig1; Hap43-repressed
PGA13	orf19.6420	5.4	7.93E-05	GPI-anchored cell wall protein involved in cell wall synthesis; required for normal cell surface properties; induced in oralpharyngeal candidasis; Spider biofilm induced; Bcr1-repressed in RPMI a/a biofilms
orf19.6951	orf19.6951	5.4	2.82E-06	Ortholog(s) have sphinganine-1-phosphate aldolase activity and role in calcium-mediated signaling, cellular response to starvation, sphingolipid metabolic process
orf19.1887	orf19.1887	5.1	4.78E-05	Ortholog(s) have sterol esterase activity, role in sterol metabolic process and integral to membrane, lipid particle localization
orf19.1861	orf19.1861	5.0	2.66E-06	Protein of unknown function; flow model biofilm induced
HSP21	orf19.822	5.0	2.04E-05	Small heat shock protein; role in stress response and virulence; fluconazole-downregulated; induced in cyr1 or ras1 mutant; stationary phase enriched protein; detected in some, not all, biofilm extracts; Spider biofilm induced
orf19.1395	orf19.1395	4.7	7.17E-06	Ortholog(s) have inorganic phosphate transmembrane transporter activity, role in phosphate ion transport, transmembrane transport and mitochondrion localization
FMP45	orf19.6489	4.6	2.66E-06	Predicted membrane protein induced during mating; mutation confers hypersensitivity to toxic ergosterol analog, to amphotericin B; alkaline repressed; repressed by alpha pheromone in SpiderM medium; rat catheter, Spider biofilm induced
AOX2	orf19.4773	4.4	1.72E-04	Alternative oxidase; cyanide-resistant respiration; induced by antimycin A, oxidants; growth; Hap43, chlamydospore formation repressed; rat catheter, Spider biofilm induced; regulated in Spider biofilms by Bcr1, Tec1, Ndt80, Brg1
GAL102	orf19.3674	4.3	1.25E-04	UDP-glucose 4,6-dehydratase; role in mannosylation of cell wall proteins; mutation confers hypersensitivity to toxic ergosterol analog; overlaps orf19.3673; Spider biofilm induced
HGT2	orf19.3668	4.3	1.08E-05	Putative MFS glucose transporter; 20 member C. albicans glucose transporter family; 12 probable membrane-spanning segments; expressed in rich medium with 2% glucose; rat catheter and Spider biofilm induced
orf19.673	orf19.673	4.2	4.27E-05	Has domain(s) with predicted FMN binding, catalytic activity, oxidoreductase activity and role in oxidation-reduction process
OPT8	orf19.5770	4.2	2.66E-06	Oligopeptide transporter; similar to Opt1 and to S. cerevisiae Ygl114wp, but not other OPTs; induced by nitric oxide, amphotericin B; expression of OPT6, 7, 8 does not complement mutants lacking Opt1, Opt2, and Opt3; Spider biofilm induced
SUL2	orf19.2738	4.1	5.10E-05	Putative sulfate transporter; transcript negatively regulated by Sfu1; amphotericin B induced; F-12/CO2 and Spider biofilm induced
HSX11	orf19.4592	3.9	1.06E-05	UDP-glucose:ceramide glucosyltransferase (glucosylceramide synthase [GCS], EC 2.4.1.80); involved in glucosylceramide biosynthesis, which is important for virulence
RCH1	orf19.5663	3.9	8.08E-06	Plasma membrane protein; involved in regulation of cytosolic calcium homeostasis; null mutation confers sensitivity to calcium and resistance to azoles and terbinafine; rat catheter biofilm induced

orf19.1117	orf19.1117	3.7	1.32E-03	Protein similar to Candida boidinii formate dehydrogenase; virulence-group-correlated expression; Hap43-repressed; Spider biofilm repressed
orf19.3922	orf19.3922	3.4	1.06E-05	Possible pyrimidine 5' nucleotidase; protein present in exponential and stationary growth phase yeast cultures; Hap43p-repressed gene
RGA2	orf19.4593	3.4	2.67E-05	Putative GTPase-activating protein (GAP) for Rho-type GTPase Cdc42; involved in cell signaling pathways controlling cell polarity; induced by low-level peroxide stress; flow model biofilm induced
AOX1	orf19.4774	3.4	8.14E-04	Alternative oxidase; low abundance; constitutively expressed; one of two isoforms (Aox1p and Aox2p); involved in a cyanide-resistant respiratory pathway present in plants, protists, and some fungi, absent in S. cerevisiae; Hap43p-repressed
OYE22	orf19.3234	3.4	1.43E-05	Putative NADPH dehydrogenase; rat catheter biofilm induced
orf19.1785	orf19.1785	3.4	4.89E-06	Protein with a PI31 proteasome regulator domain; Hap43-repressed; flow model biofilm induced
BUL4	orf19.5245	3.3	8.37E-06	Protein with a predicted BUL1 N-terminal and C-terminal domains; Bul1 binds the ubiquitin ligase Rsp5 in S. cerevisiae; Hap43-repressed gene; rat catheter biofilm induced
orf19.3448	orf19.3448	3.3	5.10E-05	Protein of unknown function; ketoconazole-repressed
PGA38	orf19.2758	3.2	2.01E-05	Putative adhesin-like GPI-anchored protein; repressed during cell wall regeneration; possibly an essential gene, disruptants not obtained by UAU1 method; rat catheter and Spider biofilm repressed
RTA3	orf19.23	3.1	2.04E-05	Similar to S. cerevisiae Rta1 (role in 7-aminocholesterol resistance) and Rsb1 (flippase); putative drug-responsive regulatory site; induced by fluphenazine, estradiol, ketoconazole, caspofungin; rat catheter biofilm induced
GAL7	orf19.3675	3.1	2.42E-04	Putative galactose-1-phoshphate uridyl transferase; downregulated by hypoxia, upregulated by ketoconazole; macrophage/pseudohyphal-repressed
orf19.670.2	orf19.670.2	3.1	2.28E-03	Protein of unknown function; hypoxia, Hap43-repressed; ketoconazole induced; induced in oralpharyngeal candidasis; 16h flow model biofilm repressed, late-stage flow model biofilm induced; rat catheter and Spider biofilm induced
orf19.6770	orf19.6770	3.1	8.08E-06	protein with ENTH Epsin domain, N-terminal; Spider biofilm repressed
orf19.7056	orf19.7056	3.0	1.14E-04	Putative protein of unknown function; transcript is upregulated in clinical isolates from HIV+ patients with oral candidiasis; regulated by Sef1, Sfu1, and Hap43
FDH1	orf19.638	3.0	1.43E-03	Formate dehydrogenase; oxidizes formate to CO2; Mig1 regulated; induced by macrophages; fluconazole-repressed; repressed by Efg1 in yeast, not hyphal conditions; stationary phase enriched; rat catheter and Spider biofilm induced
STB3	orf19.203	3.0	1.43E-05	Putative SIN3-binding protein 3 homolog; caspofungin induced; macrophage/pseudohyphal-repressed; rat catheter biofilm induced
GAC1	orf19.7053	3.0	1.25E-04	Putative regulatory subunit of ser/thr phosphoprotein phosphatase 1; fluconazole-induced; caspofungin repressed; transcript induced by Mnl1 under weak acid stress; regulated by Nrg1, Tup1; Spider and flow model biofilm induced

orf19.3089	orf19.3089	3.0	2.33E-04	Predicted mitochondrial intermembrane space protein; predicted role in phospholipid metabolism; rat catheter and Spider biofilm induced
IFE1	orf19.769	2.9	1.20E-04	Putative medium-chain alcohol dehydrogenase; rat catheter and Spider biofilm repressed
PGA62	orf19.2765	2.9	1.01E-05	Adhesin-like cell wall protein; putative GPI-anchor; fluconazole-induced; induced in high iron; induced during cell wall regeneration; Cyr1 or Ras1 repressed; Tbf1 induced
orf19.2515	orf19.2515	2.8	3.69E-05	ZZ-type zinc finger protein; rat catheter and Spider biofilm induced
PGA7	orf19.5635	2.8	2.34E-04	GPI-linked hyphal surface antigen; induced by ciclopirox olamine, ketoconazole, Rim101 at pH 8; Hap43, fluconazole; flow model biofilm induced; Spider biofilm induced; required for RPMI biofilm; Bcr1-induced in a/a biofilm
orf19.7344	orf19.7344	2.8	1.33E-05	Ortholog(s) have DNA binding, chromatin binding, histone deacetylase activity
CAT2	orf19.4591	2.8	1.91E-05	Major carnitine acetyl transferase; intracellular acetyl-CoA transport; localized in peroxisomes and mitochondria; induced in macrophages; Hog1-repressed; stationary phase enriched; farnesol-upregulated in biofilm; Spider biofilm induced
RGT1	orf19.2747	2.8	2.00E-04	Zn(II)2Cys6 transcription factor; transcriptional repressor involved in the regulation of glucose transporter genes; ortholog of S. cerevisiae Rgt1; mutants display decreased colonization of mouse kidneys
orf19.6864	orf19.6864	2.7	9.46E-05	Putative ubiquitin-protein ligase; role in protein ubiquitination; Spider biofilm induced
CWC22	orf19.1771	2.7	1.76E-05	Predicted spliceosome-associated protein; role in pre-mRNA splicing; Spider biofilm induced
HSM3	orf19.1331	2.7	2.24E-05	Ortholog(s) have role in mismatch repair, proteasome regulatory particle assembly and cytosol, nucleus, proteasome regulatory particle, base subcomplex localization
FRE7	orf19.6139	2.7	1.86E-03	Copper-regulated cupric reductase; repressed by ciclopirox olamine or 17-beta-estradiol; induced by alkaline conditions or interaction with macrophage; Spider biofilm induced
HSP78	orf19.882	2.7	1.85E-05	Heat-shock protein; regulated by macrophage response, Nrg1, Mig1, Gcn2, Gcn4, Mnl1p; heavy metal (cadmium) stress-induced; stationary phase enriched protein; rat catheter and Spider biofilm induced
GDH2	orf19.2192	2.7	5.53E-04	Putative NAD-specific glutamate dehydrogenase; fungal-specific; transcript regulated by Nrg1, Mig1, Tup1, and Gcn4; stationary phase enriched protein; flow model biofilm induced; Spider biofilm induced
orf19.4600	orf19.4600	2.6	1.27E-04	Protein of unknown function; possible mitochondrial protein; Spider biofilm induced
orf19.510	orf19.510	2.6	1.27E-04	Protein of unknown function; Spider biofilm induced
orf19.675	orf19.675	2.6	5.10E-05	Cell wall protein; induced in core stress response and core caspofungin response; iron-regulated; amphotericin B, ketoconazole, and hypoxia induced; regulated by Cyr1, Ssn6; induced in oralpharyngeal candidasis; Spider biofilm repressed
DAG7	orf19.4688	2.6	5.39E-04	Secretory protein; a-specific, alpha-factor induced; mutation confers hypersensitivity to toxic ergosterol analog; fluconazole-induced; induced during chlamydospore formation in C. albicans and C. dubliniensis
orf19.1830	orf19.1830	2.6	1.00E-03	Protein of unknown function; Hap43-induced; rat catheter and Spider biofilm induced
SAP7	orf19.756	2.6	2.72E-04	Pepstatin A-insensitive secreted aspartyl protease; self-processing; expressed in human oral infection; Ssn6p-regulated; role in murine intravenous infection; induced during, but not required for, murine vaginal infection; N glycosylated

GAL10	orf19.3672	2.6	2.04E-05	UDP-glucose 4-epimerase; galactose utilization; mutant has cell wall defects and increased filamentation; GlcNAc-, fluconazole- and ketoconazole-induced; stationary phase enriched protein; rat catheter and flow model biofilm induced
orf19.3007	orf19.3007	2.6	3.30E-05	Ortholog(s) have role in endosome organization, regulation of protein localization and BLOC-1 complex localization
orf19.215	orf19.215	2.6	2.08E-04	Component of a complex containing the Tor2p kinase; possible a role in regulation of cell growth; Spider biofilm induced
orf19.4634	orf19.4634	2.5	6.00E-04	Protein required for thiolation of uridine at wobble position of Gln, Lys, and Glu tRNAs; has a role in urmylation; S. cerevisiae ortholog has a role in invasive and pseudohyphal growth
HGT10	orf19.5753	2.5	6.96E-03	Glycerol permease involved in glycerol uptake; member of the major facilitator superfamily; induced by osmotic stress, at low glucose in rich media, during cell wall regeneration; 12 membrane spans; Hap43p-induced gene
orf19.3499	orf19.3499	2.5	2.70E-04	Secreted potein; Hap43-repressed; fluconazole-induced; regulated by Tsa1, Tsa1B under H2O2 stress conditions; induced by Mnl1p under weak acid stress; Spider biofilm induced
HSP104	orf19.6387	2.5	1.85E-05	Heat-shock protein; roles in biofilm and virulence; complements chaperone, prion activity in S. cerevisiae; guanidine-insensitive; heat shock/stress induced; repressed in farnesol-treated biofilm; sumoylation target; Spider biofilm induced
orf19.2769	orf19.2769	2.5	4.74E-04	Putative protease B inhibitor; hyphal-induced expression; Cyr1p- and Ras1p-repressed
MNN22	orf19.3803	2.5	7.03E-05	Alpha-1,2-mannosyltransferase; required for normal cell wall mannan; regulated by Tsa1, Tsa1B at 37 deg; repressed in core stress response; NO, Hog1 induced; confers sensitivity to cell wall perturbing agents; Spider biofilm repressed
MET14	orf19.946	2.5	1.37E-04	Putative adenylylsulfate kinase; predicted role in sulfur metabolism; possibly adherence-induced; protein present in exponential and stationary growth phase yeast; F-12/CO2 biofilm induced
SNZ1	orf19.2947	2.5	4.78E-05	Stationary phase protein; vitamin B synthesis; induced byyeast-hypha switch, 3-AT or in azole-resistant strain overexpressing MDR1; soluble in hyphae; regulated by Gcn4, macrophage; Spider biofilm induced; rat catheter biofilm repressed
orf19.7085	orf19.7085	2.5	3.31E-04	Protein of unknown function; induced in core stress response; induced by cadmium stress via Hog1; oxidative stress-induced via Cap1; induced by Mnl1 under weak acid stress; macrophage-repressed; rat catheter and Spider biofilm induced
CHT3	orf19.7586	2.5	9.28E-05	Major chitinase; secreted; functional homolog of S. cerevisiae Cts1p; 4 N-glycosylation motifs; possible O-mannosylation; putative signal peptide; hyphal-repressed; farnesol upregulated in biofilm; regulated by Efg1p, Cyr1p, Ras1p
orf19.6586	orf19.6586	2.5	5.33E-04	Protein of unknown function; transcript induced by benomyl or in azole-resistant strain overexpressing MDR1; Ssn6 colony morphology-related regulation; induced by NO; Hap43-repressed; rat catheter and flow model biofilm induced

orf19.5605	orf19.5605	2.5	4.69E-05	Ortholog(s) have protein binding, bridging, ubiquitin protein ligase binding activity and role in positive regulation of ubiquitin-dependent endocytosis, regulation of intracellular transport
CPA1	orf19.4630	2.5	7.40E-05	Putative carbamoyl-phosphate synthase subunit; alkaline repressed; rat catheter, Spider and flow model biofilm induced
orf19.3364	orf19.3364	2.4	7.48E-05	Ortholog of C. parapsilosis CDC317 : CPAR2_403360, Debaryomyces hansenii CBS767 : DEHA2D00814g, Pichia stipitis Pignal : PICST_32156 and Candida guilliermondii ATCC 6260 : PGUG_04611
orf19.775	orf19.775	2.4	1.94E-05	Ortholog of C. dubliniensis CD36 : Cd36_04450, C. parapsilosis CDC317 : CPAR2_105460, Debaryomyces hansenii CBS767 : DEHA2D07128g and Pichia stipitis Pignal : PICST_80203
CIT1	orf19.4393	2.4	1.30E-02	Citrate synthase; induced by phagocytosis; induced in high iron; Hog1-repressed; Efg1-regulated under yeast, not hyphal growth conditions; present in exponential and stationary phase; Spider biofilm repressed; rat catheter biofilm induced
orf19.1473	orf19.1473	2.4	3.03E-04	2-hydroxyacid dehydrogenase domain-containing protein; Hap43-repressed gene; induced by alpha pheromone in SpiderM medium
orf19.2870	orf19.2870	2.4	4.01E-04	Protein of unknown function; rat catheter and Spider biofilm induced
orf19.1430	orf19.1430	2.4	5.46E-05	Ortholog of C. parapsilosis CDC317 : CPAR2_402120, C. dubliniensis CD36 : Cd36_43870, Lodderomyces elongisporus NRLL YB-4239 : LELG_04437 and Candida orthopsilosis Co 90-125 : CORT_0E02170
SFC1	orf19.3931	2.4	6.82E-04	Putative succinate-fumarate transporter; involved in repression of growth on sorbose; alkaline induced; rat catheter biofilm induced; Spider biofilm induced
orf19.2749	orf19.2749	2.4	6.37E-05	BTB/POZ domain protein; induced by Mnl1 under weak acid stress; flow model biofilm induced; Spider biofilm induced
XOG1	orf19.2990	2.4	4.58E-05	Exo-1,3-beta-glucanase; 5 glycosyl hydrolase family member; affects sensitivity to chitin and glucan synthesis inhibitors; not required for yeast-to-hypha transition or for virulence in mice; Hap43-induced; Spider biofilm induced
GAL4	orf19.5338	2.4	7.15E-03	Zn(II)2Cys6 transcription factor; involved in control of glycolysis; ortholog of S. cerevisiae Gal4, but not involved in regulation of galactose utilization genes; caspofungin repressed; Spider biofilm repressed
RFX2	orf19.4590	2.4	1.38E-03	Transcriptional repressor; regulator of filamentation, response to DNA damage, adhesion, virulence in murine mucosal, systemic infections; RFX domain; regulated by Nrg1, UV-induced; partially complements S. cerevisiae rfx1 mutant defects
SOU1	orf19.2896	2.4	1.17E-04	Enzyme involved in utilization of L-sorbose; has sorbitol dehydrogenase, fructose reductase, and sorbose reductase activities; NAD-binding site motif; transcriptional regulation affected by chromosome 5 copy number; Hap43p-induced gene
orf19.94	orf19.94	2.3	2.14E-04	Protein of unknown function; Spider biofilm induced
DLD1	orf19.5805	2.3	1.29E-04	Putative D-lactate dehydrogenase; white cell-specific trancript; colony morphology-related gene regulation by Ssn6; Hap43-repressed; rat catheter biofilm induced; Spider biofilm repressed
orf19.3679	orf19.3679	2.3	1.15E-04	Putative protein of unknown function; stationary phase enriched protein

ADR1	orf19.2752	2.3	2.02E-04	C2H2 transcription factor; ortholog of S. cerevisiae Adr1 but mutant phenotype suggests a different set of target genes; transposon mutation affects filamentous growth; Spider biofilm induced
orf19.5572	orf19.5572	2.3	2.60E-05	Protein of unknown function; Spider biofilm repressed
orf19.1386	orf19.1386	2.3	1.23E-04	Ortholog(s) have SNAP receptor activity and role in ER to Golgi vesicle-mediated transport, retrograde vesicle-mediated transport, Golgi to ER, vesicle fusion
CHA1	orf19.1996	2.3	9.66E-05	Similar to catabolic ser/thr dehydratases; repressed by Rim101; induced in low iron; regulated on white-opaque switch; filament induced; Tn mutation affects filamentation; flow model biofilm induced; Spider biofilm repressed
GAL1	orf19.3670	2.3	5.39E-05	Galactokinase; galactose, Mig1, Tup1, Hap43 regulated; fluconazole, ketoconazole-induced; stationary phase enriched protein; GlcNAc-induced protein; farnesol, hypoxia-repressed in biofilm; rat catheter and Spider biofilm induced
orf19.4582	orf19.4582	2.3	1.25E-04	Ortholog(s) have role in U1 snRNA 3'-end processing, U4 snRNA 3'-end processing and U5 snRNA 3'-end processing, more
orf19.4702	orf19.4702	2.3	7.93E-05	Possible similarity to mutator-like element (MULE) transposase; flow model biofilm induced; expression regulated during planktonic growth
orf19.1653	orf19.1653	2.3	4.41E-05	Has domain(s) with predicted integral to membrane localization
orf19.4534	orf19.4534	2.3	2.69E-05	Putative UBX-domain (ubiquitin-regulatory domain) protein; macrophage-downregulated gene
orf19.4756	orf19.4756	2.2	5.26E-04	Ortholog of S. cerevisiae : YTP1, C. dubliniensis CD36 : Cd36_08490, C. parapsilosis CDC317 : CPAR2_801590, Candida tenuis NRRL Y-1498 : CANTEDRAFT_109732 and Debaryomyces hansenii CBS767 : DEHA2C10384g
orf19.6741	orf19.6741	2.2	3.96E-04	Putative plasma membrane protein; predicted role in cell wall integrity; regulated by Nrg1, Tup1; induced during chlamydospore formation in both C. albicans and C. dubliniensis
orf19.1349	orf19.1349	2.2	5.96E-05	Ortholog of C. dubliniensis CD36 : Cd36_22470, Candida tropicalis MYA-3404 : CTRG_01829 and Candida albicans WO-1 : CAWG_05920
LAB5	orf19.2774	2.2	4.01E-05	Ortholog(s) have role in protein lipoylation and mitochondrion localization
orf19.7210	orf19.7210	2.2	6.92E-04	Protein of unknown function; Spider biofilm induced
orf19.7619	orf19.7619	2.2	8.78E-05	Protein with a mitochondrial distribution and morphology domain; possibly an essential gene, disruptants not obtained by UAU1 method; rat catheter and Spider biofilm induced
orf19.409	orf19.409	2.2	1.05E-03	Ortholog of S. cerevisiae Aim38/Rcf2, cytochrome c oxidase subunit; plasma membrane localized; Hap43-repressed; induced in oralpharyngeal candidasis; flow model biofilm induced; Spider biofilm repressed
orf19.4593.1	orf19.4593.1	2.2	1.25E-04	Protein with a predicted role in mitochondrial respiratory chain complex II assembly; rat catheter biofilm induced
orf19.3378	orf19.3378	2.2	1.27E-04	Protein of unknown function; regulated by Tsa1, Tsa1B in minimal media at 37 degrees C
orf19.5290	orf19.5290	2.2	1.92E-04	Protein of unknown function; repressed by Sfu1; Hap43-induced gene
orf19.4575	orf19.4575	2.2	2.69E-05	Ortholog(s) have mitochondrion localization
orf19.22	orf19.22	2.2	1.09E-03	Protein with homology to peroxisomal membrane proteins; Sef1p-, Sfu1p-, and Hap43p-regulated gene

MOH1	orf19.3369	2.2	4.78E-05	Ortholog of S. cerevisiae Moh1, essential for staionary phase growth; induced by alpha pheromone in SpiderM medium and by Mnl1 under weak acid stress; possibly essential (UAU1 method); flow model biofilm induced; Spider biofilm induced
orf19.2244	orf19.2244	2.2	1.19E-04	Similar to oxidoreductases and to S. cerevisiae Yjr096wp; Sfu1 repressed; induced by benomyl treatment, Ssr1; Hap43-repressed; flow model biofilm repressed
PHHB	orf19.2079	2.2	9.66E-05	Putative 4a-hydroxytetrahydrobiopterin dehydratase; transposon mutation affects filamentous growth; flow model biofilm induced; Spider biofilm induced
orf19.3706	orf19.3706	2.2	2.96E-05	Has domain(s) with predicted oxidoreductase activity, zinc ion binding activity and role in oxidation-reduction process
orf19.7227	orf19.7227	2.1	3.13E-04	Protein phosphatase inhibitor; Hap43-repressed; homozygous Tn insertion decreases colony wrinkling but does not block hyphal growth in liquid media; mutation confers hypersensitivity to toxic ergosterol analog; Spider biofilm induced
orf19.428	orf19.428	2.1	4.65E-05	Putative serine/threonine kinase; induced during planktonic growth; rat catheter biofilm repressed
HOS3	orf19.2772	2.1	4.78E-05	Histone deacetylase; similar to S. cerevisiae Hos3p; greater expression and longer mRNA in white cells, compared to opaque cells; has conserved deacetylation motif
orf19.5207	orf19.5207	2.1	5.88E-03	Predicted diphthamide biosynthesis protein; Spider biofilm induced
orf19.7456	orf19.7456	2.1	4.03E-05	Protein of unknown function; flow model biofilm repressed
orf19.3684	orf19.3684	2.1	3.16E-04	Putative oxidoreductase; Spider biofilm induced
orf19.3869	orf19.3869	2.1	9.66E-05	Protein of unknown function; regulated by Tsa1, Tsa1B in minimal media at 37 degrees C; shows colony morphology-related gene regulation by Ssn6; Spider biofilm induced
orf19.5216	orf19.5216	2.1	3.01E-03	Has domain(s) with predicted acyl-CoA hydrolase activity and role in acyl-CoA metabolic process
orf19.25	orf19.25	2.1	2.69E-04	Ortholog(s) have tRNA (guanine) methyltransferase activity, role in tRNA methylation and cytoplasm, nucleolus localization
ADH5	orf19.2608	2.1	1.05E-04	Putative alcohol dehydrogenase; regulated by white-opaque switch; fluconazole-induced; antigenic in murine infection; regulated by Nrg1, Tup1; Hap43, macrophage repressed, flow model biofilm induced; Spider biofilm induced
orf19.4610	orf19.4610	2.1	1.74E-04	Predicted metallocarboxypeptidase; role in proteolysis; rat catheter biofilm repressed
TYE7	orf19.4941	2.1	2.93E-03	bHLH transcription factor; control of glycolysis; required for biofilm formation; hyphally regulated by Cph1, Cyr1; flucytosine, Hog1 induced; amphotericin B, caspofungin repressed; induced in flow model biofilm and planktonic cultures
BUD23	orf19.1966	2.1	2.09E-02	Putative methyltransferase; Hap43-induced; repressed by prostaglandins
PHO89	orf19.4599	2.1	1.30E-02	Putative phosphate permease; transcript regulated upon white-opaque switch; alkaline induced by Rim101; possibly adherence-induced; F-12/CO2 model, rat catheter and Spider biofilm induced
SOD1	orf19.2770.1	2.1	2.09E-04	Cytosolic copper- and zinc-containing superoxide dismutase; role in protection from oxidative stress; required for full virulence; alkaline induced by Rim101; induced by human blood; rat catheter, flow model and Spider biofilm repressed

WH11	orf19.3548.1	2.1	1.46E-03	White-phase yeast transcript; expression in opaques increases virulence/switching; mutant switches as WT; Hap43, hypoxia, ketoconazol induced; required for RPMI biofilm; Bcr1-induced in RPMI a/a biofilm; rat catheter, Spider biofilm induced
orf19.4626	orf19.4626	2.1	3.69E-05	Ortholog(s) have role in TOR signaling cascade, positive regulation of transcription from RNA polymerase I promoter and cytosol, extrinsic to membrane, nucleus localization
orf19.5735.3	orf19.5735.3	2.1	1.07E-03	Protein of unknown function; Spider biofilm induced
GPX1	orf19.87	2.1	3.94E-04	Putative thiol peroxidase; rat catheter and Spider biofilm induced
BGL2	orf19.4565	2.1	5.39E-05	Cell wall 1,3-beta-glucosyltransferase; mutant has cell-wall and growth defects, but wild-type 1,3- or 1,6-beta-glucan content; antigenic; virulence role in mouse systemic infection; rat catheter biofilm induced
orf19.4342	orf19.4342	2.1	4.93E-03	Zn2Cys6 transcription factor involved in sterol uptake; flow model biofilm induced; Spider biofilm repressed
orf19.4643	orf19.4643	2.1	2.63E-04	Ortholog of C. dubliniensis CD36 : Cd36_41430, Candida tropicalis MYA-3404 : CTRG_00187 and Candida albicans WO-1 : CAWG_03642
orf19.2067	orf19.2067	2.1	3.29E-04	Protein with a predicted role in mitochondrial iron metabolism; Hap43-repressed; expression upregulated during growth in the mouse cecum; Spider biofilm induced
orf19.7296	orf19.7296	2.0	6.29E-03	Putative cation conductance protein; similar to stomatin mechanoreception protein; plasma-membrane localized; induced by Rgt1; rat catheter and Spider biofilm induced
orf19.4569	orf19.4569	2.0	1.00E-03	Ortholog of C. dubliniensis CD36 : Cd36_42100, Debaryomyces hansenii CBS767 : DEHA2C14850g, Pichia stipitis Pignal : PICST_52615 and Spathaspora passalidarum NRRL Y-27907 : SPAPADRAFT_58608
orf19.6899	orf19.6899	2.0	2.09E-04	Putative oxidoreductase; mutation confers hypersensitivity to toxic ergosterol analog; rat catheter and Spider biofilm induced
orf19.4600.1	orf19.4600.1	2.0	9.04E-05	Protein of unknown function; flow model biofilm repressed
WAR1	orf19.1035	2.0	4.10E-04	Zn(II)2Cys6 transcription factor; plays a role in resistance to weak organic acids; required for yeast cell adherence to silicone substrate; Spider biofilm induced
orf19.2846	orf19.2846	2.0	6.38E-04	Protein of unknown function; Hap43-repressed; induced in core caspofungin response; regulated by yeast-hypha switch; Spider biofilm repressed
orf19.2204	orf19.2204	2.0	3.83E-04	Predicted membrane protein of unknown function; Spider biofilm induced
orf19.4589	orf19.4589	2.0	8.33E-05	Ortholog(s) have polyamine oxidase activity, role in pantothenate biosynthetic process, polyamine catabolic process and cytoplasm localization
orf19.7184	orf19.7184	2.0	1.36E-04	Ortholog of C. dubliniensis CD36 : Cd36_73640, C. parapsilosis CDC317 : CPAR2_702340, Candida tenuis NRRL Y-1498 : CANTEDRAFT_112965 and Debaryomyces hansenii CBS767 : DEHA2G16566g
orf19.4609	orf19.4609	2.0	4.82E-05	Putative dienelactone hydrolase; protein abundance is affected by URA3 expression in the CAI-4 strain background; protein present in exponential and stationary growth phase yeast cultures; rat catheter biofilm repressed

MET10	orf19.4076	2.0	4.78E-05	Sulfite reductase; role in sulfur amino acid metabolism; induced by human whole blood or PMNs; Hog1-induced; possibly adherence-induced; flow model, Spider model, F-12/CO2 biofilm induced
ADAEC	orf19.868	2.0	1.16E-03	Protein of unknown function; transcription is specific to white cell type
HGH1	orf19.4587	2.0	1.66E-04	Putative HMG1/2-related protein; transcript regulated by Mig1
SOD4	orf19.2062	2.0	1.54E-03	Cu and Zn-containing superoxide dismutase; role in response to host innate immune ROS; regulated on white-opaque switch; ciclopirox olamine induced; caspofungin repressed; SOD1,4,5,6 gene family; yeast-associated; Spider biofilm induced
ZCF15	orf19.2753	2.0	7.70E-05	Predicted Zn(II)2Cys6 transcription factor of unknown function; rat catheter biofilm induced
orf19.604	orf19.604	2.0	1.25E-04	Ortholog(s) have cytosol localization
orf19.2755	orf19.2755	2.0	2.12E-04	Ortholog(s) have role in proteasomal ubiquitin-dependent protein catabolic process, proteasomal ubiquitin-independent protein catabolic process and cytosol, nucleus, proteasome core complex, beta-subunit complex localization
UBC15	orf19.5337	2.0	1.32E-04	Putative E2 ubiquitin-conjugating enzyme
ZCF27	orf19.4649	2.0	3.63E-04	Putative Zn(II)2Cys6 transcription factor
PGA53	orf19.4651	2.0	9.00E-05	GPI-anchored cell surface protein of unknown function; greater mRNA abundance observed in a cyr1 homozygous null mutant than in wild type
CWH8	orf19.3682	2.0	3.72E-04	Putative dolichyl pyrophosphate (Dol-P-P) phosphatase; ketoconazole-induced; expression is increased in a fluconazole-resistant isolate; clade-associated gene expression; Hap43p-induced gene
CYT2	orf19.4578	2.0	9.83E-05	Cytochrome c1 heme lyase; transcript regulated by Nrg1; induced in high iron
orf19.4597	orf19.4597	2.0	1.58E-04	Putative F-actin-capping protein subunit beta; possibly an essential gene, disruptants not obtained by UAU1 method
orf19.4574	orf19.4574	2.0	9.28E-05	Ortholog(s) have lipid particle localization
orf19.1113	orf19.1113	2.0	2.40E-04	Ortholog of C. dubliniensis CD36 : Cd36_53540, Debaryomyces hansenii CBS767 : DEHA2G07854g, Pichia stipitis Pignal : PICST_32162 and Spathaspora passalidarum NRRL Y-27907 : SPAPADRAFT_50795
TYR1	orf19.4605	2.0	3.56E-04	Putative prepephenate dehydrogenase; enzyme of tyrosine biosynthesis; fungal-specific (no human or murine homolog)
MET15	orf19.5645	2.0	7.40E-05	O-acetylhomoserine O-acetylserine sulfhydrylase; sulfur amino acid synthesis; immunogenic; Hog1, adherence-induced; brown color of mutant in Pb(2+) medium a visual selection; chlamydospore formation induced, F-12/CO2 biofilm induced
orf19.6578	orf19.6578	2.0	1.05E-02	Predicted membrane transporter; vesicular neurotransmitter (VNT) family, major facilitator superfamily (MFS); repressed in core caspofungin response; induced in oralpharyngeal candidasis; Spider biofilm induced
orf19.3783	orf19.3783	-2.0	4.76E-03	Protein of unknown function; rat catheter biofilm induced
FGR17	orf19.5729	-2.0	1.01E-02	Putative DNA-binding transcription factor; has zinc cluster DNA-binding motif; lacks an ortholog in S. cerevisiae; transposon mutation affects filamentous growth; Hap43p-repressed gene
NRG2	orf19.6339	-2.0	3.56E-04	Transcription factor; transposon mutation affects filamentous growth

orf19.6200	orf19.6200	-2.0	6.85E-03	Pry family pathogenesis-related protein; oral infection upregulated gene; mutant has reduced capacity to damage oral epithelial cells
RNH35	orf19.6562	-2.0	9.66E-05	Putative ribonuclease H2 catalytic subunit; flucytosine induced; Spider biofilm repressed
orf19.2452	orf19.2452	-2.0	2.34E-03	Protein of unknown function; induced in high iron; repressed in core caspofungin response; ketoconazole-repressed; colony morphology-related gene regulation by Ssn6; possibly subject to Kex2 processing
orf19.1691	orf19.1691	-2.0	1.41E-02	Plasma-membrane-localized protein; filament induced; Hog1, ketoconazole, fluconazole and hypoxia-induced; regulated by Nrg1, Tup1, Upc2; induced by prostaglandins; flow model biofilm induced; rat catheter and Spider biofilm repressed
CNH1	orf19.367	-2.0	2.34E-04	Na+/H+ antiporter; required for wild-type growth, cell morphology, and virulence in a mouse model of systemic infection; not transcriptionally regulated by NaCl; fungal-specific (no human or murine homolog)
orf19.7130	orf19.7130	-2.0	2.38E-04	Protein of unknown function; Hap43-repressed gene
orf19.6715	orf19.6715	-2.0	6.71E-04	Ortholog of Candida albicans WO-1 : CAWG_03078
EBP1	orf19.125	-2.0	1.58E-02	NADPH oxidoreductase; interacts with phenolic substrates (17beta-estradiol); possible role in estrogen response; induced by oxidative, weak acid stress, NO, benomyl, GlcNAc; Cap1, Mnl1 induced; Hap43-repressed; rat catheter biofilm induced
orf19.1365	orf19.1365	-2.0	2.01E-03	Putative monooxygenase; mutation confers hypersensitivity to toxic ergosterol analog; constitutive expression independent of MTL or white-opaque status
HNT2	orf19.7419	-2.0	1.36E-03	Putative dinucleoside triphosphate hydrolase; induced upon low-level peroxide stress
orf19.2163	orf19.2163	-2.0	6.67E-04	Ortholog(s) have cytosol localization
orf19.4665	orf19.4665	-2.0	3.70E-03	Protein of unknown function; Spider biofilm induced
WOR1	orf19.4884	-2.0	2.33E-04	Transcription factor ("master switch") of white-opaque phenotypic switching; required to establish and maintain the opaque state; opaque-specific, nuclear; regulates its own expression; suggested role in regulation of adhesion factors
orf19.5103	orf19.5103	-2.1	5.39E-05	Protein with a predicted phosphoglycerate mutase family domain; Hap43-repressed; clade-associated gene expression; induced by hypoxia
RBT7	orf19.2681	-2.1	5.22E-03	Protein with similarity to RNase T2 enzymes; has putative secretion signal; expression is Tup1-repressed
orf19.4287	orf19.4287	-2.1	1.76E-03	Putative oxidoreductase; Hap43-repressed gene; clade-associated gene expression
orf19.7166	orf19.7166	-2.1	1.38E-03	Predicted mitochondrial cardiolipin-specific phospholipase; upregulated in an azole-resistant strain that overexpresses MDR1; induced by Mnl1 under weak acid stress; rat catheter and Spider biofilm induced
BUL1	orf19.5094	-2.1	3.16E-03	Protein similar but not orthologous to S. cerevisiae Bul1; a protein involved in selection of substrates for ubiquitination; mutants are viable; macrophage/pseudohyphal-induced; rat catheter biofilm induced
UBA4	orf19.2324	-2.1	4.75E-03	Putative ubiquitin activating protein; Hap43-repressed; induced by prostaglandins; clade-associated gene expression
SOD5	orf19.2060	-2.1	3.04E-03	Cu and Zn-containing superoxide dismutase; protects against oxidative stress; induced by neutrophils, hyphal growth, caspofungin, osmotic/oxidative stress; oralpharyngeal candidiasis induced; rat catheter and Spider biofilm induced

ATO6	orf19.6995	-2.1	2.40E-04	Putative fungal-specific transmembrane protein
orf19.5370	orf19.5370	-2.1	2.54E-04	Ortholog(s) have fungal-type vacuole membrane localization
VPS70	orf19.7106	-2.1	1.34E-03	Ortholog(s) have role in protein targeting to vacuole and endoplasmic reticulum localization
DIT1	orf19.1741	-2.1	1.09E-02	Ortholog(s) have catalytic activity and role in ascospore wall assembly
orf19.5190	orf19.5190	-2.2	1.95E-03	Ortholog of Candida albicans WO-1 : CAWG_05610
GAT1	orf19.1275	-2.2	7.02E-03	GATA-type transcription factor; regulator of nitrogen utilization; required for nitrogen catabolite repression and utilization of isoleucine, tyrosine and tryptophan N sources; required for virulence in a mouse systemic infection model
MEP1	orf19.1614	-2.2	5.38E-03	Ammonium permease; Mep1 more efficient permease than Mep2, Mep2 has additional regulatory role; 11 predicted transmembrane regions; low mRNA abundance; hyphal downregulated; flow model biofilm induced
orf19.7502	orf19.7502	-2.2	4.78E-05	Protein of unknown function; Hap43-induced gene; upregulated in a cyr1 null mutant; Spider biofilm induced
HYR1	orf19.4975	-2.2	1.33E-02	GPI-anchored hyphal cell wall protein; macrophage-induced; repressed by neutrophils; resistance to killing by neutrophils, azoles; regulated by Rfg1, Efg1, Nrg1, Tup1, Cyr1, Bcr1, Hap43; Spider and flow model biofilm induced
orf19.270	orf19.270	-2.2	4.70E-04	Ortholog of C. parapsilosis CDC317 : CPAR2_102150, C. dubliniensis CD36 : Cd36_82780, Pichia stipitis Pignal : psti_CGOB_00155 and Candida orthopsilosis Co 90-125 : CORT_0B03450
NAT4	orf19.4664	-2.2	1.86E-03	Putative histone acetyltransferase; involved in regulation of white-opaque switch; early-stage flow model biofilm induced; Spider biofilm induced
orf19.1427	orf19.1427	-2.2	1.22E-04	Putative transporter; fungal-specific; Spider biofilm induced
RBT1	orf19.1327	-2.3	2.61E-03	Cell wall protein with similarity to Hwp1; required for virulence; predicted glycosylation; fluconazole, Tup1 repressed; farnesol, alpha factor, serum, hyphal and alkaline induced; Rfg1, Rim101-regulated
HGT12	orf19.7094	-2.3	5.05E-03	Glucose, fructose, mannose transporter; major facilitator superfamily; role in macrophage-induced hyphal growth; detected at germ tube plasma membrane by mass spectrometry; Snf3p-induced; 12 probable transmembrane segments
PGA45	orf19.2451	-2.3	3.05E-04	Putative GPI-anchored cell wall protein; repressed in core caspofungin response; Hog1-induced; regulated by Ssn6; Mob2-dependent hyphal regulation; flow model biofilm induced
TRY6	orf19.6824	-2.3	1.27E-04	Helix-loop-helix transcription factor; regulator of yeast form adherence; required for yeast cell adherence to silicone substrate; Spider and F-12/CO2 biofilm induced; repressed by alpha pheromone in SpiderM medium
orf19.5925	orf19.5925	-2.3	1.22E-04	Ortholog of S. cerevisiae : AIM6, C. glabrata CBS138 : CAGL0C05533g, C. dubliniensis CD36 : Cd36_84610, C. parapsilosis CDC317 : CPAR2_404550 and Candida tenuis NRRL Y-1498 : CANTEDRAFT_115337
ALS2	orf19.1097	-2.3	1.75E-02	ALS family protein; role in adhesion, biofilm formation, germ tube induction; expressed at infection of human buccal epithelial cells; putative GPI-anchor; induced by ketoconazole, low iron and at cell wall regeneration; regulated by Sfu1p
FCY2	orf19.333	-2.3	1.84E-04	Purine-cytosine permease of pyrimidine salvage; mutation associated with resistance to flucytosine in clinical isolates; transposon mutation affects filamentation; farnesol-upregulated in biofilm

AAH1	orf19.2251	-2.3	1.14E-04	Adenine deaminase; purine salvage and nitrogen catabolism; colony morphology-related regulation by Ssn6; Hog1, CO2-induced; chlamydospore formation repressed in C. albicans and C. dubliniensis; rat catheter and F-12/CO2 biofilm induced
orf19.5451	orf19.5451	-2.3	1.79E-04	Ortholog of Candida guilliermondii ATCC 6260 : PGUG_05321, Candida lusitaniae ATCC 42720 : CLUG_00887 and Candida albicans WO-1 : CAWG_02354
orf19.6758	orf19.6758	-2.4	3.05E-04	Predcted glucose 1-dehydrogenase (NADP+); rat catheter biofilm repressed
CDC6	orf19.5242	-2.5	8.33E-04	Putative ATP-binding protein with a predicted role in DNA replication; member of conserved Mcm1p regulon; periodic mRNA expression, peak at cell-cycle M/G1 phase
DUR3	orf19.6656	-2.5	3.98E-04	Spermidine transporter; induced in strains from HIV patients with oral candidiasis; alkaline repressed; amphotericin B induced; colony morphology regulated by Ssn6; reduced oral epithelial cell damage by mutant; Spider biofilm induced
orf19.376	orf19.376	-2.6	8.56E-04	Protein of unknown function; Hap43-repressed; Spider biofilm induced
FCY24	orf19.7331	-2.6	2.04E-04	Putative transporter; more similar to S. cerevisiae Tpn1, which is a vitamin B6 transporter, than to purine-cytosine permeases; transcription is regulated by Nrg1; Spider biofilm induced
OPT9	orf19.2584	-2.6	5.85E-05	Probable pseudogene similar to fragments of OPT1 oligopeptide transporter gene; decreased expression in hyphae compared to yeast-form cells; transcriptionally induced upon phagocytosis by macrophage
DUR1,2	orf19.780	-2.7	5.56E-03	Urea amidolyase; hydrolyzes urea to CO2; use of urea as N source and for hyphal switch in macrophage; regulated by Nrg1/Hap43; required for virulence; promotes mouse kidney and brain colonization; rat catheter and flow model biofilm induced
PGA23	orf19.3740	-2.8	3.72E-03	Putative GPI-anchored protein of unknown function; Rim101-repressed; Cyr1-regulated; colony morphology-related gene regulation by Ssn6
orf19.5210	orf19.5210	-2.8	1.39E-04	Putative Xbp1 transcriptional repressor; binds to cyclin gene promoters in S. cerevisiae; Hap43-repressed; possibly essential, disruptants not obtained by UAU1 method
orf19.4055	orf19.4055	-2.8	3.30E-05	Protein similar to S. cerevisiae Ybr075wp; transposon mutation affects filamentous growth; clade-associated gene expression
GIT1	orf19.34	-2.9	2.42E-04	Glycerophosphoinositol permease; involved in utilization of glycerophosphoinositol as a phosphate source; Rim101-repressed; virulence-group-correlated expression
OPT1	orf19.2602	-2.9	9.28E-05	Oligopeptide transporter; transports 3-to-5-residue peptides; alleles are distinct, one has intron; suppresses S. cerevisiae ptr2-2 mutant defects; induced by BSA or peptides; Stp3p, Hog1p regulated; flow model biofilm induced
THI20	orf19.889	-2.9	4.14E-03	Putative trifunctional enzyme of thiamine biosynthesis, degradation and salvage; Spider biofilm induced
orf19.6113	orf19.6113	-2.9	3.83E-05	Protein of unknown function; transcript detected on high-resolution tiling arrays
PRM1	orf19.669	-2.9	2.80E-04	Putative membrane protein with a predicted role in membrane fusion during mating; Hap43p-repressed gene; protein induced during the mating process

CAN2	orf19.111	-3.0	6.19E-03	Basic amino acid permease; arginine metabolism; regulated by Nrg1/Tup1; caspofungin, flucytosine induced; colony morphology-related regulation by Ssn6; Hap43-repressed; rat catheter and Spider biofilm induced; promoter bound by Efg1
orf19.1449	orf19.1449	-3.0	8.33E-05	Protein of unknown function; induced in azole-resistant strain that overexpresses MDR1; protein present in exponential and stationary growth phase yeast cultures; Spider biofilm induced
orf19.7330	orf19.7330	-3.0	4.01E-05	Protein with a predicted heme oxygenase domain; Spider biofilm induced
orf19.7596	orf19.7596	-3.1	4.94E-04	Protein with a phosphoglycerate mutase family domain; Hap43-repressed gene
ALS1	orf19.5741	-3.3	2.30E-05	Cell-surface adhesin; adhesion, virulence, immunoprotective roles; band at hyphal base; Rfg1, Ssk1, Spider biofilm induced; flow model biofilm repressed; CAI-4 strain background effects; promoter bound Bcr1, Tec1, Efg1, Ndt80, and Brg1
POL93	orf19.6078	-3.3	1.00E-03	Predicted ORF in retrotransposon Tca8 with similarity to the Pol region of retrotransposons encoding reverse transcriptase, protease and integrase; downregulated in response to ciclopirox olamine; F-12/CO2 early biofilm induced
orf19.6079	orf19.6079	-3.4	1.10E-04	Predicted ORF in retrotransposon Tca8 with similarity to the Gag region encoding nucleocapsid-like protein; repressed by ciclopirox olamine; filament induced; regulated by Rfg1, Tup1; overlaps orf19.6078.1
RTA4	orf19.6595	-3.4	3.09E-04	Protein similar to S. cerevisiae Rsb1p, involved in fatty acid transport; transposon mutation affects filamentous growth; alkaline downregulated; caspofungin induced; possibly an essential gene; Hap43p-repressed
OYE23	orf19.3433	-3.4	3.06E-04	Putative NAPDH dehydrogenase; induced by nitric oxide, benomyl; oxidative stress-induced via Cap1; Hap43p-repressed; rat catheter biofilm induced
orf19.2059	orf19.2059	-3.7	1.42E-05	Protein with homology to magnesium-dependent endonucleases and phosphatases; regulated by Sef1, Sfu1, and Hap43; Spider biofilm induced
NUP	orf19.6570	-5.1	2.56E-04	Nucleoside permease; adenosine and guanosine are substrates, whereas cytidine, adenine, guanine, uridine, uracil are not; similar to a nucleoside permease of S. pombe; possibly processed by Kex2p
URA3	orf19.1716	-8.2	1.86E-03	Orotidine-5'-phosphate decarboxylase; pyrimidine biosynthesis; gene used as genetic marker; decreased expression when integrated at ectopic chromosomal locations can cause defects in hyphal growth and virulence; Spider biofilm repressed
PGA10	orf19.5674	-8.3	1.79E-04	GPI anchored membrane protein; utilization of hemin and hemoglobin for Fe in host; Rim101 at ph8/hypoxia/ketoconazole/ciclopirox/hypha-induced; required for RPMI biofilm formation, Bcr1-induced in a/a biofilm; rat catheter biofilm repressed
PLB1	orf19.689	-11.6	8.12E-04	Phospholipase B; host cell penetration and virulence in mouse systemic infection; Hog1-induced; signal sequence, N-glycosylation, and Tyr phosphorylation site; induced in fluconazole-resistant strains; rat catheter biofilm repressed

SUPPLEMENTARY TABLE II.3C_GO TERM ANALYSIS FOR THE *fcr1* MUTANT

GO term	Cluster frequency	Background frequency	adj. p-value	Gene(s) annotated to the term
Upregulated genes				
Process				
single-species biofilm formation on inanimate substrate	4 out of 7 genes, 57.1%	119 out of 13081 background genes, 0.9%	7.63E-05	PBR1:ECE1:HWP1:ALS3
intraspecies interaction between organisms	4 out of 7 genes, 57.1%	119 out of 13081 background genes, 0.9%	7.63E-05	PBR1:ECE1:HWP1:ALS3
single-species submerged biofilm formation	4 out of 7 genes, 57.1%	131 out of 13081 background genes, 1.0%	1.10E-04	PBR1:ECE1:HWP1:ALS3
single-species biofilm formation	4 out of 7 genes, 57.1%	134 out of 13081 background genes, 1.0%	1.20E-04	PBR1:ECE1:HWP1:ALS3
submerged biofilm formation	4 out of 7 genes, 57.1%	134 out of 13081 background genes, 1.0%	1.20E-04	PBR1:ECE1:HWP1:ALS3
biofilm formation	4 out of 7 genes, 57.1%	142 out of 13081 background genes, 1.1%	1.50E-04	PBR1:ECE1:HWP1:ALS3
cell adhesion	3 out of 7 genes, 42.9%	62 out of 13081 background genes, 0.5%	6.90E-04	PBR1:HWP1:ALS3
multi-organism cellular process	4 out of 7 genes, 57.1%	262 out of 13081 background genes, 2.0%	1.76E-03	PBR1:ECE1:HWP1:ALS3
biological adhesion	3 out of 7 genes, 42.9%	88 out of 13081 background genes, 0.7%	2.00E-03	PBR1:HWP1:ALS3
single organismal cell-cell adhesion	2 out of 7 genes, 28.6%	15 out of 13081 background genes, 0.1%	2.98E-03	HWP1:ALS3

single organism cell adhesion	2 out of 7 genes, 28.6%	15 out of 13081 background genes, 0.1%	2.98E-03	HWP1:ALS3
cell-cell adhesion	2 out of 7 genes, 28.6%	16 out of 13081 background genes, 0.1%	3.40E-03	HWP1:ALS3
cell adhesion involved in single-species biofilm formation	2 out of 7 genes, 28.6%	22 out of 13081 background genes, 0.2%	6.54E-03	HWP1:ALS3
cell adhesion involved in biofilm formation	2 out of 7 genes, 28.6%	25 out of 13081 background genes, 0.2%	8.48E-03	HWP1:ALS3
Function				
cell adhesion molecule binding	2 out of 7 genes, 28.6%	6 out of 13081 background genes, 0.0%	3.61E-05	HWP1:ALS3
Component				
hyphal cell wall	3 out of 7 genes, 42.9%	69 out of 13081 background genes, 0.5%	1.40E-04	ECE1:HWP1:ALS3
cell wall	3 out of 7 genes, 42.9%	163 out of 13081 background genes, 1.2%	1.85E-03	ECE1:HWP1:ALS3
fungal-type cell wall	3 out of 7 genes, 42.9%	163 out of 13081 background genes, 1.2%	1.85E-03	ECE1:HWP1:ALS3
external encapsulating structure	3 out of 7 genes, 42.9%	164 out of 13081 background genes, 1.3%	1.89E-03	ECE1:HWP1:ALS3

Downregulated genes: no GO terms retrieved

SUPPLEMENTARY TABLE II.3D_GO TERM ANALYSIS FOR THE *FCR1* OE STRAIN

GO term Upregulated genes Process	Cluster frequency	Background frequency	adj. p-value	Gene(s) annotated to the term
oxidation-reduction process	30 out of 175 genes, 17.1%	418 out of 13081 background genes, 3.2%	1.16E-05	IFE1:AOX2:AOX1:C1_11290W_A:MET3:C1_14190C_A:SOD4:C2_01630W_A:DLD1:C2_06890C_A:GDH2:MET10:C2_10070W_A:TYR1:CAT2:C4_02040W_A:SOD1:CFL2:SOU1:MET14:C5_03770C_A:GPX1:GAC1:C7_01170C_A:OYE22:ADH5:CIT1:FDH1:FRE7:CR_07780W_A
galactose catabolic process via UDP-galactose	3 out of 175 genes, 1.7%	3 out of 13081 background genes, 0.0%	6.89E-03	GAL1:GAL10:GAL7
hexose catabolic process	4 out of 175 genes, 2.3%	11 out of 13081 background genes, 0.1%	4.55E-02	GAL1:GAL10:GAL7:SOU1
galactose catabolic process	3 out of 175 genes, 1.7%	5 out of 13081 background genes, 0.0%	6.66E-02	GAL1:GAL10:GAL7
single-organism metabolic process	52 out of 175 genes, 29.7%	1382 out of 13081 background genes, 10.6%	7.28E-02	GAL1:GAL10:GAL7:C1_02220C_A:CWH8:SNZ1:XOG1:IFE1:AOX2:AOX1:C1_11290W_A:MET3:C1_14190C_A:SOD4:C2_01630W_A:DLD1:HSP21:C2_06890C_A:C2_07440C_A:GDH2:MET10:C2_10070W_A:C3_03680W_A:MET15:CPA1:TYR1:DPM3:HSX11:CAT2:C4_02040W_A:LAB5:SOD1:RGT1:MNN22:CFL2:SOU1:YDC1:C4_07140W_A:MET14:C5_03770C_A:C5_04360C_A:SFC1:GPX1:GAC1:C7_01170C_A:OYE22:ADH5:CIT1:FDH1:FRE7:CR_07780W_A:HSP104
carbon catabolite activation of transcription	5 out of 175 genes, 2.9%	23 out of 13081 background genes, 0.2%	8.49E-02	GAL1:TYE7:STB3:GAL4:ADR1
Function				

oxidoreductase activity	25 out of 175 genes, 14.3%	487 out of 13081 background genes, 3.7%	3.85E-02	IFE1:AOX2:AOX1:C1_11290W_A:SOD4:C2_01630W_A:DLD1:C2_06890C_A:GDH2:MET10:C2_10070W_A:TYR1:C4_02040W_A:SOD1:CFL2:SOU1:C5_03770C_A:GPX1:C7_01170C_A:OYE22:ADH5:FDH1:FRE7:CR_07780W_A:CR_07940W_A
alternative oxidase activity	2 out of 175 genes, 1.1%	2 out of 13081 background genes, 0.0%	8.63E-02	AOX2:AOX1
Component				
cell surface	12 out of 175 genes, 6.9%	203 out of 13081 background genes, 1.6%	7.88E-02	XOG1:SOD4:HSP21:PGA7:RBT5:PGA53:BGL2:PGA62:PGA38:HSP104:PGA13:CHT3

Downregulated genes

Process				
adhesion of symbiont to host	5 out of 73 genes, 6.8%	48 out of 13081 background genes, 0.4%	0.02437	WOR1:HYR1:URA3:ALS1:ALS2
biological adhesion	6 out of 73 genes, 8.2%	88 out of 13081 background genes, 0.7%	0.05129	WOR1:HYR1:AAH1:URA3:ALS1:ALS2
symbiosis, encompassing mutualism through parasitism	7 out of 73 genes, 9.6%	126 out of 13081 background genes, 1.0%	0.05307	WOR1:HYR1:SOD5:URA3:PLB1:ALS1:ALS2
interspecies interaction between organisms	7 out of 73 genes, 9.6%	128 out of 13081 background genes, 1.0%	0.05852	WOR1:HYR1:SOD5:URA3:PLB1:ALS1:ALS2

nitrogen utilization	3 out of 73 genes, 4.1%	14 out of 13081 background genes, 0.1%	0.07858	DUR1,2:MEP1:OPT1
Function				
substrate-specific transmembrane transporter activity	11 out of 73 genes, 15.1%	335 out of 13081 background genes, 2.6%	0.03343	DUR3:GIT1:MEP1:FCY2:CNH1:C4_04230W_A:CAN2:HGT12:NUP:OPT1:FCY24
secondary active transmembrane transporter activity	5 out of 73 genes, 6.8%	69 out of 13081 background genes, 0.5%	0.04296	GIT1:CNH1:C4_04230W_A:NUP:OPT1
Component				
cell surface	10 out of 73 genes, 13.7%	203 out of 13081 background genes, 1.6%	0.00033	PGA45:HYR1:SOD5:PGA10:RBT1:EBP1:ALS1:ALS2:PGA23:CR_10200W_A
cell wall	8 out of 73 genes, 11.0%	163 out of 13081 background genes, 1.2%	0.00314	PGA45:HYR1:SOD5:PGA10:RBT1:EBP1:ALS1:ALS2
fungal-type cell wall	8 out of 73 genes, 11.0%	163 out of 13081 background genes, 1.2%	0.00314	PGA45:HYR1:SOD5:PGA10:RBT1:EBP1:ALS1:ALS2
external encapsulating structure	8 out of 73 genes, 11.0%	164 out of 13081 background genes, 1.3%	0.00328	PGA45:HYR1:SOD5:PGA10:RBT1:EBP1:ALS1:ALS2
hyphal cell wall	5 out of 73 genes, 6.8%	69 out of 13081 background genes, 0.5%	0.01419	HYR1:SOD5:RBT1:EBP1:ALS1

		817 out of 13081		
	17 out of 73	background		DUR3:PGA45:PRM1:HYR1:SOD5:GIT1:C3_01540W_A:MEP1:CNH1:PGA10:RBT1:CAN2:EBP1
cell periphery	genes, 23.3%	genes, 6.2%	0.01601	:ALS1:ALS2:HGT12:OPT1

SUPPLEMENTARY TABLE II.4A_BOUND AND MODULATED GENES

	Binding ratio	Expression Ratio	Description
Upregulated			
HSP21	1.7532114	4.981540454	Small heat shock protein; role in stress response and virulence; fluconazole-downregulated; induced in cyr1 or ras1 mutant; stationary phase enriched protein; detected in some, not all, biofilm extracts; Spider biofilm induced
orf19.510	1.5167675	2.626096521	Protein of unknown function; Spider biofilm induced
ADH5	1.7326737	2.107098731	Putative alcohol dehydrogenase; regulated by white-opaque switch; fluconazole-induced; antigenic in murine infection; regulated by Nrg1, Tup1; Hap43, macrophage repressed, flow model biofilm induced; Spider biofilm induced
orf19.7296	1.7532114	2.048302805	Putative cation conductance protein; similar to stomatin mechanoreception protein; plasma-membrane localized; induced by Rgt1; rat catheter and Spider biofilm induced
Downregulated			
orf19.1691	1.5659086	-1.97828291	Plasma-membrane-localized protein; filament induced; Hog1, ketoconazole, fluconazole and hypoxia-induced; regulated by Nrg1, Tup1, Upc2; induced by prostaglandins; flow model biofilm induced; rat catheter and Spider biofilm repressed
orf19.4287	1.5811782	-2.06199313	Putative oxidoreductase; Hap43-repressed gene; clade-associated gene expression
UBA4	1.5594097	-2.0909447	Putative ubiquitin activating protein; Hap43-repressed; induced by prostaglandins; clade-associated gene expression
GAT1	1.6233792	-2.16147323	GATA-type transcription factor; regulator of nitrogen utilization; required for nitrogen catabolite repression and utilization of isoleucine, tyrosine and tryptophan N sources; required for virulence in a mouse systemic infection model
MEP1	2.4605827	-2.2	Ammonium permease; Mep1 more efficient permease than Mep2, Mep2 has additional regulatory role; 11 predicted transmembrane regions; low mRNA abundance; hyphal downregulated; flow model biofilm induced
FCY2	1.6278864	-2.32853384	Purine-cytosine permease of pyrimidine salvage; mutation associated with resistance to flucytosine in clinical isolates; transposon mutation affects filamentation; farnesol-upregulated in biofilm
DUR3	1.6678621	-2.53628566	Spermidine transporter; induced in strains from HIV patients with oral candidiasis; alkaline repressed; amphotericin B induced; colony morphology regulated by Ssn6; reduced oral epithelial cell damage by mutant; Spider biofilm induced
FCY24	1.5833717	-2.59529095	Putative transporter; more similar to S. cerevisiae Tpn1, which is a vitamin B6 transporter, than to purine-cytosine permeases; transcription is regulated by Nrg1; Spider biofilm induced

OPT9	2.4250256	-2.6	Probable pseudogene similar to fragments of OPT1 oligopeptide transporter gene; decreased expression in hyphae compared to yeast-form cells; transcriptionally induced upon phagocytosis by macrophage
DUR1,2	2.5526575	-2.7	Urea amidolyase; hydrolyzes urea to CO2; use of urea as N source and for hyphal switch in macrophage; regulated by Nrg1/Hap43; required for virulence; promotes mouse kidney and brain colonization; rat catheter and flow model biofilm induced
OPT1	2.4759806	-2.9	Oligopeptide transporter; transports 3-to-5-residue peptides; alleles are distinct, one has intron; suppresses S. cerevisiae ptr2-2 mutant defects; induced by BSA or peptides; Stp3p, Hog1p regulated; flow model biofilm induced
CAN2	2.0307322	-3	Basic amino acid permease; arginine metabolism; regulated by Nrg1/Tup1; caspofungin, flucytosine induced; colony morphology-related regulation by Ssn6; Hap43-repressed; rat catheter and Spider biofilm induced; promoter bound by Efg1
NUP	1.905276	-5.1	Nucleoside permease; adenosine and guanosine are substrates, whereas cytidine, adenine, guanine, uridine, uracil are not; similar to a nucleoside permease of S. pombe; possibly processed by Kex2p

SUPPLEMENTARY TABLE II.4B_GO TERM ANALYSIS FOR BOUND AND MODULATED GENES

GO_term	Cluster frequency	Background frequency	Corrected P-value	Gene(s) annotated to the term
Bound and downregulated genes				
Process				
nitrogen compound transport	7 out of 13 genes, 53.8%	228 out of 13081 background genes, 1.7%	1.71E-06	DUR3:MEP1:FCY2:CAN2:NUP:OPT1:FCY24
transmembrane transport	7 out of 13 genes, 53.8%	394 out of 13081 background genes, 3.0%	7.29E-05	DUR3:MEP1:FCY2:CAN2:NUP:OPT1:FCY24
nitrogen utilization	3 out of 13 genes, 23.1%	14 out of 13081 background genes, 0.1%	8.11E-05	DUR1,2:MEP1:OPT1
nucleobase transport	2 out of 13 genes, 15.4%	12 out of 13081 background genes, 0.1%	1.01E-02	FCY2:FCY24
organic substance transport	6 out of 13 genes, 46.2%	681 out of 13081 background genes, 5.2%	2.92E-02	DUR3:FCY2:CAN2:NUP:OPT1:FCY24
transport	7 out of 13 genes, 53.8%	1165 out of 13081 background genes, 8.9%	8.34E-02	DUR3:MEP1:FCY2:CAN2:NUP:OPT1:FCY24
Function				
substrate-specific transmembrane transporter activity	7 out of 13 genes, 53.8%	335 out of 13081 background genes, 2.6%	1.22E-05	DUR3:MEP1:FCY2:CAN2:NUP:OPT1:FCY24
transmembrane transporter activity	7 out of 13 genes, 53.8%	383 out of 13081 background genes, 2.9%	3.03E-05	DUR3:MEP1:FCY2:CAN2:NUP:OPT1:FCY24
substrate-specific transporter activity	7 out of 13 genes, 53.8%	395 out of 13081 background genes, 3.0%	3.74E-05	DUR3:MEP1:FCY2:CAN2:NUP:OPT1:FCY24
transporter activity	7 out of 13 genes, 53.8%	460 out of 13081 background genes, 3.5%	1.00E-04	DUR3:MEP1:FCY2:CAN2:NUP:OPT1:FCY24
nucleobase transmembrane transporter activity	2 out of 13 genes, 15.4%	9 out of 13081 background genes, 0.1%	2.24E-03	FCY2:FCY24
amide transmembrane transporter activity	2 out of 13 genes, 15.4%	19 out of 13081 background genes, 0.1%	1.05E-02	DUR3:OPT1

Component				
membrane	8 out of 13 genes, 61.5%	1576 out of 13081 background genes, 12.0%	1.13E-02	DUR3:C3_01540W_A:MEP1:FCY2:CAN2:NUP:OPT1:FCY24
plasma membrane	5 out of 13 genes, 38.5%	526 out of 13081 background genes, 4.0%	1.28E-02	DUR3:C3_01540W_A:MEP1:CAN2:OPT1
cell periphery	5 out of 13 genes, 38.5%	817 out of 13081 background genes, 6.2%	9.27E-02	DUR3:C3_01540W_A:MEP1:CAN2:OPT1

Bound and upregulated genes

no GO terms retrieved

SUPPLEMENTARY TABLE III.1_Tn MUTANT LIBRARY

Strain Name	Standard Name	Systematic Name
BRY429	RLM1	orf19.4662
CJN1001		orf19.6845
CJN1003	orf19.6850	orf19.6850
CJN1007	MCM1	orf19.7025
CJN242	FCR1	orf19.6817
CJN256	BAS1	orf19.6874
CJN267	RIM101	orf19.7247
CJN299	orf19.3928	orf19.3928
CJN305	CPH1	orf19.4433
CJN308	TEC1	orf19.5908
CJN322	NRG1	orf19.7150
CJN334	MSN4	orf19.4752
CJN348	MIG2	orf19.5326
CJN393	orf19.4972	orf19.4972
CJN395	AZF1	orf19.173
CJN396	PZF1	orf19.4125
CJN401	ARG81	orf19.4766
CJN403	ZNC1	orf19.3187
CJN411	PPR1	orf19.3986
CJN419	FGR27	orf19.6680
CJN427	orf19.5026	orf19.5026
CJN432	CAS5	orf19.4670
CJN434	MIG1	orf19.4318
CJN442	CRZ1	orf19.7359
CJN459	BCR1	orf19.723
CJN491	ZCF38	orf19.7518
CJN494	UME7	orf19.2745
CJN495	ZCF39	orf19.7583
CJN506	FGR17	orf19.5729
CJN511	UGA3	orf19.7570
CJN517	CZF1	orf19.3127
CJN518	ZCF25	orf19.4568
CJN523	CAS1	orf19.1135
CJN524	CPH2	orf19.1187
CJN528	LYS14	orf19.5548
CJN531	STB5	orf19.3308
CJN544	ZCF14	orf19.2647
CJN548	ZCF34	orf19.6182
CJN563	ZCF2	orf19.431
CJN571	UGA33	orf19.7317
CJN577	LYS144	orf19.5380
CJN582	ZCF6	orf19.1497
CJN592	ZCF5	orf19.1255
CJN593	ZCF17	orf19.3305
CJN598	ZCF26	orf19.4573
CJN608	CAP1	orf19.1623
CJN609		orf19.1007
CJN799	ZCF10	orf19.2280
CJN801	GAL4	orf19.5338
CJN803	ZCF28	orf19.4767
CJN805	LYS143	orf19.4776
CJN807	LYS142	orf19.4778
CJN809	orf19.5975	orf19.5975
CJN811	CRZ2	orf19.2356
CJN815	orf19.1757	orf19.1757
CJN817	STP4	orf19.909
CJN831	FGR15	orf19.2054
CJN854	orf19.2260	orf19.2260
CJN856	TAF14	orf19.798
CJN857		orf19.889
CJN863	ADA2	orf19.2331
CJN864	RTG3	orf19.2315
CJN866	orf19.1178	orf19.1178
CJN872	orf19.2393	orf19.2393
CJN874	JJJ1	orf19.2399
CJN885		orf19.3088
CJN908	orf19.2612	orf19.2612
CJN911		orf19.2674
CJN913	GCN4	orf19.1358
CJN922		orf19.1496
CJN926	FCR3	orf19.3193
CJN928	ZPR1	orf19.3300
CJN932		orf19.1589
CJN941	orf19.1565	orf19.1565
CJN943	ZCF18	orf19.3405
CJN945	RAD18	orf19.3407

CJN958	CAS4	orf19.1693
CJN966		orf19.1729
CJN975	MDM34	orf19.1826
CJN979	GCS1	orf19.3683
CJN983	SEF1	orf19.3753
CJN993	TFC3	orf19.3833
CJN997	orf19.6781	orf19.6781
DSY1691	CTA4	orf19.7374
DSY1762	ASG1	orf19.166
DSY2906	TAC1	orf19.3188
DSY2989	HAP43	orf19.681
DSY3297	CTF1	orf19.1499
DSY3326	FLC2	orf19.2217
DSY3328	MCA1	orf19.5995
DSY3329-3	SNQ2	orf19.5759
DSY3330	KNS1	orf19.4979
DSY3331	orf19.6626	orf19.6626
DSY3332		orf19.7523
DSY3333	MKC1	orf19.1813
DSY3336-4		orf19.2395
DSY3365	SUC1	orf19.7319
DSY3367	orf19.6227	orf19.6227
DSY3369	orf19.6713	orf19.6713
DSY3410-1	MNL1	orf19.6121
DSY3411-2	ZCF11	orf19.2423
DSY3412-2	ZCF1	orf19.255
DSY3413-2	ZCF15	orf19.2753
DSY3414-1	DAL81	orf19.3252
DSY3415-1	ZCF20	orf19.4145
DSY3416-1	ZCF21	orf19.4166
DSY3417-1	LEU3	orf19.4225
DSY3418-1	CTA7	orf19.4288
DSY3419-1	ZCF23	orf19.4450
DSY3420-1	ZCF31	orf19.5924
DSY3421-1	ZCF32	orf19.5940
DSY3422-8	STP2	orf19.4961
DSY3423-6	ACE2	orf19.6124
DSY3425-9	ZCF24	orf19.4524
DSY3426-2	ARG83	orf19.2748
DSY3428-8	orf19.3434	orf19.3434
DSY3430-3	orf19.217	orf19.217
DSY3438-2	orf19.702	orf19.702
DSY3439-3	SAS3	orf19.2540
DSY3447-11	ZCF8	orf19.1718
HZY14	orf19.5848	orf19.5848
HZY15	orf19.6407	orf19.6407
HZY2-1	SKO1	orf19.1032
HZY23	TEA1	orf19.6985
HZY24	ZCF35	orf19.7371
HZY29	ARO80	orf19.3012
HZY34	ZCF29	orf19.5133
HZY35	STP3	orf19.5917
HZY44	PUT3	orf19.6203
HZY5-1	orf19.861	orf19.861
HZY59	UGA32	orf19.6038
HZY60	CWT1	orf19.5849
HZY61	ZCF27	orf19.4649
HZY62	MBF1	orf19.3294
HZY63	ZCF12	orf19.2623
HZY66	RPN4	orf19.1069
HZY67	HAL9	orf19.3190
HZY7-1	CST6	orf19.6102

SUPPLEMENTARY TABLE III.2_PRIMERS USED IN THIS STUDY

	Primer ID	Position (bp relative to ATG)	Primer Sequence (5'-3')	Amplicon Size (bp)
CAS5 HA-tagging[a]	MR2549	2344	AATTGTGGTAAAAGATTTAATCGTAAAGATAATTTAAAAGCTCATTTAAAAAAGATTCATGGACTTGT GAAAGGACAAGAAGAGTTTACAAGAGTGTTGAATGAAAACAAAGAAGTTTCCagggaacaaaagctgg	1893
	MR2550	2467	AAAATCAACCATATTTCTATGATCCTAGTCATGTAATTACAAATTTGTTTAAAATACGAATTATCTATAT GGATTATACTTTAAATAATACCGTCTTTTAATGCATAGTCTATATAATGTctatagggcgaattgg	
CAS5 deletion; first round[b]	MR2741	-60	*TTATTTACTTTGCTTTTCATCCCACCCCTTTGTTGGTAA ATATAGACTTTAACATATACT*GAGCTCCACCGCGGTGGCGGCCGC T	4337
	MR2742		TTATCTATATGGATTATACTTTAAATAATACCGTCTTTTAATGCATAGTCTATATAATGTGGTACCGGG CCCCCCCTCGAGGAA	
CAS5 deletion; second round	MR2743	-120	TATTTTATTGTTGAAAGGAATAGACACTATCAATTTTTGCTATTTTATTTCTATTCTAATTTATTTACTTT GCTTTTCAT	4457
	MR2744		AAAATCAACCATATTTCTATGATCCTAGTCATGTAATTACAAATTTGTTTAAAATACGAATTATCTATAT GGATTATACT	

[a] bases in lower case represent sequences homologous to sequences from plasmid pCaMPY-3xHA

[c] double underlined bases represent annealing sequences within plasmid pSFS2A

SUPPLEMENTARY TABLE III.3A_Cas5p BINDING HITS

Systematic Name	Standard Name	Log2 Binding Ratio	Description
orf19.3707	YHB1	3.83	Verified ORF||Nitric oxide dioxygenase, acts in nitric oxide scavenging/detoxification; role in virulence in mouse; transcription activated by NO, macrophage interaction; hyphal downregulated; mRNA binds to She3p
orf19.1354	UCF1	3.79	Uncharacterized ORF||Putative protein of unknown function; mRNA binds to She3p; transcription is induced in high iron, decreased upon yeast-hyphal switch; downregulation correlates with clinical development of fluconazole resistance; Ras1p-regulated
orf19.5288	IFE2	3.43	Uncharacterized ORF||Protein described as an alcohol dehydrogenase; decreased expression in hyphae compared to yeast-form cells; Efg1p-regulated; fluconazole-induced; Hog1p-induced; increased expression in response to prostaglandins
orf19.2659	UCF1	3.22	Predicted ORF from Assembly 19; downregulation correlates with clinical development of fluconazole resistance; decreased expression in hyphae compared to yeast-form cells; Ras1p-regulated; merged with orf19.1354 in Assembly 20
orf19.3669	SHA3	3.00	Verified ORF||Protein similar to S. cerevisiae Sha3p, a serine/threonine kinase involved in glucose transport; transposon mutation affects filamentous growth; fluconazole-induced; ketoconazole-repressed; induced in by alpha pheromone; possibly essential
orf19.5626	orf19.5626	2.89	Uncharacterized ORF||Predicted ORF in Assemblies 19, 20 and 21; Plc1p-regulated; transcriptionally activated by Mnl1p under weak acid stress
orf19.1153	GAD1	2.76	Uncharacterized ORF||Protein described as glutamate decarboxylase; macrophage-downregulated gene; alkaline downregulated; amphotericin B induced; transcriptionally activated by Mnl1p under weak acid stress
orf19.7514	PCK1	2.75	Uncharacterized ORF||Phosphoenolpyruvate carboxykinase; role in gluconeogenesis; regulated by hyphal switch, carbon source; repressed on glucose; induced by fluconazole, phagocytosis, H2O2; predicted ATP-dependent, dimeric; predicted PKC phosphorylation sites
orf19.3419	MAE1	2.69	Uncharacterized ORF||Malic enzyme, mitochondrial; transcription regulated by Mig1p and Tup1p; shows colony morphology-related gene regulation by Ssn6p
orf19.3672	GAL10	2.62	Verified ORF||UDP-glucose 4-epimerase, required for galactose utilization; mutant shows cell wall defects and increased filamentation; fluconazole-induced; protein detected by mass spec in stationary phase cultures
orf19.339	NDE1	2.59	Verified ORF||Putative NADH dehydrogenase that could act alternatively to complex I in respiration; caspofungin repressed; fungal-specific (no human or murine homolog); transcription is upregulated in both intermediate and mature biofilms
orf19.670.2	orf19.670.2	2.58	Uncharacterized ORF||ORF Predicted by Annotation Working Group; hypoxia downregulated, ketoconazole induced
orf19.2192	GDH2	2.55	Uncharacterized ORF||Putative NAD-specific glutamate dehydrogenase; fungal-specific (no human or murine homolog); transcription is regulated by Nrg1p, Mig1p, Tup1p, and Gcn4p
orf19.7600	FDH3	2.54	Uncharacterized ORF||Putative protein of glycine catabolism; downregulated by Efg1p under yeast-form but not hyphal growth conditions; transcriptionally activated by Mnl1p under weak acid stress
orf19.7085	orf19.7085	2.52	Uncharacterized ORF||Predicted ORF in Assemblies 19, 20 and 21; induced in core stress response; induced by heavy metal (cadmium) stress via Hog1p; oxidative stress-induced via Cap1p; induced by Mnl1p under weak acid stress; macrophage-downregulated
orf19.6540	PFK2	2.47	Verified ORF||Beta subunit of phosphofructokinase (PFK), which is a heteromultimer of Pfk1p and Pfk2p; PFK is activated by fructose 2,6-bisphosphate or AMP, inhibited by ATP; downregulated upon phagocytosis or hyphal growth; fluconazole-induced

orf19.6882	OSM1	2.45	Verified ORF||Putative flavoprotein subunit of fumarate reductase; soluble protein in hyphae; fungal-specific (no human or murine homolog); caspofungin repressed; protein detected by mass spec in stationary phase cultures
orf19.5079	CDR4	2.43	Verified ORF||Putative transporter of ATP-binding cassette (ABC) superfamily; fluconazole, Sfu1p, Hog1p, core stress response induced; caspofungin repressed; fluconazole resistance is not affected by mutation or correlated with expression
orf19.3278	GSY1	2.40	Uncharacterized ORF||Protein described as glycogen synthase; enzyme of glycogen metabolism; transcription downregulated upon yeast-hyphal switch and regulated by Efg1p; strong oxidative stress induced; shows colony morphology-related gene regulation by Ssn6p
orf19.4784	CRP1	2.39	Verified ORF||Copper transporter of the plasma membrane; P1-type ATPase (CPx type); mediates Cu resistance; similar to proteins of Menkes and Wilson disease; copper-induced; Tbf1p-activated; suppresses Cu sensitivity of S. cerevisiae cup1 null mutant
orf19.5118	SDS24	2.38	Uncharacterized ORF||Protein described as similar to S. cerevisiae Ybr214wp; transcription regulated by Mig1p and Tup1p; fluconazole-induced
orf19.5305	RHD3	2.38	Verified ORF||GPI-anchored cell wall protein; transcription decreased upon yeast-hyphal switch; transcriptionally regulated by iron; expression greater in high iron; clade-associated gene expression; possibly an essential gene (by UAU1 method); not essential for cell wall integrity
orf19.449	orf19.449	2.36	Uncharacterized ORF||Predicted ORF in Assemblies 19, 20 and 21; possible phosphatidyl synthase; transcription reduced upon yeast-hyphal switch; protein detected by mass spec in stationary phase cultures
orf19.508	QDR1	2.35	Uncharacterized ORF||Putative transporter of antibiotic resistance; transcription is regulated by Nrg1p and Tup1p; caspofungin repressed; expression is regulated upon white-opaque switching
orf19.3670	GAL1	2.35	Verified ORF||Galactokinase; transcription regulated by galactose; transcription regulated by Mig1p and Tup1p; not required for systemic mouse virulence; farnesol-downregulated in biofilm; fluconazole-induced
orf19.3038	TPS2	2.34	Verified ORF||Trehalose-6-phosphate (Tre6P) phosphatase; mutation causes heat sensitivity, Tre6P accumulation, and decreased mouse virulence; possible drug target; two conserved phospohydrolase motifs; no human or murine homolog
orf19.868	ADAEC	2.34	Uncharacterized ORF||Transcription is specific to white cell type
orf19.6586	orf19.6586	2.34	Verified ORF||Predicted ORF in Assemblies 19, 20 and 21; increased transcription is observed upon benomyl treatment or in an azole-resistant strain that overexpresses MDR1; shows colony morphology-related gene regulation by Ssn6p; induced by nitric oxide, 17-beta-estradiol, ethynyl estradiol; macrophage-downregulated gene
orf19.3675	GAL7	2.27	Uncharacterized ORF||Predicted ORF in Assemblies 19, 20 and 21; Putative galactose-1-phoshphate uridyl transferase; downregulated by hypoxia, upregulated by ketoconazole; macrophage/pseudohyphal-repressed
orf19.409	orf19.409	2.26	1) Uncharacterized ORF||Putative catalytic epsilon subunit of the translation initiation factor eIF2B, based on similarity to S. cerevisiae Gcd6p; genes encoding translation factors are downregulated upon phagocytosis by murine macrophage. 2) Verified ORF||Plasma membrane-localized protein; similar to S. cerevisiae Ynr018Wp. 3) Predicted ORF from Assembly 19; removed from Assembly 20.
orf19.909	STP4	2.25	Verified ORF||Putative transcription factor with zinc finger DNA-binding motif; induced in core caspofungin response; shows colony morphology-related gene regulation by Ssn6p; induced by 17-beta-estradiol, ethynyl estradiol
orf19.5114	orf19.5114	2.25	Uncharacterized ORF||Predicted ORF in Assemblies 19, 20 and 21; S. cerevisiae ortholog SNX3 has phosphatidylinositol-3-phosphate binding, has role in late endosome to Golgi transport, protein localization and localizes to endosome, cytosol
orf19.6514	CUP9	2.18	Verified ORF||Protein of unknown function, upregulated in clinical isolates from HIV+ patients with oral candidiasis; transcription reduced upon yeast-hyphal switch; ketoconazole-induced; Plc1p-regulated; shows colony morphology-related Ssn6p regulation

orf19.1774	orf19.1774	2.17	Uncharacterized ORF||Predicted ORF in Assemblies 19, 20 and 21; transcription is upregulated in an RHE model of oral candidiasis; virulence-group-correlated expression
orf19.2023	HGT7	2.15	Verified ORF||Putative glucose transporter, major facilitator superfamily; glucose-, fluconazole-, Snf3p-induced, expressed at high glucose; upregulated in biofilm; C. albicans glucose transporter family comprises 20 members; 12 TM regions predicted
orf19.4907	orf19.4907	2.13	Uncharacterized ORF||Predicted ORF in Assemblies 19, 20 and 21; increased transcription is observed upon fluphenazine treatment; possibly transcriptionally regulated by Tac1p; induced by nitric oxide; fungal-specific (no human or murine homolog)
orf19.4777	DAK2	2.11	Uncharacterized ORF||Protein described as similar to dihydroxyacetone kinase; transcription is decreased upon yeast-hyphal switch; fluconazole-induced; caspofungin repressed; protein detected by mass spec in stationary phase cultures
orf19.3406	orf19.3406	2.11	Uncharacterized ORF||Predicted ORF in Assemblies 19, 20 and 21; member of conserved Mcm1p regulon
orf19.7021	GPH1	2.09	Verified ORF||Putative glycogen phosphorylase; gene regulated by Ssk1p, Mig1p, and Tup1p; fluconazole-induced; localizes to cell surface of hyphal cells, but not yeast-form cells; S. cerevisiae Gph1p is a stress-regulated protein of glycogen metabolism
orf19.6660	orf19.6660	2.08	Uncharacterized ORF||Putative protein of unknown function; mRNA binds to She3p; predicted ORF in Assemblies 19, 20 and 21
orf19.6817	FCR1	2.08	Verified ORF||Putative zinc cluster transcription factor; negative regulator of fluconazole, ketoconazole, brefeldin A resistance; transposon mutation affects filamentous growth; partially suppresses S. cerevisiae pdr1 pdr3 mutant fluconazole sensitivity
orf19.6000	CDR1	2.07	Verified ORF||Multidrug transporter of ATP-binding cassette (ABC) superfamily; transports phospholipids in an in-to-out direction; transcription induced by beta-estradiol, progesterone, corticosteroid, or cholesterol
orf19.6387	HSP104	2.06	Verified ORF||Functional homolog of S. cerevisiae Hsp104p; has chaperone and prion propagation activity in S. cerevisiae; guanidine-insensitive; heat shock/stress induced; downregulated in biofilm upon treatment with farnesol; no human or murine homolog
orf19.4527	HGT1	2.05	Verified ORF||High-affinity glucose transporter, member of major facilitator superfamily; transcription induced by progesterone and by drugs including chloramphenicol and benomyl; likely essential for growth, based on an insertional mutagenesis strategy
orf19.4779	orf19.4779	2.05	Uncharacterized ORF||Putative transporter; slightly similar to the Sit1p siderophore transporter; Gcn4p-regulated; fungal-specific (no human or murine homolog); transcriptionally activated by Mnl1p under weak acid stress
orf19.4445	orf19.4445	2.05	Verified ORF||Putative protein of unknown function; Plc1p-regulated; expression is upregulated early upon infection of reconstituted human epithelium (RHE), while expression of the C. dubliniensis ortholog is not upregulated; not required for viability
orf19.5958	CDR2	2.04	Verified ORF||Multidrug transporter, ATP-binding cassette (ABC) superfamily; transports phospholipids, in-to-out direction; low mRNA level; overexpressed in azole-resistant isolates; expression confers multidrug resistance to S. cerevisiae pdr5 mutant
orf19.2020	HGT6	2.03	Verified ORF||Putative glucose transporter of major facilitator superfamily; 20 members of C. albicans glucose transporter family; 12 probable membrane-spanning segments; core stress response, fluconazole-induced; expressed in rich medium with 2% glucose
orf19.3967	PFK1	2.02	Verified ORF||Alpha subunit of phosphofructokinase (PFK), which is Pfk1p, Pfk2p heteromultimer; PFK is activated by fructose 2,6-bisphosphate or AMP, inhibited by ATP; activity reduced on hyphal induction; phagocytosis-downregulated; fluconazole-induced

orf19.638	FDH1	2.02	Uncharacterized ORF||Putative formate dehydrogenase, oxidizes formate to produce CO2; induced during macrophage infection; fluconazole-downregulated; Mig1p regulated; downregulated by Efg1p under yeast, not hyphal, growth conditions; predicted to be cytosolic
orf19.2877	PDC11	2.01	Verified ORF||Protein similar to pyruvate decarboxylase; antigenic; at hyphal cell surface, not yeast-form cells; soluble in hyphae; regulated by Gcn4p, Efg1p, Efh1p; fluconazole-, farnesol-, biofilm-induced; repressed upon amino acid starvation
orf19.7091	orf19.7091	2.00	Uncharacterized ORF||Predicted ORF in Assemblies 19, 20 and 21; induced by nitric oxide
orf19.3302	orf19.3302	2.00	Uncharacterized ORF||Predicted ORF in Assemblies 19, 20 and 21; transcription downregulated upon yeast-hyphal switch; transcriptionally activated by Mnl1p under weak acid stress
orf19.2060	SOD5	1.99	Verified ORF||Copper- and zinc-containing superoxide dismutase; protective role against oxidative stress; induced by neutrophil contact, hyphal growth, caspofungin, osmotic or oxidative stress; member of a gene family including SOD1, SOD4, SOD5, and SOD6
orf19.4737	TPO3	1.98	Verified ORF||Possible role in polyamine transport; MFS-MDR family; transcription induced by Sfu1p, regulated upon white-opaque switching; decreased expression in hyphae compared to yeast-form cells; regulated by Nrg1p; fungal-specific
orf19.4941	TYE7	1.96	Verified ORF||Transcription factor with bHLH (basic region, helix-loop-helix) motif involved in control of glycolysis; hyphally regulated via Cph1p, Cyr1p; flucytosine, Hog1p induced; amphotericin B, caspofungin repressed
orf19.85	GPX2	1.96	Uncharacterized ORF||Similar to glutathione peroxidase; expression greater in high iron; alkaline upregulated by Rim101p; transcriptionally induced by alpha factor or interaction with macrophage; regulated by Efg1p; caspofungin repressed
orf19.2608	ADH5	1.95	Verified ORF||Putative alcohol dehydrogenase; soluble protein in hyphae; expression is regulated upon white-opaque switching; fluconazole-induced; antigenic during murine systemic infection; regulated by Nrg1p, Tup1p; macrophage-downregulated protein
orf19.1381	orf19.1381	1.94	Uncharacterized ORF||Predicted ORF in Assemblies 19, 20 and 21; S. cerevisiae ortholog LSB5 has role in actin filament organization, endocytosis, actin cortical patch localization and localizes to actin cortical patch
orf19.4631	ERG251	1.91	Verified ORF||Predicted ORF in Assemblies 19, 20 and 21; ketoconazole-induced; amphotericin B, caspofungin repressed; possibly an essential gene, disruptants not obtained by UAU1 method
orf19.7150	NRG1	1.91	Verified ORF||Transcriptional repressor; regulates hyphal genes, virulence genes, chlamydospore development, and genes involved in rescue and stress responses; effects both Tup1p-dependent (major) and -independent (minor) regulation
orf19.3668	HGT2	1.89	Verified ORF||Putative glucose transporter of the major facilitator superfamily; the C. albicans glucose transporter family comprises 20 members; 12 probable membrane-spanning segments; expressed in rich medium with 2% glucose
orf19.1117	orf19.1117	1.88	Uncharacterized ORF||Predicted ORF in Assemblies 19, 20 and 21; similar to Candida boidinii formate dehydrogenase; virulence-group-correlated expression
orf19.5908	TEC1	1.88	Verified ORF||TEA/ATTS transcription factor involved in regulation of hypha-specific genes; required for wild-type biofilm formation; regulates BCR1; directly transcriptionally regulated by Cph2p under some growth conditions; alkaline upregulated
orf19.6447	ARF1	1.87	Uncharacterized ORF||ADP-ribosylation factor, probable GTPase involved in intracellular transport; one of several C. albicans ADP-ribosylation factors; N-myristoylprotein; substrate of Nmt1p
orf19.3997	ADH1	1.87	1) Verified ORF||Alcohol dehydrogenase; at yeast-form but not hyphal cell surface; soluble in hyphae; immunogenic in human or mouse; complements S. cerevisiae adh1 adh2 adh3 mutation; regulated by growth phase, carbon source; fluconazole-, farnesol-induced. 2) Uncharacterized ORF||Predicted ORF in Assemblies 19, 20 and 21.
orf19.986	GLY1	1.87	Verified ORF||L-threonine aldolase; possibly tetrameric; complements the glycine auxotrophy of an S. cerevisiae shm1 null shm2 null gly1-1 triple mutant; macrophage/pseudohyphal-induced; the GLY1 locus has an RFLP and is triploid in strain SGY269

orf19.6816	orf19.6816	1.86	Uncharacterized ORF||Predicted ORF in Assemblies 19, 20 and 21; S. cerevisiae ortholog YJR096W has aldehyde reductase activity, has role in arabinose catabolic process, D-xylose catabolic process, cellular response to oxidative stress and localizes to cytoplasm, nucleus
orf19.3392	DOG1	1.86	Uncharacterized ORF||Putative 2-deoxyglucose-6-phosphatase; haloacid dehalogenase hydrolase/phosphatase superfamily; similar to S. cerevisiae Dog1p, Dog2p, Hor1p, and Rhr2p; regulated by Nrg1p, Tup1p
orf19.6770	orf19.6770	1.85	Uncharacterized ORF||Predicted ORF in Assemblies 19, 20 and 21
orf19.3651	PGK1	1.85	Verified ORF||Phosphoglycerate kinase; enzyme of glycolysis; localizes to cell wall and to cytoplasm; antigenic during murine or human systemic infection; biofilm, Hog1p, GCN-induced; downregulated upon phagocytosis; possible N-glycosylation at N349
orf19.675	orf19.675	1.85	Uncharacterized ORF||Similar to cell wall proteins; induced in core stress response, core caspofungin response; iron-regulated; amphotericin B induced; regulated by Cyr1p, Ssn6p; possibly spurious ORF (Annotation Working Group prediction)
orf19.542	HXK2	1.83	Uncharacterized ORF||Protein described as hexokinase II; antigenic in human; downregulated in the presence of human neutrophils; regulated by Efg1p; fluconazole-induced; shows colony morphology-related gene regulation by Ssn6p
orf19.3302	orf19.3302	1.83	Uncharacterized ORF||Predicted ORF in Assemblies 19, 20 and 21; transcription downregulated upon yeast-hyphal switch; transcriptionally activated by Mnl1p under weak acid stress
orf19.6322	ARD	1.82	Verified ORF||D-arabitol dehydrogenase, NAD-dependent (ArDH); enzyme of D-arabitol and D-arabinose catabolism; D-arabitol is a marker for active infection in humans; has conserved YXXXK motif of short-chain alcohol-polyol-sugar dehydrogenases
orf19.2414	orf19.2414	1.82	Uncharacterized ORF||Predicted ORF in Assemblies 19, 20 and 21
orf19.5285	PST3	1.81	Uncharacterized ORF||Putative flavodoxin; biofilm induced; fungal-specific (no human or murine homolog); protein detected by mass spec in stationary phase cultures
orf19.72	CTR2	1.81	Predicted ORF from Assembly 19; merged with orf19.4720 in Assembly 20; induced by nitric oxide; clade-associated gene expression
orf19.5282	orf19.5282	1.81	Uncharacterized ORF||Putative protein of unknown function; mRNA binds to She3p; decreased expression in hyphae compared to yeast-form cells; regulated by Efg1p and Efh1p; intron in 5'-UTR; transcriptionally activated by Mnl1p under weak acid stress
orf19.3040	EHT1	1.80	Uncharacterized ORF||Protein similar to S. cerevisiae Eht1p; transcription is induced in response to alpha pheromone in SpiderM medium
orf19.2803	HEM13	1.80	Verified ORF||Coproporphyrinogen III oxidase; antigenic in human/mouse; localizes to yeast-form cell surface, not hyphae; soluble in hyphae; iron-regulated expression; macrophage-downregulated; not Rfg1p regulated, farnesol-induced; possibly essential
orf19.822	HSP21	1.80	Verified ORF||Protein detected in some, not all, biofilm extracts; fluconazole-downregulated; greater mRNA abundance observed in cyr1 or ras1 homozygous null mutant than in wild type; protein detected by mass spec in stationary phase cultures
orf19.1944	GPR1	1.80	Verified ORF||Putative G-protein-coupled receptor of plasma membrane; required for wild-type hyphal growth; acts in cAMP-PKA pathway; reports differ on role in cAMP-mediated glucose signaling; Gpr1p C terminus binds Gpa2p; regulates HWP1 and ECE1
orf19.4342	orf19.4342	1.80	Uncharacterized ORF||Predicted ORF in Assemblies 19, 20 and 21
orf19.2173	MAF1	1.80	Uncharacterized ORF||Protein described as affecting nucleocytoplasmic transport and synthesis of RNA Polymerase III; decreased expression in hyphae compared to yeast-form cells; caspofungin repressed

orf19.5338	GAL4	1.79	Verified ORF||Transcription factor with zinc cluster DNA-binding motif involved in control of glycolysis; ortholog of S. cerevisiae Gal4p, but not involved in the regulation of galactose utilization genes; caspofungin repressed
orf19.4044	MUM2	1.79	Uncharacterized ORF||Protein similar to S. cerevisiae Mum2p; transcription is induced in response to alpha pheromone in SpiderM medium; transcription is regulated by Tup1p.
orf19.1193	GNP1	1.78	Uncharacterized ORF||Protein described as similar to asparagine and glutamine permease; fluconazole or caspofungin induced; transcription is regulated by Nrg1p, Mig1p, Tup1p, Gcn2p, Gcn4p, and alkaline regulated by Rim101p; fungal-specific
orf19.4720	CTR2	1.78	Uncharacterized ORF||Predicted ORF in Assemblies 19, 20 and 21; induced by nitric oxide; clade-associated gene expression
orf19.1277	orf19.1277	1.77	Uncharacterized ORF||Predicted ORF in Assemblies 19, 20 and 21; repressed by Rgt1p
orf19.7498	LEU1	1.76	Uncharacterized ORF||Protein described as 3-isopropylmalate dehydratase which is essential for fungal pathogenicity; antigenic in human; decreased expression in hyphae compared to yeast-form cells; alkaline downregulated; upregulated in the presence of human whole blood or polymorphonuclear (PMN) cells
orf19.7676	XYL2	1.76	Verified ORF||Protein described as similar to D-xylulose reductase; immunogenic in mouse; soluble protein in hyphae; Hog1p-induced; induced during cell wall regeneration; caspofungin or fluconazole-induced; Mnl1p-induced in weak acid stress
orf19.951	orf19.951	1.76	Uncharacterized ORF||Predicted ORF in Assemblies 19, 20 and 21; transcription downregulated upon yeast-hyphal switch; fluconazole-induced; possibly spurious ORF (Annotation Working Group prediction)
orf19.7229	IML2	1.75	Uncharacterized ORF||Predicted ORF in Assemblies 19, 20 and 21; S. cerevisiae ortholog YKR018C localizes to cytoplasm, nucleus
orf19.5960	NCE102	1.75	Verified ORF||Predicted ORF in Assemblies 19, 20 and 21; Protein involved in non classical protein export; localized to plasma membrane
orf19.1395	orf19.1395	1.75	Uncharacterized ORF||Predicted ORF in Assemblies 19, 20 and 21; S. cerevisiae ortholog PIC2 has inorganic phosphate transmembrane transporter activity, has role in transmembrane transport, phosphate transport and localizes to mitochondrion
orf19.903	GPM1	1.74	Verified ORF||Surface protein that binds host complement Factor H and FHL-1; phosphoglycerate mutase; antigenic in murine, human infection; biofilm-, fluconazole-, or amino acid starvation (3-aminotriazole treatment) induced, farnesol-downregulated
orf19.3171	ACH1	1.74	Verified ORF||Acetyl-coA hydrolase; acetate utilization; nonessential; soluble protein in hyphae; antigenic in human; induced on polystyrene adherence; farnesol-, ketoconazole-induced; no human or murine homolog
orf19.4998	ROB1	1.74	Verified ORF||Putative protein of unknown function; null mutant displays abnormal colony morphology and invasive growth; caspofungin repressed; predicted ORF in Assemblies 19, 20 and 21
orf19.5022	orf19.5022	1.74	Uncharacterized ORF||Predicted ORF in Assemblies 19, 20 and 21; S. cerevisiae ortholog SMF2 has di-, tri-valent inorganic cation transmembrane transporter activity and has role in manganese ion transport, cellular cobalt ion homeostasis, cobalt ion transport, cellular manganese ion homeostasis
orf19.72	CTR2	1.74	Predicted ORF from Assembly 19; merged with orf19.4720 in Assembly 20; induced by nitric oxide; clade-associated gene expression
orf19.5956	PIN3	1.73	Uncharacterized ORF||Predicted ORF in Assemblies 19, 20 and 21; Putative SH3-domain-containing protein
orf19.1861	orf19.1861	1.73	Uncharacterized ORF||Predicted ORF in Assemblies 19, 20 and 21
orf19.633	orf19.633	1.72	Uncharacterized ORF||Protein described as a putative methyltransferase; decreased expression in hyphae compared to yeast-form cells; expression regulated during planktonic growth
orf19.5286	YCP4	1.72	Uncharacterized ORF||Putative flavodoxin; fungal-specific (no human or murine homolog)

orf19.2296	orf19.2296	1.72	Uncharacterized ORF||Predicted ORF in Assemblies 19, 20 and 21; similar to mucins; ketoconazole-induced; fluconazole-downregulated; greater mRNA abundance observed in a cyr1 homozygous null mutant than in wild type; colony morphology-related gene regulation by Ssn6p
orf19.3669	SHA3	1.71	Verified ORF||Protein similar to S. cerevisiae Sha3p, a serine/threonine kinase involved in glucose transport; transposon mutation affects filamentous growth; fluconazole-induced; ketoconazole-repressed; induced in by alpha pheromone; possibly essential
orf19.2218	orf19.2218	1.71	Uncharacterized ORF||Predicted ORF from Assembly 19; merged with orf19.1861 in Assembly 20
orf19.7314	CDG1	1.71	Uncharacterized ORF||Protein described as similar to cysteine dioxygenases; expression is regulated upon white-opaque switching; transcription is upregulated in both intermediate and mature biofilms
orf19.3712	orf19.3712	1.71	Uncharacterized ORF||Predicted ORF in Assemblies 19, 20 and 21; transcriptionally activated by Mnl1p under weak acid stress
orf19.13	GLK1	1.71	Putative glucokinase; transcription is regulated upon yeast-hyphal switch; transcriptionally regulated by Efg1p; fluconazole-induced; induced in core stress response; shows colony morphology-related gene regulation by Ssn6p
orf19.2665	MSN5	1.70	Uncharacterized ORF||Predicted ORF in Assemblies 19, 20 and 21; S. cerevisiae ortholog MSN5 has importin-alpha export receptor activity, has role in tRNA re-export from nucleus, protein export from nucleus and localizes to nucleus
orf19.1187	CPH2	1.70	Verified ORF||Transcriptional activator of hyphal growth; Myc bHLH family: directly regulates Tec1p, which regulates hypha-specific genes; probably homodimeric, phosphorylated; enhances S. cerevisiae nitrogen starvation-induced pseudohyphal growth
orf19.918	CDR11	1.70	Uncharacterized ORF||Putative transporter of PDR subfamily of ABC family; Gcn4p-regulated; upregulated by Rim101p at pH 8
orf19.6928	SAP9	1.70	Verified ORF||Secreted aspartyl proteinase; roles in adhesion, cell surface integrity; induced by antifungal drugs, stationary phase, or in white-phase cells; farnesol-downregulated in biofilm; autocatalytic processing; GPI-anchor; N-glycosylated
orf19.6814	TDH3	1.70	Verified ORF||Glyceraldehyde-3-phosphate dehydrogenase; enzyme of glycolysis; binds fibronectin and laminin; at surface of yeast-form cells and hyphae; soluble in hyphae; antigenic during infection; NAD-linked; farnesol-downregulated
orf19.2050	orf19.2050	1.69	Uncharacterized ORF||Predicted ORF in Assemblies 19, 20 and 21; S. cerevisiae ortholog TGL1 has sterol esterase activity, has role in cellular lipid metabolic process, sterol metabolic process and localizes to integral to membrane, lipid particle
orf19.5113	ADH2	1.69	Verified ORF||Putative alcohol dehydrogenase; soluble protein in hyphae; fungal-specific (no human or murine homolog); expression is regulated upon white-opaque switching; regulated by Ssn6p; transcriptionally activated by Mnl1p under weak acid stress
orf19.1585	ZRT2	1.68	Uncharacterized ORF||Putative zinc transporter; ciclopirox olamine, fluconazole, and alkaline downregulated; transcriptionally induced by interaction with macrophages; amphotericin B induced; possibly an essential gene, disruptants not obtained by UAU1 method
orf19.84	CAN3	1.68	Uncharacterized ORF||Predicted ORF in Assemblies 19, 20 and 21; expression is regulated upon white-opaque switching
orf19.461	MHP1	1.67	Verified ORF||Protein similar to S. cerevisiae Mhp1p, which is involved in microtubule stabilization; transposon mutation affects filamentous growth; possibly transcriptionally regulated upon hyphal formation; possibly an essential gene (by UAU1 method)
orf19.255	ZCF1	1.67	1) Uncharacterized ORF||Predicted zinc-cluster protein of unknown function; possibly transcriptionally regulated upon hyphal formation; intron in 5'-UTR; possibly an essential gene, disruptants not obtained by UAU1 method. 2) Dubious ORF||Transcription is negatively regulated by Sfu1p; repressed by nitric oxide.
orf19.6771	UBI4	1.67	Verified ORF||Ubiquitin precursor (polyubiquitin), contains three tandem repeats of the ubiquitin peptide that are processed to individual units; transcription is induced by stress; mRNA found in yeast-form and mycelial cells at similar abundance

orf19.2005	REG1	1.66	Uncharacterized ORF||Predicted ORF in Assemblies 19, 20 and 21; macrophage/pseudohyphal-induced; possibly transcriptionally regulated upon hyphal formation
orf19.5005	OSM2	1.66	Uncharacterized ORF||Protein described as mitochondrial fumarate reductase; regulated by Ssn6p, Gcn2p, and Gcn4p; Hog1p-downregulated; protein detected by mass spec in stationary phase cultures
orf19.6116	GLK4	1.66	Uncharacterized ORF||Protein described as a glucokinase; decreased expression in hyphae compared to yeast-form cells
orf19.2876	CBF1	1.66	Verified ORF||Transcription factor that binds to a conserved sequence at ribosomal protein genes and the rDNA locus, with Tbf1p; also regulates sulfur starvation-response and other genes; binds centromeres and has a role in centromere maintenance
orf19.7544	TLO1	1.66	Uncharacterized ORF||Member of a family of telomere-proximal genes of unknown function; hyphal-induced expression
orf19.2655	BUB3	1.66	Uncharacterized ORF||Protein similar to S. cerevisiae Bub3p, which is a kinetochore checkpoint component; induced under hydroxyurea treatment
orf19.2529	orf19.2529	1.65	Uncharacterized ORF||Predicted ORF in Assemblies 19, 20 and 21; shares similarity with human Pig-H, which is involved in glycosylphosphatidylinositol assembly
orf19.5228	RIB3	1.65	Verified ORF||3,4-Dihydroxy-2-butanone 4-phosphate synthase; homodimeric enzyme of riboflavin biosynthesis; converts ribulose 5-phosphate to L-3,4-dihydroxy-2-butanone 4-phosphate; transcription regulated on yeast-hyphal switch, macrophage interaction
orf19.3363	VTC4	1.65	Uncharacterized ORF||Protein described as polyphosphate synthetase; decreased expression in hyphae compared to yeast-form cells; fungal-specific (no human or murine homolog); virulence-group-correlated expression
orf19.4451	RIA1	1.65	1) Uncharacterized ORF||ORF Predicted by Annotation Working Group; Predicted zinc-finger protein of unknown function. 2) Uncharacterized ORF||Putative translation elongation factor; genes encoding ribosomal subunits, translation factors, and tRNA synthetases are downregulated upon phagocytosis by murine macrophage.
orf19.4783	orf19.4783	1.64	Uncharacterized ORF||Predicted ORF in Assemblies 19, 20 and 21
orf19.1653	orf19.1653	1.64	Uncharacterized ORF||Predicted ORF in Assemblies 19, 20 and 21; possibly spurious ORF (Annotation Working Group prediction)
orf19.2333	orf19.2333	1.64	Uncharacterized ORF||Predicted ORF in Assemblies 19, 20 and 21; S. cerevisiae ortholog YHR009C localizes to cytoplasm
orf19.7551	ALO1	1.64	Verified ORF||D-Arabinono-1,4-lactone oxidase, involved in biosynthesis of dehydro-D-arabinono-1,4-lactone, which has a protective role against oxidative damage; required for full virulence in a mouse model of systemic infection
orf19.5958	CDR2	1.64	Verified ORF||Multidrug transporter, ATP-binding cassette (ABC) superfamily; transports phospholipids, in-to-out direction; low mRNA level; overexpressed in azole-resistant isolates; expression confers multidrug resistance to S. cerevisiae pdr5 mutant
orf19.5019	orf19.5019	1.64	Uncharacterized ORF||Predicted ORF in Assemblies 19, 20 and 21
orf19.3133	GUT2	1.63	Verified ORF||Glycerol-3-phosphate dehydrogenase; Plc1p-regulated; transcription is upregulated in both intermediate and mature biofilms
orf19.5024	GND1	1.63	Verified ORF||Putative 6-phosphogluconate dehydrogenase; soluble protein in hyphae; farnesol-, macrophage-induced protein; antigenic in mouse; protein detected by mass spec in exponential and stationary phase cultures
orf19.1715	IRO1	1.63	Verified ORF||Putative transcription factor; role in iron utilization, pathogenesis; both IRO1 and adjacent URA3 are mutated in strain CAI4; suppresses S. cerevisiae aft1 mutant low-iron growth defect; hyphal-induced; reports differ about iron regulation
orf19.4922	orf19.4922	1.63	Uncharacterized ORF||Predicted ORF in Assemblies 19, 20 and 21

orf19.5117	OLE1	1.63	Verified ORF||Fatty acid desaturase (stearoyl-CoA desaturase), essential protein involved in oleic acid synthesis; required for aerobic hyphal growth and chlamydospore formation; subject to hypoxic regulation; fluconazole-induced; caspofungin repressed
orf19.3940.1	CUP1	1.63	Verified ORF||Metallothionein, involved in copper resistance; transcription is induced by copper
orf19.4698	PTC8	1.63	Verified ORF||Predicted type 2C protein phosphatase, serine/threonine-specific; required for hyphal growth; induced under stress
orf19.610	EFG1	1.62	Verified ORF||Transcriptional repressor; required for white-phase cell type; hyphal growth, metabolism, cell-wall gene regulator; roles in adhesion, virulence; Cph1p and Efg1p have role in host cytokine response; bHLH; binds E-box; T206 phosphorylated; Enhanced Filamentous Growth
orf19.7296	orf19.7296	1.62	Verified ORF||Predicted ORF in Assemblies 19, 20 and 21; Putative cation conductance protein; similar to stomatin mechanoreception protein; induced by Rgt1p; plasma-membrane localized
orf19.3360	orf19.3360	1.62	Uncharacterized ORF||Predicted ORF in Assemblies 19, 20 and 21; possibly spurious ORF (Annotation Working Group prediction)
orf19.575	HYR3	1.61	Uncharacterized ORF||Putative GPI-anchored protein of unknown function; similar to Hyr1p; transcriptionally regulated by iron; expression greater in high iron; clade-specific repeat variation
orf19.1408	GLK4	1.61	Predicted ORF from Assembly 19; merged with orf19.6116 in Assembly 20; Protein described as a glucokinase; decreased expression in hyphae compared to yeast-form cells
orf19.1407	orf19.1407	1.61	Predicted ORF from Assembly 19; merged with orf19.6117 in Assembly 20; Predicted ORF in Assemblies 19, 20 and 21; ketoconazole and hypoxia induced
orf19.3331	ABC1	1.61	Uncharacterized ORF||Protein described as ubiquinol-cytochrome-c reductase; induced upon adherence to polystyrene
orf19.6741	orf19.6741	1.61	Uncharacterized ORF||Predicted ORF in Assemblies 19, 20 and 21; regulated by Nrg1p, Tup1p
orf19.734	GLK1	1.61	1) Uncharacterized ORF||Predicted ORF in Assemblies 19, 20 and 21. 2) Uncharacterized ORF||Putative glucokinase; transcription is regulated upon yeast-hyphal switch; transcriptionally regulated by Efg1p; fluconazole-induced; induced in core stress response; shows colony morphology-related gene regulation by Ssn6p
orf19.2021	HGT8	1.61	Verified ORF||Putative glucose transporter of the major facilitator superfamily; the C. albicans glucose transporter family comprises 20 members; 12 probable membrane-spanning segments; gene has intron; expressed in rich medium with 2% glucose
orf19.3669	SHA3	1.60	Verified ORF||Protein similar to S. cerevisiae Sha3p, a serine/threonine kinase involved in glucose transport; transposon mutation affects filamentous growth; fluconazole-induced; ketoconazole-repressed; induced in by alpha pheromone; possibly essential
orf19.1252	YME1	1.60	Uncharacterized ORF||Protein not essential for viability; similar to S. cerevisiae Yme1p, which is a mitochondrial inner membrane protease of the AAA family; S. cerevisiae ortholog YME1 has role in chronological cell aging, misfolded or incompletely synthesized protein catabolic process and localizes to i-AAA complex
orf19.395	ENO1	1.60	Verified ORF||Enolase (2-phospho-D-glycerate-hydrolyase), enzyme of glycolysis and gluconeogenesis; major cell-surface antigen; binds host plasmin/plasminogen; immunoprotective; phagocytosis, biofilm-regulated; farnesol-downregulated; possibly essential
orf19.3004	orf19.3004	1.60	Uncharacterized ORF||Predicted ORF in Assemblies 19, 20 and 21
orf19.2242	PRB1	1.59	Uncharacterized ORF||Putative endoprotease B; regulated by heat, carbon source (GlcNAc-induced), nitrogen, macrophage response, human neutrophils; putative D200-H232-S389 catalytic triad; similar to (but does not replace) S. cerevisiae vacuolar B protease Prb1p

orf19.3412	ATG15	1.59	Uncharacterized ORF||Putative lipase; fungal-specific (no human or murine homolog)
orf19.1151	orf19.1151	1.59	1) Predicted ORF from Assembly 19; induced in core stress response; merged with orf19.1152 in Assembly 20; Predicted ORF in Assemblies 19, 20 and 21; regulated by Gcn2p and Gcn4p; induced in core stress response. 2) Uncharacterized ORF||ORF Predicted by Annotation Working Group
orf19.3190	HAL9	1.58	Uncharacterized ORF||Protein with Zn(2)-Cys(6) binuclear cluster; gene in zinc cluster region of Chr. 5; transcriptionally activated by Mnl1p in weak acid; similar to S. cerevisiae Hal9p, which is a putative transcription factor involved in salt tolerance
orf19.3706	orf19.3706	1.58	Uncharacterized ORF||Predicted ORF in Assemblies 19, 20 and 21
orf19.6713	orf19.6713	1.58	Uncharacterized ORF||Predicted ORF in Assemblies 19, 20 and 21
orf19.1785	orf19.1785	1.58	Uncharacterized ORF||Predicted ORF in Assemblies 19, 20 and 21
orf19.2398	orf19.2398	1.58	Uncharacterized ORF||Predicted ORF in Assemblies 19, 20 and 21; possible increased transcription in an azole-resistant strain that overexpresses CDR1 and CDR2; possibly transcriptionally regulated by Tac1p; induced by Mnl1p under weak acid stress
orf19.6881	YTH1	1.58	Verified ORF||Protein described as an mRNA cleavage and polyadenylation specificity factor; transcription is regulated upon yeast-hyphal switch; decreased expression in hyphae compared to yeast-form cells; fluconazole or flucytosine induced
orf19.5911	CMK1	1.57	Uncharacterized ORF||Expression is regulated upon white-opaque switching; biochemically purified Ca2+/CaM-dependent kinase is soluble, cytosolic, monomeric, and serine-autophosphorylated
orf19.7124	RVS161	1.57	Verified ORF||Protein required for endocytosis; contains a BAR domain, which is found in proteins involved in membrane curvature; null mutant exhibits defects in hyphal growth, virulence, cell wall integrity, and actin patch localization
orf19.4774	AOX1	1.57	Verified ORF||Alternative oxidase; low abundance; constitutively expressed; one of two isoforms (Aox1p and Aox2p); involved in a cyanide-resistant respiratory pathway present in plants, protists, and some fungi, although absent from S. cerevisiae
orf19.7481	MDH1	1.57	Verified ORF||Protein described as malate dehydrogenase, mitochondrial; transcription regulated by Mig1p and Tup1p, white-opaque switching; induced in high iron, biofilm; regulated upon phagocytosis; antigenic during murine or human infection
orf19.3678	orf19.3678	1.57	Uncharacterized ORF||Protein not essential for viability
orf19.6745	TPI1	1.57	1) Uncharacterized ORF||Predicted ORF in Assemblies 19, 20 and 21; Ortholog of S. cerevisiae YMR262W. 2) Verified ORF||Triose-phosphate isomerase; antigenic in mouse or human; mutation affects filamentous growth; biofilm-induced; macrophage-downregulated protein; detected by mass spec in exponential and stationary phase cultures; possibly an essential gene.
orf19.4540	UBC8	1.57	Uncharacterized ORF||Protein similar to S. cerevisiae Ubc8p; transcription is induced in response to alpha pheromone in SpiderM medium
orf19.5961	orf19.5961	1.57	Uncharacterized ORF||Predicted ORF in Assemblies 19, 20 and 21; described as similar to S. cerevisiae Nas6p proteasome component; induced upon adherence to polystyrene; regulated by Gcn2p and Gcn4p
orf19.7502	orf19.7502	1.57	Uncharacterized ORF||Predicted ORF in Assemblies 19, 20 and 21; greater mRNA abundance observed in a cyr1 homozygous null mutant than in wild type; possibly spurious ORF (Annotation Working Group prediction)
orf19.3888	PGI1	1.56	Verified ORF||Protein described as glucose-6-phosphate isomerase, enzyme of glycolysis; antigenic in human; regulated by Efg1p; induced in biofilm, upon adherence to polystyrene; downregulated in the presence of human neutrophils, upon phagocytosis
orf19.4843	orf19.4843	1.56	Uncharacterized ORF||Predicted ORF in Assemblies 19, 20 and 21; S. cerevisiae ortholog FRE8 has oxidoreductase activity, oxidizing metal ions and has role in cellular metal ion homeostasis

orf19.7561	DEF1	1.56	Verified ORF||Protein required for filamentous growth and for escape from epithelial cells and dissemination in an RHE model; transcription induced in oral candidiasis clinical isolates; induced by fluconazole, high cell density; hyphally regulated
orf19.4942	orf19.4942	1.56	Dubious ORF||Predicted ORF in Assemblies 19, 20 and 21
orf19.2175	orf19.2175	1.56	Uncharacterized ORF||Predicted ORF in Assemblies 19, 20 and 21; induced by nitric oxide
orf19.4546	HOL4	1.56	Uncharacterized ORF||Protein described as an ion transporter; alkaline upregulated by Rim101p; Plc1p-regulated; caspofungin repressed
orf19.5551	MIF2	1.56	Verified ORF||Centromere-associated protein; similar to CENP-C proteins; Cse4p and Mif2p colocalize at C. albicans centromeres
orf19.1862	orf19.1862	1.55	Uncharacterized ORF||Possible stress protein; increased transcription is associated with CDR1 and CDR2 overexpression or fluphenazine treatment; transcription regulated by Sfu1p, Nrg1p, Tup1p
orf19.4672	orf19.4672	1.55	Dubious ORF||Predicted ORF in Assemblies 19, 20 and 21
orf19.2762	AHP1	1.55	Verified ORF||Putative alkyl hydroperoxide reductase; immunogenic in mouse; biofilm-induced; fluconazole-induced; amphotericin B, caspofungin, alkaline downregulated; induced in core stress response; regulated by Ssk1p, Nrg1p, Tup1p, Ssn6p, Hog1p
orf19.2026	UBP13	1.55	Uncharacterized ORF||Predicted ORF in Assemblies 19, 20 and 21; Ortholog of S. cerevisiae UBP13
orf19.2602	OPT1	1.55	Verified ORF||Oligopeptide transporter; transports 3-to-5-residue peptides; alleles are distinct, one has intron; not ABC or PTR type transporter; suppresses S. cerevisiae ptr2-2 mutant defects; induced by BSA or peptides; Stp3p, Hog1p regulated
orf19.86	orf19.86	1.55	Uncharacterized ORF||Putative glutathione peroxidase; peroxide-induced; induced in response to peroxide, exposure to neutrophils and macrophage blood fractions; downregulated during infection of macrophages
orf19.54	RHD1	1.55	Verified ORF||Putative beta-mannosyltransferase, required for the addition of beta-mannose to the acid-labile fraction of cell wall phosphopeptidomannan; member of a 9-gene family; transcriptionally regulated on yeast-hyphal and white-opaque switches; Repressed during Hyphae Development
orf19.5843	orf19.5843	1.55	Uncharacterized ORF||Predicted ORF in Assemblies 19, 20 and 21; Plc1p-regulated; greater mRNA abundance observed in a cyr1 homozygous null mutant than in wild type; possibly spurious ORF (Annotation Working Group prediction)
orf19.671	PSP1	1.55	Uncharacterized ORF||Protein repressed during the mating process
orf19.5741	ALS1	1.55	Verified ORF||Adhesin; ALS family of cell-surface glycoproteins; adhesion, virulence roles; immunoprotective; in band at hyphal base; amyloid domain; biofilm-induced; Rfg1p, Ssk1p, growth-regulated; strain background affects expression
orf19.5552	orf19.5552	1.55	Uncharacterized ORF||Predicted ORF in Assemblies 19, 20 and 21; S. cerevisiae ortholog CRT10 has role in regulation of transcription from RNA polymerase II promoter, global
orf19.2730	orf19.2730	1.55	Uncharacterized ORF||Predicted ORF in Assemblies 19, 20 and 21
orf19.5334	orf19.5334	1.55	Uncharacterized ORF||Predicted ORF in Assemblies 19, 20 and 21; transcription regulated upon yeast-hyphal switch
orf19.6837	FMA1	1.54	Uncharacterized ORF||Predicted ORF in Assemblies 19, 20 and 21; Protein similar to oxidoreductases; transcription is upregulated in response to treatment with ciclopirox olamine; upregulation correlates with clinical development of fluconazole resistance
orf19.4372	orf19.4372	1.54	Uncharacterized ORF||Predicted ORF in Assemblies 19, 20 and 21
orf19.4432	KSP1	1.54	Verified ORF||Putative protein of unknown function; mRNA binds to She3p and is localized to hyphal tips; mutation confers hypersensitivity to amphotericin B; predicted ORF in Assemblies 19, 20 and 21
orf19.3441	FRP6	1.54	Uncharacterized ORF||Transcription is regulated by Nrg1p and Tup1p; regulated by Ssn6p; upregulated in the presence of human neutrophils

orf19.7329	orf19.7329	1.53	Uncharacterized ORF||Predicted ORF in Assemblies 19, 20 and 21; S. cerevisiae ortholog UBC7 has ubiquitin-protein ligase activity and has role in chromatin assembly or disassembly, ER-associated protein catabolic process, fungal-type cell wall organization
orf19.6927	PEP8	1.53	Verified ORF||Protein similar to S. cerevisiae Pep8p, which is involved in retrograde transport; transposon mutation affects filamentous growth
orf19.1788	XKS1	1.53	Uncharacterized ORF||Predicted ORF from Assembly 19, 20 and 21; increased expression in response to prostaglandins
orf19.3641	CAN3	1.53	Expression is regulated upon white-opaque switching; merged with orf19.84 in Assembly 20
orf19.4752	MSN4	1.53	Uncharacterized ORF||Putative zinc finger transcription factor; similar to S. cerevisiae Msn4p, but not a significant stress response regulator in C. albicans; partly complements STRE-activation defect of S. cerevisiae msn2 msn4 double mutant
orf19.4657	orf19.4657	1.53	Uncharacterized ORF||Predicted ORF in Assemblies 19, 20 and 21; S. cerevisiae ortholog NEM1 has phosphoprotein phosphatase activity and has role in regulation of lipid biosynthetic process, nuclear envelope organization, ascospore formation
orf19.2270	SMF12	1.53	Uncharacterized ORF||Protein not essential for viability; similar to S. cerevisiae Smf1p, which is a manganese transporter; Gcn4p-regulated; alkaline upregulated; caspofungin repressed
orf19.4127	orf19.4127	1.53	Uncharacterized ORF||Predicted ORF in Assemblies 19, 20 and 21; S. cerevisiae ortholog LSB3 has role in actin cortical patch localization and localizes to cellular bud neck, mitochondrion
orf19.2743	orf19.2743	1.53	Uncharacterized ORF||Predicted ORF in Assemblies 19, 20 and 21
orf19.5054	orf19.5054	1.52	Uncharacterized ORF||Putative quinolinate phosphoribosyl transferase, involved in NAD biosynthesis
orf19.4318	MIG1	1.52	Verified ORF||Transcriptional repressor; regulates genes for utilization of carbon sources; Tup1p-dependent and -independent functions; upregulated in biofilm; hyphal downregulated; caspofungin repressed; functional homolog of S. cerevisiae Mig1p
orf19.6842	TUS1	1.52	Uncharacterized ORF||Predicted ORF in Assemblies 19, 20 and 21; transcriptionally activated by Mnl1p under weak acid stress
orf19.4438	RME1	1.52	Uncharacterized ORF||Protein similar to S. cerevisiae meiotic regulator Rme1p; white-specific transcription; upregulation correlates with clinical development of fluconazole resistance; transcription is not regulated during rat oral infection
orf19.4444	PHO15	1.52	Verified ORF||Protein described as 4-nitrophenyl phosphatase, possible histone H2A phosphatase; involved in regulation of white-opaque switching; hyphal downregulated; induced in core stress response; induced by heavy metal (cadmium) stress via Hog1p
orf19.220	PIR1	1.52	Verified ORF||Structural protein of cell wall; 1,3-beta-glucan-linked; O-glycosylated by Pmt1p; N-mannosylated; tandem repeats; heterozygous mutant has cell wall defects; hyphal repressed; Hog1p, fluconazole, hypoxia induced; iron, Efg1p, Plc1p regulated
orf19.4035	PGA4	1.52	Verified ORF||GPI-anchored cell surface protein, similar to S. cerevisiae Gas1p; fungal-specific (no human or murine homolog); transcription is upregulated in RHE model of oral candidiasis
orf19.3656	COX15	1.52	Verified ORF||Cytochrome oxidase assembly protein, Transcription is regulated by Nrg1p and Tup1p; alkaline downregulated
orf19.6706	GYP7	1.52	Uncharacterized ORF||Predicted ORF in Assemblies 19, 20 and 21; similar to S. cerevisiae Gyp7p (GTPase-activating protein for Ypt1p); caspofungin-induced
orf19.5626	orf19.5626	1.52	Uncharacterized ORF||Predicted ORF in Assemblies 19, 20 and 21; Plc1p-regulated; transcriptionally activated by Mnl1p under weak acid stress
orf19.4773	AOX2	1.52	Verified ORF||Alternative oxidase; induced by antimycin A, some oxidants; growth- and carbon-source-regulated; one of two isoforms (Aox1p and Aox2p); involved in cyanide-resistant respiratory pathway that is absent from S. cerevisiae
orf19.3355	ISN1	1.51	Uncharacterized ORF||Putative inosine 5'-monophosphate 5'-nucleotidase; fungal-specific (no human or murine homolog)

orf19.173	orf19.173	1.51	Verified ORF||Putative transcription factor with zinc finger DNA-binding motif; transcriptionally activated by Mnl1p under weak acid stress
orf19.6608	orf19.6608	1.51	Uncharacterized ORF||Predicted ORF in Assemblies 19, 20 and 21; downregulation correlates with clinical development of fluconazole resistance
orf19.3822	SCS7	1.51	Verified ORF||Protein described as ceramide hydroxylase; transcription is regulated by Nrg1p; transcriptionally regulated by iron; expression greater in high iron; fluconazole-induced
orf19.4055	orf19.4055	1.51	Verified ORF||Protein similar to S. cerevisiae Ybr075wp; transposon mutation affects filamentous growth; clade-associated gene expression
orf19.1800	orf19.1800	1.51	Uncharacterized ORF||Predicted ORF in Assemblies 19, 20 and 21; Ortholog of S. cerevisiae YPR157W
orf19.79	orf19.79	1.51	Predicted ORF from Assembly 19; removed from Assembly 20
orf19.5640	PEX5	1.51	Verified ORF||Protein of the Pex5p family; required for PTS1-mediated peroxisomal protein import, fatty acid beta-oxidation; similar to S. cerevisiae Pas10p peroxisomal targeting receptor; macrophage/pseudohyphal-repressed
orf19.7247	RIM101	1.51	Verified ORF||Transcription factor involved in alkaline pH response; required for alkaline-induced hyphal growth; role in virulence in mouse systemic infection; activated by C-terminal proteolytic cleavage; mediates both positive and negative regulation
orf19.871	orf19.871	1.51	Uncharacterized ORF||Predicted ORF in Assemblies 19, 20 and 21; S. cerevisiae ortholog LST4 has protein transporter activity, has role in Golgi to plasma membrane transport, intracellular protein transport and localizes to vesicle coat
orf19.1220	RVS167	1.51	Verified ORF||Protein involved in endocytosis; contains a BAR domain; null mutant exhibits defects in hyphal growth, virulence, cell wall integrity, and actin patch localization; cosediments with phosphorylated Myo5p
orf19.6763	SLK19	1.51	Verified ORF||Alkaline-induced protein of plasma membrane; affects cell aggregation, cell wall; similar to S. cerevisiae Slk19p (a kinetochore protein with roles in mitosis, meiosis); required for wild-type virulence in mouse; macrophage-downregulated
orf19.882	HSP78	1.51	Uncharacterized ORF||Protein described as a heat-shock protein; transcriptionally regulated by macrophage response; transcription is regulated by Nrg1p, Mig1p, Gcn2p, Gcn4p, Mnl1p; heavy metal (cadmium) stress-induced
orf19.988	orf19.988	1.50	Uncharacterized ORF||Predicted ORF in Assemblies 19, 20 and 21; fungal-specific (no human or murine homolog); transcription is upregulated in clinical isolates from HIV+ patients with oral candidiasis; possibly transcriptionally regulated upon hyphal formation
orf19.6117	orf19.6117	1.50	Uncharacterized ORF||Predicted ORF in Assemblies 19, 20 and 21; ketoconazole and hypoxia induced
orf19.6338	orf19.6338	1.50	Dubious ORF||Predicted ORF in Assemblies 19, 20 and 21
orf19.4555	ALS4	1.50	Verified ORF||ALS family protein; role in adhesion and wild-type germ tube induction; growth and temperature regulated; expressed during infection of human buccal epithelial cells; down-regulated upon vaginal contact; putative GPI-anchored
orf19.980	orf19.980	1.50	Uncharacterized ORF||Predicted ORF in Assemblies 19, 20 and 21
orf19.1267	orf19.1267	1.50	Uncharacterized ORF||Predicted ORF in Assemblies 19, 20 and 21; Ortholog of S. cerevisiae CAJ1
orf19.5730	orf19.5730	1.50	Uncharacterized ORF||Predicted ORF in Assemblies 19, 20 and 21; clade-associated gene expression
orf19.3325	orf19.3325	1.50	Uncharacterized ORF||Protein described as glycogen synthesis initiator; regulated by Efg1p and Efh1p; Hog1p-downregulated; shows colony morphology-related gene regulation by Ssn6p; increased expression in response to prostaglandins
orf19.5813	orf19.5813	1.50	Uncharacterized ORF||Predicted ORF in Assemblies 19, 20 and 21; expression upregulated during growth in the mouse cecum

SUPPLEMENTARY TABLE III.3B_GO ANALYSIS FOR Cas5p BINDING HITS

GO term	Cluster Frequency	Background Frequency	adj. p-value	Gene(s) annotated to the term
Process				
pyruvate metabolic process	16 out of 230 genes, 7.0%	26 out of 6473 background genes, 0.4%	1.25E-14	ADH2:ENO1:GPM1:NDE1:TDH3:TPI1:PDC11:PFK1:ADH1:PGK1:MAE1:PFK2:HXK2:PGI1:GLK1:CDG1
single-organism carbohydrate catabolic process	21 out of 230 genes, 9.1%	53 out of 6473 background genes, 0.8%	1.44E-14	GAL1:GAL10:GAL7:ADH2:ENO1:GPM1:NDE1:C3_06860C_A:TDH3:TPI1:XKS1:PDC11:PFK1:ADH1:ARD:PGK1:GPH1:PFK2:HXK2:PGI1:GLK1
carbohydrate catabolic process	21 out of 230 genes, 9.1%	55 out of 6473 background genes, 0.8%	3.58E-14	GAL1:GAL10:GAL7:ADH2:ENO1:GPM1:NDE1:C3_06860C_A:TDH3:TPI1:XKS1:PDC11:PFK1:ADH1:ARD:PGK1:GPH1:PFK2:HXK2:PGI1:GLK1
monosaccharide metabolic process	18 out of 230 genes, 7.8%	40 out of 6473 background genes, 0.6%	2E-13	GAL1:GAL10:GAL7:ADH2:ENO1:GPM1:GAL4:NDE1:C3_06860C_A:XKS1:PDC11:ARD:PGK1:PCK1:MDH1:HXK2:PGI1:GLK1
oxidoreduction coenzyme metabolic process	20 out of 230 genes, 8.7%	70 out of 6473 background genes, 1.1%	1.27E-10	ABC1:C1_07840W_A:ADH2:ENO1:GND1:GPM1:C2_08100W_A:NDE1:TDH3:TPI1:PDC11:GUT2:PFK1:ADH1:PGK1:C6_03620C_A:PFK2:HXK2:PGI1:GLK1
hexose metabolic process	15 out of 230 genes, 6.5%	35 out of 6473 background genes, 0.5%	1.68E-10	GAL1:GAL10:GAL7:ADH2:ENO1:GPM1:GAL4:NDE1:PDC11:PGK1:PCK1:MDH1:HXK2:PGI1:GLK1
nicotinamide nucleotide metabolic process	18 out of 230 genes, 7.8%	56 out of 6473 background genes, 0.9%	2.26E-10	C1_07840W_A:ADH2:ENO1:GND1:GPM1:C2_08100W_A:NDE1:TDH3:TPI1:PDC11:GUT2:PFK1:ADH1:PGK1:PFK2:HXK2:PGI1:GLK1
glycolytic process	11 out of 230 genes, 4.8%	16 out of 6473 background genes, 0.2%	2.83E-10	ENO1:GPM1:TDH3:TPI1:PFK1:ADH1:PGK1:PFK2:HXK2:PGI1:GLK1
pyridine nucleotide metabolic process	18 out of 230 genes, 7.8%	57 out of 6473 background genes, 0.9%	3.21E-10	C1_07840W_A:ADH2:ENO1:GND1:GPM1:C2_08100W_A:NDE1:TDH3:TPI1:PDC11:GUT2:PFK1:ADH1:PGK1:PFK2:HXK2:PGI1:GLK1
pyridine-containing compound metabolic process	19 out of 230 genes, 8.3%	65 out of 6473 background genes, 1.0%	3.36E-10	ISN1:C1_07840W_A:ADH2:ENO1:GND1:GPM1:C2_08100W_A:NDE1:TDH3:TPI1:PDC11:GUT2:PFK1:ADH1:PGK1:PFK2:HXK2:PGI1:GLK1

single-organism carbohydrate metabolic process	32 out of 230 genes, 13.9%	204 out of 6473 background genes, 3.2%	4.84E-10	C1_01360C_A:GAL1:GAL10:GAL7:TPS2:RHD1:ADH2:ENO1:GPM1:HSP21:GAL4:NDE1:C3_06860C_A:TDH3:TPI1:XKS1:PDC11:GUT2:PFK1:ADH1:PGA4:ARD:PGK1:GPH1:PFK2:PCK1:MDH1:GSY1:HXK2:PGI1:GLK1:HSP104
oxidation-reduction process	44 out of 230 genes, 19.1%	408 out of 6473 background genes, 6.3%	1.13E-08	C1_01360C_A:ABC1:ADH2:OLE1:AOX2:AOX1:C1_10840C_A:RIB3:OSM2:SOD5:OSM1:GDH2:C2_08100W_A:UCF1:C2_10070W_A:NDE1:HEM13:C3_06860C_A:TDH3:PEX5:ERG251:SCS7:PDC11:GUT2:C5_03770C_A:ADH1:COX15:GPX2:C6_00850W_A:MAE1:C6_03620C_A:GPH1:MDH1:GSY1:ADH5:FDH1:IFE2:GLK1:CR_07780W_A:YHB1:CDG1:ALO1:FDH3:XYL2
monocarboxylic acid metabolic process	24 out of 230 genes, 10.4%	133 out of 6473 background genes, 2.1%	2.27E-08	EHT1:ADH2:OLE1:ENO1:GPM1:NDE1:TDH3:TPI1:PEX5:ERG251:SCS7:PDC11:ACH1:PFK1:ADH1:PGK1:MAE1:C6_03620C_A:PFK2:HXK2:FDH1:PGI1:GLK1:CDG1
carbohydrate metabolic process	33 out of 230 genes, 14.3%	251 out of 6473 background genes, 3.9%	3.07E-08	C1_01360C_A:GAL1:GAL10:GAL7:TPS2:RHD1:ADH2:ENO1:GPM1:HSP21:GAL4:NDE1:C3_06860C_A:TDH3:TPI1:XKS1:PDC11:GUT2:PFK1:ADH1:PGA4:ARD:PGK1:GPH1:PFK2:PCK1:MDH1:GSY1:HXK2:PGI1:GLK1:GLK4:HSP104
generation of precursor metabolites and energy	23 out of 230 genes, 10.0%	133 out of 6473 background genes, 2.1%	0.000000148	C1_01360C_A:ADH2:ENO1:AOX2:AOX1:RIB3:GPM1:UCF1:NDE1:TDH3:TPI1:PDC11:PFK1:ADH1:COX15:PGK1:GPH1:PFK2:MDH1:GSY1:HXK2:PGI1:GLK1
glucose metabolic process	10 out of 230 genes, 4.3%	19 out of 6473 background genes, 0.3%	0.000000155	ADH2:ENO1:GPM1:NDE1:PDC11:PGK1:PCK1:MDH1:HXK2:PGI1
monosaccharide catabolic process	9 out of 230 genes, 3.9%	15 out of 6473 background genes, 0.2%	0.000000271	GAL1:GAL10:GAL7:ADH2:NDE1:C3_06860C_A:XKS1:PDC11:ARD

single-organism process	159 out of 230 genes, 69.1%	3192 out of 6473 background genes, 49.3%	0.000000393	C1_01360C_A:ABC1:ISN1:HOL4:HGT1:HGT2:SHA3:GAL1:GAL10:GAL7:TPS2:EHT1:TUS1:RHD1:C1_07220W_A:RME1:KSP1:C1_07840W_A:CDR4:ADH2:C1_08340C_A:OLE1:SDS24:ENO1:CTR2:TPO3:MSN4:AOX2:AOX1:C1_09210C_A:CRP1:C1_09780C_A:C1_10360C_A:GLY1:C1_10840C_A:GAD1:RIB3:TYE7:ROB1:OSM2:C1_13840W_A:GND1:RIM101:SOD5:C2_00740C_A:UBP13:HGT7:HGT8:HGT6:REG1:ZRT2:STP4:GPM1:C2_03500W_A:ADAEC:HSP21:C2_04850C_A:OSM1:SMF12:GDH2:C2_08100W_A:MAF1:UCF1:C2_09590C_A:C2_09710C_A:C2_10070W_A:ZSF1:GAL4:IRO1:NDE1:PEP8:HEM13:TEC1:CDR2:NCE102:CDR1:FCR1:C3_06860C_A:TDH3:UBI4:TPI1:PEX5:PTC8:C4_01300W_A:ERG251:AHP1:C4_02570C_A:MSN5:VTC4:SCS7:XKS1:YME1:PDC11:CBF1:GUT2:C5_00180W_A:GPR1:HAL9:ACH1:MIG1:BUB3:C5_03770C_A:CUP1:PFK1:ADH1:PGA4:MUM2:C5_05510C_A:ARD:CPH2:GNP1:COX15:PGK1:CAN3:GPX2:C6_00850W_A:MAE1:ATG15:C6_01780C_A:MIF2:C6_03620C_A:ALS1:RVS167:ALS4:RVS161:GPH1:PFK2:CUP9:NRG1:PCK1:LEU1:MDH1:GSY1:CR_01430W_A:OPT1:ADH5:CR_03730C_A:QDR1:HXK2:CRG1:FDH1:IFE2:PST3:SRR1:MHP1:PGI1:GLK1:CR_07480W_A:CR_07780W_A:YHB1:EFG1:HSP104:ARF1:CDG1:CR_09340W_A:ALO1:DEF1:FDH3:XYL2
cofactor metabolic process	23 out of 230 genes, 10.0%	154 out of 6473 background genes, 2.4%	0.00000298	ABC1:C1_07840W_A:ADH2:ENO1:GND1:GPM1:C2_08100W_A:NDE1:HEM13:TDH3:TPI1:PDC11:GUT2:ACH1:PFK1:ADH1:COX15:PGK1:C6_03620C_A:PFK2:HXK2:PGI1:GLK1
coenzyme metabolic process	21 out of 230 genes, 9.1%	132 out of 6473 background genes, 2.0%	0.00000465	ABC1:C1_07840W_A:ADH2:ENO1:GND1:GPM1:C2_08100W_A:NDE1:TDH3:TPI1:PDC11:GUT2:ACH1:PFK1:ADH1:PGK1:C6_03620C_A:PFK2:HXK2:PGI1:GLK1
response to oxidative stress	21 out of 230 genes, 9.1%	136 out of 6473 background genes, 2.1%	0.00000808	GAL10:TPS2:OLE1:MSN4:GAD1:GND1:SOD5:HSP21:C2_08100W_A:CMK1:CDR2:CDR1:C3_06860C_A:AHP1:GPX2:C6_00850W_A:SRR1:YHB1:HSP104:ALO1:FDH3
response to chemical	55 out of 230 genes, 23.9%	717 out of 6473 background genes, 11.1%	0.0000121	HOL4:HGT1:SHA3:GAL1:GAL10:TPS2:PHO15:KSP1:CDR4:OLE1:TPO3:MSN4:DAK2:C1_09210C_A:GAD1:TYE7:OSM2:GND1:RIM101:SOD5:UBP13:HGT7:C2_02920W_A:HSP21:YTH1:C2_08100W_A:GAL4:HEM13:TEC1:CMK1:CDR2:CDR1:FCR1:C3_06860C_A:AHP1:CBF1:GPR1:ACH1:MIG1:SUT1:PGA4:CPH2:C6_00850W_A:C7_01430C_A:NRG1:OPT1:CR_02510W_A:QDR1:HXK2:YHB1:EFG1:HSP104:CR_09340W_A:ALO1:FDH3

single-organism catabolic process	31 out of 230 genes, 13.5%	289 out of 6473 background genes, 4.5%	0.0000199	GAL1:GAL10:GAL7:EHT1:ADH2:ENO1:GAD1:GPM1:NDE1:C3_06860C_A:TDH3:TPI1:PEX5:VTC4:XKS1:PDC11:PFK1:ADH1:ARD:PGK1:ATG15:C6_03620C_A:GPH1:PFK2:HXK2:FDH1:PGI1:GLK1:CDG1:CR_09340W_A:FDH3
response to stimulus	83 out of 230 genes, 36.1%	1368 out of 6473 background genes, 21.1%	0.0000659	HOL4:HGT1:SHA3:GAL1:GAL10:TPS2:TUS1:PHO15:KSP1:CDR4:OLE1:ENO1:TPO3:MSN4:DAK2:C1_09210C_A:GAD1:TYE7:ROB1:OSM2:GND1:RIM101:SOD5:UBP13:HGT7:REG1:ZRT2:C2_02920W_A:HSP78:ADAEC:HSP21:YTH1:C2_08100W_A:PIR1:GAL4:SAP9:PEP8:HEM13:TEC1:CMK1:CDR2:CDR1:FCR1:C3_06860C_A:TDH3:UBI4:SLK19:TPI1:PTC8:AHP1:CBF1:GPR1:HAL9:ACH1:MIG1:SUT1:ADH1:PGA4:C5_05510C_A:CPH2:PGK1:GPX2:C6_00850W_A:ALS1:RVS167:ALS4:RVS161:GPH1:C7_01430C_A:NRG1:OPT1:CR_02510W_A:QDR1:HXK2:SRR1:MHP1:YHB1:EFG1:HSP104:ARF1:CR_09340W_A:ALO1:FDH3
response to host defenses	11 out of 230 genes, 4.8%	41 out of 6473 background genes, 0.6%	0.0000933	ENO1:RIM101:SOD5:SAP9:TDH3:TPI1:ADH1:PGK1:ALS1:YHB1:EFG1
response to host	11 out of 230 genes, 4.8%	41 out of 6473 background genes, 0.6%	0.0000933	ENO1:RIM101:SOD5:SAP9:TDH3:TPI1:ADH1:PGK1:ALS1:YHB1:EFG1
cellular response to chemical stimulus	46 out of 230 genes, 20.0%	584 out of 6473 background genes, 9.0%	0.00011	HGT1:GAL1:GAL10:TPS2:PHO15:KSP1:OLE1:TPO3:MSN4:DAK2:GAD1:TYE7:OSM2:GND1:RIM101:SOD5:UBP13:HGT7:C2_02920W_A:HSP21:GAL4:HEM13:TEC1:CMK1:CDR2:CDR1:FCR1:C3_06860C_A:AHP1:CBF1:GPR1:MIG1:SUT1:PGA4:CPH2:C6_00850W_A:C7_01430C_A:NRG1:OPT1:CR_02510W_A:HXK2:YHB1:EFG1:HSP104:ALO1:FDH3
gluconeogenesis	6 out of 230 genes, 2.6%	9 out of 6473 background genes, 0.1%	0.00012	ENO1:GPM1:PGK1:PCK1:MDH1:PGI1
cellular response to oxidative stress	18 out of 230 genes, 7.8%	121 out of 6473 background genes, 1.9%	0.00017	GAL10:TPS2:OLE1:MSN4:GAD1:GND1:SOD5:HSP21:CMK1:CDR2:CDR1:C3_06860C_A:AHP1:C6_00850W_A:YHB1:HSP104:ALO1:FDH3
regulation of defense response	9 out of 230 genes, 3.9%	27 out of 6473 background genes, 0.4%	0.00017	HGT1:ENO1:RIM101:SAP9:TDH3:TPI1:ADH1:PGK1:ALS1
response to external biotic stimulus	11 out of 230 genes, 4.8%	44 out of 6473 background genes, 0.7%	0.0002	ENO1:RIM101:SOD5:SAP9:TDH3:TPI1:ADH1:PGK1:ALS1:YHB1:EFG1

response to other organism	11 out of 230 genes, 4.8%	44 out of 6473 background genes, 0.7%	0.0002	ENO1:RIM101:SOD5:SAP9:TDH3:TPI1:ADH1:PGK1:ALS1:YHB1:EFG1
response to defenses of other organism involved in symbiotic interaction	11 out of 230 genes, 4.8%	44 out of 6473 background genes, 0.7%	0.0002	ENO1:RIM101:SOD5:SAP9:TDH3:TPI1:ADH1:PGK1:ALS1:YHB1:EFG1
symbiosis, encompassing mutualism through parasitism	18 out of 230 genes, 7.8%	125 out of 6473 background genes, 1.9%	0.00028	ENO1:RIM101:SOD5:GPM1:ZCF1:SAP9:TEC1:TDH3:TPI1:ADH1:CPH2:PGK1:ALS1:ALS4:NRG1:YHB1:EFG1:DEF1
hexose biosynthetic process	6 out of 230 genes, 2.6%	10 out of 6473 background genes, 0.2%	0.00029	ENO1:GPM1:PGK1:PCK1:MDH1:PGI1
monosaccharide biosynthetic process	6 out of 230 genes, 2.6%	10 out of 6473 background genes, 0.2%	0.00029	ENO1:GPM1:PGK1:PCK1:MDH1:PGI1
response to external stimulus	35 out of 230 genes, 15.2%	398 out of 6473 background genes, 6.1%	0.00035	SHA3:GAL1:GAL10:TPS2:OLE1:ENO1:MSN4:TYE7:RIM101:SOD5:UBP13:REG1:ZRT2:GAL4:SAP9:PEP8:FCR1:TDH3:TPI1:PTC8:CBF1:GPR1:MIG1:ADH1:C5_05510C_A:PGK1:ALS1:RVS161:NRG1:HXK2:SRR1:MHP1:YHB1:EFG1:ALO1
interspecies interaction between organisms	18 out of 230 genes, 7.8%	127 out of 6473 background genes, 2.0%	0.00036	ENO1:RIM101:SOD5:GPM1:ZCF1:SAP9:TEC1:TDH3:TPI1:ADH1:CPH2:PGK1:ALS1:ALS4:NRG1:YHB1:EFG1:DEF1
oxoacid metabolic process	32 out of 230 genes, 13.9%	350 out of 6473 background genes, 5.4%	0.00049	EHT1:ADH2:OLE1:ENO1:GLY1:GAD1:GPM1:GDH2:NDE1:TDH3:TPI1:PEX5:ERG251:VTC4:SCS7:PDC11:CBF1:ACH1:PFK1:ADH1:PGK1:MAE1:C6_03620C_A:PFK2:LEU1:MDH1:HXK2:FDH1:PGI1:GLK1:CDG1:FDH3
organic acid metabolic process	32 out of 230 genes, 13.9%	351 out of 6473 background genes, 5.4%	0.00052	EHT1:ADH2:OLE1:ENO1:GLY1:GAD1:GPM1:GDH2:NDE1:TDH3:TPI1:PEX5:ERG251:VTC4:SCS7:PDC11:CBF1:ACH1:PFK1:ADH1:PGK1:MAE1:C6_03620C_A:PFK2:LEU1:MDH1:HXK2:FDH1:PGI1:GLK1:CDG1:FDH3
response to oxygen-containing compound	14 out of 230 genes, 6.1%	80 out of 6473 background genes, 1.2%	0.00054	SHA3:OLE1:MSN4:SOD5:C2_08100W_A:CBF1:GPR1:ACH1:MIG1:C6_00850W_A:NRG1:CR_02510W_A:EFG1:HSP104
hexose catabolic process	6 out of 230 genes, 2.6%	11 out of 6473 background genes, 0.2%	0.00063	GAL1:GAL10:GAL7:ADH2:NDE1:PDC11

monosaccharide transport	9 out of 230 genes, 3.9%	31 out of 6473 background genes, 0.5%	0.00066	HGT1:HGT2:SHA3:GAL1:HGT7:HGT8:HGT6:HXK2:GLK1
hexose transport	9 out of 230 genes, 3.9%	31 out of 6473 background genes, 0.5%	0.00066	HGT1:HGT2:SHA3:GAL1:HGT7:HGT8:HGT6:HXK2:GLK1
interaction with host	12 out of 230 genes, 5.2%	60 out of 6473 background genes, 0.9%	0.00079	ENO1:RIM101:SOD5:GPM1:SAP9:TDH3:TPI1:ADH1:PGK1:ALS1:YHB1:EFG1
carboxylic acid metabolic process	31 out of 230 genes, 13.5%	340 out of 6473 background genes, 5.3%	0.0008	EHT1:ADH2:OLE1:ENO1:GLY1:GAD1:GPM1:GDH2:NDE1:TDH3:TPI1:PEX5:ERG251:SCS7:PDC11:CBF1:ACH1:PFK1:ADH1:PGK1:MAE1:C6_03620C_A:PFK2:LEU1:MDH1:HXK2:FDH1:PGI1:GLK1:CDG1:FDH3
nucleotide metabolic process	20 out of 230 genes, 8.7%	164 out of 6473 background genes, 2.5%	0.00097	ISN1:GAL7:C1_07840W_A:ADH2:ENO1:GND1:GPM1:C2_08100W_A:NDE1:TDH3:TPI1:PDC11:GUT2:PFK1:ADH1:PGK1:PFK2:HXK2:PGI1:GLK1
glucose transport	8 out of 230 genes, 3.5%	25 out of 6473 background genes, 0.4%	0.00121	HGT1:HGT2:SHA3:HGT7:HGT8:HGT6:HXK2:GLK1
purine nucleoside monophosphate metabolic process	14 out of 230 genes, 6.1%	87 out of 6473 background genes, 1.3%	0.00156	ADH2:ENO1:GPM1:NDE1:TDH3:TPI1:PDC11:PFK1:ADH1:PGK1:PFK2:HXK2:PGI1:GLK1
purine ribonucleoside monophosphate metabolic process	14 out of 230 genes, 6.1%	87 out of 6473 background genes, 1.3%	0.00156	ADH2:ENO1:GPM1:NDE1:TDH3:TPI1:PDC11:PFK1:ADH1:PGK1:PFK2:HXK2:PGI1:GLK1
nucleoside phosphate metabolic process	20 out of 230 genes, 8.7%	169 out of 6473 background genes, 2.6%	0.00157	ISN1:GAL7:C1_07840W_A:ADH2:ENO1:GND1:GPM1:C2_08100W_A:NDE1:TDH3:TPI1:PDC11:GUT2:PFK1:ADH1:PGK1:PFK2:HXK2:PGI1:GLK1
modulation by symbiont of host defense response	8 out of 230 genes, 3.5%	26 out of 6473 background genes, 0.4%	0.0017	ENO1:RIM101:SAP9:TDH3:TPI1:ADH1:PGK1:ALS1
modulation by organism of defense response of other organism involved in symbiotic interaction	8 out of 230 genes, 3.5%	26 out of 6473 background genes, 0.4%	0.0017	ENO1:RIM101:SAP9:TDH3:TPI1:ADH1:PGK1:ALS1

ribonucleoside monophosphate metabolic process	14 out of 230 genes, 6.1%	90 out of 6473 background genes, 1.4%	0.00237	ADH2:ENO1:GPM1:NDE1:TDH3:TPI1:PDC11:PFK1:ADH1:PGK1:PFK2:HXK2:PGI1:GLK1
single-organism cellular process	130 out of 230 genes, 56.5%	2699 out of 6473 background genes, 41.7%	0.0024	C1_01360C_A:ABC1:ISN1:HOL4:HGT1:HGT2:SHA3:GAL1:GAL10:GAL7:TPS2:EHT1:TUS1:RHD1:RME1:KSP1:C1_07840W_A:ADH2:C1_08340C_A:OLE1:SDS24:ENO1:CTR2:TPO3:MSN4:AOX2:AOX1:C1_09210C_A:CRP1:C1_09780C_A:C1_10360C_A:GLY1:GAD1:RIB3:TYE7:C1_13840W_A:GND1:RIM101:C2_00740C_A:UBP13:HGT7:HGT8:HGT6:REG1:ZRT2:GPM1:ADAEC:HSP21:C2_04850C_A:SMF12:GDH2:C2_08100W_A:MAF1:UCF1:C2_09590C_A:C2_09710C_A:ZSF1:GAL4:IRO1:NDE1:PEP8:HEM13:TEC1:CDR2:NCE102:CDR1:FCR1:TDH3:UBI4:TPI1:PEX5:PTC8:C4_01300W_A:ERG251:AHP1:C4_02570C_A:VTC4:SCS7:YME1:PDC11:CBF1:GUT2:C5_00180W_A:GPR1:ACH1:MIG1:BUB3:CUP1:PFK1:ADH1:PGA4:MUM2:C5_05510C_A:ARD:CPH2:GNP1:COX15:PGK1:CAN3:MAE1:ATG15:MIF2:C6_03620C_A:RVS161:GPH1:PFK2:NRG1:LEU1:MDH1:GSY1:CR_01430W_A:OPT1:CR_03730C_A:QDR1:HXK2:CRG1:FDH1:PST3:SRR1:MHP1:PGI1:GLK1:CR_07480W_A:EFG1:HSP104:ARF1:CDG1:CR_09340W_A:ALO1:FDH3
purine nucleoside metabolic process	15 out of 230 genes, 6.5%	103 out of 6473 background genes, 1.6%	0.00244	ISN1:ADH2:ENO1:GPM1:NDE1:TDH3:TPI1:PDC11:PFK1:ADH1:PGK1:PFK2:HXK2:PGI1:GLK1
purine ribonucleoside metabolic process	15 out of 230 genes, 6.5%	103 out of 6473 background genes, 1.6%	0.00244	ISN1:ADH2:ENO1:GPM1:NDE1:TDH3:TPI1:PDC11:PFK1:ADH1:PGK1:PFK2:HXK2:PGI1:GLK1
positive regulation of defense response	7 out of 230 genes, 3.0%	20 out of 6473 background genes, 0.3%	0.00287	ENO1:RIM101:TDH3:TPI1:ADH1:PGK1:ALS1
induction by symbiont of host defense response	7 out of 230 genes, 3.0%	20 out of 6473 background genes, 0.3%	0.00287	ENO1:RIM101:TDH3:TPI1:ADH1:PGK1:ALS1
induction by organism of defense response of other organism involved in symbiotic interaction	7 out of 230 genes, 3.0%	20 out of 6473 background genes, 0.3%	0.00287	ENO1:RIM101:TDH3:TPI1:ADH1:PGK1:ALS1
positive regulation by symbiont of host defense response	7 out of 230 genes, 3.0%	20 out of 6473 background genes, 0.3%	0.00287	ENO1:RIM101:TDH3:TPI1:ADH1:PGK1:ALS1

positive regulation by organism of defense response of other organism involved in symbiotic interaction	7 out of 230 genes, 3.0%	20 out of 6473 background genes, 0.3%	0.00287	ENO1:RIM101:TDH3:TPI1:ADH1:PGK1:ALS1
nucleoside monophosphate metabolic process	14 out of 230 genes, 6.1%	92 out of 6473 background genes, 1.4%	0.0031	ADH2:ENO1:GPM1:NDE1:TDH3:TPI1:PDC11:PFK1:ADH1:PGK1:PFK2:HXK2:PGI1:GLK1
modification of morphology or physiology of other organism	8 out of 230 genes, 3.5%	28 out of 6473 background genes, 0.4%	0.00318	ENO1:RIM101:SAP9:TDH3:TPI1:ADH1:PGK1:ALS1
modification by symbiont of host morphology or physiology	8 out of 230 genes, 3.5%	28 out of 6473 background genes, 0.4%	0.00318	ENO1:RIM101:SAP9:TDH3:TPI1:ADH1:PGK1:ALS1
modification of morphology or physiology of other organism involved in symbiotic interaction	8 out of 230 genes, 3.5%	28 out of 6473 background genes, 0.4%	0.00318	ENO1:RIM101:SAP9:TDH3:TPI1:ADH1:PGK1:ALS1
carbohydrate transport	9 out of 230 genes, 3.9%	37 out of 6473 background genes, 0.6%	0.00339	HGT1:HGT2:SHA3:GAL1:HGT7:HGT8:HGT6:HXK2:GLK1
response to biotic stimulus	27 out of 230 genes, 11.7%	295 out of 6473 background genes, 4.6%	0.00401	SHA3:OLE1:ENO1:ROB1:RIM101:SOD5:SAP9:PEP8:TEC1:FCR1:TDH3:TPI1:PTC8:GPR1:HAL9:ADH1:C5_05510C_A:CPH2:PGK1:ALS1:RVS167:RVS161:NRG1:SRR1:MHP1:YHB1:EFG1
NADH metabolic process	5 out of 230 genes, 2.2%	9 out of 6473 background genes, 0.1%	0.00512	ADH2:C2_08100W_A:NDE1:PDC11:GUT2
purine ribonucleotide metabolic process	14 out of 230 genes, 6.1%	96 out of 6473 background genes, 1.5%	0.00519	ADH2:ENO1:GPM1:NDE1:TDH3:TPI1:PDC11:PFK1:ADH1:PGK1:PFK2:HXK2:PGI1:GLK1
multi-organism process	40 out of 230 genes, 17.4%	546 out of 6473 background genes, 8.4%	0.00542	TPS2:OLE1:ENO1:TYE7:ROB1:RIM101:SOD5:GPM1:HSP21:IRO1:ZCF1:SAP9:PEP8:TEC1:NCE102:TDH3:UBI4:SLK19:TPI1:RHD3:ADH1:PGA4:CPH2:PGK1:ALS1:RVS167:ALS4:RVS161:NRG1:OPT1:ADH5:QDR1:CRG1:SRR1:YHB1:EFG1:HSP104:ALO1:DEF1:FDH3
ribonucleoside metabolic process	15 out of 230 genes, 6.5%	110 out of 6473 background genes, 1.7%	0.00564	ISN1:ADH2:ENO1:GPM1:NDE1:TDH3:TPI1:PDC11:PFK1:ADH1:PGK1:PFK2:HXK2:PGI1:GLK1

purine nucleotide metabolic process	14 out of 230 genes, 6.1%	97 out of 6473 background genes, 1.5%	0.00588	ADH2:ENO1:GPM1:NDE1:TDH3:TPI1:PDC11:PFK1:ADH1:PGK1:PFK2:HXK2:PGI1:GLK1
small molecule metabolic process	44 out of 230 genes, 19.1%	631 out of 6473 background genes, 9.7%	0.0063	ABC1:ISN1:GAL7:EHT1:C1_07840W_A:ADH2:OLE1:ENO1:GLY1:GAD1:RIB3:GND1:C2_00740C_A:GPM1:GDH2:C2_08100W_A:NDE1:TDH3:TPI1:PEX5:ERG251:VTC4:SCS7:PDC11:CBF1:GUT2:C5_00180W_A:ACH1:PFK1:ADH1:ARD:PGK1:MAE1:C6_03620C_A:PFK2:LEU1:MDH1:HXK2:FDH1:PGI1:GLK1:CDG1:ALO1:FDH3
glycolytic fermentation	4 out of 230 genes, 1.7%	5 out of 6473 background genes, 0.1%	0.00636	ADH2:NDE1:PDC11:GLK1
ethanol metabolic process	4 out of 230 genes, 1.7%	5 out of 6473 background genes, 0.1%	0.00636	ADH2:NDE1:PDC11:FDH3
response to abiotic stimulus	26 out of 230 genes, 11.3%	287 out of 6473 background genes, 4.4%	0.00735	HGT1:TPS2:OLE1:MSN4:TYE7:OSM2:RIM101:HSP78:HSP21:PIR1:HEM13:UBI4:SLK19:PTC8:GPR1:ACH1:PGA4:CPH2:ALS1:ALS4:RVS161:GPH1:NRG1:SRR1:EFG1:HSP104
ribonucleotide metabolic process	14 out of 230 genes, 6.1%	100 out of 6473 background genes, 1.5%	0.00845	ADH2:ENO1:GPM1:NDE1:TDH3:TPI1:PDC11:PFK1:ADH1:PGK1:PFK2:HXK2:PGI1:GLK1
regulation of response to stress	16 out of 230 genes, 7.0%	129 out of 6473 background genes, 2.0%	0.00961	HGT1:KSP1:ENO1:RIM101:SAP9:TDH3:TPI1:GPR1:MIG1:SUT1:ADH1:PGK1:ALS1:NRG1:SRR1:EFG1
ribose phosphate metabolic process	15 out of 230 genes, 6.5%	115 out of 6473 background genes, 1.8%	0.00982	ADH2:ENO1:GND1:GPM1:NDE1:TDH3:TPI1:PDC11:PFK1:ADH1:PGK1:PFK2:HXK2:PGI1:GLK1
nucleoside metabolic process	15 out of 230 genes, 6.5%	118 out of 6473 background genes, 1.8%	0.01347	ISN1:ADH2:ENO1:GPM1:NDE1:TDH3:TPI1:PDC11:PFK1:ADH1:PGK1:PFK2:HXK2:PGI1:GLK1
organic substance catabolic process	37 out of 230 genes, 16.1%	508 out of 6473 background genes, 7.8%	0.01456	UBC8:GAL1:GAL10:GAL7:EHT1:PHO15:ADH2:ENO1:GAD1:UBP13:REG1:GPM1:PRB1:ZSF1:NDE1:SAP9:C3_06860C_A:TDH3:TPI1:PEX5:XKS1:YME1:PDC11:PFK1:ADH1:ARD:PGK1:C6_03620C_A:GPH1:PFK2:HXK2:FDH1:PGI1:GLK1:CDG1:CR_09340W_A:FDH3

Function

oxidoreductase activity	41 out of 230 genes, 17.8%	422 out of 6473 background genes, 6.5%	3.71E-07	FMA1:ADH2:OLE1:AOX2:AOX1:C1_09780C_A:C1_10840C_A:OSM2:GND1:SOD5:OSM1:GDH2:C2_08100W_A:C2_10070W_A:NDE1:HEM13:C3_06860C_A:TDH3:ERG251:AHP1:C4_02570C_A:SCS7:GUT2:C5_03770C_A:ADH1:ARD:COX15:GPX2:C6_00850W_A:MAE1:C6_03620C_A:MDH1:ADH5:FDH1:IFE2:CR_07780W_A:YHB1:CDG1:ALO1:FDH3:XYL2
oxidoreductase activity, acting on CH-OH group of donors	14 out of 230 genes, 6.1%	71 out of 6473 background genes, 1.1%	2.65E-05	ADH2:GND1:C2_10070W_A:C3_06860C_A:GUT2:C5_03770C_A:ADH1:ARD:MAE1:MDH1:ADH5:FDH1:ALO1:FDH3
oxidoreductase activity, acting on the CH-OH group of donors, NAD or NADP as acceptor	13 out of 230 genes, 5.7%	67 out of 6473 background genes, 1.0%	9.18E-05	ADH2:GND1:C2_10070W_A:C3_06860C_A:C5_03770C_A:ADH1:ARD:MAE1:MDH1:ADH5:FDH1:ALO1:FDH3
carbohydrate kinase activity	6 out of 230 genes, 2.6%	11 out of 6473 background genes, 0.2%	1.40E-04	GAL1:XKS1:PFK1:PFK2:HXK2:GLK1
nucleic acid binding transcription factor activity	21 out of 230 genes, 9.1%	225 out of 6473 background genes, 3.5%	8.38E-03	RME1:MSN4:TYE7:ROB1:RIM101:STP4:GAL4:ZCF1:NDE1:TEC1:FCR1:C4_02570C_A:CBF1:HAL9:MIG1:SUT1:CPH2:CUP9:NRG1:CR_02510W_A:EFG1
sequence-specific DNA binding transcription factor activity	21 out of 230 genes, 9.1%	225 out of 6473 background genes, 3.5%	8.38E-03	RME1:MSN4:TYE7:ROB1:RIM101:STP4:GAL4:ZCF1:NDE1:TEC1:FCR1:C4_02570C_A:CBF1:HAL9:MIG1:SUT1:CPH2:CUP9:NRG1:CR_02510W_A:EFG1
alcohol dehydrogenase (NAD) activity	3 out of 230 genes, 1.3%	3 out of 6473 background genes, 0.0%	8.59E-03	ADH2:ADH1:FDH3

Component				
cell periphery	60 out of 230 genes, 26.1%	686 out of 6473 background genes, 10.6%	1.64E-09	HGT1:HGT2:CDR4:ADH2:ENO1:C1_08610C_A:TPO3:AOX2:C1_09210C_A:CRP1:SOD5:HGT7:HGT8:HGT6:ZRT2:GPM1:C2_04850C_A:SMF12:C2_07640W_A:UCF1:PIR1:C2_09710C_A:NDE1:SAP9:HEM13:PIN3:CDR2:NCE102:CDR1:TDH3:UBI4:SLK19:TPI1:C3_07470W_A:ERG251:AHP1:RHD3:PDC11:GUT2:HYR3:GPR1:ADH1:PGA4:COX15:PGK1:C6_03620C_A:ALS1:RVS167:ALS4:RVS161:GPH1:OPT1:QDR1:YCP4:PST3:PGI1:GLK1:CR_08990C_A:ALO1:XYL2

plasma membrane	45 out of 230 genes, 19.6%	477 out of 6473 background genes, 7.4%	1.01E-07	HGT1:HGT2:CDR4:ADH2:ENO1:C1_08610C_A:TPO3:AOX2:C1_09210C_A:CRP1:HGT7:HGT8:HGT6:ZRT2:SMF12:C2_07640W_A:NDE1:SAP9:CDR2:NCE102:CDR1:TDH3:UBI4:SLK19:TPI1:C3_07470W_A:ERG251:AHP1:RHD3:PDC11:GUT2:GPR1:ADH1:PGA4:COX15:PGK1:C6_03620C_A:OPT1:QDR1:YCP4:PST3:PGI1:GLK1:CR_08990C_A:ALO1
hyphal cell wall	14 out of 230 genes, 6.1%	55 out of 6473 background genes, 0.8%	5.95E-07	ENO1:SOD5:GPM1:TDH3:TPI1:AHP1:RHD3:PDC11:ADH1:PGA4:PGK1:ALS1:GPH1:XYL2
membrane raft	8 out of 230 genes, 3.5%	21 out of 6473 background genes, 0.3%	4.45E-05	NCE102:CDR1:SLK19:C3_07470W_A:RVS161:QDR1:YCP4:PST3
cell wall	19 out of 230 genes, 8.3%	142 out of 6473 background genes, 2.2%	7.45E-05	ENO1:SOD5:GPM1:PIR1:SAP9:HEM13:TDH3:TPI1:AHP1:RHD3:PDC11:HYR3:ADH1:PGA4:PGK1:ALS1:ALS4:GPH1:XYL2
fungal-type cell wall	19 out of 230 genes, 8.3%	142 out of 6473 background genes, 2.2%	7.45E-05	ENO1:SOD5:GPM1:PIR1:SAP9:HEM13:TDH3:TPI1:AHP1:RHD3:PDC11:HYR3:ADH1:PGA4:PGK1:ALS1:ALS4:GPH1:XYL2
external encapsulating structure	19 out of 230 genes, 8.3%	144 out of 6473 background genes, 2.2%	9.29E-05	ENO1:SOD5:GPM1:PIR1:SAP9:HEM13:TDH3:TPI1:AHP1:RHD3:PDC11:HYR3:ADH1:PGA4:PGK1:ALS1:ALS4:GPH1:XYL2
membrane region	8 out of 230 genes, 3.5%	29 out of 6473 background genes, 0.4%	7.30E-04	NCE102:CDR1:SLK19:C3_07470W_A:RVS161:QDR1:YCP4:PST3
intrinsic component of plasma membrane	11 out of 230 genes, 4.8%	59 out of 6473 background genes, 0.9%	8.00E-04	HGT1:HGT2:HGT7:HGT8:HGT6:SAP9:CDR1:SLK19:RHD3:PGA4:OPT1
yeast-form cell wall	9 out of 230 genes, 3.9%	39 out of 6473 background genes, 0.6%	9.30E-04	ENO1:PIR1:HEM13:TDH3:RHD3:ADH1:PGA4:ALS1:ALS4
plasma membrane part	14 out of 230 genes, 6.1%	100 out of 6473 background genes, 1.5%	1.45E-03	HGT1:HGT2:HGT7:HGT8:HGT6:C2_07640W_A:SAP9:NCE102:CDR1:SLK19:RHD3:PGA4:PGK1:OPT1
integral component of plasma membrane	8 out of 230 genes, 3.5%	40 out of 6473 background genes, 0.6%	9.37E-03	HGT1:HGT2:HGT7:HGT8:HGT6:CDR1:SLK19:OPT1

cell surface	19 out of 230 genes, 8.3%	199 out of 6473 background genes, 3.1%	1.08E-02	ENO1:SOD5:GPM1:HSP21:SAP9:HEM13:CDR1:TDH3:TPI1:RHD3:PDC11:HYR3:ADH1:PGA4:PGK1:ALS1:ALS4:GPH1:HSP104

SUPPLEMENTARY TABLE III.4A_MODULATED GENES AT LOW CELL DENSITY

Standard Name	Systematic Name	FC (cas5ΔΔ$_s$/wt) at low density	adj.P.Val	Description
HWP1	orf19.1321	3.64	9.01E-03	Hyphal cell wall protein; host transglutaminase substrate; opaque-, a-specific, alpha-factor induced; at MTLa side of conjugation tube; virulence complicated by URA3 effects; Bcr1-repressed in RPMI a/a biofilms; Spider biofilm induced
PGA31	orf19.5302	3.62	8.34E-04	Cell wall protein; putative GPI anchor; expression regulated upon white-opaque switch; induced by Congo Red and cell wall regeneration; Bcr1-repressed in RPMI a/a biofilms
orf19.6484	orf19.6484	3.32	3.05E-03	Ortholog of C. parapsilosis CDC317 : CPAR2_808370, C. dubliniensis CD36 : Cd36_72070, Candida orthopsilosis Co 90-125 : CORT_0C00800 and Candida albicans WO-1 : CAWG_05577
ECE1	orf19.3374	3.18	1.29E-02	Hypha-specific protein; regulated by Rfg1, Nrg1, Tup1, Cph1, Efg1, Hog1, farnesol, phagocytosis; fluconazole-induced; rat catheter and Spider biofilm induced; flow model biofilm repressed; Bcr1-repressed in RPMI a/a biofilms
orf19.251	orf19.251	2.52	5.81E-05	ThiJ/PfpI protein; binds human immunoglobulin E; alkaline, fluconazole, Hog1 repressed; induced in core stress response,; hypoxia, oxidative stress via Cap1, Hap43 induced; stationary-phase enriched; rat catheter, Spider biofilm induced
DDR48	orf19.4082	2.16	6.03E-03	Immunogenic stress-associated protein; filamentation regulated; induced by benomyl/caspofungin/ketoconazole or in azole-resistant strain; Hog1, farnesol, alkaline repressed; stationary phase enriched; Spider, flow model biofilm induced
RBR1	orf19.535	2.07	9.03E-02	Glycosylphosphatidylinositol (GPI)-anchored cell wall protein; required for filamentous growth at acidic pH; expression repressed by Rim101 and activated by Nrg1; Hap43-induced
orf19.3338	orf19.3338	2.01	2.93E-03	Protein of unknown function; Bcr1-repressed in RPMI a/a biofilms; rat catheter and Spider biofilm induced; ORF deleted and merged with orf19.3337
SOD4	orf19.2062	1.99	8.75E-02	Cu and Zn-containing superoxide dismutase; role in response to host innate immune ROS; regulated on white-opaque switch; ciclopirox olamine induced; caspofungin repressed; SOD1,4,5,6 gene family; yeast-associated; Spider biofilm induced
ASR1	orf19.2344	1.96	6.57E-02	Heat shock protein; transcript regulated by cAMP, osmotic stress, ciclopirox olamine, ketoconazole; repressed by Cyr1, Ras1; colony morphology-related regulated by Ssn6; stationary phase enriched; Hap43-induced; Spider biofilm induced
LDG3	orf19.6486	1.94	6.03E-03	Putative LDG family protein; F-12/CO2 early biofilm induced
SAP7	orf19.756	1.77	7.34E-03	Pepstatin A-insensitive secreted aspartyl protease; self-processing; expressed in human oral infection; Ssn6p-regulated; role in murine intravenous infection; induced during, but not required for, murine vaginal infection; N-glycosylated

ALS3	orf19.1816	1.68	7.73E-02	Cell wall adhesin; epithelial adhesion, endothelial invasion; alleles vary in adhesiveness; immunoprotective in mice; binds SspB adhesin of S. gordonii in mixed biofilm; induced in/required for Spider biofilm; flow model biofilm repressed
orf19.3499	orf19.3499	1.61	6.44E-02	Secreted potein; Hap43-repressed; fluconazole-induced; regulated by Tsa1, Tsa1B under H2O2 stress conditions; induced by Mnl1p under weak acid stress; Spider biofilm induced
YHM1	orf19.685	1.61	9.03E-02	Putative mitochondrial carrier protein; fungal-specific (no human or murine homolog); Hap43p-repressed gene
FAD3	orf19.4933	1.60	2.87E-02	Omega-3 fatty acid desaturase; production of alpha-linolenic acid, a major component of membranes; caspofungin induced; Plc1-regulated; colony morphology-related gene regulation by Ssn6; Spider biofilm induced, flow model biofilm repressed
CTR1	orf19.3646	1.58	1.29E-02	Copper transporter; transcribed in low copper; induced Mac1, Tye7, macrophage interaction, alkaline pH via Rim101; 17-beta-estradiol repressed; complements S. cerevisiae ctr1 ctr3 copper transport mutant; flow model/Spider biofilm induced
orf19.828	orf19.828	1.57	1.15E-01	Putative ribosomal protein, large subunit, mitochondrial precursor; repressed by prostaglandins; Spider biofilm repressed
SEN2	orf19.2735	1.53	3.94E-03	Putative tRNA splicing endonuclease subunit; mutation confers hypersensitivity to toxic ergosterol analog and to amphotericin B; 5'-UTR intron; Hap43-induced; Spider biofilm induced
orf19.1774	orf19.1774	-1.51	1.54E-02	Predicted dehydrogenase; transcript upregulated in an RHE model of oral candidiasis; virulence-group-correlated expression; Spider biofilm repressed
ATX1	orf19.2369.1	-1.53	9.01E-03	Putative cytosolic copper metallochaperone; flucytosine induced; Ssr1-repressed; rat catheter biofilm induced
PGA26	orf19.2475	-1.59	5.23E-02	GPI-anchored adhesin-like protein of the cell wall; role in cell wall integrity; required for normal virulence; induced in high iron and during cell wall regeneration; Hap43-repressed
SWE1	orf19.4867	-1.67	9.83E-03	Putative protein kinase with a role in control of growth and morphogenesis, required for full virulence; mutant cells are small, rounded, and sometimes binucleate; not required for filamentous growth; mutant is hypersensitive to caspofungin
FDH1	orf19.638	-1.69	8.82E-03	Formate dehydrogenase; oxidizes formate to CO2; Mig1 regulated; induced by macrophages; fluconazole-repressed; repressed by Efg1 in yeast, not hyphal conditions; stationary phase enriched; rat catheter and Spider biofilm induced
DAG7	orf19.4688	-1.77	9.72E-03	Secretory protein; a-specific, alpha-factor induced; mutation confers hypersensitivity to toxic ergosterol analog; fluconazole-induced; induced during chlamydospore formation in C. albicans and C. dubliniensis
PCL2	orf19.403	-1.98	7.34E-03	Cyclin homolog; reduced expression observed upon depletion of Cln3; farnesol regulated; periodic mRNA expression, peak at cell-cycle G1/S phase; Hap43-induced; rat catheter biofilm repressed
PGA6	orf19.4765	-2.17	5.11E-02	GPI-anchored cell wall adhesin-like protein; induced by high iron; upregulated upon Als2 depletion; mRNA binds She3 and is localized to hyphal tips; Spider biofilm repressed

SUPPLEMENTARY TABLE III.4B_MODULATED GENES AT HIGH CELL DENSITY

Standard Name	Systematic Name	FC (cas5ΔΔ$_s$/wt) at high density	adj.P.Val	Description
PHO89	orf19.4599	7.07	3.35E-08	Putative phosphate permease; transcript regulated upon white-opaque switch; alkaline induced by Rim101; possibly adherence-induced; F-12/CO2 model, rat catheter and Spider biofilm induced
HWP1	orf19.1321	6.37	3.74E-06	Hyphal cell wall protein; host transglutaminase substrate; opaque-, a-specific, alpha-factor induced; at MTLa side of conjugation tube; virulence complicated by URA3 effects; Bcr1-repressed in RPMI a/a biofilms; Spider biofilm induced
SOD5	orf19.2060	6.11	8.22E-07	Cu and Zn-containing superoxide dismutase; protects against oxidative stress; induced by neutrophils, hyphal growth, caspofungin, osmotic/oxidative stress; oralpharyngeal candidiasis induced; rat catheter and Spider biofilm induced
orf19.3338	orf19.3338	5.82	5.49E-08	Protein of unknown function; Bcr1-repressed in RPMI a/a biofilms; rat catheter and Spider biofilm induced; ORF deleted and merged with orf19.3337
ECE1	orf19.3374	5.79	4.92E-06	Hypha-specific protein; regulated by Rfg1, Nrg1, Tup1, Cph1, Efg1, Hog1, farnesol, phagocytosis; fluconazole-induced; rat catheter and Spider biofilm induced; flow model biofilm repressed; Bcr1-repressed in RPMI a/a biofilms
IHD1	orf19.5760	5.66	6.35E-08	GPI-anchored protein; alkaline, hypha-induced; regulated by Nrg1, Rfg1, Tup1 and Tsa1, Tsa1B in minimal media at 37; oralpharyngeal candidasis induced ; Spider biofilm induced; regulated in Spider biofilms by Tec1, Efg1, Ndt80, Rob1, Brg1
ALS1	orf19.5741	5.59	2.69E-07	Cell-surface adhesin; adhesion, virulence, immunoprotective roles; band at hyphal base; Rfg1, Ssk1, Spider biofilm induced; flow model biofilm repressed; CAI-4 strain background effects; promoter bound Bcr1, Tec1, Efg1, Ndt80, and Brg1
POL93	orf19.6078	4.72	3.86E-07	Predicted ORF in retrotransposon Tca8 with similarity to the Pol region of retrotransposons encoding reverse transcriptase, protease and integrase; downregulated in response to ciclopirox olamine; F-12/CO2 early biofilm induced
PHR1	orf19.3829	4.68	3.35E-08	Cell surface glycosidase; may act on cell-wall beta-1,3-glucan prior to beta-1,6-glucan linkage; role in systemic, not vaginal virulence (neutral, not low pH); high pH or filamentation induced; Bcr1-repressed in RPMI a/a biofilm
CYS3	orf19.6402	4.62	7.21E-08	Cystathionine gamma-lyase; induced by alkaline, amphotericin B, cadmium stress, oxidative stress via Cap1; possibly adherence-induced; Hog1 regulated; reduced levels in stationary phase yeast cells; Spider and flow model biofilm induced

UTP18	orf19.7154	4.48	1.06E-07	Putative U3 snoRNA-associated protein; Hap43-induced; repressed in core stress response; physically interacts with TAP-tagged Nop1
NOG1	orf19.7384	4.48	2.21E-08	Putative GTPase; mutation confers hypersensitivity to 5-fluorocytosine (5-FC), 5-fluorouracil (5-FU), and tubercidin (7-deazaadenosine); repressed by prostaglandins; Hap43-induced
orf19.3337	orf19.3337	4.39	1.84E-06	Protein of unknown function; merged with orf19.3338; rat catheter, flow and Spider model biofilm induced; promoter bound by Bcr1, Efg1, Ndt80, and Rob1; orf19.3338 Bcr1- repressed in RPMI a/a biofilms
UTP4	orf19.1633	4.34	1.48E-06	Putative U3 snoRNA-associated protein; Hap43-induced; physically interacts with TAP-tagged Nop1; Spider biofilm induced
SRP40	orf19.2859	4.31	5.59E-07	Putative chaperone of small nucleolar ribonucleoprotein particles; macrophage/pseudohyphal-induced; rat catheter biofilm induced
TSR1	orf19.6417	4.29	5.49E-07	Component of 20S pre-rRNA processing unit; repressed by prostaglandins
RPL7	orf19.3867	4.28	1.02E-07	Ribosomal protein L7; repressed upon phagocytosis by murine macrophages; Hap43-induced; rat catheter and Spider biofilm induced
RPA34	orf19.4896	4.23	8.82E-06	Putative RNA polymerase I subunit; rat catheter biofilm induced
GPD2	orf19.691	4.17	9.83E-07	Surface protein similar to glycerol 3-P dehydrogenase; binds host Factor H, FHL-1, plasminogen; regulated by Ssn6, Nrg1, Efg1; induced by cell wall regeneration, macrophage/pseudohyphal growth, core stress response; Spider biofilm induced
HBR3	orf19.6955	4.16	8.35E-07	Essential protein; regulated by hemoglobin; S. cerevisiae ortholog is essential; Hap43p-induced gene
NSA1	orf19.2185	4.10	1.10E-07	Putative 66S pre-ribosomal particles conmponent; Hap43-induced; repressed by prostaglandins
orf19.2917	orf19.2917	4.07	4.92E-06	Putative GTPase; heterozygous null mutant exhibits resistance to parnafungin in the C. albicans fitness test; Hap43p-induced gene
YTM1	orf19.4815	4.06	5.27E-08	Protein similar to S. cerevisiae Ytm1p, which is involved in biogenesis of the large ribosomal subunit; transposon mutation affects filamentous growth; protein level decreases in stationary phase cultures; Hap43p-induced gene
orf19.1030	orf19.1030	4.06	1.15E-07	Putative peptidyl-prolyl cis-trans isomerase
ELF1	orf19.7332	4.05	4.63E-07	Putative mRNA export protein; Walker A and B (ATP/GTP binding) motifs; required for wild-type morphology, growth; expressed in hyphal, pseudohyphal, and yeast form; Hap43-induced; Spider and flow model biofilm induced
GUK1	orf19.1115	4.04	1.02E-07	Putative guanylate kinase; identified in extracts from biofilm and planktonic cells; protein level decrease in stationary phase cultures; Hap43p-induced gene

TEC1	orf19.5908	3.98	3.04E-07	TEA/ATTS transcription factor; white cell pheromone response, hyphal gene regulation; required for Spider and RPMI biofilm formation; regulates BCR1; Cph2 regulated transcript; alkaline, rat catheter, Spider, flow model biofilm induced
RHR2	orf19.5437	3.95	2.67E-06	Glycerol 3-phosphatase; roles in osmotic tolerance, glycerol accumulation in response to salt; Spider/flow model biofilm induced; regulated by macrophage, stress, yeast-hyphal switch, pheromone, Gcn4, Hog1, Nrg1, Tup1
RRP9	orf19.2830	3.94	3.92E-06	Ribosomal protein; mutation confers resistance to 5-fluorocytosine (5-FC), 5-fluorouracil (5-FU), and tubercidin (7-deazaadenosine); physically interacts with TAP-tagged Nop1; Hap43-induced; Spider biofilm induced
orf19.6079	orf19.6079	3.94	9.83E-07	Predicted ORF in retrotransposon Tca8 with similarity to the Gag region encoding nucleocapsid-like protein; repressed by ciclopirox olamine; filament induced; regulated by Rfg1, Tup1; overlaps orf19.6078.1
RLP24	orf19.4191	3.91	2.03E-07	Putative ribosomal protein; Hap43-induced; essential gene; heterozygous mutation confers hypersensitivity to 5-fluorocytosine (5-FC), 5-fluorouracil (5-FU), and tubercidin (7-deazaadenosine); Spider biofilm induced
RNR1	orf19.5779	3.88	8.59E-06	Ribonucleotide reductase large subunit; induced in low iron; transposon mutation affects filamentous growth; farnesol upregulated in biofilm; regulated by cell cycle, tyrosol, cell density; regulated by Sef1, Sfu1, and Hap43
ARX1	orf19.3015	3.80	1.56E-07	Putative ribosomal large subunit biogenesis protein; repressed in core stress response; repressed by prostaglandins
orf19.6247	orf19.6247	3.76	7.21E-08	Ortholog(s) have chromatin binding activity
NOP5	orf19.1199	3.71	1.06E-07	Ortholog of S. cerevisiae Nop58; involved in pre-rRNA process; Tn mutation affects filamentous growth; macrophage/pseudohyphal-induced; physically interacts with TAP-tagged Nop1; Spider biofilm repressed
RRP15	orf19.563	3.70	9.83E-07	Putative nucleolar protein; constituent of pre-60S ribosomal particles; Hap43-induced; repressed by prostaglandins
MPP10	orf19.1915	3.67	8.75E-08	Putative SSU processome and 90S preribosome component; repressed in core stress response; repressed by prostaglandins
CIC1	orf19.124	3.66	2.32E-06	Putative proteasome-interacting protein; rat catheter biofilm induced
RPA135	orf19.7062	3.65	1.15E-07	Putative RNA polymerase I subunit A135; repressed by prostaglandins
KRR1	orf19.661	3.62	2.20E-07	Putative nucleolar protein; repressed benomyl treatment or in an azole-resistant strain that overexpresses MDR1; F-12/CO2 early biofilm induced
RRS1	orf19.6014	3.62	6.66E-07	Putative ribosome biogenesis and nuclear export protein; Hap43p-induced gene; mutation confers hypersensitivity to 5-fluorocytosine (5-FC), 5-fluorouracil (5-FU), and tubercidin (7-deazaadenosine)

DBP3	orf19.4870	3.59	9.37E-06	Putative ATP-dependent DEAD-box RNA helicase; Hap43-induced; repressed by prostaglandins; Spider biofilm induced
orf19.5905	orf19.5905	3.57	1.35E-07	Protein of unknown function; Hap43-induced; F-12/CO2 early biofilm induced
SPB1	orf19.76	3.56	1.06E-07	Putative AdoMet-dependent methyltransferase; Hap43-induced; repressed by prostaglandins; possibly essential gene, disruptants not obtained by UAU1 method; Spider biofilm induced
DRS1	orf19.7635	3.55	7.21E-08	Putative nucleolar DEAD-box protein; Hap43-induced; mutation confers hypersensitivity to 5-fluorouracil (5-FU), tubercidin (7-deazaadenosine); Tbf1-induced; repressed in core stress response
ENA2	orf19.6070	3.54	3.38E-06	Putative sodium transporter; induced by ciclopirox olamine; alkaline induced by Rim101; repressed by high-level peroxide stress; induced in oral candidiasis clinical isolates; possibly essential gene; rat catheter and Spider biofilm induced
PWP2	orf19.3276	3.54	8.35E-08	Putative 90S pre-ribosomal component; repressed in core stress response; repressed by prostaglandins; physically interacts with TAP-tagged Nop1; Hap43-induced
MIS12	orf19.7534	3.51	2.73E-07	Mitochondrial C1-tetrahydrofolate synthase precursor
orf19.7398	orf19.7398	3.48	8.22E-07	Protein of unknown function' Hap43-induced gene; repressed by prostaglandins
RPF2	orf19.3553	3.47	2.67E-06	Putative pre-rRNA processing protein; Hap43p-induced gene; mutation confers hypersensitivity to 5-fluorocytosine (5-FC), 5-fluorouracil (5-FU), and tubercidin (7-deazaadenosine)
NIP7	orf19.3478	3.46	1.72E-06	Putative nucleolar protein with role in ribosomal assembly; hyphal-induced; Hap43-induced; Spider biofilm induced
orf19.7546	orf19.7546	3.45	7.32E-06	Protein involved in rRNA processing; required for maturation of the 35S primary transcript of pre-rRNA and for cleavage leading to mature 18S rRNA; Spider biofilm induced
orf19.2319	orf19.2319	3.44	2.05E-05	Putative nucleolar protein with a predicted role in pre-rRNA processing; Hap43-induced gene; repressed in core stress response
orf19.6828	orf19.6828	3.44	3.81E-06	Ortholog(s) have role in rRNA processing and nucleolus, preribosome, large subunit precursor localization
UTP9	orf19.6710	3.43	1.08E-06	Small-subunit processome protein; Ssr1-induced; repressed by prostaglandins; physically interacts with TAP-tagged Nop1
HOM3	orf19.1235	3.39	3.11E-06	Putative L-aspartate 4-P-transferase; fungal-specific (no human or murine homolog); regulated by Gcn2 and Gcn4; early-stage flow model biofilm induced
NOG2	orf19.5732	3.38	7.28E-06	Putative nucleolar GTPase; repressed by prostaglandins; Hap43-induced, rat catheter and Spider biofilm induced
UTP21	orf19.1566	3.37	1.16E-06	Putative U3 snoRNP protein; Hap43-induce; physically interacts with TAP-tagged Nop1; Spider biofilm induced

TSR2	orf19.2998	3.37	1.02E-07	Protein with a predicted role in pre-rRNA processing; repressed by prostaglandins
orf19.3547	orf19.3547	3.36	2.03E-07	Ortholog(s) have mRNA 3'-UTR binding, translation repressor activity, nucleic acid binding activity, role in negative regulation of translation, ribosomal large subunit biogenesis and large ribosomal subunit, nucleolus localization
TIF3	orf19.3423	3.36	5.75E-05	Putative translation initiation factor; genes encoding ribosomal subunits, translation factors, and tRNA synthetases are downregulated upon phagocytosis by murine macrophage
orf19.6662	orf19.6662	3.35	2.61E-07	Putative coenzyme Q (ubiquinone) binding protein; transcript is upregulated in clinical isolates from HIV+ patients with oral candidiasis
PHO84	orf19.655	3.34	7.77E-04	High-affinity phosphate transporter; transcript regulated by white-opaque switch; Hog1, ciclopirox olamine or alkaline induced; caspofungin, stress repressed; upregulated in RHE model; Spider and flow model biofilm induced, Hap43-induced
POL1	orf19.5873	3.32	1.18E-07	Putative DNA directed DNA polymerase alpha; RNA abundance regulated by cell cycle, tyrosol and cell density; rat catheter biofilm induced
MAK5	orf19.3540	3.32	7.28E-06	Putative nucleolar DEAD-box RNA helicase; oxidative stress-repressed via Cap1; repressed by prostaglandins
YMC1	orf19.4447	3.31	1.34E-06	Putative inner mitochondrial membrane transporter; flucytosine induced; Spider biofilm repressed
UTP5	orf19.7599	3.31	1.72E-06	Putative U3 snoRNA-associated protein; Hap43p-induced gene; mutation confers resistance to 5-fluorocytosine (5-FC), 5-fluorouracil (5-FU), and tubercidin (7-deazaadenosine); physically interacts with TAP-tagged Nop1p
SMC1	orf19.4367	3.30	4.66E-07	Protein similar to chromosomal ATPases; RNA abundance regulated by tyrosol and cell density; cell-cycle regulated periodic mRNA expression
POP3	orf19.7657	3.30	4.62E-06	Putative RNase MRP and nuclear RNase P component; decreased repressed by prostaglandins; Spider biofilm induced
DUT1	orf19.3322	3.28	2.59E-06	dUTP pyrophosphatase; cell-cycle regulated if expressed in S. cerevisiae; upstream MluI and SCB elements; 17-beta-estradiol, ethynyl estradiol, macrophage induced; decreased in stationary phase yeast; rat catheter, Spider biofilm repressed
BMS1	orf19.2504	3.28	8.87E-07	Putative GTPase; Hap43-induced gene; mutation confers resistance to 5-fluorocytosine (5-FC); flucytosine induced; repressed by prostaglandins; Spider biofilm induced
RPL11	orf19.2232	3.23	1.44E-05	Ribosomal protein; repressed by phagocytosis; colony morphology-related gene regulation by Ssn6; Hap43-induced; Spider biofilm repressed
UTP8	orf19.5436	3.22	3.04E-07	Essential nucleolar protein; involved in tRNA export from the nucleus and ribosomal small subunit biogenesis; physically interacts with TAP-tagged Nop1; Spider biofilm induced

MAK16	orf19.5500	3.22	3.90E-06	Putative constituent of 66S pre-ribosomal particles; Hap43-induced; repressed by prostaglandins; Spider biofilm induced
OGG1	orf19.7190	3.22	8.44E-06	Mitochondrial glycosylase/lyase; repairs oxidative damage to mitochondrial DNA, contributes to UVA resistance, role in base-excision repair; Spider biofilm induced
HCA4	orf19.2712	3.21	1.06E-07	Putative role in regulation of cell wall biogenesis; Hap43p-induced gene; possibly an essential gene, disruptants not obtained by UAU1 method; flow model and rat catheter biofilm induced
IMH3	orf19.18	3.21	2.38E-06	Inosine monophosphate (IMP) dehydrogenase; enzyme of GMP biosynthesis; target of mycophenolic acid and mizoribine monophosphate; antigenic during infection; repressed in core stress response; snoRNA snR54 encoded within IMH3 intron
SIT1	orf19.2179	3.20	1.21E-06	Transporter of ferrichrome siderophores, not ferrioxamine B; required for human epithelial cell invasion in vitro, not for mouse systemic infection; regulated by iron, Sfu1, Rfg1, Tup1, Hap43; rat catheter and Spider biofilm induced
HMX1	orf19.6073	3.19	3.04E-07	Heme oxygenase; utilization of hemin iron; transcript induced by heat, low iron, or hemin; repressed by Efg1; induced by low iron; upregulated by Rim101 at pH 8; Hap43-induced; Spider and flow model biofilm induced
PRI2	orf19.2885	3.19	3.14E-05	Putative DNA primase; gene adjacent to and divergently transcribed with CDC68; Hap43-induced; Spider biofilm repressed
RPS27	orf19.6286.2	3.17	4.04E-05	Putative ribosomal protein; repressed upon phagocytosis by murine macrophage; Spider biofilm repressed
POL30	orf19.4616	3.16	1.57E-05	Similar to proliferating cell nuclear antigen (PCNA); RNA abundance regulated by tyrosol, cell density; induced by flucytosine, interaction with macrophages; stationary phase enriched protein; rat catheter and Spider biofilm repressed
YDJ1	orf19.506	3.14	5.44E-07	Putative type I HSP40 co-chaperone; heavy metal (cadmium) stress-induced
FET3	orf19.4211	3.13	3.05E-03	Multicopper oxidase; for growth in low iron, prostaglandin E2 synthesis; ketoconazole/caspofungin/amphotericin B repressed; Sef1/Sfu1/Hap43 regulated; reports differ if functional homolog of ScFet3; rat catheter and Spider biofilm induced
orf19.2330	orf19.2330	3.13	1.32E-06	Putative U3 snoRNA-associated protein; Hap43-induced; transposon mutation affects filamentous growth; repressed by prostaglandins
orf19.1961	orf19.1961	3.11	3.04E-07	Planktonic growth-induced gene
RPA190	orf19.1839	3.10	4.85E-07	Putative RNA polymerase I subunit A190; Hap43p-induced gene; flucytosine induced
GCD11	orf19.4223	3.09	1.18E-07	Gamma subunit of translation initiation factor eIF2; involved in identification of the start codon; likely essential for growth, based on an insertional mutagenesis strategy; Spider biofilm repressed

CNT	orf19.4118	3.07	1.72E-06	CNT family H(+)/nucleoside symporter; transports adenosine, uridine, inosine, guanosine, tubercidin; variant alleles for high/low-affinity isoforms; S or G at residue 328 affects specificity; Spider, flow model biofilm induced
DOT4	orf19.3370	3.06	3.26E-06	Protein similar to ubiquitin C-terminal hydrolase; localizes to cell surface of hyphal cells, but not yeast-form cells; repressed upon high-level peroxide; Hap43p-induced; rat catheter biofilm induced
FRE7	orf19.6139	3.04	3.06E-05	Copper-regulated cupric reductase; repressed by ciclopirox olamine or 17-beta-estradiol; induced by alkaline conditions or interaction with macrophage; Spider biofilm induced
NOP6	orf19.6236	3.04	3.86E-07	Putative ortholog of S. cerevisiae Nop6; role in ribosomal small subunit biogenesis; Spider biofilm induced
orf19.2320	orf19.2320	3.04	6.37E-06	Putative serine/threonine-protein kinase; possibly an essential gene, disruptants not obtained by UAU1 method
orf19.4283	orf19.4283	3.03	3.92E-06	Ortholog(s) have role in translational initiation and cytosol, eukaryotic 43S preinitiation complex, eukaryotic translation initiation factor 3 complex, eIF3e, eukaryotic translation initiation factor 3 complex, eIF3m, nucleus localization
WOR3	orf19.467	3.02	5.01E-06	Transcription factor; modulator of white-opaque switch; induced in opaque cells; promoter bound by Wor1; overexpression at 25 degr shifts cells to opaque state; deletion stabilizes opaque cells at higher temperatures; Spider biofilm induced
NOP13	orf19.6766	3.02	6.79E-07	Ortholog of S. cerevisiae Nop13; a nucleolar protein found in preribosomal complexes; Hap43-induced gene; rat catheter biofilm induced
orf19.4760	orf19.4760	3.02	1.82E-05	Putative protein-histidine N-methyltransferase; Spider biofilm induced
WRS1	orf19.5226	3.00	1.87E-05	Putative tRNA-Trp synthetase; genes encoding ribosomal subunits, translation factors, tRNA synthetases are downregulated upon phagocytosis by murine macrophages
ERB1	orf19.1047	2.99	8.55E-05	Protein with a predicted role in ribosomal large subunit biogenesis; mutation confers hypersensitivity to 5-fluorocytosine (5-FC), 5-fluorouracil (5-FU), and tubercidin (7-deazaadenosine); hyphal, macrophage repressed
NOC4	orf19.1902	2.98	1.91E-07	Putative nucleolar protein; Hap43-induced; mutation confers resistance to 5-fluorocytosine (5-FC), 5-fluorouracil (5-FU), and tubercidin (7-deazaadenosine); Spider biofilm induced
ENP1	orf19.5507	2.98	5.42E-06	Protein required for pre-rRNA processing and 40S ribosomal subunit synthesis; associated with U3 and U14 snoRNAs; transposon mutation affects filamentous growth; repressed by prostaglandins; Spider biofilm induced
orf19.6090	orf19.6090	2.97	9.19E-08	Putative nucleolar protein with a predicted role in pre-rRNA processing and ribosome biogenesis; repressed by nitric oxide; required for flow model biofilm formation; Spider biofilm repressed

NEP1	orf19.665	2.97	9.83E-07	Ortholog(s) have rRNA (pseudouridine) methyltransferase activity
TRP4	orf19.3099	2.96	3.91E-06	Predicted enzyme of amino acid biosynthesis; upregulated in biofilm; regulated by Gcn2p and Gcn4p; S. cerevisiae ortholog is Gcn4p regulated
PMS1	orf19.1605	2.95	3.25E-05	Putative DNA mismatch repair factor; ortholog of S. cerevisiae PMS1 which is an ATP-binding protein involved in DNA mismatch repair
GUA1	orf19.4813	2.95	1.72E-06	Putative GMP synthase, involved in the final step of guanine biosynthesis; soluble protein in hyphae; flucytosine induced; macrophage-downregulated protein abundance; protein level decreases in stationary phase cultures
PES1	orf19.4093	2.95	9.83E-04	Pescadillo homolog required for yeast cell growth, lateral yeast growth on filamentous cells and virulence in mice; hyphal cells grow normally in mutant; mutation confers hypersensitivity to 5-fluorocytosine, 5-fluorouracil, tubercidin
IRR1	orf19.7232	2.94	4.07E-07	Putative cohesin complex subunit; cell-cycle regulated periodic mRNA expression
orf19.7488	orf19.7488	2.93	3.11E-06	Component of the SSU processome; predicted role in pre-18S rRNA processing; Spider biofilm induced
FAD2	orf19.118	2.93	3.10E-06	Delta-12 fatty acid desaturase, involved in production of linoleic acid, which is a major component of membranes
orf19.4459	orf19.4459	2.90	7.39E-05	Predicted heme-binding stress-related protein; Tn mutation affects filamentous growth; induced during chlamydospore formation in C. albicans and C. dubliniensis; Spider biofilm induced
NSA2	orf19.7424	2.89	3.02E-06	Putative protein constituent of 66S pre-ribosomal particles; Hap43-induced; repressed by prostaglandins
PPT1	orf19.1673	2.89	1.88E-05	Putative serine/threonine phosphatase; induced in high iron
orf19.3088	orf19.3088	2.89	3.26E-06	bZIP transcription factor; possibly transcriptionally regulated upon hyphal formation; Hap43; F-12/CO2 early biofilm induced; Spider biofilm induced
RPL82	orf19.2311	2.87	9.83E-07	Predicted ribosomal protein; genes encoding cytoplasmic ribosomal subunits, translation factors, and tRNA synthetases are downregulated upon phagocytosis by murine macrophage
orf19.3690.2	orf19.3690.2	2.87	7.05E-06	Ribosomal 60S subunit protein; Spider biofilm repressed
PGA30	orf19.5303	2.87	1.09E-03	GPI-anchored protein of cell wall
NOC2	orf19.5850	2.87	2.24E-05	Putative nucleolar complex protein; Hap43-induced; transposon mutation affects filamentous growth; mutation confers hypersensitivity to 5-fluorouracil (5-FU), tubercidin (7-deazaadenosine); repressed in core stress response
orf19.3831	orf19.3831	2.84	4.41E-04	Ortholog(s) have telomerase inhibitor activity, role in box C/D snoRNA 3'-end processing, negative regulation of telomere maintenance via telomerase and nucleolus, nucleoplasm localization

orf19.3393	orf19.3393	2.84	4.15E-07	Putative DEAD-box helicase; Hap43-induced; Spider biofilm induced
orf19.4517	orf19.4517	2.82	6.28E-06	Protein of unknown function; Hap43-induced gene
RRN3	orf19.1923	2.82	2.20E-06	Protein with a predicted role in recruitment of RNA polymerase I to rDNA; caspofungin induced; flucytosine repressed; repressed in core stress response; repressed by prostaglandins
orf19.2657	orf19.2657	2.82	5.02E-04	
KRE30	orf19.2183	2.82	1.81E-05	YEF3-subfamily ABC family protein; predicted not to be a transporter; repressed in core stress response; mutation confers hypersensitivity to amphotericin B
SAS10	orf19.2717	2.82	6.34E-06	Putative U3-containing small subunit processome complex subunit; Hap43p-induced gene; mutation confers resistance to 5-fluorocytosine (5-FC); repressed upon high-level peroxide stress
PWP1	orf19.4640	2.81	1.13E-05	Putative rRNA processing protein; Hap43-induced; repressed in core stress response
RFC4	orf19.7658	2.81	8.75E-08	Putative heteropentameric replication factor C subunit; flucytosine induced; periodic mRNA expression, peak at cell-cycle G1/S phase
LAC1	orf19.7354	2.81	7.15E-07	Ceramide synthase; required for biosynthesis of ceramides with C18:0 fatty acids, which serve as precursors for glucosylsphingolipids; caspofungin induced
NAN1	orf19.2688	2.80	1.95E-06	Putative U3 snoRNP protein; Hap43p-induced gene; physically interacts with TAP-tagged Nop1p
DBP7	orf19.6902	2.78	1.13E-06	Putative ATP-dependent DEAD-box RNA helicase; Hap43-induced; rat catheter biofilm induced
orf19.3778	orf19.3778	2.77	2.56E-06	Protein with a predicted role in ribosome biogenesis; mutation confers hypersensitivity to 5-fluorocytosine (5-FC), 5-fluorouracil (5-FU); repressed in core stress response; repressed by prostaglandins; Hap43-induced
RPS16A	orf19.2994.1	2.77	6.44E-05	Putative 40S ribosomal subunit; macrophage/pseudohyphal-induced after 16 h; Spider biofilm repressed
orf19.7593	orf19.7593	2.77	6.95E-06	Putative asparaginase; predicted role in asparagine catabolism; Spider biofilm induced
ENP2	orf19.6686	2.77	2.15E-04	Putative nucleolar protein; essential; heterozygous mutation confers resistance to 5-fluorocytosine (5-FC), 5-fluorouracil (5-FU), and tubercidin (7-deazaadenosine); Hap43-induced; Spider biofilm induced
RPS10	orf19.2179.2	2.76	2.77E-05	Ribosomal protein S10; downregulated in the presence of human whole blood or PMNs; Spider biofilm repressed
GIN1	orf19.658	2.76	2.38E-06	Protein involved in regulation of DNA-damage-induced filamentous growth; putative component of DNA replication checkpoint; ortholog of S. cerevisiae Mrc1p, an S-phase checkpoint protein; Hap43p-induced gene

RPL9B	orf19.236	2.76	2.90E-05	Ribosomal protein L9; repressed upon phagocytosis by murine macrophages; repressed by nitric oxide; protein levels decrease in stationary phase; Hap43-induced; Spider biofilm repressed
orf19.1791	orf19.1791	2.75	3.26E-06	Putative protein with a predicted role in 60S ribosomal subunit biogenesis; Hap43p-induced gene; ortholog of S. cerevisiae MAK11
PRT1	orf19.6584	2.74	2.18E-04	Putative translation initiation factor eIF3; mutation confers hypersensitivity to roridin A, verrucarin A; genes encoding ribosomal subunits, translation factors, tRNA synthetases are downregulated upon phagocytosis by murine macrophages
SUI3	orf19.7161	2.74	3.69E-05	Putative translation initiation factor; genes encoding ribosomal subunits, translation factors, and tRNA synthetases are downregulated upon phagocytosis by murine macrophage
orf19.2594	orf19.2594	2.73	1.32E-06	Ortholog(s) have RNA polymerase I activity, role in transcription of nuclear large rRNA transcript from RNA polymerase I promoter and DNA-directed RNA polymerase I complex, cytosol localization
orf19.1578	orf19.1578	2.73	4.63E-07	Ortholog of S. cereviaie Rrp5, an RNA binding protein involved in synthesis of 18S and 5.8S rRNAs; Hap43-induced gene
RPS7A	orf19.1700	2.72	6.47E-04	Ribosomal protein S7; genes encoding cytoplasmic ribosomal subunits, translation factors, and tRNA synthetases are downregulated upon phagocytosis by murine macrophage; Spider biofilm repressed
KTI12	orf19.2385	2.71	1.52E-06	Protein similar to S. cerevisiae Kti12p, which associates with Elongator complex; has a role in resistance to killer toxin; predicted Kex2p substrate; Hap43p-induced gene
POL2	orf19.2365	2.70	6.95E-04	DNA polymerase epsilon; transcript induced by interaction with macrophage; transcript is regulated by Tup1; periodic mRNA expression, peak at cell-cycle G1/S phase
SAM4	orf19.386	2.70	1.81E-06	Putative S-adenosylmethionine-homocysteine methyltransferase; Hap43-repressed; alkaline induced; Spider biofilm repressed
DBP2	orf19.171	2.69	5.83E-05	Putative DEAD-box family ATP-dependent RNA helicase; flucytosine induced; repressed in core stress response
CSI2	orf19.5232	2.69	3.18E-03	Putative 66S pre-ribosomal particle component; Hap43-induced; essential for growth; transposon mutation affects filamentous growth; Spider biofilm induced
orf19.2796	orf19.2796	2.69	1.82E-05	Ortholog(s) have DNA-directed DNA polymerase activity, role in DNA replication initiation, telomere capping and alpha DNA polymerase:primase complex, cytosol, nuclear envelope localization
orf19.1626	orf19.1626	2.67	7.40E-06	Deoxyhypusine synthase; catalyzes formation of deoxyhypusine, the first step in hypusine biosynthesis; Spider biofilm repressed
orf19.3205	orf19.3205	2.66	3.38E-06	Mitochondrial ribosomal protein of the large subunit; rat catheter biofilm induced

CCT7	orf19.3206	2.66	6.66E-07	Cytosolic chaperonin Cct ring complex; protein is present in exponential and stationary growth phase yeast cultures; sumoylation target
RLI1	orf19.3034	2.66	3.20E-06	Member of RNase L inhibitor (RLI) subfamily of ABC family; predicted not to be a transporter; regulated by Sef1p, Sfu1p, and Hap43p
orf19.5991	orf19.5991	2.66	2.41E-04	Ortholog(s) have role in maturation of 5.8S rRNA from tricistronic rRNA transcript (SSU-rRNA, 5.8S rRNA, LSU-rRNA), maturation of LSU-rRNA from tricistronic rRNA transcript (SSU-rRNA, 5.8S rRNA, LSU-rRNA)
orf19.2090	orf19.2090	2.66	9.70E-05	Ortholog of S. cerevisiae Ecm16, an essential DEAH-box ATP-dependent RNA helicase specific to the U3 snoRNP required for 18S rRNA synthesis; Hap43-induced; Spider biofilm induced
RPA12	orf19.2287	2.65	4.09E-07	Putative DNA-directed RNA polymerase I; induced upon adherence to polystyrene
orf19.5802	orf19.5802	2.65	4.91E-06	Ortholog(s) have role in maturation of SSU-rRNA and cytoplasm, nucleus localization
orf19.5038	orf19.5038	2.65	1.11E-06	Predicted tRNA (guanine) methyltransferase activity; Spider biofilm induced
orf19.6907	orf19.6907	2.63	1.91E-04	Ortholog(s) have DNA binding activity and cytoplasm, nuclear chromatin localization
orf19.7494	orf19.7494	2.63	7.39E-05	Protein of unknown function; cell-cycle regulated periodic mRNA expression
SEN2	orf19.2735	2.63	1.32E-06	Putative tRNA splicing endonuclease subunit; mutation confers hypersensitivity to toxic ergosterol analog and to amphotericin B; 5'-UTR intron; Hap43-induced; Spider biofilm induced
orf19.7011	orf19.7011	2.62	2.16E-04	Ortholog(s) have 90S preribosome, cytoplasm, mitotic spindle pole body, nucleolus localization
SKN1	orf19.7362	2.61	3.33E-07	Protein with a role in beta-1,6-glucan synthesis; probable N-glycosylated type II membrane protein; transcript and mRNA length change induced by yeast-hypha transition; induced by Rim101, caspofungin; rat catheter and Spider biofilm induced
orf19.4479	orf19.4479	2.61	2.20E-07	Putative U3-containing 90S preribosome subunit; Hap43-induced; repressed in core stress response; Spider biofilm induced
RPS15	orf19.5927	2.61	2.00E-06	Putative ribosomal protein; macrophage/pseudohyphal-induced after 16 h; repressed upon phagocytosis by murine macrophage; Spider biofilm repressed
orf19.1646	orf19.1646	2.58	1.88E-06	Ortholog(s) have rRNA primary transcript binding activity
orf19.3100	orf19.3100	2.58	6.42E-07	Protein with t-SNARE domains and a microtubule associated domain; Hap43-induced gene; repressed by alpha pheromone in SpiderM medium
RPS4A	orf19.5341	2.58	1.06E-05	Predicted ribosomal protein; repressed upon phagocytosis by murine macrophage; positively regulated by Tbf1; Spider biofilm repressed
RMS1	orf19.2654	2.58	2.04E-07	Putative lysine methyltransferase; Hap43-induced; protein induced during mating; possibly essential, disruptants not obtained by UAU1 method; rat catheter and Spider biofilm induced

RPL30	orf19.3788.1	2.58	1.55E-05	Ribosomal 60S subunit protein; pre-rRNA processing; pre-mRNA alternatively spliced to productive/unproductive transcripts; temp-regulated splicing; colony morphology-related regulation by Ssn6, Tup1, Nrg1 regulated; Spider biofilm repressed
EXO1	orf19.926	2.58	6.95E-06	Putative exodeoxyribonuclease; cell-cycle regulated periodic mRNA expression
orf19.6418	orf19.6418	2.58	8.22E-07	Ortholog(s) have role in ribosomal large subunit biogenesis and cytoplasm, nucleus localization
INO1	orf19.7585	2.58	1.46E-05	Inositol-1-phosphate synthase; antigenic in human; repressed by farnesol in biofilm or by caspofungin; upstream inositol/choline regulatory element; glycosylation predicted; rat catheter, flow model induced; Spider biofilm repressed
REI1	orf19.59	2.57	5.40E-06	Putative cytoplasmic pre-60S factor; Hap43-induced; repressed by prostaglandins
MAL2	orf19.7668	2.56	4.94E-06	Alpha-glucosidase; hydrolyzes sucrose for sucrose utilization; transcript regulated by Suc1, induced by maltose, repressed by glucose; Tn mutation affects filamentous growth; upregulated in RHE model; rat catheter and Spider biofilm induced
orf19.1833	orf19.1833	2.56	7.89E-05	Ortholog(s) have pseudouridine synthase activity, role in box H/ACA snoRNA 3'-end processing, rRNA pseudouridine synthesis, snRNA pseudouridine synthesis and 90S preribosome, box H/ACA snoRNP complex, cytosol localization
orf19.345	orf19.345	2.56	2.13E-02	Succinate semialdehyde dehydrogenase; for utilization of gamma-aminobutyrate (GABA) as a nitrogen source; part of 4-aminobutyrate and glutamate degradation pathways; rat catheter biofilm induced
orf19.7618	orf19.7618	2.55	1.77E-05	Putative nucleolar protein with a predicted role in pre-18S rRNA processing; Plc1p-regulated; Spider biofilm induced
ECM331	orf19.4255	2.55	9.85E-05	GPI-anchored protein; mainly at plasma membrane, also at cell wall; Hap43, caspofungin-induced; Plc1-regulated; Hog1, Rim101-repressed; colony morphology-related regulated by Ssn6; induced by ketoconazole and hypoxia
NOP1	orf19.3138	2.54	5.31E-04	Nucleolar protein; flucytosine induced; Hap43-induced; Spider biofilm repressed
RPS21	orf19.3334	2.54	5.35E-05	Protein component of the small (40S) subunit; repressed upon phagocytosis by murine macrophage; positively regulated by Tbf1; Spider biofilm repressed
orf19.2673	orf19.2673	2.54	1.26E-05	Ortholog(s) have role in DNA repair and Smc5-Smc6 complex, cytoplasm, nucleus localization
orf19.29	orf19.29	2.52	1.06E-04	Ortholog of S. cerevisiae Tah11, a DNA replication licensing factor required for pre-replication complex assembly; rat catheter, flow model and Spider biofilm induced
RPF1	orf19.2667	2.52	6.32E-04	Putative nucleolar protein with a predicted role in the assembly and export of the large ribosomal subunit; essential for growth; rat catheter and Spider biofilm induced
RPL18	orf19.5982	2.52	1.06E-04	Predicted ribosomal protein; Plc1p-regulated, Tbf1-activated; repressed upon phagocytosis by murine macrophage; Hap43p-induced; Spider biofilm repressed

GPX2	orf19.85	2.51	1.88E-04	Similar to glutathione peroxidase; induced in high iron; alkaline induced by Rim101; induced by alpha factor or interaction with macrophage; regulated by Efg1; caspofungin repressed; Spider biofilm induced
orf19.4793	orf19.4793	2.51	1.47E-06	Putative ribosome-associated protein; ortholog of S. cerevisiae Tma16; Hap43-induced gene; Spider biofilm induced
NMD3	orf19.706	2.51	2.15E-05	Putative nonsense-mediated mRNA decay protein; repressed in core stress response; repressed by prostaglandins
orf19.4492	orf19.4492	2.50	6.95E-06	Ortholog(s) have role in nuclear division, rRNA processing and mitotic spindle pole body, nuclear periphery, nucleolus, preribosome, large subunit precursor localization
DIM1	orf19.5010	2.50	1.83E-03	Putative 18S rRNA dimethylase; predicted role in rRNA modification and processing; Hap43-induced; likely to be essential for growth based on insertional mutagenesis strategy; F-12/CO2 early biofilm induced
DRG1	orf19.5083	2.50	3.96E-06	Member of the DRG family of GTP-binding proteins; involved in regulation of invasive filamentous growth
CLN3	orf19.1960	2.50	1.81E-05	G1 cyclin; depletion abolishes budding and causes hyphal growth defects; farnesol regulated, functional in S. cerevisiae; possibly essential (UAU1 method); other biofilm induced; Spider biofilm induced
CDC46	orf19.5487	2.49	3.02E-06	Putative hexameric MCM complex subunit; predicted role in control of cell division; periodic mRNA expression. peak at cell-cycle M/G1 phase; regulated by tyrosol, cell density, Plc1; repressed by alpha pheromone in SpiderM medium
orf19.95	orf19.95	2.49	2.18E-04	Ortholog of S. cerevisiae : PRM5, C. dubliniensis CD36 : Cd36_60980, C. parapsilosis CDC317 : CPAR2_603060, Candida tenuis NRRL Y-1498 : CANTEDRAFT_113703 and Debaryomyces hansenii CBS767 : DEHA2F10032g
orf19.512	orf19.512	2.49	3.93E-03	Ortholog of S. cerevisiae Kre33; essential; S. cerevisiae ortholog is essential and is required for biogenesis of the small ribosomal subunit
orf19.6886	orf19.6886	2.49	4.00E-04	Ortholog(s) have rRNA binding activity, role in maturation of LSU-rRNA from tricistronic rRNA transcript (SSU-rRNA, 5.8S rRNA, LSU-rRNA), ribosomal large subunit export from nucleus and nucleolus localization
orf19.6477	orf19.6477	2.48	4.46E-05	Ortholog(s) have tRNA (guanine-N7-)-methyltransferase activity, role in tRNA methylation and cytosol, nucleus, tRNA methyltransferase complex localization
orf19.1486	orf19.1486	2.48	6.48E-04	Protein with a life-span regulatory factor domain; regulated by Sef1, Sfu1, and Hap43; flow model biofilm induced; Spider biofilm induced
SDA1	orf19.6648	2.48	2.52E-04	Predicted nuclear protein involved in actin cytoskeleton organization, passage through Start, 60S ribosome biogenesis; rat catheter biofilm induced; Hap43-induced
SIK1	orf19.7569	2.48	5.80E-07	Putative U3 snoRNP protein; Hap43p-induced gene; physically interacts with TAP-tagged Nop1p

orf19.3463	orf19.3463	2.47	4.78E-06	Putative GTPase; role in 60S ribosomal subunit biogenesis; Spider biofilm induced
MRT4	orf19.5550	2.47	3.03E-06	Putative mRNA turnover protein; Hap43-induced; mutation confers hypersensitivity to tubercidin (7-deazaadenosine); rat catheter biofilm induced
orf19.6996	orf19.6996	2.47	1.99E-05	Predicted mannosyltransferase; Hap43-repressed; Spider biofilm induced
TBF1	orf19.801	2.46	6.95E-04	Essential transcription factor; induces ribosomal protein genes and the rDNA locus; acts with Cbf1 at subset of promoters; recruits Fhl1 and Ifh1 to promoters; role is analogous to that of S. cerevisiae Rap1; Spider biofilm induced
orf19.3481	orf19.3481	2.44	1.37E-06	Putative mitochondrial ATP-dependent RNA helicase of the DEAD-box family, transcription is activated in the presence of elevated CO2
orf19.1687	orf19.1687	2.43	2.48E-06	Ortholog of S. cerevisiae Prp43, an RNA helicase in the DEAH-box family that functions in both RNA polymerase I and polymerase II transcript metabolism; Hap43-induced gene
RPS22A	orf19.6265	2.43	1.52E-04	Predicted ribosomal protein; repressed upon phagocytosis by murine macrophage; Spider biofilm repressed
SUR2	orf19.5818	2.43	2.16E-06	Putative ceramide hydroxylase; predicted enzyme of sphingolipid biosynthesis; regulated by Tsa1, Tsa1B under H2O2 stress conditions; Spider and flow model biofilm induced
CTP1	orf19.5870	2.43	1.67E-06	Putative citrate transport protein; flucytosine induced; amphotericin B repressed, caspofungin repressed; Hap43p-induced gene
HUT1	orf19.6803	2.42	1.00E-03	Ortholog(s) have UDP-galactose transmembrane transporter activity, role in UDP-galactose transmembrane transport, UDP-glucose transport, regulation of protein folding in endoplasmic reticulum and endoplasmic reticulum localization
ADE8	orf19.5789	2.42	7.07E-06	Putative phosphoribosylglycinamide formyl-transferase, enzyme of amino acid biosynthesis pathway; upregulated in biofilm; S. cerevisiae ortholog is Gcn4p regulated; protein enriched in stationary phase yeast-form cultures
ECM1	orf19.5299	2.41	7.61E-05	Putative pre-ribosomal factor; decreased mRNA abundance observed in cyr1 homozygous mutant hyphae; induced by heavy metal (cadmium) stress; Hog1p regulated
orf19.1122	orf19.1122	2.41	4.99E-05	Protein of unknown function; induced by alpha pheromone in SpiderM medium; Spider biofilm induced
UTP13	orf19.4268	2.39	2.94E-05	Putative U3 snoRNA-associated protein; Hap43-induced; repressed in core stress response; physically interacts with TAP-tagged Nop1
orf19.4375	orf19.4375	2.39	3.67E-05	Ortholog(s) have S-adenosylmethionine-dependent methyltransferase activity, role in chromatin silencing at rDNA, nicotinamide metabolic process and cytosol localization
orf19.3354	orf19.3354	2.39	1.77E-02	Ortholog(s) have structural constituent of ribosome activity and 90S preribosome, cytosolic small ribosomal subunit, nucleolus localization

RPS9B	orf19.838.1	2.38	1.87E-06	Predicted ribosomal protein; repressed upon phagocytosis by murine macrophage; transcript possibly regulated upon hyphal formation; Spider biofilm repressed
orf19.1116	orf19.1116	2.38	3.93E-04	Protein of unknown function; planktonic growth-induced gene
orf19.6737	orf19.6737	2.37	3.16E-04	Protein of unknown function; mutants are viable; induced in a cyr1, ras1, or efg1 homozygous null
orf19.4149.1	orf19.4149.1	2.37	2.99E-05	Protein component of the small (40S) ribosomal subunit; Spider biofilm repressed
IFH1	orf19.4282	2.37	1.38E-04	Transcription factor; forms a heterodimer with Fhl11 that is tethered to promoters by Tbf1; positively regulates rRNA and ribosomal protein gene transcription; Spider biofilm induced
RNR21	orf19.5801	2.34	7.32E-06	Ribonucleoside-diphosphate reductase; regulated by tyrosol and cell density; ciclopirox olamine, fluconazole or flucytosine induced; regulated by Sef1, Sfu1, and Hap43
GDA1	orf19.7394	2.34	4.39E-05	Golgi membrane GDPase, required for wild-type O-mannosylation, not N-glycosylation; required for wild-type hyphal induction, cell wall, and cell surface charge; not required for HeLa cell adherence; functional homolog of S. cerevisiae Gda1p
BUD21	orf19.5430	2.34	9.81E-06	Small-subunit processome component; repressed by prostaglandins
URA7	orf19.3941	2.34	1.25E-04	CTP synthase 1; flucytosine induced; protein present in exponential and stationary growth phase yeast cultures
TIF5	orf19.4261	2.34	7.54E-07	Putative translation initiation factor; repressed upon phagocytosis by murine macrophage; Spider biofilm repressed
orf19.4900	orf19.4900	2.34	7.69E-06	Ortholog(s) have alpha-1,3-mannosyltransferase activity and role in protein O-linked glycosylation
orf19.7664	orf19.7664	2.34	7.43E-06	Ortholog(s) have nucleolus localization
orf19.4563	orf19.4563	2.33	5.52E-06	Protein of unknown function; repressed by prostaglandins; Hap43-induced, Spider biofilm induced
orf19.6220.4	orf19.6220.4	2.33	1.74E-04	Ribosomal 60S subunit protein; Spider biofilm repressed
ATO1	orf19.6169	2.33	2.15E-05	Putative fungal-specific transmembrane protein; induced by Rgt1; Spider biofilm induced
PDR17	orf19.5839	2.32	1.32E-05	Fungal-specific protein (no human or murine homolog); role in sensitivity to fluconazole, specifically
orf19.6291	orf19.6291	2.32	7.62E-07	Ortholog(s) have DNA binding, DNA-dependent ATPase activity, chromatin binding activity
orf19.4835	orf19.4835	2.32	3.29E-05	Ortholog(s) have role in endonucleolytic cleavage in 5'-ETS of tricistronic rRNA transcript (SSU-rRNA, 5.8S rRNA and LSU-rRNA), more

DIP2	orf19.5106	2.32	9.57E-06	Putative small ribonucleoprotein complex; Tn mutation affects filamentous growth; physically interacts with TAP-tagged Nop1; heterozygous null mutant exhibits resistance to parnafungin; Hap43-induced gene; Spider biofilm induced
APN2	orf19.1836	2.32	1.72E-06	Putative class II abasic (AP) endonuclease; flucytosine induced
SPB4	orf19.6298	2.31	4.20E-06	Putative ATP-dependent RNA helicase; flucytosine repressed; Spider biofilm induced
MCD1	orf19.7634	2.31	3.67E-06	Alpha-kleisin cohesin complex subunit; for sister chromatid cohesion in mitosis and meiosis; repressed by alpha pheromone in SpiderM medium; periodic cell-cycle expression; Hap43-repressed; rat catheter and Spider biofilm repressed
orf19.7552	orf19.7552	2.31	1.20E-05	Putative U3-containing small subunit processome complex protein; Hap43-induced gene; repressed in core stress response; Spider biofilm induced
NOP14	orf19.5959	2.31	1.01E-03	Putative nucleolar protein; Hap43-induced; mutation confers resistance to 5-fluorocytosine (5-FC), 5-fluorouracil (5-FU), and tubercidin (7-deazaadenosine); heterozygous mutant is resistant to parnafungin; Spider biofilm induced
RAD53	orf19.6936	2.30	7.90E-06	Protein involved in regulation of DNA-damage-induced filamentous growth; putative component of cell cycle checkpoint; ortholog of S. cerevisiae Rad53p, protein kinase required for cell-cycle arrest in response to DNA damage
CDC13	orf19.6072	2.30	2.07E-04	Essential protein with similarity to S. cerevisiae Cdc13p, involved in telomere maintenance
ERF1	orf19.3541	2.30	3.32E-06	Putative translation release factor 1, which interacts with stop codons and promotes release of nascent peptides from ribosomes; Hap43p-induced gene
orf19.6526	orf19.6526	2.30	2.88E-06	Ortholog(s) have COPI-coated vesicle, Golgi apparatus localization
NIP1	orf19.4635	2.29	6.74E-05	Putative translation initiation factor; mutation confers hypersensitivity to roridin A and verrucarin A; genes encoding ribosomal subunits, translation factors, and tRNA synthetases are downregulated upon phagocytosis by murine macrophage
RRP8	orf19.3630	2.28	9.16E-04	Ribosomal protein; Hap43-induced; F-12/CO2 early biofilm and rat catheter biofilm induced
DEF1	orf19.7561	2.28	2.30E-05	RNA polymerase II regulator; role in filamentation, epithelial cell escape, dissemination in RHE model; induced by fluconazole, high cell density; Efg1/hyphal regulated; role in adhesion, hyphal growth on solid media; Spider biofilm induced
ZCF3	orf19.1168	2.28	1.14E-04	Zn(II)2Cys6 domain transcription factor; required for filamentous growth, resistance to rapamycin and flucytosine; possibly an essential gene, disruptants not obtained by UAU1 method; Hap43-repressed; Spider and flow model biofilm induced
ERG12	orf19.4809	2.28	1.49E-05	Ortholog(s) have mevalonate kinase activity and role in ergosterol biosynthetic process, farnesyl diphosphate biosynthetic process, mevalonate pathway, isopentenyl diphosphate biosynthetic process, mevalonate pathway

orf19.6840	orf19.6840	2.28	1.68E-03	Protein of unknown function; transcript detected in high-resolution tiling arrays; transcription induced by alpha pheromone in SpiderM medium; Spider and early-stage flow model biofilm induced
SER2	orf19.5838	2.27	6.09E-06	Ortholog(s) have phosphoserine phosphatase activity, role in L-serine biosynthetic process and cytoplasm, nucleus localization
DPB2	orf19.7564	2.27	3.55E-05	Probable subunit of DNA polymerase II (DNA polymerase epsilon), similar to S. cerevisiae Dpb2p; essential for viability; rat catheter biofilm induced
orf19.500	orf19.500	2.26	3.72E-05	Ortholog(s) have tRNA (adenine-N1-)-methyltransferase activity, role in tRNA methylation and nucleus, tRNA (m1A) methyltransferase complex localization
orf19.3798	orf19.3798	2.26	1.19E-05	Ortholog(s) have tRNA (guanine-N7-)-methyltransferase activity, role in tRNA methylation and nucleolus, tRNA methyltransferase complex localization
orf19.1697	orf19.1697	2.25	1.55E-03	Ortholog(s) have role in cytoplasmic translation and cytoplasm, polysomal ribosome localization
orf19.3124	orf19.3124	2.25	3.19E-06	Ortholog(s) have mRNA binding, metalloaminopeptidase activity, role in negative regulation of gene expression, protein initiator methionine removal involved in protein maturation and cytosolic ribosome, nucleolus localization
orf19.6355	orf19.6355	2.24	4.44E-05	Ortholog(s) have role in ribosome biogenesis and cytosol, nucleolus localization
orf19.1708	orf19.1708	2.24	3.74E-06	Protein of unknown function; Spider biofilm induced
orf19.1305	orf19.1305	2.23	4.91E-06	Ortholog(s) have tRNA (guanine) methyltransferase activity, role in tRNA methylation and mitochondrial matrix, nucleus localization
GPD1	orf19.1756	2.23	5.14E-06	Glycerol-3-phosphate dehydrogenase; glycerol biosynthesis; regulated by Efg1; regulated by Tsa1, Tsa1B under H2O2 stress conditions; Sflow model and Spider biofilm induced
SUI2	orf19.6213	2.23	1.20E-05	Translation initiation factor eIF2, alpha chain; genes encoding ribosomal subunits, translation factors, and tRNA synthetases are downregulated upon phagocytosis by murine macrophage; stationary phase enriched protein
orf19.5049	orf19.5049	2.22	1.11E-06	Putative U3-containing 90S preribosome processome complex subunit; Hap43-induced gene; rat catheter and Spider biofilm induced; F-12/CO2 early biofilm induced
SWI6	orf19.4725	2.21	1.72E-06	Putative component of the MBF and SBF transcription complexes involved in G1/S cell-cycle progression; periodic mRNA expression, peak at cell-cycle G1/S phase
FTR2	orf19.7231	2.21	2.48E-04	High-affinity iron permease; probably interacts with ferrous oxidase; regulated by iron level, ciclopirox olamine, amphotericin B, caspofungin; complements S. cerevisiae ftr1 iron transport defect; Hap43-repressed; Spider biofilm induced
orf19.501	orf19.501	2.21	1.17E-03	Ortholog(s) have nucleus, preribosome, large subunit precursor localization
orf19.3304	orf19.3304	2.20	1.71E-05	Exosome non-catalytic core component; involved in 3'-5' RNA processing and degradation in the nucleus and cytoplasm; Spider biofilm induced

CAN3	orf19.84	2.20	3.58E-03	Predicted amino acid transmembrane transporter; transcript regulated by white-opaque switch; Hap43-repressed gene
orf19.4792	orf19.4792	2.20	1.42E-04	Protein with a regulator of G-protein signaling domain; Plc1-regulated; Spider biofilm induced; rat catheter biofilm repressed
orf19.5934	orf19.5934	2.19	1.50E-04	Ortholog(s) have DNA topoisomerase type I activity
CDC21	orf19.3549	2.18	4.21E-05	Putative thymidylate synthase; flucytosine induced; rat catheter biofilm repressed; Spider biofilm repressed
orf19.823	orf19.823	2.18	5.27E-06	Protein of unknown function; Spider biofilm induced
ERG2	orf19.6026	2.18	3.62E-05	C-8 sterol isomerase; enzyme of ergosterol biosynthesis; converts fecosterol to episterol; mutant is hypersensitive to multiple drugs; ketoconazole-induced; flow model and Spider biofilm repressed
RPS24	orf19.5466	2.17	8.46E-03	Predicted ribosomal protein; hyphal downregulated; repressed upon phagocytosis by murine macrophage; transcriptionally activated by Tbf1; Spider biofilm repressed
IDI1	orf19.2775	2.16	2.75E-06	Ortholog(s) have isopentenyl-diphosphate delta-isomerase activity, role in farnesyl diphosphate biosynthetic process and cytosol, nucleus localization
ILV2	orf19.1613	2.16	9.76E-07	Putative acetolactate synthase; regulated by Gcn4p; induced by amino acid starvation (3-AT treatment); stationary phase enriched protein
STP4	orf19.909	2.16	1.09E-04	C2H2 transcription factor; induced in core caspofungin response; colony morphology-related gene regulation by Ssn6; induced by 17-beta-estradiol, ethynyl estradiol; rat catheter and Spider biofilm induced
orf19.4030	orf19.4030	2.16	1.43E-05	Ortholog(s) have DNA primase activity, single-stranded DNA binding activity, role in DNA replication, synthesis of RNA primer, telomere maintenance and alpha DNA polymerase:primase complex localization
RPL43A	orf19.3942.1	2.15	8.80E-06	Putative ribosomal protein, large subunit; repressed by human whole blood or PMNs; colony morphology-related gene regulation by Ssn6; Spider biofilm repressed
orf19.5207	orf19.5207	2.15	3.92E-06	Predicted diphthamide biosynthesis protein; Spider biofilm induced
SMC6	orf19.6568	2.15	2.01E-04	Putative structural maintenance of chromosomes (SMC) protein; Hap43-induced; cell-cycle regulated periodic mRNA expression; S. cerevisiae ortholog not cell-cycle regulated; Spider biofilm induced
RPS19A	orf19.5996.1	2.15	4.23E-04	Putative ribosomal protein S19; protein level decreases in stationary phase cultures; Spider biofilm repressed
ASC1	orf19.6906	2.15	3.32E-06	40S ribosomal subunit similar to G-beta subunits; glucose or N starvation induced filamentation; required for virulence in mice; snoRNA snR24 encoded in ASC1 intron; repressed in stationary phase; GlcNAc-induced; Spider biofilm repressed

ACC1	orf19.7466	2.15	2.41E-04	Putative acetyl-coenzyme-A carboxylases; regulated by Efg1; amphotericin B repressed; caspofungin repressed; 5'-UTR intron; gene used for strain identification by multilocus sequence typing; Hap43-induced; flow model biofilm repressed
MAL31	orf19.3981	2.15	2.33E-04	Putative high-affinity maltose transporter; transcript is upregulated in clinical isolates from HIV+ patients with oral candidiasis; alkaline induced; Spider biofilm induced
BUD22	orf19.3287	2.15	2.74E-05	Protein with a predicted role in 18S rRNA maturation and small ribosomal subunit biogenesis; repressed in core stress response; repressed by prostaglandins
orf19.5126	orf19.5126	2.15	9.23E-05	Putative adhesin-like protein
orf19.813	orf19.813	2.14	1.67E-06	Protein of unknown function; mutants are viable; Hap43-induced gene; oxidative stress-induced via Cap1; rat catheter and Spider biofilm induced
orf19.6882.1	orf19.6882.1	2.14	2.85E-06	Ribosomal 60S subunit protein; Spider biofilm repressed
ARO3	orf19.1517	2.14	1.04E-04	3-deoxy-D-arabinoheptulosonate-7-phosphate synthase; aromatic amino acid synthesis; GCN-regulated; feedback-inhibited by phe if expressed in S. cerevisiae; decreased in stationary phase; flow model biofilm repressed
orf19.6813	orf19.6813	2.14	6.44E-05	Protein of unknown function; Hap43-induced gene
RPL15A	orf19.493	2.14	6.40E-05	Putative ribosomal protein; repressed upon phagocytosis by murine macrophage; positively regulated by Tbf1; Spider biofilm repressed
PEA2	orf19.1835	2.14	1.79E-06	Putative coiled-coil polarisome; predicted role in polarized morphogenesis, cell fusion, and low affinity Ca2+ influx; rat catheter biofilm induced
orf19.5517	orf19.5517	2.13	1.35E-05	Similar to alcohol dehydrogenases; induced by benomyl treatment, nitric oxide; induced in core stress response; oxidative stress-induced via Cap1; Spider biofilm repressed
orf19.2489	orf19.2489	2.13	2.30E-05	Putative karyopherin beta; repressed by nitric oxide
CAR1	orf19.3934	2.13	2.28E-05	Arginase; arginine catabolism; transcript regulated by Nrg1, Mig1, Tup1; colony morphology-related regulation by Ssn6; alkaline induced; protein decreased in stationary phase; sumoylation target; flow model biofilm induced
orf19.3797	orf19.3797	2.13	2.20E-04	Ortholog(s) have structural constituent of ribosome activity and mitochondrial large ribosomal subunit localization
orf19.3470	orf19.3470	2.12	1.12E-05	Putative flavodoxin; similar to S. cerevisiae Tyw1, an iron-sulfer protein required for synthesis of Wybutosine modified tRNA; predicted Kex2 substrate; Spider biofilm induced
UAP1	orf19.4265	2.12	1.00E-04	UDP-N-acetylglucosamine pyrophosphorylase, catalyzes biosynthesis of UDP-N-acetylglucosamine from UTP and N-acetylglucosamine 1-phosphate; functional homolog of S. cerevisiae Qri1p; alkaline upregulated

FAD3	orf19.4933	2.12	1.51E-05	Omega-3 fatty acid desaturase; production of alpha-linolenic acid, a major component of membranes; caspofungin induced; Plc1-regulated; colony morphology-related gene regulation by Ssn6; Spider biofilm induced, flow model biofilm repressed
KRE1	orf19.4377	2.11	1.77E-05	Cell wall glycoprotein; beta glucan synthesis; increases glucan content in S. cerevisiae kre1, complements killer toxin sensitivity; caspofungin induced; Spider/rat catheter/flow model biofilm induced; Bcr1-repressed in RPMI a/a biofilms
orf19.915	orf19.915	2.11	1.81E-05	Protein of unknown function; Spider biofilm induced
TRP3	orf19.5243	2.11	3.91E-06	Putative bifunctional enzyme with predicted indole-3-glycerol-phosphate synthase and anthranilate synthase activities; regulated by Gcn2p and Gcn4p
MUP1	orf19.5280	2.11	1.39E-02	Putative high affinity methionine permease; alkaline upregulated by Rim101; Spider biofilm induced
HSL1	orf19.4308	2.10	6.36E-05	Probable protein kinase involved in determination of morphology during the cell cycle of both yeast-form and hyphal cells via regulation of Swe1p and Cdc28p; required for full virulence and kidney colonization in mouse systemic infection
orf19.2930	orf19.2930	2.10	2.71E-03	Predicted translation initiation factor; role in translational initiation; Spider biofilm repressed
orf19.7291	orf19.7291	2.09	2.19E-04	Ortholog(s) have tRNA (adenine-N1-)-methyltransferase activity, role in tRNA methylation and cytosol, nucleus, tRNA (m1A) methyltransferase complex localization
GIT2	orf19.1978	2.09	6.47E-06	Putative glycerophosphoinositol permease; fungal-specific; repressed by alpha pheromone in SpiderM medium; Hap43-repressed; Spider biofilm induced
ERG6	orf19.1631	2.09	1.38E-04	Delta(24)-sterol C-methyltransferase, converts zymosterol to fecosterol, ergosterol biosynthesis; mutation confers nystatin resistance; Hap43, GlcNAc-, fluconazole-induced; upregulated in azole-resistant strain; Spider biofilm repressed
orf19.4161	orf19.4161	2.09	8.05E-04	Ortholog(s) have role in DNA repair and Smc5-Smc6 complex, nucleus localization
orf19.7422	orf19.7422	2.09	3.26E-06	Ortholog(s) have RNA binding activity and nucleus localization
MPS1	orf19.7293	2.09	1.10E-05	Monopolar spindle protein, a putative kinase; essential for growth; periodic mRNA expression, peak at cell-cycle S/G2 phase
CNS1	orf19.6052	2.08	5.98E-04	Putative co-chaperone; Hap43p-induced gene; mutation confers hypersensitivity to radicicol
orf19.4069	orf19.4069	2.07	3.04E-03	Protein of unknown function; repressed by alpha pheromone in SpiderM medium
orf19.7215	orf19.7215	2.07	1.96E-06	Nucleolar protein; component of the small subunit processome containing the U3 snoRNA; involved in pre-18S rRNA processing; flow model biofilm repressed
NCE103	orf19.1721	2.07	4.67E-04	Carbonic anhydrase; converts of CO2 to bicarbonate; essential for virulence in host niches with limited CO2, normal white-opaque switch; Mnl1-induced in weak acid stress; Hap43-induced gene; F-12/CO2, rat catheter, Spider biofilm induced
orf19.5169	orf19.5169	2.07	2.42E-03	Ortholog(s) have cytosol, nucleus localization

orf19.2017	orf19.2017	2.06	3.70E-05	Ortholog(s) have RNA polymerase I activity and role in regulation of cell size, transcription elongation from RNA polymerase I promoter, transcription of nuclear large rRNA transcript from RNA polymerase I promoter
YHB5	orf19.3710	2.06	1.07E-03	Flavohemoglobin-related protein; not required for normal NO resistance; predicted globin/FAD-binding/NAD(P)-binding domains but lacks some conserved residues of flavohemoglobins; filament induced; rat catheter and Spider biofilm induced
RPS13	orf19.4193.1	2.06	1.62E-06	Putative ribosomal protein of the small subunit
orf19.1404	orf19.1404	2.06	1.30E-05	Predicted tRNA dihydrouridine synthase; Spider biofilm induced
RPC19	orf19.172	2.05	5.16E-06	Putative RNA polymerases I and III subunit AC19; Hap43-induced; rat catheter biofilm induced
UBI3	orf19.3087	2.04	2.46E-05	Fusion of ubiquitin with the S34 protein of the small ribosomal subunit; mRNA decreases upon heat shock, appears to be degraded; functional homolog of S. cerevisiae RPS31; Hap43-induced; Spider biofilm repressed
VRG4	orf19.1232	2.04	3.06E-04	GDP-mannose transporter; essential; required for glycosylation, hyphal growth; functional homolog of S. cerevisiae Vrg4p, which imports GDP-mannose from cytoplasm to Golgi for protein and lipid mannosylation; no mammalian homolog
PGA45	orf19.2451	2.03	4.15E-04	Putative GPI-anchored cell wall protein; repressed in core caspofungin response; Hog1-induced; regulated by Ssn6; Mob2-dependent hyphal regulation; flow model biofilm induced
RPS18	orf19.7018	2.03	2.26E-04	Predicted ribosomal protein; repressed upon phagocytosis by murine macrophage; repressed by nitric oxide; Hap43-induced; Spider biofilm repressed
FUN12	orf19.5081	2.02	2.26E-06	Functional homolog of S. cerevisiae Fun12 translation initiation factor eIF5B; genes encoding ribosomal subunits, translation factors, and tRNA synthetases are downregulated upon phagocytosis by murine macrophage
DBF4	orf19.5166	2.02	2.27E-04	Putative Cdc7p-Dbf4p kinase complex regulatory subunit; Hap43p-induced gene; macrophage/pseudohyphal-repressed; cell-cycle regulated periodic mRNA expression; S. cerevisiae ortholog is not cell-cycle regulated
PGA6	orf19.4765	2.02	3.33E-03	GPI-anchored cell wall adhesin-like protein; induced by high iron; upregulated upon Als2 depletion; mRNA binds She3 and is localized to hyphal tips; Spider biofilm repressed
NDT80	orf19.2119	2.02	7.54E-06	Ortholog of Ndt80; meiosis-specific transcription factor; activator of CDR1 induction by antifungal drugs; required for wild-type drug resistance and for Spider biofilm formation; transcript induced by antifungal drug treatment
orf19.773	orf19.773	2.01	1.10E-05	Protein similar to S. cerevisiae Rsa3 predicted nucleolar protein involved in maturation of pre-60S ribosomal particles; rat catheter and Spider biofilm induced

orf19.3902	orf19.3902	2.01	2.30E-05	Protein of unknown function; repressed by fluphenazine treatment or in an azole-resistant strain that overexpresses CDR1 and CDR2; Spider biofilm induced
MCM3	orf19.1901	2.01	4.21E-03	Putative DNA replication protein; periodic mRNA expression, peak at cell-cycle M/G1 phase; Spider biofilm induced
MAK21	orf19.5912	2.01	2.84E-04	Putative 66S pre-ribosomal particle subunit; mutation confers hypersensitivity to tubercidin (7-deazaadenosine)
SSF1	orf19.6589	2.01	1.12E-05	Protein involved in ribosome biogenesis; ortholog of S. cerevisiae Ssf1; Hap43-induced; rat catheter and Spider biofilm induced
RIO2	orf19.6369	2.00	6.49E-06	Putative serine kinase with a predicted role in the processing of the 20S pre-rRNA into mature 18S rRNA; null mutants are hypersensitive to caspofungin
orf19.3037	orf19.3037	2.00	1.91E-05	Putative poly(A)-binding protein; regulated by Gcn4p; induced in response to amino acid starvation (3-AT treatment); protein present in exponential and stationary growth phase yeast cultures
NAT4	orf19.4664	2.00	1.30E-04	Putative histone acetyltransferase; involved in regulation of white-opaque switch; early-stage flow model biofilm induced; Spider biofilm induced
IMP4	orf19.603	1.99	3.46E-03	Putative SSU processome component; Hap43-induced; repressed by prostaglandins; Spider biofilm induced
PBR1	orf19.6274	1.99	1.86E-05	Protein of unknown function; required for cohesion, adhesion, and RPMI biofilm formation; induced by alpha pheromone in white cells; fluconazole-induced; Spider biofilm induced
THR1	orf19.923	1.99	1.65E-04	Putative homoserine kinase; regulated by Tup1; amphotericin B repressed; regulated by Gcn2 and Gcn4; Spider biofilm repressed
PDS5	orf19.2216	1.99	1.27E-05	Putative protein with a predicted role in establishment and maintenance of sister chromatid condensation and cohesion; cell-cycle regulated periodic mRNA expression
YOX1	orf19.7017	1.98	6.48E-03	Putative homeodomain-containing transcription factor; transcriptional repressor; periodic mRNA expression, peak at cell-cycle G1/S phase
RPL35	orf19.5964.2	1.98	2.99E-05	Ribosomal protein; downregulation correlates with clinical development of fluconazole resistance; colony morphology-related gene regulation by Ssn6; Hap43-induced; Spider biofilm repressed
RPL12	orf19.1635	1.98	2.10E-05	Ribosomal protein L12, 60S ribosomal subunit; downregulated by human whole blood or polymorphonuclear cells; genes encoding cytoplasmic ribosomal subunits are downregulated upon phagocytosis by macrophage; Tbf1p-activated; Hap43p-induced
orf19.3556	orf19.3556	1.97	1.55E-06	Transportin or cytosolic karyopherin beta; Spider biofilm induced
ERG25	orf19.3732	1.97	1.81E-05	Putative C-4 methyl sterol oxidase; C4-demethylation of ergosterol biosynthesis intermediates, based on similarity to S. cerevisiae Erg25; fluconazole-induced; induced in azole-resistant strain; rat catheter and Spider biofilm induced

orf19.158	orf19.158	1.97	2.41E-04	Ortholog of S. cerevisiae Apd1; required for normal localization of actin patches and normal tolerance of sodium ions and hydrogen peroxide; Hap43-induced; Spider biofilm induced
VAS1	orf19.1295	1.97	1.01E-04	Putative tRNA-Val synthetase; genes encoding ribosomal subunits, translation factors, and tRNA synthetases are downregulated upon phagocytosis by murine macrophage
BRG1	orf19.4056	1.97	3.18E-05	Transcription factor; recruits Hda1 to hypha-specific promoters; Tn mutation affects filamentation; Hap43-repressed; Spider and flow model biofilm induced; required for Spider biofilm formation; Bcr1-repressed in RPMI a/a biofilms
ARO2	orf19.1986	1.97	4.99E-06	Putative chorismate synthase; fungal-specific (no human or murine homolog); protein level decreased in stationary phase yeast cultures; GlcNAc-induced protein
RPS21B	orf19.3325.3	1.97	5.55E-05	Ribosomal protein S21; regulated by Nrg1, Tup1; colony morphology-related gene regulation by Ssn6; positively regulated by Tbf1, Hap43; Spider biofilm repressed
RNR22	orf19.1868	1.97	6.45E-04	Putative ribonucleoside diphosphate reductase;colony morphology-related gene regulation by Ssn6; transcript regulated by tyrosol and cell density; Hap43-repressed; Spider biofilm induced
orf19.687	orf19.687	1.96	5.41E-04	Ortholog of C. dubliniensis CD36 : Cd36_62090, C. parapsilosis CDC317 : CPAR2_602150, Candida tenuis NRRL Y-1498 : CANTEDRAFT_112751 and Debaryomyces hansenii CBS767 : DEHA2F11814g
MCM6	orf19.2611	1.96	1.44E-04	Putative MCM DNA replication initiation complex component; mRNA expression peak at cell-cycle M/G1 phase; regulated by tyrosol and cell density; repressed by alpha pheromone in SpiderM medium; Hap43-induced gene
orf19.1834	orf19.1834	1.96	4.15E-04	Ortholog of C. dubliniensis CD36 : Cd36_09960, C. parapsilosis CDC317 : CPAR2_212580, Debaryomyces hansenii CBS767 : DEHA2G11770g and Pichia stipitis Pignal : PICST_51041
RPL38	orf19.2111.2	1.96	1.56E-04	60S ribosomal ribosomal protein subunit; genes encoding cytoplasmic ribosomal subunits, translation factors, tRNA synthetases are downregulated upon phagocytosis by murine macrophage
orf19.1830	orf19.1830	1.96	3.80E-04	Protein of unknown function; Hap43-induced; rat catheter and Spider biofilm induced
orf19.2362	orf19.2362	1.94	2.61E-04	Putative 90S preribosome component; Hap43p-induced gene; possibly an essential gene, disruptants not obtained by UAU1 method
orf19.809	orf19.809	1.94	1.01E-05	Ortholog(s) have role in maturation of LSU-rRNA from tricistronic rRNA transcript (SSU-rRNA, 5.8S rRNA, LSU-rRNA) and nucleolus, preribosome localization
NMD5	orf19.4188	1.93	1.35E-04	Karyopherin; carrier protein involved in nuclear import of proteins; repressed in core stress response; Hap43-induced; Spider biofilm induced
orf19.7425	orf19.7425	1.93	2.20E-04	Ortholog(s) have uracil DNA N-glycosylase activity, role in DNA repair and mitochondrion, nucleus localization

KTI11	orf19.6873.1	1.93	7.83E-04	Zn-ribbon protein; required for synthesis of diphthamide on translation factor eEF2; involved in modification of wobble nucleosides in tRNAs; rat catheter and Spider biofilm induced
RPL23A	orf19.3504	1.93	7.48E-05	Ribosomal protein; downregulated upon phagocytosis by murine macrophage; Hap43-induced; sumoylation target; Spider biofilm repressed
RPL5	orf19.6541	1.93	1.47E-02	Ribosomal protein; repressed upon phagocytosis by murine macrophages; Hap43-induced; Spider biofilm repressed
orf19.5020	orf19.5020	1.92	2.84E-05	Protein of unknown function; Hap43-induced; Spider biofilm induced
orf19.1447	orf19.1447	1.92	4.53E-04	Ortholog of C. dubliniensis CD36 : Cd36_16290, C. parapsilosis CDC317 : CPAR2_214050, Candida tenuis NRRL Y-1498 : CANTEDRAFT_92180 and Debaryomyces hansenii CBS767 : DEHA2A01738g
RPS3	orf19.6312	1.92	4.37E-03	Ribosomal protein S3; Hog1, Hap43-induced; grepressed upon phagocytosis by murine macrophage; present in exponential and stationary phase cells; Spider biofilm repressed
orf19.5308	orf19.5308	1.92	6.90E-05	Protein of unknown function; induced by Rgt1
WOR2	orf19.5992	1.91	9.54E-05	Zn(II)2Cys6 transcription factor; regulator of white-opaque switching; required for maintenance of opaque state; Hap43-induced
FEN1	orf19.6343	1.90	7.07E-05	Putative fatty acid elongase; predicted role in sphingolipid biosynthesis; possibly an essential gene, disruptants not obtained by UAU1 method; Spider and flow model biofilm induced
orf19.2308	orf19.2308	1.90	1.68E-03	Putative 6-phosphofructo-2-kinase; catalyzes synthesis of fructose-2,6-bisphosphate; Hap43-repressed; flow model, rat catheter and Spider biofilm induced
RPL6	orf19.3003.1	1.90	1.41E-05	Ortholog of S. cerevisiae ribosomal subunit, Rpl6B; transposon mutation affects filamentous growth; translation-related genes are downregulated upon phagocytosis by murine macrophage; Hap43-induced; Spider biofilm repressed
TIF35	orf19.7236	1.89	9.62E-05	Putative translation initiation factor; repressed upon phagocytosis by murine macrophage; Spider biofilm repressed
RPO26	orf19.2643	1.89	7.89E-05	Putative RNA polymerase subunit; heterozygous null mutant exhibits resistance to parnafungin in the C. albicans fitness test
PTP3	orf19.7610	1.89	1.06E-05	Putative protein tyrosine phosphatase; hypha induced; alkaline induced; regulated by Efg1, Ras1, cAMP pathways; mutants are viable; Spider biofilm induced; rat catheter biofilm repressed; flow model biofilm repressed
orf19.3854	orf19.3854	1.89	1.13E-05	Ortholog of S. cerevisiae Sat4; amphotericin B induced; clade-associated gene expression; Spider biofilm induced
orf19.6556	orf19.6556	1.89	1.04E-04	Protein of unknown function; rat catheter, flow model and Spider biofilm induced

HMT1	orf19.3291	1.89	4.27E-03	Major type I protein arginine methyltransferases (PRMT); involved in asymmetric dimethylation of arginine residues; involved in nuclear export of Npl3; Spider biofilm repressed
ZUO1	orf19.2709	1.89	4.45E-06	Ortholog of S. cerevisiae Zuo1; a cytosolic ribosome-associated chaperone; likely to be essential for growth, based on an insertional mutagenesis strategy; Spider biofilm repressed
SSZ1	orf19.3812	1.89	8.99E-06	Putative HSP70 chaperone; protein level decreases in stationary phase cultures; Spider biofilm repressed
RPL29	orf19.2310.1	1.89	1.30E-03	Ribosomal protein L29; induced upon germ tube formation; colony morphology-related gene regulation by Ssn6; intron in 5'-UTR; Spider biofilm repressed
HAS1	orf19.3962	1.89	3.55E-03	Functional homolog of S. cerevisiae Has1p, which is a nucleolar protein of the DEAD-box ATP-dependent RNA helicase family that is involved in biogenesis of the ribosome, particularly the small (40S) subunit; caspofungin-downregulated
orf19.6705	orf19.6705	1.88	5.49E-04	Putative guanyl nucleotide exchange factor with Sec7 domain; required for normal filamentous growth; regulated by yeast-hyphal switch; filament induced; regulated by Nrg1, Tup1, Mob2, Hap43; mRNA binds She3; Spider biofilm induced
AAH1	orf19.2251	1.88	1.46E-05	Adenine deaminase; purine salvage and nitrogen catabolism; colony morphology-related regulation by Ssn6; Hog1, CO2-induced; chlamydospore formation repressed in C. albicans and C. dubliniensis; rat catheter and F-12/CO2 biofilm induced
orf19.496	orf19.496	1.88	4.73E-05	Ortholog(s) have DNA-dependent ATPase activity, dinucleotide insertion or deletion binding, guanine/thymine mispair binding activity, role in mismatch repair, mitochondrial DNA repair and mitochondrion localization
orf19.6610	orf19.6610	1.87	1.38E-05	Ortholog(s) have microtubule binding, structural constituent of cytoskeleton activity
orf19.2246	orf19.2246	1.87	1.90E-05	Ortholog(s) have cytosol, nucleus localization
orf19.3581	orf19.3581	1.87	6.99E-05	Ortholog(s) have histone binding activity, role in DNA replication-dependent nucleosome assembly and CAF-1 complex, cytoplasm, nucleus localization
orf19.7545	orf19.7545	1.87	1.39E-03	Protein similarity to mutator-like element (MULE) transposase
SFL2	orf19.3969	1.86	7.73E-06	Predicted transcription factor; required for filamentous growth, for virulence in RHE model but not in mice; induced upon RHE infection but C. dubliniensis ortholog is not; Spider biofilm induced
TIF11	orf19.5351	1.86	3.81E-06	Translation initiation factor eIF1a; possibly transcriptionally regulated upon hyphal formation; genes encoding ribosomal subunits, translation factors, and tRNA synthetases are downregulated upon phagocytosis by murine macrophage
RPS8A	orf19.6873	1.86	1.05E-03	Small 40S ribosomal subunit protein; induced by ciclopirox olamine; repressed upon phagocytosis by murine macrophage; 5'-UTR intron; Hap43-induced; Spider biofilm repressed

orf19.413	orf19.413	1.86	6.86E-05	Protein of unknown function; induced by Sfu1; Spider biofilm induced
HTS1	orf19.4051	1.86	3.81E-06	Putative tRNA-His synthetase; downregulated upon phagocytosis by murine macrophage; stationary phase enriched protein; Spider biofilm repressed
FRP1	orf19.5634	1.85	4.80E-04	Ferric reductase; alkaline-induced by Rim101; iron-chelation-induced by CCAAT-binding factor; fluconazole-repressed; ciclopirox-, hypoxia-, Hap43-induced; colony morphology-related regulation by Ssn6; Spider and flow model biofilm induced
TOP1	orf19.96	1.84	3.83E-04	DNA topoisomerase I; required for wild-type growth and for wild-type mouse virulence; sensitive to camptothecin; induced upon adherence to polystyrene; rat catheter biofilm induced
FAS2	orf19.5949	1.84	1.46E-05	Alpha subunit of fatty-acid synthase; required for virulence in mouse systemic infection and rat oropharyngeal infection models; regulated by Efg1; fluconazole-induced; amphotericin B repressed; flow model and Spider biofilm repressed
orf19.2544	orf19.2544	1.84	2.81E-05	Ortholog(s) have aminoacyl-tRNA hydrolase activity, role in negative regulation of proteasomal ubiquitin-dependent protein catabolic process and mitochondrial outer membrane localization
CEF3	orf19.4152	1.84	3.74E-03	Translation elongation factor 3; antigenic in humans; predicted C-term nucleotide-binding active site; protein on surface of yeast, not hyphae; polystyrene adherence induced; higher protein amount in stationary phase; possibly essential
orf19.494	orf19.494	1.84	7.77E-04	Putative RNA-binding protein; role in assembly of box H/ACA snoRNPs and thus pre-rRNA processing; Spider biofilm induced
orf19.4771	orf19.4771	1.83	4.01E-04	Protein of unknown function; Spider biofilm induced
DCK1	orf19.815	1.83	2.61E-05	Putative guanine nucleotide exchange factor; required for embedded filamentous growth; activates Rac1; has a DOCKER domain; similar to adjacent DCK2 and to S. cerevisiae Ylr422wp; regulated by Nrg1; Spider biofilm induced
PGA13	orf19.6420	1.83	4.80E-03	GPI-anchored cell wall protein involved in cell wall synthesis; required for normal cell surface properties; induced in oralpharyngeal candidasis; Spider biofilm induced; Bcr1-repressed in RPMI a/a biofilms
ABP140	orf19.3676	1.83	1.31E-05	Ortholog of S. cerevisiae actin-binding protein Abp140; Hap43-induced; F-12/CO2 early biofilm induced
CHS2	orf19.7298	1.83	1.67E-04	Chitin synthase; nonessential; required for wild-type chitin deposition in hyphae; transcript regulated during dimorphic transition; Chs1 and Chs2, but not Chs3, are inhibited by the protoberberine HWY-289; flow model biofilm repressed
orf19.3477	orf19.3477	1.83	2.51E-03	Putative pseudouridine synthase; predicted role in snRNA pseudouridine synthesis, tRNA pseudouridine synthesis; Spider biofilm induced
orf19.1606	orf19.1606	1.83	5.27E-03	Protein of unknown function; Plc1-regulated

GAP4	orf19.4456	1.82	1.65E-03	Putative amino acid permease; hyphal induced; regulated by Hap43, Gcn2 and Gcn4; colony morphology-related gene regulation by Ssnp; detected at plasma membrane of yeast and germ tube by mass spec; Spider biofilm induced
AGP2	orf19.4679	1.81	1.45E-04	Amino acid permease; hyphal repressed; white-opaque switch regulated; induced in core caspofungin response, during cell wall regeneration, by flucytosine; regulated by Sef1, Sfu1, and Hap43; rat catheter and Spider biofilm induced
orf19.3559	orf19.3559	1.81	3.45E-04	S. cerevisiae ortholog Mrps35p is a structural constituent of ribosome and localizes to mitochondrial small ribosomal subunit; the snoRNA CD39 is encoded within the MRPS35 intron
SOD3	orf19.7111.1	1.81	1.40E-02	Cytosolic manganese-containing superoxide dismutase; protects against oxidative stress; repressed by ciclopirox olamine, induced during stationary phase when SOD1 expression is low; Hap43-repressed; Spider and flow model biofilm induced
SUV3	orf19.4519	1.81	6.15E-04	RNA helicase; mitochondrial RNA catabolism; required for chlamydospore formation, embedded hyphal growth, wild-type respiratory growth, alkaline-induced morphogenesis and SD or Spider biofilm formation; rat catheter biofilm induced
orf19.475	orf19.475	1.80	6.13E-04	Putative rRNA processing protein; rat catheter biofilm induced
TYS1	orf19.2694	1.80	2.04E-05	Putative tRNA-Tyr synthetase; downregulated upon phagocytosis by murine macrophages; stationary phase enriched protein; Spider biofilm repressed
NOP4	orf19.5198	1.80	1.62E-02	Putative nucleolar protein; Hap43-induced; mutation confers hypersensitivity to 5-fluorocytosine (5-FC), 5-fluorouracil (5-FU), and tubercidin (7-deazaadenosine); represses in core stress response
CDC6	orf19.5242	1.80	1.08E-02	Putative ATP-binding protein with a predicted role in DNA replication; member of conserved Mcm1p regulon; periodic mRNA expression, peak at cell-cycle M/G1 phase
orf19.4964	orf19.4964	1.79	6.03E-04	Ortholog(s) have role in cellular bud site selection, mRNA export from nucleus, mRNA splicing, via spliceosome and RES complex localization
MCM2	orf19.4354	1.79	4.16E-05	Phosphorylated protein of unknown function; transcription is periodic with a peak at M/G1 phase of the cell cycle
RSM22	orf19.414	1.79	1.11E-04	Predicted mitochondrial small ribosomal subunit; rat catheter and Spider biofilm induced
RPP2B	orf19.5928	1.79	2.86E-05	Conserved acidic ribosomal protein; possibly involved in regulation of translation elongation; interacts with Rpp1A; 1 of 4 similar C. albicans proteins (Rpp1A, Rpp1B, Rpp2A, Rpp2B); macrophage/pseudohyphal-induced; Spider biofilm repressed
RPL37B	orf19.667.1	1.78	7.50E-05	Ribosomal protein L37; Hap43-induced; Spider biofilm repressed
orf19.5698	orf19.5698	1.78	7.53E-06	Putative mitochondrial ribosomal protein of the large subunit; transcript is upregulated in clinical isolates from HIV+ patients with oral candidiasis; Spider biofilm repressed

RPL10A	orf19.3465	1.78	3.00E-05	Predicted ribosomal protein; downregulated upon phagocytosis by murine macrophages; Hap43-induced; Spider biofilm repressed
orf19.263.1	orf19.263.1	1.78	2.10E-03	Protein of unknown function; gene has intron; Spider biofilm induced
OPT4	orf19.176	1.78	5.71E-03	Oligopeptide transporter; detected at germ tube plasma membrane; transcript inducede during phagocytosis by macrophages; fungal-specific; Hap43-repressed; merged with orf19.2292 in Assembly 20; rat catheter and Spider biofilm induced
MET14	orf19.946	1.78	4.92E-05	Putative adenylylsulfate kinase; predicted role in sulfur metabolism; possibly adherence-induced; protein present in exponential and stationary growth phase yeast; F-12/CO2 biofilm induced
RFC5	orf19.2029	1.78	1.92E-05	Putative heteropentameric replication factor C subunit; periodic mRNA expression, peak at cell-cycle G1/S phase
RCL1	orf19.1886	1.77	1.66E-05	Putative U3-containing 90S preribosome processome complex subunit; Hap43-induced; essential; S. cerevisiae ortholog is essential; represses in core stress response;
SMC5	orf19.2417	1.77	3.46E-05	Protein similar to S. cerevisiae Smc5p, which is involved in DNA repair; transposon mutation affects filamentous growth
orf19.962	orf19.962	1.76	1.23E-03	Protein with a fungal RNA polymerase I subunit RPA14 domain; proposed to play a role in the recruitment of pol I to the promoter; Hap43-induced gene
YML6	orf19.7019	1.76	1.32E-03	Putative mitochondrial ribosomal protein; induced upon adherence to polystyrene
PTC8	orf19.4698	1.76	4.73E-04	Predicted type 2C protein phosphatase, ser/thr-specific; required for hyphal growth; transcript induced by stress; flow model biofilm induced; Spider biofilm induced
NOP8	orf19.1091	1.76	4.58E-04	Ortholog of S. cereviiae Nop8; has a role in ribosomal large subunit biogenesis; rat catheter and Spider biofilm induced
orf19.6691	orf19.6691	1.75	2.56E-04	Putative ember of the multi-drug and toxin extrusion (MATE) family of the multidrug/oligosaccharidyl-lipid/polysaccharide exporter superfamily; Spider biofilm induced
RPS6A	orf19.4660	1.74	1.54E-02	Ribosomal protein 6A; localizes to cell surface of yeast cells but not hyphae; repressed upon phagocytosis by murine macrophage; possibly essential; Hap43-induced; Spider biofilm repressed
CCN1	orf19.3207	1.74	2.14E-02	G1 cyclin; required for hyphal growth maintenance (not initiation); cell-cycle regulated transcription (G1/S); Cdc28p-Ccn1p initiates Cdc11p S394 phosphorylation on hyphal induction; expression in S. cerevisiae inhibits pheromone response
RPS14B	orf19.6265.1	1.74	2.63E-03	Putative ribosomal protein; repressed upon phagocytosis by murine macrophage; transcript positively regulated by Tbf1; Spider biofilm repressed

orf19.6565	orf19.6565	1.74	8.09E-05	Conserved mitochondrial inner membrane insertase; mediates insertion of mitochondrial and nuclear-encoded proteins from the matrix into the inner membrane; Spider biofilm repressed
NCS2	orf19.4399	1.74	4.10E-03	Putative cytosolic thiouridylase subunit; Spider biofilm induced
orf19.5704	orf19.5704	1.74	8.44E-04	Ortholog(s) have rRNA binding activity, role in mitochondrial RNA processing, mitochondrial genome maintenance, rRNA metabolic process and mitochondrion localization
orf19.7370	orf19.7370	1.74	5.50E-03	Possible G-protein coupled receptor; vacuolar membrane transporter for cationic amino acids; PQ-loop motif; rat catheter and Spider biofilm induced
orf19.2575	orf19.2575	1.73	2.35E-04	Putative S-adenosylmethionine-dependent methyltransferase; Hap43p-induced gene
CCT3	orf19.4004	1.73	2.99E-05	Putative cytosolic chaperonin Cct ring complex subunit; mutation confers hypersensitivity to cytochalasin D
DNA2	orf19.1192	1.73	1.93E-04	Protein similar to S. cerevisiae Dna2p, which is a DNA replication factor involved in DNA repair; induced under hydroxyurea treatment
orf19.4376	orf19.4376	1.73	3.30E-04	Protein of unknown function; Spider biofilm induced
ASH2	orf19.3964	1.72	1.66E-05	Ortholog(s) have histone methyltransferase activity (H3-K4 specific) activity and role in cellular response to cadmium ion, chromatin silencing at telomere, detoxification of cadmium ion, histone H3-K4 trimethylation, telomere maintenance
ECM22	orf19.2623	1.72	1.06E-04	Zn(II)2Cys6 transcription factor; rat catheter and Spider biofilm induced
GCV2	orf19.385	1.71	9.54E-05	Glycine decarboxylase P subunit; protein of glycine catabolism; repressed by Efg1; Hog1-induced; induced by Rim101 at acid pH; transcript induced in elevated CO2; stationary phase enriched protein
FRS2	orf19.2960	1.71	5.16E-06	Putative tRNA-Phe synthetase; downregulated upon phagocytosis by murine macrophage; protein present in exponential and stationary growth phase yeast cultures; Spider biofilm repressed
orf19.4889	orf19.4889	1.71	1.67E-04	Predicted MFS family membrane transporter, member of the drug:proton antiporter (12 spanner) (DHA1) family; Spider biofilm induced
orf19.1815	orf19.1815	1.71	8.18E-03	Ortholog of S. cerevisae/S. pombe Tif6; constituent of 66S pre-ribosomal particles; Spider biofilm induced
orf19.154	orf19.154	1.71	1.00E-04	Putative ortholog of S. cerevisiae Utp30; a U3-containing 90S preribosome complex protein; Hap43-induced; Spider biofilm induced
orf19.5067	orf19.5067	1.71	2.09E-04	Predicted nuclear exosome-associated nucleic acid binding protein; rat catheter and Spider biofilm induced
PLB1	orf19.689	1.70	1.49E-05	Phospholipase B; host cell penetration and virulence in mouse systemic infection; Hog1-induced; signal sequence, N-glycosylation, and Tyr phosphorylation site; induced in fluconazole-resistant strains; rat catheter biofilm repressed

orf19.4960	orf19.4960	1.70	2.33E-05	Ortholog(s) have spermine synthase activity, role in pantothenate biosynthetic process, spermine biosynthetic process and cytoplasm localization
orf19.3869	orf19.3869	1.69	1.91E-05	Protein of unknown function; regulated by Tsa1, Tsa1B in minimal media at 37 degrees C; shows colony morphology-related gene regulation by Ssn6; Spider biofilm induced
orf19.5271	orf19.5271	1.69	4.19E-03	Protein of unknown function; Hap43-induced gene
RPS5	orf19.4336	1.69	1.96E-02	Ribosomal protein S5; macrophage/pseudohyphal-induced after 16 h; downregulated upon phagocytosis by murine macrophage; Hap43-induced; Spider biofilm repressed
orf19.270	orf19.270	1.69	4.49E-03	Ortholog of C. parapsilosis CDC317 : CPAR2_102150, C. dubliniensis CD36 : Cd36_82780, Pichia stipitis Pignal : psti_CGOB_00155 and Candida orthopsilosis Co 90-125 : CORT_0B03450
TOP2	orf19.2873	1.69	6.71E-06	DNA topoisomerase II; catalyzes ATP-dependent DNA relaxation and decatenation in vitro; Y842 predicted to be catalytic; functional homolog of S. cerevisiae Top2p; sensitive to amsacrine or doxorubicin; farnesol-upregulated in biofilm
orf19.3061.1	orf19.3061.1	1.69	4.51E-04	Ortholog of S. cerevisiae Rps22Ap and Rps22Bp; gene contains 5' UTR intron
ACS2	orf19.1064	1.69	7.21E-06	Acetyl-CoA synthetase; antigenic during human and murine infection; induced by Efg1; macrophage-induced protein; soluble protein in hyphae; gene contains intron; flow model and Spider biofilm repressed
RBT4	orf19.6202	1.68	3.37E-05	Pry family protein; required for virulence in mouse systemic/rabbit corneal infections; not filamentation; mRNA binds She3, is localized to hyphal tips; Hap43-induced; in both yeast and hyphal culture supernatants; Spider biofilm induced
orf19.2724	orf19.2724	1.68	7.93E-04	Protein of unknown function; flow model, rat catheter and Spider biofilm induced; Hap43-repressed
orf19.1414	orf19.1414	1.68	5.38E-06	Protein of unknown function; transcript is upregulated in an RHE model of oral candidiasis; Hap43-repressed
orf19.2286	orf19.2286	1.68	1.14E-04	Putative deoxyhypusine hydroxylase; ketoconazole-induced; protein level decreases in stationary phase cultures; required for biofilm formation; Spider biofilm repressed
orf19.2761	orf19.2761	1.68	4.45E-03	Putative glycosylphosphatidylinositol (GPI) anchor assembly protein; transposon insertion causes decreased colony wrinkling but does not block true hyphal growth; induced by nitric oxide independent of Yhb1p
orf19.4435	orf19.4435	1.68	1.12E-05	Ortholog(s) have structural constituent of cytoskeleton activity, role in microtubule nucleation and spindle pole body localization
SMP3	orf19.5792	1.67	1.54E-03	Mannosyltransferase of glycosylphosphatidylinositol (GPI) biosynthesis; catalyzes mannosylation of Man3-GPI precursor; essential for viability; 8-9 transmembrane regions predicted; has HQEXRF motif; functional homolog of S. cerevisiae Smp3p
orf19.7624	orf19.7624	1.67	1.44E-03	Ortholog(s) have role in rRNA processing and 90S preribosome, nucleolus localization

orf19.6227	orf19.6227	1.66	4.71E-03	Ortholog of C. dubliniensis CD36 : Cd36_06390, C. parapsilosis CDC317 : CPAR2_209040, Candida tenuis NRRL Y-1498 : CANTEDRAFT_114052 and Debaryomyces hansenii CBS767 : DEHA2D14300g
TIF34	orf19.2967	1.66	1.65E-05	Putative translation initiation factor eIF3, p39 subunit; mutation confers hypersensitivity to roridin A, verrucarin A; downregulated upon phagocytosis by murine macrophages; Spider biofilm repressed
orf19.7088	orf19.7088	1.66	8.37E-05	Ortholog(s) have single-stranded telomeric DNA binding activity, role in regulation of translational fidelity, telomere maintenance, threonylcarbamoyladenosine metabolic process and cytosol, nucleus localization
UME6	orf19.1822	1.66	2.27E-04	Zn(II)2Cys6 transcription factor; role in hyphal extension, virulence, adherence to plastic; filament induced; regulated by Nrg1/Tup1/Rfg1, alkaline conditions; expression promotes highly filamentous biofilms; rat catheter biofilm induced
orf19.3536	orf19.3536	1.66	3.96E-04	Ortholog(s) have acetylglucosaminyltransferase activity, role in protein N-linked glycosylation and Golgi medial cisterna localization
orf19.4301	orf19.4301	1.66	6.57E-04	Ortholog(s) have role in chromatin silencing at rDNA, chromatin silencing at silent mating-type cassette, chromatin silencing at telomere, regulation of transcription from RNA polymerase II promoter and nucleus localization
TIM23	orf19.1361	1.66	2.90E-04	Protein involved in mitochondrial matrix protein import
orf19.1802	orf19.1802	1.65	7.05E-06	Putative termination and polyadenylation protein; repressed by prostaglandins; Spider biofilm induced
orf19.355	orf19.355	1.65	3.16E-04	Has domain(s) with predicted oxidoreductase activity and role in oxidation-reduction process
orf19.2639	orf19.2639	1.65	1.81E-04	Ortholog(s) have structural constituent of ribosome activity and mitochondrial large ribosomal subunit localization
RPL24A	orf19.3789	1.65	2.19E-04	Predicted ribosomal protein; downregulated upon phagocytosis by murine macrophage; intron in 5'-UTR; Hap43-induced; Spider biofilm repressed
CHT2	orf19.3895	1.65	2.34E-05	GPI-linked chitinase; required for normal filamentous growth; repressed in core caspofungin response; fluconazole, Cyr1, Efg1, pH-regulated; mRNA binds She3 and is localized to yeast-form buds and hyphal tips; Spider biofilm repressed
SEC14	orf19.941	1.64	3.36E-05	Essential protein; functional homolog of S. cerevisiae Sec14p, a Golgi phosphatidylinositol/phosphatidylcholine transfer protein that regulates choline-phosphate cytidyltransferase and thereby affects secretion; biofilm-regulated
MTS1	orf19.4831	1.64	3.39E-05	Sphingolipid C9-methyltransferase; catalyzes methylation of the 9th carbon in the long chain base component of glucosylceramides; glucosylceramide biosynthesis is important for virulence; Spider biofilm repressed

orf19.6751	orf19.6751	1.64	2.12E-04	Ortholog(s) have tRNA methyltransferase activity, role in cytoplasmic translation, tRNA methylation and cytoplasm localization
FGR6-4	orf19.3490	1.64	1.38E-02	Protein lacking an ortholog in S. cerevisiae; member of a family encoded by FGR6-related genes in the RB2 repeat sequence; transposon mutation affects filamentous growth
orf19.7107	orf19.7107	1.64	2.88E-04	Ortholog(s) have role in ribosomal large subunit biogenesis and cytoplasm, nucleus, ribosome localization
orf19.5356	orf19.5356	1.64	7.11E-06	Protein with a predicted role in cell wall integrity; repressed in core stress response
FTH2	orf19.3227	1.63	2.09E-03	Putative iron transporter; similar to S. cerevisiae Fth1p
CTR1	orf19.3646	1.63	2.66E-04	Copper transporter; transcribed in low copper; induced Mac1, Tye7, macrophage interaction, alkaline pH via Rim101; 17-beta-estradiol repressed; complements S. cerevisiae ctr1 ctr3 copper transport mutant; flow model/Spider biofilm induced
PIF1	orf19.6133	1.62	6.39E-05	Putative DNA helicase; decreased transcription is observed upon fluphenazine treatment
orf19.4666	orf19.4666	1.62	4.35E-03	Protein of unknown function; hyphal-induced expression, regulated by Cyr1, Ras1, Efg1; Spider biofilm induced
orf19.6748	orf19.6748	1.62	6.94E-03	Ortholog(s) have role in ascospore formation, cellular response to cadmium ion, detoxification of cadmium ion
orf19.7504	orf19.7504	1.62	1.14E-04	Ortholog of S. cerevisiae Rts3; a component of the protein phosphatase type 2A complex; Plc1-regulated; induced in core caspofungin response; Spider biofilm induced
TRM2	orf19.3327	1.62	7.72E-06	Putative tRNA methyltransferase; repressed by prostaglandins; Spider biofilm induced
orf19.1075	orf19.1075	1.62	1.49E-02	Protein of unknown function; Spider biofilm induced
orf19.4634	orf19.4634	1.62	7.43E-06	Protein required for thiolation of uridine at wobble position of Gln, Lys, and Glu tRNAs; has a role in urmylation; S. cerevisiae ortholog has a role in invasive and pseudohyphal growth
PMI1	orf19.1390	1.61	4.17E-04	Phosphomannose isomerase; cell wall biosynthesis enzyme; drug target; functional homolog of S. cerevisiae, E. coli phosphomannose isomerase; Gcn4-regulated; induced on adherence to polystyrene, phagocytosis; 3-AT, Spider biofilm repressed
orf19.3721	orf19.3721	1.61	1.62E-03	Protein of unknown function; Spider biofilm induced
TCP1	orf19.401	1.61	4.25E-04	Chaperonin-containing T-complex subunit, induced by alpha pheromone in SpiderM medium; stationary phase enriched protein
DED1	orf19.7392	1.61	3.63E-05	Predicted ATP-dependent RNA helicase; RNA strand annealing activity; Spider biofilm induced
RPS17B	orf19.2329.1	1.61	3.69E-05	Ribosomal protein 17B; downregulated upon phagocytosis by murine macrophages; Hap43-induced; Spider biofilm repressed
orf19.4665	orf19.4665	1.61	7.43E-06	Protein of unknown function; Spider biofilm induced

RPL4B	orf19.7217	1.61	5.43E-04	Ribosomal protein 4B; repressed upon phagocytosis by murine macrophage; Spider biofilm repressed
RPL21A	orf19.840	1.60	1.15E-04	Putative ribosomal protein; repressed upon phagocytosis by murine macrophage; Spider biofilm repressed
CHS3	orf19.4937	1.60	2.20E-04	Major chitin synthase of yeast and hyphae; synthesizes short-chitin fibrils; Chs4-activated; transcript induced at yeast-hyphal transition; Chs1 and Chs2, but not Chs3, are inhibited by the protoberberine HWY-289; Spider biofilm induced
MSH6	orf19.4945	1.60	3.21E-04	Protein similar to S. cerevisiae Msh6p, which is involved in mismatch repair; repressed under Cdc5p depletion; Hap43p-induced gene
ZFU2	orf19.6781	1.60	1.35E-02	Zn(II)2Cys6 transcription factor; regulator of yeast form adherence; mutants display increased colonization of mouse kidneys; required for yeast cell adherence to silicone substrate; Spider biofilm induced
NOP10	orf19.596.1	1.60	4.21E-06	Small nucleolar ribonucleoprotein; flucytosine induced
RPS25B	orf19.6663	1.60	1.11E-04	Ribosomal protein; macrophage/pseudohyphal-induced after 16 h; repressed upon phagocytosis by murine macrophage; transcript positively regulated by Tbf1; 5'-UTR intron; Hap43-induced; Spider biofilm repressed
LEA1	orf19.1260	1.60	2.20E-05	Predicted component of U2 snRNP; induced by alpha pheromone in SpiderM medium
PAM18	orf19.4190	1.59	1.13E-04	Predicted component of the presequence translocase-associated import motor (PAM complex) involved in protein import into mitochondrial matrix; rat catheter biofilm induced
RPL3	orf19.1601	1.59	1.21E-03	Ribosomal protein, large subunit; induced by ciclopirox olamine treatment; genes encoding cytoplasmic ribosomal subunits are downregulated upon phagocytosis by murine macrophages; Hap43-induced gene; Spider biofilm repressed
LHP1	orf19.2795	1.59	6.27E-03	Ortholog(s) have tRNA binding activity, role in regulation of ascospore formation, tRNA 3' trailer cleavage, endonucleolytic and nucleolus, nucleoplasm localization
orf19.5578	orf19.5578	1.59	2.50E-04	Ortholog of C. dubliniensis CD36 : Cd36_63050 and Candida albicans WO-1 : CAWG_05094
ASF1	orf19.3715	1.59	3.20E-05	Protein similar to S. cerevisiae Asf1p, a chromatin assembly complex component; likely to be essential for growth, based on an insertional mutagenesis strategy
MSI3	orf19.2435	1.59	1.44E-05	Essential HSP70 family protein; required for fluconazole resistance and calcineurin-dependent transcription; interacts with Cgr1; transcript regulated by iron; rat catheter biofilm induced; farnesol repressed in biofilm; sumoylation target
RPL42	orf19.4909.1	1.58	1.50E-02	Putative 60S ribosomal subunit protein; colony morphology-related gene regulation by Ssn6; Spider biofilm repressed

FAS1	orf19.979	1.58	6.47E-04	Beta subunit of fatty-acid synthase; multifunctional enzyme; Hap43, fluconazole-induced; amphotericin B, caspofungin repressed; macrophage/pseudohyphal-induced; flow model and Spider biofilm repressed
orf19.7166	orf19.7166	1.58	1.50E-04	Predicted mitochondrial cardiolipin-specific phospholipase; upregulated in an azole-resistant strain that overexpresses MDR1; induced by Mnl1 under weak acid stress; rat catheter and Spider biofilm induced
SEP7	orf19.3680	1.58	1.41E-05	Septin, required for wild-type invasive growth in vitro but not required for virulence in a mouse model of systemic infection; localizes to hyphal septum or bud neck; Asn-rich; aberrant gel mobility; phosphorylated in vitro by Gin4p
orf19.2923	orf19.2923	1.58	1.14E-03	Predicted membrane transporter, member of the drug:proton antiporter (14 spanner) (DHA2) family, MFS superfamily; induced by alpha pheromone in SpiderM medium
RPS12	orf19.6785	1.58	5.77E-04	Acidic ribosomal protein S12; regulated by Gcn4, activated by Tbf1; repressed by amino acid starvation (3-AT); protein abundance is affected by URA3 expression in CAI-4 strain background; sumoylation target; Spider biofilm repressed
orf19.5628	orf19.5628	1.58	1.78E-03	Mitochondrial dicarboxylate transporter; possibly an essential gene, disruptants not obtained by UAU1 method
ZCF17	orf19.3305	1.58	1.90E-03	Putative Zn(II)2Cys6 transcription factor
CAM1	orf19.7382	1.58	1.35E-04	Putative translation elongation factor eEF1 gamma; protein level decreased in stationary phase cultures; Spider biofilm repressed
RPL16A	orf19.6085	1.57	1.71E-04	Ribosomal protein; transposon mutation affects filamentous growth; repressed upon phagocytosis by murine macrophages; Hap43-induced; Spider biofilm repressed
orf19.688	orf19.688	1.57	4.90E-05	Mitochondrial ribosomal protein of the small subunit; S. cerevisiae ortholog is essential for viability; Spider biofilm repressed
orf19.5057	orf19.5057	1.57	7.13E-03	Ortholog of C. dubliniensis CD36 : Cd36_07380 and Candida albicans WO-1 : CAWG_00634
orf19.3141	orf19.3141	1.57	3.99E-03	Ortholog(s) have role in ER to Golgi vesicle-mediated transport and cytoplasmic mRNA processing body, endoplasmic reticulum membrane, extrinsic to membrane localization
orf19.4932	orf19.4932	1.57	2.46E-04	Ortholog(s) have role in mitochondrial translation and mitochondrion localization
RPL28	orf19.2864.1	1.57	4.25E-04	Putative ribosomal protein; Plc1-regulated; downregulated upon phagocytosis by murine macrophage; Spider biofilm repressed
orf19.341	orf19.341	1.57	5.45E-03	Putative spermidine export pump; fungal-specific (no human or murine homolog)
orf19.3582	orf19.3582	1.57	8.64E-05	Ortholog(s) have protein-lysine N-methyltransferase activity, role in peptidyl-lysine dimethylation, vesicle-mediated transport and cytosol, nucleus localization
LTV1	orf19.7650	1.56	1.12E-03	Putative GSE complex component; repressed by prostaglandins
orf19.5510	orf19.5510	1.56	2.05E-05	Ortholog(s) have role in chromatin silencing at telomere, negative regulation of transcription from RNA polymerase II promoter by pheromones and CHRAC localization

ERP5	orf19.2322.3	1.56	8.59E-06	Protein involved in ER to Golgi transport; rat catheter and Spider biofilm repressed
AAT22	orf19.4669	1.56	7.35E-05	Aspartate aminotransferase; nitrogen metabolism; similar but not orthologous to S. cerevisiae Aat2; clade-associated gene expression; protein levels decrease in stationary phase yeast; mutant is viable; flow model biofilm repressed
orf19.7459	orf19.7459	1.55	6.39E-05	Putative mitochondrial protein with a predicted role in respiratory growth; fluconazole-induced; ketoconazole-repressed; mutants display a strong defect in flow model biofilm formation; Spider biofilm induced
orf19.547	orf19.547	1.55	5.46E-03	Ortholog(s) have 5'-flap endonuclease activity, single-stranded DNA specific 5'-3' exodeoxyribonuclease activity
HIS7	orf19.5505	1.55	1.66E-05	Putative imidazole glycerol phosphate synthase; histidine biosynthesis; no human/murine homolog; transcription induced by histidine starvation; regulated by Gcn2p and Gcn4p; higher protein level in stationary phase
orf19.7502	orf19.7502	1.55	9.62E-04	Protein of unknown function; Hap43-induced gene; upregulated in a cyr1 null mutant; Spider biofilm induced
PRP39	orf19.1492	1.55	1.12E-02	Putative component of the U1 snRNP; involved in splicing; Hap43-induced gene; Spider biofilm induced
CLG1	orf19.6146	1.55	7.54E-06	Putative cyclin-like protein; transcription is regulated upon yeast-hyphal switch
RPP1A	orf19.2992	1.55	1.66E-02	Conserved acidic ribosomal protein; likely role in regulation of translation elongation; interacts with Rpp2B; 1 of 4 similar C. albicans ribosomal proteins (Rpp1A, Rpp1Bp, Rpp2A, Rpp2B); Hap43-induced; Spider biofilm repressed
orf19.4805	orf19.4805	1.55	1.16E-04	Putative membrane protein; induced by alpha pheromone in SpiderM medium; Hap4-induced gene; Spider biofilm induced
YNK1	orf19.4311	1.55	1.94E-03	Nucleoside diphosphate kinase (NDP kinase); homo-hexameric; soluble protein in hyphae; flucytosine induced; biofilm induced; macrophage-induced protein; stationary phase enriched protein; Spider biofilm repressed
FGR6-3	orf19.4712	1.54	1.73E-02	Protein lacking an ortholog in S. cerevisiae; member of a family encoded by FGR6-related genes in the RB2 repeat sequence; transposon mutation affects filamentous growth
orf19.7069	orf19.7069	1.54	4.17E-04	Putative AdoMet-dependent proline methyltransferase; Hap43-induced; required for normal flow model biofilm growth; Spider biofilm repressed
HCM1	orf19.4853	1.54	2.75E-05	Protein with forkhead domain; similar to S. cerevisiae Hcm1p; Hap43p-induced gene
orf19.6415.1	orf19.6415.1	1.54	3.86E-03	Ortholog(s) have structural constituent of ribosome activity and cytosolic small ribosomal subunit, nucleus localization

FGR6-10	orf19.1234	1.54	9.27E-03	Protein lacking an ortholog in S. cerevisiae; member of a family encoded by FGR6-related genes in the RB2 repeat sequence; transposon mutation affects filamentous growth
orf19.4160	orf19.4160	1.54	5.05E-03	Ortholog(s) have serine-type endopeptidase activity, role in glycoprotein metabolic process, mitochondrial tRNA threonylcarbamoyladenosine modification and mitochondrion localization
MLH1	orf19.4162	1.53	2.30E-03	Putative mismatch repair protein; cell-cycle regulated periodic mRNA expression
orf19.6730	orf19.6730	1.53	5.62E-03	Ortholog(s) have nucleolus localization
RNH35	orf19.6562	1.53	1.12E-04	Putative ribonuclease H2 catalytic subunit; flucytosine induced; Spider biofilm repressed
RPC31	orf19.2831	1.53	2.63E-05	Putative RNA polymerase III subunit C31; repressed by nitric oxide; induced during infection of murine kidney, compared to growth in vitro; has murine homolog
TRP5	orf19.4718	1.53	2.71E-05	Predicted tryptophan synthase; identified in detergent-resistant membrane fraction (possible lipid raft component); predicted N-terminal acetylation; Gcn4p-regulated; S. cerevisiae ortholog is Gcn4p regulated; upregulated in biofilm;
YVH1	orf19.4401	1.52	2.46E-03	Putative dual specificity phosphatase (phosphoserine/threonine and phosphotyrosine phosphatase); required for wild-type growth rate and for wild-type virulence in mouse model of systemic infection; Hap43p-induced gene
orf19.5455	orf19.5455	1.52	1.80E-04	Ortholog(s) have mRNA binding, small GTPase regulator activity
orf19.6752	orf19.6752	1.52	7.98E-04	Ortholog(s) have structural constituent of ribosome activity and mitochondrial small ribosomal subunit localization
orf19.3220	orf19.3220	1.52	1.98E-04	Putative rRNA processing protein; Spider biofilm induced
orf19.2260	orf19.2260	1.52	4.07E-05	Putative transcription factor with zinc finger DNA-binding motif
orf19.4532	orf19.4532	1.52	1.44E-04	Protein of unknown function; present in exponential and stationary growth phase yeast cultures
GDH3	orf19.4716	1.52	4.23E-03	NADP-glutamate dehydrogenase; Nrg1, Plc1 regulated; hypha, hypoxia, Efg1-repressed; Rim101-induced at pH 8; GlcNAc, ciclopirox, ketoconazole induced; exp and stationary phase protein; Spider biofilm repressed; rat catheter biofilm induced
CDC60	orf19.2560	1.51	2.20E-05	Cytosolic leucyl tRNA synthetase; conserved amino acid and ATP binding class I signature, tRNA binding, proofreading motifs; likely essential for growth; interacts with benzoxaborole antifungals; present in exponential and stationary phase
orf19.7301	orf19.7301	1.51	3.62E-04	Has domain(s) with predicted DNA binding, nucleic acid binding activity
RRN11	orf19.718	1.51	9.37E-06	Putative RNA polymerase I subunit; rat catheter biofilm induced; Spider biofilm induced
orf19.2676	orf19.2676	1.51	2.34E-02	Predicted hexameric RecA-like ATPase Elp456 Elongator subcomplex subunit; required for modification of wobble nucleosides in tRNA; Spider biofilm induced

PHO87	orf19.2454	1.51	2.26E-04	Putative phosphate permease; transcript repressed by Rim101 at pH 8; regulated by white-opaque switch; caspofungin repressed; virulence-group-correlated expression; flow model biofilm induced
GAP1	orf19.4304	1.51	8.99E-05	Amino acid permease; antigenic in human/mouse; 10-12 transmembrane regions; regulated by nitrogen source; alkaline, GlcNAc, phagocytosis induced; WT virulence in mice; Spider and flow model biofilm induced
TCC1	orf19.6734	1.51	1.14E-04	Putative transcription factor/corepressor; regulation of filamentation and virulence; interacts with Tup1; regulates hypha-specific gene expression; contains 4 tetratricopeptide repeat (TPR) motifs; flucytosine repressed; Tbp1-induced
orf19.445	orf19.445	1.51	4.72E-04	Protein of unknown function; repressed by prostaglandins
PMM1	orf19.2937	1.50	2.94E-05	Phosphomannomutase; enzyme of O- and N-linked mannosylation; interconverts mannose-6-phosphate and mannose-l-phosphate; functional homolog of S. cerevisiae Sec53; antigenic in mice; Hap43-induced; flow model and Spider biofilm repressed
orf19.6736	orf19.6736	1.50	4.10E-03	Protein required for mitochondrial ribosome small subunit biogenesis; role in maturation of SSU-rRNA; Spider biofilm induced
SPE3	orf19.2250	1.50	1.84E-05	Putative spermidine synthase; predicted role in pantothenate and spermidine biosynthesis; Spider biofilm repressed
MCD4	orf19.5244	1.50	1.41E-05	Protein of major facilitator superfamily; has phosphodiesterase/nucleotide pyrophosphatase domain; similar to S. cerevisiae Mcd4p, which acts in GPI anchor biosynthesis; possibly an essential gene, disruptants not obtained by UAU1 method
orf19.2115	orf19.2115	1.50	5.25E-05	Putative molybdopterin-converting factor; fungal-specific (no human or murine homolog)
orf19.3042	orf19.3042	1.50	5.59E-04	Protein of unknown function; Hap43-induced; rat catheter biofilm induced
HGT10	orf19.5753	-1.50	1.24E-03	Glycerol permease involved in glycerol uptake; member of the major facilitator superfamily; induced by osmotic stress, at low glucose in rich media, during cell wall regeneration; 12 membrane spans; Hap43p-induced gene
SSU1	orf19.7313	-1.50	1.07E-03	Protein similar to S. cerevisiae Ssu1 sulfite transport protein; Tn mutation affects filamentous growth; regulated by Gcn2 and Gcn4; induced by nitric oxide; Hap43-repressed; Spider and flow model biofilm induced
SSP96	orf19.5145	-1.50	4.80E-04	Putative flavin-containing monooxygenase; F-12/CO2 early biofilm induced
GYP1	orf19.3811	-1.50	1.63E-03	Putative Cis-golgi GTPase-activating protein; transcript regulated by Nrg1, Mig1, and Tup1
orf19.7598	orf19.7598	-1.50	4.46E-03	Ortholog(s) have histone acetyltransferase activity, role in histone acetylation and Ada2/Gcn5/Ada3 transcription activator complex localization
orf19.3329	orf19.3329	-1.50	1.13E-02	Ortholog(s) have sphingosine-1-phosphate phosphatase activity, role in calcium-mediated signaling and endoplasmic reticulum localization

DAL52	orf19.3208	-1.50	4.11E-03	Putative allantoate permease; mutant is viable; similar but not orthologous to S. cerevisiae Dal5
orf19.5129	orf19.5129	-1.51	4.21E-04	Ortholog of C. dubliniensis CD36 : Cd36_72910, C. parapsilosis CDC317 : CPAR2_704100, Candida tenuis NRRL Y-1498 : CANTEDRAFT_113193 and Debaryomyces hansenii CBS767 : DEHA2E23100g
SKN2	orf19.348	-1.51	1.77E-05	Protein with a potential role in beta-1,6 glucan biosynthesis; similarity to Kre6 and Skn1; possibly essential, disruptants not obtained by UAU1 method; Hap43-induced; flow model biofilm induced; rat catheter biofilm repressed
orf19.4699	orf19.4699	-1.51	5.55E-03	Putative phospholipase of patatin family; similar to S. cerevisiae Tgl3p; predicted Kex2p substrate
ADH3	orf19.4505	-1.51	2.61E-04	Putative NAD-dependent (R,R)-butanediol dehydrogenase; regulated by white-opaque switch; induced by nitric oxide independent of Yhb1; Spider biofilm induced
BMT8	orf19.860	-1.51	7.28E-06	Putative beta-mannosyltransferase, member of a 9-gene family including characterized BMT genes with roles in beta-1,2-mannosylation of cell wall phosphopeptidomannan; transposon insertion in promoter region causes decreased colony wrinkling
NHX1	orf19.4201	-1.51	3.03E-04	Protein similar to S. cerevisiae Nhx1p, which is an Na+/H+ exchanger required for intracellular sequestration of Na+
VMA7	orf19.806	-1.52	1.41E-03	Putative subunit of the V-ATPase complex, which is involved in control of vacuolar pH; highly similar to S. cerevisiae Vma7p; interacts with phosphatidylinositol 3-kinase Vps34p
orf19.4680	orf19.4680	-1.52	1.17E-05	Possile protease; mutation confers hypersensitivity to toxic ergosterol analog
orf19.4894	orf19.4894	-1.52	1.07E-04	Protein with similarity to S. cerevisiae Yer010cp, a protein of unknown function belonging to the prokaryotic RraA family; repressed by benomyl; Hap43-induced; Spider biofilm induced
OYE22	orf19.3234	-1.52	2.29E-05	Putative NADPH dehydrogenase; rat catheter biofilm induced
IFC3	orf19.3749	-1.52	2.81E-05	Oligopeptide transporter; transcript induced by macrophage phagocytosis, BSA or peptides; fluconazole-induced; induced by Rim101 at pH 8; virulence-group-correlated expression; Hap43-repressed; Spider biofilm induced
orf19.4550	orf19.4550	-1.52	9.05E-05	Predicted MFS membrane transporter, member of the drug:proton antiporter (12 spanner) (DHA1) family; flow model biofilm induced
orf19.7131	orf19.7131	-1.52	8.96E-04	Butyrobetaine dioxygenase, the fourth enzyme of the carnitine biosynthesis pathway
HAP42	orf19.1481	-1.52	1.50E-04	Predicted transcription factor; possibly an essential gene, disruptants not obtained by UAU1 method
orf19.398	orf19.398	-1.53	5.32E-03	Ortholog of C. dubliniensis CD36 : Cd36_08040, C. parapsilosis CDC317 : CPAR2_207180, Candida tenuis NRRL Y-1498 : CANTEDRAFT_114140 and Debaryomyces hansenii CBS767 : DEHA2G13992g

CPY1	orf19.1339	-1.53	5.68E-05	Carboxypeptidase Y; transcript regulated at yeast-hypha transition or macrophage response; induced human neutrophils; regulated by Gcn2 and Gcn4; putative N-glycosylation
orf19.1477	orf19.1477	-1.54	6.19E-04	Protein of unknown function; possible ER protein; Hap43p-repressed; Spider biofilm induced
orf19.4504	orf19.4504	-1.54	2.98E-03	Has domain(s) with predicted oxidoreductase activity, transferase activity, transferring acyl groups other than amino-acyl groups, zinc ion binding activity and role in oxidation-reduction process
orf19.1417	orf19.1417	-1.54	2.17E-03	Ortholog of C. dubliniensis CD36 : Cd36_43970, C. parapsilosis CDC317 : CPAR2_401720, Candida tenuis NRRL Y-1498 : CANTEDRAFT_102588 and Debaryomyces hansenii CBS767 : DEHA2G16698g
orf19.4609	orf19.4609	-1.55	2.07E-04	Putative dienelactone hydrolase; protein abundance is affected by URA3 expression in the CAI-4 strain background; protein present in exponential and stationary growth phase yeast cultures; rat catheter biofilm repressed
SPO72	orf19.4119	-1.55	7.86E-05	Protein described as similar to S. cerevisiae sporulation protein; ortholog of S. cerevisiae Atg2, an autophagic vesicle formation protein; up-regulation associated with azole resistance; Spider biofilm induced
orf19.371	orf19.371	-1.55	1.44E-03	Ortholog of C. dubliniensis CD36 : Cd36_40110, C. parapsilosis CDC317 : CPAR2_402300, Candida tenuis NRRL Y-1498 : CANTEDRAFT_94507 and Debaryomyces hansenii CBS767 : DEHA2F05588g
ADH2	orf19.5113	-1.55	7.24E-04	Alcohol dehydrogenase; soluble in hyphae; expression regulated by white-opaque switching; regulated by Ssn6; indued by Mnl1 in weak acid stress; protein enriched in stationary phase yeast cultures; Spider biofilm induced
orf19.5943	orf19.5943	-1.55	9.50E-04	Ortholog(s) have role in peroxisome organization and peroxisomal membrane localization
orf19.6790	orf19.6790	-1.56	5.30E-05	Ortholog(s) have mRNA binding activity, role in 3'-UTR-mediated mRNA destabilization, mitochondrion organization and cytoplasmic mRNA processing body, cytoplasmic stress granule, cytosol, perinuclear region of cytoplasm localization
orf19.2691	orf19.2691	-1.56	3.09E-03	Planktonic growth-induced gene
CAT1	orf19.6229	-1.56	5.43E-04	Catalase; resistance to oxidative stress, neutrophils, peroxide; role in virulence; regulated by iron, ciclopirox, fluconazole, carbon source, pH, Rim101, Ssn6, Hog1, Hap43, Sfu1, Sef1, farnesol, core stress response; Spider biofilm induced
orf19.5003	orf19.5003	-1.56	9.61E-04	Ortholog(s) have GTPase regulator activity and cytoplasm, nuclear envelope localization
orf19.1654	orf19.1654	-1.56	2.44E-04	Predicted membrane protein; induced by prostaglandins
ZCF38	orf19.7518	-1.57	3.74E-05	Putative Zn(II)2Cys6 transcription factor

orf19.5125	orf19.5125	-1.57	5.21E-04	Protein of unknown function; induced by ketoconazole; Spider, F-12/CO2 and flow model biofilm induced
ANT1	orf19.6254	-1.57	8.55E-03	Peroxisomal adenine nucleotide transporter; role in beta-oxidation of medium-chain fatty acid and peroxisome proliferation; rat catheter biofilm induced
PTC4	orf19.6638	-1.58	1.01E-03	Type PP2C serine/threonine phosphatase; localized to mitochondria; mutation causes sensitivity to sodium, potassium and azole drugs; decreased expression in hyphae compared to yeast-form cells
orf19.6596	orf19.6596	-1.58	9.92E-05	Putative esterase; possibly transcriptionally regulated by Tac1; induced by Mnl1 under weak acid stress; protein present in exponential and stationary growth phase yeast cultures; Spider biofilm repressed
ALS9	orf19.5742	-1.58	1.98E-03	ALS family cell-surface glycoprotein; expressed during infection of human epithelial cells; confers laminin adhesion to S. cerevisiae; highly variable; putative GPI-anchor; Hap43-repressed
ATC1	orf19.6214	-1.58	1.14E-04	Cell wall acid trehalase; catalyzes hydrolysis of the disaccharide trehalose; similar to S. cerevisiae vacuolar acid trehalase (Ath1p); Hap43p-repressed gene
orf19.510	orf19.510	-1.59	2.96E-03	Protein of unknown function; Spider biofilm induced
orf19.1764	orf19.1764	-1.59	1.56E-03	Protein of unknown function; rat catheter and Spider biofilm induced
orf19.5842.1	NA	-1.59	1.89E-05	NA
FMP27	orf19.3422	-1.60	2.33E-03	Putative mitochondrial protein; mRNA binds She3
orf19.1240	orf19.1240	-1.60	4.14E-05	Ortholog of S. cerevisiae : YPR117W, C. glabrata CBS138 : CAGL0D04510g, C. dubliniensis CD36 : Cd36_45200, C. parapsilosis CDC317 : CPAR2_500480 and Candida tenuis NRRL Y-1498 : CANTEDRAFT_120679
orf19.6941	orf19.6941	-1.60	5.98E-06	Putative diacylglycerol acyltransferase; catalyzes the terminal step of triacylglycerol formation; flow model biofilm induced; Spider biofilm induced
orf19.3728	orf19.3728	-1.60	1.23E-02	Ortholog(s) have protein phosphatase 1 binding, protein phosphatase type 1 regulator activity, role in chromosome segregation, regulation of phosphoprotein phosphatase activity and cytoplasm localization
orf19.1150	orf19.1150	-1.60	6.99E-05	GATA-like transcription factor; oral infection induced; mutant has reduced capacity to damage oral epithelial cells; regulated by Gcn2 and Gcn4; Spider biofilm induced
LPG20	orf19.771	-1.60	3.09E-04	Aldo-keto reductase family protein; similar to aryl alcohol dehydrogenases; osmotic stress-induced, correlates with overexpression of MDR1 in fluconazole-resistant isolate; stationary phase enriched protein
orf19.5523	orf19.5523	-1.61	4.91E-06	Ortholog of C. dubliniensis CD36 : Cd36_62780, C. parapsilosis CDC317 : CPAR2_601690, Candida tenuis NRRL Y-1498 : CANTEDRAFT_113271 and Debaryomyces hansenii CBS767 : DEHA2A06644g

orf19.1933	orf19.1933	-1.61	1.13E-05	Ortholog(s) have role in peroxisome organization and peroxisomal membrane localization
orf19.7547	orf19.7547	-1.61	3.42E-04	Ortholog(s) have phosphatidylinositol-3-phosphate binding, ubiquitin-protein ligase activity, role in protein ubiquitination and cytosol, fungal-type vacuole membrane, late endosome, nucleus localization
RHD1	orf19.54	-1.61	1.53E-03	Putative beta-mannosyltransferase required for the addition of beta-mannose to the acid labile fraction of cell wall phosphopeptidomannan; 9-gene family memebr; regulated on yeast-hypha and white-opaque switches; Spider biofilm repressed
orf19.673	orf19.673	-1.61	3.44E-04	Has domain(s) with predicted FMN binding, catalytic activity, oxidoreductase activity and role in oxidation-reduction process
orf19.2063	orf19.2063	-1.61	5.93E-05	Ortholog of C. parapsilosis CDC317 : CPAR2_213140, C. dubliniensis CD36 : Cd36_15600, Lodderomyces elongisporus NRLL YB-4239 : LELG_01226 and Debaryomyces hansenii CBS767 : DEHA2B02442g
orf19.4676	orf19.4676	-1.62	1.45E-03	Protein with homology to mitochondrial intermembrane space proteins; regulated by Sef1p-, Sfu1p-, and Hap43p
PEX14	orf19.1805	-1.62	1.75E-05	Ortholog(s) have protein binding, bridging activity, role in protein import into peroxisome matrix, docking and peroxisomal membrane localization
orf19.6508	orf19.6508	-1.64	7.72E-06	Ortholog(s) have protein transporter activity, role in Golgi to plasma membrane transport, intracellular protein transport and vesicle coat localization
AUT7	orf19.2480.1	-1.64	2.35E-05	Putative autophagosome protein; macrophage/pseudohyphal-repressed; alternatively spliced intron in 5' UTR; Spider biofilm induced
DAG7	orf19.4688	-1.64	4.09E-04	Secretory protein; a-specific, alpha-factor induced; mutation confers hypersensitivity to toxic ergosterol analog; fluconazole-induced; induced during chlamydospore formation in C. albicans and C. dubliniensis
PDR16	orf19.1027	-1.64	1.95E-03	Phosphatidylinositol transfer protein; induction correlates with CDR1, CDR2 overexpression/azole resistance; fluphenazine, 17-beta-estradiol, ethynyl estradiol, NO induced; farnesol-downregulated in biofilm; rat catheter biofilm induced
RIM8	orf19.6091	-1.65	2.11E-04	Beta-arrestin-like protein; involved in pH response; required for pathogenesis, activation of Rim101 and alkaline pH-induced hyphal growth; colony morphology-related gene regulation by Ssn6p negative feedback regulation target
orf19.5522	orf19.5522	-1.65	2.97E-04	Ortholog of C. dubliniensis CD36 : Cd36_62760, C. parapsilosis CDC317 : CPAR2_601700, Candida tenuis NRRL Y-1498 : CANTEDRAFT_115220 and Debaryomyces hansenii CBS767 : DEHA2A06666g
orf19.1776	orf19.1776	-1.65	3.38E-05	Putative pantetheine-phosphate adenylyltransferase (PPAT); which catalyzes 4th step in coenzyme A biosynthesis from pantothenate; rat catheter biofilm repressed

STE11	orf19.844	-1.66	2.84E-04	Protein similar to S. cerevisiae Ste11p; mutants are sensitive to growth on H2O2 medium
orf19.164	orf19.164	-1.66	6.25E-04	Ortholog(s) have lipase activity and peroxisomal matrix localization
FCR1	orf19.6817	-1.66	9.54E-05	Transcription factor; repressor of fluconazole/ketoconazole/brefeldin A resistance; Tn mutation enhances filamentation; partially rescues S. cerevisiae pdr1 pdr3 fluconazole sensitivity; rat catheter biofilm induced/Spider biofilm repressed
orf19.7204	orf19.7204	-1.66	2.30E-05	Ortholog(s) have cytoplasm localization
ARG4	orf19.6689	-1.66	4.44E-04	Argininosuccinate lyase, catalyzes the final step in the arginine biosynthesis pathway; alkaline downregulated; flow model biofilm induced; Spider biofilm induced
ECM42	orf19.6500	-1.66	1.77E-05	Ornithine acetyltransferase; Gcn2, Gcn4-regulated; clade-specific gene expression; possibly essential gene, disruptants not obtained by UAU1 method; Spider biofilm induced
orf19.1307	orf19.1307	-1.67	7.91E-04	Predicted membrane protein; rat catheter biofilm induced
orf19.4609	orf19.4609	-1.67	2.19E-03	Putative dienelactone hydrolase; protein abundance is affected by URA3 expression in the CAI-4 strain background; protein present in exponential and stationary growth phase yeast cultures; rat catheter biofilm repressed
LIP1	orf19.4821	-1.68	3.69E-04	Secreted lipase, member of a lipase gene family whose members are expressed differentially in response to carbon source and during infection; may have a role in nutrition and/or in creating an acidic microenvironment
orf19.4911	orf19.4911	-1.68	2.01E-06	BED zinc finger protein; predicted DNA binding protein; Spider biofilm repressed
orf19.4580	orf19.4580	-1.68	3.24E-04	Protein of unknown function; Hap43-repressed gene
orf19.6816	orf19.6816	-1.68	9.54E-05	Putative xylose and arabinose reductase; flow model biofilm induced; Spider biofilm repressed
orf19.4090	orf19.4090	-1.68	1.09E-03	Predicted membrane transporter, member of the fucose:proton symporter (FHS) family, major facilitator superfamily (MFS)
orf19.2168	orf19.2168	-1.68	2.20E-03	Putative sterol deacetylase; flow model biofilm induced; rat catheter biofilm repressed
orf19.1381	orf19.1381	-1.68	8.99E-06	Ortholog of S. cerevisiae/S. pombe Lsb5; predicted role in actin cortical patch localization, actin filament organization, endocytosis; flow model biofilm induced; Spider biofilm repressed
orf19.4174	orf19.4174	-1.69	2.67E-06	Ortholog(s) have nicotinamide riboside transmembrane transporter activity, role in nicotinamide riboside transport, transmembrane transport and fungal-type vacuole membrane localization
orf19.4031	orf19.4031	-1.69	1.46E-05	Ortholog(s) have cytoplasm localization
ZCF13	orf19.2646	-1.70	5.06E-05	Predicted Zn(II)2Cys6 transcription factor; similar to but not the true ortholog of S. cerevisiae Hap1; mutants display decreased colonization of mouse kidneys

ATO2	orf19.2496	-1.70	4.35E-04	Putative fungal-specific transmembrane protein; fluconazole repressed, Hap43-repressed; flow model biofilm induced; Spider biofilm induced
orf19.3156	orf19.3156	-1.70	9.76E-04	Protein of unknown function; induced by Mnl1 under weak acid stress
orf19.3226	orf19.3226	-1.72	4.25E-05	Ortholog(s) have role in intracellular sterol transport and fungal-type vacuole lumen localization
COX11	orf19.1416	-1.73	1.08E-05	Cytochrome oxidase assembly protein; transcript regulated by Nrg1; protein repressed during the mating process; Hap43-repressed gene; rat catheter biofilm induced
PEX8	orf19.2805	-1.73	2.23E-06	Putative peroxisomal biogenesis factor; expression regulated during planktonic growth
YDC1	orf19.3104	-1.74	9.41E-05	Alkaline dihydroceramidase; involved in sphingolipid metabolism; Mob2-dependent hyphal regulation; transcript is regulated by Nrg1 and Mig1; Hap43-repressed
orf19.137	orf19.137	-1.74	2.12E-03	Putative transferase involved in phospholipid biosynthesis; induced by alpha pheromone in SpiderM medium
FAA2-3	orf19.7156	-1.74	4.46E-03	Predicted acyl CoA synthetase
LEU5	orf19.2117	-1.74	2.20E-06	Putative mitochondrial carrier protein; Hap43-repressed; rat catheter biofilm induced
orf19.4368	orf19.4368	-1.74	3.58E-04	Has domain(s) with predicted hydrolase activity and role in cellular process
orf19.577	orf19.577	-1.74	2.43E-05	Predicted protein tyrosine phosphatase; rat catheter biofilm induced
orf19.4610	orf19.4610	-1.74	1.12E-05	Predicted metallocarboxypeptidase; role in proteolysis; rat catheter biofilm repressed
COX17	orf19.2006.1	-1.75	3.76E-04	Putative copper metallochaperone; Hap43p-repressed gene; rat catheter biofilm induced; Spider biofilm induced
orf19.4229	orf19.4229	-1.76	1.69E-06	Putative polyphosphate phosphatase; role in hydrolysis of diphosphorylated inositol polyphosphates and diadenosine polyphosphates; Spider biofilm induced
orf19.6498	orf19.6498	-1.76	1.21E-04	Ortholog(s) have role in RNA polymerase II complex localization to nucleus, RNA polymerase III complex localization to nucleus and DNA-directed RNA polymerase II, holoenzyme, cytoplasm localization
MODF	orf19.5029	-1.76	4.83E-04	Ortholog(s) have mitochondrion localization
OPT8	orf19.5770	-1.76	2.41E-04	Oligopeptide transporter; similar to Opt1 and to S. cerevisiae Ygl114wp, but not other OPTs; induced by nitric oxide, amphotericin B; expression of OPT6, 7, 8 does not complement mutants lacking Opt1, Opt2, and Opt3; Spider biofilm induced
orf19.2262	orf19.2262	-1.76	4.81E-03	Protein similar to quinone oxidoreductases; induced by benomyl treatment, nitric oxide; oxidative stress-induced via Cap1; stationary-phase enriched protein; Spider biofilm induced
orf19.1121	orf19.1121	-1.77	6.21E-05	Has domain(s) with predicted hydrolase activity
IFF4	orf19.7472	-1.77	6.75E-04	Adhesin-like cell surface protein; putative GPI-anchor; null mutant germ tubes show decreased adhesion to plastic substrate; mutants are viable; Hap43-repressed gene

orf19.511	orf19.511	-1.78	8.12E-04	Ortholog(s) have ribosylnicotinamide kinase activity, role in NAD biosynthesis via nicotinamide riboside salvage pathway, nicotinamide riboside metabolic process and cytosol, nucleus localization
ZCF15	orf19.2753	-1.78	4.41E-04	Predicted Zn(II)2Cys6 transcription factor of unknown function; rat catheter biofilm induced
NIT2	orf19.7279	-1.78	2.06E-04	Putative carbon-nitrogen hydrolase; rat catheter biofilm repressed
orf19.1887	orf19.1887	-1.78	9.32E-05	Ortholog(s) have sterol esterase activity, role in sterol metabolic process and integral to membrane, lipid particle localization
orf19.1158	orf19.1158	-1.78	5.96E-05	Ortholog of S. cerevisiae Yft2 required for normal ER membrane biosynthesis; Hap43-repressed gene
orf19.4768	orf19.4768	-1.79	4.04E-05	Protein of unknown function; Spider biofilm induced
SAP3	orf19.6001	-1.80	2.09E-04	Secreted aspartyl proteinase, acts in utilization of protein as nitrogen source; assessment of virulence role complicated by URA3 effects; regulated by growth phase; produced by opaque phase cells; alpha-pheromone repressed
BPH1	orf19.6261	-1.80	6.09E-04	Ortholog of S. cerevisiae Bph1; a putative ortholog of human Chediak-Higashi syndrome protein and murine beige gene implicated in disease syndromes involving defective lysosomal trafficking; mutant is viable
POT1	orf19.7520	-1.81	5.05E-03	Putative peroxisomal 3-oxoacyl CoA thiolase; transcript regulated by Nrg1 and Mig1; farnesol regulated; Hap43-repressed
VCX1	orf19.405	-1.81	1.45E-04	Putative H+/Ca2+ antiporter; Spider biofilm repressed
SOD1	orf19.2770.1	-1.81	1.67E-03	Cytosolic copper- and zinc-containing superoxide dismutase; role in protection from oxidative stress; required for full virulence; alkaline induced by Rim101; induced by human blood; rat catheter, flow model and Spider biofilm repressed
PEX12	orf19.2009	-1.82	7.34E-06	Ortholog(s) have ubiquitin-protein ligase activity, role in protein import into peroxisome matrix and integral to peroxisomal membrane localization
STP3	orf19.5917	-1.82	4.20E-04	Transcription factor; regulates SAP2, OPT1 expression and thereby protein catabolism for nitrogen source; activated via amino-acid-induced proteolytic processing; macrophage/pseudohyphal-repressed; Spider biofilm repressed
orf19.4916	orf19.4916	-1.83	3.38E-05	Protein of unknown function; induced by alpha pheromone in SpiderM medium
orf19.2414	orf19.2414	-1.83	1.29E-03	Ortholog of S. cerevisiae Mpm1; a mitochondrial intermembrane space protein of unknown function; Hap43-repressed; Spider biofilm induced
orf19.4121	orf19.4121	-1.83	3.88E-05	Predicted thioesterase/thiol ester dehydrase-isomerase; Spider biofilm induced
orf19.5572	orf19.5572	-1.83	1.10E-04	Protein of unknown function; Spider biofilm repressed
orf19.931	orf19.931	-1.83	1.09E-03	Ortholog of Candida albicans WO-1 : CAWG_04452
orf19.3910	orf19.3910	-1.84	1.90E-03	Has domain(s) with predicted RNA binding, ribonuclease T2 activity
orf19.4842	orf19.4842	-1.84	3.72E-04	Protein of unknown function; Spider biofilm induced

CPA1	orf19.4630	-1.84	1.06E-04	Putative carbamoyl-phosphate synthase subunit; alkaline repressed; rat catheter, Spider and flow model biofilm induced
orf19.2737	orf19.2737	-1.84	2.78E-03	Carbohydrate kinase domain-containing protein; Spider biofilm induced
orf19.2686	orf19.2686	-1.84	3.23E-06	Ortholog(s) have carboxypeptidase activity, role in nitrogen compound metabolic process, proteolysis involved in cellular protein catabolic process and fungal-type vacuole lumen localization
orf19.2125	orf19.2125	-1.85	9.68E-04	Protein of unknown function; GlcNAc-induced protein; Spider biofilm induced; rat catheter biofilm repressed
MDH1-3	orf19.5323	-1.85	6.28E-06	Predicted malate dehydrogenase; farnesol regulated; protein present in exponential and stationary growth phase yeast; Hap43p-repressed gene
orf19.5809	orf19.5809	-1.85	6.51E-05	Putative arylformamidase, enzyme of the NAD biosynthesis pathway; Gcn4p-regulated
YMX6	orf19.5713	-1.86	1.07E-03	Putative NADH dehydrogenase; macrophage-downregulated gene; induced by nitric oxide; rat catheter biofilm induced
orf19.5446	orf19.5446	-1.86	3.30E-06	Putative protein of unknown function; transcript is upregulated in clinical isolates from HIV+ patients with oral candidiasis; regulated by Ssn6
PEX13	orf19.7282	-1.87	6.58E-06	Protein required for peroxisomal protein import mediated by PTS1 and PTS2 targeting sequences; transcript induced in an RHE model of oral candidiasis; Hap43-repressed gene
PXA1	orf19.7500	-1.88	2.79E-05	Putative peroxisomal, half-size adrenoleukodystrophy protein (ALD or ALDp) subfamily ABC family transporter
CWC22	orf19.1771	-1.88	2.75E-06	Predicted spliceosome-associated protein; role in pre-mRNA splicing; Spider biofilm induced
orf19.178	orf19.178	-1.89	6.57E-06	Ortholog of C. dubliniensis CD36 : Cd36_32460, C. parapsilosis CDC317 : CPAR2_205480, Candida tenuis NRRL Y-1498 : CANTEDRAFT_115156 and Debaryomyces hansenii CBS767 : DEHA2E22154g
HGT2	orf19.3668	-1.89	2.04E-05	Putative MFS glucose transporter; 20 member C. albicans glucose transporter family; 12 probable membrane-spanning segments; expressed in rich medium with 2% glucose; rat catheter and Spider biofilm induced
PHO100	orf19.4424	-1.89	2.43E-03	Putative inducible acid phosphatase; DTT-extractable and observed in culture supernatant in low-phosphate conditions; slight effect on murine virulence; virulence-group-correlated expression; N-glycosylated; F-12/CO2 early biofilm induced
orf19.1314	orf19.1314	-1.90	5.66E-06	Protein of unknown function; planktonic growth-induced gene
orf19.7596	orf19.7596	-1.91	3.33E-04	Protein with a phosphoglycerate mutase family domain; Hap43-repressed gene
orf19.2769	orf19.2769	-1.91	7.50E-05	Putative protease B inhibitor; hyphal-induced expression; Cyr1p- and Ras1p-repressed
orf19.4901	orf19.4901	-1.92	4.59E-04	Predicted methyltransferase; Spider biofilm induced

ALK8	orf19.10	-1.92	3.02E-06	Alkane-inducible cytochrome P450; catalyzes hydroxylation of lauric acid to hydroxylauric acid; overproduction causes fluconazole resistance in WT and causes multidrug resistance in a cdr1 cdr2 double mutant; rat catheter biofilm repressed
EBP7	orf19.5816	-1.92	2.71E-05	Putative NADPH oxidoreductase; mutation confers hypersensitivity to toxic ergosterol analog; oxidative stress-induced via Cap1p
orf19.90	orf19.90	-1.92	7.54E-06	Ortholog(s) have cytoplasm localization
GAP2	orf19.6993	-1.92	1.11E-03	General amino acid permease; ketoconazole, flucytosine repressed; Ssy1-dependent histidine induction; regulated by Nrg1, Tup1; colony morphology-related gene regulation by Ssn6; Spider and flow model biofilm induced
ECM29	orf19.6773	-1.93	1.10E-05	Putative scaffold protein; assists in association of the proteasome core particle with the regulatory particle; ortholog of S. cerevisiae Ecm29; transposon mutation affects filamentous growth; flow model biofilm repressed
ASR1	orf19.2344	-1.93	4.13E-03	Heat shock protein; transcript regulated by cAMP, osmotic stress, ciclopirox olamine, ketoconazole; repressed by Cyr1, Ras1; colony morphology-related regulated by Ssn6; stationary phase enriched; Hap43-induced; Spider biofilm induced
orf19.1308	orf19.1308	-1.93	2.49E-03	Predicted membrane transporter, member of the drug:proton antiporter (14 spanner) (DHA2) family, major facilitator superfamily (MFS)
orf19.5730	orf19.5730	-1.94	1.15E-04	Putative phenylacrylic acid decarboxylase; clade-associated gene expression
POX1-3	orf19.1652	-1.95	5.93E-05	Predicted acyl-CoA oxidase; farnesol regulated; stationary phase enriched protein; Spider biofilm induced
STD1	orf19.6173	-1.95	5.88E-05	Putative transcription factor; involved in control of glucose-regulated gene expression; repressed by Rgt1; Spider biofilm induced
PIR1	orf19.220	-1.95	1.27E-05	1,3-beta-glucan-linked cell wall protein; N-mannosylated, O-glycosylated by Pmt1; cell wall defect in het mutant; Hog1/fluconazole/hypoxia induced; iron/Efg1/Plc1/temp regulated; flow model biofilm induced; hyphal, Spider biofilm repressed
PEX2	orf19.3546	-1.95	7.43E-06	Ortholog(s) have ubiquitin-protein ligase activity, role in protein import into peroxisome matrix and peroxisomal membrane localization
orf19.3922	orf19.3922	-1.96	2.81E-03	Possible pyrimidine 5' nucleotidase; protein present in exponential and stationary growth phase yeast cultures; Hap43p-repressed gene
PEX5	orf19.5640	-1.97	7.69E-06	Pex5p family protein; required for PTS1-mediated peroxisomal protein import, fatty acid beta-oxidation; similar to S. cerevisiae Pas10p peroxisomal targeting receptor; macrophage/pseudohyphal-repressed; Hap43p-repressed
UGT51C1	orf19.2616	-1.98	2.59E-04	UDP-glucose:sterol glucosyltransferase; enzyme of sterol glucoside (membrane-bound lipid) biosynthesis; has UDP-sugar binding domain; activity is UDP-glucose-specific in vitro; enzyme does not use UDP-mannose; Mig1-regulated

PXA2	orf19.5255	-1.98	3.37E-05	Putative peroxisomal, half-size adrenoleukodystrophy protein (ALD or ALDp) subfamily ABC transporter; Gcn4p-regulated
orf19.6973	orf19.6973	-2.00	6.09E-06	ATP-dependent LON protease family member; Hap43-repressed gene; regulated by Gcn2 and Gcn4; Spider biofilm induced
ZCF2	orf19.431	-2.00	9.92E-05	Zn(II)2Cys6 transcription factor; regulates sulfite tolerance through expression of SSU1 and CDG1; Hap43-repressed; Spider biofilm induced
orf19.3029	orf19.3029	-2.00	5.22E-04	Predicted 3-hydroxyisobutyryl-CoA hydrolase; mitochondrially localized; Spider biofilm induced
PHR2	orf19.6081	-2.01	1.20E-04	Glycosidase; role in vaginal not systemic infection (low pH not neutral); low pH, high iron, fluconazole, Hap43-induced; Rim101-repressed at pH8; rat catheter biofilm induced; Bcr1-repressed in RPMI a/a biofilms
GAL10	orf19.3672	-2.02	6.13E-04	UDP-glucose 4-epimerase; galactose utilization; mutant has cell wall defects and increased filamentation; GlcNAc-, fluconazole- and ketoconazole-induced; stationary phase enriched protein; rat catheter and flow model biofilm induced
orf19.5250	orf19.5250	-2.03	2.78E-05	Has domain(s) with predicted cofactor binding activity
ASR2	orf19.7284	-2.04	2.40E-04	Adenylyl cyclase and stress responsive protein; induced in cyr1 or ras1 mutant; stationary phase enriched protein; Spider biofilm induced
LAP3	orf19.539	-2.04	2.09E-03	Putative aminopeptidase; positively regulated by Sfu1; clade-associated gene expression; virulence-group-correlated expression; induced by alpha pheromone in SpiderM medium; Hap43-induced; Spider and flow model biofilm induced
orf19.3047	orf19.3047	-2.04	3.16E-03	Protein kinase-related protein, required for normal sensitivity to caspofungin
CGR1	orf19.2722	-2.04	3.70E-06	Negative regulator of yeast-form growth; HSP70 family member; induced by growth cessation at yeast-hyphal transition or in planktonic growth; physically interacts with Msi3p; similar to rat anti-aging gene, SMP30, stationary phase enriched
orf19.3661	orf19.3661	-2.05	4.24E-05	Putative deubiquitinating enzyme; induced by Mnl1 under weak acid stress
orf19.2620	orf19.2620	-2.05	3.74E-05	Ortholog of C. dubliniensis CD36 : Cd36_33120 and Candida albicans WO-1 : CAWG_02046
orf19.3352	orf19.3352	-2.05	5.68E-05	Has domain(s) with predicted oxidoreductase activity and role in metabolic process
RME1	orf19.4438	-2.07	3.90E-05	Zinc finger protein; controls meiosis in S. cerevisae; white-specific transcript; upregulation correlates with clinical development of fluconazole resistance; Upc2-regulated in hypoxia; flow model biofilm induced; Spider biofilm repressed
RTA3	orf19.23	-2.08	1.94E-05	Similar to S. cerevisiae Rta1 (role in 7-aminocholesterol resistance) and Rsb1 (flippase); putative drug-responsive regulatory site; induced by fluphenazine, estradiol, ketoconazole, caspofungin; rat catheter biofilm induced

CAT2	orf19.4591	-2.09	4.02E-05	Major carnitine acetyl transferase; intracellular acetyl-CoA transport; localized in peroxisomes and mitochondria; induced in macrophages; Hog1-repressed; stationary phase enriched; farnesol-upregulated in biofilm; Spider biofilm induced
orf19.304	orf19.304	-2.10	1.74E-05	Putative transporter similar to MDR proteins; fungal-specific; Spider biofilm induced
orf19.3679	orf19.3679	-2.11	1.13E-04	Putative protein of unknown function; stationary phase enriched protein
GST2	orf19.2693	-2.11	4.07E-05	Glutathione S transferase; induced by benomyl and in populations of cells exposed to fluconazole over multiple generations; regulated by Nrg1, Tup1; induced by nitric oxide; stationary phase enriched; Spider biofilm induced
EHT1	orf19.3040	-2.12	7.21E-06	Putative acyl-coenzymeA:ethanol O-acyltransferase; regulated by Sef1, Sfu1, and Hap43; induced by alpha pheromone in SpiderM medium; Spider biofilm induced; promoter bound by Ndt80
orf19.2846	orf19.2846	-2.14	1.23E-03	Protein of unknown function; Hap43-repressed; induced in core caspofungin response; regulated by yeast-hypha switch; Spider biofilm repressed
RHD3	orf19.5305	-2.14	1.42E-06	GPI-anchored yeast-associated cell wall protein; induced in high iron; clade-associated gene expression; not essential for cell wall integrity; fluconazole-repressed; flow model and Spider biofilm repressed
CTN1	orf19.4551	-2.14	5.73E-05	Carnitine acetyl transferase; required for growth on nonfermentable carbon sources, not for hyphal growth or virulence in mice; induced in macrophage; macrophage/pseudohyphal-repressed after 16 hr; rat catheter, Spider biofilm induced
orf19.2204	orf19.2204	-2.14	1.42E-06	Predicted membrane protein of unknown function; Spider biofilm induced
orf19.5295	orf19.5295	-2.15	1.07E-03	Protein with a predicted endonuclease/exonuclease/phosphatase family domain and a carbon catabolite repressor protein 4 domain; induced by alpha pheromone in SpiderM medium
ARG8	orf19.3770	-2.16	3.46E-04	Putative acetylornithine aminotransferase; Gcn2, Gcn4 regulated; rat catheter biofilm induced; Spider biofilm induced
orf19.6788	orf19.6788	-2.16	5.94E-07	Protein with a predicted role in cotranslational protein targeting to membrane; induced during chlamydospore formation in both C. albicans and C. dubliniensis
IFU5	orf19.2568	-2.16	7.32E-06	Predicted membrane protein; estradiol-induced; upregulation associated with CDR1 and CDR2 overexpression or fluphenazine; putative drug-responsive regulatory site; similar to S. cerevisiae Wwm1p; Hap43-repressed; Spider biofilm repressed
orf19.4886	orf19.4886	-2.17	1.12E-05	Putative adhesin-like protein; Hap43-repressed; rat catheter and Spider biofilm induced
orf19.3544	orf19.3544	-2.18	1.68E-05	Putative protein of unknown function; Hap43p-repressed gene
orf19.6797	orf19.6797	-2.18	7.54E-06	Ortholog of C. dubliniensis CD36 : Cd36_86960, C. parapsilosis CDC317 : CPAR2_808800, Candida tenuis NRRL Y-1498 : CANTEDRAFT_113621 and Debaryomyces hansenii CBS767 : DEHA2F02486g
orf19.5449	orf19.5449	-2.20	6.95E-06	Predicted integral membrane protein; Spider biofilm induced

orf19.7196	orf19.7196	-2.21	1.14E-06	Putative vacuolar protease; upregulated in the presence of human neutrophils; Spider biofilm induced
CSO99	orf19.2883	-2.21	1.87E-06	Protein of unknown function; Hap43-repressed gene; protein not conserved in S. cerevisiae
PRC2	orf19.4135	-2.23	3.06E-05	Putative carboxypeptidase; induced by human neutrophils; Spider biofilm induced
orf19.3610	orf19.3610	-2.23	1.28E-05	Protein of unknown function; upregulation correlates with clinical development of fluconazole resistance; regulated by Sef1, Sfu1, and Hap43
orf19.1461	orf19.1461	-2.24	4.83E-04	S. pombe ortholog SPCC576.01c is a predicted sulfonate dioxygenase; possibly transcriptionally regulated upon hyphal formation; Spider biofilm induced
GAL7	orf19.3675	-2.24	3.32E-06	Putative galactose-1-phoshphate uridyl transferase; downregulated by hypoxia, upregulated by ketoconazole; macrophage/pseudohyphal-repressed
POT1-2	orf19.2046	-2.26	4.95E-04	Putative peroxisomal 3-ketoacyl CoA thiolase; Hap43-repressed
YWP1	orf19.3618	-2.26	5.35E-03	Secreted yeast wall protein; possible role in dispersal in host; mutation increases adhesion and biofilm formation; propeptide; growth phase, phosphate, Ssk1/Ssn6/Efg1/Efh1/Hap43 regulated; mRNA binds She3; flow and Spider biofilm repressed
orf19.11	orf19.11	-2.27	2.88E-06	Protein of unknown function; transcript regulated by Mig1 and Tup1; rat catheter biofilm induced
orf19.1356	orf19.1356	-2.29	1.16E-06	Ortholog(s) have thiosulfate sulfurtransferase activity, role in tRNA wobble position uridine thiolation and mitochondrion localization
LYP1	orf19.651	-2.32	1.13E-06	Putative permease; amphotericin B induced; flucytosine repressed; possibly an essential gene, disruptants not obtained by UAU1 method
PDK2	orf19.7281	-2.34	7.43E-06	Putative pyruvate dehydrogenase kinase; mutation confers hypersensitivity to amphotericin B
CYB2	orf19.5000	-2.38	2.86E-05	Putative cytochrome b2 precursor; induced in high iron; alkaline repressed; colony morphology-related gene regulation by Ssn6; Hap43-repressed; pider biofilm induced
orf19.2284	orf19.2284	-2.38	1.87E-05	Protein with an FMN-binding domain; Hap43-repressed; flow model biofilm induced
HGT13	orf19.7093	-2.42	2.30E-05	Predicted sugar transporter, involved in glycerol utilization; member of the major facilitator superfamily; 12 transmembrane; gene has intron; oxidative stress-induced via Cap1p; expressed in rich medium, 2% glucose
orf19.5565	orf19.5565	-2.44	1.14E-03	Putative 3-hydroxyisobutyrate dehydrogenase; rat catheter and Spider biofilm induced
ZCF16	orf19.2808	-2.44	4.15E-06	Predicted Zn(II)2Cys6 transcription factor; mutants are viable; rat catheter biofilm induced
orf19.3627	orf19.3627	-2.45	9.33E-07	Ortholog of C. dubliniensis CD36 : Cd36_22640, C. parapsilosis CDC317 : CPAR2_406910, Candida tenuis NRRL Y-1498 : CANTEDRAFT_104937 and Debaryomyces hansenii CBS767 : DEHA2D02706g

PEX4	orf19.4041	-2.45	4.85E-07	Putative peroxisomal ubiquitin conjugating enzyme; regulated by Sef1, Sfu1, and Hap43; rat catheter biofilm induced; Spider biofilm induced
CMK1	orf19.5911	-2.46	1.43E-05	Putative calcium/calmodulin-dependent protein kinase II; expression regulated upon white-opaque switching; biochemically purified Ca2+/CaM-dependent kinase is soluble, cytosolic, monomeric, and serine-autophosphorylated; Hap43p-repressed
PEX1	orf19.6460	-2.46	5.52E-06	Ortholog(s) have ATPase activity, protein heterodimerization activity, role in protein import into peroxisome matrix, receptor recycling and cytosol, peroxisomal membrane localization
orf19.1395	orf19.1395	-2.47	2.05E-05	Ortholog(s) have inorganic phosphate transmembrane transporter activity, role in phosphate ion transport, transmembrane transport and mitochondrion localization
PRN1	orf19.2467	-2.49	1.99E-04	Protein with similarity to pirins; induced by benomyl and in response to alpha pheromone in SpiderM medium; transcript induced by Mnl1 in weak acid stress; rat catheter and Spider biofilm induced
orf19.1890	orf19.1890	-2.55	3.26E-06	Ortholog(s) have role in medium-chain fatty acid biosynthetic process
HXT5	orf19.4384	-2.57	8.48E-04	Putative sugar transporter; induced by ciclopirox olamine; Snf3-induced; alkaline repressed; colony morphology-related gene regulation by Ssn6; possibly essential gene
orf19.3684	orf19.3684	-2.60	2.63E-05	Putative oxidoreductase; Spider biofilm induced
DLD1	orf19.5805	-2.64	5.70E-06	Putative D-lactate dehydrogenase; white cell-specific trancript; colony morphology-related gene regulation by Ssn6; Hap43-repressed; rat catheter biofilm induced; Spider biofilm repressed
CRC1	orf19.2599	-2.64	1.13E-06	Mitochondrial carnitine carrier protein
orf19.3139	orf19.3139	-2.66	1.12E-05	Putative NADP-dependent oxidoreductase; Hap43-repressed; induced by benomyl treatment; oxidative stress-induced via Cap1; rat catheter biofilm repressed
orf19.6793	orf19.6793	-2.67	1.00E-04	Protein of unknown function; Sef1, Sfu1, and Hap43 regulated; rat catheter and Spider biofilm induced
CIT1	orf19.4393	-2.71	6.85E-04	Citrate synthase; induced by phagocytosis; induced in high iron; Hog1-repressed; Efg1-regulated under yeast, not hyphal growth conditions; present in exponential and stationary phase; Spider biofilm repressed; rat catheter biofilm induced
orf19.1430	orf19.1430	-2.71	1.82E-06	Ortholog of C. parapsilosis CDC317 : CPAR2_402120, C. dubliniensis CD36 : Cd36_43870, Lodderomyces elongisporus NRLL YB-4239 : LELG_04437 and Candida orthopsilosis Co 90-125 : CORT_0E02170
HGT19	orf19.5447	-2.72	5.43E-04	Putative MFS glucose/myo-inositol transporter; 20 member family; 12 transmembrane segments, extended N terminus; expressed in rich medium; Hap43, phagocytosis, rat catheter, Spider and flow model biofilm induced
orf19.692	orf19.692	-2.72	6.66E-07	Protein of unknown function; Hap43-repressed gene; rat catheter and Spider biofilm induced

orf19.2244	orf19.2244	-2.81	2.15E-05	Similar to oxidoreductases and to S. cerevisiae Yjr096wp; Sfu1 repressed; induced by benomyl treatment, Ssr1; Hap43-repressed; flow model biofilm repressed
orf19.5290	orf19.5290	-2.83	2.03E-07	Protein of unknown function; repressed by Sfu1; Hap43-induced gene
ARG1	orf19.7469	-2.83	1.34E-05	Argininosuccinate synthase; arginine synthesis; Gcn4, Rim101 regulated; induced by amino acid starvation (3-AT), benomyl treatment; stationary phase enriched protein; repressed in alkalinizing medium; rat catheter, Spider biofilm induced
orf19.4873	orf19.4873	-2.85	1.15E-07	Protein of unknown function; transcript regulated by white-opaque switch; flow model biofilm induced; Spider biofilm induced
FOX2	orf19.1288	-2.88	2.49E-06	3-hydroxyacyl-CoA epimerase; fatty acid beta-oxidation; induced by phagocytosis; regulated by Mig1, by white-opaque switch, by DNA methylation; transcriptional activation by oleate requires Ctf1; rat catheter and Spider biofilm induced
orf19.1709	orf19.1709	-2.89	4.90E-06	Sterol carrier domain protein; alkaline downregulated; colony morphology-related gene regulation by Ssn6; Spider biofilm induced
orf19.4807	orf19.4807	-2.91	1.13E-06	Ortholog(s) have inorganic diphosphatase activity, role in aerobic respiration and mitochondrion localization
orf19.5587	orf19.5587	-2.91	2.38E-06	Protein of unknown function; transcript is upregulated in clinical isolates from HIV+ patients with oral candidiasis
orf19.4287	orf19.4287	-2.95	1.76E-07	Putative oxidoreductase; Hap43-repressed gene; clade-associated gene expression
GCA1	orf19.4899	-3.09	2.77E-05	Extracellular/plasma membrane-associated glucoamylase; expressed in rat oral infection; regulated by carbohydrates, pH, galactose; promotes biofilm matrix formation; flow model biofilm induced; Bcr1 repressed in RPMI a/a biofilms
orf19.4370	orf19.4370	-3.10	5.80E-07	Protein of unknown function; induced by nitric oxide; oxidative stress-induced via Cap1; fungal-specific (no human or murine homolog)
FMA1	orf19.6837	-3.11	4.99E-06	Putative oxidoreductase; induced by ciclopirox olamine; upregulation correlates with clinical development of fluconazole resistance; Spider biofilm repressed
ECI1	orf19.6445	-3.14	1.02E-07	Protein similar to S. cerevisiae Eci1p, which is involved in fatty acid oxidation; transposon mutation affects filamentous growth; expression is regulated upon white-opaque switching
PEX6	orf19.3573	-3.19	5.80E-07	Ortholog(s) have ATPase activity, protein heterodimerization activity, role in protein import into peroxisome matrix, receptor recycling, replicative cell aging and cytosol, nucleus, peroxisome localization
FOX3	orf19.1704	-3.19	5.59E-07	Putative peroxisomal 3-oxoacyl CoA thiolase; transcript regulated by white-opaque switch; Spider biofilm induced
orf19.7288	orf19.7288	-3.22	1.28E-06	Protein with predicted oxidoreductase and dehydrogenase domains; Hap43-repressed; Spider biofilm induced

orf19.3621	orf19.3621	-3.23	4.09E-06	Possible pseudogene; similar to Ywp1p; ORF extended upstream from the initiating Met of orf19.3621 has a stop codon in the region corresponding to the Ywp1p signal peptide; disruption causes no apparent phenotype; no expression detected
orf19.7091	orf19.7091	-3.29	4.91E-06	Protein of unknown function; induced by nitric oxide; Spider biofilm repressed
PXP2	orf19.1655	-3.31	2.75E-06	Putative acyl-CoA oxidase; enzyme of fatty acid beta-oxidation; induced during macrophage infection; opaque specific transcript; putative peroxisome targeting signal; Spider biofilm induced
FAA21	orf19.272	-3.35	5.25E-07	Predicted acyl CoA synthetase; upregulated upon phagocytosis; transcript regulated by Nrg1 and Mig1
RBR1	orf19.535	-3.35	3.21E-04	Glycosylphosphatidylinositol (GPI)-anchored cell wall protein; required for filamentous growth at acidic pH; expression repressed by Rim101 and activated by Nrg1; Hap43-induced
GCA2	orf19.999	-3.38	6.42E-07	Predicted extracellular glucoamylase; induced by ketoconazole; possibly essential, disruptants not obtained by UAU1 method; promotes biofilm matrix formation; Spider biofilm induced; Bcr1-induced in RPMI a/a biofilms
orf19.633	orf19.633	-3.40	1.89E-05	Putative methyltransferase; decreased expression in hyphae compared to yeast; expression regulated during planktonic growth; flow model biofilm induced; Hap43-repressed gene
orf19.1985	orf19.1985	-3.45	6.15E-07	Has aminoglycoside phosphotransferase and protein kinase domains; rat catheter and flow model biofilm induced
GAL1	orf19.3670	-3.50	2.52E-06	Galactokinase; galactose, Mig1, Tup1, Hap43 regulated; fluconazole, ketoconazole-induced; stationary phase enriched protein; GlcNAc-induced protein; farnesol, hypoxia-repressed in biofilm; rat catheter and Spider biofilm induced
IFD3	orf19.3311	-3.55	2.73E-07	Putative aldo/keto reductase; Mig1-regulated
orf19.5525	orf19.5525	-3.69	1.06E-07	Putative oxidoreductase; protein levels affected by URA3 expression in CAI-4 strain background; Efg1, Efh1 regulated; Rgt1-repressed; protein present in exponential and stationary growth phase yeast; rat catheter biofilm repressed
orf19.7029	orf19.7029	-3.70	6.42E-07	Putative guanine deaminase; mutation confers hypersensitivity to toxic ergosterol analog; Spider biofilm induced
TES15	orf19.5215	-3.81	2.48E-06	Putative acyl-CoA thioesterase; Hap43-repressed; Spider biofilm induced
PGA10	orf19.5674	-4.09	5.80E-07	GPI anchored membrane protein; utilization of hemin and hemoglobin for Fe in host; Rim101 at ph8/hypoxia/ketoconazole/ciclopirox/hypha-induced; required for RPMI biofilm formation, Bcr1-induced in a/a biofilm; rat catheter biofilm repressed
orf19.6838	orf19.6838	-4.23	5.78E-06	Putative protein of unknown function, transcript upregulated in clinical isolates from HIV+ patients with oral candidiasis; Spider biofilm induced

HSP30	orf19.4526	-4.24	1.20E-07	Putative heat shock protein; fluconazole repressed; amphotericin B induced; Spider biofilm induced; rat catheter biofilm induced
ARG3	orf19.5610	-4.26	9.49E-07	Putative ornithine carbamoyltransferase; Gcn4-regulated; Hap43-induced; repressed in alkalinizing medium; rat catheter and Spider biofilm induced
orf19.2114	orf19.2114	-4.74	4.22E-06	Predicted uricase; ortholog of S. pombe SPCC1223.09; Spider biofilm induced
GCY1	orf19.6757	-4.83	3.58E-07	Aldo/keto reductase; mutation confers hypersensitivity to toxic ergosterol analog; farnesol-repressed; stationary phase enriched protein; flow model biofilm induced; Spider biofilm repressed
HGT17	orf19.4682	-6.02	9.13E-10	Putative MFS family glucose transporter; 20 members in C. albicans; 12 probable membrane-spanning segments; induced at low (0.2%, compared to 2%) glucose in rich media; Spider biofilm induced

SUPPLEMENTARY TABLE III.4C_GO ANALYSIS FOR GENES MODULATED AT HIGH CELL DENSITY**

GO_term	Cluster frequency	Background frequency	Corrected P-value	Gene(s) annotated to the term
Downregulated genes_High density				
fatty acid oxidation	11 out of 259 genes, 4.2%	14 out of 6473 background genes, 0.2%	7.02E-11	ANT1:MDH1-3:FOX2:PXP2:POX1-3:PEX5:CAT2:POT1:PEX14:ALK8:ECI1
lipid oxidation	11 out of 259 genes, 4.2%	14 out of 6473 background genes, 0.2%	7.02E-11	ANT1:MDH1-3:FOX2:PXP2:POX1-3:PEX5:CAT2:POT1:PEX14:ALK8:ECI1
fatty acid beta-oxidation	10 out of 259 genes, 3.9%	12 out of 6473 background genes, 0.2%	3.42E-10	ANT1:MDH1-3:FOX2:PXP2:POX1-3:PEX5:CAT2:POT1:PEX14:ECI1
monocarboxylic acid catabolic process	15 out of 259 genes, 5.8%	36 out of 6473 background genes, 0.6%	1.18E-09	CTN1:EHT1:ANT1:C1_10240C_A:MDH1-3:FOX2:PXP2:POX1-3:PEX5:CAT2:C6_03620C_A:POT1:CRC1:PEX14:ECI1
fatty acid catabolic process	11 out of 259 genes, 4.2%	18 out of 6473 background genes, 0.3%	5.32E-09	EHT1:ANT1:MDH1-3:FOX2:PXP2:POX1-3:PEX5:CAT2:POT1:PEX14:ECI1
monocarboxylic acid metabolic process	26 out of 259 genes, 10.0%	133 out of 6473 background genes, 2.1%	5.45E-09	RIM8:CTN1:EHT1:ANT1:ADH2:C1_10240C_A:CYB2:C2_02950W_A:PEX6:C2_07410W_A:MDH1-3:FOX2:PXP2:POX1-3:FAA21:PEX5:CAT2:C6_03620C_A:PEX1:C7_04310C_A:POT1:CRC1:PEX14:ALK8:ECI1:PEX13
fatty acid metabolic process	18 out of 259 genes, 6.9%	63 out of 6473 background genes, 1.0%	1.24E-08	EHT1:ANT1:PEX6:C2_07410W_A:MDH1-3:FOX2:PXP2:POX1-3:FAA21:PEX5:CAT2:PEX1:POT1:CRC1:PEX14:ALK8:ECI1:PEX13

cellular lipid catabolic process	14 out of 259 genes, 5.4%	36 out of 6473 background genes, 0.6%	2.06E-08	EHT1:ANT1:MDH1-3:FOX2:PXP2:POX1-3:PEX5:C4_00950C_A:CAT2:YDC1:POT1:CR_02570C_A:PEX14:ECI1
organic acid catabolic process	18 out of 259 genes, 6.9%	69 out of 6473 background genes, 1.1%	6.65E-08	CTN1:EHT1:ANT1:ADH2:C1_10240C_A:MDH1-3:FOX2:PXP2:POX1-3:PEX5:CPA1:CAT2:C6_03620C_A:POT1:CRC1:LAP3:PEX14:ECI1
carboxylic acid catabolic process	18 out of 259 genes, 6.9%	69 out of 6473 background genes, 1.1%	6.65E-08	CTN1:EHT1:ANT1:ADH2:C1_10240C_A:MDH1-3:FOX2:PXP2:POX1-3:PEX5:CPA1:CAT2:C6_03620C_A:POT1:CRC1:LAP3:PEX14:ECI1
small molecule catabolic process	20 out of 259 genes, 7.7%	87 out of 6473 background genes, 1.3%	7.18E-08	CTN1:EHT1:ANT1:ADH2:C1_10240C_A:MDH1-3:FOX2:PXP2:POX1-3:PEX5:CPA1:CAT2:C5_02220C_A:C6_03620C_A:POT1:CRC1:LAP3:PEX14:ECI1:CR_09670C_A
lipid modification	13 out of 259 genes, 5.0%	33 out of 6473 background genes, 0.5%	8.80E-08	ANT1:C2_08170W_A:MDH1-3:FOX2:PXP2:POX1-3:PEX5:CAT2:POT1:UGT51C1:PEX14:ALK8:ECI1
lipid catabolic process	15 out of 259 genes, 5.8%	47 out of 6473 background genes, 0.7%	1.07E-07	EHT1:ANT1:LIP1:MDH1-3:FOX2:PXP2:POX1-3:PEX5:C4_00950C_A:CAT2:YDC1:POT1:CR_02570C_A:PEX14:ECI1
single-organism catabolic process	35 out of 259 genes, 13.5%	289 out of 6473 background genes, 4.5%	1.58E-06	CTN1:GAL1:GAL10:GAL7:EHT1:AUT7:ANT1:CAT1:ATC1:ADH2:LIP1:C1_10240C_A:C2_00180C_A:SPO72:MDH1-3:FOX2:PXP2:POX1-3:C3_06860C_A:GCY1:PEX5:C4_00950C_A:CPA1:CAT2:YDC1:C5_02220C_A:C6_03620C_A:C7_00870W_A:POT1:CRC1:CR_02570C_A:LAP3:PEX14:ECI1:CR_09670C_A
protein import into peroxisome matrix	8 out of 259 genes, 3.1%	14 out of 6473 background genes, 0.2%	9.03E-06	PEX12:PEX2:PEX6:PEX5:PEX4:PEX1:PEX14:PEX13

peroxisomal transport	8 out of 259 genes, 3.1%	16 out of 6473 background genes, 0.2%	3.61E-05	PEX12:PEX2:PEX6:PEX5:PEX4:PEX1:PEX14:PEX13
protein targeting to peroxisome	8 out of 259 genes, 3.1%	16 out of 6473 background genes, 0.2%	3.61E-05	PEX12:PEX2:PEX6:PEX5:PEX4:PEX1:PEX14:PEX13
protein localization to peroxisome	8 out of 259 genes, 3.1%	16 out of 6473 background genes, 0.2%	3.61E-05	PEX12:PEX2:PEX6:PEX5:PEX4:PEX1:PEX14:PEX13
establishment of protein localization to peroxisome	8 out of 259 genes, 3.1%	16 out of 6473 background genes, 0.2%	3.61E-05	PEX12:PEX2:PEX6:PEX5:PEX4:PEX1:PEX14:PEX13
oxidation-reduction process	39 out of 259 genes, 15.1%	408 out of 6473 background genes, 6.3%	1.40E-04	CTN1:ANT1:CAT1:ADH2:C1_09440W_A:C1_11290W_A:C2_01540W_A:EBP7:DLD1:ADH3:C2_04480W_A:C2_05130W_A:C2_06890C_A:C2_07070W_A:C2_07270W_A:MDH1-3:FOX2:PXP2:POX1-3:C3_06860C_A:GCY1:PEX5:CAT2:SOD1:COX11:C4_06710W_A:C5_02690W_A:C6_02560W_A:YMX6:C6_03620C_A:C7_03780C_A:C7_04310C_A:POT1:OYE22:CIT1:PEX14:ALK8:ECI1:CR_08920W_A
peroxisome organization	12 out of 259 genes, 4.6%	48 out of 6473 background genes, 0.7%	1.50E-04	ANT1:PEX12:PEX2:PEX6:SPO72:C3_04800C_A:PEX5:C5_01350W_A:PEX4:PEX1:PEX14:PEX13
oxoacid metabolic process	35 out of 259 genes, 13.5%	350 out of 6473 background genes, 5.4%	2.10E-04	RIM8:CTN1:EHT1:ANT1:ADH2:C1_10240C_A:CYB2:C2_02950W_A:PEX6:C2_07410W_A:MDH1-3:FOX2:PXP2:POX1-3:FAA21:PEX5:CPA1:CAT2:ARG8:C5_02220C_A:ARG3:C6_03620C_A:ECM42:PEX1:ARG4:C7_04310C_A:POT1:ARG1:CRC1:CIT1:LAP3:PEX14:ALK8:ECI1:PEX13
organic acid metabolic process	35 out of 259 genes, 13.5%	351 out of 6473 background genes, 5.4%	2.30E-04	RIM8:CTN1:EHT1:ANT1:ADH2:C1_10240C_A:CYB2:C2_02950W_A:PEX6:C2_07410W_A:MDH1-3:FOX2:PXP2:POX1-3:FAA21:PEX5:CPA1:CAT2:ARG8:C5_02220C_A:ARG3:C6_03620C_A:ECM42:PEX1:ARG4:C7_04310C_A:POT1:ARG1:CRC1:CIT1:LAP3:PEX14:ALK8:ECI1:PEX13

carboxylic acid metabolic process	34 out of 259 genes, 13.1%	340 out of 6473 background genes, 5.3%	3.20E-04	RIM8:CTN1:EHT1:ANT1:ADH2:C1_10240C_A:CYB2:C2_02950W_A:PEX6:C2_07410W_A:MDH1-3:FOX2:PXP2:POX1-3:FAA21:PEX5:CPA1:CAT2:ARG8:ARG3:C6_03620C_A:ECM42:PEX1:ARG4:C7_04310C_A:POT1:ARG1:CRC1:CIT1:LAP3:PEX14:ALK8:ECI1:PEX13
lipid metabolic process	29 out of 259 genes, 11.2%	267 out of 6473 background genes, 4.1%	4.40E-04	EHT1:PDR16:ANT1:LIP1:C1_11620W_A:PEX6:C2_07410W_A:C2_07440C_A:C2_08170W_A:MDH1-3:FOX2:PXP2:POX1-3:FAA21:C3_03760W_A:PEX5:C4_00950C_A:CAT2:SOD1:YDC1:PEX1:POT1:CRC1:UGT51C1:CR_02570C_A:PEX14:ALK8:ECI1:PEX13
cellular lipid metabolic process	27 out of 259 genes, 10.4%	244 out of 6473 background genes, 3.8%	7.60E-04	EHT1:PDR16:ANT1:C1_11620W_A:PEX6:C2_07410W_A:C2_08170W_A:MDH1-3:FOX2:PXP2:POX1-3:FAA21:C3_03760W_A:PEX5:C4_00950C_A:CAT2:SOD1:YDC1:PEX1:POT1:CRC1:UGT51C1:CR_02570C_A:PEX14:ALK8:ECI1:PEX13
monosaccharide transport	9 out of 259 genes, 3.5%	31 out of 6473 background genes, 0.5%	1.33E-03	HGT2:GAL1:C2_09280C_A:HGT19:STD1:HGT17:HGT10:HGT13:HXT5
hexose transport	9 out of 259 genes, 3.5%	31 out of 6473 background genes, 0.5%	1.33E-03	HGT2:GAL1:C2_09280C_A:HGT19:STD1:HGT17:HGT10:HGT13:HXT5
arginine metabolic process	6 out of 259 genes, 2.3%	12 out of 6473 background genes, 0.2%	1.83E-03	CPA1:ARG8:ARG3:ECM42:ARG4:ARG1
small molecule metabolic process	49 out of 259 genes, 18.9%	631 out of 6473 background genes, 9.7%	1.95E-03	RIM8:CTN1:GAL7:C1_02220C_A:EHT1:PDR16:ANT1:ADH2:C1_10240C_A:CYB2:C2_00180C_A:C2_02950W_A:PEX6:C2_07410W_A:C2_07440C_A:C2_08170W_A:C2_10060C_A:MDH1-3:FOX2:PXP2:POX1-3:FAA21:PEX5:CPA1:CAT2:ARG8:C5_02220C_A:C5_04360C_A:C6_02560W_A:HPD1:ARG3:C6_03620C_A:C7_00870W_A:ECM42:PEX1:ARG4:C7_04310C_A:POT1:ARG1:CRC1:UGT51C1:CIT1:CR_04230W_A:LAP3:PEX14:ALK8:ECI1:PEX13:CR_09670C_A
carbohydrate transport	9 out of 259 genes, 3.5%	37 out of 6473 background genes, 0.6%	6.67E-03	HGT2:GAL1:C2_09280C_A:HGT19:STD1:HGT17:HGT10:HGT13:HXT5

arginine biosynthetic process	5 out of 259 genes, 1.9%	9 out of 6473 background genes, 0.1%	6.84E-03	CPA1:ARG3:ECM42:ARG4:ARG1
monosaccharide catabolic process	6 out of 259 genes, 2.3%	15 out of 6473 background genes, 0.2%	8.97E-03	GAL1:GAL10:GAL7:ADH2:C3_06860C_A:GCY1
transmembrane transport	31 out of 259 genes, 12.0%	348 out of 6473 background genes, 5.4%	1.19E-02	C1_01750W_A:HGT2:VCX1:PXA2:LEU5:PEX12:VMA7:PEX2:PEX6:C2_09280C_A:C2_09590C_A:HGT19:C3_03070W_A:GAP2:PEX5:C4_00680W_A:HGT17:C4_03700W_A:DAL52:PEX4:NHX1:HGT10:OPT8:HGT13:PEX1:OPT3:HXT5:PEX14:LYP1:PEX13:SSU1
organic substance catabolic process	40 out of 259 genes, 15.4%	508 out of 6473 background genes, 7.8%	1.33E-02	CTN1:C1_02040C_A:GAL1:GAL10:GAL7:EHT1:ANT1:ATC1:ADH2:LIP1:C1_10240C_A:GCA1:C2_00180C_A:MDH1-3:FOX2:PXP2:POX1-3:SAP3:C3_05360C_A:C3_06860C_A:GCY1:PEX5:C4_00950C_A:CPA1:CAT2:C4_03050C_A:YDC1:C5_02220C_A:HPD1:C6_03620C_A:C7_00870W_A:C7_03860W_A:POT1:CRC1:CR_02570C_A:CIT1:LAP3:PEX14:ECI1:CR_09670C_A

Upregulated genes_High density

ribosome biogenesis	154 out of 578 genes, 26.6%	298 out of 6473 background genes, 4.6%	3.21E-84	RRS1:C1_01160C_A:RPS21B:RPS21:RPS16A:TSR2:RPL6:ARX1:RLI1:C1_04040C_A:ERB1:NOP4:C1_04710C_A:REI1:RPS14B:NOP6:C1_07960W_A:FUN12:DIP2:YTM1:C1_09710C_A:DBP3:C1_10620W_A:RPS17B:C1_10880W_A:C1_10950C_A:C1_10970W_A:NEP1:KRR1:CSI2:C1_12680W_A:DIM1:C1_14080W_A:MPP10:C2_00410C_A:UTP21:C2_02540W_A:C2_03000C_A:RPS9B:C2_04120C_A:C2_04570W_A:C2_04700C_A:MAK5:C2_05160C_A:RPF2:RPS8A:C2_05750W_A:MAK16:RPL11:NOC4:RCL1:NSA1:KRE30:RPS10:RRP8:PES1:RRP15:RPL3:RPS24:UTP8:BUD21:BMS1:RPS7A:C3_01560W_A:C3_02020W_A:RPL12:UTP4:HBR3:MAK21:RPS15:NOP14:RPL35:C3_05160C_A:RPS19A:CAM1:NOG1:NSA2:C3_06760W_A:C3_07550C_A:UTP9:RLP24:RPS6A:PWP1:SAS10:HCA4:ZUO1:NAN1:RPF1:ECM1:SSZ1:C4_04820C_A:RPL30:C4_05010W_A:C4_05330C_A:C4_06210C_A:NOP1:UBI3:C5_01540W_A:SPB4:TIF5:UTP13:RPS5:C5_03920C_A:HAS1:NOP5:RPS13:CIC1:C6_01890C_A:C6_02230W_A:NIP7:C6_02380W_A:MRT4:NOG2:SPB1:NOP8:C7_00160C_A:RPS18:DBP7:RPL5:ENP2:ENP1:UTP18:BUD22:PWP2:CR_01780W_A:DBP2:YVH1:CR_03940W_A:CR_04110W_A:CR_04170W_A:CR_04240C_A:RPS3:NOC2:SDA1:RPL7:NMD3:CR_07030C_A:CR_07080W_A:RPS27:NOP10:RIO2:TSR1:CR_08500W_A:ELF1:SSF1:CR_09740W_A:CR_09800C_A:SIK1:UTP5:CR_10410C_A:CR_10470C_A:DRS1:LTV1:POP3
ribonucleoprotein complex biogenesis	160 out of 578 genes, 27.7%	369 out of 6473 background genes, 5.7%	3.31E-73	RRS1:C1_01160C_A:RPS21B:RPS21:RPS16A:TSR2:RPL6:ARX1:RLI1:C1_04040C_A:ERB1:NOP4:C1_04710C_A:REI1:RPS14B:NOP6:SUI2:C1_07960W_A:FUN12:DIP2:YTM1:C1_09710C_A:DBP3:C1_10620W_A:RPS17B:C1_10880W_A:C1_10950C_A:C1_10970W_A:NEP1:KRR1:CSI2:C1_12680W_A:DIM1:C1_14080W_A:MPP10:C2_00410C_A:PRP39:UTP21:C2_02540W_A:C2_03000C_A:RPS9B:C2_04120C_A:C2_04570W_A:C2_04700C_A:MAK5:C2_05160C_A:RPF2:RPS8A:C2_05750W_A:MAK16:RPL11:NOC4:RCL1:NSA1:KRE30:RPS10:RRP8:PES1:RRP15:RPL3:TIF11:RPS24:UTP8:BUD21:BMS1:RPS7A:C3_01560W_A:C3_02020W_A:RPL12:UTP4:HBR3:MAK21:RPS15:NOP14:RPL35:C3_05160C_A:RPS19A:CAM1:NOG1:NSA2:C3_06760W_A:C3_07550C_A:UTP9:RLP24:RPS6A:PWP1:SAS10:HCA4:ZUO1:NAN1:RPF1:ECM1:SSZ1:C4_04820C_A:RPL30:C4_05010W_A:C4_05330C_A:C4_06210C_A:NOP1:UBI3:C5_01540W_A:SPB4:GCD11:TIF5:UTP13:RPS5:C5_03920C_A:HAS1:NOP5:RPS13:CIC1:TIF3:C6_01890C_A:C6_02230W_A:NIP7:C6_02380W_A:MRT4:NOG2:SPB1:NOP8:C7_00160C_A:RPS18:DBP7:RPL5:ENP2:ENP1:SUI3:UTP18:BUD22:PWP2:CR_01780W_A:DBP2:YVH1:CR_03940W_A:CR_04110W_A:CR_04170W_A:CR_04240C_A:RPS3:NOC2:SDA1:RPL7:NMD3:CR_07030C_A:CR_07080W_A:RPS27:NOP10:RIO2:TSR1:CR_08500W_A:ELF1:SSF1:CR_09740W_A:CR_09800C_A:SIK1:UTP5:CR_10410C_A:CR_10470C_A:DRS1:LTV1:POP3

ncRNA metabolic process	153 out of 578 genes, 26.5%	400 out of 6473 background genes, 6.2%	2.3E-60	RRS1:C1_01160C_A:RPS21B:TRM2:ABP140:FRS2:RPS16A:TSR2:C1_04040C_A:ERB1:NOP4:RPS14B:LHP1:C1_07960W_A:FUN12:DIP2:C1_09710C_A:DBP3:RPA34:C1_10620W_A:RPA190:C1_10880W_A:C1_10950C_A:C1_10970W_A:NEP1:KRR1:WRS1:DIM1:C1_14080W_A:RRN3:MPP10:C2_00170C_A:C2_00410C_A:C2_01070W_A:UTP21:C2_02540W_A:C2_03000C_A:RPS9B:C2_04120C_A:TBF1:C2_04570W_A:MAK5:RPF2:RPS8A:KTI11:C2_05750W_A:MAK16:VAS1:C2_07040W_A:RPA12:NOC4:RCL1:RRP8:PES1:RRP15:C2_09500W_A:RPS24:UTP8:BUD21:BMS1:C3_01560W_A:C3_02020W_A:UTP4:HBR3:NOP14:RPL35:C3_05160C_A:NOG1:NSA2:C3_06760W_A:C3_07400W_A:C3_07550C_A:UTP9:C4_00810C_A:RPS6A:PWP1:C4_01500W_A:SEN2:SAS10:HCA4:ZUO1:TYS1:NAN1:C4_03140C_A:RPF1:C4_03730C_A:C4_03830W_A:C4_04520W_A:SSZ1:C4_04810C_A:RPL30:C4_05330C_A:C4_06210C_A:NOP1:UBI3:C5_01540W_A:SPB4:UTP13:IFH1:RPO26:C5_03920C_A:HAS1:HTS1:NOP5:RPS13:TOP1:C6_01890C_A:C6_02290C_A:C6_02350C_A:NIP7:MRT4:C6_03440W_A:SPB1:NOP8:RPA135:RPS18:DBP7:C7_02340C_A:ENP2:ENP1:UTP18:BUD22:PWP2:CDC60:CR_01780W_A:CR_01950W_A:RPC19:DBP2:RPC31:KTI12:NCS2:CR_03940W_A:CR_04110W_A:CR_04160C_A:CR_04170W_A:RPL7:RRN11:CR_07030C_A:CR_07080W_A:RPS27:NOP10:RIO2:TSR1:CR_08940W_A:SSF1:CR_09740W_A:CR_09800C_A:SIK1:UTP5:CR_10410C_A:CR_10470C_A:DRS1:POP3
ncRNA processing	130 out of 578 genes, 22.5%	298 out of 6473 background genes, 4.6%	2.5E-58	RRS1:C1_01160C_A:RPS21B:TRM2:ABP140:RPS16A:TSR2:C1_04040C_A:ERB1:NOP4:RPS14B:LHP1:C1_07960W_A:FUN12:DIP2:C1_09710C_A:DBP3:C1_10620W_A:C1_10880W_A:C1_10950C_A:C1_10970W_A:NEP1:KRR1:DIM1:C1_14080W_A:MPP10:C2_00170C_A:C2_00410C_A:UTP21:C2_02540W_A:C2_03000C_A:RPS9B:C2_04120C_A:C2_04570W_A:MAK5:RPF2:RPS8A:KTI11:C2_05750W_A:MAK16:NOC4:RCL1:RRP8:PES1:RRP15:C2_09500W_A:RPS24:UTP8:BUD21:BMS1:C3_01560W_A:C3_02020W_A:UTP4:HBR3:NOP14:RPL35:C3_05160C_A:NOG1:NSA2:C3_06760W_A:C3_07400W_A:C3_07550C_A:UTP9:C4_00810C_A:RPS6A:PWP1:C4_01500W_A:SEN2:SAS10:HCA4:ZUO1:NAN1:C4_03140C_A:RPF1:C4_03730C_A:C4_03830W_A:C4_04520W_A:SSZ1:C4_04810C_A:RPL30:C4_05330C_A:C4_06210C_A:NOP1:UBI3:C5_01540W_A:SPB4:UTP13:C5_03920C_A:HAS1:NOP5:RPS13:C6_01890C_A:C6_02290C_A:C6_02350C_A:NIP7:MRT4:SPB1:NOP8:RPS18:DBP7:C7_02340C_A:ENP2:ENP1:UTP18:BUD22:PWP2:CR_01780W_A:DBP2:KTI12:NCS2:CR_03940W_A:CR_04160C_A:CR_04170W_A:RPL7:CR_07030C_A:CR_07080W_A:RPS27:NOP10:RIO2:TSR1:CR_08940W_A:SSF1:CR_09740W_A:CR_09800C_A:SIK1:UTP5:CR_10410C_A:CR_10470C_A:DRS1:POP3

rRNA processing	108 out of 578 genes, 18.7%	205 out of 6473 background genes, 3.2%	4.5E-58	RRS1:C1_01160C_A:RPS21B:RPS16A:TSR2:C1_04040C_A:ERB1:NOP4:RPS14B:C1_07960W_A:FUN12:DIP2:C1_09710C_A:DBP3:C1_10620W_A:C1_10880W_A:C1_10950C_A:C1_10970W_A:NEP1:KRR1:DIM1:C1_14080W_A:MPP10:C2_00410C_A:UTP21:C2_02540W_A:C2_03000C_A:RPS9B:C2_04120C_A:C2_04570W_A:MAK5:RPF2:RPS8A:C2_05750W_A:MAK16:NOC4:RCL1:RRP8:PES1:RRP15:RPS24:UTP8:BUD21:BMS1:C3_01560W_A:C3_02020W_A:UTP4:HBR3:NOP14:RPL35:C3_05160C_A:NOG1:NSA2:C3_06760W_A:C3_07550C_A:UTP9:RPS6A:PWP1:SAS10:HCA4:ZUO1:NAN1:RPF1:SSZ1:RPL30:C4_05330C_A:C4_06210C_A:NOP1:UBI3:C5_01540W_A:SPB4:UTP13:C5_03920C_A:HAS1:NOP5:RPS13:C6_01890C_A:NIP7:MRT4:SPB1:NOP8:RPS18:DBP7:ENP2:ENP1:UTP18:BUD22:PWP2:CR_01780W_A:DBP2:CR_03940W_A:CR_04170W_A:RPL7:CR_07030C_A:CR_07080W_A:RPS27:NOP10:RIO2:TSR1:SSF1:CR_09740W_A:CR_09800C_A:SIK1:UTP5:CR_10410C_A:CR_10470C_A:DRS1:POP3
rRNA metabolic process	109 out of 578 genes, 18.9%	217 out of 6473 background genes, 3.4%	7.7E-56	RRS1:C1_01160C_A:RPS21B:RPS16A:TSR2:C1_04040C_A:ERB1:NOP4:RPS14B:C1_07960W_A:FUN12:DIP2:C1_09710C_A:DBP3:C1_10620W_A:C1_10880W_A:C1_10950C_A:C1_10970W_A:NEP1:KRR1:DIM1:C1_14080W_A:MPP10:C2_00410C_A:UTP21:C2_02540W_A:C2_03000C_A:RPS9B:C2_04120C_A:C2_04570W_A:MAK5:RPF2:RPS8A:C2_05750W_A:MAK16:NOC4:RCL1:RRP8:PES1:RRP15:RPS24:UTP8:BUD21:BMS1:C3_01560W_A:C3_02020W_A:UTP4:HBR3:NOP14:RPL35:C3_05160C_A:NOG1:NSA2:C3_06760W_A:C3_07550C_A:UTP9:RPS6A:PWP1:SAS10:HCA4:ZUO1:NAN1:RPF1:SSZ1:RPL30:C4_05330C_A:C4_06210C_A:NOP1:UBI3:C5_01540W_A:SPB4:UTP13:C5_03920C_A:HAS1:NOP5:RPS13:C6_01890C_A:NIP7:MRT4:C6_03440W_A:SPB1:NOP8:RPS18:DBP7:ENP2:ENP1:UTP18:BUD22:PWP2:CR_01780W_A:DBP2:CR_03940W_A:CR_04170W_A:RPL7:CR_07030C_A:CR_07080W_A:RPS27:NOP10:RIO2:TSR1:SSF1:CR_09740W_A:CR_09800C_A:SIK1:UTP5:CR_10410C_A:CR_10470C_A:DRS1:POP3

RNA processing	136 out of 578 genes, 23.5%	440 out of 6473 background genes, 6.8%	4E-40	RRS1:C1_01160C_A:RPS21B:TRM2:ABP140:RPS16A:TSR2:C1_04040C_A:ERB1:NOP4:RPS14B:LHP1:C1_07960W_A:FUN12:DIP2:C1_09710C_A:DBP3:C1_10620W_A:C1_10880W_A:C1_10950C_A:C1_10970W_A:NEP1:KRR1:C1_13380W_A:DIM1:C1_14080W_A:MPP10:C2_00170C_A:C2_00410C_A:PRP39:UTP21:C2_02540W_A:C2_03000C_A:RPS9B:C2_04120C_A:SUV3:C2_04570W_A:MAK5:RPF2:RPS8A:KTI11:C2_05750W_A:MAK16:NOC4:RCL1:RRP8:PES1:RRP15:C2_09500W_A:RPS24:UTP8:BUD21:BMS1:C3_01560W_A:C3_02020W_A:UTP4:HBR3:NOP14:RPL35:C3_05160C_A:NOG1:DED1:NSA2:C3_06760W_A:C3_07400W_A:C3_07550C_A:UTP9:C4_00810C_A:RPS6A:PWP1:C4_01500W_A:SEN2:SAS10:HCA4:ZUO1:NAN1:C4_03140C_A:RPF1:C4_03730C_A:C4_03830W_A:C4_04520W_A:SSZ1:C4_04810C_A:RPL30:C4_05330C_A:LEA1:C4_06210C_A:NOP1:UBI3:C5_01540W_A:SPB4:UTP13:C5_03920C_A:HAS1:NOP5:RPS13:C6_01890C_A:C6_02290C_A:C6_02350C_A:NIP7:MRT4:C6_03440W_A:SPB1:NOP8:RPS18:DBP7:C7_02340C_A:ENP2:ENP1:UTP18:BUD22:PWP2:CR_01780W_A:DBP2:KTI12:NCS2:CR_03940W_A:CR_04160C_A:CR_04170W_A:RPL7:CR_07030C_A:CR_07080W_A:RPS27:NOP10:RIO2:TSR1:CR_08940W_A:SSF1:CR_09740W_A:CR_09800C_A:SIK1:UTP5:CR_10410C_A:CR_10470C_A:DRS1:POP3

gene expression	227 out of 578 genes, 39.3%	1100 out of 6473 background genes, 17.0%	2.44E-38	RPL16A:RRS1:HMT1:C1_01160C_A:RPS21B:TRM2:RPS21:RPS42:ABP140:C1_02330C_A:C1_02430C_A:FRS2:TIF34:RPP1A:RPS16A:TSR2:RPL6:RLI1:C1_03370W_A:C1_03620C_A:C1_04040C_A:ERB1:NOP4:RSM22:RPS14B:RPS22A:C1_06890C_A:SUI2:LHP1:C1_07960W_A:FUN12:DRG1:DIP2:C1_09710C_A:DBP3:RPA34:RPL42:C1_10620W_A:RPA190:RPS17B:C1_10880W_A:C1_10950C_A:C1_10970W_A:RPL29:RPL37B:NEP1:KRR1:WRS1:C1_13060C_A:C1_13380W_A:DIM1:C1_14080W_A:RPL4B:TIF35:RRN3:MPP10:NDT80:C2_00170C_A:RPL38:C2_00410C_A:C2_01070W_A:PRP39:UTP21:C2_02540W_A:C2_03000C_A:RPL21A:RPS9B:C2_04120C_A:TBF1:SUV3:C2_04570W_A:C2_04700C_A:MAK5:ERF1:RPF2:RPS8A:KTI11:C2_05710C_A:C2_05750W_A:MAK16:VAS1:RPL11:RPA12:NOC4:RCL1:RRP8:PES1:RRP15:RPL3:C2_09500W_A:RPS4A:TIF11:RPS24:UTP8:BUD21:BMS1:RPS7A:C3_01520C_A:C3_01560W_A:C3_02020W_A:RPL12:UTP4:RPL9B:HBR3:RPS15:RPP2B:NOP14:RPL35:RPL18:C3_05160C_A:RPS19A:CAM1:NOG1:DED1:NSA2:C3_06760W_A:RPS12:C3_07390C_A:C3_07400W_A:C3_07550C_A:UTP9:C4_00810C_A:RPS6A:PWP1:NIP1:C4_01500W_A:SEN2:SAS10:HCA4:ZUO1:TYS1:NAN1:C4_03140C_A:RPF1:C4_03730C_A:C4_03830W_A:C4_04520W_A:SSZ1:C4_04810C_A:RPL30:C4_05330C_A:OFD1:LEA1:C4_06210C_A:NOP1:C4_06850C_A:UBI3:C5_00030W_A:C5_01540W_A:CEF3:SPB4:GCD11:TIF5:UTP13:IFH1:C5_02660C_A:RPS5:RPO26:C5_03920C_A:RPL43A:HAS1:ASH2:HTS1:NOP5:RPS13:TOP1:CIC1:TIF3:C6_01890C_A:C6_01980C_A:RPL23A:RPL10A:C6_02290C_A:C6_02350C_A:NIP7:MRT4:C6_03440W_A:SPB1:NOP8:C7_00490C_A:RPA135:YML6:RPS18:DBP7:PRT1:RPL5:C7_02340C_A:ENP2:ENP1:SUI3:UTP18:BUD22:PWP2:CDC60:CR_01780W_A:CR_01950W_A:RPC19:DBP2:RPC31:RPL28:KTI12:NCS2:CR_03940W_A:RPL15A:CR_04160C_A:CR_04170W_A:RPS3:RPL7:RRN11:CR_07030C_A:CR_07080W_A:RPS27:NOP10:RIO2:CR_08480C_A:TSR1:CR_08940W_A:ELF1:SSF1:CR_09740W_A:CR_09800C_A:SIK1:UTP5:CR_10410C_A:CR_10470C_A:DRS1:POP3
ribosomal small subunit biogenesis	64 out of 578 genes, 11.1%	108 out of 6473 background genes, 1.7%	3.48E-37	RRS1:RPS21B:RPS16A:TSR2:C1_04040C_A:RPS14B:NOP6:FUN12:DIP2:C1_09710C_A:RPS17B:C1_10880W_A:C1_10950C_A:NEP1:KRR1:DIM1:C1_14080W_A:MPP10:C2_00410C_A:C2_02540W_A:C2_03000C_A:RPS9B:C2_04700C_A:RPS8A:NOC4:RCL1:PES1:RPS24:UTP8:BUD21:C3_01560W_A:C3_02020W_A:UTP4:HBR3:NOP14:RPS19A:C3_07550C_A:UTP9:RPS6A:SAS10:NAN1:UBI3:C5_01540W_A:UTP13:C5_03920C_A:HAS1:NOP5:RPS13:RPS18:ENP2:ENP1:UTP18:BUD22:PWP2:CR_04240C_A:CR_07030C_A:RPS27:RIO2:ELF1:CR_09740W_A:CR_09800C_A:UTP5:CR_10410C_A:LTV1

ribosomal large subunit biogenesis	57 out of 578 genes, 9.9%	88 out of 6473 background genes, 1.4%	6.26E-36	RRS1:RPL6:RLI1:ERB1:NOP4:C1_04710C_A:REI1:YTM1:DBP3:CSI2:C2_02540W_A:C2_04120C_A:MAK5:C2_05160C_A:RPF2:C2_05750W_A:MAK16:RPL11:NSA1:RRP8:PES1:RRP15:RPL3:C3_01560W_A:RPL12:MAK21:RPL35:C3_05160C_A:NOG1:NSA2:RLP24:RPF1:C4_05010W_A:C4_05330C_A:SPB4:HAS1:CIC1:C6_01890C_A:C6_02230W_A:NIP7:C6_02380W_A:MRT4:SPB1:NOP8:C7_00160C_A:DBP7:RPL5:YVH1:CR_03940W_A:CR_04170W_A:NOC2:SDA1:RPL7:CR_07080W_A:CR_08500W_A:SSF1:DRS1
nucleic acid metabolic process	210 out of 578 genes, 36.3%	1025 out of 6473 background genes, 15.8%	4.74E-34	POL93:CDC13:RRS1:C1_01160C_A:DUT1:RPS21B:TRM2:ABP140:FRS2:RPS16A:TSR2:C1_04040C_A:ERB1:NOP4:RPS14B:C1_06630W_A:C1_07490C_A:LHP1:C1_07960W_A:FUN12:DIP2:C1_09710C_A:DBP3:RPA34:C1_10620W_A:APN2:RPA190:C1_10880W_A:C1_10950C_A:C1_10970W_A:NEP1:KRR1:GIN1:CDC6:WRS1:MSH6:C1_13380W_A:DIM1:C1_14080W_A:RRN3:MPP10:NDT80:C2_00170C_A:C2_00410C_A:RFC5:C2_01070W_A:PRP39:UTP21:C2_02540W_A:C2_03000C_A:RNR1:RPS9B:C2_04120C_A:TBF1:SUV3:C2_04570W_A:MAK5:ERF1:RPF2:RPS8A:KTI11:C2_05750W_A:CDC46:MAK16:C2_06530W_A:VAS1:C2_07040W_A:RPA12:NOC4:MCM3:RCL1:PDS5:RRP8:PES1:RRP15:PMS1:C2_09500W_A:RPS24:UTP8:BUD21:BMS1:C3_01560W_A:C3_02020W_A:UTP4:HBR3:RAD53:POL1:C3_04740C_A:NOP14:RPL35:C3_05160C_A:NOG1:DED1:NSA2:C3_06400C_A:C3_06760W_A:C3_07400W_A:C3_07550C_A:UTP9:MLH1:C4_00800W_A:C4_00810C_A:RPS6A:PWP1:C4_01500W_A:POL30:SEN2:SAS10:HCA4:ZUO1:TYS1:NAN1:C4_03140C_A:C4_03170W_A:RPF1:C4_03730C_A:C4_03830W_A:C4_04520W_A:SSZ1:C4_04810C_A:RPL30:C4_05330C_A:OFD1:LEA1:C4_06210C_A:PRI2:TOP2:NOP1:UBI3:EXO1:C5_01540W_A:SPB4:TIF5:UTP13:IFH1:RPO26:C5_03920C_A:HAS1:ASH2:C5_05350W_A:HTS1:DNA2:NOP5:RPS13:TOP1:C6_01890C_A:C6_02290C_A:C6_02350C_A:NIP7:C6_02380W_A:MRT4:C6_03440W_A:SPB1:NOP8:C7_00330C_A:RPA135:RPS18:DBP7:SMC6:RNH35:C7_02340C_A:DBF4:ENP2:ENP1:OGG1:UTP18:BUD22:PWP2:CDC60:CR_01780W_A:CR_01950W_A:MCM6:RPC19:DBP2:RPC31:SMC5:KTI12:NCS2:SMC1:MCM2:CR_03940W_A:CR_04110W_A:CR_04120C_A:CR_04160C_A:CR_04170W_A:CR_04560C_A:RPL7:RRN11:POL2:CR_07030C_A:CR_07080W_A:PIF1:CR_07600W_A:RPS27:NOP10:RIO2:TSR1:CR_08940W_A:SSF1:CR_09740W_A:CR_09800C_A:DPB2:SIK1:UTP5:CR_10410C_A:CR_10470C_A:MCD1:DRS1:POP3:RFC4

maturation of SSU-rRNA	56 out of 578 genes, 9.7%	91 out of 6473 background genes, 1.4%	1.81E-33	RRS1:RPS21B:RPS16A:TSR2:C1_04040C_A:RPS14B:FUN12:DIP2:C1_09710C_A:C1_10880W_A:C1_10950C_A:NEP1:KRR1:DIM1:C1_14080W_A:MPP10:C2_00410C_A:C2_02540W_A:C2_03000C_A:RPS9B:RPS8A:NOC4:RCL1:PES1:RPS24:UTP8:BUD21:C3_01560W_A:C3_02020W_A:UTP4:HBR3:NOP14:C3_07550C_A:UTP9:RPS6A:SAS10:NAN1:UBI3:C5_01540W_A:UTP13:C5_03920C_A:HAS1:NOP5:RPS13:RPS18:ENP1:UTP18:BUD22:PWP2:CR_07030C_A:RPS27:RIO2:CR_09740W_A:CR_09800C_A:UTP5:CR_10410C_A
RNA metabolic process	174 out of 578 genes, 30.1%	767 out of 6473 background genes, 11.8%	9.79E-33	RRS1:C1_01160C_A:RPS21B:TRM2:ABP140:FRS2:RPS16A:TSR2:C1_04040C_A:ERB1:NOP4:RPS14B:LHP1:C1_07960W_A:FUN12:DIP2:C1_09710C_A:DBP3:RPA34:C1_10620W_A:RPA190:C1_10880W_A:C1_10950C_A:C1_10970W_A:NEP1:KRR1:WRS1:C1_13380W_A:DIM1:C1_14080W_A:RRN3:MPP10:NDT80:C2_00170C_A:C2_00410C_A:RFC5:C2_01070W_A:PRP39:UTP21:C2_02540W_A:C2_03000C_A:RPS9B:C2_04120C_A:TBF1:SUV3:C2_04570W_A:MAK5:ERF1:RPF2:RPS8A:KTI11:C2_05750W_A:MAK16:VAS1:C2_07040W_A:RPA12:NOC4:RCL1:RRP8:PES1:RRP15:C2_09500W_A:RPS24:UTP8:BUD21:BMS1:C3_01560W_A:C3_02020W_A:UTP4:HBR3:POL1:NOP14:RPL35:C3_05160C_A:NOG1:DED1:NSA2:C3_06760W_A:C3_07400W_A:C3_07550C_A:UTP9:C4_00810C_A:RPS6A:PWP1:C4_01500W_A:POL30:SEN2:SAS10:HCA4:ZUO1:TYS1:NAN1:C4_03140C_A:RPF1:C4_03730C_A:C4_03830W_A:C4_04520W_A:SSZ1:C4_04810C_A:RPL30:C4_05330C_A:OFD1:LEA1:C4_06210C_A:PRI2:NOP1:UBI3:C5_01540W_A:SPB4:TIF5:UTP13:IFH1:RPO26:C5_03920C_A:HAS1:ASH2:C5_05350W_A:HTS1:DNA2:NOP5:RPS13:TOP1:C6_01890C_A:C6_02290C_A:C6_02350C_A:NIP7:C6_02380W_A:MRT4:C6_03440W_A:SPB1:NOP8:RPA135:RPS18:DBP7:RNH35:C7_02340C_A:ENP2:ENP1:UTP18:BUD22:PWP2:CDC60:CR_01780W_A:CR_01950W_A:RPC19:DBP2:RPC31:KTI12:NCS2:CR_03940W_A:CR_04110W_A:CR_04160C_A:CR_04170W_A:CR_04560C_A:RPL7:RRN11:POL2:CR_07030C_A:CR_07080W_A:RPS27:NOP10:RIO2:TSR1:CR_08940W_A:SSF1:CR_09740W_A:CR_09800C_A:SIK1:UTP5:CR_10410C_A:CR_10470C_A:DRS1:POP3:RFC4
maturation of SSU-rRNA from tricistronic rRNA transcript (SSU-rRNA, 5.8S rRNA, LSU-rRNA)	52 out of 578 genes, 9.0%	81 out of 6473 background genes, 1.3%	2.93E-32	RRS1:RPS21B:RPS16A:TSR2:C1_04040C_A:RPS14B:FUN12:DIP2:C1_09710C_A:C1_10880W_A:C1_10950C_A:NEP1:KRR1:DIM1:C1_14080W_A:MPP10:C2_00410C_A:C2_02540W_A:RPS9B:RPS8A:NOC4:RCL1:PES1:RPS24:UTP8:BUD21:C3_01560W_A:C3_02020W_A:UTP4:HBR3:NOP14:UTP9:RPS6A:SAS10:NAN1:C5_01540W_A:UTP13:C5_03920C_A:HAS1:NOP5:RPS13:RPS18:ENP1:UTP18:PWP2:CR_07030C_A:RPS27:RIO2:CR_09740W_A:CR_09800C_A:UTP5:CR_10410C_A

cellular aromatic compound metabolic process	234 out of 578 genes, 40.5%	1292 out of 6473 background genes, 20.0%	8.08E-30	POL93:HMX1:CDC15:RKI1:C1_01160C_A:DUT1:RPS21B:TRM2:ABP140:PRS2:RPS16A:TSR2:C1_04040C_A:ERB1:NOP4:RPS14B:C1_06630W_A:C1_07490C_A:LHP1:C1_07960W_A:FUN12:DIP2:SAM4:GUA1:C1_09710C_A:DBP3:RPA34:C1_10620W_A:APN2:RPA190:C1_10880W_A:C1_10950C_A:C1_10970W_A:NEP1:KRR1:GIN1:TRP3:CDC6:WRS1:MSH6:C1_13380W_A:DIM1:C1_14080W_A:RRN3:MPP10:NDT80:C2_00170C_A:C2_00410C_A:RFC5:C2_01070W_A:PRP39:ARO3:UTP21:C2_02540W_A:C2_03000C_A:RNR21:ADE8:RNR1:RPS9B:C2_04120C_A:TBF1:SUV3:C2_04570W_A:MAK5:ERF1:CDC21:RPF2:RPS8A:KTI11:C2_05750W_A:CDC46:MAK16:IMH3:C2_06530W_A:VAS1:AAH1:C2_07040W_A:RPA12:NOC4:MCM3:RCL1:RNR22:PDS5:RRP8:PES1:RRP15:PMS1:C2_09500W_A:PMI1:GPD1:RPS24:UTP8:BUD21:BMS1:C3_01560W_A:C3_02020W_A:UTP4:HBR3:RAD53:POL1:C3_04740C_A:NOP14:RPL35:C3_05160C_A:NOG1:DED1:GDA1:NSA2:C3_06400C_A:C3_06760W_A:C3_07400W_A:C3_07550C_A:UTP9:MLH1:C4_00800W_A:C4_00810C_A:RPS6A:PWP1:C4_01500W_A:POL30:SEN2:SAS10:HCA4:ZUO1:TYS1:NAN1:C4_03140C_A:C4_03170W_A:RPF1:C4_03730C_A:C4_03830W_A:C4_04520W_A:SSZ1:C4_04810C_A:RPL30:C4_05330C_A:OFD1:LEA1:TRP5:C4_06210C_A:PRI2:TOP2:NOP1:TRP4:UBI3:EXO1:C5_01540W_A:SPB4:TIF5:UAP1:UTP13:IFH1:YNK1:RPO26:C5_03920C_A:URA7:HAS1:ASH2:C5_05350W_A:HTS1:DNA2:NOP5:RPS13:TOP1:C6_01890C_A:C6_02290C_A:C6_02350C_A:NIP7:C6_02380W_A:MRT4:C6_03440W_A:SPB1:NOP8:C7_00330C_A:RPA135:RPS18:DBP7:SMC6:RNH35:C7_02340C_A:DBF4:ENP2:C7_03590C_A:ENP1:HIS7:OGG1:UTP18:MIS12:BUD22:PWP2:CDC60:CR_01780W_A:CR_01950W_A:MCM6:RPC19:DBP2:RPC31:SMC5:KTI12:NCS2:SMC1:MCM2:CR_03940W_A:CR_04110W_A:CR_04120C_A:CR_04160C_A:CR_04170W_A:CR_04560C_A:RPL7:RRN11:POL2:CR_07030C_A:CR_07080W_A:PIF1:CR_07600W_A:RPS27:ARO2:NOP10:RIO2:TSR1:CR_08940W_A:CR_09520C_A:SSF1:CR_09740W_A:CR_09800C_A:DPB2:SIK1:UTP5:CR_10410C_A:CR_10470C_A:MCD1:DRS1:POP3:RFC4

nucleobase-containing compound metabolic process	225 out of 578 genes, 38.9%	1219 out of 6473 background genes, 18.8%	1.42E-29	POL93:CDC13:RRS1:C1_01160C_A:DUT1:RPS21B:TRM2:ABP140:FRS2:RPS16A:TSR2:C1_04040C_A:ERB1:NOP4:RPS14B:C1_06630W_A:C1_07490C_A:LHP1:C1_07960W_A:FUN12:DIP2:SAM4:GUA1:C1_09710C_A:DBP3:RPA34:C1_10620W_A:APN2:RPA190:C1_10880W_A:C1_10950C_A:C1_10970W_A:NEP1:KRR1:GIN1:CDC6:WRS1:MSH6:C1_13380W_A:DIM1:C1_14080W_A:RRN3:MPP10:NDT80:C2_00170C_A:C2_00410C_A:RFC5:C2_01070W_A:PRP39:UTP21:C2_02540W_A:C2_03000C_A:RNR21:ADE8:RNR1:RPS9B:C2_04120C_A:TBF1:SUV3:C2_04570W_A:MAK5:ERF1:CDC21:RPF2:RPS8A:KTI11:C2_05750W_A:CDC46:MAK16:IMH3:C2_06530W_A:VAS1:AAH1:C2_07040W_A:RPA12:NOC4:MCM3:RCL1:RNR22:PDS5:RRP8:PES1:RRP15:PMS1:C2_09500W_A:PMI1:GPD1:RPS24:UTP8:BUD21:BMS1:C3_01560W_A:C3_02020W_A:UTP4:HBR3:RAD53:POL1:C3_04740C_A:NOP14:RPL35:C3_05160C_A:NOG1:DED1:GDA1:NSA2:C3_06400C_A:C3_06760W_A:C3_07400W_A:C3_07550C_A:UTP9:MLH1:C4_00800W_A:C4_00810C_A:RPS6A:PWP1:C4_01500W_A:POL30:SEN2:SAS10:HCA4:ZUO1:TYS1:NAN1:C4_03140C_A:C4_03170W_A:RPF1:C4_03730C_A:C4_03830W_A:C4_04520W_A:SSZ1:C4_04810C_A:RPL30:C4_05330C_A:OFD1:LEA1:C4_06210C_A:PRI2:TOP2:NOP1:UBI3:EXO1:C5_01540W_A:SPB4:TIF5:UAP1:UTP13:IFH1:YNK1:RPO26:C5_03920C_A:URA7:HAS1:ASH2:C5_05350W_A:HTS1:DNA2:NOP5:RPS13:TOP1:C6_01890C_A:C6_02290C_A:C6_02350C_A:NIP7:C6_02380W_A:MRT4:C6_03440W_A:SPB1:NOP8:C7_00330C_A:RPA135:RPS18:DBP7:SMC6:RNH35:C7_02340C_A:DBF4:ENP2:C7_03590C_A:ENP1:OGG1:UTP18:BUD22:PWP2:CDC60:CR_01780W_A:CR_01950W_A:MCM6:RPC19:DBP2:RPC31:SMC5:KTI12:NCS2:SMC1:MCM2:CR_03940W_A:CR_04110W_A:CR_04120C_A:CR_04160C_A:CR_04170W_A:CR_04560C_A:RPL7:RRN11:POL2:CR_07030C_A:CR_07080W_A:PIF1:CR_07600W_A:RPS27:NOP10:RIO2:TSR1:CR_08940W_A:SSF1:CR_09740W_A:CR_09800C_A:DPB2:SIK1:UTP5:CR_10410C_A:CR_10470C_A:MCD1:DRS1:POP3:RFC4

cellular component biogenesis	181 out of 578 genes, 31.3%	870 out of 6473 background genes, 13.4%	5.43E-29	RRS1:C1_01160C_A:RPS21B:RPS21:ABP140:SEP7:RPS16A:TSR2:RPL6:ARX1:RLI1:C1_03790C_A:C1_04040C_A:ERB1:NOP4:C1_04710C_A:REI1:RPS14B:NOP6:SUI2:C1_07360W_A:C1_07960W_A:FUN12:DIP2:YTM1:C1_09710C_A:DBP3:C1_10620W_A:RPS17B:C1_10880W_A:C1_10950C_A:C1_10970W_A:NEP1:KRR1:CDC6:CSI2:C1_12680W_A:CHS3:DIM1:C1_14080W_A:MPP10:C2_00410C_A:PRP39:UTP21:C2_02540W_A:C2_03000C_A:SMP3:RPS9B:C2_04120C_A:C2_04570W_A:C2_04700C_A:MAK5:C2_05160C_A:RPF2:C2_05510C_A:RPS8A:C2_05750W_A:CDC46:MAK16:C2_06530W_A:RPL11:NOC4:MCM3:RCL1:NSA1:KRE30:RPS10:RRP8:PES1:RRP15:RPL3:PMI1:TIF11:RPS24:UTP8:BUD21:BMS1:RPS7A:C3_01560W_A:C3_02020W_A:RPL12:UTP4:HBR3:MAK21:RPS15:NOP14:RPL35:C3_05160C_A:RPS19A:CAM1:NOG1:GDA1:NSA2:C3_06760W_A:C3_07550C_A:UTP9:RLP24:RPS6A:PWP1:SAS10:HCA4:ZUO1:NAN1:RPF1:ECM1:SSZ1:C4_04820C_A:RPL30:C4_05010W_A:C4_05330C_A:C4_06210C_A:NOP1:UBI3:C5_01540W_A:SPB4:GCD11:TIF5:UTP13:RPS5:C5_03920C_A:HAS1:NOP5:RPS13:CIC1:TIF3:C6_01890C_A:C6_02230W_A:NIP7:C6_02380W_A:MRT4:NOG2:SPB1:NOP8:C7_00160C_A:RPS18:DBP7:C7_01600W_A:RPL5:ENP2:ENP1:SUI3:UTP18:BUD22:PWP2:CR_01780W_A:MCM6:DBP2:YVH1:MCM2:CR_03940W_A:CR_04110W_A:CR_04170W_A:CR_04240C_A:RPS3:NOC2:SDA1:RPL7:NMD3:CR_07030C_A:CR_07080W_A:CR_07600W_A:RPS27:ASF1:NOP10:RIO2:TSR1:CR_08500W_A:MPS1:CHS2:ELF1:CR_09520C_A:SSF1:CR_09740W_A:CR_09800C_A:SIK1:UTP5:CR_10410C_A:CR_10470C_A:DRS1:LTV1:POP3

cellular macromolecule metabolic process	312 out of 578 genes, 54.0%	2038 out of 6473 background genes, 31.5%	7.06E-29	RPL16A:POL93:CDC13:CNS1:RRS1:HMT1:C1_01160C_A:DUT1:RPS21B:TRM2:RPS21:RPS42:ABP140:C1_02330C_A:C1_02430C_A:FRS2:TIF34:RPP1A:RPS16A:TSR2:RPL6:RLI1:C1_03620C_A:C1_03790C_A:C1_04040C_A:ERB1:ACS2:NOP4:RSM22:MSI3:RPS14B:RPS22A:C1_06630W_A:C1_06890C_A:SUI2:C1_07490C_A:LHP1:VRG4:C1_07960W_A:FUN12:DRG1:DIP2:TCP1:C1_09040C_A:C1_09710C_A:DBP3:RPA34:MNN12:RPL42:C1_10620W_A:APN2:RPA190:RPS17B:C1_10880W_A:C1_10950C_A:C1_10970W_A:RPL29:RPL37B:NEP1:KRR1:GIN1:MCD4:CDC6:WRS1:C1_13060C_A:CHS3:MSH6:C1_13380W_A:DIM1:C1_14080W_A:RPL4B:TIF35:RRN3:MPP10:NDT80:C2_00170C_A:RPL38:C2_00410C_A:RFC5:C2_01070W_A:PRP39:UTP21:C2_02540W_A:C2_03000C_A:SMP3:RNR1:RPL21A:RPS9B:C2_04120C_A:TBF1:SUV3:C2_04570W_A:C2_04700C_A:C2_05050C_A:MAK5:ERF1:RPF2:C2_05520W_A:RPS8A:KTI11:C2_05710C_A:C2_05750W_A:C2_05840W_A:CDC46:MAK16:C2_06530W_A:VAS1:RPL11:C2_07040W_A:C2_07290W_A:RPA12:NOC4:MCM3:RCL1:PDS5:RRP8:PES1:RRP15:RPL3:PMS1:C2_09500W_A:PMI1:RPS4A:TIF11:RPS24:UTP8:BUD21:BMS1:RPS7A:C3_01520C_A:C3_01560W_A:PPT1:C3_02020W_A:RPL12:UTP4:C3_02180C_A:RPL9B:HBR3:RAD53:POL1:RPS15:RPP2B:C3_04740C_A:NOP14:RPL35:RPL18:C3_05160C_A:RPS19A:MNN14:SKN1:CAM1:NOG1:DED1:GDA1:NSA2:C3_06400C_A:C3_06760W_A:RPS12:C3_07390C_A:C3_07400W_A:C3_07550C_A:UTP9:MLH1:C4_00800W_A:C4_00810C_A:PTC8:NAT4:RPS6A:PWP1:NIP1:C4_01500W_A:POL30:C4_02420C_A:SEN2:SAS10:HCA4:ZUO1:TYS1:NAN1:C4_03140C_A:C4_03170W_A:RPF1:DOT4:C4_03730C_A:C4_03830W_A:C4_04520W_A:SSZ1:C4_04810C_A:RPL30:C4_05330C_A:OFD1:LEA1:C4_06210C_A:PRI2:TOP2:NOP1:C4_06850C_A:UBI3:C5_00030W_A:EXO1:C5_01540W_A:CEF3:SPB4:CCT7:GCD11:TIF5:UTP13:IFH1:C5_02660C_A:HSL1:YNK1:RPS5:RMS1:RPO26:C5_03920C_A:RPL43A:HAS1:ASH2:CCT3:C5_05350W_A:HTS1:DNA2:NOP5:RPS13:TOP1:CIC1:TIF3:C6_01890C_A:C6_01980C_A:RPL23A:RPL10A:C6_02290C_A:C6_02350C_A:NIP7:C6_02380W_A:MRT4:C6_03440W_A:SPB1:NOP8:C7_00330C_A:C7_00490C_A:RPA135:YML6:RPS18:DBP7:PRT1:SMC6:RNH35:RPL5:C7_02340C_A:DBF4:ENP2:ENP1:OGG1:SUI3:UTP18:BUD22:PWP2:CDC60:CR_01780W_A:CR_01950W_

heterocycle metabolic process	233 out of 578 genes, 40.3%	1305 out of 6473 background genes, 20.2%	1.34E-28	POL93:HMX1:CDC13:RR31:C1_01160C_A:DUT1:RPS21B:TRM2:ABP140:PRS2:RPS16A:TSR2:C1_04040C_A:ERB1:NOP4:RPS14B:C1_06630W_A:C1_07490C_A:LHP1:C1_07960W_A:FUN12:DIP2:SAM4:GUA1:C1_09710C_A:DBP3:RPA34:C1_10620W_A:APN2:RPA190:C1_10880W_A:C1_10950C_A:C1_10970W_A:NEP1:KRR1:GIN1:TRP3:CDC6:WRS1:MSH6:C1_13380W_A:DIM1:C1_14080W_A:RRN3:MPP10:NDT80:C2_00170C_A:C2_00410C_A:RFC5:C2_01070W_A:PRP39:UTP21:C2_02540W_A:C2_03000C_A:RNR21:ADE8:RNR1:RPS9B:C2_04120C_A:TBF1:SUV3:C2_04570W_A:MAK5:ERF1:CDC21:RPF2:RPS8A:KTI11:C2_05750W_A:CDC46:MAK16:IMH3:C2_06530W_A:VAS1:AAH1:C2_07040W_A:RPA12:NOC4:MCM3:RCL1:RNR22:PDS5:RRP8:PES1:RRP15:PMS1:C2_09500W_A:PMI1:GPD1:RPS24:UTP8:BUD21:BMS1:C3_01560W_A:C3_02020W_A:UTP4:HBR3:RAD53:POL1:C3_04740C_A:NOP14:RPL35:C3_05160C_A:NOG1:DED1:GDA1:NSA2:C3_06400C_A:C3_06760W_A:C3_07400W_A:C3_07550C_A:UTP9:MLH1:C4_00800W_A:C4_00810C_A:RPS6A:PWP1:C4_01500W_A:POL30:SEN2:SAS10:HCA4:ZUO1:TYS1:NAN1:C4_03140C_A:C4_03170W_A:RPF1:C4_03730C_A:C4_03830W_A:C4_04520W_A:SSZ1:C4_04810C_A:RPL30:C4_05330C_A:OFD1:LEA1:TRP5:C4_06210C_A:PRI2:TOP2:NOP1:TRP4:UBI3:EXO1:C5_01540W_A:SPB4:TIF5:UAP1:UTP13:IFH1:YNK1:RPO26:C5_03920C_A:URA7:HAS1:ASH2:C5_05350W_A:HTS1:DNA2:NOP5:RPS13:TOP1:C6_01890C_A:C6_02290C_A:C6_02350C_A:NIP7:C6_02380W_A:MRT4:C6_03440W_A:SPB1:NOP8:C7_00330C_A:RPA135:RPS18:DBP7:SMC6:RNH35:C7_02340C_A:DBF4:ENP2:C7_03590C_A:ENP1:HIS7:OGG1:UTP18:MIS12:BUD22:PWP2:CDC60:CR_01780W_A:CR_01950W_A:MCM6:RPC19:DBP2:RPC31:SMC5:KTI12:NCS2:SMC1:CR_03760W_A:MCM2:CR_03940W_A:CR_04110W_A:CR_04120C_A:CR_04160C_A:CR_04170W_A:CR_04560C_A:RPL7:RRN11:POL2:CR_07030C_A:CR_07080W_A:PIF1:CR_07600W_A:RPS27:NOP10:RIO2:TSR1:CR_08940W_A:CR_09520C_A:SSF1:CR_09740W_A:CR_09800C_A:DPB2:SIK1:UTP5:CR_10410C_A:CR_10470C_A:MCD1:DRS1:POP3:RFC4

cellular nitrogen compound metabolic process	240 out of 578 genes, 41.5%	1368 out of 6473 background genes, 21.1%	1.64E-28	POL93:HMX1:CDC13:RRS1:C1_01160C_A:DUT1:RPS21B:TRM2:ABP140:FRS2:RPS16A:TSR2:C1_04040C_A:ERB1:NOP4:RPS14B:C1_06630W_A:C1_07490C_A:LHP1:C1_07960W_A:FUN12:DIP2:SAM4:GUA1:MTS1:C1_09710C_A:DBP3:RPA34:C1_10620W_A:APN2:RPA190:C1_10880W_A:C1_10950C_A:C1_10970W_A:NEP1:KRR1:GIN1:TRP3:CDC6:WRS1:MSH6:C1_13330C_A:C1_13380W_A:DIM1:C1_14080W_A:RRN3:MPP10:NDT80:C2_00170C_A:C2_00410C_A:RFC5:C2_01070W_A:PRP39:UTP21:C2_02540W_A:C2_03000C_A:RNR21:ADE8:RNR1:RPS9B:C2_04120C_A:TBF1:SUV3:C2_04570W_A:MAK5:ERF1:CDC21:RPF2:RPS8A:KTI11:C2_05750W_A:CDC46:MAK16:IMH3:C2_06530W_A:VAS1:SPE3:AAH1:C2_07040W_A:RPA12:NOC4:MCM3:RCL1:RNR22:PDS5:RRP8:PES1:RRP15:PMS1:C2_09500W_A:PMI1:GPD1:RPS24:UTP8:BUD21:BMS1:C3_01560W_A:C3_02020W_A:UTP4:HBR3:RAD53:POL1:C3_04740C_A:NOP14:RPL35:C3_05160C_A:LAC1:NOG1:DED1:GDA1:NSA2:C3_06400C_A:C3_06760W_A:C3_07400W_A:C3_07550C_A:UTP9:MLH1:C4_00800W_A:C4_00810C_A:RPS6A:PWP1:C4_01500W_A:POL30:SEN2:SAS10:HCA4:ZUO1:TYS1:NAN1:C4_03140C_A:C4_03170W_A:RPF1:C4_03730C_A:C4_03830W_A:C4_04520W_A:SSZ1:C4_04810C_A:RPL30:C4_05330C_A:OFD1:LEA1:TRP5:C4_06210C_A:PRI2:TOP2:NOP1:TRP4:UBI3:SEC14:EXO1:C5_01540W_A:SPB4:TIF5:UAP1:UTP13:IFH1:YNK1:RPO26:C5_03920C_A:URA7:HAS1:ASH2:C5_05350W_A:HTS1:DNA2:NOP5:RPS13:TOP1:C6_01890C_A:C6_02290C_A:C6_02350C_A:NIP7:C6_02380W_A:MRT4:C6_03440W_A:SPB1:NOP8:C7_00330C_A:RPA135:RPS18:DBP7:SMC6:RNH35:C7_02340C_A:DBF4:ENP2:C7_03590C_A:ENP1:HIS7:OGG1:UTP18:MIS12:BUD22:PWP2:CDC60:CR_01780W_A:CR_01950W_A:MCM6:RPC19:DBP2:RPC31:SMC5:KTI12:NCS2:SMC1:CR_03760W_A:MCM2:CR_03940W_A:CR_04110W_A:CR_04120C_A:CR_04160C_A:CR_04170W_A:CR_04560C_A:RPL7:RRN11:POL2:CR_07030C_A:CR_07080W_A:PIF1:CR_07600W_A:RPS27:NOP10:RIO2:TSR1:CR_08940W_A:CHS2:CR_09520C_A:SSF1:CR_09740W_A:CR_09800C_A:DPB2:SIK1:CR_10170C_A:UTP5:CR_10410C_A:CR_10470C_A:MCD1:DRS1:POP3:RFC4

organic cyclic compound metabolic process	239 out of 578 genes, 41.3%	1360 out of 6473 background genes, 21.0%	1.82E-28	POL93:HMX1:CDC13:ERG2:RRS1:C1_01160C_A:DUT1:RPS21B:TRM2:ABP140:PRS2:RPS16A:TSR2:C1_04040C_A:ERB1:NOP4:RPS14B:C1_06630W_A:C1_07490C_A:LHP1:C1_07960W_A:FUN12:DIP2:SAM4:ERG12:GUA1:C1_09710C_A:DBP3:RPA34:C1_10620W_A:APN2:RPA190:C1_10880W_A:C1_10950C_A:C1_10970W_A:NEP1:KRR1:GIN1:TRP3:CDC6:WRS1:MSH6:C1_13380W_A:DIM1:C1_14080W_A:RRN3:MPP10:NDT80:C2_00170C_A:C2_00410C_A:RFC5:C2_01070W_A:PRP39:ARO3:UTP21:C2_02540W_A:C2_03000C_A:RNR21:ADE8:RNR1:RPS9B:C2_04120C_A:TBF1:SUV3:C2_04570W_A:MAK5:ERF1:CDC21:RPF2:RPS8A:KTI11:C2_05750W_A:CDC46:MAK16:IMH3:C2_06530W_A:VAS1:AAH1:C2_07040W_A:RPA12:NOC4:MCM3:RCL1:RNR22:PDS5:RRP8:PES1:RRP15:PMS1:C2_09500W_A:PMI1:GPD1:RPS24:UTP8:BUD21:BMS1:C3_01560W_A:C3_02020W_A:UTP4:ERG6:HBR3:RAD53:POL1:C3_04740C_A:NOP14:RPL35:C3_05160C_A:NOG1:DED1:GDA1:NSA2:C3_06400C_A:C3_06760W_A:C3_07400W_A:C3_07550C_A:UTP9:MLH1:C4_00800W_A:C4_00810C_A:RPS6A:PWP1:C4_01500W_A:POL30:SEN2:SAS10:HCA4:ZUO1:TYS1:NAN1:C4_03140C_A:C4_03170W_A:RPF1:C4_03730C_A:C4_03830W_A:C4_04520W_A:SSZ1:C4_04810C_A:RPL30:C4_05330C_A:OFD1:LEA1:TRP5:C4_06210C_A:PRI2:TOP2:NOP1:TRP4:UBI3:EXO1:C5_01540W_A:SPB4:TIF5:UAP1:UTP13:IFH1:YNK1:RPO26:C5_03920C_A:URA7:HAS1:ASH2:C5_05350W_A:HTS1:DNA2:NOP5:RPS13:TOP1:C6_01890C_A:C6_02290C_A:C6_02350C_A:NIP7:C6_02380W_A:MRT4:C6_03440W_A:SPB1:NOP8:C7_00330C_A:RPA135:RPS18:DBP7:SMC6:RNH35:C7_02340C_A:DBF4:ENP2:C7_03590C_A:ENP1:HIS7:OGG1:UTP18:MIS12:BUD22:PWP2:CDC60:CR_01780W_A:CR_01950W_A:MCM6:ERG25:RPC19:DBP2:RPC31:SMC5:KTI12:NCS2:SMC1:CR_03760W_A:MCM2:CR_03940W_A:CR_04110W_A:CR_04120C_A:CR_04160C_A:CR_04170W_A:CR_04560C_A:RPL7:RRN11:POL2:CR_07030C_A:CR_07080W_A:PIF1:CR_07600W_A:RPS27:ARO2:NOP10:RIO2:TSR1:CR_08940W_A:CR_09520C_A:SSF1:CR_09740W_A:CR_09800C_A:DPB2:SIK1:UTP5:CR_10410C_A:CR_10470C_A:MCD1:DRS1:POP3:RFC4

nitrogen compound metabolic process	256 out of 578 genes, 44.3%	1527 out of 6473 background genes, 23.6%	1.02E-27	POL93:HMX1:CDC15:RRS1:C1_01160C_A:DUT1:RPS21B:TRM2:ABP140:FRS2:RPS16A:TSR2:C1_04040C_A:ERB1:NOP4:RPS14B:C1_06630W_A:C1_07490C_A:LHP1:C1_07960W_A:FUN12:DIP2:GCV2:SAM4:GUA1:MTS1:C1_09710C_A:DBP3:RPA34:C1_10620W_A:APN2:RPA190:C1_10880W_A:C1_10950C_A:C1_10970W_A:NEP1:KRR1:GIN1:TRP3:CDC6:WRS1:FEN1:CHS3:MSH6:C1_13330C_A:C1_13380W_A:DIM1:C1_14080W_A:RRN3:MPP10:NDT80:C2_00170C_A:C2_00410C_A:RFC5:C2_01070W_A:PRP39:ARO3:UTP21:C2_02540W_A:SER2:SUR2:C2_03000C_A:RNR21:ADE8:RNR1:RPS9B:C2_04120C_A:TBF1:SUV3:C2_04570W_A:MAK5:ERF1:CDC21:RPF2:RPS8A:KTI11:C2_05750W_A:CDC46:MAK16:IMH3:C2_06530W_A:VAS1:SPE3:AAH1:C2_07040W_A:RPA12:NOC4:MCM3:RCL1:RNR22:PDS5:RRP8:PES1:RRP15:PMS1:C2_09500W_A:PMI1:GPD1:RPS24:UTP8:BUD21:BMS1:C3_01560W_A:C3_02020W_A:UTP4:ILV2:C3_03470W_A:HBR3:RAD53:POL1:C3_04740C_A:NOP14:RPL35:C3_05160C_A:LAC1:NOG1:DED1:GDA1:NSA2:C3_06400C_A:C3_06760W_A:C3_07400W_A:C3_07550C_A:UTP9:MLH1:C4_00800W_A:C4_00810C_A:AAT22:RPS6A:PWP1:C4_01500W_A:POL30:SEN2:SAS10:HCA4:ZUO1:TYS1:NAN1:C4_03140C_A:C4_03170W_A:RPF1:C4_03730C_A:C4_03830W_A:C4_04520W_A:SSZ1:C4_04810C_A:RPL30:C4_05330C_A:OFD1:HOM3:LEA1:TRP5:GDH3:C4_06210C_A:PRI2:TOP2:NOP1:TRP4:UBI3:MET14:SEC14:EXO1:THR1:C5_01540W_A:SPB4:TIF5:UAP1:UTP13:IFH1:YNK1:RPO26:C5_03920C_A:CAR1:URA7:HAS1:ASH2:C5_05350W_A:HTS1:DNA2:NOP5:RPS13:TOP1:C6_01890C_A:C6_02290C_A:C6_02350C_A:NIP7:C6_02380W_A:MRT4:C6_03440W_A:SPB1:NOP8:C7_00330C_A:RPA135:RPS18:DBP7:SMC6:RNH35:C7_02340C_A:DBF4:ENP2:C7_03590C_A:ENP1:HIS7:OGG1:UTP18:MIS12:BUD22:PWP2:CDC60:CR_01780W_A:CR_01950W_A:MCM6:RPC19:DBP2:RPC31:SMC5:KTI12:NCS2:SMC1:CR_03760W_A:MCM2:CR_03940W_A:CR_04110W_A:CR_04120C_A:CR_04160C_A:CR_04170W_A:CR_04560C_A:RPL7:RRN11:POL2:CR_07030C_A:CR_07080W_A:PIF1:CR_07600W_A:RPS27:ARO2:NOP10:RIO2:CYS3:TSR1:CR_08940W_A:CHS2:CR_09520C_A:SSF1:CR_09740W_A:CR_09800C_A:DPB2:SIK1:CR_10170C_A:UTP5:CR_10410C_A:CR_10470C_A:MCD1:DRS1:POP3:RFC4

macromolecule metabolic process	315 out of 578 genes, 54.5%	2120 out of 6473 background genes, 32.8%	1.38E-26	RPL16A:POL93:CDC13:CNS1:RRS1:HMT1:C1_01160C_A:DUT1:RPS21B:TRM2:RPS21:RPS42:ABP140:C1_02330C_A:C1_02430C_A:FRS2:TIF34:RPP1A:RPS16A:TSR2:RPL6:RLI1:C1_03370W_A:C1_03620C_A:C1_03790C_A:C1_04040C_A:ERB1:ACS2:NOP4:RSM22:MSI3:RPS14B:RPS22A:C1_06630W_A:C1_06890C_A:SUI2:C1_07490C_A:LHP1:VRG4:C1_07960W_A:FUN12:DRG1:DIP2:TCP1:C1_09040C_A:C1_09710C_A:DBP3:RPA34:MNN12:RPL42:C1_10620W_A:APN2:RPA190:RPS17B:C1_10880W_A:C1_10950C_A:C1_10970W_A:RPL29:RPL37B:NEP1:KRR1:GIN1:MCD4:CDC6:WRS1:C1_13060C_A:CHS3:MSH6:C1_13380W_A:DIM1:C1_14080W_A:RPL4B:TIF35:RRN3:MPP10:NDT80:C2_00170C_A:RPL38:C2_00410C_A:RFC5:C2_01070W_A:PRP39:UTP21:C2_02540W_A:C2_03000C_A:SMP3:RNR1:RPL21A:RPS9B:C2_04120C_A:TBF1:SUV3:C2_04570W_A:C2_04700C_A:C2_05050C_A:MAK5:ERF1:RPF2:C2_05520W_A:RPS8A:KTI11:C2_05710C_A:C2_05750W_A:C2_05840W_A:CDC46:MAK16:C2_06530W_A:VAS1:RPL11:C2_07040W_A:C2_07290W_A:RPA12:NOC4:MCM3:RCL1:PDS5:RRP8:PES1:RRP15:RPL3:PMS1:C2_09500W_A:PMI1:RPS4A:TIF11:RPS24:UTP8:BUD21:BMS1:RPS7A:C3_01520C_A:C3_01560W_A:PPT1:C3_02020W_A:RPL12:UTP4:C3_02180C_A:RPL9B:HBR3:RAD53:POL1:RPS15:RPP2B:C3_04740C_A:FAS2:NOP14:RPL35:RPL18:C3_05160C_A:RPS19A:MNN14:SKN1:CAM1:NOG1:DED1:GDA1:NSA2:C3_06400C_A:C3_06760W_A:RPS12:C3_07390C_A:C3_07400W_A:C3_07550C_A:UTP9:MLH1:C4_00800W_A:C4_00810C_A:PTC8:NAT4:RPS6A:PWP1:NIP1:C4_01500W_A:POL30:C4_02420C_A:SEN2:SAS10:HCA4:ZUO1:TYS1:NAN1:C4_03140C_A:C4_03170W_A:RPF1:DOT4:C4_03730C_A:C4_03830W_A:C4_04520W_A:SSZ1:C4_04810C_A:RPL30:C4_05330C_A:OFD1:LEA1:C4_06210C_A:PRI2:TOP2:NOP1:C4_06850C_A:UBI3:C5_00030W_A:EXO1:C5_01540W_A:CEF3:SPB4:CCT7:GCD11:TIF5:UTP13:IFH1:C5_02660C_A:HSL1:YNK1:RPS5:RMS1:RPO26:C5_03920C_A:RPL43A:HAS1:ASH2:CCT3:C5_05350W_A:HTS1:DNA2:NOP5:RPS13:TOP1:CIC1:TIF3:C6_01890C_A:C6_01980C_A:RPL23A:RPL10A:C6_02290C_A:C6_02350C_A:NIP7:C6_02380W_A:MRT4:C6_03440W_A:SPB1:NOP8:C7_00330C_A:C7_00490C_A:RPA135:YML6:RPS18:DBP7:PRT1:SMC6:RNH35:RPL5:C7_02340C_A:DBF4:ENP2:ENP1:OGG1:SUI3:UTP18:BUD22:PWP2:CDC60:CR_01

primary metabolic process	368 out of 578 genes, 63.7%	2697 out of 6473 background genes, 41.7%	6.69E-26	RPL16A:POL93:CDC13:CNS1:ERG2:RRS1:HMT1:C1_01160C_A:DUT1:RPS21B:TRM2:RPS21:RPS42:ABP140:C1_02330C_A:C1_02430C_A:PMM1:FRS2:TIF34:RPP1A:RPS16A:TSR2:RPL6:RLI1:C1_03620C_A:C1_03790C_A:C1_04040C_A:ERB1:ACS2:NOP4:RSM22:MSI3:RPS14B:RPS22A:C1_06630W_A:C1_06890C_A:SUI2:C1_07490C_A:LHP1:VRG4:C1_07960W_A:FUN12:DRG1:DIP2:GCV2:SAM4:TCP1:C1_09040C_A:ERG12:GUA1:MTS1:C1_09710C_A:DBP3:RPA34:MNN12:RPL42:C1_10620W_A:APN2:RPA190:RPS17B:C1_10880W_A:C1_10950C_A:C1_10970W_A:RPL29:C1_11080W_A:RPL37B:NEP1:KRR1:GIN1:MCD4:TRP3:CDC6:WRS1:FEN1:C1_13060C_A:FAD3:CHS3:MSH6:C1_13380W_A:DIM1:C1_14080W_A:RPL4B:TIF35:RRN3:MPP10:NDT80:C2_00170C_A:RPL38:C2_00410C_A:RFC5:C2_01070W_A:PRP39:ARO3:UTP21:C2_02540W_A:SER2:SUR2:C2_03000C_A:RNR21:SMP3:ADE8:RNR1:RPL21A:RPS9B:C2_04120C_A:TBF1:SUV3:C2_04570W_A:C2_04700C_A:C2_05050C_A:MAK5:ERF1:CDC21:RPF2:C2_05520W_A:RPS8A:KTI11:C2_05710C_A:C2_05750W_A:C2_05840W_A:CDC46:MAK16:IMH3:C2_06530W_A:VAS1:RPL11:AAH1:C2_07040W_A:C2_07290W_A:RPA12:NOC4:MCM3:RCL1:RNR22:PDS5:RRP8:PES1:RRP15:RPL3:PMS1:C2_09500W_A:PMI1:GPD1:RPS4A:TIF11:RPS24:RHR2:UTP8:BUD21:BMS1:RPS7A:C3_01520C_A:C3_01560W_A:PPT1:C3_02020W_A:RPL12:UTP4:ERG6:C3_02180C_A:ILV2:RPL9B:C3_03470W_A:HBR3:RAD53:POL1:RPS15:RPP2B:C3_04740C_A:FAS2:NOP14:RPL35:RPL18:C3_05160C_A:RPS19A:MNN14:LAC1:SKN1:CAM1:NOG1:DED1:GDA1:NSA2:C3_06400C_A:C3_06760W_A:RPS12:C3_07390C_A:C3_07400W_A:C3_07550C_A:UTP9:MLH1:C4_00800W_A:C4_00810C_A:PTC8:AAT22:NAT4:RPS6A:PWP1:NIP1:C4_01500W_A:POL30:IDI1:C4_02420C_A:SEN2:SAS10:HCA4:ZUO1:TYS1:NAN1:C4_03140C_A:C4_03170W_A:RPF1:DOT4:C4_03730C_A:C4_03830W_A:C4_04520W_A:PHR1:SSZ1:C4_04810C_A:RPL30:C4_05330C_A:OFD1:HOM3:LEA1:TRP5:GDH3:C4_06210C_A:PRI2:TOP2:NOP1:C4_06850C_A:TRP4:UBI3:C5_00030W_A:FAS1:MET14:SEC14:EXO1:THR1:C5_01540W_A:CEF3:SPB4:CCT7:GCD11:TIF5:UAP1:UTP13:IFH1:C5_02660C_A:HSL1:YNK1:RPS5:RMS1:RPO26:C5_03920C_A:CHT2:CAR1:URA7:RPL43A:HAS1:ASH2:CCT3:C5_05350W_A:HTS1:DNA2:NOP5:FET3:RPS13:TOP1:FAD2:CIC1:TIF3:C6_01890C_A:C6_019

cellular metabolic process	377 out of 578 genes, 65.2%	2815 out of 6473 background genes, 43.5%	3.3E-25	RPL16A:POL93:HMX1:CDC13:CNS1:ERG2:RRS1:HMT1:C1_01160C_A:DUT1:RPS21B:TRM2:RPS21:RPS42:ABP140:C1_02330C_A:C1_02430C_A:FRS2:TIF34:RPP1A:RPS16A:TSR2:RPL6:RLI1:C1_03620C_A:C1_03790C_A:C1_04040C_A:ERB1:ACS2:NOP4:RSM22:PHO87:MSI3:RPS14B:RPS22A:C1_06630W_A:C1_06890C_A:SUI2:C1_07490C_A:LHP1:VRG4:C1_07960W_A:FUN12:DRG1:DIP2:GCV2:SAM4:TCP1:C1_09040C_A:ERG12:GUA1:MTS1:C1_09710C_A:DBP3:RPA34:MNN12:RPL42:C1_10620W_A:APN2:RPA190:RPS17B:C1_10880W_A:C1_10950C_A:C1_10970W_A:RPL29:C1_11080W_A:RPL37B:NEP1:KRR1:GIN1:PHO84:MCD4:TRP3:CDC6:WRS1:FEN1:C1_13060C_A:FAD3:CHS3:MSH6:C1_13330C_A:C1_13380W_A:DIM1:C1_14080W_A:RPL4B:TIF35:RRN3:MPP10:NDT80:C2_00170C_A:RPL38:C2_00410C_A:SOD5:RFC5:C2_01070W_A:PRP39:ARO3:UTP21:C2_02540W_A:SER2:SUR2:C2_03000C_A:RNR21:SMP3:ADE8:RNR1:RPL21A:RPS9B:C2_04120C_A:TBF1:SUV3:C2_04570W_A:C2_04700C_A:C2_05050C_A:MAK5:ERF1:CDC21:RPF2:C2_05520W_A:RPS8A:KTI11:C2_05710C_A:C2_05750W_A:C2_05840W_A:CDC46:MAK16:IMH3:C2_06530W_A:VAS1:RPL11:SPE3:AAH1:C2_07040W_A:C2_07290W_A:RPA12:NOC4:MCM3:RCL1:RNR22:PDS5:RRP8:PES1:RRP15:RPL3:PMS1:C2_09500W_A:PMI1:GPD1:RPS4A:TIF11:RPS24:C3_00170C_A:RHR2:UTP8:BUD21:BMS1:RPS7A:C3_01520C_A:C3_01560W_A:PPT1:C3_02020W_A:RPL12:UTP4:ERG6:C3_02180C_A:ILV2:RPL9B:C3_03470W_A:HBR3:RAD53:POL1:RPS15:RPP2B:C3_04740C_A:FAS2:NOP14:RPL35:RPL18:C3_05160C_A:RPS19A:MNN14:LAC1:SKN1:CAM1:NOG1:DED1:GDA1:NSA2:C3_06400C_A:C3_06700C_A:C3_06760W_A:RPS12:C3_07390C_A:C3_07400W_A:C3_07550C_A:UTP9:MLH1:C4_00800W_A:C4_00810C_A:PTC8:AAT22:NAT4:RPS6A:PWP1:NIP1:C4_01500W_A:POL30:IDI1:C4_02420C_A:SEN2:SAS10:HCA4:ZUO1:TYS1:NAN1:C4_03140C_A:C4_03170W_A:RPF1:DOT4:C4_03730C_A:C4_03830W_A:C4_04520W_A:SSZ1:C4_04810C_A:RPL30:C4_05330C_A:OFD1:HOM3:LEA1:TRP5:GDH3:C4_06210C_A:PRI2:TOP2:NOP1:C4_06850C_A:TRP4:UBI3:C5_00030W_A:FAS1:MET14:SEC14:EXO1:THR1:C5_01540W_A:CEF3:SPB4:CCT7:GCD11:TIF5:UAP1:UTP13:IFH1:C5_02660C_A:HSL1:YNK1:RPS5:RMS1:RPO26:C5_03530C_A:C5_03920C_A:CAR1:URA7:RPL43A:HAS1:ASH2:CCT3:C5_05350W_A

organic substance metabolic process	380 out of 578 genes, 65.7%	2862 out of 6473 background genes, 44.2%	1.05E-24	RPL16A:POL93:HMX1:CDC13:CNS1:ERG2:RRS1:HMT1:C1_01160C_A:DUT1:RPS21B:TRM2:RPS21:RPS42:ABP140:C1_02330C_A:C1_02430C_A:PMM1:FRS2:TIF34:RPP1A:RPS16A:TSR2:RPL6:RLI1:C1_03370W_A:C1_03620C_A:C1_03790C_A:C1_04040C_A:ERB1:ACS2:NOP4:RSM22:PHO87:MSI3:RPS14B:RPS22A:C1_06630W_A:C1_06890C_A:SUI2:C1_07490C_A:LHP1:VRG4:C1_07960W_A:FUN12:DRG1:DIP2:GCV2:SAM4:TCP1:C1_09040C_A:ERG12:GUA1:MTS1:C1_09710C_A:DBP3:RPA34:MNN12:RPL42:C1_10620W_A:APN2:RPA190:RPS17B:C1_10880W_A:C1_10950C_A:C1_10970W_A:RPL29:C1_11080W_A:RPL37B:NEP1:KRR1:GIN1:PHO84:MCD4:TRP3:CDC6:WRS1:FEN1:C1_13060C_A:FAD3:CHS3:MSH6:C1_13330C_A:C1_13380W_A:DIM1:C1_14080W_A:RPL4B:TIF35:RRN3:MPP10:NDT80:C2_00170C_A:RPL38:C2_00410C_A:RFC5:C2_01070W_A:PRP39:ARO3:UTP21:C2_02540W_A:SER2:SUR2:C2_03000C_A:RNR21:SMP3:ADE8:RNR1:RPL21A:RPS9B:C2_04120C_A:TBF1:SUV3:C2_04570W_A:C2_04700C_A:C2_05050C_A:MAK5:ERF1:CDC21:RPF2:C2_05520W_A:RPS8A:KTI11:C2_05710C_A:C2_05750W_A:C2_05840W_A:CDC46:MAK16:IMH3:C2_06530W_A:VAS1:RPL11:SPE3:AAH1:C2_07040W_A:C2_07290W_A:RPA12:NOC4:MCM3:RCL1:RNR22:PDS5:RRP8:PES1:RRP15:RPL3:PMS1:C2_09500W_A:PMI1:GPD1:RPS4A:TIF11:RPS24:C3_00170C_A:RHR2:UTP8:BUD21:BMS1:RPS7A:C3_01520C_A:C3_01560W_A:PPT1:C3_02020W_A:RPL12:UTP4:ERG6:C3_02180C_A:ILV2:RPL9B:C3_03470W_A:HBR3:RAD53:POL1:RPS15:RPP2B:C3_04740C_A:FAS2:NOP14:RPL35:RPL18:C3_05160C_A:RPS19A:MNN14:LAC1:SKN1:CAM1:NOG1:DED1:GDA1:NSA2:C3_06400C_A:C3_06760W_A:RPS12:C3_07390C_A:C3_07400W_A:C3_07550C_A:UTP9:MLH1:C4_00800W_A:C4_00810C_A:PTC8:AAT22:NAT4:RPS6A:PWP1:NIP1:C4_01500W_A:POL30:IDI1:C4_02420C_A:SEN2:SAS10:HCA4:ZUO1:TYS1:NAN1:C4_03140C_A:C4_03170W_A:RPF1:DOT4:C4_03730C_A:C4_03830W_A:C4_04520W_A:PHR1:SSZ1:C4_04810C_A:RPL30:C4_05330C_A:OFD1:HOM3:LEA1:TRP5:GDH3:C4_06210C_A:PRI2:TOP2:NOP1:C4_06850C_A:TRP4:UBI3:C5_00030W_A:FAS1:MET14:SEC14:EXO1:THR1:C5_01540W_A:CEF3:SPB4:CCT7:GCD11:TIF5:UAP1:UTP13:IFH1:C5_02660C_A:HSL1:YNK1:RPS5:RMS1:RPO26:C5_03530C_A:C5_03920C_A:CHT2:CAR1:URA7:RPL43A:HAS1:ASH2:CCT3:C5_053
maturation of 5.8S rRNA	41 out of 578 genes, 7.1%	75 out of 6473 background genes, 1.2%	4.57E-21	RRS1:C1_01160C_A:RPS21B:C1_04040C_A:C1_07960W_A:DIP2:C1_09710C_A:DBP3:C1_10880W_A:NEP1:KRR1:C1_14080W_A:MPP10:C2_02540W_A:MAK5:RPF2:MAK16:NOC4:RCL1:RRP15:BUD21:C3_01560W_A:C3_02020W_A:NOP14:C3_05160C_A:NSA2:SAS10:RPF1:C4_05330C_A:UTP13:C5_03920C_A:NOP5:SPB1:RPS18:ENP1:UTP18:PWP2:RPL7:CR_07080W_A:CR_09800C_A:CR_10410C_A

maturation of 5.8S rRNA from tricistronic rRNA transcript (SSU-rRNA, 5.8S rRNA, LSU-rRNA)	41 out of 578 genes, 7.1%	75 out of 6473 background genes, 1.2%	4.57E-21	RRS1:C1_01160C_A:RPS21B:C1_04040C_A:C1_07960W_A:DIP2:C1_09710C_A:DBP3:C1_10880W_A:NEP1:KRR1:C1_14080W_A:MPP10:C2_02540W_A:MAK5:RPF2:MAK16:NOC4:RCL1:RRP15:BUD21:C3_01560W_A:C3_02020W_A:NOP14:C3_05160C_A:NSA2:SAS10:RPF1:C4_05330C_A:UTP13:C5_03920C_A:NOP5:SPB1:RPS18:ENP1:UTP18:PWP2:RPL7:CR_07080W_A:CR_09800C_A:CR_10410C_A
maturation of LSU-rRNA from tricistronic rRNA transcript (SSU-rRNA, 5.8S rRNA, LSU-rRNA)	25 out of 578 genes, 4.3%	31 out of 6473 background genes, 0.5%	2.06E-18	NOP4:DBP3:C2_02540W_A:C2_04120C_A:MAK5:RPF2:C2_05750W_A:MAK16:RRP15:C3_01560W_A:RPL35:C3_05160C_A:NSA2:RPF1:C4_05330C_A:HAS1:C6_01890C_A:NIP7:SPB1:NOP8:DBP7:CR_04170W_A:RPL7:CR_07080W_A:SSF1
ribosome assembly	31 out of 578 genes, 5.4%	49 out of 6473 background genes, 0.8%	4.48E-18	RPL6:C1_04710C_A:RPS14B:FUN12:RPS17B:CSI2:RPF2:RPL11:RPL3:BMS1:C3_02020W_A:RPL12:MAK21:RPF1:C4_05010W_A:C4_05330C_A:UBI3:C5_01540W_A:SPB4:TIF5:C6_02230W_A:NIP7:C6_02380W_A:MRT4:RPL5:YVH1:CR_03940W_A:CR_07080W_A:RPS27:SSF1:DRS1

metabolic process	388 out of 578 genes, 67.1%	3152 out of 6473 background genes, 48.7%	7.65E-18	RPL16A:POL93:HMX1:CDC13:CNS1:ERG2:RRS1:HMT1:C1_01160C_A:DUT1:RPS21B:TRM2:RPS21:RPS42:ABP140:C1_02330C_A:C1_02430C_A:PMM1:FRS2:TIF34:RPP1A:RPS16A:TSR2:RPL6:RLI1:C1_03370W_A:C1_03620C_A:C1_03790C_A:C1_04040C_A:ERB1:ACS2:NOP4:RSM22:PHO87:MSI3:RPS14B:RPS22A:C1_06630W_A:C1_06890C_A:SUI2:C1_07490C_A:LHP1:VRG4:C1_07960W_A:FUN12:DRG1:DIP2:GCV2:SAM4:TCP1:C1_09040C_A:ERG12:GUA1:MTS1:C1_09710C_A:DBP3:RPA34:MNN12:RPL42:C1_10620W_A:APN2:RPA190:RPS17B:C1_10880W_A:C1_10950C_A:C1_10970W_A:RPL29:C1_11080W_A:RPL37B:NEP1:KRR1:GIN1:PHO84:MCD4:TRP3:CDC6:WRS1:FEN1:C1_13060C_A:FAD3:CHS3:MSH6:C1_13330C_A:C1_13380W_A:DIM1:C1_14080W_A:RPL4B:TIF35:RRN3:MPP10:NDT80:C2_00170C_A:RPL38:C2_00410C_A:SOD5:RFC5:C2_01070W_A:PRP39:ARO3:UTP21:C2_02540W_A:SER2:SUR2:C2_03000C_A:RNR21:SMP3:ADE8:RNR1:RPL21A:RPS9B:C2_04120C_A:TBF1:SUV3:C2_04570W_A:C2_04700C_A:C2_05050C_A:MAK5:ERF1:CDC21:RPF2:C2_05520W_A:RPS8A:KTI11:C2_05710C_A:C2_05750W_A:C2_05840W_A:CDC46:MAK16:IMH3:C2_06530W_A:VAS1:RPL11:SPE3:AAH1:C2_07040W_A:C2_07290W_A:RPA12:NOC4:MCM3:RCL1:RNR22:PDS5:RRP8:PES1:RRP15:RPL3:PMS1:C2_09500W_A:PMI1:GPD1:RPS4A:TIF11:RPS24:C3_00170C_A:RHR2:UTP8:BUD21:BMS1:RPS7A:C3_01520C_A:C3_01560W_A:PPT1:C3_02020W_A:RPL12:UTP4:ERG6:C3_02180C_A:ILV2:RPL9B:C3_03470W_A:C3_03570C_A:HBR3:RAD53:POL1:RPS15:RPP2B:C3_04740C_A:FAS2:NOP14:RPL35:RPL18:C3_05160C_A:RPS19A:MNN14:LAC1:SKN1:CAM1:NOG1:DED1:GDA1:NSA2:C3_06400C_A:C3_06700C_A:C3_06760W_A:RPS12:C3_07390C_A:C3_07400W_A:C3_07550C_A:UTP9:FRP1:MLH1:C4_00800W_A:C4_00810C_A:PTC8:AAT22:NAT4:RPS6A:PWP1:NIP1:C4_01500W_A:POL30:IDI1:C4_02420C_A:SEN2:SAS10:HCA4:ZUO1:TYS1:NAN1:C4_03140C_A:C4_03170W_A:RPF1:DOT4:C4_03730C_A:C4_03830W_A:C4_04520W_A:PHR1:SSZ1:C4_04810C_A:RPL30:C4_05330C_A:OFD1:HOM3:LEA1:TRP5:GDH3:C4_06210C_A:PRI2:TOP2:NOP1:C4_06850C_A:TRP4:UBI3:C5_00030W_A:FAS1:MET14:SEC14:EXO1:THR1:C5_01540W_A:CEF3:SPB4:CCT7:GCD11:TIF5:UAP1:UTP13:IFH1:C5_02660C_A:HSL1:YNK1:RPS5:RMS1:RPO26:C5_03530C_A:C5_03920C_A:CHT
maturation of LSU-rRNA	26 out of 578 genes, 4.5%	35 out of 6473 background genes, 0.5%	1.31E-17	NOP4:DBP3:C2_02540W_A:C2_04120C_A:MAK5:RPF2:C2_05750W_A:MAK16:RRP15:C3_01560W_A:RPL35:C3_05160C_A:NSA2:RPF1:C4_05330C_A:SPB4:HAS1:C6_01890C_A:NIP7:SPB1:NOP8:DBP7:CR_04170W_A:RPL7:CR_07080W_A:SSF1

cellular process	461 out of 578 genes, 79.8%	4064 out of 6473 background genes, 62.8%	3.05E-17	C1_00160C_A:RPL16A:POL93:HMX1:CDC13:CNS1:ERG2:RRS1:HMT1:C1_01160C_A:DUT1:RPS21B:TRM2:RPS21:RPS42:ABP140:SEP7:C1_02330C_A:C1_02430C_A:PMM1:FRS2:TIF34:RPP1A:RPS16A:TSR2:RPL6:RLI1:C1_03620C_A:C1_03790C_A:C1_03870C_A:C1_04040C_A:ERB1:ACS2:NOP4:C1_04710C_A:REI1:BRG1:RSM22:PHO87:MSI3:UME6:PBR1:RPS14B:RPS22A:C1_06630W_A:C1_06890C_A:SUI2:RBT4:GAP4:YMC1:C1_07360W_A:C1_07490C_A:LHP1:VRG4:FGR6-3:C1_07960W_A:FUN12:DRG1:DIP2:GCV2:SAM4:TCP1:SWI6:C1_09040C_A:ERG12:GUA1:YTM1:MTS1:C1_09710C_A:HCM1:DBP3:C1_10200C_A:RPA34:MNN12:RPL42:C1_10620W_A:PEA2:APN2:RPA190:RPS17B:C1_10880W_A:C1_10950C_A:C1_10970W_A:RPL29:C1_11080W_A:RPL37B:NEP1:KRR1:GIN1:PHO84:ZCF3:MUP1:MCD4:TRP3:CDC6:CSI2:WRS1:FEN1:C1_13060C_A:FAD3:CHS3:MSH6:C1_13330C_A:C1_13380W_A:DIM1:C1_14080W_A:RPL4B:FTR2:IRR1:TIF35:RRN3:MPP10:NDT80:C2_00170C_A:RPL38:C2_00410C_A:SOD5:RFC5:C2_01070W_A:PRP39:ARO3:UTP21:C2_02540W_A:PDR17:SER2:SUR2:C2_03000C_A:RNR21:SMP3:ADE8:RNR1:RPL21A:RPS9B:DCK1:C2_04120C_A:TBF1:SUV3:C2_04570W_A:C2_04700C_A:C2_05050C_A:MAK5:ERF1:CDC21:RPF2:C2_05270W_A:C2_05510C_A:C2_05520W_A:RPS8A:KTI11:C2_05710C_A:C2_05750W_A:C2_05840W_A:CNT:CDC46:MAK16:IMH3:C2_06530W_A:VAS1:RPL11:SPE3:AAH1:C2_07040W_A:C2_07290W_A:RPA12:NOC4:MCM3:RCL1:RNR22:PDS5:KRE30:SIT1:RRP8:PES1:RRP15:RPL3:PMS1:C2_09500W_A:PMI1:TIM23:GPD1:FGR6-4:RPS4A:TIF11:C2_10740C_A:RPS24:C3_00170C_A:RHR2:UTP8:BUD21:BMS1:NCE103:RPS7A:C3_01520C_A:C3_01560W_A:PPT1:C3_02020W_A:RPL12:UTP4:ERG6:C3_02180C_A:ILV2:RPL9B:C3_03440C_A:C3_03470W_A:HBR3:RAD53:CTP1:POL1:TEC1:MAK21:RPS15:RPP2B:C3_04740C_A:FAS2:NOP14:RPL35:RPL18:C3_05160C_A:WOR2:RPS19A:MNN14:LAC1:SKN1:C3_05900W_A:CAM1:NOG1:DED1:GDA1:NSA2:C3_06400C_A:C3_06700C_A:C3_06760W_A:HUT1:RPS12:ZFU2:C3_07390C_A:C3_07400W_A:C3_07420W_A:C3_07550C_A:TCC1:UTP9:FRP1:RLP24:PAM18:MLH1:C4_00800W_A:C4_00810C_A:PTC8:AGP2:AAT22:NAT4:RPS6A:PWP1:NIP1:C4_01500W_A:POL30:PHO89:IDI1:C4_02420C_A:SEN2:SAS10:HCA4:ZUO1:TYS
RNA phosphodiester bond hydrolysis, endonucleolytic	29 out of 578 genes, 5.0%	46 out of 6473 background genes, 0.7%	1.02E-16	RRS1:RPS21B:C1_04040C_A:LHP1:DIP2:C1_09710C_A:DBP3:C1_10880W_A:NEP1:KRR1:C1_14080W_A:MPP10:C2_02540W_A:NOC4:RCL1:BUD21:C3_02020W_A:NOP14:SAS10:UTP13:C5_03920C_A:NOP5:RPS18:ENP1:UTP18:PWP2:RPS27:CR_09800C_A:CR_10410C_A

endonucleolytic cleavage involved in rRNA processing	28 out of 578 genes, 4.8%	43 out of 6473 background genes, 0.7%	1.22E-16	RRS1:RPS21B:C1_04040C_A:DIP2:C1_09710C_A:DBP3:C1_10880W_A:NEP1:KRR1:C1_14080W_A:MPP10:C2_02540W_A:NOC4:RCL1:BUD21:C3_02020W_A:NOP14:SAS10:UTP13:C5_03920C_A:NOP5:RPS18:ENP1:UTP18:PWP2:RPS27:CR_09800C_A:CR_10410C_A
endonucleolytic cleavage of tricistronic rRNA transcript (SSU-rRNA, 5.8S rRNA, LSU-rRNA)	28 out of 578 genes, 4.8%	43 out of 6473 background genes, 0.7%	1.22E-16	RRS1:RPS21B:C1_04040C_A:DIP2:C1_09710C_A:DBP3:C1_10880W_A:NEP1:KRR1:C1_14080W_A:MPP10:C2_02540W_A:NOC4:RCL1:BUD21:C3_02020W_A:NOP14:SAS10:UTP13:C5_03920C_A:NOP5:RPS18:ENP1:UTP18:PWP2:RPS27:CR_09800C_A:CR_10410C_A
endonucleolytic cleavage in ITS1 to separate SSU-rRNA from 5.8S rRNA and LSU-rRNA from tricistronic rRNA transcript (SSU-rRNA, 5.8S rRNA, LSU-rRNA)	26 out of 578 genes, 4.5%	39 out of 6473 background genes, 0.6%	1.06E-15	RRS1:RPS21B:C1_04040C_A:DIP2:C1_09710C_A:C1_10880W_A:NEP1:KRR1:C1_14080W_A:MPP10:C2_02540W_A:NOC4:RCL1:BUD21:C3_02020W_A:NOP14:SAS10:UTP13:C5_03920C_A:NOP5:RPS18:ENP1:UTP18:PWP2:CR_09800C_A:CR_10410C_A
cleavage involved in rRNA processing	33 out of 578 genes, 5.7%	65 out of 6473 background genes, 1.0%	3.03E-15	RRS1:C1_01160C_A:RPS21B:C1_04040C_A:C1_07960W_A:DIP2:C1_09710C_A:DBP3:C1_10880W_A:NEP1:KRR1:C1_14080W_A:MPP10:C2_02540W_A:NOC4:RCL1:BUD21:C3_02020W_A:NOP14:SAS10:UTP13:C5_03920C_A:NOP5:RPS18:ENP1:UTP18:PWP2:RPL7:CR_07030C_A:RPS27:NOP10:CR_09800C_A:CR_10410C_A

cellular biosynthetic process	203 out of 578 genes, 35.1%	1318 out of 6473 background genes, 20.4%	3.63E-15	RPL16A:POL93:ERG2:DUT1:RPS21B:RPS21:RPS42:C1_02330C_A:C1_02430C_A:FRS2:TIF34:RPP1A:RPS16A:RPL6:RLI1:C1_03620C_A:ACS2:RSM22:RPS14B:RPS22A:C1_06630W_A:C1_06890C_A:SUI2:C1_07490C_A:VRG4:FUN12:DRG1:SAM4:ERG12:GUA1:MTS1:RPA34:MNN12:RPL42:RPA190:RPS17B:RPL29:RPL37B:GIN1:MCD4:TRP3:CDC6:WRS1:FEN1:C1_13060C_A:FAD3:CHS3:C1_13330C_A:RPL4B:TIF35:RRN3:NDT80:RPL38:RFC5:C2_01070W_A:ARO3:SER2:SUR2:RNR21:SMP3:ADE8:RNR1:RPL21A:RPS9B:TBF1:SUV3:C2_04700C_A:C2_05050C_A:ERF1:CDC21:RPS8A:KTI11:C2_05710C_A:C2_05840W_A:CDC46:IMH3:C2_06530W_A:VAS1:RPL11:SPE3:AAH1:RPA12:MCM3:PES1:RPL3:PMI1:GPD1:RPS4A:TIF11:RPS24:RHR2:RPS7A:C3_01520C_A:RPL12:ERG6:ILV2:RPL9B:RAD53:POL1:RPS15:RPP2B:C3_04740C_A:FAS2:RPL35:RPL18:RPS19A:MNN14:LAC1:SKN1:CAM1:DED1:GDA1:RPS12:C3_07390C_A:C3_07400W_A:RPS6A:NIP1:POL30:IDI1:C4_02420C_A:ZUO1:TYS1:SSZ1:RPL30:OFD1:HOM3:TRP5:GDH3:PRI2:TOP2:TRP4:UBI3:C5_00030W_A:FAS1:MET14:SEC14:THR1:C5_01540W_A:CEF3:GCD11:TIF5:UAP1:IFH1:C5_02660C_A:YNK1:RPS5:RPO26:C5_03530C_A:URA7:RPL43A:ASH2:C5_05350W_A:HTS1:DNA2:FET3:RPS13:TOP1:FAD2:CIC1:TIF3:C6_01980C_A:RPL23A:RPL10A:C7_00490C_A:RPA135:YML6:RPS18:PRT1:RNH35:RPL5:DBF4:C7_03590C_A:HIS7:OGG1:SUI3:MIS12:ACC1:CDC60:CR_01950W_A:MCM6:ERG25:RPC19:RPC31:RPL28:KRE1:MCM2:CR_03940W_A:RPL15A:CR_04160C_A:CR_04560C_A:RPS3:RRN11:POL2:RPS27:ARO2:CYS3:CR_08480C_A:CHS2:CR_09520C_A:DPB2:INO1:MCD1:RFC4
translation	91 out of 578 genes, 15.7%	403 out of 6473 background genes, 6.2%	8.66E-15	RPL16A:RPS21B:RPS21:RPS42:C1_02330C_A:C1_02430C_A:FRS2:TIF34:RPP1A:RPS16A:RPL6:RLI1:C1_03620C_A:RSM22:RPS14B:RPS22A:C1_06890C_A:SUI2:FUN12:DRG1:RPL42:RPS17B:RPL29:RPL37B:WRS1:C1_13060C_A:RPL4B:TIF35:RPL38:RPL21A:RPS9B:C2_04700C_A:ERF1:RPS8A:C2_05710C_A:VAS1:RPL11:RPL3:RPS4A:TIF11:RPS24:RPS7A:C3_01520C_A:RPL12:RPL9B:RPS15:RPP2B:RPL35:RPL18:RPS19A:CAM1:DED1:RPS12:C3_07390C_A:C3_07400W_A:RPS6A:NIP1:ZUO1:TYS1:SSZ1:RPL30:OFD1:UBI3:C5_00030W_A:C5_01540W_A:CEF3:GCD11:TIF5:C5_02660C_A:RPS5:RPL43A:HTS1:RPS13:CIC1:TIF3:C6_01980C_A:RPL23A:RPL10A:C7_00490C_A:YML6:RPS18:PRT1:RPL5:SUI3:CDC60:RPL28:RPL15A:CR_04160C_A:RPS3:RPS27:CR_08480C_A

biosynthetic process	208 out of 578 genes, 36.0%	1384 out of 6473 background genes, 21.4%	2.16E-14	RPL16A:POL93:ERG2:DUT1:RPS21B:RPS21:RPS42:C1_02330C_A:C1_02430C_A:PMM1:FRS2:TIF34:RPP1A:RPS16A:RPL6:RLI1:C1_03620C_A:ACS2:RSM22:RPS14B:RPS22A:C1_06630W_A:C1_06890C_A:SUI2:C1_07490C_A:VRG4:FUN12:DRG1:SAM4:ERG12:GUA1:MTS1:RPA34:MNN12:RPL42:RPA190:RPS17B:RPL29:RPL37B:GIN1:MCD4:TRP3:CDC6:WRS1:FEN1:C1_13060C_A:FAD3:CHS3:C1_13330C_A:RPL4B:TIF35:RRN3:NDT80:RPL38:RFC5:C2_01070W_A:ARO3:SER2:SUR2:RNR21:SMP3:ADE8:RNR1:RPL21A:RPS9B:TBF1:SUV3:C2_04700C_A:C2_05050C_A:ERF1:CDC21:RPS8A:KTI11:C2_05710C_A:C2_05840W_A:CDC46:IMH3:C2_06530W_A:VAS1:RPL11:SPE3:AAH1:C2_07290W_A:RPA12:MCM3:PES1:RPL3:PMI1:GPD1:RPS4A:TIF11:RPS24:RHR2:RPS7A:C3_01520C_A:RPL12:ERG6:C3_02180C_A:ILV2:RPL9B:RAD53:POL1:RPS15:RPP2B:C3_04740C_A:FAS2:RPL35:RPL18:RPS19A:MNN14:LAC1:SKN1:CAM1:DED1:GDA1:RPS12:C3_07390C_A:C3_07400W_A:AAT22:RPS6A:NIP1:POL30:IDI1:C4_02420C_A:ZUO1:TYS1:SSZ1:RPL30:OFD1:HOM3:TRP5:GDH3:PRI2:TOP2:TRP4:UBI3:C5_00030W_A:FAS1:MET14:SEC14:THR1:C5_01540W_A:CEF3:GCD11:TIF5:UAP1:IFH1:C5_02660C_A:YNK1:RPS5:RPO26:C5_03530C_A:URA7:RPL43A:ASH2:C5_05350W_A:HTS1:DNA2:FET3:RPS13:TOP1:FAD2:CIC1:TIF3:C6_01980C_A:RPL23A:RPL10A:C6_02290C_A:C7_00490C_A:RPA135:YML6:RPS18:PRT1:RNH35:RPL5:DBF4:C7_03590C_A:HIS7:OGG1:SUI3:MIS12:ACC1:CDC60:CR_01950W_A:MCM6:ERG25:RPC19:RPC31:RPL28:KRE1:MCM2:CR_03940W_A:RPL15A:CR_04160C_A:CR_04560C_A:RPS3:RRN11:POL2:RPS27:ARO2:CYS3:CR_08480C_A:CHS2:CR_09520C_A:DPB2:INO1:MCD1:RFC4

organic substance biosynthetic process	203 out of 578 genes, 35.1%	1341 out of 6473 background genes, 20.7%	2.93E-14	RPL16A:POL93:ERG2:DUT1:RPS21B:RPS21:RPS42:C1_02330C_A:C1_02430C_A:PMM1:FRS2:TIF34:RPP1A:RPS16A:RPL6:RLI1:C1_03620C_A:ACS2:RSM22:RPS14B:RPS22A:C1_06630W_A:C1_06890C_A:SUI2:C1_07490C_A:VRG4:FUN12:DRG1:SAM4:ERG12:GUA1:MTS1:RPA34:MNN12:RPL42:RPA190:RPS17B:RPL29:RPL37B:GIN1:MCD4:TRP3:CDC6:WRS1:FEN1:C1_13060C_A:FAD3:CHS3:C1_13330C_A:RPL4B:TIF35:RRN3:NDT80:RPL38:RFC5:C2_01070W_A:ARO3:SER2:SUR2:RNR21:SMP3:ADE8:RNR1:RPL21A:RPS9B:TBF1:SUV3:C2_04700C_A:C2_05050C_A:ERF1:CDC21:RPS8A:C2_05710C_A:CDC46:IMH3:C2_06530W_A:VAS1:RPL11:SPE3:AAH1:RPA12:MCM3:PES1:RPL3:PMI1:GPD1:RPS4A:TIF11:RPS24:RHR2:RPS7A:C3_01520C_A:RPL12:ERG6:ILV2:RPL9B:RAD53:POL1:RPS15:RPP2B:C3_04740C_A:FAS2:RPL35:RPL18:RPS19A:MNN14:LAC1:SKN1:CAM1:DED1:GDA1:RPS12:C3_07390C_A:C3_07400W_A:RPS6A:NIP1:POL30:IDI1:C4_02420C_A:ZUO1:TYS1:SSZ1:RPL30:OFD1:HOM3:TRP5:GDH3:PRI2:TOP2:TRP4:UBI3:C5_00030W_A:FAS1:MET14:SEC14:THR1:C5_01540W_A:CEF3:GCD11:TIF5:UAP1:IFH1:C5_02660C_A:YNK1:RPS5:RPO26:C5_03530C_A:URA7:RPL43A:ASH2:C5_05350W_A:HTS1:DNA2:FET3:RPS13:TOP1:FAD2:CIC1:TIF3:C6_01980C_A:RPL23A:RPL10A:C6_02290C_A:C7_00490C_A:RPA135:YML6:RPS18:PRT1:RNH35:RPL5:DBF4:C7_03590C_A:HIS7:OGG1:SUI3:MIS12:ACC1:CDC60:CR_01950W_A:MCM6:ERG25:RPC19:RPC31:RPL28:KRE1:MCM2:CR_03940W_A:RPL15A:CR_04160C_A:CR_04560C_A:RPS3:RRN11:POL2:RPS27:ARO2:CYS3:CR_08480C_A:CHS2:CR_09520C_A:DPB2:INO1:MCD1:RFC4
macromolecule biosynthetic process	153 out of 578 genes, 26.5%	904 out of 6473 background genes, 14.0%	6.34E-14	RPL16A:POL93:DUT1:RPS21B:RPS21:RPS42:C1_02330C_A:C1_02430C_A:FRS2:TIF34:RPP1A:RPS16A:RPL6:RLI1:C1_03620C_A:RSM22:RPS14B:RPS22A:C1_06630W_A:C1_06890C_A:SUI2:C1_07490C_A:VRG4:FUN12:DRG1:RPA34:MNN12:RPL42:RPA190:RPS17B:RPL29:RPL37B:GIN1:MCD4:CDC6:WRS1:C1_13060C_A:CHS3:RPL4B:TIF35:RRN3:NDT80:RPL38:RFC5:C2_01070W_A:SMP3:RNR1:RPL21A:RPS9B:TBF1:SUV3:C2_04700C_A:C2_05050C_A:ERF1:RPS8A:C2_05710C_A:CDC46:C2_06530W_A:VAS1:RPL11:RPA12:MCM3:PES1:RPL3:PMI1:RPS4A:TIF11:RPS24:RPS7A:C3_01520C_A:RPL12:RPL9B:RAD53:POL1:RPS15:RPP2B:C3_04740C_A:FAS2:RPL35:RPL18:RPS19A:MNN14:SKN1:CAM1:DED1:GDA1:RPS12:C3_07390C_A:C3_07400W_A:RPS6A:NIP1:POL30:C4_02420C_A:ZUO1:TYS1:SSZ1:RPL30:OFD1:PRI2:TOP2:UBI3:C5_00030W_A:C5_01540W_A:CEF3:GCD11:TIF5:IFH1:C5_02660C_A:RPS5:RPO26:RPL43A:ASH2:C5_05350W_A:HTS1:DNA2:RPS13:TOP1:CIC1:TIF3:C6_01980C_A:RPL23A:RPL10A:C7_00490C_A:RPA135:YML6:RPS18:PRT1:RNH35:RPL5:DBF4:OGG1:SUI3:CDC60:CR_01950W_A:MCM6:RPC19:RPC31:RPL28:KRE1:MCM2:CR_03940W_A:RPL15A:CR_04160C_A:CR_04560C_A:RPS3:RRN11:POL2:RPS27:CR_08480C_A:CHS2:DPB2:MCD1:RFC4

cellular macromolecule biosynthetic process	152 out of 578 genes, 26.3%	899 out of 6473 background genes, 13.9%	9.23E-14	RPL16A:POL93:DUT1:RPS21B:RPS21:RPS42:C1_02330C_A:C1_02430C_A:FRS2:TIF34:RPP1A:RPS16A:RPL6:RLI1:C1_03620C_A:RSM22:RPS14B:RPS22A:C1_06630W_A:C1_06890C_A:SUI2:C1_07490C_A:VRG4:FUN12:DRG1:RPA34:MNN12:RPL42:RPA190:RPS17B:RPL29:RPL37B:GIN1:MCD4:CDC6:WRS1:C1_13060C_A:CHS3:RPL4B:TIF35:RRN3:NDT80:RPL38:RFC5:C2_01070W_A:SMP3:RNR1:RPL21A:RPS9B:TBF1:SUV3:C2_04700C_A:C2_05050C_A:ERF1:RPS8A:C2_05710C_A:CDC46:C2_06530W_A:VAS1:RPL11:RPA12:MCM3:PES1:RPL3:PMI1:RPS4A:TIF11:RPS24:RPS7A:C3_01520C_A:RPL12:RPL9B:RAD53:POL1:RPS15:RPP2B:C3_04740C_A:RPL35:RPL18:RPS19A:MNN14:SKN1:CAM1:DED1:GDA1:RPS12:C3_07390C_A:C3_07400W_A:RPS6A:NIP1:POL30:C4_02420C_A:ZUO1:TYS1:SSZ1:RPL30:OFD1:PRI2:TOP2:UBI3:C5_00030W_A:C5_01540W_A:CEF3:GCD11:TIF5:IFH1:C5_02660C_A:RPS5:RPO26:RPL43A:ASH2:C5_05350W_A:HTS1:DNA2:RPS13:TOP1:CIC1:TIF3:C6_01980C_A:RPL23A:RPL10A:C7_00490C_A:RPA135:YML6:RPS18:PRT1:RNH35:RPL5:DBF4:OGG1:SUI3:CDC60:CR_01950W_A:MCM6:RPC19:RPC31:RPL28:KRE1:MCM2:CR_03940W_A:RPL15A:CR_04160C_A:CR_04560C_A:RPS3:RRN11:POL2:RPS27:CR_08480C_A:CHS2:DPB2:MCD1:RFC4
ncRNA 5'-end processing	22 out of 578 genes, 3.8%	32 out of 6473 background genes, 0.5%	2.01E-13	C1_04040C_A:DIP2:C1_09710C_A:C1_10880W_A:NEP1:C1_14080W_A:MPP10:C2_02540W_A:NOC4:RCL1:BUD21:C3_02020W_A:NOP14:SAS10:UTP13:C5_03920C_A:NOP5:UTP18:PWP2:RPL7:CR_09800C_A:CR_10410C_A
rRNA 5'-end processing	22 out of 578 genes, 3.8%	32 out of 6473 background genes, 0.5%	2.01E-13	C1_04040C_A:DIP2:C1_09710C_A:C1_10880W_A:NEP1:C1_14080W_A:MPP10:C2_02540W_A:NOC4:RCL1:BUD21:C3_02020W_A:NOP14:SAS10:UTP13:C5_03920C_A:NOP5:UTP18:PWP2:RPL7:CR_09800C_A:CR_10410C_A
ribonucleoprotein complex subunit organization	46 out of 578 genes, 8.0%	136 out of 6473 background genes, 2.1%	2.81E-13	RPL6:RLI1:C1_04710C_A:RPS14B:SUI2:FUN12:RPS17B:CSI2:PRP39:RPF2:RPL11:RPL3:TIF11:BMS1:C3_01560W_A:C3_02020W_A:RPL12:MAK21:C3_05160C_A:NOG1:DED1:RLP24:RPF1:C4_05010W_A:C4_05330C_A:UBI3:C5_01540W_A:SPB4:GCD11:TIF5:TIF3:C6_02230W_A:NIP7:C6_02380W_A:MRT4:RPL5:SUI3:DBP2:YVH1:CR_03940W_A:CR_04110W_A:CR_04170W_A:CR_07080W_A:RPS27:SSF1:DRS1
RNA 5'-end processing	22 out of 578 genes, 3.8%	33 out of 6473 background genes, 0.5%	5.53E-13	C1_04040C_A:DIP2:C1_09710C_A:C1_10880W_A:NEP1:C1_14080W_A:MPP10:C2_02540W_A:NOC4:RCL1:BUD21:C3_02020W_A:NOP14:SAS10:UTP13:C5_03920C_A:NOP5:UTP18:PWP2:RPL7:CR_09800C_A:CR_10410C_A

				CDC15:RRS1:C1_01160C_A:RPS21B:RPS21:ABP140:SLF7:PMM1:RPS10A:TSR2:RPL6:ARX1:RLI1:C1_03790C_A:C1_04040C_A:ERB1:ACS2:NOP4:C1_04710C_A:REI1:RPS14B:C1_06630W_A:NOP6:SUI2:C1_07360W_A:C1_07490C_A:C1_07960W_A:FUN12:DIP2:YTM1:C1_09710C_A:HCM1:DBP3:C1_10620W_A:RPA190:RPS17B:C1_10880W_A:C1_10950C_A:C1_10970W_A:NEP1:KRR1:GIN1:CDC6:CSI2:C1_12680W_A:C1_13060C_A:CHS3:MSH6:DIM1:C1_14080W_A:IRR1:MPP10:NDT80:C2_00410C_A:RFC5:C2_01070W_A:PRP39:UTP21:C2_02540W_A:C2_03000C_A:SMP3:RPS9B:DCK1:C2_04120C_A:TBF1:SUV3:C2_04570W_A:C2_04700C_A:MAK5:ERF1:C2_05160C_A:RPF2:C2_05270W_A:C2_05510C_A:RPS8A:C2_05750W_A:CDC46:MAK16:C2_06530W_A:RPL11:C2_07290W_A:NOC4:MCM3:RCL1:PDS5:NSA1:KRE30:RPS10:RRP8:PES1:RRP15:RPL3:PMS1:PMI1:TIM23:TIF11:C2_10740C_A:RPS24:C3_00170C_A:UTP8:BUD21:BMS1:RPS7A:C3_01560W_A:C3_02020W_A:RPL12:UTP4:ERG6:HBR3:POL1:MAK21:RPS15:C3_04740C_A:NOP14:RPL35:C3_05160C_A:RPS19A:LAC1:CAM1:NOG1:DED1:GDA1:NSA2:C3_06760W_A:C3_07550C_A:UTP9:RLP24:PAM18:MLH1:C4_00810C_A:NAT4:RPS6A:PWP1:POL30:SAS10:HCA4:ZUO1:NAN1:RPF1:DOT4:HWP1:ECM1:PHR1:SSZ1:C4_04820C_A:RPL30:C4_05010W_A:C4_05330C_A:OFD1:C4_06210C_A:PRI2:TOP2:NOP1:UBI3:SEC14:EXO1:CLN3:C5_01540W_A:CEF3:SPB4:GCD11:TIF5:UTP13:RPS5:C5_03920C_A:HAS1:ASH2:C5_05350W_A:HTS1:DNA2:NOP5:RPS13:TOP1:CIC1:TIF3:C6_01890C_A:C6_02230W_A:NIP7:C6_02380W_A:MRT4:C6_03440W_A:NOG2:SPB1:NOP8:C7_00160C_A:C7_00330C_A:RPS18:DBP7:C7_01600W_A:RPL5:DBF4:ENP2:ENP1:OGG1:SUI3:UTP18:BUD22:PWP2:CR_01780W_A:MCM6:DBP2:YVH1:SMC1:MCM2:CR_03940W_A:CR_04110W_A:CR_04120C_A:CR_04170W_A:YDJ1:CR_04240C_A:CR_04560C_A:RPS3:NOC2:SDA1:RPL7:NMD3:POL2:CR_07030C_A:CR_07080W_A:PIF1:CR_07600W_A:RPS27:ASF1:NOP10:RIO2:TSR1:CR_08500W_A:PGA13:MPS1:CHS2:ELF1:CR_09520C_A:SSF1:CR_09740W_A:CR_09800C_A:SIK1:UTP5:CR_10410C_A:CR_10470C_A:MCD1:DRS1:LTV1:POP3:RFC4
cellular component organization or biogenesis	244 out of 578 genes, 42.2%	1778 out of 6473 background genes, 27.5%	1.03E-12	
endonucleolytic cleavage to generate mature 5'-end of SSU-rRNA from (SSU-rRNA, 5.8S rRNA, LSU-rRNA)	21 out of 578 genes, 3.6%	31 out of 6473 background genes, 0.5%	1.6E-12	C1_04040C_A:DIP2:C1_09710C_A:C1_10880W_A:NEP1:C1_14080W_A:MPP10:C2_02540W_A:NOC4:RCL1:BUD21:C3_02020W_A:NOP14:SAS10:UTP13:C5_03920C_A:NOP5:UTP18:PWP2:CR_09800C_A:CR_10410C_A
ribosomal large subunit assembly	20 out of 578 genes, 3.5%	29 out of 6473 background genes, 0.4%	4.56E-12	RPL6:C1_04710C_A:CSI2:RPF2:RPL11:RPL3:RPL12:MAK21:RPF1:C4_05010W_A:C4_05330C_A:SPB4:C6_02230W_A:C6_02380W_A:MRT4:RPL5:YVH1:CR_03940W_A:SSF1:DRS1

ribonucleoprotein complex assembly	43 out of 578 genes, 7.4%	129 out of 6473 background genes, 2.0%	5.12E-12	RPL6:C1_04710C_A:RPS14B:SUI2:FUN12:RPS17B:CSI2:PRP39:RPF2:RPL11:RPL3:TIF11:BMS1:C3_02020W_A:RPL12:MAK21:C3_05160C_A:NOG1:RLP24:RPF1:C4_05010W_A:C4_05330C_A:UBI3:C5_01540W_A:SPB4:GCD11:TIF5:TIF3:C6_02230W_A:NIP7:C6_02380W_A:MRT4:RPL5:SUI3:DBP2:YVH1:CR_03940W_A:CR_04110W_A:CR_04170W_A:CR_07080W_A:RPS27:SSF1:DRS1
RNA phosphodiester bond hydrolysis	35 out of 578 genes, 6.1%	93 out of 6473 background genes, 1.4%	3.09E-11	RRS1:C1_01160C_A:RPS21B:C1_04040C_A:LHP1:C1_07960W_A:DIP2:C1_09710C_A:DBP3:C1_10880W_A:NEP1:KRR1:C1_14080W_A:MPP10:C2_02540W_A:NOC4:RCL1:BUD21:C3_02020W_A:NOP14:SAS10:UTP13:C5_03920C_A:NOP5:RPS18:ENP1:UTP18:PWP2:RPL7:CR_07030C_A:RPS27:NOP10:CR_09800C_A:CR_10410C_A:POP3
endonucleolytic cleavage in 5'-ETS of tricistronic rRNA transcript (SSU-rRNA, 5.8S rRNA, LSU-rRNA)	19 out of 578 genes, 3.3%	29 out of 6473 background genes, 0.4%	9.67E-11	C1_04040C_A:DIP2:C1_09710C_A:C1_10880W_A:NEP1:C1_14080W_A:MPP10:C2_02540W_A:NOC4:RCL1:C3_02020W_A:NOP14:SAS10:UTP13:C5_03920C_A:NOP5:UTP18:PWP2:CR_09800C_A
nucleic acid phosphodiester bond hydrolysis	37 out of 578 genes, 6.4%	112 out of 6473 background genes, 1.7%	6.24E-10	RRS1:C1_01160C_A:RPS21B:C1_04040C_A:LHP1:C1_07960W_A:DIP2:C1_09710C_A:DBP3:APN2:C1_10880W_A:NEP1:KRR1:C1_14080W_A:MPP10:C2_02540W_A:NOC4:RCL1:BUD21:C3_02020W_A:NOP14:SAS10:UTP13:C5_03920C_A:NOP5:RPS18:ENP1:UTP18:PWP2:CR_04560C_A:RPL7:CR_07030C_A:RPS27:NOP10:CR_09800C_A:CR_10410C_A:POP3
rRNA-containing ribonucleoprotein complex export from nucleus	24 out of 578 genes, 4.2%	51 out of 6473 background genes, 0.8%	1.22E-09	RRS1:RPS21:ARX1:RLI1:C1_04040C_A:C2_05750W_A:KRE30:RPS10:RPS15:RPS19A:NOG1:ZUO1:RPF1:ECM1:C4_06210C_A:RPS5:C6_02230W_A:NOG2:RPS18:RPS3:SDA1:NMD3:CR_07080W_A:LTV1
organelle assembly	33 out of 578 genes, 5.7%	105 out of 6473 background genes, 1.6%	5.49E-08	SEP7:RPL6:C1_04710C_A:RPS14B:FUN12:RPS17B:CSI2:RPF2:RPL11:RPL3:BMS1:C3_02020W_A:RPL12:MAK21:RPF1:C4_05010W_A:C4_05330C_A:UBI3:C5_01540W_A:SPB4:TIF5:C6_02230W_A:NIP7:C6_02380W_A:MRT4:RPL5:YVH1:CR_03940W_A:CR_07080W_A:RPS27:MPS1:SSF1:DRS1
RNA modification	29 out of 578 genes, 5.0%	93 out of 6473 background genes, 1.4%	1.05E-06	TRM2:ABP140:C1_10620W_A:NEP1:DIM1:C2_00170C_A:KTI11:RRP8:C2_09500W_A:C3_07400W_A:C4_00810C_A:C4_01500W_A:C4_03140C_A:C4_03730C_A:C4_03830W_A:C4_04810C_A:NOP1:C6_02290C_A:C6_02350C_A:SPB1:C7_02340C_A:CR_01780W_A:KTI12:NCS2:CR_04110W_A:CR_04160C_A:CR_04170W_A:NOP10:CR_08940W_A

ribonucleoprotein complex localization	30 out of 578 genes, 5.2%	101 out of 6473 background genes, 1.6%	1.99E-06	RRS1:HMT1:RPS21:ARX1:RLI1:C1_03370W_A:C1_04040C_A:RPA190:C1_13380W_A:C2_05750W_A:KRE30:RPS10:UTP8:RPS15:RPS19A:NOG1:ZUO1:RPF1:ECM1:C4_06210C_A:RPS5:C6_02230W_A:NOG2:RPS18:RPS3:SDA1:NMD3:CR_07080W_A:ELF1:LTV1
ribonucleoprotein complex export from nucleus	30 out of 578 genes, 5.2%	101 out of 6473 background genes, 1.6%	1.99E-06	RRS1:HMT1:RPS21:ARX1:RLI1:C1_03370W_A:C1_04040C_A:RPA190:C1_13380W_A:C2_05750W_A:KRE30:RPS10:UTP8:RPS15:RPS19A:NOG1:ZUO1:RPF1:ECM1:C4_06210C_A:RPS5:C6_02230W_A:NOG2:RPS18:RPS3:SDA1:NMD3:CR_07080W_A:ELF1:LTV1
nuclear export	30 out of 578 genes, 5.2%	103 out of 6473 background genes, 1.6%	3.35E-06	RRS1:HMT1:RPS21:ARX1:RLI1:C1_03370W_A:C1_04040C_A:RPA190:C1_13380W_A:C2_05750W_A:KRE30:RPS10:UTP8:RPS15:RPS19A:NOG1:ZUO1:RPF1:ECM1:C4_06210C_A:RPS5:C6_02230W_A:NOG2:RPS18:RPS3:SDA1:NMD3:CR_07080W_A:ELF1:LTV1
DNA replication	33 out of 578 genes, 5.7%	121 out of 6473 background genes, 1.9%	3.42E-06	POL93:DUT1:C1_06630W_A:C1_07490C_A:GIN1:CDC6:RFC5:RNR1:SUV3:CDC46:C2_06530W_A:MCM3:PES1:RAD53:POL1:C3_04740C_A:POL30:PRI2:TOP2:C5_05350W_A:DNA2:TOP1:RNH35:DBF4:OGG1:MCM6:MCM2:CR_03940W_A:CR_04560C_A:POL2:DPB2:MCD1:RFC4
DNA-dependent DNA replication	29 out of 578 genes, 5.0%	98 out of 6473 background genes, 1.5%	4.13E-06	C1_06630W_A:C1_07490C_A:GIN1:CDC6:RFC5:SUV3:CDC46:C2_06530W_A:MCM3:PES1:RAD53:POL1:C3_04740C_A:POL30:PRI2:TOP2:C5_05350W_A:DNA2:TOP1:RNH35:DBF4:MCM6:MCM2:CR_03940W_A:CR_04560C_A:POL2:DPB2:MCD1:RFC4
assembly of large subunit precursor of preribosome	8 out of 578 genes, 1.4%	8 out of 6473 background genes, 0.1%	4.97E-06	RPF2:C3_05160C_A:NOG1:RLP24:SPB4:NIP7:CR_04170W_A:CR_07080W_A
ribosome localization	18 out of 578 genes, 3.1%	43 out of 6473 background genes, 0.7%	9.39E-06	RRS1:ARX1:RLI1:C1_04040C_A:C2_05750W_A:KRE30:NOG1:ZUO1:RPF1:ECM1:C4_06210C_A:C6_02230W_A:NOG2:RPS3:SDA1:NMD3:CR_07080W_A:LTV1
establishment of ribosome localization	18 out of 578 genes, 3.1%	43 out of 6473 background genes, 0.7%	9.39E-06	RRS1:ARX1:RLI1:C1_04040C_A:C2_05750W_A:KRE30:NOG1:ZUO1:RPF1:ECM1:C4_06210C_A:C6_02230W_A:NOG2:RPS3:SDA1:NMD3:CR_07080W_A:LTV1
ribosomal subunit export from nucleus	18 out of 578 genes, 3.1%	43 out of 6473 background genes, 0.7%	9.39E-06	RRS1:ARX1:RLI1:C1_04040C_A:C2_05750W_A:KRE30:NOG1:ZUO1:RPF1:ECM1:C4_06210C_A:C6_02230W_A:NOG2:RPS3:SDA1:NMD3:CR_07080W_A:LTV1

translational initiation	16 out of 578 genes, 2.8%	36 out of 6473 background genes, 0.6%	0.000023	C1_02430C_A:TIF34:RLI1:SUI2:FUN12:TIF35:TIF11:DED1:NIP1:GCD11:TIF5:C5_02660C_A:TIF3:PRT1:SUI3:CR_04160C_A
nucleocytoplasmic transport	36 out of 578 genes, 6.2%	151 out of 6473 background genes, 2.3%	0.0000323	RRS1:HMT1:RPS21:ARX1:RLI1:C1_03370W_A:C1_04040C_A:REI1:C1_05630C_A:RPA190:C1_13380W_A:C2_05270W_A:C2_05750W_A:KRE30:RPS10:UTP8:RPS15:RPS19A:NOG1:NMD5:ZUO1:RPF1:ECM1:C4_06210C_A:RPS5:C6_02230W_A:NOG2:RPS18:ACC1:RPS3:SDA1:NMD3:CR_07080W_A:CR_08500W_A:ELF1:LTV1
nuclear transport	36 out of 578 genes, 6.2%	152 out of 6473 background genes, 2.3%	0.0000389	RRS1:HMT1:RPS21:ARX1:RLI1:C1_03370W_A:C1_04040C_A:REI1:C1_05630C_A:RPA190:C1_13380W_A:C2_05270W_A:C2_05750W_A:KRE30:RPS10:UTP8:RPS15:RPS19A:NOG1:NMD5:ZUO1:RPF1:ECM1:C4_06210C_A:RPS5:C6_02230W_A:NOG2:RPS18:ACC1:RPS3:SDA1:NMD3:CR_07080W_A:CR_08500W_A:ELF1:LTV1
DNA strand elongation	14 out of 578 genes, 2.4%	31 out of 6473 background genes, 0.5%	0.00014	RFC5:MCM3:POL30:TOP2:EXO1:DNA2:TOP1:RNH35:MCM6:MCM2:CR_04560C_A:POL2:DPB2:RFC4
DNA strand elongation involved in DNA replication	13 out of 578 genes, 2.2%	28 out of 6473 background genes, 0.4%	0.00027	RFC5:MCM3:POL30:TOP2:DNA2:TOP1:RNH35:MCM6:MCM2:CR_04560C_A:POL2:DPB2:RFC4
RNA methylation	14 out of 578 genes, 2.4%	34 out of 6473 background genes, 0.5%	0.00058	ABP140:NEP1:RRP8:C3_07400W_A:C4_03730C_A:C4_03830W_A:C4_04810C_A:NOP1:SPB1:C7_02340C_A:CR_01780W_A:CR_04160C_A:CR_04170W_A:CR_08940W_A
transcription of nuclear large rRNA transcript from RNA polymerase I promoter	9 out of 578 genes, 1.6%	16 out of 6473 background genes, 0.2%	0.00282	RPA34:RPA190:RRN3:C2_01070W_A:RPA12:TOP1:RPA135:CR_01950W_A:RRN11
cytoplasmic translational initiation	6 out of 578 genes, 1.0%	7 out of 6473 background genes, 0.1%	0.00412	TIF34:FUN12:TIF35:TIF11:DED1:TIF5
tRNA modification	19 out of 578 genes, 3.3%	68 out of 6473 background genes, 1.1%	0.00575	TRM2:ABP140:C2_00170C_A:KTI11:C2_09500W_A:C3_07400W_A:C4_00810C_A:C4_01500W_A:C4_03140C_A:C4_03730C_A:C4_03830W_A:C4_04810C_A:C6_02290C_A:C6_02350C_A:C7_02340C_A:KTI12:NCS2:CR_04160C_A:CR_08940W_A

macromolecule methylation	20 out of 578 genes, 3.5%	75 out of 6473 background genes, 1.2%	0.0071	HMT1:ABP140:C1_09040C_A:NEP1:C2_05520W_A:RRP8:C3_07400W_A:C4_03730C_A:C4_03830W_A:C4_04810C_A:NOP1:RMS1:ASH2:SPB1:C7_00490C_A:C7_02340C_A:CR_01780W_A:CR_04160C_A:CR_04170W_A:CR_08940W_A
tRNA processing	23 out of 578 genes, 4.0%	95 out of 6473 background genes, 1.5%	0.00851	TRM2:ABP140:LHP1:C2_00170C_A:KTI11:C2_09500W_A:C3_07400W_A:C4_00810C_A:C4_01500W_A:SEN2:C4_03140C_A:C4_03730C_A:C4_03830W_A:C4_04810C_A:NOP1:C6_02290C_A:C6_02350C_A:C7_02340C_A:KTI12:NCS2:CR_04160C_A:CR_08940W_A:POP3
methylation	20 out of 578 genes, 3.5%	76 out of 6473 background genes, 1.2%	0.00885	HMT1:ABP140:C1_09040C_A:NEP1:C2_05520W_A:RRP8:C3_07400W_A:C4_03730C_A:C4_03830W_A:C4_04810C_A:NOP1:RMS1:ASH2:SPB1:C7_00490C_A:C7_02340C_A:CR_01780W_A:CR_04160C_A:CR_04170W_A:CR_08940W_A
tRNA metabolic process	30 out of 578 genes, 5.2%	147 out of 6473 background genes, 2.3%	0.0149	C1_01160C_A:TRM2:ABP140:FRS2:LHP1:WRS1:C2_00170C_A:KTI11:VAS1:C2_09500W_A:C3_07400W_A:C4_00810C_A:C4_01500W_A:SEN2:TYS1:C4_03140C_A:C4_03730C_A:C4_03830W_A:C4_04810C_A:NOP1:HTS1:C6_02290C_A:C6_02350C_A:C7_02340C_A:CDC60:KTI12:NCS2:CR_04160C_A:CR_08940W_A:POP3

**** As stated in materials and methods, the gene lists were uploaded to CGD for GO term analysis. Sometimes, some genes cannot be included in the analysis either because of an annotation problem or because the software couldn't assign a GO term to them. Consequently, the software excludes these genes in the final results. For this reason I have 259 genes instead of 261 in the GO term analysis for the downregulated genes. Similarly, 578 genes were analyzed rather than 579 for the upregulated genes.**